A COMPARATIVE APPROACH TO THE DEVELOPMENT OF ANCIENT COPPER SUPPY NETWORKS IN OMAN AND OBSIDIAN SUPPLY NETWORKS IN ETHIOPIA

by
Ioana A. Dumitru

A dissertation submitted to Johns Hopkins University in conformity with the requirements for the degree of Doctor of Philosophy

Baltimore, Maryland
October 2019

Abstract

This dissertation adopts a comparative framework to the study of ancient raw material supply networks of copper in Oman (ca. 2500 BCE – 1800 CE) and obsidian in Ethiopia (ca. 800 BCE – 825 CE). A Social Network Analysis (SNA) approach is used to reveal the structures of supply networks, charting their diachronic developments and identifying fluctuations in the network positions of individual nodes as well as alterations in network sub-groups.

Using formal centrality and centralization measures (e.g. degree, betweenness, closeness) this study reveals largely decentralized networks of production in both study areas. These findings can tentatively be used to argue against the notion of elite control over production. Additionally, the longitudinal dataset reveals remarkable stability in network structures over time.

In the absence of evidence of elite control of this economic sector, one must identify the mechanisms that would have engendered the trust necessary for the reproduction of this economic system and for the maintenance of social order.

This dissertation turns to social networks, and social relationships themselves, as the mechanisms that integrated economic interactions, bringing about social order and maintaining stability. Counter to both formalist and substantivist economic theories, social network theories conceptualize exchange not in terms of atomized decision-making, driven either by a pursuit of utility maximization or solely by internalized patterns of behavior, but rather in terms of ever-changing interactions embedded within networks of ongoing personal relationships. Where these relationships are concerned, it is not merely economic gains that are the focus of economic interactions, but also social gains, such as a good reputation. These social gains are understood as

deterrents against malfeasance, as individuals would have a vested interest to operate fairly to maintain reputations for trustworthiness.

A final aim of this dissertation is to understand the spatial dimensions of the productive resources that form the basis of the case studies being investigated. To this end, high-resolution geological resource maps were created for the study regions in Oman and Ethiopia through analysis of Hyperion hyperspectral satellite imagery.

Advisor: Michael J. Harrower

Second Reader: Glenn M. Schwartz

Committee Chair: Benjamin Zaitchik

Readers: Marian Feldman, Matthew Peeples

To my friends in Ethiopia and Oman

And to Cătălina Bogdan, without whom I would not be here.

Acknowledgements

This dissertation would not have been possible without the help of a number of people and institutions. The greatest thanks must go to the people of Ethiopia and Oman. The friendships and professional partnerships I have forged along the way have changed me both as a person and as a scholar. I am tremendously grateful and fortunate to have the opportunity to work in such wonderful places and with such incredible people.

My dissertation work was supported both intellectually and financially by two larger archaeological projects: The Archaeological Water Histories of Oman (ARWHO) project and The Southern Red Sea Archaeological Histories (SRSAH) Project, led by Michael Harrower.

The research undertaken in the writing of this dissertation was also supported by a number of grants. A grant from the Sigma Xi foundation that I received in 2013 allowed me to explore some of the initial questions that subsequently laid the foundations of my dissertation. A NASA-ROSES Grant (NNX13A048G) to Michael Harrower supported fieldwork in both Oman and Ethiopia and satellite imagery analysis in the Spatial Observation Lab for Archaeological Research (SOLAR) at Johns Hopkins University. Excavations in Ethiopia were also supported through a Cotsen Excavation Grant from the Archaeological Institute of America (2015) and a Committee for Research and Exploration Grant from the National Geographic Society (2016).

I am grateful to the Sultanate of Oman, Ministry of Heritage and Culture for permission and support of this work. Special thanks go to Sultan Al-Bakri, Khamis Al-Asmi, Mohammed Al-Waili, and Suleiman Al-Jabri. Ceramic analyses informed identification of the time periods represented at the sites under investigation in this study and were undertaken by Jennifer Swerida (American University in Beirut) and Eli Dollarhide (Research Institute, NYU Abu Dhabi). Reconstruction of slag technologies would not have been possible without the support and expertise of Lucian Petrescu (University of Bucharest) and Joseph W. Lehner (University of Sydney). I am also grateful to the support of a brilliant group of colleagues: Smiti Nathan (Life Design Lab, Johns Hopkins University), Alexander Sivitskis (Samtse College of Education, Bhutan), Frances Wiig (The University of New South Wales), Abigail Buffington (College of William and Mary), Mehrnoush Soroush (Harvard University), Wolfgang Alders (University of California, Berkeley), and Avary K. Taylor (Johns Hopkins University). You all made data collection an extremely enjoyable and rewarding task.

Work in Ethiopia was made possible through the support of the Authority for Research and Conservation of Cultural Heritage (ARCCH), Tigrai Culture and Tourism Bureau, and Aksum University. I am grateful for the tremendous support of Kifle Zerue, Aley Woldeselassie, Habtamu Mekonnen, Seminew Asrat, Gidey Gebreegziabher, Fantahun Zelelew, Mekonnen Gebre-Meskel, Tesfay Aragie, and the people of Edaga Rabu and Ahferom Woreda. Ceramic analyses informed identification of the time periods represented at the sites under investigation in this study and were

undertaken by Cinzia Perlingieri (CoDA), Gabriella Giovannone (Università degli Studi di Napoli "L'Orientale"), Rachel Moy (University of California Los Angeles), and Habtamu Mekonnen (Simon Fraser University). Lithic analyses would not have been possible without the help of Lucas R. Martindale Johnson (Far Western Anthropological Research Group, Inc.), who identified the obsidian groups from p-XRF data that I collected in the field. Morphological analysis of lithics was conducted by Elizabeth A. Peterson (Vancouver Police Museum) following a morphological typology established by Steve Brandt (University of Florida) for the Eastern Tigrai Archaeological Project (ETAP) directed by Catherine D'Andrea (Simon Fraser University). I am truly grateful for their support and expertise.

I would like to thank my dissertation chair, Benjamin Zaitchik, and my advisors, Michael Harrower and Glenn Schwartz, as well as my dissertation readers, Marian Feldman and Matthew Peeples, for their comments, suggestions, and thoughtful questions during the dissertation writing process and the defense.

The person to whom I owe the most thanks for the completion of this dissertation is my primary advisor, Michael Harrower, who patiently mentored me through the PhD process. I cannot thank him enough for the opportunities he opened up for me, for his personal investment in my training and success, for his encouragements and helpful advice (even when I did not listen). When I started in the Near Eastern Studies department, I was intending to do my dissertation in Turkey, so it is safe to say that [redacted] years later, the fact that I am an archaeologist working in Oman and Ethiopia is entirely due to his guidance. As cheesy as it may sound, working with him not only changed my scholarly scope, it changed my life, for without him I would not have met my life partner, Jacob Bongers.

My enormous gratitude also goes to Glenn Schwartz for his insightful and thoughtful comments on my dissertation. Nearly every page of my dissertation has benefitted from his meticulous commentary. I am a more careful and diligent scholar because of him and for that I am truly grateful.

My deepest appreciation also goes to the many other outstanding scholars who have contributed to my education, both at Bryn Mawr College and Johns Hopkins University. My undergraduate career was shaped by the mentorship I received from Peter Magee, Astrid Lindenlauf, and James C. Wright, in the Department of Classical and Near Eastern Archaeology, and from Robert Dostal, Michael Krausz, and Bharath Vallabha, in the Department of Philosophy. I will forever remember with great fondness the debates on constructivism I had with Professor Vallabha and the guidance I received from Professor Krausz when I could not decide between pursuing graduate studies in Philosophy or Archaeology. I think I made the right choice! I am also indebted to Nicholas Rauh (Purdue University) with whom I did fieldwork in Turkey throughout my undergraduate career. Going further back still, I am truly grateful for the wonderful experiences I had while participating in my first fieldwork in Romania (Giurgiu – Malu Roșu and Histria) and am particularly thankful for the wonderfully kind reception into the field that I received from Emilian (Socrate) Alexandrescu (University of Bucharest), from the late Alexandru Suceveanu, and from Alexandru Avram (Le Mans University).

I am also tremendously grateful to have had a wonderful group of friends and colleagues who have supported me throughout this process. In particular I would like to thank my cohort members, William Reed and Adam Bean. I will remember our Akkadian classes and especially the carrots and whiskey tasting with great fondness for many years to come. Megan Lewis and Jill Waller, thank you for your friendship and for the great fun we had in the field at Tayinat. I could not have asked for better companions to share my pre-comps summer with and would even consider forgiving one of you for the grave mistake of stealing my clothespin (you know who you are). Erin Villareal, this department may have made me a doctor, but it was you who made me a reverend and for that I am truly grateful. Laurel Poolman, thank you for feeding me and for bringing Abe into my life. Avary Taylor, did you go to Bryn Mawr? Smiti Nathan, Morgan Moroney, Maggie Bryson, Mike Chapin, Karlene Shippelhoute, Lingxin Zhang, Bianca Hand, Nicholas Gill, Paige Paulsen, Richard Essam, Stephanie Cooper, Tori Finlayson, Gaultier Mouron, Jem Swerida, Tiffany Earley Spadoni, and Marina Escolano-Poveda I will always much rather be with you guys at CVP than anywhere else.

Special thanks must also go to Douglas Comer without whose support and friendship the last three years of my grad school career would have been less pleasant. You are probably the best employer I will ever have, and I am truly grateful to have worked with you.

To my Calvert family, Jacob, Rania, Rosanne, Anna, Raquel, Michele, Jaime, Hannah, and Gabri – I really could go on for another 500 pages about you guys. Perhaps more than anyone, you all have shaped my little baby adult self. You have been there with me through some joyous and very difficult moments; you put up with me while I recited whole *Office* scenes under my breath. You fed me and kept me upright (both literally and figuratively) particularly during my last months of dissertation. Meeting you will forever be the best thing to come out of my time in Baltimore.

Rosanne, my implausible twin, the Jim to my Dwight, the Rory to my Lorelai, I can only hope that what I have taken from you in terms of life lessons about being a responsible adult I have given back to you in the form of mischief and shenanigans. My greatest dream will forever be starting a commune with you and Patrick.

Anna, the truest *Gilmore Girls* fan there ever was, what can I even say about you? Not much, as it turns out, for you seem to have stolen (for your own *Acknowledgements*) all of the most memorable and mentionable moments of our friendship. On paper, sleeping on the floor of the lab and going to buy greasy pizza at 3:00 AM does not seem like the best of times, and yet I think those are the moments I will remember most fondly from my time at Hopkins. You made even the hardest grad school days fun and truly are my Platonic soulmate. I think I first knew this that day in the History Seminar when the dawning realization of the often-ridiculous nature of our pursuits befell you and you could not stop laughing. To this day, one of the most dangerous things I could ever do would be to look your way during a lecture.

Thank you must also go to my family for your support and love through these most joyous and most difficult times. My mother, Elena, is the person I picture in the audience when I give a talk. Her presence, even if imagined, turns even the scariest of rooms into a place of love and acceptance. Your belief in me carries me through when my own falters. My father, Mircea, has

arguably played the biggest role in shaping me both as a human and as a scholar. I am an archaeologist because you are a philosopher, a constructivist because you are a realist, a dyed-in-the-wool leftist because you are a centrist. Motanul Vasile is my moral kernel. Words cannot express how grateful I am to have you as parents. Finally, a huge debt of gratitude goes to my partner, Jacob. Nothing about the future scares me because of you. This dissertation is also dedicated to you.

I have recently alighted upon the notion that accolades are merely functional *substitutes* for love and group acceptance. That being said, having this one sure is nice!

Contents

List of Tables

List of Figures

Chapter 1

Introduction

1.1. Context of Research

This dissertation sets out to accomplish four complementary goals. Employing a Social Network Analysis approach (SNA), it examines the structures of copper and obsidian supply networks outlining their diachronic developments and identifying fluctuations in the network positions of individual nodes as well as transformations in network sub-groups. Relatedly, this study attempts to reveal aspects of underlying network topology, defined as the emergent properties of networks. This latter aim is undertaken through a cross-cultural comparison of the copper supply network that developed in north-east Oman (ca. 2500 BCE – 1800 CE) and the obsidian supply network that developed in the central zone of the northern Tigray region, in northern Ethiopia (ca. 800 BCE – 825 CE) (Fig. 1.1). Theoretically, the aim of this dissertation is to explore the validity of adopting a social network approach as an alternative to traditional theories of market exchange and to substantivist theories of economic interaction. A final aim this dissertation sets out to accomplish is to understand the spatial dimensions of the productive resources that form the basis of the case studies being investigated.

This dissertation compares socio-economic networks that emerged within two different cultural contexts in Oman and in Ethiopia, where copper and obsidian were extracted, processed, and distributed to consumers. Although the formation of production and distribution networks is impacted by unique historical particulars, cross-cultural commonalities ostensibly do exist among

Figure 1.1 Geographical Position of Research Areas in Oman (ArWHO) and Ethiopia (SRSAH).

contexts that share environmental, technological, and social constraints (Trigger 2003; Barjamovic 2011, Feinman 2013).

Cross-cultural comparative studies have a long history within archaeology and anthropology (Mead 1928, Geertz 1971, Sahlins 2004, Adams 1974, and Earle 1997). This approach has drawn some criticism from archaeologists who associate cross-cultural comparison with neoevolutionism (Fried 1967, Service 1971, Steward 1972). However, while neoevolutionism made frequent use of cross-cultural comparisons, the comparative framework itself is a stand-alone methodology that does not necessitate the implications of neoevolutionism (Drennan et al. 2012). Indeed, the primary contention with neoevolutionism, its preoccupation with normative societal types, is avoided by most recent comparative studies, which focus instead on particular

archaeological studies undertaken at various spatial or societal scales (Drennan et al. 2012: 2, Harrower 2016, Smith 2011).

The cross-cultural comparison employed in conjunction with a network approach is more distant still from neoevolutionist approaches; this is because the subjects of comparison are bounded archaeological networks, abstractions devised to proxy economic interaction that do not investigate the impacts of a plethora of interlocking socio-economic phenomena, but rather a single relationship chosen for the construction of the networks.

Even so, the case studies selected in Oman and Ethiopia are characterized by several similarities outside of the bounds of the networks themselves, which further solidify their selection for comparison. The supply networks are both located in mountainous regions, with the copper network developing in the Ad-Dhahirah Governorate of northern Oman and the obsidian network in the Tigray Region in the northern Ethiopian highlands. Both have histories of engaging in local, regional, and long-distance terrestrial and maritime trade conducted in the Arabian Gulf and in the Red Sea, respectively. Socio-politically, both regions were characterized by the development of so-called secondary civilizations, Magan (in Oman) and the Aksumite Empire (in Ethiopia), both of which are often defined in relation to interactions with more powerful neighbors in Yemen, Sudan, and Egypt along the Red Sea, and Iraq, Iran, and the Indian subcontinent, in the Arabian Gulf and broader Indian Ocean (Cleuziou and Méry 2002, Cleuziou and Tosi 2007, Fattovich 2000, Fattovich 2010, Magee 2014, Potts 1993).

Socio-political organization of research areas – These regions differ in terms of the level of socio-political complexity and stratification attained: the Omani case study is defined by initial lower levels of hierarchy (Fleming 2004, Jacobsen 1943) than are observed in regional Bronze Age neighbors, while northern Ethiopia is characterized from the beginning of the Pre-Aksumite

period by evidence of marked social stratification (Fattovich 2010, Phillipson 2012, Finneran 2013).

Oman – Archaeological evidence dating to the Southeast Arabian Bronze Age (ca. 3200 – 1300 BCE) reveals a mixed subsistence economy with evidence of agricultural intensification (Al-Jahwari 2009), pastoralism (McCorriston et al. 2012), hunting and foraging (Charpentier 2008, Potts 2009, McCorriston 2006), and fishing (Beech 2004). This period's economy is characterized by fluctuations in the degree of agricultural intensification, sedentism, and transhumant lifestyles (Cleuziou 1981, Cleuziou and Tosi 2007) and by the endurance of a mixed subsistence strategy (Højgaard 1980).

While many contemporaneous centers in the ancient Near East were characterized by hierarchical systems of socio-political organization, Bronze Age societies in Oman demonstrated lower levels of hierarchy (Fleming 2004; Jacobsen 1943). Instead of a strict hierarchy, it has been theorized (Cleuziou 2002, McCorriston 2011, Magee 2014) that Bronze Age social groups were organized according to a sentiment of social cohesion inculcated through kinship and group ties. This theory of a shared social sentiment of cohesion and solidarity has been constructed around a notion, termed *'aṣabîyah* ("group feeling"), and defined by the Arab historian Ibn Khaldun in his book *Muqaddimah* (also known as the *Prolegomena* in the Western world). In this book, the 14th century historian argues for a cyclical theory of world history (Khaldun 1377/ Rosenthal 1958).

Arguably one of his most famous contributions to scholarship, the notion of *'aṣabîyah* does not originate with Ibn Khaldun; indeed, it is rather the positive light in which the term is portrayed that appears to be particular to his scholarship. The term derives from the word '*aṣabah* meaning *agnate* or a male relative connected through the father's family (Rosenthal 1958: lxxviii). As such, one original meaning of the term may have been a feeling of solidarity with one's agnates. In Ibn

Khaldun's work, the term seems to expand in meaning through its association with the etymologically related terms *'iṣâbah* and *'uṣbah* meaning more generally "group" (Rosenthal 1958: lxxviii). As such, a feeling of solidarity, while primarily reserved for one's kin is here being used to connect one to a non-kin social group.

This term was more frequently used in Muslim literature with the pejorative sense of "bias" referring to situations in which one's preference for one's group or family members would lead one to disregard their shortcomings and misdeeds. Indeed, Muslim contemporary scholars associated the notion with unsophisticated elements of pre-Islamic societies. Enlightened to this understanding of the term, Ibn Khaldun argued for the need to discern between '*aṣabîyah* as "bias" in the pre-Islamic sense and innate '*aṣabîyah* that characterizes human nature. This discussion, unsurprisingly, arises in the context of trying to understand the rise of social complexity.

For the historian, the more '*aṣabîyah* one group had, the higher their chances of success (Khaldun 1377/ Rosenthal 1958). Similarly, the more '*aṣabîyah* one individual or family had within the community, the higher their chances would be to rise the ranks of leadership. In this manner, Ibn Khaldun explains the formation of hierarchy within a society, but is careful to suggest that one's leadership roles would eventually be removed if they are to lose community support.[1]

Importantly, Ibn Khaldun makes clear that this term is meant to understand the evolution of socio-political complexity in pre-Islamic societies, as early Muslim states were to be understood as arising in connection with a pure and unworldly notion of a state (Khaldun 1377/ Rosenthal 1958).

[1] In this sense, Ibn Khaldun's explanation is not far from the argument recently put forth by Stanish (2017) according to which pre-state leaders did not obtain their positions through force and coercion but rather as a result of their position within society and the high regard they were held in by their social group.

A reconstruction of Bronze Age social organization relies heavily on mortuary contexts (Benton 2006, Cleuziou 2002, 2003, 2007, 2009, Cleuziou and Tosi 2007, Giraud & Cleuziou 2009, al-Jahwari 2008). Communal Hafit beehive tombs (Frifelt 1975, de Cardi, Collier, and Doe 1976, Vogt 1985) and Umm an-Nar tombs (Cleuziou 2002, 2003, 2007, 2009, Cleuziou and Tosi 2007, al-Jahwari 2008:329, Lancaster and Lancaster 1992, Potts 2008, 2009, Rouse and Weeks 2011) contained osteal assemblages representative of multiple ages and sex groups. Additionally, grave goods do not seem to have been used to demarcate a social hierarchy during this period.[2] A shift in community structure seems to occur during the subsequent Wadi Suq period. This is suggested both by the settlement structure and by mortuary architecture. Unlike previous periods, available evidence from Wadi Suq settlements indicates the abandonment of a settlement plan centered around a highly visible megalithic tower. Visibility does not seem to be a consideration in the construction of Wadi Suq tombs either. Associated with the Hafit and Umm an-Nar periods, constructing communal tombs in highly visible points in the landscape is arguably considered a strategy used to communicate a lack of social stratification. Discontinuing this practice suggests that whereas tombs remained communal, mortuary architecture was no longer used to communicate a lack of social hierarchy.

Iron Age subsistence strategies reveal a familiar pattern of mixed economic strategies. As in previous periods, fishing occurred on the coast and farming in inland oases. Less is known about Iron Age pastoralism (Potts 1990). Important technological developments appear to characterize

[2] This picture is somewhat complicated by textual evidence from Mesopotamia. Textual records from the reign of Šulgi, for instance, mention a *lugal* of Magan (lu_2-gal Ma_2-gan^{ki}; Legrain 1947). Another text dating to the reign of Amar-Sin mentions an *ensi* ($ensi_2$) of Magan (Sigrist 1988). However, this is not necessarily to be taken as indicative of the structure of Bronze Age society. In the absence of corroborating material evidence, it can be suggested that Mesopotamians may have been casting their interactions with the people of Magan in terms understandable within the ideologies generated by their highly socially structured societies. Further work needs to be undertaken to reconcile this evidence.

this period. The introduction of the falaj irrigation system and the domestication of the camel during the Iron II period (Magee 2004) appear to lead to settlement growth and increased inter-regional interaction.

Socio-politically, the Iron Age is characterized by some evidence of hierarchical organization, although the notion of '*aṣabîyah* is also used in reference to this time period. A 7th century BCE Neo-Assyrian text dating to the reign of Assurbanipal records the visit of king Padê from the land of Qadê (identified as Oman), who travels to the court at Nineveh, bringing with him tribute (Thompson 1933). Padê traveled for six months from the city in which he dwelt, Iske,[3] to arrive at Nineveh. The extent to which power was centralized in the hands of one ruler, however, remains to be determined. Evidence of social stratification and political complexity can also be seen in the material record and in particular in the architectural evidence. During the Iron II period, large buildings were discovered throughout Southeast Arabia. These buildings have evidence of large halls which would have allowed gatherings to take place.

Before the Islamic Period, Southeast Arabia was under Sasanian control. During this period, large-scale maritime trade flourished in the Gulf (al-Naboodah 1992). Oman was considered to have immense strategic importance to the Sasanians because of its position at the mouth of the Gulf. Sasanians were able to control maritime trade in the Gulf by occupying important ports, such as the one at Sohar and at Diba, which also became important administrative and military centers (Wilkinson 1973).

The importance of long-distance maritime trade to the development of socio-political complexity during the Sasanian and Early Islamic period can also be deduced from the fact that the port city of Sohar became the seat of government during these periods (al-Naboodah 1992).

[3] It has been suggested that Iske refers to the modern town of Izki, located in the interior of Oman and locally identified as the oldest town in Oman (Wilkinson 1983, Potts 1990).

The Riddah Wars from the beginning of the Islamic period temporarily halted trade activities. These recommenced during the Umayyad period, but were now under the control of the Umayyad Caliphate. During the later Abbasid period, Oman regains its centrality in maritime trade within the Gulf and the wider Indian Ocean. Oman's importance continues throughout the Islamic Period. The principal exports throughout this period were copper, pearls, dates, and frankincense. The main imports of this period were precious minerals (gold from Africa, silver from Persia), ivory from East Africa, textiles (from India, Persia, and China), timber for ship building and furniture making (from India and East Africa), perfume (from Tibet and China), and slaves (from East Africa) (al-Naboodah 1992). While the importance of maritime trade was undoubtedly great, agriculture and water management remained the basis of the economy (Hoyland 2002).

The introduction of Islam led to many social changes occurring within the socio-political context of the state. Islamic culture encouraged a departure from tribal rules and regulations (such as the aforementioned '*aṣabîyah*) in favor of overriding divine laws.

Ethiopia – By contrast, the economic and socio-political context in northern Ethiopia was characterized from the beginning by marked social stratification. Developing during the first millennium BCE, the Pre-Aksumite polity of the northern Ethiopian highlands has been characterized as the first Ethiopian complex society[4] (Fattovich 2010, Phillipson 2012, Finneran 2013). The base of the economy was agricultural with evidence of intensive local production traditions where lithics and ceramics are concerned (Fattovich 1978, 1990, Munro-Hay 1993, Phillipson 1998, Finneran 2007). Cattle rearing dominated the Pre-Aksumite economy, a characteristic that continued into the Aksumite period (Phillipson 1998, Cain 2000). Plant cultivation included a combination of local African crops (t'ef and sorghum) and cereals imported

[4] A parallel developmental trajectory results in the formation of the Ona culture in the Eritrean highlands (Curtis 2009, Schmidt and Curtis 2001, Schmidt 2009).

from Western Asia (wheat, barley, lentils, and flax; Bard et al. 1997, Phillipson 2000a, D'Andrea 2008, D'Andrea et al. 2008, 2011, Schmidt et al. 2008, Beldados and Costantini 2011).

The origins of the Pre-Aksumite polity are still passionately debated, with some scholars highlighting local influences and others foreign South Arabian influences. Interactions with South Arabia are evidenced by the discovery of objects with South Arabian script as well as South Arabian architectural elements and elite objects (Fattovich 1988, 1990, 2009, 2010, Munro-Hay 1993). The nature of these interactions, however, remains disputed with some arguing for the colonization of the Tigrayan highlands by South Arabian social groups (Finneran 2013) and others suggesting autochthonous Ethiopian adoption of certain aspects of South Arabian culture and religion (Curtis 2004, 2008). Where socio-political organization is concerned, Pre-Aksumite inscriptions make reference to both a kingdom of D'MT (de Contenson 1981), which may or may not have had a South Arabian origin, and to local rulers called MLK (*malik*) or king and MKRB (*mukkarib*), interpreted to mean "unifier" (Beeston 1972).

The ensuing Aksumite economy was characterized by an agricultural and pastoral base (D'Andrea 2008, Harrower et al. 2010, Phillipson 1998, D'Andrea et al. 1999). While domestic animals included sheep, goats, donkeys, camels, and chickens, cattle rearing continued to have an outsized importance in the Aksumite economy, with cattle becoming a symbol of Aksumite identity (Phillipson 1998, Cain 2000). The same combination of local and imported cultivated plants that characterized Pre-Aksumite agriculture persists into the Aksumite period. These agricultural imports into northern Ethiopia are considered the culmination of long-distance trade exchanges throughout the Red Sea region and the wider Indian Ocean area (Hanotte et al. 2002; MacDonald 1992).

While not remaining static over time[5] (Munro-Hay 1991), the entire period of the Kingdom of Aksum is characterized by a high degree of social complexity and by a relatively high level of stability[6] over time (Phillipson 1998). The structure of Aksumite society has been compared to a pyramid model of social stratification, which finds the king at the top[7] of the hierarchy and his family members occupying important administrative and political positions immediately below (Munro-Hay 1991, Phillipson 2012). This hierarchy and social stratification is supported by the discovery of elite centers with palatial structures, elite tombs, and inscriptions.

The archaeological record is replete with examples of non-royal elite structures of various sizes and degrees of affluence which have been used by scholars to argue for the existence of a strong middle class (Phillipson 1998). Another important social class for which we have a considerable amount of evidence, as seen in Chapter 2, is that of skilled craft specialists who engaged in ceramic and lithic production as well as metallurgy (Phillipson 1998). Finally, texts record the existence of a slave class, integrated into Aksumite economy as a result of expansions into neighboring southern Sudan (Sadr 1991).

Raw material supply networks – The facet of the supply network that is being investigated is raw material production. In Oman, slag assemblages constitute material proxies for production. Slag is a by-product of the smelting process that has been geochemically analyzed to reconstruct smelting technologies. These reconstructed technologies were in turn used to generate networks of settlements linked by evidence of comparable implementation of shared technological knowledge.

[5] The socio-political structure was particularly susceptible to changes following the conversion of Aksumite kings to Christianity, for instance.
[6] The absence of walled settlements and the Aksumite engagement in long-distance trade endeavors has been used by scholars as evidence for stability (Phillipson 1998).
[7] There is some evidence that, on occasion, greater power was held by generals who usurped the authority of the king (e.g. King Kaleb's general Abreha in the 6th century CE).

In Ethiopia, obsidian assemblages that are largely made up of lithic debris serve as proxies for production. Lithic debris constitutes material evidence of knapping and is characterized by the presence of angular waste, flakes, and occasional finished tool types. Several geochemically distinct obsidian groups have been reconstructed from the Ethiopian lithic assemblage. These groups were used to construct networks of affiliation based on shared material culture. Thus, while both networks investigate production, they differ in terms of what is being diffused through the network: in Ethiopia it is the raw material itself that is circulating through the network, whereas in Oman it is the diffusion of information relating to copper smelting practices that is the subject of this investigation. Notwithstanding, considerable overlap potentially existed between networks of technological diffusion, networks of copper ore distribution, and networks of product exchange. Similarly, there was also potential overlap between networks of obsidian raw material diffusion, networks of production, and networks through which knowledge of obsidian knapping circulated. However, owing to dataset particulars, it is networks of production sites that are the focus of this investigation.

A nominalist approach has been adopted to demarcate network boundaries. That is, the entities under investigation are defined on the basis of shared attributes (Laumann et al. 1992, Peeples 2019) and, in contrast with realist networks, categorized as real-world social groups characterized by often culturally specific shared norms, rules, and feelings (Homans et al. 1968, Bandyopadhyay et al. 2011).

Nominalist groups, however, have realist referents. Where the case studies being investigated are concerned, these referents were communities of production engaging in large-scale, organized raw material exploitation and production, likely for the purpose of regional and long-distance exchange.

Cultural context – In Oman, cycles of intensive copper production correspond to periods of increased socio-political complexity occurring during the Bronze Age, Iron Age, and Islamic Period. Because of this correlation, some have argued that the cyclical nature of Omani copper production was impacted by broad, inter-regional dynamics involving increasing demand for copper and bronze throughout the Ancient Near East (Potts 1993, Weeks 2003, Cleuziou and Tosi 2007, Giardino 2017). In accordance with this position, early evidence of widespread copper production during the third millennium BCE (2700-2000 BCE) appears to coincide with evidence of increased trade connections between Magan (identified as Oman) and Sumer (Begemann et al. 2010, Cleuziou and Tosi 2007, Weeks 2003, Peake 1928, Potts 1999). Approximately 10,000 tons of slag were recorded for this period, producing an estimated 2,000 – 4,000 tons of copper (Hauptmann 1985).

Around the beginning of the second millennium BCE, Mesopotamian cuneiform records reveal that most trade activities with regions in the Lower Sea (identified as the Arabian Gulf in Mesopotamian sources; Frayne 1993: 27: 2.1.1.1) were occurring through the intermediary of Dilmun (identified as Bahrain). The last mention of a Mesopotamian trade partner in the Arabian Gulf dates to the reign of Samsu-iluna (1744 BCE) and refers to Dilmun. Approximately 400 years later, however, Oman observed another resurgence in local copper production during the Iron Age I and II periods (ca 1300 – 600 BCE). Additionally, the presence of tin-bronzes in later Iron Age assemblages suggests a revitalization of long-distance trade networks (al-Shanfari and Weisgerber 1989). The scale of Iron Age production increased significantly as compared to Bronze Age production, with tens of thousands of tons of slag being recorded at several sites in the Omani interior (e.g. Raki, Weisgerber and Yule 1999).

Around 300 BCE, production in Oman once again appears to have been halted and available data suggests this interruption may have lasted for nearly 1000 years (Cleuziou and Tosi 2007: 303). Large-scale copper production is once again recoded during the Islamic Period and can be divided into two periods of florescence, during the Early Islamic period (800 – 900 CE) and during the Late Islamic Period (1100 – 1800 CE). As it related to scale, Islamic production supersedes all previous periods of production, with several sites being characterized by 100,000 tons of slag (Hauptmann 1985).

Whether these fluctuations in production are tied to internal socio-political developments or due to external factors related to broader regional tendencies remains a greatly debated question (Weeks 2003). This study, however, is focused on regional interactions and, as such, the extent to which broader socio-political dynamics may have impacted local histories of production is not within its scope.

In Ethiopia, the period under investigation includes the first millennium BCE and the first millennium CE and has been divided into two broad phases: the Pre-Aksumite period and the Aksumite period. The Aksumite period has in turn been sub-divided into six sub-phases: Proto-Aksumite, Early Aksumite, Classic Aksumite, Middle Aksumite, Late Aksumite, and Post-Aksumite (Fattovich 1990; Fattovich et al. 2000; Munro-Hay 1993; L. Phillipson 1998, 2000b).

Characterized by both indigenous and foreign elements, three lithic traditions are associated with the Pre-Aksumite period (ca. 800 – 360 BCE): a microlithic tradition, a macrolithic tradition, and a possible hybrid micro-macro tradition (L. Phillipson 2009a). Microlithic assemblages contain a variety of obsidian forms, including backed crescents and bladelets. Notable variability in Pre-Aksumite lithic forms, both within and between assemblages, has been interpreted as evidence of non-specialized production (L. Phillipson 2000, 2009).

The microlithic industry of the Pre-Aksumite period is the only tradition to continue into later periods, an observation which has led some to argue for a continuation in population groups between periods (L. Phillipson 2009). Evidence of cultural continuity between the Pre-Aksumite and later Aksumite periods has also been theorized based on the discovery of so-called 'Likanos' flake assemblages at Kidane Mehret (Aksum). 'Likanos' assemblages made entirely of obsidian were discovered in both Pre-Aksumite and Late Aksumite contexts (Finneran 2007: 56, L. Phillipson 2009: 109 – 113).

While difficult to differentiate between Pre- and Proto-Aksumite (ca. 360 – 130 BCE) assemblages, evidence of increased direct percussion appears to differentiate Proto- from Pre-Aksumite lithics. Coupled with evidence of flakes characterized by smaller striking platforms, this evidence has been used to suggest an increase in skill among Proto-Aksumite knappers (L. Phillipson 2009b: 112). Despite this theorized increase in skill levels, Proto-Aksumite assemblages do not indicate broader economic changes when compared to Pre-Aksumite lithics. One must, however, lead with skepticism when considering interpretations of the Proto-Aksumite. This is because, much of the evidence dated to this period is highly localized, being confined to the area of Bieta Giyorgis at Aksum, and, as such, generalizations are problematic (L. Phillipson 2000b: 112).

Overall, the Aksumite period is characterized by a slight decrease in lithic usage when compared to previous periods (L. Phillipson 2000). Despite this diminution, stone tools continue to be used throughout all Aksumite sub-periods, are seemingly better represented in later periods, and survive the introduction of metals.

Aksumite lithic assemblages appear to be dominated by so-called Gudit chert scrapers (DW Phillipson 1977, L. Phillipson 2009:120, 2000a: 52-57, Puglisi 1946). Part of the microlithic

tradition, Gudit scrapers are remarkably uniform and standardized. Obsidian backed bladelets and flakes, as well as small triangular points are also contained in Aksumite assemblages.

A remarkable degree of similarity exists between Early (ca. 130 BCE – 160 CE) and Classic Aksumite (ca. 160 – 380 BCE) lithic assemblages which does not support classification to time period in the absence of other elements of material culture (L. Phillipson 2009b: 113 – 114). It is presently unclear whether this pattern is suggestive of continuity in lithic traditions or whether it is owing to issues relating to sample size, sampling strategy, or multi-period assemblages (L. Phillipson 2009b: 113).

The Early and Classic Aksumite periods are characterized by a trajectory from generalized towards specialized lithic production as evidenced by an increase in what appear to be small specialized workshops. Lithic production dating to these periods is also characterized by an increase in uniformity both within assemblages, in terms of tool type, and between assemblages (L. Phillipson 2009b: 113). These patterns have been suggested to reveal the professionalization of lithic manufacturing and the commoditization of all facets of the supply network, including raw material exploitation, transportation, and production (L. Phillipson 2009b).

While this observation about an increase in specialization and a rise in the production of more uniform assemblages presents interesting interpretive prospects, it is important to note that these patterns rely on often multi-period surface finds uncovered in the vicinity of the site of Aksum and, as such, generalizations should be undertaken cautiously.

This observed trajectory towards standardization culminates during the Middle Aksumite Period (ca. 380 – 580 CE) and has been characterized by the production of highly uniform lithics. During this period and during the Late Aksumite period (ca. 580 – 825 CE) production appears to occur at a number of specialized sites, each of which concentrated on the production of a specific

tool type. Another pattern characterized by a perceived decrease in consumption may result from sampling from multi-period sites (L. Phillipson 2009b: 114 – 115).

Characterized by largely overlapping lithic forms, it has been argued that Late Aksumite assemblages can be differentiated from Middle Aksumite assemblages through the presence of highly standardized Gudit scrapers. These scrapers have evidence of repeated resharpening which has been interpreted as further indication of a trend towards hyper-specialization. Produced using locally sourced chert, a refusal to replace these tools does not appear to be owing to the value or the scarcity of the material. As such, it has been proposed that it was in fact a shortage of specialists that created this pattern (Hirth and Andrews 2002: 9; Phillipson 2009: 115).

Theoretical and methodological context – The theoretical foundations of this study were largely influenced by theories affiliated with the network approach that developed in a number of different disciplines. The network approach is an umbrella term with both methodological and theoretical implications that evolved slightly different iterations within the various fields that employ it (including economics, sociology, anthropology, etc.). On the one hand, this framework provides a methodological blueprint (originating in graph theory) for analyzing and visualizing patterns of human interaction. On the other hand, it provides a theoretical foundation for analyzing human behavior.

The theories adapted herein are influenced by network approaches in sociology (Bandyopadhyay et al. 2011, Collins 1988) and new economic sociology (Granovetter 1985) and by particular applications in archaeology (Brughmans 2010, 2013, Knappett 2013, Mills et al. 2015, Mills 2017, Mizoguchi 2013, Peeples 2019, etc.).

Of interest to this dissertation was a defense of the validity of employing social networks as an alternative to Neoclassical (Bandyopadhyay et al. 2011, Collins 1988) and substantivist

theories of economic interaction. In contrast to Neoclassical economics, social network theories do not theorize economic interactions in terms of utility maximization but rather in the context of interactions embedded within networks of ongoing personal relationships (Granovetter 1985). Social networks developing out of recurring social relations preserve trust and maintain social order in the context of economic interactions. Originally developed by Granovetter to explain "imperfectly competitive markets" (1985: 488), the notion that economic activity is embedded in a social network of relations is particularly applicable to studies of ancient economies, and indeed a version of the embeddedness theory predates this iteration within archaeology and anthropology by decades (Barber 1995, Malinowski 1922/ 2014, Polanyi 1944). Granovetter's argument is that individuals will prefer to engage in economic interactions with social actors that have a reputation for fairness. This notion is also supported by empirical investigations studying human cooperation (Nowak et al. 2000; Stanish 2017: 48). This preference, it is argued, would provide social actors with an incentive to behave fairly and refrain from engaging in misconduct, thereby maintaining social order. Participation in economic activities would, therefore, involve economic partners with culturally determined reciprocal expectations (Granovetter 1985, Turner 1987, Homans 1961, Blau 1964).

This network approach also evades many of the drawbacks of substantivist economic theories, foremost among which is the outsized focus on understanding equilibrium within systems. Influenced by Malinowski's functionalism, a centering of the notion of systemic stability does not provide Substantivists with a good blueprint for studying tensions or change within a system. Formulated in contrast to a structuralist-functionalist approach, the network approach provides scholars with a model for analyzing tensions, power dynamics, and imbalance within a system.

Far from developing an idealized notion of economic interactions, the network approach is a bottom-up methodology that provides a robust design for studying and understanding economic transactions. According to this notion, malfeasance is not entirely overcome through social networks as trust can be abused for personal gain by bad actors (Granovetter 1985). Indeed, this allowance coheres with a social network approach that recognizes the existence of and need for studying social tensions.

1.2. Focus of the Study

The primary focus of this study is gaining an understanding of the internal structures of supply networks and of the distribution of power within networks.

In network analysis, powerful actors are identified by the advantageous positions they occupy in relation to other actors within the networks. As will be demonstrated, the same network position, analyzed according to different metrics and assumptions, can reveal different types of advantages.

For instance, one of the most common network measures, degree centrality, assumes that the most central actors will also be the most powerful because they will have more occasions to influence other actors (Freeman 1978). Other measures of degree centrality, like Bonacich's beta-centrality (1987), however, argue that being characterized by the same degree does not inherently make actors equally important. The assumption inherent in this beta-centrality measure is that not only is a node's centrality a function of its own direct connections, it is also impacted by the number of connections that characterize the nodes it is connected to. However, whether or not the best-connected node of a sub-set of well-connected nodes has more influence than the best-connected node of a sub-set of isolated nodes remains a topic of debate that should be determined by theorizing based on the socio-cultural context of the network.

1.3. Value of the Research

The value of this research lies primarily in its theoretical and methodological contributions. Theoretically, it represents a new attempt in a burgeoning area of network studies at understanding the diachronic development of networks at scales of thousands of years (Coward 2010, Peeples 2019, Mills et al. 2013, Ryan and D'Angelo 2018, Suitor et al. 1997, Wissink and Mazzucato 2017). Because of its ability to analyze the development of networks across large time spans, archaeology is uniquely positioned to contribute to broader questions within network studies.

Cross-cultural studies of ancient economies can also impact the development of economic theories more broadly. Knowledge of ancient economic systems that developed in Africa and Arabia have not often been taken into consideration by economists. Diachronic and cross-cultural approaches to ancient economies can generate a tremendous amount of empirical data that can be used to nuance theories related to the development of economic processes. Echoing Granovetter, I argue that it is likely that "the level of embeddedness of economic behavior […] has changed less with "modernization" than [substantivists] believe" (Granovetter 1985: 482). As such, insights from premarket economic systems can prove useful in understanding long-term processes of development as well as contemporary economic situations. Cross-cultural approaches are also useful in illuminating the interplay and coexistence of various economic mechanisms and forms of integration, a notion that is readily accepted for the ancient economy, yet seldom entertained for contemporary economic systems.

Methodologically, the contribution of this dissertation is represented by an uncommon combination of a suite of methods (SNA, GIS, and remote sensing for rock and mineral prospectivity analysis) which, when jointly applied, provide a rigorous approach to modeling raw

material supply chains, both in terms of the networks that develop around their production and trade and in terms of determining prospective locations for exploited resources.

1.4. Dissertation Organization

This dissertation is divided into eight chapters. Chapter 2 provides an overview of the background and history of scholarship relating to the diachronic development of supply networks of copper in northern Oman (ca. 2500 BCE – 1800 CE) and of obsidian in northern Ethiopia (ca. 800 BCE – 825 CE) with the aim of providing regional context for the comparative examinations of material supply networks.

Chapter 3 outlines the theoretical relationship between network theories and traditional anthropological, archaeological, economic, and sociological theories relating to the ancient economy. The goal of the chapter is to use a network theory framework to reevaluate notions about ancient economies originating from both Neoclassical and substantivist schools of economic thought. The social network model has recently been proposed as a counterpart to theories of market exchange (Bandyopadhyay et al. 2011, Collins 1988) and I contend that it possesses advantages over substantivist economic theories as well. This is because the network model provides a reasonable solution to understanding how trust and social order are maintained in systems of economic interaction.

Chapter 4 outlines the methods used to collect and analyze data for this dissertation. The first part of the chapter delineates the methodological parameters associated with the theories framing this study: the comparative and network analysis approaches. The second part of the chapter summarizes recording and analysis strategies and includes sections on: (1) satellite imagery analysis (employed in the creation of preliminary exploratory geological resource maps), (2) field

methods related to archaeological survey and ground-truthing of prospectivity maps, and (3) methods relating to geochemical analyses using portable X-ray Fluorescence devices.

A large portion of the data analyzed for this dissertation was collected as part of two NASA-funded projects: the Archaeological Water Histories of Oman (ArWHO) project and the Southern Red Sea Archaeological Histories (SRSAH) project. Through a combination of systematic and reconnaissance surveys and archaeological excavations, these projects generated datasets that represent the entirety of the data universes that became the foundations for the archaeological networks in Oman and Ethiopia. Chapter 5 summarizes aspects of research generated by these two projects as these relate to the network datasets analyzed for this dissertation. The aim of this chapter is, therefore, to provide insights into sampling strategies and sample sizes.

Chapter 6 outlines the process of creating geological resource maps to model the spatial distribution of copper and obsidian resources in Oman and Ethiopia. Gaining an understanding of the geography of the raw materials whose supply networks are under investigation in this dissertation was deemed important for understanding broader landscapes of interaction between ancient communities of production and their raw material environments. A high-resolution representation of landscapes characterized by complex mineralization and rock formation processes was unattainable merely using traditional geological maps. This is because available geological maps for Ethiopia, and to a lesser extent for Oman, generally identify the locations of resources with the larger geological units they are embedded into. As such, the need arose for high resolution spectral mapping through analysis of Hyperion hyperspectral satellite imagery. This chapter outlines the steps taken to create the resource maps and includes details regarding detection workflows, ground-truthing surveys, as well as more general information about the geology of the al-Hajar mountains of northeast Oman and the volcanic landscapes of the Danakil depression and

the Eastern Rift Valley, both of which represent host environments for the materials whose production is analyzed in this dissertation.

The goals of Chapter 7 are two-fold: (1) to examine and analyze the structures of copper and obsidian supply networks and their diachronic developments in Oman and Ethiopia, charting long-term fluctuations in the network position of individual nodes and changes in relationships between network sub-groups, and (2) to reveal aspects of network topology (emergent properties of networks) through comparison of the Omani and Ethiopian networks. Finally, Chapter 8 concludes this research outlining results and discussing prospects for future research.

This dissertation also contains two appendices: Appendix I presents the database used in the creation of the copper network and Appendix II contains data used in the formulation of the obsidian network.

Chapter 2

Background and History of Scholarship

2.1. Introduction

While ancient production and trade have long been studied as proxies for understanding the cross-cultural development of social complexity (Adams 1975, Freidel and Reilly III 2010, Rathje 1975, Sabloff and Freidel 1975), these dynamics are less known in Oman and Ethiopia. This chapter outlines the background for comparative and diachronic examinations of raw material supply networks with the aim of understanding economic complexity, broadly defined as a system that facilitates the transfer of a commodity from its source to its locus of consumption (Earle 2002).

2.2. Regional History and Diachronic Development of Metallurgy in Southeast Arabia

The first modern archaeological survey in Oman was undertaken in 1958 by P.V. Glob and T.G. Bibby (Bibby 1970). Modern scholarly interest into the area, however, is evidenced even earlier in the works of H. Peake who's 1928 publication suggested that the source of Sumerian copper-alloy objects originated in Oman. Since then, over four decades of archaeological research have established that extractive metallurgy and sociopolitical complexity arose in Oman roughly contemporaneously during the late fourth – early third millennia BCE (Berthoud and Cleuziou 1983, Cleuziou 1996, Weeks 2003, Cleuziou and Tosi 2007, Giardino 2017). This is largely in contrast to the trajectory observed in other areas of the world, like Anatolia, the Levant, and Iran, where the rise of sociopolitical complexity often preceded the development of extractive

metallurgy by a few millennia (Hauptmann 2007; Helwing 2014; Lehner and Yener 2014; Thornton 2014).

In the 1970s, scholars affiliated with the Deutsches Bergbau Museum (DBM) in Bochum began research on the development of archaeometallurgy in Oman (Hauptmann 1985; Weisgerber 1977, 1981). Gerd Weisgerber who first arrived in Oman in 1977 initiated a program of survey and excavation undertaken in conjunction with Prospection (Oman) Ltd. That recorded 115 ancient smelting sites (Weisgerber 1977, 1978, 1980).

Some of the earliest copper objects in Oman have been uncovered in contexts that date to the Hafit period (Early Bronze Age) to the fourth millennium BCE (Begemann et al. 2010, Cleuziou and Tosi 2007) (see Table 2.1 for Omani archaeological chronology).[8] An initial phase of more intense copper production, however, is not identified until the Umm an-Nar period (Early Bronze Age) dating back to the middle of the third millennium BCE (Hauptmann 1985, Weisgerber 1981a, 1983); this phase corresponds with an increase in the consumption of copper in southern Mesopotamia (Begemann et al. 2010). As further described below, research undertaken on sites dated to the third and second millennia BCE indicates production of 10,000 tons of slag, corresponding to between 2,000 and 4,000 tons of copper (Begemann et al. 2010, Hauptmann 1985: 95, 116, Weeks 2004: 34). During the second millennium, Wadi Suq (Middle Bronze Age) copper production entered a period of decline, but scant available evidence points to a continuation in smelting technologies albeit at a smaller scale (Begemann et al. 2010).

[8] Before proceeding with this section, it is important to point out that the chronology of Oman is the subject of considerable debate. Broadly speaking, this dissertation adopts the chronology put forth by Kennet 2004, Magee 1996, Whitcomb 1978, and Potts 1992. However, when reporting on German archaeometallurgical findings, I will occasionally report the chronology they published and cite it accordingly (Begemann et al. 2010: 138: Table 1; see Table 2.1b).

The Iron Age I and II periods, dated to between 1300 and 600 BCE, mark a second major phase of copper production. Some of the largest Iron Age sites are characterized by slag heaps with over 40,000 tons of slag (Hauptmann 1985: 107, 116). A third distinct phase of copper production occurs in the early and late Islamic periods. This period is characterized by the smelting of massive sulfide ores, which produced between 40,000 – 150,000 tons of slag each at sites such as Lasail, Arja, Semdah, Raki, and Tawi Raki (Hauptmann 1985: 100). With slag heaps containing in excess of 100,000 tons of slag, some of the largest copper producing sites discovered in Oman date to the Islamic period. At the other end of the spectrum, this period is characterized by comparatively small sites that only generated a few tons of slag, indicating short-term production (Hauptmann 1985: 100).

Table 2.1: Oman Archaeological Chronology (a) (Kennet 2004, Magee 1996, Whitcomb 1978, Potts 1992) and (b) Chronology of Copper-producing periods (Begemann 2010 et al: 138):

Period	**Date Range**
Hafit	3200 – 2500 BCE
Umm an-Nar	2500 – 2000 BCE
Wadi Suq	2000 – 1300 BCE
Iron Age I	1300 – 1000 BCE
Iron Age II	1100 – 600 BCE
Iron Age III	600 – 300 BCE
Early Islamic	635 – 1000 CE
Middle Islamic	1000 – 1300 CE
Late Islamic	1300 – 1800 CE

(a)

Period	**Date Range**
Hafit	c.3200–2600 BC
Umm an-Nar	c.2600–2000 BC
Wadi Suq	c.2000–1250 BC
Iron Age (Lizq/ Rumeilah)	c.1250–500 BC
Early Islamic	c.800–1100 AD

(b)

The three main periods of copper production in Oman roughly coincide with periods of heightened sociopolitical complexity during the Bronze Age, Iron Age, and the Islamic period. Some have postulated links between copper production and heightened sociopolitical complexity and speculated that long-term trends may have been related to broader inter-regional developmental trajectories, including demand for bronze (Potts 1993, Weeks 2003, Cleuziou and

Tosi 2007, Giardino 2017). Indeed, the initial development of widespread copper mining and production in ancient Oman roughly coincides with the region's burgeoning trade connections with Sumer, with more evidence of contacts between the two areas during the third millennium BCE – a period of dramatically expanding sociopolitical complexity in Mesopotamia (Peake 1928, Weeks 2003, Cleuziou and Tosi 2007). Whether local phases of increased and decreased copper production in Oman recurred periodically due to internal circumstances, or were due to external factors, remains a point of considerable uncertainly and debate (Weeks 2003).

The traditional narrative linking sociopolitical complexity in Southeast Arabia to commercial interactions with southern Mesopotamia has its roots in some of the earliest metal sourcing studies in the Near East. Early research on ancient metallurgy was originally undertaken, in part, to identify sources used in the manufacture of copper objects discovered in Mesopotamia (Witter 1938). Based on the high nickel content present in both Mesopotamian artifacts and analyzed Omani sources, early studies identified Oman as a likely copper source. While other copper deposits in the Near East have similar characteristics and, indeed, not all Omani sources are characterized by a high nickel content, subsequent research confirmed Oman as an important early source of copper (Cheng and Schwitter 1957; Muhly 1973, Tosi 1975).

2.2.1. Brief Overview of Mining in Oman

In Oman, early ore extraction has been linked to Neolithic flint nodule exploitation (Giardino 2017: 84). It is thought that the suite of techniques associated with the mining of flint nodules, including open-cast and underground mining, had a direct impact of the development of similar techniques used in the exploitation of copper ores. Additionally, it has been argued that what potentially drew ancient miners to copper-rich outcrops were the bright colors of the gossans which were a result of weathering (Giardino 2017). The link between visual appearance and the

selection of ore bodies for exploitation has also been made in connection to the beginnings of metallurgy in other regions of the world (see Radivojević and Rehren 2016).

Evidence of both surface and underground mining has been identified in ancient Oman. Early prehistoric opencast mines have been discovered at Maysar, Gebel Saleli, Huqain, Tawi Ubaylah, Wadi Miadin, Bilad Al-Maidin, and Nujum (Giardino 2017: 88; Weisgerber 2008). Opencast mining has also been uncovered at Nujum, while underground mining techniques appear to have been employed at Wadi Miadin (Weisgerber 2007: 198, fig. 206; Weisgerber 2008).

Although many early mines were subsequently destroyed through continued exploitation in later periods, the evidence we do have suggests that these were located where the ore was surficially exposed. Early miners used lithic tools (likely hafted stone hammers) (Pickin and Timberlake 1988) to exploit the ore along a vein and mined the outcrop until it disappeared under the surface of the ground or until the surrounding matrix became too unstable to mine (Craddock 1995: 31-69). These stone hammers left concave or rounded marks on mine walls. Following the gradual introduction of metal mining tools these rounded strokes were replaced by long and deep incision.

In addition to hammering, ancient miners sometimes used fires to fracture bedrock and lessen the difficulty inherent in extracting ore. This method was originally described in the seminal sixteenth century CE treatise on mining and metallurgy De Re Metallica by German metallurgist and mineralogist Georgius Agricola. As Craddock (1995: 33) describes, fires set on bedrock were left to burn for hours and would fracture rock to as much as 30 centimeters below surface.

After the ore was mined, processing of the metal included a set of stages. The first steps can be grouped under the category of ore beneficiation, which involved crushing and hand-sorting the ore from the gangue (Merkel 1985: 164-168; Giardino 2010: 55-56). Gangue is the rock or

mineral matrix co-occurring with and encasing the metallic ore. Undertaken close to mines, this process is evinced by heaps of debris and by a characteristic beneficiation assemblage which contained mortars, pounders, and mining tools and was often discovered in proximity to mined ore sources (Craddock 1995: 156 – 167). This process resulted in ore pebbles that are easier and require less fuel to smelt than larger blocks. Ethnographic evidence suggests that ore beneficiation could potentially be undertaken by women and children (Hinton et al. 2003).

2.2.2. Brief Overview of Smelting in Oman

Archaeometallurgists reconstruct copper smelting techniques through a complex multi-proxy method that involves a geochemical characterization of copper slag. In Oman, A. Hauptmann (1985) has discovered broad chemical and morphological patterns in copper slags that are diagnostic to time period, thereby allowing scholars to establish diachronic developments in smelting technologies. These patterns have been used to determine a timeline for the development of copper smelting. Morphologically, smaller slags are associated with the Bronze Age, tapped slags (weighing up to ten kilograms) are associated with the Iron Age, and bowl slags are diagnostic of the Middle Islamic period (Weisgerber 2008).

Reconstructing the smelting process in antiquity is a complex multi-proxy process based on interpretations of chemical differences and similarities between ores, slag, furnace wall materials, fuel charcoal, and metal objects. The smelting process can be divided into a progression of solid state and liquid state chemical reactions that occurred under strongly reducing conditions, in environments in which ambient air pressure and temperature reached up to ca. 1300˚C. The purpose of the process was the concentration of metal from metal oxides and sulfides, which can only occur under conditions of very low oxygen and in an atmosphere rich in carbon monoxide.

These conditions were typically achieved in a furnace or a crucible together with charcoal and an air draft.

The smelting process involves the application of heat in combination with a chemical reduction agent to decompose ore. This process results in the separation of the metal from the other elements that make up the gangue which are eliminated either as gasses or as slag. Ancient smelting practices often used a source of carbon, such as charcoal, as a reducing agent, although animal dung has also been attested as an alternative (Craddock 1995: 196) especially in arid or semi-arid environments, where wood may not have been as plentiful (Miller 1984).

Where oxides are concerned, this smelting process involved two stages: the first is a stage in which carbon monoxide is produced. During this first stage, oxygen molecules from inside the furnace bond with carbon molecules from the roasting charcoal, producing carbon monoxide. During the second stage, molecules of carbon monoxide bond once again with molecules of oxygen to produce carbon dioxide. To more easily separate the gangue from the metal, a flux (commonly an iron oxide) is often added to the molten material, resulting in the metal itself and in slag, defined as the non-metallic waste material that is removed.

In the case of sulfide metal ores, the smelting process is preceded by a roasting phase. Roasting is a technique used to heat a sulfide ore to a high temperature in the presence of oxygen and with the goal of removing the sulfur as sulfur dioxide and converting the sulfide into an oxide, which can then be smelted. Whereas smelting generally occurs in furnaces, sulfide ores are set upon an exposed fire during the roasting process. While removing the sulfur, this process of oxidization can also remove other elements such as arsenic, antimony, and bismuth (Giardino 2017: 93). This is a typical reduction reaction; the origin of the term lies in the fact that the amount

of oxygen bonded with the metal is reduced. The temperature at which this type of reaction is successful in producing metal varies with the metal involved.

Ancient pyrotechnological systems were not always able to achieve the circumstances necessary for the reduction of some oxides (such as silica, alumina, titanium, chromium, alkali, and alkali earth oxides). These elements, therefore, often remained in the slag together with a certain amount of iron oxide which had been used as a flux. Thus, the presence and quantities of these elements found in slag reveals production technologies.

2.2.3. Hafit Period (ca. 3200 – 2500 BCE)

Although intensification of copper production does not begin until the subsequent Umm an-Nar period, some of the earliest evidence of smaller scale copper production in Oman comes from Hafit period sites (Early Bronze Age). Ancient Oman underwent an important transformation during the Hafit period evidenced by distinctive circular cairn tombs that exhibit remarkable similarity across Southeast and Southwest Arabia. Hafit period occupations are known at sites including Hili 8 (in the United Arab Emirates), Ras al-Hadd 6 (on the southeastern coast of Oman), and Bat (in northern Oman). The most diagnostic feature of this period, Hafit 'beehive' tombs (Frifelt 1975; de Cardi et al. 1976), are circular, single-chambered structures constructed in highly visible, elevated locations. These above-ground tombs contained single or multiple interments and sometimes grave goods, which occasionally included copper objects, weapons, and tools, as well as ornaments and other objects made from semi-precious stones and shells. Indeed, early evidence of metal was discovered in a Hafit period tomb, Grave 1 at Maysar-25 (Weisgerber 1981: 198-200; 2008: 1615, fig. 4). This evidence was in the form of a copper needle that was analyzed by Prange (2001) and revealed to have been very pure in copper content, with trace element presence recorded at under 0.2%. Evidence of contact with Mesopotamia has also been attested among the

Hafit funerary assemblages, as indicated by the presence of Jemdet Nasr pots in Hafit tombs (e.g. Ras al-Jinz 10) (Cleuziou and Tosi 2007: 113 – 115; Potts 1986).

Despite being located appreciable distances from the inland copper sources, some of the earliest evidence of Hafit copper consumption and production has been discovered at the coastal sites of Ras al-Hamra, Ras al-Hadd, and Ras al-Jinz. The earliest consumption of copper has been uncovered at Ras al-Hamra (RH-10) in a context dated to between the end of the fifth millennium BCE to the second half of the fourth millennium BCE (Giardino 2015: 117). The earliest evidence of production comes from the site of Ras al-Hadd (HD-6) and has been dated to the late fourth and early third millennia BCE (Cattani 2003). The HD-6 assemblage is composed of ingot fragments, finished, and unfinished copper tools and weapons, the latter category suggesting most securely the likelihood of metalworking occurring at the site. Cold-hammered copper tools were used in the production of beads (Azzarà 2013). Because HD-6 was a coastal settlement, copper fishhooks likewise made up a large part of the assemblage. The introduction of copper fishhooks seems to have disrupted an earlier Neolithic tradition of fishhooks made from *Pinctada margaritifera* shells, most notably found at HD-5 (Bavutti et al. 2015: 3). This alteration to an established local practice illustrates Southeast Arabia's expanding engagement with copper.

Excepting the discovery of a bun ingot from Ras al-Hadd 1 (HD-1) (Craddock et al. 2003)[9], the lack of substantial evidence of smelting coupled with the presence of ingot fragments at coastal sites suggests that copper ingots were imported from the interior of Oman. While fishing villages were flourishing along the coast, the interior was populated by nomadic pastoralists. Economic interdependencies between inhabitants of the coast and the interior likely arose as a result of the different resources available across disparate ecologies (Magee 2014: 275; Murra 1968).

[9] Chemical analyses reveal that this bun ingot contained 2% arsenic and 0.6% nickel and was thus likely smelted from Samail ophiolite ores.

Foodstuffs such as dates, wheat, barley, and perhaps sorghum, millet, and pulses, could feasibly only be cultivated in interior oasis environments, whereas nomadic herders could provide meat, dairy, wool, and skins, and coastal fisherfolk produced cured-fish, shark, dugong, oil, and fish fat (Cleuziou and Tosi 2007). These interdependencies arguably led to the development of complex multi-scalar integration of the different regions, exemplified by similarities in Early Bronze Age Hafit material culture found in different environments. Material integration has also been observed in metal assemblages from contemporaneous sites located across Oman, including HD-6 and Hili 8 (Cleuziou and Tosi 2007: 93).

In the interior of Oman, a number of sites have yielded evidence of copper production. The oasis settlement of Bat revealed early metalworking in the form of crucible fragments and copper slag. Evidence of late fourth millennium BCE small scale copper production has been uncovered in association with the Bronze Age towers of Kasr al-Khafaji (1146), Matariya (1147), and 1156 (Thornton et al. 2016: 44, 123, 132; Leigh 2016). Other evidence of early metal production from the interior of the country originated at the site of Batin, located in Wadi Nam near Ibra (Yule and Weisgerber 1996, Weisgerber 2008). More recently important new evidence of copper production has been found at Al-Khashbah (Schmidt and Döpper 2019).

Chemical analyses undertaken on Hafit period copper objects from HD-6 reveal low iron levels (0.03%) suggesting an imperfect smelting process, during which desired reducing conditions were not achieved (Giardino 2017: 55). The major impurity in these objects is arsenic and nickel, suggesting that these objects were likely made with local copper from the al-Hajar ophiolite (Prange 2001:95; Cattani 2003; Begemann et al. 2010).

2.2.4. Umm an-Nar Period (ca. 2500 – 2000 BCE)

Beginning in the middle of the third millennium BCE, the first phase of copper intensification dates to the Umm an-Nar period (Early Bronze Age) and reaches its zenith around 2000 BCE (Begemann et al. 2010, Hauptmann 1985). The Umm an-Nar period derives its name from archaeological remains on Umm an-Nar Island (UAE), where the characteristic assemblage was initially defined. The Umm an-Nar period is characterized by a high degree of regional integration in both portable and non-portable material culture (Charpentier et al. 2013; Potts 2012). Enduring cultural similarities validate the notion of a continuation of economic interdependency defined by tower-settlements, black-on-red and black-on-buff painted ceramics, and above-ground collective tombs sometimes made of small well-cut stones.

A great deal of evidence links copper production to Umm an-Nar towers (Cable and Thornton 2013, Thornton et al. 2016). Metallurgy became increasingly more sophisticated during the Umm an-Nar period. Early copper smelting is thought to have relied on secondary copper minerals, as the multistep technological process required to smelt copper sulfides likely developed during the later third millennium BCE (Hauptmann 1985). By the third and second millennia BCE, small slag fragments were composed of partially reduced and self-fluxing ores, which together demonstrate that a liquid slag process was incomplete. Since metallic copper was not fully released from the slag during the smelting process, Hauptmann argues that these slags were crushed and prills of copper were collected for re-melting at a later stage.

Evidence of smelting, including crucibles, molds, and casting residue, has been uncovered at several different sites spanning Southeast Arabia, including at Ras al-Jinz (RJ-2) on the southern coast, at Maysar, in the interior of the country, on Umm an-Nar Island, off the coast of Abu Dhabi (Weisgerber 1983: 271; Frifelt 1995: 70, 188-191; Weeks 1997: 17-20), at Bilad al Maaidin near

Samad ash Shan, (Begemann et al. 2010, Hauptmann 1985), at al Aqir near Bahla (Hauptmann 1987, Weisgerber and Yule 2003), and at Arja, Assayab, and Tawi Ubaylah in Wadi Jizzi (Begemann et al. 2010)

The best-known Umm an-Nar period smelting site is Maysar. Situated in central Oman in Maysar valley, the site of Maysar is in the vicinity of the Semail Ophiolite of the southern al-Hajar mountains. Initially settled during the Hafit period, the site's economic focus turned to copper production during the Umm an-Nar period. Characterized by an Umm an-Nar tower and by domestic and mortuary structures dating from the Bronze Age to the Iron Age, the site was excavated between 1979 and 1982 by the DBM. The metallurgical assemblage uncovered through survey and excavation incorporates copper ingot fragments, furnace fragments, charcoal, crucibles, molds, slag, and finished copper objects (Weisgerber 1983). The discovery of an Indus Valley seal at Maysar-1 is evidence of long-distance trade occurring in association with copper production during this time period.

Excavations at Maysar reveal a great deal about Omani metallurgy during the third millennium BCE. Indeed, excavations of House 1 were particularly illuminating and revealed a furnace 40 cm in diameter and approximately 50 cm high (Weisgerber 1983). House 4 at Maysar produced a hoard of copper ingots. Bronze Age copper ingots are made of almost pure copper, with trace remains of impurities such as sulfur, iron, nickel, and arsenic (Prange 2001: tab. 37; Hauptmann 1985: 80-83, tab. 21; Hauptmann et al. 1988: 41-42, tab. 4.1). These ingots were plano-convex in form, a shape characteristic for the Arabian Bronze Age, which was produced by pouring molten metal from a crucible into a rounded hole in the ground.

To match the archaeological metal to a copper source, lead isotope analyses were undertaken on six of the twenty-two ingots from the Maysar hoard. The lead isotope composition

of these ingots – 208Pb/206Pb; 207Pb/206Pb and 204Pb/206Pb; 207Pb/206Pb – does not match the composition of any known Omani copper source. This discovery suggests that the copper was either derived from a hitherto unidentified Omani copper source or that it arrived into Southeast Arabia through long-distance trade (Prange 2001: 91-98, 102, tab. 30; Weeks 2003; Weeks 2008: 91- 94; Begemann et al. 2010: 153-154). Interestingly, geochemical analyses of finished copper objects found at Maysar indicate that, unlike the ingots, they were made of Omani copper (Prange 2001; Weisgerber 2008).

Although the importation of copper into a region rich in autochthonous copper sources may seem unlikely, this situation is not without precedent in the ancient world. During the Late Bronze Age, for instance, Cypriot oxhide ingots circulated throughout the Mediterranean and were consumed in regions with autochthonous copper supplies (Giardino 1995; Gale 1991: 212-224; Muhly 2009: 26-30; Schiavo et al. 2009). A possible foreign source has not been uncovered, although sources in Saudi Arabia have been proposed (Weeks 2007: 94).

Metallographic and SEM analyses undertaken on the slag assemblage from Maysar provide good evidence for change in smelting technology between the Hafit and Umm an-Nar periods. While slags from both periods share similarities in terms of bulk chemistry and microstructure, both containing comparable measures of silicon dioxide, iron oxide, magnesium oxide, and calcium oxide, their compositions differ significantly in copper content. Whereas Hafit period slags contained copper content that can reach up to 31%, Umm an-Nar period slags contain on average less than 2% and no more than 7% copper (Hauptmann et al. 1988: 37-40; Giardino 2017: 104). These contrasting copper amounts indicate advancements in smelting technology, revealing that unlike Hafit period slags, which were produced in high oxidizing conditions, Umm an-Nar

slags resulted from a strong reducing atmosphere and were produced in furnaces that reached minimum temperatures of around 1100 °C.

Geochemical analyses have revealed that most of the metal objects dated to this period were made almost entirely of pure copper, with trace amounts of arsenic (2 – 3%; Giardino 2017: 80). While exemplified by few items, tin-bronze alloys are introduced during this period. Given the absence of tin sources in Southeast Arabia, tin-bronze alloys are a further indication of long-distance trade associated with copper production. A source for the tin has not yet been identified, although possible candidate sources in the Near East include southern Anatolia, western Iran, Uzbekistan, Tajikistan, and Afghanistan (Thornton and Giardino 2012).

2.2.5. Wadi Suq Period (ca. 2000 – 1300 BCE)

The international trade network that connected Oman to the rest of the ancient Near East began to crumble during the first few centuries of the second millennium BCE. Although increasingly challenged, the traditional scholarly narrative has attributed deterioration of economic relations between Mesopotamia and the southern Gulf region to allegedly increased trade relations between Mesopotamia and Cyprus (Constantinou 1982; Giardino 2000; Knapp 2013; Merrillees 1984; Muhly 2005; Pulak 2000).

There are marked cultural and demographic changes between the Umm an-Nar and Wadi Suq (Middle Bronze Age) periods, with mortuary architecture demonstrating perhaps the greatest differences between the two periods. Wadi Suq assemblages first identified along Wadi Suq in the piedmont hinterlands southwest of the port city of Sohar, are dispersed across UAE, Oman, and on Masirah Island. In comparison with their Umm an-Nar counterparts, Wadi Suq sites are smaller and more sparsely distributed across Southeast Arabia (Cleuziou and Tosi 2007: 258, fig. 274; Yule et al. 1994).

The limited evidence of Wadi Suq metallurgy reveals a continuation in smelting technology from the previous period (Begemann et al. 2010). The discovery of two sites in Wadi Samad, Bir Kalher and Wadi Sahl, reveals a slag type that is indistinguishable from Umm an-Nar slag. Additionally, furnace fragments from Bir Khaler dated through thermoluminescence to 1310 ± 250 BCE (Wagner and Yule 2007) are identical to Umm an-Nar fragments from Maysar 1 and from Bilad al Maaidin (Weisgerber 1981b: 210, Abb. 44). Despite this continuity in smelting technologies, it is difficult to ascertain the scale of copper production during the Wadi Suq period because few metallurgical sites have been definitively attributed to the Wadi Suq period. Indeed, the possibility of multi-period production at sites that have been attributed only to the Umm an-Nar period cannot be dismissed. However, evidence from the site of Bir Kalher indicates a smaller scale of production, as suggested by the presence of a relatively small slag heap, amounting to 200 tons (Kroll 1981; Weisgerber 2007: 195). Evidence of copper consumption, on the other hand, is plentiful during the Wadi Suq Period as indicated by substantial metal assemblages from mortuary contexts. Tomb W1 from al-Wasit in Wadi Jizzi, for instance, contained 58 copper-based objects (primarily weapons) which were analyzed using ICP-OES and found to have been made almost entirely of pure copper with up to 3% nickel content (Prange 2001; Yule and Weisgerber 2015; al-Shanfari and Weisgerber 1989; Weisgerber 2007: 195-196). Four of the analyzed objects were typically Iron Age bronze daggers which contained significant quantities of tin, indicating that this collective interment was in use for a long period of time.

2.2.6. Iron Age I or Nizwa Period (ca. 1300 – 1100 BCE)

An abundance of metal objects made of tin-bronze in later Iron Age assemblages emphasizes the region's re-connection with inter-regional long-distance trade networks (al-Shanfari and Weisgerber 1989). Between 1200 and 800 BCE, the eastern Mediterranean region

and the ancient Near East underwent tremendous upheaval, which contributed to the transformation of interregional relations during the first millennium BCE. In Oman, the end of the Wadi Suq period gave way to the development of a new homogenous culture that spread across the country. Together with significant cultural differences, this period witnessed demographic changes, with an increase in population density and a renewed focus on copper production that included the development of new smelting techniques. The Iron Age in Oman has been subdivided into three phases: Iron Age I (cf. Nizwa period; ca. 1300 – 1100 BCE), Iron Age II (cf. Lizq; ca. 1100 – 600 BCE), and Iron Age III (cf. Samad period; ca. 600 – 300 BCE) (Giardino 2017: 114).

Traditional scholarship on Omani metallurgy attributes the reinvigoration of copper production beginning in Iron Age I in part to the new practice of exploiting new ore types from the enrichment zones of massive ore bodies (Weisgerber 1988; Prange 2001; Weeks 2003; Weisgerber 2008) and in part to the introduction of a new smelting technology from Cyprus that involved a multiple step process for exploiting chalcopyritic ores (Giardino 2017, Weisgerber 2007).

Early scholarship in Southeast Arabia focused largely on the beginnings of metallurgy and, as such, less is known about Iron Age and Islamic production. Scholarly inattention is not, however, matched by a paucity of evidence as, indeed, there is a growing body of research to suggest an increase of consumption during this time period (Esposti et al. 2016, etc; Hermann et al. 2012; Yule et al. 2001).

The evidence we do have suggests that by the second millennium BCE, some slags demonstrate increased use of copper sulfide minerals. However, these were apparently still smelted together with secondary copper minerals in a process that did not include a second copper matte production stage. Indeed, the process by which a matte production stage was reached is more

confidently associated with the early Islamic period but is *possibly* also evident during the Iron Age.

Iron Age production in Oman is documented by Hauptmann with just two analyses published in his 1985 monograph. Hauptmann nevertheless theorized an increase in the consumption of copper iron sulfides, possibly from extensive mining supplemented with a lower quantity of secondary minerals. In this sense, Iron Age copper production represented an intermediate phase incorporating both Bronze Age technologies and innovations in sulfide processing. It remains unclear whether a fully formed copper matte stage of production developed during this time period. Differentiating between slag associated with the different sub-phases of the Iron Age is generally difficult in the absence of other items of material culture.

The Iron Age I has been largely characterized based on research undertaken at two sites in the United Arab Emirates: Shimal and Kalba. Cultural traits associated with this first phase include crudely made, hand-thrown ceramics characterized by coarse, grit tempered paste, simple forms, and no decorations.

The so-called "warrior" grave uncovered at Jabal al-Hawra east of the modern town of Nizwa is an important example of metallurgy attributed to this time period. Discovered by an Omani farmer in the 1970s, this grave contained a large metal assemblage which incorporated copper and copper-based weapons and pieces of jewelry, including a tin bronze battle-axe, three daggers (two of which were tin bronzes) (Prange 2001: tabs. 32, 36), twenty-seven arrowheads, one razor, one ring, and two copper-based bangles. Other non-metal offerings included a ceramic bowl, a calcite stamp seal, carnelian beads, and three softstone vessels (al-Shanfari and Weisgerber 1989; Cleuziou and Tosi 2007, Giardino 2017).

The more recent discovery of two collective Iron Age I graves at Daba al-Bayah in the Musandam Peninsula (Oman) expands our knowledge of metallurgy and metal consumption during this period. Each comprising the redeposited remains of hundreds of individuals of different ages and sexes, these collective graves (LCG-1 and LCG-2) contained thousands of grave goods including bronze tools, objects, and ornaments, objects made from silver and gold, thousands of beads, and a Kassite Eye-Stone amulet bead inscribed with cuneiform and dedicated to the healer goddess Gula (Frenez et al. 2017, Genchi 2019, Giardino 2017).

An object that dominated these metal assemblages, the copper and copper-based arrowhead, can be found in both the Daba and Nizwa contexts. Their ubiquity has been used to suggest the importance of military endeavors during this time period and the high esteem in which archers appear to have been held during the Arabian Iron Age (Giardino 2017: 114).

Research at the site of ‘Uqdat al-Bakrah (Safah) has also clarified aspects of Iron Age metal production. Located on the eastern edge of the Rub al-Khali, hundreds of copper and bronze objects were found surrounding hundreds of pits. While research on the function of these pits is ongoing, some have suggested that they appear to have been used for either charcoal production or melting of what appear to be predominantly recycled items (Aksoy 2018, Genchi et al. 2018: 238; Gernez et al. 2018). XRF analyses of sixty objects from ‘Uqdat al-Bakrah indicate that most objects were made of almost pure copper, with a quarter being made of tin bronze. Additionally, there is no evidence of objects composed of arsenical copper and an inconsequential number of objects registered less than 1% nickel. These findings indicate a different source from the one that was being used in some previous periods for Iron Age copper objects (Giardino 2017: 117).

2.2.7. Iron Age II or Lizq Period (ca. 1100 – 600 BCE)

The second phase of the Iron Age demonstrates a return to the cultural integration that characterized the region during the Bronze Age and to large scale copper production. Like their Early Bronze Age counterparts, Iron Age II settlements can be found throughout all ecological zones of Southeast Arabia, indicating population increase and economic diversification stimulated human cooperation (Cleuziou and Tosi 2007: 284).

Although many aspects of Iron Age subsistence economies remain obscure, the proliferation of oasis settlements undoubtedly involved new forms of animal husbandry and more advanced irrigation agriculture. Indeed, one major factor that differentiates Iron Age society and trade from the Bronze Age was the domestication of the camel at the end of the second or beginning of the first millennium BCE (Magee 2014: 204). Camel transport, which allowed merchants to move goods much faster and much further and enabled them to across previously less-integrated ecologies (e.g. deserts), led to unprecedented economic integration. Additionally, the introduction of qanat/ falaj (underground infiltration gallery) irrigation systems made access to water more reliable, leading to agricultural intensification and influencing settlement patterns (Al-Tikriti 2002; Boucharlat 2003). Magee compares the economic environment created by the introduction of these two factors to the situation that arose in fourth millennium southern Mesopotamia (Magee 2014: 235), crediting the rise of Uruk city-states to a combination of agricultural and trade-related factors (Algaze 2001). It has been argued that in Southeast Arabia, these factors led to an increase in social stratification and to an attendant attempt to offset the effects of hierarchy and maintain social cohesion (Magee 2014). In addition to oasis settlements, this period is also characterized by fortified hillforts such as the one discovered at Lizq, this sub-period's type site (Cleuziou and Tosi 2007: 287), and by large buildings, some with as many as 50 internal partitions which have been

interpreted as spaces where communal activities would have taken place (e.g. Hili 14; Cleuziou and Tosi 2007: 288).

Iron Age II funerary architecture is largely characterized by individual interments and by a range of different types of mortuary features. Typified by above-ground structures constructed in rectangular, round, or oval configurations, Iron Age interments also appear to have at times recycled or reused elements of previous mortuary structures (Cleuziou and Tosi 2007: 290). Iron Age mortuary assemblages include a wealth of ceramic and copper objects as well as ornaments made from various materials, the distribution of which suggests either the absence of a clearly defined hierarchical system or the hesitance to symbolize differences in social status through mortuary goods (Cleuziou and Tosi 2007: 290 – 291).

Indeed, unlike the evidence from domestic architecture and from textual sources that raises the possibility of some level of social stratification, echoes of egalitarianism as characterized for the Bronze Age are similarly seen in scholarship on the Iron Age (Magee 2014: 235).

The best-known metallurgical assemblage dating to the Iron Age II period is the so-called Ibri/Selme hoard (Cleuziou and Tosi 2007: 292, Giardino 2017: 136, Yule and Weisgerber 2001). One of the largest metal hoards in the ancient Near East, this assemblage comprises 550 metal objects, including weapons, vessels, and items of personal decoration. It has been suggested that the hoard, uncovered in a re-used Umm an-Nar grave at Selme near the town of Ibri, resulted from Iron Age grave robbing (Giardino 2017: 137). A. Hauptmann and M. Prange analyzed 86 objects from the hoard by Inductively Coupled Plasma Optical Emission Spectrometry (ICP-OES) and by Atomic Absorption Spectrometry (AAS) (Prange and Hauptmann 2001: tab. 9). Findings revealed that nearly all of the objects were tin bronzes and their chemical composition supports the use of Omani ores in their production (Prange and Hauptmann 2001: fig. 21). Begemann et al. (2010:

141) caution against an over-interpretation of these results, indicating that the nature of the hoard as well as the specific object types chosen for analysis (mostly bangles) may not necessarily be representative of the composition of other metal object that were in circulation during the Iron Age II period.

This period also witnesses the development of new mining and smelting techniques (Hauptmann 1985). Important Iron Age II smelting sites have been discovered at Lasail, Arja, Bayda, Assayab, Tawi Ubaylah, Gabal Saleli, Mullaq, Wadi Salh, Muaidin, Mahab, Semdah, Tawi Leshe, Tawi Rakah (Begemann et al. 2010).

2.2.8. Iron Age III or Samad Period (ca. 600 – 300 BCE)

Although the nature of Persian control over Oman is not well understood at the moment, broad changes that have been attributed to Persian rule begin to be observed in Oman after 600 BCE (Cleuziou and Tosi 2007: 297. Around 300 BCE, copper production in Oman seems to have been interrupted. According to current data, metallurgical activities may have nearly ceased for roughly 1000 years (Cleuziou and Tosi 2007: 303); but the possibility of Parthian and Sassanian exploitation cannot be entirely ruled out prior to the early Islamic production (Weisgerber 2008: 6). This decline in copper production coincides with regional geopolitical upheavals, particularly the collapse of the neighboring Achaemenid Empire, which fell to Alexander the Great (Cleuzious and Tosi 2007: 281-298; Yule and Weisgerber 2015: 42-43).

2.2.9. Early Islamic Period (ca. 635 – 1000 CE)

The third period of copper production begins during the 9th to 10th centuries CE. Within two hundred years, an industrial, multi-stage copper production technology developed (Weisgerber 1980, Ibrahim and ElMahi 2000) and was found across most major ore regions and

produced at least a total of 600,000 – 650,000 tons of slag (Hauptmann 1985: 100). This technological development involved a roast reduction process, where ores and matte slags were roasted together in permanent installations. Roasted ores were smelted to produce copper matte, which was then roasted again and reduced, producing nearly optimal fayalitic slags.

By far the best-represented period in terms of metallurgical production, the Early Islamic period is characterized by mining via underground galleries, buttressed by wooden beams, and vertical shafts through which metallic ore was extracted with windlasses (Weisgerber 1980). Early Islamic metallurgy incorporated roasting, undertaken in pits with internal partitions (e.g. 'Arja; Weisgerber 1987), and smelting in furnaces measuring ca. 1.4 meters in height and 60 cm in diameter. A combination of natural draughts and tuyères were used to maintain temperatures within furnaces, which expelled their outputs as metal or slag in the front of the furnace (Weisgerber 1978; Weisgerber 1980a, b; Hauptmann 1985). It has been theorized that the scale of production was so great that it contributed to significant deforestation and attendant landscape degradation (Eckstein et al. 1987).

2.2.10. Middle Islamic (ca. 1000 – 1300 CE) and Late Islamic Periods (ca. 1300 – 1800 BCE)

Evidence of copper production is more difficult to identify after the 12th century CE. It has been suggested that smelters began recycling slag from earlier slag heaps that they subsequently re-melted (Weisgerber 1978). Indeed, metallurgical landscapes associated with the Middle and Late Islamic periods appear quite distinct from their earlier counterparts, being characterized by slag fields with shallow ground cover and not by slag heaps. This change is associated with smelting in bowl furnaces. Dug into the ground, bowl furnaces had a diameter of ca. 25 – 30 cm and produced so-called bowl slags with the same measurements that weighed between 13 and 16

kilograms (Weisgerber 1978). There is also evidence of re-smelting of Early Islamic slag, as indicated by the circular depressions characteristic of many Early Islamic slag heaps.

2.3. Overview of Interregional Interactions

This sub-section provides a brief overview of textual and archaeological evidence for interregional interactions between Southeast Arabia and other polities and civilizations of the Persian Gulf.

2.3.1. Textual Evidence

Where trade is concerned, the textual evidence suggests interactions involving ancient Sumer, on one side, and Dilmun, Magan and Meluḫḫa on the other. Identified as Bahrain, Oman/UAE, and the Indus Valley, respectively, Dilmun, Magan and Meluḫḫa begin to be mentioned in relation to trade with Sumer in the middle of the third millennium BCE (Parpola et al. 1977; Reade 1995; Possehl 1996). During the third millennium and the early second millennium BCE, the Arabian Gulf, which was referred to as the Lower Sea in Mesopotamian sources (Frayne 1993: 27: 2.1.1.1), was central to a trade network that connected city-states in Mesopotamia with the states of the Lower Sea, in a system of interchange within which copper appears to have had primacy (Oppenheim 1954; Bibby 1970; see Potts 1990; Edens 1992: 130; Glassner 1996; Ratnagar 2004).

Cuneiform texts dating from the Jemdet Nasr to the Old Babylonian periods document the exchange of textiles, grain, silver, oil and Mesopotamian manufactured goods for copper, ivory, wood and semi-precious stones with Dilmun, Magan, and Meluḫḫa (Leemans 1960: 10 – 12; Oppenheim 1954). In the case of Magan and Dilmun, their most important export seems to have been copper, while Meluḫḫa was primarily an exporter of semi-precious stones. Magan is

mentioned as the main supplier of copper from the Sargonic to the Ur III period (2350 – 2000 BCE) while Dilmun appears to have taken the lead throughout the remainder of the aforementioned period.

Dilmun appears in cuneiform texts in 2500 BCE for the first time and is referred to as a supplier of wood by Ur-Nanshe, King of Lagash. Texts dated to his successors, Lugal-anda and Urukagina, mention merchants of Lagash trading textiles, resins, oils and silver from state storehouses, in exchange for goods in Dilmun such as copper, onions, linen, resin and bronze 'marine spoons' (Weisgerber 1986).

By the Old Akkadian Period, we learn from Sargonic texts of the merchant ships from Dilmun, Magan, and Meluḫḫa that were docked in the quay at Akkad (Hirsch 1963, Potts 1990). These texts also reveal that copper was shipped directly from Magan and that Meluḫḫans involved in the trade were predominantly sailors or interpreters (Weisgerber 1981a, 1983). Texts from the reign of Gudea of Lagash, mention the interaction between Mesopotamia and Magan as revolving around the trade of copper, diorite, and wood. Finally, King Naram-Sin of Akkad is mentioned as battling Magan for predominance in the Gulf. A late third millennium BCE (2024 BCE) text mentions the merchant Lu-Enlil from Ur as receiving 15 garments and two thirds of a talent of wool from the temple of Nanna, so that he may purchase copper from Magan.

During the Ur III period (c. 2112 – 2004 BCE), commercial interactions between southern Mesopotamia and Magan continued, with the latter being recorded as an exporter of onions, goats, oil, wood, reed, and copper. Dilmun, however, appears to have temporarily lost its function as an entrepôt.[10] Textual evidence records southbound sea voyages undertaken by Sumerian merchants, with no mention of Magan ships making voyages to southern Mesopotamia. The main export

[10] At present, it is unclear what may have occasioned this momentary disruption (see Begemann et al. 2010).

recorded seems to have been copper and luxury items from Meluḫḫa. It has been argued that these Meluḫḫan goods were being traded through Magan, as Meluḫḫan ships were not recorded as docking in southern Mesopotamia (Begemann et al. 2010: 137).

Textual records dating to the reign of Ibbi-Sin (ca. 2028 – 2004 BCE) reveal a return of trade relationships between southern Mesopotamia and Dilmun This change has been linked to the rise of Dilmun's status to that of a regional power, one that was able to control sea traffic between the northern and southern reaches of the Gulf. This period has been associated with the development of a trading emporium on the island of Bahrain. The merchants of Dilmun used cuneiform for their records and an Indus Valley-derived system of weights.

Present textual evidence indicates that Dilmun was mentioned for the last time in a record from the reign of Samsu'iluna (1744 BCE), with the entry: "…12 measures of purified copper from Alasia and Dilmun." This text mentions the copper supplier that would play an important role in trade in the Mediterranean and Ancient Near East for the next 500 years, Alashiya (identified with modern-day Cyprus) (Potts 1990; Crawford 1998). Although this narrative is increasingly being challenged, following this period, neither Dilmun, nor Magan, nor Meluḫḫa are ever mentioned in Mesopotamian textual resources as trading partners.

Oman appears once again in Akkadian records in 640 BCE when Padê, the king of Qadê, visited Assurbanipal in Nineveh. Padê's town of origin is recoded as having been Izke, and Qadê has been identified as the first millennium name ascribed to Oman by the Assyrians.

The next historical reference to copper production in southeastern Arabia comes from the tenth century CE Arab historian and geographer, Abdul Hasan Ali Al-Masʾudi, who visited the port-town of Sohar, in modern-day Oman, and documented the production of copper in the region. Other Arabic historical texts record laws and regulations surrounding copper mines, focusing

primarily on regulations surrounding the ownership of mines, and mentioning the risks incurred and the gains acquired (Weisgerber 1987).

Following these medieval texts, the next mention of mining operations in Oman comes from the writings of eighteenth and nineteenth century European travelers such as Carsten Niebuhr and J.R. Wellsted (Potts 1990: 114 – 115).

2.3.2. Archaeological Evidence

Ubaid ceramics were uncovered at several prehistoric coastal settlements in the United Arab Emirates (Shepherd-Popescu 2003) and were attested at the Hafit period cemetery of Ras Al-Jinz, RJ-6 (Cleuziou and Tosi 2007: 92, 115, fig. 95; Giardino 2017: 61).

Scant evidence of Uruk-period ceramics was uncovered at the coastal site of Ras al-Hamra (RH5) (Méry 1995). Indeed, the Uruk Expansion does not seem to have reached Oman, possibly because the expansion was not characterized by a seafaring component (Algaze 2005, Rothman 2001).

During the Hafit period, intensified interactions with Mesopotamia are suggested by the overwhelming presence of Jemdet Nasr or Early Dynastic I-style ceramics in Hafit tombs (Méry 1991, 2000; Méry and Schneider 1996, 2001; Cleuziou and Méry 2002). These Jemdet Nasr or EDI-style ceramic assemblages contained a smaller number of imported items and a larger number of local reproductions, which were often poorly fired, handmade, and constructed with coarser fabrics (Frifelt 1970, 1975; Possehl 2009).

During the early Umm an-Nar period, Mesopotamian ceramics of Early Dynastic II-III types are found in abundance on Umm an-Nar Island (Frifelt 1991, 50; 1995: 121-188). Conversely, coastal sites during the Umm an-Nar period are characterized by few such ceramics, with a small number of examples of storage and transport jars having been uncovered at Ras al-

Jinz (Cleuziou & Tosi 1993: 757). Penetration of imported Mesopotamian ceramics into the interior of the country is almost non-existent.

The early Umm an-Nar period also sees some of the strongest evidence for contacts with Meluḫḫa (Cleuziou 1992). This evidence appears in the form of black-slipped storage jars, which are diagnostic of the Harappan civilization, during the second half of the third millennium BCE (Cleuziou & Méry 2002: 291). Harappan-style ceramics were found throughout Oman during this period (Cleuziou & Méry 2002: 291).

It has been suggested that some Harappans temporarily settled alongside ancient Omanis at coastal sites, such as Ras al-Hadd (Cleuziou & Tosi 2007: 235-239) and Ras al-Jinz (Cleuziou & Tosi 2000, 2007: 229-235 and 245-247). This supposition is supported by substantial Harappan assemblages dated to the second half of the third millennium BCE. Their potentially seasonal settling at coastal sites may have been related to their inability to return to the Indus Valley during the monsoon (see Cleuziou and Tosi 2007: 191, 209).

Mesopotamian imports are also lacking during the Late Umm an-Nar period. Instead, most ceramic imports originate from Baluchistan, Harappa (Edens 1993: 341; Méry 1996: 170), and Dilmun, whence Barbar pottery has been uncovered at coastal sites in the United Arab Emirates (Méry et al. 1998), with no examples being found in Oman's interior.

During the subsequent Wadi Suq period, Mesopotamian and Dilmunite pottery was uncovered at coastal UAE sites, such as Tell Abraq (Potts 1993: 429-433). Interactions with Harappa were maintained through this period as evidenced by the discovery of Late Harappan ceramics at coastal Omani sites, such as Ras al-Jinz (Cleuziou & Tosi 2007: 272).

Finally, interactions between southeastern Arabia and Iran, while seldom discussed, have nonetheless been attested on occasion (de Cardi 1970: 268 – 269; Potts 2003, 2005), with an

emphasis placed on the similarities between early Hafit ceramics and Iranian pottery dated to the local Yahya VA/ IVC period (Méry 1996, 2000).

When compared with Mesopotamian copper-based objects with known material signatures (Begemann et al. 2010, Begemann and Schmitt-Strecker 2009, Lutz and Pernicka 2004), lead isotope analyses undertaken on an Omani metallurgical assemblage reveal that Omani copper was used in the production of Mesopotamian objects from the Uruk period to the Akkadian period. Omani copper appears to have been particularly favored during the Akkadian period, during which time half of the objects analyzed were made using Omani copper. Comprising 90 items associated with the archaeometallurgical process, this assemblage included finished objects, ingots, slag, and ores (Begemann et al. 2010, Prange 2001). Omani sources are not exclusively used in the production of Mesopotamian objects. One third of the analyzed Mesopotamian objects dating to the first half of the third millennium BCE, for instance, contained As/Ni quantities that are incompatible with Omani ores (Begemann et al. 2010).

2.3.3. Discussion

Textual and archaeological evidence associated with the Arabian Gulf have been used to construct a narrative in which the increase in socio-political and economic complexity in third millennium southern Mesopotamia led to a rise in maritime Gulf trade and an attendant decrease in the use of terrestrial trade routes, finally ending in the decline of the network of routes connecting northern Iran to southern Mesopotamia (Possehl 1986: 88; T. Potts 1993).

This burgeoning maritime trade appears to have contributed to tremendous changes within both the southern Gulf region and the Indus Valley. In Dilmun, third millennium BCE trade led to the development of the Barbar Culture, which was strongly connected to both southern

Mesopotamia and Magan. In Magan, this trade appears to have led to the development of the Umm an-Nar culture, which was likewise linked with southern Mesopotamia and the Indus Valley.

Considering the purported scale of this trade, a profound southern Mesopotamian presence is largely imperceptible in the material culture of Oman. Scholars like Weisgerber suggest that this is likely due to the interception of goods by Dilmun and to the fact that, unlike the Meluḫḫans who waited for months in Southeast Arabia for the monsoon's passage, ancient Mesopotamians did not have to spend any significant amounts of time in the area. These explanations, however, do not account for the fact that the presumed goods that were being traded in exchange for copper and other recorded commodities remain largely undetected in the archaeological record of Oman. This absence of evidence could, of course, be owing to the fact that many imports may have been perishables like grain and textiles that left few traces in the archaeological record (see Crawford 1973). Indeed, cuneiform texts corroborate this interpretation recording the export of textiles, grain, and oil among the goods that were traded into the southern Gulf region (Leemans 1960: 10 – 12; Oppenheim 1954).

To contextualize this absence, it is worth noting that Mesopotamian imports are also conspicuously absent from Harappan sites (During-Caspers 1984; Chakrabarti 1990; Possehl 2002). A Harappan presence in Oman, on the other hand, is more strongly attested in the form of ceramics and seals with Indus Valley script and iconography, which have been attested at several coastal sites and at inland Bronze Age sites such as the copper producing site of Maysar-1.

2.4. Regional History and Diachronic Development of Obsidian Exploitation and Production in Ethiopia

This section provides an overview of archaeological studies of the Pre-Aksumite and Aksumite periods with a focus on lithic technologies, and in particular on obsidian use. Obsidian is an

extrusive igneous rock that forms through the rapid cooling of felsic lava. Generally glassy-black in appearance, obsidian can present in a variety of colors when formed in the presence of different impurities (such as iron, magnetite, cristobalite, etc.). Obsidian's desirability results from its sharpness, predictable conchoidal fracture, and aesthetic appeal. Although geologically rare, obsidian is often disproportionately represented in many ancient contexts worldwide and, in comparison with copper, it is comparatively easy to trace to its source, which makes it a useful for understanding long-distance interaction (Renfrew et al. 1965, 1966, 1968, 1969; Tripcevich 2007). While largely utilized in the production of tools and weapons, its pleasing appearance has also made obsidian a material that has been sought after for the production of elite objects (Nicholson and Shaw 2000: 46 – 47).

2.4.1. Brief Overview of Obsidian Exploitation in Ethiopia

Obsidian exploitation can be viewed as following a *chaîne opératoire* of production that begins with prospecting and quarrying. Quarrying falls on a continuum from *ad hoc* endeavors to specialized exploitation by individuals connected into a network aimed to supply knappers with raw materials (Torrence 1986). The degree of specialization is likely influenced by socio-economic, political, cultural, and technological factors as well as by the spatial distribution and density of sources. An initial process of core preparation potentially took place at or near a quarry (Bradley and Edmonds 2005) and served a number of functions, chief among which were load management and quality assurance (Tripcevich 2007).

The ensuing reduction process can be divided into several culture-dependent steps, which are also necessitated by the geologic features of the raw material (Tripcevich 2007; Sellet 1993: 108). The size and general shape of a nodule depends on the quality of the material as well as on the methods employed in its extraction (Tripcevich 2007: 676). Following extended usage,

obsidian tools often need to be retouched. Determining whether knowledge of retooling and repairing was either generalized or specialized informs how we interpret material culture traces and how we more broadly understand the developmental trajectory of this technology.

In Ethiopia, obsidian exploitation is first identified in connection with Early Stone Age (ESA) Mode 2 ('Acheulean') hand-axes manufactured in the Melka Kunture area of central Ethiopia (Agazi et al. 2006; Finneran 2007: 38). During the Middle Stone Age (MSA) a trade network developed, linking sources and sites at distances of over several hundreds of kilometers (Merrick et al. 1994; Assefa et al. 2008, Agazi et al. 2011; Brandt et al. 2012).

In northern Ethiopia, isolated finds of potential ESA chert bifaces in the area surrounding Aksum indicate some degree of habitation dating to this period (e.g. LP40, L. Phillipson 2009: 28, fig. 17; L. Phillipson 2000c: 13 – 15). Lithics associated with MSA traditions are somewhat better represented although these are still few in number; because they have been uncovered in redeposited contexts, it would be imprudent to draw firm conclusions based on their presence (L. Phillipson 2009: 109).

Roughly around 10,000 years ago, climatic conditions in northern Ethiopia began allowing for more permanent settlements. The sociopolitical landscape of this region during the third and second millennia BCE was characterized by a diffuse population, by the presence of lithic workshops in the vicinity of streams and of hills and by rockshelters arranged in the sides of hills (e.g. Baahti Nebait on the western slope of Bieta Giyorgis, D.W. Phillipson et al. 2000: 17 – 26; Fattovich 2009: 1).

Several cultural chronologies have been proposed for northern Ethiopia which, although differing slightly in the limits between periods, do not have significant differences. The chronological sequence for this region relies of ceramic typologies, numismatic studies, and

radiocarbon dating (Fattovich 1990, Fattovich et al. 2000, Bard et al. 2014). The period of interest for this dissertation encompasses the first millennium BCE and the first millennium CE. This period has been divided into two phases (Pre-Aksumite and Aksumite). The Aksumite period in turn has been sub-divided into six sub-phases: Proto-Aksumite, Early Aksumite, Classic Aksumite, Middle Aksumite, Late Aksumite, and Post-Aksumite (Fattovich 1990; Fattovich et al. 2000; Munro-Hay 1993; D.W. Phillipson 1998). In terms of material culture, these phases are characterized by differences or slight dissimilarities in ceramic and lithic traditions, architectural styles, and inscriptions. The chronology I will be following in this dissertation is based on the Bard et al. 2014 publication (Table 2.2).

Table 2.2: Pre-Aksumite & Aksumite chronologies based on radiocarbon dates from Aksum (after Bard et al. 2014):

Period	Date Range
Pre-Aksumite	800-360 BCE
Proto-Aksumite	360-130 BCE
Early Aksumite	130 BCE-160 CE
Classic Aksumite	160-380 CE
Middle Aksumite	380-580 CE
Late Aksumite	580-825 CE
Post-Aksumite	825-900 CE

During the early first millennium BCE, large towns associated with the Ancient Ona (Trignali 1965; Munro-Hay and Trignali 1991; Schmidt and Curtis 2001; Schmidt et al. 2008) and Pre-Aksumite (Anfray 1990; Munro-Hay 1993; Fattovich 1990, 2010) cultures began to develop in the highlands of northern Ethiopia and Eritrea (D'Andrea et al. 2008; Finneran 2007; Harrower and D'Andrea 2014). Their origins are still vigorously debated, with some emphasizing first millennium BCE influences from South Arabian kingdoms (Anfray 1990; Gerlach 2012), and others seeing the Pre-Aksumite society as a fundamentally indigenous development. Most elements of the archaeological record are locally derived, yet local African elites also proactively

co-opted foreign architectural and religious elements from South Arabia (Curtis 2004; Phillipson 2012) and possibly were influenced by second and third millennium BCE links with pastoral societies of the Gash River region of eastern Sudan (Fattovich 1988).

A great deal of debate surrounds scholarship about the initial Pre-Aksumite iteration of socio-political complexity. Disagreements arise surrounding both the importance of different cultural influences on the development of this polity as well as the appropriateness of the current terminology used to refer to this culture and time period ("Pre-Aksumite" vs. "pre-Aksumite" vs. *D'MT*; Finneran 2007: 118 – 119; Harrower and D'Andrea 2014: 517)[11]. Proponents of the notion of an "Ethio-Sabaean" polity emphasize material culture affinities between Sabaean settlements in southwestern Arabia and mid-first millennium BCE contexts in northern Ethiopia and refer to epigraphic South Arabian inscriptions that record the presence of a kingdom of *D'MT* (generally vocalized as 'Damaat'; Rossini 1928; Anfray 1967, 1968). Nevertheless, topics that appear to have achieved a semblance of scholarly consensus include: (1) the chronological limits of this period, (2) the continuity into the later Aksumite period of certain material culture elements, including lithic traditions (Fattovich 1990; Finneran 2007; L. Phillipson 2009), and (3) the need to investigate indigenous African influences, alongside South Arabian, Sudanese, and possible Egyptian influences (Finneran 2007: 119, Harrower and D'Andrea 2014: 517, Fattovich 2012a, 2012b).

This polity had important centers at Yeha (Tigray, Ethiopia) and Matara (Eritrea; Fattovich 1990b). In Tigray, we begin to see evidence of ox-plough agriculture and a reliance on free-threshing wheat, bread wheat, emmer, barley, and legumes, with a gradual increase in the

[11] Pre-Aksumite with a capital *P* would be most appropriately used to refer to an aspect of material culture that characterizes the period preceding the Aksumite period, which also continued into the Aksumite period. Whereas, pre-Aksumite would more appropriately be used to designate elements that preceded the Aksumite period, but that did not continue being used during it.

consumption of tef (Fattovich 2009: 1). The most important animal domesticates appear to have been cattle, sheep, and goats. The settlement pattern associated with this time period was characterized by small villages and hamlets, often located along hillslopes (Fattovich 2009: 1).

The end of the first millennium BCE sees a decrease in the importance of Yeha and changes in some mortuary practices, ceramic traditions, as well as a decline in the use of monumental inscriptions (Harrower and D'Andrea 2014: 518). Starting around the end of the fifth century BCE and the beginning of the fourth century BCE, coherent cultural elements appear to consolidate around Aksum, as illustrated by excavations undertaken at the elite cemetery of Bieta Giyorgis (Fattovich and Bard 2001). These changes are paralleled in Eritrea, where an abandonment of Ona sites has been recorded (Curtis 2008).

Beginning on the cusp of the fourth century BCE and ending around the latter half of the first century BCE, the next period is referred to as the Proto-Aksumite period (in particular by the excavators of Bieta Giyorgis), although it is currently unclear whether this cultural phenomenon is representative of broadly identifiable changes in Tigray or whether it is more accurately circumscribed narrowly around the site of Aksum.

The late first millennium BCE also sees the development of long-distance trade as a significant facet of the economy. The importance of long-distance trade continues steadily through the first half of the first millennium CE, achieves a peak during the mid-first millennium CE, and observes a decline during the late first millennium CE (Fattovich 2009: 2).

The Aksumite kingdom was established as a local power in the early first millennium CE and incrementally spread across the northern Horn of Africa. The early part of the first millennium CE saw the developments of the royal cemetery in the so-called Stelae Park located at the base of the Bieta Giyorgis hill. By the mid-first millennium CE, Aksum had become the capital of a vast

territorial state, which adopted Christianity as a state religion in the fourth century CE. Between the fourth and sixth centuries CE the church of Enda Marian Tsion, constructed in Aksum, was central to Ethiopian Christianity.

Subdivided into four phases, the Aksumite period begins around 130 BCE and ends roughly around 825 CE. During this period, notable events include the fourth century CE conversion of the kingdom to Christianity and the rise of Islam during the Late Aksumite period. Although not conquered by Islam, the kingdom's decline has been linked to a loss of dominance and control over trade in the Red Sea region and broader Indian Ocean area.

At the height of its power between the third and sixth centuries CE, Aksum was the capital of a large literate civilization whose influence and trade connections extended over northern Ethiopia (at least as far as Meroe in southern Sudan), over southwestern Arabia, and as far as the Indian subcontinent. One of Africa's most powerful complex societies, Aksum's power and influence was gained and consolidated through military expeditions to Sudan and Yemen and through the maintenance of long-distance trade relations with regions in the Red Sea, Indian Ocean, and Mediterranean (Anfray 2012a, 2012b, Finneran 2007).

As was the case in Oman, the northern Ethiopian and Eritrean landscape comprised of several ecological zones that generated specific economic strategies and whose collaboration led to the development of regional networks of socioeconomic interaction (Finneran 2007).

Aksum's political organization has been described using the "pyramid" model of hierarchy which saw the monarch at the top of the political structure with various administrative and military functions often being filled by members of the royal family (Munro-Hay 1991; D.W. Phillipson 1998, 2012). This model is backed by the discovery of elite mortuary contexts, palaces, stelae, and inscriptions.

The broader society appears to have been highly stratified and comprised of agro-pastoralists (who produced both for subsistence and for commerce), craft specialists, as well as wealthier individuals. Specialized production has been attested in the domains of ceramic, lithic, metal production, as well as architectural construction, etc. Social stratification has been revealed through the investigation of domestic architecture (discovered around Aksum, Adulis, Matara) and mortuary contexts (Finneran 2007; D.W. Phillipson 2012).

While long-distance trade is often cited as a main factor contributing to the wealth and social stratification of the kingdom, less is known regarding its organization on a local level and more recent research suggests that the basis of the economy was agro-pastoral production in excess of subsistence needs (D.W. Phillipson 1998: 55; D'Andrea 2008; Harrower et al. 2010). Notably, cattle rearing appears to have been economically and socio-culturally important for the Aksumites, and ox-ploughing has been proposed as an important factor towards incremental expansion of agricultural output (McCann 1995).

Raw material exploitation, production, and consumption were significant elements of Aksumite economy (Pankhurst 1961, Connah 1987, Munro-Hay 1991). Obsidian used for lithic production during the Aksumite period was imported into the Ethiopian highlands either from the Afar region or from sources in Eritrea. Except for the work of R. Fattovich (2009) and the recent dissertation of H. Solomon-Woldekiros (2014), the local networks that would have been used for the internal circulation of obsidian, ceramics, and salt are an under-studied aspect of research into Aksumite trade.

Although characterized by a slight decrease in lithic consumption as compared to earlier periods (L. Phillipson 2000), stone tools were used across all Aksumite periods, but are arguably

better represented in later periods, particularly in contexts that have been dated to the fifth or early sixth century CE (L. Phillipson 2000: 61).

In terms of tool type, scrapers are best represented during the Aksumite period by so-called Gudit scrapers and semi-circular steep scrapers characterizing Aksumite lithic assemblages (L. Phillipson 2009:120; 2000a: 52-57). First identified by Puglisi in 1946 in the Gudit Stelae Field in Aksum, Gudit scrapers have since been more closely studied by L. Phillipson and identified at other sites in the area. Also circumscribed within the category of the Mode 5 microlithic industry, Gudit scrapers are characterized by remarkable uniformity and standardization, are commonly found in Aksumite assemblages, are generally made of local chert, and are easily identified by minute denticulation along their edges, which has been interpreted as a result of continuous retooling and resharpening (Puglisi 1946, L. Phillipson 2000: 52, Finneran 2007: 53). L. Phillipson has suggested, based on experimental archaeology that Gudit scrapers are well-suited for wood and ivory working as well as carving soft stone. The marks revealed through these archaeological experiments have been interpreted as resembling those identified on sixth century CE worked ivory and carved steatite (L. Phillipson 2000a: 52).

Semi-circular steep scrapers are made of what L. Phillipson has termed poor quality chert and are themselves often poorly made, prompting her to suggest restricted access to quality resources. Phillipson goes further, suggesting that these poor-quality scrapers were potentially used by individuals performing forced labor tasks (L. Phillipson 2000a: 57). Generally limited to surface collections, circumscribed to a small area located northwest of the Gudit Stelae Field, these tools have been described as having double-beveled edges with shallow and overlapping knapping scars. L. Phillipson reveals similarities between this form and modern scrapers used by hide-workers in southern Ethiopia (L. Phillipson 2000a: 57).

Finally, obsidian backed bladelets, flakes, and small triangular points represent another category of well-represented tool type. Often uncovered in association with a workshop (e.g. Mai Agam, Phillipson 2009), the triangular points have been interpreted as potentially having been associated with defense-related activities (Phillipson and Sulas 2005, Phillipson 2009). One item of this assemblage was identified as a polishing stone for ceramics (Phillipson 2000: 58 – 59).

An important excavated context dating to the sixth century CE from Kidane Mehret (D site) has revealed a lithic assemblage containing both Gudit and steep-convex scrapers, as well as three other types of shallow scrapers, three types of backed microliths, and four core typologies. Notably, over two-thirds of the tools in the assemblage were made of obsidian (L. Phillipson 2000a: 57).

Aksum's standing gradually declined during the late first millennium CE. While no longer the capital of the kingdom, Aksum remained the religious center of Christian Ethiopia, a position it holds to this day. This time period also saw the gradual disintegration of long-distance trade networks (Fattovich 2009: 2). Following this period, the center of power moved south.

Although lithic traditions have been under-studied and under-published, recent publications following decades of research allow us to identify basic patterns and to chart a developmental tradition (Peterson 2017). Firstly, a decrease in variability of form, coupled with an increase in quantity of lithics, has been observed as one moves from the Pre-Aksumite period into the Early and Classic Aksumite phases (L. Phillipson 2009). This pattern has been used as a proxy for reflecting on population growth and attendant settlement pattern change in the area surrounding Aksum. Secondly, during the Middle and Late Aksumite periods, a reduction in variability of lithic types is accompanied by an apparent reduction in both loci of production and consumption. Thirdly, the Post-Aksumite period is characterized by a near complete absence of lithic production

(L. Phillipson 2009). A final trend observed is one towards increased specialization and towards the restriction of knowledge surrounding lithic production techniques (L. Phillipson 2009a). As shall be explained in greater detail in the following section, studies of lithic traditions in northern Ethiopia are characterized by a dearth of quantitative data, making verification and comparative approaches difficult to undertake (Curtis 2010).

2.4.2. Pre-Aksumite Period (ca. 800 – 360 BCE)

Largely produced through the analysis of surface collections recorded by surveys around Aksum and Yeha, a number of publications address Pre-Aksumite and Aksumite lithic traditions (L. Phillipson 2000, 2009a, 2009b, 2012, 2013a, 2013b). Notwithstanding its limitations, including a lack of quantitative data and metrical analysis (Curtis 2010), the book *Using Stone Tools: The Evidence from Aksum, Ethiopia* (L. Phillipson 2009b) is the lengthiest published study of Pre-Aksumite and Aksumite lithic traditions to date.

While acknowledging significant regional variations and temporal changes that are under-studied and under-published, Laurel Phillipson discerns three lithic traditions in material culture associated with the Pre-Aksumite (Phillipson 2009a: 48). These are: (1) a microlithic tradition, (2) a macrolithic tradition, and (3) a possible micro-macro tradition. These traditions reveal both indigenous and foreign elements. Their differences and co-occurrence have been used to suggest the existence of different groups cohabitating northern Ethiopia (Phillipson 2009b). Although arguably contemporaneous, according to Phillipson these traditions are unrelated on a technical and morphological basis (L. Phillipson 2009b: 109 – 117).

The first lithic tradition, the so-called microlithic tradition, is supposedly an indigenous development with mid-Holocene antecedents and few changes noticed between LSA and Pre-Aksumite assemblages (Phillipson 2009a: 48 – 50), revealing a great degree of cultural continuity.

This tradition continued into the Aksumite period through to the end of the Late Aksumite. Revealingly, this tradition apparently remained nearly unchanged following the introduction of ceramics into the area. Obsidian also played an important role in the Pre-Aksumite microlithic tradition; one that continued into Aksumite times (Phillipson 2009b).

The microlithic tradition is associated with Africa's Mode 5 industry. A preference for obsidian characterizes Mode 5 lithics in northern Ethiopia and the Rift Valley from as early as ca. 27.5 kya (Gasse and Street 1978; Finneran 2007: 51). The main tool types represented in these early materials, uncovered near the Bulbula River in the Lake Ziway region, are backed blades, end scrapers, and burins. A detailed cultural sequence for the microlithic tradition in the Lake Besaka region has been established by Steve Brandt on the basis of excavations at four sites (Brandt 1980; Clark and Williams 1978). Termed the 'Ethiopian Blade Tool Tradition', this cultural sequence charts three developmental phases beginning around 22 – 19 kya. The extent to which patterns observed in the development of the Ethiopia Blade Tool Tradition can be generalized to encompass the Aksum region remains unclear.

In Tigray, the cultural sequence of lithic production has been developed through excavations and research undertaken at rockshelters surrounding the Aksum conurbation, including at Anqqer Baahti, Baahti Nebait, and Gobedra (Finneran et al. 2000a, 2000b). The lowest levels at Anqqer Baahti revealed Mode 4 mudstone blades and circular scrapers, with higher levels progressing towards a majority of microlithic tools. At Baahti Nebait, an early layer characterized by the Mode 4 blade industry was overlaid by a Mode 5 aceramic deposit, a sterile layer, and a ceramic Mode 5 microlithic industry. An analogous sequence was obtained at the Gobedra rockshelter (Finneran 2007: 51).

In Tigray, the Pre-Aksumite microlithic tradition comprises obsidian backed crescents, bladelets, and convex chert scrapers and is characterized by small quantities of points. Surface collections and excavated contexts from Kidane Mehret reveal both direct percussion and bipolar manufacturing technique that utilized hard and narrow implements for knapping. L. Phillipson argues for a remarkable variability in lithic types both within and between assemblages and notes that certain assemblages demonstrated more skill, uniformity, and refinement in terms of finished objects (e.g. Kidane Mehret excavated contexts; L. Phillipson 2009: 49, 55; L. Phillipson 2000). These traits are used as proxies to suggest that Pre-Aksumite lithic production was a non-specialist endeavor.

A tool type manufactured almost exclusively out of obsidian is the so-called 'Likanos' flake uncovered in both Pre-Aksumite and Late Aksumite contexts at Kidane Mehret. Produced through bipolar percussion, this tool type reinforces the notion of cultural continuity, revealing the consistent and prolonged consumption of obsidian in the Tigrayan highlands (Finneran 2007: 56, L. Phillipson 2009: 109 – 113).

Of the three lithic traditions attributed to the first millennium BCE, it is only the microlithic tradition that continues into later periods, demonstrating a degree of continuity that is unparalleled by any other category of material culture (Fattovich et al. 2000).

The second lithic tradition, the so-called macrolithic tradition, is characterized by bifacial stone hoes and by large flakes, produced using hammer percussion on multi-platform or sub-radial cores (Phillipson 2009a: 49). The raw material used to produce these tools is sandy chert (L. Phillipson 2009b: 111). Unlike the microlithic tradition, which continues into the Aksumite period, the macrolithic tradition has only been attested in association with Pre-Aksumite material culture and seems not to have had any quantifiable influence on subsequent lithic technologies. Terming this

a Pre-Aksumite (with a capital *P*) lithic tradition is problematic for this reason; however, because it was uncovered at sites with evidence of Pre-Aksumite material culture, many scholars deem this designation appropriate (L. Phillipson 2009: 110 – 111).

This tradition has been uncovered at two sites: Hwalti and Melka (de Contenson 2005, L. Phillipson 2009b: 111). Termed "archaic" by Phillipson, this tradition does not bear any resemblance to older indigenous traditions dating to the LSA and has been interpreted as a foreign cultural element introduced by a non-local population with ties to South Arabian kingdoms (2000a: 49). The connection to South Arabia has been made because of the lithic tradition's co-occurrence alongside Sabaean architectural, epigraphic, and sculptural elements uncovered at Hwalti (2009a: 50; Fattovich 1997: 283).

A third lithic tradition identified by Phillipson dates to the Pre-Aksumite period and combines elements of the micro- and macrolithic lithic industries. Comprising entirely of surface finds, this tradition is thus far not sufficiently well-represented in the material culture of the region to allow a secure characterization. L. Phillipson suggests that these micro-macro contexts represent a distinct tradition as opposed to instances of concurrent use of the two aforementioned traditions. Phillipson argues that this designation is appropriate because of the infrequency with which they occur and because of certain morphological differences between tools associated with these contexts and those associated with the other two traditions (L. Phillipson 20009a: 50 – 51; L. Phillipson 2009b).

2.4.3. Proto-Aksumite Period (ca. 360 – 130 BCE)

The fourth century BCE witnessed a gradual shift in the material culture of northern Ethiopia. From the end of the Pre-Aksumite period to the beginning of the Aksumite period, this transitional period, entitled the Proto-Aksumite is characterized by a different settlement pattern, by changes

in mortuary architecture, and by a disappearance of Sabaean material cultural elements (Fattovich and Bard 1994, 2001; Manzo 2003). The Proto-Aksumite was largely defined based on material identified at Bieta Giyorgis (Fattovich and Bard 1994) and the extent to which this material is representative of a cultural phenomenon that spread across the entire region remains unclear.

In terms of the lithic tradition, the microlithic industry described for the Pre-Aksumite period continued into the Proto-Aksumite, indicating a continuation in population between periods. Lack in uniformity both within and between assemblages, suggests that production remained outside of the exclusive bounds of specialists (L. Phillipson 2009b: 112). Phillipson does however note an increase in the quality of tools, which, if borne out by more in-depth studies, could potentially help differentiate between microlithic assemblages dating to the Pre- and Proto-Aksumite. Overall, Proto-Aksumite tools appear to have been knapped using more controlled direct percussion than in previous periods and flakes with smaller striking platforms suggest the use of narrower or pointier hammers (L. Phillipson 2009b: 112). Adept knapping was also observed in an assemblage of fine chalcedony crescents discovered in OAZ IX vertical pit graves on Bieta Giyorgis (L. Phillipson 2009a: 53; L. Phillipson 2009b: 112).

Proto-Aksumite lithic assemblages are also characterized by the presence of small cores with deeply stepped edges, from which were detached flakes with prominently tanged butts that could be easily hafted without retouching (L. Phillipson 2000b: 112). Diagnostic of the Proto- and Early Aksumite periods, these flakes also sometimes appear in Classic Aksumite assemblages.

Proto-Aksumite assemblages also contain some of the last points discovered in the region. Characterized by variation in form and discovered in association with short crescents interpreted as arrow barbs, these points are believed to have been used to hunt wild game in the surrounding

landscape, a practice which seems to have died out after the Early Aksumite period (L. Phillipson 2000b: 112).

The Proto-Aksumite lithic assemblage does not suggest significant changes in the economic system from the Pre-Aksumite period. However, one must offer interpretations cautiously as Proto-Aksumite materials are narrowly circumscribed around the Bieta Giyorgis area of Aksum and often hail from disturbed contexts, surface collections, or multi-period sites (L. Phillipson 2000b: 112).

2.4.4. Early Aksumite (ca. 130 BCE – 160 CE) and Classic Aksumite Periods (ca. 160 – 380 BCE)

Current evidence indicates that a distinction between Early and Classic Aksumite lithic assemblages is presently impossible (L. Phillipson 2009b: 113 – 114). Whether attributable to problems of sampling strategy, issues inherent in surface collections, factors associated with multi-period sites, or conversely indicative of actual continuity of lithic tradition, the types of minute differences that have allowed differentiation between Proto- and Early Aksumite assemblages cannot be discerned when comparing Early and Classic Aksumite assemblages (L. Phillipson 2009b: 113).

Continuing the tradition of bipolar flaking of small cores that has its antecedents in the Pre- and Proto-Aksumite periods, Early and Classic Aksumite knappers employed a wider-range of percussion methods, including both indirect and direct methods. Early and Classic Aksumite tools have evidence of knapping by means of different sizes of hammers, evidence of pressure flaking, and even evidence of rubbing with a hone to remove protuberances (L. Phillipson 2009b: 113). Small, steep scrapers characterize the assemblages of this period.

While potentially having its roots in the Proto-Aksumite period, a pattern from generalized to specialized lithic production begins to consolidate more clearly during the Early and Classic Aksumite periods. This pattern towards increased specialization is characterized by the appearance of small specialized workshops (e.g. Mai Agam on Bieta Giyorgis), an increase in uniformity both within a tool type category and between lithic assemblages, more intensive exploitation of specific quarry sites, etc. (L. Phillipson 2009b: 113).

According to Phillipson, this process illuminates changes in the socio-economic structure of society. Phillipson argues that specialization in the production of tool types indicates a trend towards the commoditization of all aspects of lithic manufacturing including raw material exploitation, transportation, and production. The quantities of materials recorded suggest to Phillipson that small workshops existed where a small number of knappers worked to produce specialized, uniform assemblages. Phillipson points out that these were likely part-time engagements and that knappers also undertook agro-pastoral activities.

It is worth noting that this pattern relies on certain surface collections from multi-period sites uncovered in a narrowly circumscribed region, surrounding Aksum. Additionally, Phillipson does not provide quantitative information regarding lithic assemblages. For these reasons, these interpretations cannot presently be considered conclusive.

2.4.5. Middle Aksumite Period (ca. 380 – 580 CE)

The trend towards standardization reaches its peak during this time period and has been defined through the presence of highly uniform lithics. Throughout the Middle Aksumite and into the Late Aksumite period, production occurred at a few specialized sites, each of which appears to have been engaged in the production of a specific tool type. Phillipson interprets a perceived decrease in consumption as resulting from a decrease in reliance on lithics coupled with a reduction in the

number of specialized knappers. An inability to properly identify lithics from multi-occupational sites to their appropriate time period could also be contributing towards creating this perceived pattern (L. Phillipson 2009b: 114 – 115).

Other aspects related to the lithic supply chain, such as quarrying and transportation, also appear to be following a trend towards increased specialization. Phillipson interprets these patterns as further evidence of the trend towards the commoditization, hyper-specialization, and even monetization of the economy.

"Small, slightly splayed, scrapers with steeply-trimmed edges" (L. Phillipson 2000b: 114) are tool types that, while found throughout all Aksumite periods are better represented in Classic, Middle, and perhaps also Late Aksumite contexts. These scrapers are smaller than Gudit scrapers and are identified through resharpening scars and smooth edges. Use-wear analyses conducted on this ubiquitous tool type have proven inconclusive. Nonetheless, Phillipson suggests a range of possible uses for these tools, including: (1) used by potters to shape vessels, (2) used in the preparation of leather goods or vellum for manuscripts, (3) used to hollow out dry gourds, etc. (L. Phillipson 2009: 115). In the absence of additional use-wear studies and owing to their frequent discovery in surface assemblages it is difficult, at this time, to further narrow down their potential uses.

2.4.6. Late Aksumite Period (ca. 580 – 825 CE)

While largely characterized by remarkable similarities in tool types with the previous Middle Aksumite period, Phillipson suggests that Late Aksumite contexts could be differentiated by the discovery of Gudit scrapers. Highly standardized and often found in association with both Classical and Late Aksumite ceramics, Gudit scrapers were continuously resharpened suggesting

that their replacement was less desirable and possibly costlier than their repair (Hirth and Andrews 2002: 9; Phillipson 2009: 115).

Manufactured out of locally outcropping chert, it was not the high value or scarcity of their raw material that contributed to their infrequency. Rather, Phillipson argues it was a dearth of specialists that contributed to their rarity (Hirth and Andrews 2002: 9; Phillipson 2009: 115) and, because such a deficiency peaks during the Late Aksumite period, it would therefore stand to reason that Gudit scrapers were being produced almost exclusively at this time. It follows that steep scrapers are more appropriately associated with the earlier Classic and Middle Aksumite periods. This hypothesis aligns itself with Phillipson's broader theory that the number of specialist workshops and knappers decreased throughout the Middle Aksumite, reaching its zenith during the Late Aksumite period.

While not fully understood, it has been proposed that the function of Gudit scrapers was as a rasp in the manufacturing of ivory, soft stone, or wooden objects (Phillipson 2000a, 2000b, 2004). While scrapers are often associated with hide production in Ethiopia (Brandt 1996, Gallagher 1977), Phillipson argues that unlike the small, splayed steep scraper, the Gudit scraper was unlikely to have been used for hide production. Noting the presence of spurs on Gudit scrapers, Peterson (2017: 299) argues that they too were likely used to process hides, rather than harder materials. This is because spurs are associated with scrapers that have traditionally been interpreted as having been used for hide-working (Weedman 2002).

2.5. Overview of Interregional Interactions

This sub-section provides a brief overview of textual and archaeological evidence for interregional interactions between the northern Horn of Africa and other polities and civilizations of the Red Sea region.

2.5.1. Textual Evidence

In addition to several indigenous sources, textual evidence referring to Aksum, Ethiopia, or the northern Horn of Africa, more broadly, originates in Egypt, in the Mediterranean, and in Arabia, among other places.

Epigraphic South Arabian sources dating to the Pre-Aksumite mid-first millennium BCE, document ideological themes. Such inscriptions have been uncovered in association with all major Pre-Aksumite centers. Later monumental Aksumite inscriptions record religious and political themes, such as the heroism of kings. These inscriptions underscore the development of an indigenous South Semitic language and script, Ge'ez, influenced by Sabaean. In the aftermath of the adoption of Christianity, Greek began to be used more frequently, including Greek numerals and the specific Greek Boustrophedon (or ox-turning) script, characterized by lines that are read alternately from right to left and left to right, like a bull ploughing a field. This style was later replaced by a left-right style (Finneran 2007: 26).

Following the fall of the Aksumite Empire and until the rise of the Zagwe dynasty, a so-called 'Dark Age' is characterized by the absence of textual evidence. The next important genre of texts develops throughout the late Medieval period and includes the thirteenth century *Yekunno Amlak*, which records the restoration of the Solomonic dynasty, following the defeat of the Zagwe, and the *Kebra Negast* (lit. *Glory of the Kings*), a text that attempts to create a metanarrative of

Ethiopian history for the purpose of legitimizing the rulership of the second Solomonic dynasty and of connecting it to Ethiopia's Christian past (Munro-Hay 2001).

The earliest Egyptian sources refer broadly to the Land of Punt, a geographical area that has been identified (at least in part) with the northern Horn of Africa, and in particular with the Sudanese/Eritrean coasts and part of the northern Ethiopian interior (Kitchen 1971). During the Old Kingdom, Egypt imported slaves, myrrh, and wood from Punt.

Later Middle and New Kingdom sources, including the reliefs on the walls of the temple of Queen Hatshepsut at Deir el-Bahri, testify to the existence of political and diplomatic relations between Egyptian representatives and local rulers (Finneran 2007: 18). Being desertic and flat, the landscape depicted indicates that the events recorded in the relief occurred in a coastal, rather than a mountainous hinterland region (Phillips 1997). Puntite commodities imported into Egypt during this period include gold, incense, ebony, ostrich feathers, pelts, and cinnamon; all but the last item can be found in Ethiopia (Pankhurst 1997: 12; Finneran 2007: 18). In exchange for these goods, Egyptian sources record trade in Egyptian jewels and metals (Kitchen 1971).

During the fourth century BCE, an expedition to Punt records the importation of African elephants needed by Ptolemy I Soter in the battles against Seleucid Mesopotamia. Indeed, a commander of this expedition, Philon, recorded this voyage in the *Aethiopica*, a source that has not survived into the present (Sergew 1972: 47).

Mentions of Punt cease to appear during the Late Ptolemaic period. During this period, Egypt's focus appears to shift towards relations with the Mediterranean. Despite this interruption in economic activities, religious links with Egypt appear to have persisted, as the Coptic Patriarch of Egypt was the head of the Ethiopian Orthodox Church until the latter became autocephalous in 1959 (Finneran 2007: 24).

Greek becomes the koiné language of late first millennium BCE Red Sea trade and maintains this position for nearly a millennium. The first attestation of the word *Aethiopia* (from Αἰθίοψ, literally meaning 'burnt faces') appears in Greek translations of the Hebrew Old Testament. The Hebrew word being translated was Kush and, as such, *Aethiopia* was used to refer to the region of Sudan where the Napatan and the later Meroitic kingdoms developed from the mid-late first millennium BCE to the fourth century CE (Edwards 2004: 78 – 9). The New Testament (Acts 8: 27) mentions the Kandake (or Queen) of Ethiopia, a Meroitic title for a female ruler or elite woman. This mention also refers to Sudan.

Other sources from the eastern Mediterranean that use the term Ethiopia either to refer to Sudan or, more broadly, to Africa south of Egypt include Homer (1.22), who mentioned the distant Ethiopians and Herodotus (11.29; Levine 1974: 1 – 5), who also emphasized the remoteness of Ethiopia, as well as its capital at Meroe. Strabo (Strabo XVII 820, 789, 827) and Pliny (*Naturalis Historia*, V 10: 53 – 4) both provide geographical information about the Horn of Africa. Strabo mentions the existence of three Ethiopian kingdoms, including the Kingdom of Candance, Upper Ethiopia, and Southern Ethiopia. Pliny, on the other hand, mentions the settlement of Adulis as well as the three tributaries of the Nile: Astapus (Blue Nile, originating in Ethiopia), Astaboras (Atbara, in northeastern Sudan), Astasobas (White Nile, forming in South Sudan).

Possibly one of the most important sources on the Red Sea in antiquity is represented by the first century CE trading manual, compiled by an anonymous Alexandrian, and entitled the *Periplus of the Erythraean Sea* (Huntingford 1980). This text discusses the port of Adulis and mentions Aksum as well as a settlement in between the two entitled Koloë and recently identified with Qohaito (Voigt 1999). In addition to slaves, the commodities circulating from the interior through the port at Adulis were ivory, tortoise shells, rhino horn, ivory, hippopotamus hides, and apes.

Finneran notes the similarities between Puntite trade and first century CE trade (Finneran 2007: 22). Given the title βασιλεύς (Basileus, king) the ruler of the area was Zoskales, who was fluent in Greek and educated with regards to Greek culture. Obsidian (ὁ ὀψιανὸς λίθος) is mentioned in the subsequent section and placed near a bay located 800 stades south of Adulis and hypothesized as having been Hauchil Bay. Aksum is also mentioned in connection with rulership by Ptolemy in the mid-second century CE (IV: 7 – 8).

Following its conversion to Christianity, northern Ethiopia is better integrated into the Byzantine network of the eastern Mediterranean (Finneran 2007: 22) and is even called upon by Byzantine rulers for support. Indeed, according to Procopius, Justinian appears to have asked King Kaleb of Aksum to intervene in support of the Christians being persecuted in Himyar (Hatke 2012).

Relations between Aksum and Arabia continued into the seventh century CE (Christides 1994). Significantly, members of the family of the Prophet Mohammed undertook a *hijra* to Aksum, where they had been promised refuge by a king, identified with the ruler Armah. A 10th century text mentions the Queen of Habasha (an Arabic name for Ethiopia that persists to this day; De Goeje 1873).

2.5.2. Archaeological Evidence

Evidence of obsidian circulation throughout the southern Red Sea region and wider Indian Ocean has been identified as early as the middle Holocene (Khalidi et al. 2010; Zarins 1996). Ethiopian obsidian has been found in Yemeni contexts dating to the sixth millennium BCE. Exemplified by shared use of obsidian geometric microliths, which likely originate in Africa, contacts between opposite coasts of the Red Sea intensified throughout the third through first millennia BCE (Fattovich 2010; Khalidi et al. 2010; Zarins 1987, 1989). Cultural affiliations have also been noted in the affinities that exist between second millennium BCE ceramic assemblages

from Ethiopia and from the Sabir Culture in Yemen's Aden region (Buffa and Vogt 2001; Vogt and Sedov 1998). Indeed, some scholars note cross-cultural similarities across the southern Red Sea region (Fattovich 2010, 2012). Fattovich suggests interpreting these durable contacts as representative of a so-called Tihama cultural exchange sphere which included the circulation of obsidian, ceramics, and plants across the southern Red Sea region, including areas in Ethiopia, Eritrea, Sudan, and Arabia (Fattovich 1996, 1997; Finneran 2007: 66). This model highlights the role of the Red Sea as a facilitator of contact between Africa and Arabia and suggests that the cooperation and interaction that facilitated the circulation of commodities was of a socio-economic and cultural rather than political nature (Fattovich 2000: 22; Finneran 2007: 144). Accepting this model has implication for how we view the development of the DMT during the first millennium BCE, countering the notion of South Arabian domination of large parts of the northern Horn of Africa.

The circulation of obsidian in the southern Red Sea region appears to have intensified throughout the first millennium BCE and CE. Analyses undertaken on archaeological obsidian collected along the Tihama coast of Yemen revealed that the material was not a geochemical match for the three known Arabian obsidian sources, namely Jebel Isbil and Jebel Lisi in Yemen, and Jebel Abyad in Saudi Arabia (Francaviglia 1990, 1996). Francaviglia suggested a possible Ethiopian or Eritrean source for the Yemeni obsidian samples. More recent work undertaken in Yemen supports Francaviglia's conclusions. Khalidi has proposed several potential obsidian sources for the Tihama assemblages; these include Arafali, Alid, Dubbi, and Ado Ale, all located near the Eritrean coastal plain (Khalidi 2009).

Per Zarins, archaeological obsidian from the Hadramawt of eastern Yemen matches obsidian from Arafali volcano. Located near the Gulf of Zula and the Aksumite port town of Adulis, the

volcano Alid cannot be discounted as a possible source. Indeed, while Adulis thrived during the Aksumite period, the site may have been in use as a port during the third and second millennia BCE as well (Zarins 1989; Khalidi 2009).

Ethiopia likely supplied Egypt with obsidian as well (Bavay et al. 2000; Zarins 1996) and, as recounted in the previous section was likely part of the Land of Punt that supplied Egypt with luxury commodities (Kitchen 1971). Despite this, there is a dearth of evidence of Egyptian material culture in the Horn of Africa. What we do have consists of: (1) the Cippus, stela of Horus, given to the eighteenth century Scottish traveler James Bruce upon his visit to Aksum (Phillips 1997; Finneran 2007: 19), (2) an amulet figurine of Harpocrates/Horus uncovered at Matara; this item could also be Nubian (Phillips 1995), and (3) an Egyptian ship discovered at Wadi Gawasis and interpreted as having been involved in trade with Punt (Fattovich and Bard 2006).

Lithic studies also reveal technical and typological similarities between assemblages uncovered in Tigray, and in particular at the site of Seglamen, and those discovered in the Gash Delta of eastern Sudan. These finds have been used to create the narrative of a fifth millennium BCE movement of agro-pastoralists from Sudan into northern Ethiopia (Phillipson 2017).

Chapter 3

A Network Approach to Ancient Economies

3.1. Introduction

In this chapter I explore the use of a network approach for the study of economic activity. I will argue that a traditional Neoclassical market approach has significant shortcomings, and I will also challenge the Substantivist alternative. My contention is that a network approach to studying economic activity bypasses many of the drawbacks that characterize other economic theories.

The network approach to economic interaction does not assume an idealized market nor indeed a non-market economic system but is rather a bottom-up approach investigating who is interacting with whom and with what amount of regularity. Indeed, I explore the notion that the network framework is arguably the most robust method we currently have for understanding economic interaction.

Characterized by both methodological and theoretical implications, the network approach is an umbrella term that followed somewhat different trajectories within several fields in the sciences, social sciences, and humanities. Methodological aspects related to the network approach provide a blueprint (with roots in graph theory) for analyzing and visualizing interactions between social actors. The network approach also generates a theoretical foundation for analyzing social relations.

To fully understand an economic system, it becomes necessary to identify mechanisms of integration by which trust between economic partners can be achieved and social order maintained. Towards this end, in this chapter I combine network theories with economic, sociological,

anthropological, and archaeological theories meant to build up an understanding of these important topics. I argue that people's economic activities are embedded in their networks of social relationships and that trust emerges and is maintained through repeated economic exchanges[12] with partners whose reputation is known to them either as a result of personal interactions or through information acquired from trusted intermediaries. In other words, people's economic activities depend on the nature and quality of their social relationships. I further argue that reciprocal expectations between economic partners underlie exchange and that these expectations are often socially and culturally determined (Granovetter 1985, Turner 1987, Homans 1961, Blau 1964). Because of this cultural valence, an understanding of the culture-historical milieu of exchange is likely to produce more sophisticated and robust interpretations of economic interactions.

This chapter is divided into five sections. The first section contains a brief introduction to network analysis (3.1) and is followed by a lengthier presentation of the history of major traditions related to network research (3.2). The third section (3.3) succinctly introduces basic characteristics of network studies in archaeology. The fourth section (3.4) is further sub-divided into three parts and functions as a network appraisal of various economic theories that are used in archaeological and anthropological studies. The first part of the fourth section (3.4.1) will provide a network assessment of structuralist exchange theories. While developing an early conception of economic interaction at the level of society, the structuralist exchange theory focused on distinguishing the manner in which actors engaged in economic interactions and on elucidating the characteristics of their social connections. From a network theory perspective, the structuralist models proposed by

[12] Unless explicitly stated, the term *exchange* is not used in the classical sense of market exchange but is rather used to refer to economic interactions.

Mauss (1925/ 2002) are understood to be closed networks and despite not being directly applicable to the context of my research, structuralist network thinking is a useful metaphor with indirect application to this work. Because these models developed through a consideration of small pre-state segmentary populations, it is apposite to briefly categorize the more socially complex economic and socio-political contexts that have been reconstructed for the two research areas in Oman and Ethiopia (3.4.1.1). The second part of the fourth section will contain a network appraisal of Classical and Neoclassical economic theories (3.4.2) and will be followed by a network appraisal of Substantivists theories (3.4.3). Finally, the fifth section will present a synthesis of the embedded, culturally dependent, network theory of the economy that I am arguing for in this dissertation (3.5).

3.2. Introduction to Network Analysis

Network analysis contributes a theoretical foundation and a suite of techniques for analyzing and visualizing patterns of human relationships (such as patterns related to raw material supply chains) and for assessing the significance and ramifications of those relationships (Wasserman and Faust 1994). A focus on the connection between these associations, rather than on the characteristics of the social units being analyzed, can reveal patterns that may not otherwise be accessible.

Employing mathematical and statistical methods, network approaches analyze empirical datasets to reveal network structure and the impact of such structure on members of the network (Freeman 2004, Peeples 2019, Collins 1988). Networks are constructed from social actors or nodes and their ties or connections. Nodes can represent individuals, communities, polities, etc. Ties, on

the other hand, consist of a variety of different social relationships: commercial, kin-based, information based, etc.

3.3. Brief History of Major Traditions of Network Research

A recognizable tradition of archaeological network studies began to form in the last decade (Brughmans and Peeples 2017, Peeples 2019). The application of various network measures and approaches to archaeological questions has a longer history, however, and derived influences from network-related methods and approaches that developed within the disciplines of geography, mathematics, sociology, computer science, etc. (Peeples 2019). Within the broader humanistic and sociological endeavor, the earliest such approaches date to the early 20th century (Moreno 1934; see Freeman 2004 and Peeples 2019). Within mathematics, the related field of graph theory has had a lengthier development, being used for nearly 300 years (see Biggs et al. 1986).

Although having slightly different developmental trajectories in archaeology and anthropology, the late adoption of network methods as compared to the social and physical sciences, for instance, is characteristic of the method's evolution within both disciplines. Knappett (2013) attributes the eventual rise of network studies within anthropology and archaeology to several reasons all of which can broadly be subsumed under a so-called global vs. a local academic reason. While these disciplinary dynamics will be illustrated in the following sections, it is worth beginning by pointing out one important contextual factor that spurred the adoption of network approaches within the twin disciplines. Globally, the context that gave rise to network analyses was characterized by the expansion (in the mid-1980s) of the World Wide Web and of social networking sites in particular. Later in the 1990s, the publication of the seminal "small-worlds"

paper by sociologist Duncan J. Watts and mathematician Steven Strogatz (1998) would have unquantifiable effects on the academy.

In what follows, I will briefly discuss four of the more significant pillars that support archaeological network studies: graph theory, social network analysis (SNA), complex networks scientific approaches, and relational sociology.

Graph Theory – At their core, all network approaches fundamentally analyze the structure of dyadic relationships between different units of analysis. Likewise, all formal network approaches rely on a graph theoretical foundation. Within graph theory, a sub-field of discrete mathematics, such relationships are visualized through the means of algebraic matrices and analyzed using a specific suite of mathematical methods (Peeples 2019).

Some of the earliest mentions of graph theory in archaeological work began to occur in the late 1960s (see Peeples 2019). These were not, however, fully integrated methodologically within a research program aimed at understanding patterns of interaction until the mid-1970s when archaeologists in Oceania began creating geographic networks to compare archaeological patterns with biogeographical patterns to understand human diversity in the Northern Solomons (Terrell 1976, 1977a, 1977b) and to understand the centrality of settlements in Papua New Guinea (Irwin 1978). Because of the early application of formal network analysis in Oceania, its popularity among archaeologists in the region continues to this day (Hage 1977; Hage and Harary 1983, 1991, 1996; Hunt 1988; see Peeples 2019).

Until the mid-2000s, when formal graph theoretical methods began permeating archaeological network approaches, a small number of projects employing graph theory were conducted and published, including notably one on Uruk period Iran where graph theory was used for regional

analysis of the Susiana Plains using data from Wright and Johnson's Middle Uruk Project (Rothman 1987). While this method was adopted particularly from New Geography, it was nonetheless used to understand social and economic interactions.

Social Network Analysis (SNA) – Starting in the 1940s, Social Network Analysis (SNA) began to develop as a well-defined academic field within the social sciences. Disciplinarily, SNA is differentiated from other network studies in that it focuses on relations between social entities, in particular, and specifically on the relationship between network position, network structure, and traits of individual social actors. This field proposed a relational shift from an intellectual focus on the attributes of social actors to a focus on understanding types of relationships between actors as well as the structure of those relationships (Peeples 2019).

This field owes a great deal to various traditions within social anthropology and sociology. Incipient empirical studies on social networks were conducted by the Manchester School of British Social Anthropology (Barnes 1954; Bott 1971, 2017) as a result of which several early theories were developed (Boissevain 1979, Nadel 2013). Within the British School of Social Anthropology, the aim of network analysis was to provide an explanatory framework and apposite methods for studying cultural change and adaptation. This trend came as a response to what socio-cultural anthropologists of the time saw as the problem of understanding cultural patterns as static, fixed, and unchanging. In other words, a focus on cultural continuity was not giving way to a burgeoning interest in cultural change (Firth 2013). Differentiating between social structure, which provides rigidity and continuity with the past, and social organization, which leads to change and variation, British social anthropologists considered social relations that emerged as a result of social organization as the proper focus of network analysis (Whitten and Wolf 1973).

Later, during the 1960s, the Harvard Department of Social Relations laid the foundations for combining theoretical social network approaches with quantitative measures employed to bolster and verify these theories (White 2008). The aim of these early studies was to highlight the structure of relationships alongside the traits of individual social actors within networks. Both foci were seen as equally consequential in revealing social processes; however, a preference for studying structure was declared, as this facet was understood as being understudied both within the social sciences and within socio-cultural anthropology (see Peeples 2019).

By the middle of the 1970s, the field of Social Network Analysis aligned a suite of theories with specific formal and mathematical measures, while maintaining its close relationship with sociology. Access to this new toolset led scholars within anthropology to privilege the study of quantifiable questions relating to social processes and network structure (Brint 1992). The enthusiasm over undertaking quantifiable analyses was not unanimously shared by anthropologists. Many who saw this focus as a negation of the importance of the individual scale, which dealt with the attributes of entities and with questions of agency, chose to eschew network analyses (Santoro 2008, Knox et al. 2006) and because the disciplinary trend bent in the direction of individualism, network analyses did not gain secure footing in anthropology until much later.

A few decades later, in the mid-1990s, the so-called New York School of relational sociology is credited with making a concerted effort to include analysis of agency and culture alongside analysis of network structure (Mische 2011). According to Peeples (2019: 14), the work of the relational sociology school is foundational to the way contemporary network studies are undertaken in the social sciences, anthropology, and archaeology. These network studies investigate the role of culture and history on the formation of networks, arguing that the effects on an entity associated with occupying a specific network position are culturally and historically

dependent and, as such, a study of network structure is incomplete in the absence of an understanding of the culture-historical context within which social relationships develop.

Complex Networks Science – A third significant pillar influencing archaeological network studies is the interdisciplinary field with ties to physics, mathematics, and computer science (Newman 2011, 2018; Brandes et al. 2013) and a focus on the structure, characteristics, and dynamics of complex systems. Beginning in the 1960s, this field can be traced back to research undertaken in the Los Alamos National Laboratory (the former Manhattan Project) and at the Santa Fe Institute in New Mexico. Initially, the field of complex networks science developed separately from network approaches in other disciplines (Scott 2011).

Sharing in their understanding of the defining role of the structure of relationships in impacting the conduct of related entities, complex network science and SNA focus on different scales of analysis, largely owing to their different disciplinary origins (Peeples 2019). The focus of SNA tends to be on understanding eminently social processes like the position of entities within a network's hierarchy and the impact this position may have on the properties and outcomes of these entities. In contrast, complex network approaches tend to operate on a larger scale, focusing on the emergent properties of networks themselves. This dual focus is not often incorporated into the same research program. In recent years this joint approach has been on the rise (Scott 2011, Watts 2004; see Peeples 2019) and, indeed, describes my own aspirations in approaching this project, both with an interest in understanding the structure of individual networks and in viewing them comparatively to aid in identifying potential emergent network elements.

The complex networks approach aims to identify meaningful properties characterizing networks per se which are not the result of the properties characterizing the nodes of the network (Peeples 2019). Complex network scientists are further interested in determining whether network

rules exist that determine the relationship between network structure and the development of networks (Strogatz 2001). Recent empirical research in a variety of fields suggests that real-world networks (such as the internet, air transport networks, the human brain, etc.) can be generally described according to such emergent properties (Park and Willinger 2005, Rocha 2017, Papo et al. 2014).

Complex network approaches have revealed several structural elements that characterize many real-world networks. Two such examples are the so-called small-world structure and the scale-free structure. The notion of a small-world structure is already familiar to us from work undertaken in the late-1960s within social psychology, where the idea of the *small-world problem* (Milgram 1967) developed and was subsequently analyzed through a number of well-known experiments also referred to as the *six degrees of separation* studies (Travers and Milgram 1977).

Also referred to as the "rich get richer phenomenon" (Peeples 2019: 10), the network with a scale-free structure is defined as a system in which a small number of entities with the highest degree centrality maintain their central position when new entities connect into the network because the latter preferentially link with these prominent nodes, thereby reinforcing their advantageous positions.

In addition to these two, a third prevalent focus has been on understanding the community structure of networks (Newman 2004). Community structure identifies groups of entities within a network that are more closely connected to each other than they are to entities from other so-called communities (Radivojević and Grujić 2017).

Archaeological Networks – Despite occasional forays into network studies within archaeology (Rothman 1987, Terrell 1976, 1977a, 1977b, Irwin 1978) a distinct tradition geared specifically

towards answering archaeological questions only started developing in the field around 2010 (Brughmans 2010). Peeples connects this florescence of network approaches to the recent development of network analysis software, like UCINET (launched 2012), Pajek 1.00 (launched 2004), Gephi (launched 2008), etc., that made undertaking formal measures more accessible to archaeologists.

These developments arose within a broader intellectual context that saw a surge in the use of network approaches in the sciences. Peeples identifies distinct trajectories within archaeological network approaches developing in Europe and the United States. Whereas in Europe, archaeological network studies more often than not draw from the complex networks tradition, in the United States archaeologists have been more influenced by SNA (see Brughmans and Peeples 2017). Regardless of where the tradition has been developing, archaeological network approaches seem to be defined by a trait unique to the manner in which these studies have been conducted within the discipline; that is, a willingness to combine network theories with methods from the social and physical sciences (Knappett 2013) that is not matched by network studies in other fields.

Knappett attributes the late development of a tradition of archaeological networks analysis not only to the centering of agency theories within the discipline but also to a longstanding academic divide between archaeology and sociology, to which I would add physics, and mathematics – all parent-fields to network approaches. Indeed, archaeology traditionally cross-pollinates with anthropology and geography, both fields in which network approaches had a limited impact.

This late adoption may also have been linked to the existence of other popular theories that dealt with similar questions regarding regional interactions. Archaeologists interested in understanding the impact of inter-regional interactions on cultural change, for instance, often adopted a World-Systems lens. Such an approach, however, has a series of drawbacks. One of the

theory's weaknesses is that it provides few indications as to how one might go about studying intra-regional interactions (Stein 2002; Knappett 2013). One additional troubling assumption that lies at the foundation of this theory is the notion of a core and a periphery. Problematically, these categories are habitually ascribed to the cultures under investigation from the framing of a study. An additional criticism levied at World Systems Theory is that by virtue of identifying zones of interaction, there is an inbuilt assumption that commodities, for instance, flow from one zone to another in a uniform manner. Such assumptions obfuscate the likely complicated interactions that characterized inter-regional interactions and outright erase dynamics of *intra*-regional interaction. Where inter-regional interactions (relating particularly to trade and exchange) are concerned, scholars have identified these limiting issues and have been developing appealing theoretical solutions (Oka and Kusimba 2008; Bauer and Agbe-Davies 2010). These new theoretical models and many like them would benefit greatly from integrating network methodologies and there is an exciting future for them within the field.

It is also important to remember that all archaeological network studies to date have been undertaken by first generation adopters and, as such, the heterogeneity characteristic of the methods and approaches employed is to be expected (Brughmans 2010). Although some degree of uniformity will ultimately be achieved, network analysis should nonetheless continue to be seen as the umbrella that unites a plethora of related techniques and theories underneath.

Concerted attempts to unify and standardize terminology, goals, and methodology are currently being undertaken by scholars who caution about analytical challenges and issues deriving from the uncritical adoption of network approaches (Brughmans 2010, 2013; Knappett 2013; Peeples et al. 2016). Most issues stem from four distinct challenges identified by Peeples et al. (2016: 59). These are: (1) issues surrounding the uncritical use of artefacts as proxies for social units or processes in

the construction of network relations, (2) issues surrounding the difficulty of assessing contemporaneity among units of analysis, (3) issues surrounding boundary specifications, and (4) issues surrounding incomplete datasets. While these are discipline-wide challenges, in network studies these problems are perceived as occasions to develop more robust methodological and theoretical solutions that would simplify the archaeologist's inevitable predicament summarized by David Clarke as being that of recovering "unobservable hominid behavior patterns from indirect traces in bad samples" (1973: 17).

Current network studies are diverse and robust; networks have been used to understand settlement patterns (Verhagen et al. 2013), economic relationships and interactions (Knappett et al. 2008, Livarda and Orengo 2015), transportation networks (White and Barber 2012), resource procurement and distribution (Golitko et al. 2012, Golitko and Feinman 2015), networks of interaction (Carter et al. 2013), adaptive network strategies (Gjesfjeld and Phillips 2013), social identities and social change (Peeples 2011, 2018; Hart and Engelbrecht 2012), the role of geographic and social factors in social organization and change (Coward and Knappett 2013), regional (Knappett 2012, Mills et al. 2013 a and b, Peeples 2011) and diachronic variations (Mills et al. 2013 a and b), and migration and demographic change across a variety of spatial scales (Mills et al. 2015).

The future of network analyses looks to be replete with exciting potentialities and challenging issues. One such challenge which, if met, will contribute greatly to furthering network studies both within the discipline and cross-disciplinarily is the formulation of research programs devoted to the synthesis of an SNA approach with a complex networks approach (Peeples 2019). The former focuses on understanding relationships between social units and the impact of network position on

these relationships while the latter is geared towards revealing definitory elements of networks *qua* networks. It is in this disciplinary trajectory that I aim to place this current project.

3.4. Basics of Network Studies in Archaeology

As was demonstrated in the previous section, network analysis is the umbrella that unites underneath a multitude of different approaches, methods, and theories with distinct disciplinary origins. In this section I will briefly delineate a few select elemental principles of network studies that are relevant to my own theoretical and methodological goals in this dissertation. These goals are to combine elements of SNA and complex networks studies with the twofold aim of (1) identifying and explaining correlations between network position and the attributes of social units as well as the impact of network hierarchy on the development of social relationships and (2) revealing the emergent properties of networks.

According to Boissevain, network analytical investigations can generally be subsumed under five considerations: (1) identifying which social units are connected, (2) identifying the nature of their relationships, (3) identifying the pattern formed by these related social units, (4) identifying the impact of that pattern on the behavior of the social units, and finally (5) identifying the relationship between the pattern and other societal factors (Boissevain 1979: 392).

The foundational aspect of network studies is an emphasis on connections between units of analysis. An important assumption of these studies is that these connections develop interdependently and have structuring effects on the behavior of the interconnected units.

One early view regarding the virtues of network studies was that analysts would be able to identify all manners in which social units connected to one another, which would remove the

temptation of prioritizing a certain type of relationship in favor of another (Boissevain 1979: 392). That is seldom, if ever, the way in which network studies are conducted, however. This is because social networks are not the same as social groups. Indeed, the concept of a social group, within a network studies context, can be divided into two categories: a *realist* social group and a *nominalist* social group. The former refers to a real-world entity comprised of social actors that are consistently more closely connected to each other than to non-group members. Social groups are characterized by shared feelings, norms, and rules (Homans 1968, Bandyopadhyay et al. 2011) that are often culturally specific.

Nominalist groups, on the other hand, are bounded categories created by scholars and researchers according to particular characteristics. The latter are the subject of network studies (see Wasserman and Faust 1994). The referents according to which nominalist groups are verified are, in the case of archaeological networks, culture-historical reconstructions of ancient realist social groups. Where this project is concerned, an understanding of these realist social groups is presented in Chapter 1.

While not focusing on all manner of connections between social units, the relationships that are prioritized become the focus of the study. This represents an important shift from previous approaches and methodologies where the attributes of the units of analysis themselves were prioritized. These relations are formally analyzed and visualized using a graph theoretical approach.

An impressive breadth of measures is available to those conducting formal network analyses. This approach can be used to conduct exploratory analyses which are useful in identifying quantifiable aspects relating to network structure, such as the position of nodes within the network, the total number of connections identified within the network, the number of connections incident

upon each node, network size, network density, etc. In addition to these characteristics, network analyses can be used to identify powerful and influential social actors as well as power brokers, cliques, and nodes that act as bridges between different sub-groupings within a network. In short, network analysis can be used to reveal tensions between the nodes of a network as it relates to differential access to resources, power, and influence.

Importantly, network analysis is formulated in contrast with both a structuralist-functionalist approach and an institutional approach. An ability to focus on tensions and power is an important corrective measure against the obsession with stability that characterizes structuralist-functionalism. With its focus on understanding how balance and social order *could* be maintained, structuralist-functionalism (Durkheim 1984/2014) often fell into the pitfall of believing that social order *was* maintained. Indeed, it is at this juncture that I must briefly turn to the widest context out of which the network approach emerged. In Hegelian dialectical terms, if structuralist-functionalism is the thesis, the network approach can be seen as its antithesis, a counterproposition necessitated by the structural-functionalist proposition.

One of the most deep-seated assumptions inherent in structuralist-functionalist theory is the idea of equilibrium. Structuralist-functionalists are primed by the nature of their framework to understand the way different parts of society function together. When seeking out this understanding the temptation to focus on evidence that highlights a functioning system is inescapable. But, of course, few would deny that the system does not in fact always function well and arguably malfunctions frequently. Equilibrium is not always achieved, and evidence of social order being imperiled in plentiful. By focusing on ways to analyze tension and understand differential access to resources and power within social groups, network analysis provides the

framework and methods that generate an interest in identifying precisely those indications of social tension within the system and inure the scholar to the idea of the constancy of change.

Network analysis is also formulated in contrast to the institutional approach, which encourages dealing with different institutions separately. Instead, network analysis is able to fracture the boundaries between institutions in order to gain a more holistic view. The network approach can be described as a category bursting approach in that it allows for the creation of an analytical unit from its constituent parts rather than attempting to force an abstract institutional unit on particular elements.

3.5. Network Studies and Economic Theory

The goal of this section is to use a network analysis framework to reevaluate economic theories developed within the fields of anthropology, sociology, and economics itself. Each sub-section will begin with a brief background of the economic theory in question and will end with an appraisal of the theory that focuses on revealing weaknesses in the original theory and postulating potential network solutions.

3.6. Networks and Structuralist Exchange Theories

One can observe a link between *networks* in a metaphorical sense (Whitten and Wolf 1973) and anthropological theories of exchange (see Collins 1988) as developed by the French structuralists Marcel Mauss and Claude Lévi-Strauss, who were instrumental in defining a conception of economic interaction at the macro-level of the social group. This structuralist exchange theory was concerned with identifying actors engaging in economic interactions and

elucidating characteristics of their social connections (Mauss 1925/ 2002, Lévi-Strauss 1949/ 1969).

The structuralist exchange theory is a systemic approach[13] to studying social groups, which contends that society is not merely a collection of individuals whose personal needs must be satisfied to achieve equilibrium. Rather, society must instead be seen as a *superordinate system* composed of a number of different sectors, each one characterized by specific behaviors and needs, and each one operating jointly with the rest to achieve social stability (Durkheim 1893/ 1984). This theory develops around a desire to understand culturally determined non-competitive instances of exchange taking place in so-called archaic tribal societies, where gift exchanges (Mauss 1925/ 2002) and intermarriages (Lévi-Strauss 1949/ 1969) were regulated by social customs.

Published by Mauss in 1925, *An essay on the gift: the form and reason of exchange in archaic societies* became foundational for future anthropological theories of *reciprocity* and *gift exchange*. Mauss' principal tenet is the idea that gift exchange between groups of people structures social

[13] Because of his impact on the field of anthropology, the *systemic approach* is most closely linked with Émile Durkheim, the French sociologist, associated with the foundation of the academic discipline. Durkheim designates society as the unit of research within the systemic approach, arguing that societies are differentiated by extent of division of labor (1893/1984). In quintessential French political philosophical fashion, Durkheim's program was created in direct and vehement opposition to the English tradition of liberal though, and in particular contrasted with Utilitarianism, a school of thought most closely associated with the early classical Utilitarians Jeremy Bentham and J.S. Mill. Both Bentham and Mill were hedonists, equating happiness with the pursuit of pleasure and associating each individual's primary goal with attaining this happiness. French socialists understood *individualism* as sanctioning isolationist attitudes on the part of individual members of a community, a hazardous process whose cost included the potential diminution of social cohesion. Unlike other French socialist scholars, Durkheim did attempt to incorporate the individual within the systemic approach (Douglas 2002: XV). Durkheim's utilitarian critics popularize an arguably sophistic representation of his theory of society, suggesting that the sociologist "really believed that society is a kind of separate intelligence that determines the thoughts and actions of its members as the mind does those of the body it is lodged in" (Douglas 2002: XV). Instead Douglas suggests that Durkheim's colleagues in the French school did not themselves adopt this interpretation, nor did they read it into Durkheim's own work. Rather, Durkheim's underlying purpose was to investigate shared social norms. Additionally, Durkheim's attempt was to establish a scientific methodology for sociology by applying positivism to discovering so-called "social facts." Durkheim's work was influential to anthropologists and archaeologists, aided in part by the contributions of his nephew, Marcel Mauss.

relationships. Through a comparative exploration of several so-called archaic societies, primarily focusing on peoples of the Pacific Northwest, Mauss developed the notion of reciprocal exchange.

Continuing Durkheim's refutation of English Utilitarianism, Mauss depicts the theory of utility maximization as being specifically circumscribed to market economies. In its stead, Mauss proposed a reciprocal gift economy predicated upon the obligation to both give and receive gifts, a mechanism described as leading to the creation, not only of wealth and social alliances, but also to the cultivation of social solidarity. Gift exchanges operated at several societal levels, occurring between individuals and sub-groups alike.

The comparative approach marshalled by Mauss allowed the anthropologist to infer the existence of several similarities between the gift economies that developed in a number of different socio-economic contexts. Out of this comparative approach emerged the notion that, at their core, so-called archaic societies maintained their stability on the basis of collective exchange practices. Mauss' gift economy was predicated upon the idea that exchange practices served a dual function: to satisfy the needs of the individual and to satisfy the needs of the collectivity.[14]

Maussian gift exchange formed the basis of these societies having both a ritual (see Durkheim) and moral valence. While the ritual aspect provided the blueprint for how often and under what circumstances the exchange was to take place, the moral valence was meant to ensure cooperation between social actors. This notion harkens back to Durkheim's theory of "pre-contractual solidarity" (Durkheim 1893), which suggests that in the absence of trust and social solidarity rational exchange cannot be undertaken successfully.

[14] Like Durkheim's work, Mauss' *Gift* was meant as a work pertinent to issues of public policy. Particularly, it developed a theory of human solidarity and proposed social welfare programs as a response to the morality lost in the process of repudiating gift economies in favor of market systems.

The moral aspect, on the other hand, resides in the obligation of reciprocity that underscored gift giving. Indeed, it was the cycle of reciprocal gift giving and receiving that perpetuated the economic system. In network terms, this gift exchange built the ties of social and economic connection that linked members of the social group together. In contrast to the Utilitarian, Classical, and Neoclassical view of the economy, the gift giving economy did not necessarily lead to anyone accruing material dominance, as there seems to be evidence of items of equal value as well as symbolic gifts being exchanged between social partners. This is because the goal of this interaction was to accrue social gains rather than economic gains. These social gains were in the form of group alliance, social solidarity, and ultimately peace.

For Mauss, the system functioned properly because of the cultural ideology that rewarded those that played by the rules with social recognition, while punishing bad actors with a loss of status. In effect, gifted items as well as ceremonies of gift exchange were imbued with symbolic meaning which indicated that homeostasis would be achieved and maintained provided the exchange and its reciprocation were conscientiously undertaken in culturally specific ways.[15]

[15] One such example is that of the Melanesian Kula ring (Malinowski 1922/ 1966, Mauss 1925/2002), a case study that inspired Mauss. Malinowski details socially driven motivations, illuminating two important impetuses: the desire for prestige and the desire for status: "Work and effort, instead of being merely a means to an end, are, in a way an end in themselves" (Malinowski 1922/ 1966: 60). In contrast to Mauss' systemic methodology, Malinowski's individualist approach understood the social organization of the economy as centering around behaviors and practices that were effectively motivated by individual pursuits of prestige and status and by a desire to amplify social solidarity. Social solidarity was reified in part through systems of distribution, formalized by means of ceremonies, ritual practices, and customs, such as the Kula. To reiterate, Malinowski's individualistic approach does not occupy itself with understanding the individual in the absence of their social context; rather, the approach is termed individualistic because of the assumption that satisfying individual needs creates social stability (Parry 1986: 454). Malinowski's "primitive societies" are influenced by interwoven motivations derived from religion, magic, myth, and economy, giving rise to the notion that economic systems were embedded within their socio-cultural milieus. This notion of embeddedness later influences structuralist and substantivist theories as well as theories within the emerging field of New Economic Sociology. From embeddedness scholars interested in social networks, like the American sociologist Mark Granovetter, derive the notion that the network, made up of countless social relations, is the structuring principle responsible for maintaining social order, a problem which is paramount for economic anthropologists. I shall return to this notion at greater length later in the chapter (Granovetter 1985: 491).

Four different types of exchange systems are characterized by Mauss and later expounded upon by Sahlins (2017). While their initial iteration presented these systems as an evolutionary sequence of types, one need not accept this interpretation. The first system is characterized by so-called "total services" (Fr. *prestations*) and "total counter-services" in which all goods are exchanged through ritualized gift giving ceremonies. This type of a system is described as forming the foundation of continued relationships between different segmentary population groups (Mauss 1925/ 2002: vii).

A second economic system based on gift giving is the two-level system of exchange (cf. Malinowski's Kula ring). Within this system, trust and solidary are first achieved through ritualized gift giving ceremonies and are subsequently reestablished periodically. Within this system of solidarity (see Durkheim 1893), utilitarian market-type activities can then occur. This type of system is suggested as providing the framework for barter activities in societies characterized by the absence of a utilitarian division of labor (Collins 1988).

A third system, the potlach, is characterized as competitive gift exchange. This occurs in environments in which social partners enter a cycle of providing each other with bigger and bigger gifts in an effort to out-compete one another. Such a system has frequently been criticized by Western observers particularly for its propensity towards total economic ruination.

Finally, the fourth system is the market system, where supply and demand are the price setting mechanisms and where gift giving is relegated to the private sphere, losing its utility for building social solidarity.

From a network theory perspective, these models are understood to be closed networks (Collins 1988). These networks of reciprocal gift giving developed as a result of repeated and continuous

exchanges. Arguably these models provide a blueprint for understanding symbolic as well as utilitarian (in the Millian sense) economic exchanges.

Structuralist network thinking is a useful metaphor with indirect application to this work. Mauss' structuralist and systemic models suggest that comparing the structure of different exchange systems can reveal the elemental properties of those systems and uncover the manner in which different types of social relationships impact social actors and the structure of the system. In essence, this is a form of early network thinking.

3.7. Network Appraisal of Classical and Neoclassical Economic Theories

Unlike the structural models presented above, the focus of Classical and Neoclassical Economic theories is on individual motivations and desires and relies on the notion that satisfying individual needs creates social stability.[16] This theory relies on the concept of the *Homo economicus*.

Homo economicus and the methodology this concept sanctioned constituted a bridge between the Classical political economy,[17] characterized by the works of Smith and Ricardo, and Neoclassical economics. That bridge was built by John Stuart Mill.

[16] It is important to note that the individualist approach also appears in Malinowski, whose embedded understanding of the economy contributed to the later development of the *Substantivist* school.

[17] The field of political economy came into being with the purpose of answering the following question: why are some nations wealthier than others? Such knowledge was desired so that the economic habits and choices of successful, wealthy nations could be replicated to achieve similar outcomes and increased wealth. Writing in An Inquiry into the Nature and Causes of the Wealth of Nations (1776/ 2001), the Scottish moral philosopher and political economist Adam Smith revealed a conception of human nature that has its basis in the Hobbesian view. Accepting the Aristotelian conception of humans as social animals, Smith adopted the Hobbesian notion that humans act in their own self-interest (Meyers 1983), a notion which, in my view, was altogether descriptive for Hobbes, and elevated it to a prescriptive position in his own writings. For Smith, self-interest, if managed in an appropriate manner and stimulated through apposite incentives (Rashid 1985: 332), could lead both the individual and the nation at large to achieve the greater good. For Smith, it was the division of labor within a society that was the key to attaining national wealth. Division of labor enhanced cooperation and increased productivity within the different sectors of the economy. While division of labor was the mechanism for achieving a wealthy nation, the basis for cooperation resided within humans

Arising from the intellectual landscape occasioned by Hobbes and molded by Smith, Ricardo, and Malthus, the notion of *Homo economicus* was first fully defined by the nineteenth century English philosopher and political economist John Stuart Mill (Persky 1995: 222)[18]. Writing in 1836 in his *On the Definition of Political Economy; and on the Methods of Investigation Proper to It*, Mill purposefully defines this abstract human, and her motivations for making choices, along very narrow lines to make possible a deductive methodology of investigating economic interactions. Mill's abstract human is not afforded the entire breadth of humanity, with the culture and history attendant upon a real human; instead, Mill's abstraction operates according to four motivations: wealth accumulation, desire for leisure, a yearning for luxury, and a need to procreate (Mill 1836: 321, Persky 1995). Mill does concede that humans respond to other motivations, calling these, however, "disturbing causes" (Mill 1844: V. 58) and maintaining that their investigation must not be properly undertaken according to this single economic deductive methodology that he was developing. Persky claims that Mill considered the formulation of a *methodology* to deal with so-called "disturbing causes" as "both unnecessary and hopelessly indeterminate" (Persky 1995: 223). Rather, "disturbing causes" were for Mill relegated to the realm of applied economics; that is, their consideration need not be subject to the development of

themselves, within an innate "propensity in human nature" to "truck, barter, exchange one thing for another" (Smith 1776/ 2001: Chapter 2). Smith's theory of economic interaction and his notion of the interplay between ego-directed behavior and division of labor can be summarized through an excerpt from Chapter 2 of Wealth of Nations: "…It is not from the benevolence of the butcher, the brewer, or the baker that we expect our dinner, but from their regard to their own interest. We address ourselves, not to their humanity, but to their self-love, and never talk to them of our own necessities, but of their advantages." (Smith 1776/ 2001: Chapter 2). Smith's work has had a formidable and lasting impact on the fields of political economy and Classical economic thought and, while he was not the one to inaugurate the concept of Homo economicus, which instead was fully defined a few decades later in the works of J.S. Mill, implications of a rational agent who behaved self-interestedly surfaced in Smith's work.

[18] To be clear, J.S. Mill never used the term *Homo economicus* himself. The term was initially used derisively by Mill's critics (Leslie 1879). In his 1995 retrospective on the origin of the term, the American economist Joseph Persky stipulates in a footnote that he uncovered "the first use of the Latin *homo economicus* […] in Vilfredo Pareto's *Manual* (1906, pp. 12 – 14)", admitting, however, that he had not undertaken extensive research to track the origins of this saying (Persky 1995). Persky points to fellow economist Joseph Schumpeter, who noted that Bartolomeo Frigerio had used the related *economo prudente* already in 1692, calling the term a "common sense forerunner of the Economic Man" (1954: 156).

a deductive methodology, but rather they are more properly considered at the stage of applying the theory to a specific situation[19].

One important virtue that network theories have over such Classical economic models is the ability to avoid the methodological pitfall of creating a heuristic like the *Homo economicus* which allows analysis of only four categories of economic motivations. Indeed, unlike Classical economic models, network studies are empirical and, if constructed properly, are capable of analyzing a multitude of social and economic behaviors.

Critiques of Mill's concept arose nearly instantaneously[20] and almost from the very beginning a much-deflated version of Mill's already abstract human was being popularized.[21] Perhaps unsurprisingly, critics zeroed in on one motivation for their assessments: the desire for wealth accumulation. This understanding of *Homo economicus* as a creature that only operates according to *one* motivation persisted into modern economic thought and can be observed as late as the works of John Neville Keynes (1890/ 2017), who sees *Homo economicus* as being thoroughly focused on wealth accumulation. While Mill's concept was admittedly abstract, those that followed in his

[19] One must not forget that Mill's primary purpose in developing this abstract subject and this *a priori* deductive methodology was to understand the interactions between economic humans and their institutions. Indeed, for Mill differences in economic behaviors emerged from differences between the interactions of economic humans (with their patented four core motivations) and the different types of economic institutions that existed cross-culturally and diachronically.

[20] Indeed, responses to the Hobbesian notion of the human condition, a conception which is foundational to Mill's concept of the economic human, predate Mill's formulation. Because reflections on the human condition are not merely in the purview of the philosopher or the political economist, one can spot critiques of the Hobbesian notion across the works of the Romantic movement. Samuel Taylor Coleridge addressed Malthusians directly, accusing them of "never listening to the tone and unerring impulses of our better natures" (Coleridge 1884). The literary critic and writer William Hazlitt accused the English utilitarian philosopher and social reformer Jeremy Bentham of reducing "the theory and practice of human life to a caput mortuum of reason and dull, plodding technical calculation" (Hazlitt [1825] 1998: 80).

[21] Victorian morals were similarly perturbed by the characterization of the human condition as supremely self-interested (Goschen 1893). In his 1888 book, A History of Political Economy, the Irish economist and poet John Kells Ingram described the economic human, so defined by Mill, as a fictitious individual who focused all of his energy on wealth accumulation (Ingram 1888: 218). In so doing, Ingram is one of the first to popularize a much-deflated characterization of Mill's abstraction.

field (both critics and followers alike), made of *Homo economicus* an even barer caricature, often forgetting that Mill had attributed to the creature three additional motivations (Persky 1995: 223).

The tradition that developed in the wake of Mill's concept of *Homo economicus* identified the individual with the idea of *rationality*.[22] That is, unlike Mill's *Homo economicus*, who was only motivated by four incentives, the economic humans that populated scholarship within economics and economic anthropology were not necessarily characterized by *what* they choose, but rather by the fact that the choices made are done so in a rational manner, one aimed at maximizing advantage in every single economic interaction.

While for Mill *Homo economicus* was merely a heuristic tool that would allow for the formulation of an *a priori* deductive methodology, the economic human as the apotheosis of a rational agent was often seen as a demonstrable reality first by political economists within the Millian tradition and later by economists and economic anthropologists alike. This willingness to be convinced of the reality of economic humans coheres with the world in which these theories developed: the world of nineteenth century Western Europe and North America; a world replete with industrious humans continually trucking, bartering, and producing; a strikingly Western industrial world. This notion of the rational human was foundational to the development of the so-called canonical model of Classical economics.

This notion has withstood the test of time and, while there are many who would put *Homo economicus* on the endangered list, it remains the case that the idea that equates rational behavior

[22] This statement overlooks the complicated and nuanced ways in which the concept of the economic human developed in the works of scholars within the fields of economics and economic anthropology. However, the aspect of this theory that equates an individual's self-interest and will towards maximizing utility with every economic interaction with *rationality* carries through into the beginnings of economic anthropology and is a catalyst for both supporting and reactionary frameworks.

with a desire to maximize utility in every economic interaction continues to have an outsized impact on the field of economics (Persky 1995).

More recently, attempts have been made to reform this Utilitarian notion from within the field of economics itself (Leontieff 1982, Thurow 1983, Shubik 1984, Collins 1988). Yet, rather than challenging the notion of utility maximization, these works instead interrogate the purported system that allows rational humans to seek out this goal while maintaining social order: the market system and the Neoclassical notion that it will deliver the fairest and most productive distribution of resources commensurate with capital and labor investments. Discrepancies between the reality of significant economic inequality that characterizes market systems and the Neoclassical idea that these types of systems are the fairest have led scholars to question the notion that competitive markets will bring about social order. However, even these criticisms uphold the idea behind *Homo economicus*.

Because economics seems unable to reconcile these macro-scale traits of the market system, some have suggested the problem is within macroeconomics itself, while others dispute this notion arguing that the problem lies in the idea that prices in market systems are set through cycles of supply and demand (Williamson 1975). Such inequalities, Williamson argues, arise particularly in uncertain economic environments: contexts in which too much time and effort is spent bargaining for the best deal, or in which social actors are unable to make decisions as a result of too much or too little information (March and Simon 1958), or indeed as a result of the existence of bad actors. This uncertainty can lead certain economic actors to form organizations or hierarchies which allow them to attenuate some of these risks and thereby no longer follow market principles.

These hierarchies can be seen as networks because they rely on economic actors engaging repeatedly with one another. Williamson's theory goes a long way towards dealing with the

problem of the existence of inequality within the market system and it does so by proposing what can be described as a metaphorical network. However, this theory does not represent a sufficient departure from the problematic assumption underlying Neoclassical economics that a tendency towards the highest amount of productivity and fairness is the driving mechanism of the market system. Indeed, one of the problems with Williamson's theory is that it glorifies the inner workings of the hierarchy (much in the same way the market system is itself idealized), assuming productivity and efficiency and leaving no room for interior tensions and power struggles.

Despite the weaknesses in Williamson's theory, it undoubtedly represents a step in the right direction, one that leads towards a reformulation of economic theory through the framework of network theory.

Quite opportunely, network analysis was applied explicitly by American economist Ronald Burt (1982, 1983) to contemporary business networks. By investigating the relationships between boards of directors, Burt revealed the network structure of American manufacturing businesses and was able to show a correlation between higher profitability and companies that were capable of attracting their preferred trade partners (either suppliers or customers). In effect, what was being demonstrated was the impact business relationships had on the structure of the corporations themselves and on their success, as measured through profits. The better the relationship, as between a company and its preferred partners, the higher the profits. Based on his research, Burt argues for a correlation between economic success and stability, on the one hand, and the quality and strength of social relationships, on the other hand. My own study assumes the validity of this correlation.

3.8. Network Appraisal of Substantivist Theories

While the notion that adopting market principles will generate the fairest and most efficient system has been challenged in recent years, few Neoclassical challenges are directed towards the notion of utility maximization as exemplified through the heuristic of the *Homo economicus*. Within anthropology, however, a fatal blow to the concept was already dealt through the development of functionalism (Malinowski 1941).

For Malinowskian functionalists,[23] the best way to understand a society is through an analogy with a living organism, where its different constitutive parts, such as the political sphere, the religious sphere, and the economic sphere, etc., *function* together harmoniously and rely upon each other, in the same way that the different parts of a biological organism function collectively.

Developing during the first half of the twentieth century, Malinowski's functionalism was biocultural and focused on the needs of the individual. Malinowski developed a so-called theory of needs, proposing for each a cultural response (Malinowski 1941).[24] One of Malinowski's main goals was to broaden the concept of rationality so that it applied to the behaviors of non-Western peoples. Malinowski contended that Trobriand Islanders (and other non-Western societies) behaved rationally, according to deliberate and culturally specific behaviors, which had their own

[23] Conversely, the functionalism developed by Radcliffe-Brown considered the constitutive processes of human life and human interactions as the main units of analysis for anthropologists. Radcliffe-Brown argued that process qua process essentially implies the existence of a state of change and was therefore interested in exploring pattern repetition and social stability. In other words, while a process brings about change, fixed and stable patterns indicate sameness and thus imply a deficit of incompatible or opposing processes and even the existence of potential co-adaptational processes, which function together to maintain social stability. Adopting the notion of co-adaptation from biology, his interest was in how practices functioned to bring about social homeostasis (Radcliffe-Brown 1957).

[24] First, individuals need to be able to reproduce, to nourish themselves, and to have shelter. The cultural response for these individual needs was to develop various mechanisms for food production and collection, to develop the institution of marriage, and to develop methods for defense. Secondly, Malinowski suggested that instrumental needs (those associated with the renewal of institutional personnel and with the development of institutional charters and regulations) were met by education, by rules of social control, by economics, and by political organization. Finally, Malinowski suggested that integrative needs (associated with intellectual and pragmatic concerns regarding one's life and one's future circumstances) were met through the cultural development of religion, magic, art, science, etc.

explicit function in society. In effect, Malinowski reasoned that rationality was not solely in the purview of *Homo economicus* and that the traits elevated by social Darwinists were not the only available attributes of an individual that could be said to behave rationally.[25]

Malinowski specifically addressed the notion of *Homo economicus* arguing that "the real native of flesh and bone differs from the shadowy Primitive Economic Man, on whose imaginary behavior many of the scholastic deductions of abstract economics are based" (Malinowski 1966 [1922]: 61 – 62). Diverging from the orthodoxy of Classical economics, Malinowski described the so-called "primitive economy" of the Trobriand Islanders as operating in accordance with "definite and very complex rules" (Malinowski 1966 [1922]: 98 – 99).[26]

Adopting many of Malinowski's observations about non-Western economic actors, the Austro-Hungarian economic historian and anthropologist, Karl Polanyi published *The Great Transformation* (1944), a seminal work that became foundational for the Substantivist school. Importantly, the *substantive* and the *formal* definitions of economic, were predicated on two different systems of reference: the formal meaning "derives from logic" and the substantive

[25] Malinowski and other anthropologists emboldened by this rhetoric sought to rehabilitate behaviors that had hitherto been described as irrational and peculiar by Western observers. Actions associated with ritual and superstition, for instance, instead of being dismissed as illogical, were interpreted as having their own specific function and their own internal coherence within the cultural context that originated them. Thus, a narrative emerged by which it was recognized that different cultural groups developed at times contrasting yet always rational behaviors to match the requirements of their respective socio-cultural milieus.

[26] Malinowski's concept of a successful "primitive economy" was conceptually indebted to both a Rousseauian theory of the state of nature, wherein individual needs were satisfied by a stable economic system, and a Hobbesian theory of the state of nature, in which individuals toiled for their gains. Unlike Hobbesian natural humans, Malinowski's non-Western individuals did not exist in a constant and unavoidable state of conflict. Furthermore, unlike Hobbes and the scholars in the Hobbesian school, Malinowski rejected the idea of economic scarcity in "primitive economies" (Plattner 1989:13; Stanish 2017: 29). This idea was based on Malinowski's observation that Trobriand Islanders produced a surplus of goods. The absence of scarcity, a notion later adopted by Polanyi and the substantivist school, was an important way in which Malinowski departed from formal economics. Diverging further from formal economics, Malinowski argued that socially driven motivations rest at the foundation of "primitive economies" and not, as the canonical model suggests, eminently ego-driven impetuses. This interpretation does not outright reject the existence of veritable instances of selfish economic behavior. Indeed, Malinowski presents examples of individuals shunning their social duties; he does, however, argue that, as a result of a lack of scarcity within the economic system, individuals within non-Western societies did not primarily need to be motivated by selfish behaviors, but were instead much more likely to be moved by desires to gratify social needs.

meaning "derives from fact." That is to say: "the formal meaning implies a set of rules referring to choice between the alternative uses of insufficient means. The substantive meaning implies neither choice nor insufficiency of means; man's livelihood may or may not involve the necessity of choice and, if choice there be, it need not be induced by the limiting effect of a 'scarcity' of means" (Polanyi 1957: 243).

Scarcity was not the only precept born out of political economy that Polanyi fiercely disagreed with. Indeed, his disdain towards Adam Smith's notions that humans supposedly innately engaged in "barter, truck, and exchange [which he called] entirely apocryphal" (Polanyi 1957/ 2001: 46) cannot be overstated; neither can his derision at the thought that market capitalism was to be seen as the exalted conclusion of the teleological economic journey of humans: "The habit of looking at the past ten thousand years as well as at the array of early societies as a mere prelude to the true history of our civilization which started approximately with the publication of the Wealth of Nations in 1776, is, to say the least, out of date" (Polanyi 1957/ 2001: 47).

A great deal of *The Great Transformation* is spent exploring the emergence of market capitalism in nineteenth century England and its later diffusion to other parts of the industrialized world. Polanyi saw *market capitalism* as an exchange system that was unique in its *disembeddedness* from the social fabric and considered many of the precepts arising out of the discipline of economics as being exclusively matched to the market economic system. Writ large, market economy is a system in which the value of all commodities is seen to be established through self-regulating mechanisms of supply and demand. That value can ultimately be converted into a single standard, money. In developing his substantivist model, Polanyi was attempting to discover

ways to frame and analyze human economic action that were divorced from what he saw as an essentially modern, deeply Western, and decidedly dangerous economic framework.[27]

Polanyi maintained that before the development of market economy, exchange systems were *embedded* in the social fabric of the group, a notion that he borrowed from Malinowski. The *first* crucial distinction between market and pre-market systems has to do with differential access to two of the three primary factors of production[28], namely land (including natural resources and raw materials) and labor (Polanyi 1944). *Factors* of production are those resources utilized to yield output or *consumer goods* and are sometimes called *producer goods*. According to Polanyi and those that followed in his tradition, whereas in a market economic system, land and labor are commoditized and can be converted into the single standard, money, in non-market economies, access to land and labor is socially determined through one's place within the community.

A *second* substantivist argument against the existence of premodern market exchange has to do with the question of maintaining *social order* in a system envisioned by Polanyi as inevitably producing strife and social discontent. Polanyi differentiates between three different types of exchange: (1) *operational exchange*, or the type of exchange characterized by a simple change of location or changing of hands, (2) *decisional exchange*, the act of appropriating commodities at a "set rate", which integrates the economy by means of "factors which fix that rate, not by the market

[27] Because he spoke directly to the issues facing scholars of pre-capitalist economies and because he was following in the footsteps of scholars like "Comte, Quetelet, Marx, Maine, Weber, Malinowski, Durkheim and Freud" (Polanyi et al. 1957: 239), who had been purposeful in their attempts to understand the "relationships between man as biological entity and the unique structure of symbols and techniques that resulted in maintaining his existence", or the relationship between humans and their socio-cultural context, the tools of Polanyi's program were more readily adopted by scholars of ancient economies, anthropologists and archaeologists in particular.

[28] While in Classical economics factors are divided into two categories: primary (land, labor, capital) and secondary (materials, energy), other economic schools of thought adjoin other resources to the list of factors (such as technology, entrepreneurship, etc.). For the sake of clarity, it is important to note that the term "factor" itself was not in use by Classical economists, but was rather coined by Neoclassical economists and retroactively read into works of Classical economy.

mechanism" (Polanyi 1957/ 2001: 255), and (3) *integrative exchange*, or the act of appropriating commodities at a "bargained rate" (Polanyi 1957: 255). Polanyi maintained that it is the act of bargaining, or what he calls "higgling-haggling" (Polanyi 1957/ 2001: 255), a behavior which defines market systems, that would imperil community solidarity, engender social discontent, and would therefore be inconceivable in pre-capitalist systems.[29]

To elucidate these points further, according to Polanyi the mechanisms that could manifest utility and stability and by which economic integration occurred were embedded in either "formal and informal social institutions or "supporting structures" that served to regulate economic behavior and prevent antagonism" (Garraty 2010: 12). Called *forms of* integration (Polanyi 1957a: 250), the mechanisms in question are reciprocity, redistribution, and exchange. For Polanyi, the first two forms of integration dominated pre-capitalist societies and, while not entirely discounting the existence of market exchange in these societies, the latter was not thought to have been a dominant or successful mechanism therein.[30] The differences between these mechanisms lie in who had control of resources, production, and commodity distribution[31].

Reciprocity describes the movement of goods between groups that are symmetrically positioned within society. For Polanyi, who adapted this concept from Malinowski and Thurnwald, "reciprocity needs to be understood as a social whole through a claimed mutual dependency [and

[29] Throughout his entire career, Polanyi was committed to the cause of individual freedom and to understanding its role within the context of industrialized societies. It is from an understanding of this central focus that we must approach Polanyi's work. One of Polanyi's initial aims was to develop methods for analyzing and understanding events such as the Great Depression and the rise of fascism in Europe in the 1930s and 1940s (Goldfrank 1990: 87). An additional goal was to develop a theory of comparative economics that could aptly be utilized to understand all manner of economic systems (Polanyi 1957; Halperin 1988, 1994, Stanfield 1986, 1990).

[30] A fourth form of integration, which is currently characterized by less research, is householding.

[31] The importance of investigating these differences cannot be overstated and misconceptions surrounding the ways in which these key differences structure economic systems can result in a "trap of false equations" (Isaac 2012: 18). George Dalton expressed this issue rather pleasingly: "To call a cat a quadruped and then to say that because cats and dogs are both quadrupeds, I shall call them all cats, does not change the nature of cats. Neither does it confuse dogs; it merely confuses the reader" (Dalton 1966: 733-4).

is fundamental to] the definition of the solidarity-based economy" (Servet 2007). This form of integration presupposes that the society in question is characterized by groups existing in relationships of symmetry with each other.

Redistribution is characterized by patterns of economic behavior involving a center into which goods are collected and out of which goods are distributed. Expectedly, redistribution necessitates the existence of some form of centralized institution.[32] Broadly speaking, exchange involves the existence of at least two engaged parties and a minimum of one object being exchanged.

Exchange as a form of integration can only occur, according to Polanyi, within a system in which price-making markets exist (Polanyi 1957: 254 – 255). Finally, *householding* can be defined as production being undertaken at the level of the household for use within the household and can arguably only occur within a well-established agricultural system (Polanyi 1957: 254; Gudeman 2012; Gudeman 2016).

While the trappings of modern market exchange are marketplaces and media of exchange, scholars are careful to point out that some form of market exchange could have been undertaken in the absence of both media of exchange and of physical marketplaces[33]. At this point, it bears mentioning that a non-market economy is not characterized by the absence of a *marketplace*. Indeed, the presence of market*places* is well attested both archaeologically and textually in many

[32] Scholars differentiate between central redistribution, associated often with middle-range societies and undertaken by their ruling bodies, and command economies, often associated with states (Ericson 2008: 1 – 2; La Lone 1982: 294 – 299) and characterized by centralized institutional control over production and distribution of goods.

[33] Concepts such as market system, market exchange, and marketplace are slippery, carrying with them a plethora of vernacular as well as specialized meanings (Hodges 1988). Indeed, the most elusive of the concepts, the term market itself, has arguably seldom been unproblematically represented (Lie 1991: 342, Garraty and Stark 2010: 5). This is likely the case because these terms are what archaeologists Christopher P. Garrity and Barbara Stark have called "historically contingent "moving targets" that require some amount of arbitrary acceptance of key defining components." (Garraty and Stark 2010: 4). For archaeologists and anthropologists "the challenge is to develop a definition that, on the one hand, is not so broad that it encompasses virtually any exchange situation and, on the other hand, is not so narrow that it equates markets with modern capitalism." (Garraty and Stark 2010: 4).

pre-capitalist societies. Currency was also used in several pre-capitalist economies (including in Aksumite Ethiopia). However, in Polanyi's view what was lacking was the self-adjusting, supply and demand mechanism characterizing the modern capitalist system. Moreover, the use of currency in pre-capitalist economies is considered by the substantivist group to have been relegated to narrowly circumscribed sectors of the economy and was certainly not in use where access to land and labor were concerned.

The type of market exchange that does not necessitate the use of media of exchange is called barter. *Barter* is defined as exchange undertaken, in the absence of media of exchange, with the aim of maximizing utility. By and large there are two types of narrative surrounding the development of barter. Largely agreeable to individualists, the bottom-up approach argues that regular and continuous dyadic instances of barter contributed to the reification of marketplaces and market systems. Conversely, proponents of the top-down approach argue that centralized institutions fostered barter by promoting entrepreneurs and merchants and sponsoring their ventures, thereby leading to the development of market exchange in an accretionary fashion. There are many who have argued that barter or market exchange developed within the geographical and temporal spaces created by ritual behavior, as during ceremonial gatherings and public events (Hassig 1982).

Indeed, substantivists did not outright dismiss the possibility of barter or market exchange; rather, what they argued was that instances of exchange were so irregular and unlikely that their role within the socio-economic context would have been negligible and their mark upon material culture imperceptible (Dalton 1982: 185 – 186). It is within this small space left by substantivists that many contemporary scholars of pre-capitalist markets are operating, with many agreeing with the notion that market exchange was likely not a dominant economic mechanism and was

conceivably attendant upon other social, cultural, or ritual procedures. Despite the auxiliary nature of many instances of market exchange, an attempt is being made to investigate instances thereof.

Each different form of integration has traditionally been more closely associated with one type of socio-political system or another. As such, acephalous societies are more closely associated with reciprocity. Chiefdoms and non-capitalist states are commonly associated with redistribution and reciprocity. Capitalist market economies have some evidence of reciprocity and redistribution alongside the representative evidence of exchange. Indeed, it is very likely that pre-capitalist economies were multicentric (Garraty and Stark 2012), allowing for the coexistence of multiple spheres of many different forms of integration. Finally, it is important to note that the forms of integration do not represent any developmental stages or any temporal sequence.

Once again, the individualists and the systemic methodologists disagree regarding the emergence of these forms of integration. Individualists argue that it is patterns of repeated economic behaviors that individuals engage in that, taken collectively, reify one or another form of integration. In other words, individuals frequently engaging in mutually beneficial economic activities lead to the development of reciprocal integration. Similarly, continuous collection and sharing of goods among individuals, over time, leads to redistributive forms of integration. Finally, unceasing instances of barter are thought by individualists to reify exchange as a form of integration.

Scholars who adopt a systemic methodology contend that cumulative dyadic economic relationships are not sufficient in creating forms of integration. Polanyi, for instance, argues for the existence of "definite institutional arrangements, such as symmetrical organizations, central points and market systems, respectively" as a precondition for the development of the reciprocal, redistributive, and exchange forms of integration (Polanyi 1957: 251). The model they propose

sees reciprocal activities functioning to integrate society *only* in the presence of *symmetrically organized structures*, such as *kinship groups* (Polanyi 1957: 251). Similarly, redistribution only functions to integrate society in a context within which a *communal allocative center* already exists. So too must a system of price-making markets predate the existence of exchange as a form of integration.[34] In other words, institutions must exist as scaffolding for the individual economic acts to successfully integrate society in one particular form or another. These institutions do not arise as a result of these behaviors, but rather there must be some other socio-political phenomenon at work that contributes to bringing about them. Polanyi describes this socio-political phenomenon as a "vital element of organization and validation [arising from] an altogether different type of behavior" (Polanyi 1957a: 251 – 252).

Finally, Polanyi's *third* argument against the existence of premodern market exchange has to do with his contention that premodern societies were technologically unable to communicate effectively and in a timely manner information relevant to market conditions (knowledge related to pricing, and supply and demand, necessary for the making of informed choices).

Substantivism holds up well in the face of a network theory appraisal. There are, however, certain improvements that a network approach can bring to substantivist economic theory. Network theory can contribute to several discussions within this substantivist school of though. In what follows I will discuss a network evaluation of the following topics: (1) tensions between the individualist and systemic methods; (2) the related issues of acquiring trust and maintaining social

[34] Whether a substantivist or a formalist, Polanyi's stance against the existence of market exchange in pre-capitalist societies, is a notion that all scholars of the ancient economy have had to contend with. Polanyi's enduring critique coupled with the equifinality problem (which will be discussed at greater lengths in the section to follow) has made the study of premodern market exchange a toilsome task. Indeed, many scholars who do not a priori dismiss the existence of market exchange in ancient economies, are cautious to attribute a prominent role to this economic mechanism (Garraty and Stark 2010).

order, (3) analytical problems surrounding societies with multiple apparent forms of integration, and (4) the problem of equifinality of patterns.

Individualist versus systemic methods – Firstly, where the tension between the individualist and systemic scale is concerned, network theory is able to operate seamlessly between the two scales and reveals the dialectic that exists between individual actors, whose behaviors are structured by their position within the network they are part of, and the network itself, which in turn is structured by the nature of the relationships between constituent actors.

In adopting a systemic methodology, Polanyi argues for the existence of institutions[35] as preconditions for the development of certain modes of exchange (Polanyi 1957: 251). Institutionalists believe that social order is maintained as a result of efficient institutional development (Schotter 2008). New Institutional Economists (NIE),[36] however, are quick to point out that institutions do not in fact "produce trust but instead are a functional substitute for it". The notion of institutions as precondition reminds one of Durkheim's "pre-contractual solidarity" (Durkheim 1893/ 1984). Both theories express the same idea, namely that exchange cannot occur

[35] A key belief of institutionalists is that "although behavior patterns have been described as resulting from "conscious, deliberate choice making on the part of people holding and using power to establish structure", through repetition the "institutions" become habitual. The original conscious decision-making processes which brought them into being are forgotten, and the "institutions" appear and are thought to be "natural" and "eternal." (Waller 1982: 759 – 760). Most institutional economists see institutions as being resistant to change and as being "essentially static" (Ayres 1952: 49). Each institution has traditional customs which are seldom questioned and whose existence is explained through moralizing stories (Ayres 1978: 156).

[36] New institutional economics (NIE) continues the project begun by classical institutional economists, maintaining the focus on the "institution", the "ceremonial function", or traditional customs. While institutional economics had taken a step away from Neoclassical economics, through the work of English economist Ronald Coase, new institutional economics took a step back towards Neoclassical economics, incorporating many of the methods thereof. "New institutional economics" emerged as a term in a 1975 book by American economist Oliver E. Williamson entitled Markets and Hierarchies, Analysis and Antitrust Implications: A Study in the Economics of Internal Organization. Importantly, NIE scholars dichotomize between *institutions* and *organization*. Whereas, "institutions" are seen as being the rules and customs that regulate behavior and configure interactions, "organizations" are composed of individuals arranged hierarchically and working towards a certain goal and against other competing groups of individuals (Coase 1937).

successfully and continually in the absence of trust between economic partners. They differ, however, in their respective explanations of how that trust is achieved and maintained.

Acquiring trust and maintaining social order – Network theory can also provide a coherent and arguably more compelling solution to the question of achieving and maintaining trust, and this theory is best exemplified in a paper credited with launching the field of New Economic Sociology,[37] Granovetter's 1985 "Economic Action and Social Structure: The Problem of Embeddedness". While Granovetter explicitly focuses on embeddedness in modern market societies, his insights are particularly relevant to pre-capitalist societies. Concerning the creation and maintenance of trust, Granovetter's notion of embeddedness foregrounds the importance of social relationships between economic actors and the networks these relationships engendered (Granovetter 1985: 490). Plainly, Granovetter argues that social actors are inclined to engage in economic interactions with other social actors whose reputation is known to them and that knowledge is gained either through repeated social and economic interaction or is acquired through the intermediary of trusted informants. In other words, people's economic activities are embedded in their networks of social relationships and whether they can trust one another depends on the

[37] Broadly defined, economic sociology is a field characterized by a focus on studying the economic processes in terms of their social causes and effects. Economic sociology is not claimed by economics, being firmly relegated to the field of sociology. However, this sub-field is arguably located at the juncture between the two fields. The term was first used at the end of the nineteenth century by the English economist W. S. Jevons (Jevons 1879) and has since notably been attributed to the works of Durkheim and Weber. Economic sociology arose in response to modernity. Within many humanistic fields, modernity refers both to an epoch of history (the modern period) and to a set of socio-cultural developments associated with that period. The modern era broadly encompasses the Enlightenment of the seventeenth and eighteenth centuries and arguably ends by the middle of the twentieth century. The term as well as the duration of the period is often characterized differently by different fields of thought. Broadly, modernity refers to the socio-cultural impact of modern traits, such as heightened rationalization, industrialization, the rise of market economy, the rise of socialist beliefs, a strong belief in the inevitability of technological progress, individualism, freedom, and equality, etc. (Berman 2010, 15–36; Foucault 1977: 170 – 177). Sociology, specifically reacted to the rise of market economy and to the characteristics attendant thereunto (rationalization, industrialization, individualism, etc.) and crystalized this reaction in the form of a strong critique. The focus was specifically on understanding the social causes of these modern developments and their social effects. The beginnings of the contemporary period of economic sociology, also called New Economic Sociology (NES) can be traced back to the 1985 article published by the American sociologist and economist Mark Granovetter and entitled *Economic Action and Social Structure: The Problem of Embeddedness*.

nature and quality of those social relationships. Thus, in a move reminiscent of Mauss, Granovetter is arguing for the importance of social gains in economic interactions.

One point that is often falsely attributed to Granovetter, and indeed to other economic sociologists, is that people's social relationships will always lead them to trust one another. This idealized notion would be an apt solution to the issue of social order that Polanyi so problematically resolves[38]. However, Granovetter does not make that claim, stating rather that when one trusts other people, one is in fact made *more* vulnerable to bad actors. Thus, it is the nature of those social relationships that will determine whether the trust is misplaced or not. While this may seem like a problem, for researchers of ancient economies intent on discovering a solution to the social order issue, network theorists would argue that, influenced by Malinowski's functionalism, substantivists are too focused on understanding how societies achieve equilibrium to consider the effects of social tensions leading to disequilibrium. In a sense, Polanyi's version of economic interaction is itself an idealized form, one which too often seeks evidence of stability within the system, to consider the prevalence of instability. The various measures available to network theorists, however, allow and encourage the investigation of inequality and differential power dynamics within networks.

The problem of multiple economic forms of integration – Different forms of integration can characterize an economic system, co-occurring across different, contemporaneous economic sectors, thereby making the task of identifying an overriding form difficult and making categorization (based on one form of integration) at times impossible. For Polanyi, the answer regarding which form of integration prevails in a society has to do with the way land and labor are

[38] Recall that Polanyi's solution to the social order problem was to argue against the existence of premodern market exchange, as it would inevitably produce strife and social discontent.

integrated. That is, non-market societies are to be identified as such if land and labor are not commoditized, but are instead accessed through kinship or community ties. However, this approach is presented with a problem when other sectors of the economy are integrated through a different mechanism and often differently integrated sectors cannot be simultaneously studied.

Network analysis does not operate within the constraints of these categories. Empirically based, network studies take bottom-up approaches to each case study and can provide insights into economic interactions without needing to resolve this issue. This approach is particularly useful where cross-cultural comparisons are concerned as it does not encounter the problem of needing to find an overriding mechanism of integration in order to compare economic systems.

Problem of Equifinality of Patterns – When attempting to identify forms of integration within the archaeological record, the problem of *equifinality* of patterns inevitably arises. Equifinality is the concept that an end state can be achieved through a number of different paths; for this reason, a tremendous amount of data must be marshalled to allow for the investigation of different forms of integration (Hirth 1998). For instance, scholars who accept the possibility of market exchange in pre-capitalist economies signal difficulties inherent in identifying whether the observed patterns indicate market exchange or centralized redistribution (Garraty and Stark 2010; Earle 1977: 215; Blanton and Fargher 2012). Traditional approaches to the study of economic mechanisms and their associated political structures, like central-place theory (Christaller 1933/ 1966) and regional falloff analyses (Renfrew 1975, 1977), have had difficulties in dealing with the equifinality problem. Christaller's method is particularly inefficient at differentiating centers that develop within a market society and centers of redistribution often characterizing middle-range societies. Spatial falloff or distance-decay patterns are equally inadequate at differentiating patterns created

through market exchange versus centralized redistribution (Garraty and Stark 2010). This is because both mechanisms are often characterized by some level of centralization (Hirth 1998).

The equifinality of patterns problem is further compounded by the aforementioned problem of multiple contemporaneous economic mechanisms integrating different sectors of the economy. For instance, some level of market-type exchange can exist where certain commodities are concerned, while other commodities could circulate through reciprocity (among social or kinship group), other types of commodities could be produced as a result of household production, etc. (Earle 1977, Halperin 1991, Polanyi 1944: 53, 1957: 250 – 256). Undoubtedly the economic interactions in such an environment would be difficult to disentangle through traditional approaches.

Network methods once again provide a solution to the problem of the equifinality of patterns. As an eminently bottom-up approach, capable of integrating multiple spatial scales, network analysis marshals its own specific catalog of terms to describe emergent patterns. These patterns materialize as a result of formal graph theoretical analyses and, as such, are more easily quantified and compared.

3.9. Synthesis

In this chapter I combine network theories with traditional anthropological, archaeological, economic, and sociological theories of the ancient economy and attempt to evaluate the latter through the prism of the former. While challenging elements of the two schools of thought, the model I propose for understanding ancient economies draws from Structuralist and Substantivist theories as well as from New Economic Sociology. My social network appraisal of economic theories is also indebted to Collins' (1988) sociological reformulation of economics.

Social networks have recently been accepted as counterparts to theories of market exchange (Collins 1988, Bandyopadhyay et al. 2011) and I propose utilizing social networks as alternatives to Substantivist economic theories as well. Social network theory provides an elegant solution to the trust and social order problem. Counter to market theories, social network theories conceptualize exchange not in terms of utility maximization but rather in terms of interactions occurring between economic partners that are embedded within a network of ongoing personal relationships in which individuals have an economic as well as a social reason to maintain trustworthiness.

The approach I am adapting sees actions as being socially embedded in "ongoing systems of social relations" (Granovetter 1985: 487). It is my contention that social networks engendered by recurring social relations and interactions preserve trust, avert malfeasance, and maintain social order in economic dealings. This notion, while emerging as a result of micro-economic studies of contemporary "imperfectly competitive markets" (Granovetter 1985: 488) is exceedingly applicable to studies of ancient economies for which the preference for doing business with individuals with a reputation for fairness has emerged in more recent empirical studies on the nature of human cooperation (Nowak et al. 2000; Stanish 2017: 48ff). This inclination of transacting with individuals with a good reputation has been proposed as a convincing reason for avoiding malfeasance and maintaining social order.

At this juncture it is important to mention that the social network response to the problem of social order does not negate the existence of malfeasance and disorder; doing so would plunge us into another type of idealized economic scenario.

Chapter 4

Research Methods and Data Recording Strategies

4.1. Introduction

To investigate the development of socio-economic networks of exploitation, production, and trade of obsidian in Ethiopia and copper in Oman, this research was conducted using a multi-stage and multi-proxy approach. Data collection combined field research with laboratory analyses and relied on published and unpublished survey data. The databases that were created represent not only my own research, but also the contribution of many archaeologists and the collaboration of multiple projects that have been active for many years.

The databases created for formal network analysis contain sites with evidence of shared slag typologies in Oman and shared obsidian groups, in Ethiopia, and were amassed through archaeological and geological surveys. Affiliation data was generated through geochemical characterization of slag and obsidian using portable X-ray Fluorescence instruments.

While these databases were created for the network analysis component of this dissertation, the related goal of gaining a high-resolution understanding of the distribution of copper sources in Oman and obsidian sources in Ethiopia was undertaken through analysis of Hyperion hyperspectral satellite imagery and led to the production of prospective maps of obsidian and copper distribution. Relational data was integrated with spatial data to produce maps that aim to model Ethiopian and Omani geographies of raw material exploitation, production, and trade.

This chapter outlines the methods used in the collection and analysis of these datasets. In the first part of the chapter (section 4.2), I will briefly present the methodological parameters associated with the broadest theories that frame this dissertation: the comparative approach and the network analysis approach. The second part of the chapter (sections 4.3 – 4.5) describes data recording and analysis strategies and includes sections on satellite imagery analysis for creating preliminary exploratory geological resource maps, archaeological and geological field methods, and methods relating to geochemical analysis using pXRF.

4.2. Modelling Network Connectivity Through Space and Time

This project employs a cross-cultural, multiscalar, and diachronic approach to modelling the dynamics of socio-economic networks at three regional scales and across two cultural spheres. The social relations defined by means of Social Network Analysis (SNA) measures will be linked back to physical space through the use of Geographic Information System (GIS).

4.2.1. Social Network Analysis Methods

A network analysis approach is being employed in an attempt to engage with one of the main goals of this dissertation: to reveal the structure of social networks and the impact of network positions on the behavior and development of social actors.

In addition to contributing a theoretical foundation, network analysis provides a suite of techniques for analyzing and visualizing patterns of interaction in social networks. This dissertation employs two types of network measures: node centrality (and accompanying graph centralization measures) and measures of connectedness and cohesion. Interpretation of results

along with a lengthier methodological explanation is included in Chapter 7.[39] Analyses were undertaken using the UCINET software package and graph visualizations were generated using NetDraw.

Network analyses take a bottom-up approach to studying social interactions and, because they are based in deductive methodologies, are particularly well suited for cross-cultural comparisons where the desired outcome is a move away from general societal types and economic mechanisms of integration.

4.2.2. Comparative Approach

The broadest framing device for this study is the cross-cultural comparison. Integrated with network measures, the cross-cultural comparative approach aims to address the second goal of this dissertation: that of attempting to reveal aspects of network typology, or the emergent properties of networks in themselves. In complex network terms, comparison is the method by which network topology can be studied. In addition to the cross-cultural comparative approach, this study utilizes overlapping spatio-temporal levels to address network dynamics at varying scales.

4.2.3. Multiscalar Approach

Spatially, this study investigates socio-economic networks of production and change at three increasingly large scales: microscale, mesoscale, and macroscale. The microscale of individual archaeological sites and the mesoscale of the systematic survey areas were the subjects of formal

[39] I elected to go into greater detail regarding network methods in Chapter 7, rather than in this current chapter, because a lengthy discussion which contextualizes the chosen measures and their inherent assumptions is necessarily informed by particulars of the networks under investigation and, as such, is a better fit for a chapter in which those particulars are revealed and theorized.

network investigations. Conversely, the macroscale is represented by the wider cultural spheres into which the two networks were embedded and is being used to provide context for the structural developments revealed by the two networks. Micro and mesoscalar data were compiled through archaeological surveys undertaken in northern Tigray (SRSAH survey, see section 4.4.1) and northern Oman (ArWHO Survey, see section 4.4.2), while the level of the macroscale is being theorized through literature review.

These three scales allow one to investigate relational patterns as these emerge and develop contrastingly between different sets of nodes (individual sites, network subgroups, larger networks). The multiscalar approach illuminates the plasticity of the concept of a network; different scales produce different relational patterns, allowing for a more robust understanding of a network's organization and of its structuring principles (Mills et al. 2015).

4.2.4. Diachronic Approach

For each area of interest, formal analyses were employed to reveal diachronic fluctuations in the positions of nodes within each time period's network as well as elements of change and continuity in the structure of networks as these developed throughout the millennia.

Formal network analyses were used in conjunction with these longitudinal datasets with the aim of understanding the manner in which networks developed through time and the impact those changes had on the structural positions of multi-period nodes (see Ryan and D'Angelo 2017, Suitor et al. 1997).

Several limitations hinder confidence in interpretations based on data from multi-period sites in archaeology. One common problem that characterizes the current study as well, is the issue of

contemporaneity. This is because a significant portion of the obsidian and slag assemblages that form the basis of the networks were comprised through surface collection from multi-period sites, for which uncertainties surrounding issues of contemporaneity cannot at present be resolved. As such, the results and interpretations presented in this dissertation are tentative. This research is intended to be a starting point for the use of this particular methodology, the results of which will need to be refined in the future.

For this reason, longitudinal network studies should be undertaken with a great deal of caution. Indeed, rather than reconstructing direct dyadic relationships, these studies are likely revealing trends over time. These trends are established as a result of the sustained and recurring patterns of interactions between pairs of sites across long intervals of time (Peeples 2019: 34).

Where this study is concerned, tracing the development of these socio-economic networks of production and trade through time may conceivably reveal which aspects of the networks remained consistent throughout time and which aspects were altered over time, thereby allowing one to theorize about the impacts of local environments or culture historical conditions on their development (Wilson 2008).

4.2.5. Geographic Information System (GIS)

Used in conjunction with GIS, an SNA approach provided a way of linking traditional ideas about communities defined by spatial analyses with communities defined by shared participation in different kinds of social networks (Mills et al. 2015, Yaeger and Canuto 2000), thereby framing the leap from spatial relations to social relations (Knappett 2011).

The spatial component of these scales of inquiry (microscale, mesoscale, and macroscale) was visualized using ArcGIS Pro, which was used to generate layouts that integrated spatio-relational evidence of production with maps that indicate the prospective locations of copper and obsidian resources.

4.3. Hyperspectral image processing of EO-1 Hyperion data for rock and mineral prospectivity analysis

These maps indicating prospective locations of copper and obsidian resources were produced through satellite imagery analysis. Hyperion hyperspectral satellite images of Oman and Ethiopia were analyzed to detect and map copper and obsidian sources, respectively. Traditional mapping of copper and obsidian, which alternatively identifies sources as either points on a map or with the large geological formations (e.g. mountain ranges) that they are part of, does not account for the complexities of the copper mineralization process or of the obsidian formation processes that result in spatially heterogeneous landscapes, often characterized by granular and sporadic distribution of comingled raw materials. Satellite imagery mapping allows the remote surveillance of large geographical areas in a fairly inexpensive and expeditious way, and facilitates the mapping of relatively inaccessible landscapes, whether that inaccessibility is due to safety concerns or geographical remoteness. Finally, hyperspectral satellite imagery has potential to produce detailed and precise maps which are representative of the patchy distribution of many raw materials. Certainly, establishing accuracy, where this method is concerned, still depends upon ground-truthing. However, as the methodology improves and is better understood over time, confidence may be achieved with minimal highly-targeted ground-truthing. Remote prospection depends upon the analysis of a dataset supplied by a hyperspectral satellite by means of a software package that specializes in analyzing satellite imagery (ERDAS Imagine, ENVI). This method does not attempt

to link archaeological objects to sources, but rather to map the distribution of raw materials across landscapes and to facilitate the modelling of possible interactions between humans and their raw material environments.

4.3.1. Spectroscopy

The science behind hyperspectral imagery analysis is spectroscopy. Spectroscopy is used to study the constituents of matter and relies on patterns of reflectance and absorption, across specific wavelengths, as proxies for determining geochemical composition and physical properties (Borengasser et al. 2007, Clark 1999). Reflectance spectroscopy can be used to derive mineralogical information about an area without much prior geochemical knowledge of the analysis area. In this study, reflectance spectroscopy was used to detect the presence of copper minerals and obsidian sources in Hyperion satellite imagery of the two study areas.

Photons that are reflected from grain surfaces, refracted through particles, or emitted from grain surfaces are scattered into the atmosphere, where they can be detected by reflectance spectrometers mounted on satellites orbiting in space (Clark 1999). Photons that are not scattered are absorbed by matter. The wavelength-dependency of absorption lies at the core of imaging spectroscopy, allowing analysts to ascertain the geochemical composition of matter by measuring scattered photons and identifying which parts of the electromagnetic spectrum are being absorbed.

Image spectroscopy functions according to the following principle: minerals (or other materials) are detected by identifying spectral characteristics which are determined by chemical bonds that are particular to the material in question (Goetz and Srivastava 1985). Once detected, these spectral characteristics are matched to different minerals or rocks through the application of a number of classification methods.

These so-called spectral characteristics that are used to identify specific mineral constituents are absorption features that occur in the visible (VIS), near-infrared (NIR), short-wave infrared (SWIR), and thermal infrared (TIR) regions of the electromagnetic (EM) spectrum and are often referred to as spectral signatures (Kruse 1988, Crowley et al. 1989, Kruse et al. 1993b, Swayze 1997, Crósta et al. 1998, Dalton et al. 2004).

Spectral absorption features can be used to identify mineral composition because features are regulated by electromagnetic transitions and vibrational processes that result from the interaction of EM energy with the atomic level of a material. Taken in isolation, atoms and ions have determined energy states. When an atom absorbs a photon, however, the energy state within its structure changes, setting in motion an electronic transition.

There are four types of electronic transitions: crystal field effects, charge transfer absorption, conductive bands, and color centers. Crystal field effects create diagnostic spectral features for minerals containing transition elements with unfilled electron shells. Charge transfer absorption takes place when the absorption of a photon impels an electron to move between ions or between ions and ligands. Conductive bands are related to electrons with two energy levels and result in absorption features in the VIS and NIR. Finally, color centers result from the irradiation of imperfect crystals (Clark 1999).

For the VIS and NIR portions of the EM spectrum, these absorption features are generally determined by crystal field effects in transition elements. Whereas for the SWIR, the diagnostic absorption features are determined by the presence of water (H_2O), hydroxyl (OH), carbonates, and sulfates. The nature of these interactions is uniquely determined by the chemical composition of matter.

The wavelength range that is represented by the Hyperion hypercube is contained between 0.4 and 2.5 μm. This range is divided into the VIS (0.4 – 0.7 μm), the NIR (0.7 – 1.1 μm), and the SWIR (1.1 – 2.5 μm).

Material mapping was undertaken by means of commercial remote sensing packages, such as ERDAS Imagine 2016 and 2018 and ENVI 5.3. These software packages contain spectral libraries collected by the United States Geological Survey (USGS) and by NASA's Jet Propulsion Laboratory (JPL). These packages are equipped with a number of classification methods for extracting spectral information from remotely sensed data and matching it with spectral signatures selected by the analyst. Often these spectral signatures are derived from perfect specimens, measured in ideal laboratory conditions. Remotely sensed surfaces, however, often produce spectral features that are dissimilar from their laboratory counterparts owing to atmospheric conditions.

A further confounding factor is engendered by a particular characteristic of remotely sensed data, namely the fact that its spatial resolution decreases proportionately with its increase in spectral resolution. Where hyperspectral imagery is concerned, each 30-meter pixel exemplifies a portion of the surface of the Earth that likely contains a multitude of elements with different spectral properties. These large pixels represent comingled surfaces, characterized by a number of different elements that each absorb and reflect electromagnetic radiation in distinct and dissimilar ways. To differentiate between these different elements, algorithms have been developed to extract spectral information at a sub-pixel level (Giles et al. 2009, Mertens et al. 2006, Thornton et al. 2006, Verhoeye & De Wolf 2002).

4.3.2. Earth Observing (EO-1) Hyperion Sensor

There are four technical specifications that determine the capabilities of spectrometers: spectral range, spectral bandwidth, spectral sampling, and signal-to-noise ratio (S/N).

The spectral range of a spectrometer represents the portion of the electromagnetic spectrum that can be measured by the instrument. Determining the spectrometer that is most appropriate for one's spectral analyses relies on knowledge of the absorption features of study materials. The electromagnetic spectrum is divided into five sections: ultraviolet (UV) between 0.0001 and 0.4 μm, visible light between 0.4 and 0.5 μm, near-infrared (NIR) between 0.7 and 3.0 μm, mid-infrared (MIR) between 3.0 and 30 μm, far-infrared (FIR) between 30 μm and 1 mm. Within the field of remote sensing, the portion of the electromagnetic spectrum between 0.4 and 1.00 μm is called the visible-near-infrared (VNIR) and the portion between 1.0 and 2.5 μm is termed the short-wave-infrared (SWIR) portion. The hyperspectral Hyperion sensor used in this study measures the spectral range between 0.4 μm and 2.5 μm, corresponding to the portion between violet in the visible light spectral field and shortwave infrared.

The spectral bandwidth of a spectrometer is defined as the width of one spectral channel in the spectrometer. Narrow absorption features, that are often signatures characteristic of specific materials, are more accurately detected and measured by narrow spectral bandwidths. *Spectrometers* appropriately termed are those instruments that contain channels measuring contiguous ranges of the electromagnetic spectrum. Hyperion, the instrument upon which this study relies, is a hyperspectral spectrometer containing 220 contiguous spectral channels that are divided into intervals of 0.011 μm. This technical specification allows Hyperion to resolve narrow absorption features that are particularly important for the type of rock and mineral characterization that remote sensing relies on.

The spectral sampling capabilities of a spectrometer consist in the distances in wavelength ranges between the spectral bandpass profiles for each spectral channel. A channel within a spectrometer measures only the light within a pre-established wavelength range, being designed to ignore light from outside this pre-established spectral range or bandpass. Despite this, light from outside of the desired wavelength range can unintentionally be measured as a result of scattering or because of faulty blocking filters (Clark 1999). A Gaussian distribution commonly characterizes a bandpass profile. The resolution of a spectrometer is in equal parts determined by its spectral sampling and its bandpass width.

Finally, the signal-to-noise ratio (S/N) capability of a spectrometer is characterized by three aspects: the sensitivity of the instrument, its spectral bandwidth (Swayze *et al.* 1997), and the spectral traits (i.e. the intensity of scattered photons) of the features that are being measured. For Hyperion, the S/N is 190 to 40 as the wavelengths increase (cf. Beck 2003).

The dataset we are currently using is generated by the Hyperion hyperspectral instrument, on-board NASA's Earth-Observing 1 (EO-1) satellite that was launched in the year 2000. The Hyperion instrument provides spectral data via a push broom sensor, perpendicular to the flight direction of the EO-1 satellite. NASA's Hyperion hyperspectral satellite imagery has already successfully been used by scholars to detect and map copper (Savage et al. 2012). The spatial resolution of Hyperion images is of 30 square meters. Additionally, the instrument can image a 750 km^2 area. This high spectral resolution allows for the characterization of the surface of the Earth in terms of its various geological components according to their known spectral responses or signatures. As a result of this sophisticated spectral information, hyperspectral satellite imagery is a useful data source for remotely detecting surface deposits of copper ore and obsidian outcrops.

4.4. Field Methods

In this section, I will discuss the field methodologies employed in the collection of the datasets investigated in this dissertation. The datasets I am analyzing were collected as part of the Southern Red Sea Archaeological Histories (SRSAH) project and the Archaeological Water Histories of Oman (ArWHO) project. I have worked on both the SRSAH and ArWHO projects, led by M. Harrower. These two projects adapt satellite remote sensing and geospatial technologies to examine the role of water availability and irrigation, and more generally water histories, in the origins and long-term trajectories of ancient complex societies in Oman and Ethiopia.

4.4.1. The Southern Red Sea Archaeological Histories (SRSAH) Project

The obsidian dataset analyzed for this dissertation was assembled as a result of the work undertaken by the SRSAH survey and excavation teams. Since 2009, the SRSAH project has been investigating the development of Pre- to Late-Aksumite societies in the area surrounding Yeha and employing survey methods that combine both systematic and opportunistic reconnaissance sampling (Harrower & D'Andrea 2014).[40] The goal of the first season was to re-locate sites identified by the previous surveys of Francis Anfray and Joseph Michels as well as to record anew some of the largest and most easily recognizable archaeological sites in the area. Following this first season, a 100 km^2 survey area was selected for systematic survey and subsequently divided into 1x1 km sectors. Beginning in 2012, a stratified random sampling approach was employed

[40] The methodology employed by the SRSAH survey was initially devised for the neighboring Eastern Tigrai Archaeological Project (ETAP) led by Catherine D'Andrea (for which Harrower served as Director of Archaeological Survey from 2005-2008). Methodological consistency with the ETAP project ensures comparability of results and is helping to generate wider understanding of Pre- to Late-Aksumite societies in the region.

towards the survey of this area. Using Microsoft Excel, 50 survey sectors were randomly selected by generating 50 random numbers from 1 to 100.

A "coin toss" was then simulated to determine the orientation (North-South or East-West) of each 0.1 km^2 (1000 x 100 meter) survey transect by generating random integers between 0 and 1 (0 assigns a North-South transect while 1 assigns an East-West transect). The last 3 digits of the UTM coordinates for every survey transect were also randomly selected. The southwest corner of every survey transect was designated as the "point of origin" because the coordinates of the three other corners (northwest, southeast, northeast) could be calculated relative to the coordinates of the southwest corner. To randomly select the last 3 digits of UTM coordinates for the southwest northing and easting, numbers between 0 and 900 were also randomly generated in Microsoft Excel. Using this stratified random sampling approach, 5% of this area was surveyed.

To discover and document sites within each 1000 x 100 meter transect, six field crew members standing 17 meters apart walked lengthwise through each transect, dividing the landscape into survey units determined by landform class. Two crew members standing at the ends of each transect carried handheld Garmin Etrex GPS units to ensure that they and the rest of the team, remained within the transect boundaries. Using a Trimble GeoXH GPS unit, one crew member recorded sites and landform boundaries. Whenever a landform change was encountered, crewmembers stopped surveying. Artifacts collected within the boundaries of one landform class were consolidated within transect bags (divided by landform class and artifact type). Landscape photographs were taken, and the crewmember equipped with the GeoXH GPS mapped the boundary of the recently surveyed landform. Survey units were thus designated with a letter, proceeding alphabetically from the letter "a" in each sector.

Survey units were differentiated by landform categories defined as follows:

(1) Sediment Plateau – Areas that are predominantly covered by soil and sometimes low terraces and characterized by a slope with an angle that is <5º.

(2) Sediment Slope – Areas from 5 to 25º slope commonly used for farming and grazing that are often terraced.

(3) Bedrock Slope – Areas of exposed bedrock from 10 to 90º slope that are at times partially covered by sediment, scree and/or talus.

(4) Scree Slope – Areas of abundant angular clasts often of a low (<20º) gradient lying below prominent highland areas.

(5) Valley Bottom – Low lying drainage networks often carrying water in the rainy season and characterized by copious grass and other foliage.

Sites discovered systematically within survey transects and those discovered opportunistically outside survey transects were divided into 3 main types:

(1) Find Spots: Isolated, small sites that when intensively examined yielded at least 15-20 pottery sherds in 2-3 minutes. A Trimble GPS point was taken in the center of each site.

(2) Artifact Scatters: Sites exhibiting higher and more extensive artifact densities that are generally no more than 2 hectares in size. The Trimble GPS was used to take a point at the center and map the areal extent of each site.

(3) Settlement Sites: Sites that are generally larger than 2 hectares and usually contain highly visible features including remnants of architecture such as a debris field indicative of collapsed buildings, hearths, standing stones, pillar bases or other monuments. The Trimble GPS was used to take a point at the center and map the areal extent of each site. Artifacts including predominantly lithic stone tools and ceramics were collected, bagged, and tagged according to survey unit number and site number. A sample of each ceramic ware as well

as diagnostic sherds and lithics were collected. In addition to names solicited through inquiries with local people, sites were referred to according to their three-digit sector number followed by a three-digit site number that begins anew for each sector (e.g. Beta Samati 006- 001).

While the obsidian dataset utilized in this study is largely comprised of archaeological obsidian collected through survey, the geochemical analysis also relies on 46 pieces of obsidian uncovered during excavations at the site of Beta Samati, located to the northeast of the eight century BCE megalithic ruins of Yeha. Excavations began at the 20-hectare site in 2011 and, over the course of four excavation seasons (2011, 2012, 2015, and 2016) revealed a multi-period site with residential and monumental architecture spanning the time period from the 6th century BCE to the 6th century CE. Thirty-six of the forty-six analyzed obsidian pieces from Beta Samati were discovered in association with a basilica context, while the rest were associated with domestic architecture.

4.4.1.1. SRSAH Ceramic Analysis

Ceramic analyses informed identification of the time periods represented at the sites under investigation in this study and were undertaken by Cinzia Perlingieri (CoDA), Gabriella Giovannone (Università degli Studi di Napoli "L'Orientale"), Rachel Moy (University of California Los Angeles), Habtamu Mekonnen Taddesse (Simon Fraser University), and Jennifer Swerida (Johns Hopkins University).

Ceramics collected during the SRSAH 2011 field season, especially those uncovered in excavations at the site of Beta Samati, formed the basis for a developing understanding of the Pre-Aksumite, Aksumite, and ethnographic pottery tradition in the study region. The employed classification system divides all sherds (diagnostic and non-diagnostic) into one of four broad

wares on the basis of sherd fabric, temper, and color. The content of each ware was subdivided according to sherd quality (coarse, common, medium-fine, and fine) as determined by grain size, firing quality, surface treatment, etc. Diagnostic sherds were further classified into distinctive forms based on vessel shape. Rather than attempting to apply ceramic typologies developed for other regions, the broad classification system employed during the SRSAH 2011 season relied wholly on internal data. The resultant ceramic sequence and typology was therefore independent and regionally specific. In later seasons, the SRSAH ceramic typology increased in refinement, with the contribution of Cinzia Perlingieri's ceramic typology, which was developed over decades of archaeological research in northern Ethiopia.

4.4.2. The Archaeological Water Histories of Oman (ArWHO) Project

The copper dataset, analyzed for this dissertation, was amassed through 4 years of systematic random survey, ground-truthing of copper prospectivity maps, and judgmental geological and archaeological survey targeted at investigating evidence of copper exploitation and production in the ArWHO systematic survey area. An additional component of the ground-truthing program was the survey of a randomly selected area (covered by analyzed satellite imagery) to determine the prevalence of false positives.

The ArWHO project examines the role of water in ancient Oman in relation to the development of settlements, copper mining, trade, and territoriality. Archaeologists have long identified irrigation as one of several primary factors involved in the origins of the world's earliest civilizations. The Archaeological Water Histories of Oman (ArWHO) project utilizes archaeological survey, satellite imagery and geospatial analysis to examine the role of water availability and irrigation in the origins and long-term histories of ancient societies.

The ArWHO survey strategy has involved both systematic stratified random sampling and wider judgmental reconnaissance aimed at elucidating site distribution patterns with respect to environments, water resources, and chronologies. These efforts are not only leading to the discovery of important new sites, but just as crucially are helping determine which areas were specifically targeted by ancient populations for different purposes such as hunting, camping, herding, farming, copper mining and settlement, and which areas were less frequently utilized.

A stratified random strategy was devised to sample 5% of a 100 km^2 area to match SRSAH Project research in Ethiopia. Similar methodologies thus allow comparability and facilitate analysis of site distributions across these two environmentally, culturally and historically different regions.

The 100 km^2 systematic survey area was divided into 1x1 km sectors. The ArWHO survey was conducted essentially according to the same procedures as described in section 4.4.1 (above). Some minor modifications were made to account for different landform characteristics and types of archaeological sites. To maximize discovery of ancient settlement, tower, and mining sites, opportunistic reconnaissance was also conducted. In addition to surveyor judgment and the reports of local inhabitants, our efforts drew on Google Earth imagery, ASTER satellite imagery, ASTER-based water flow accumulation models, and Hyperion satellite imagery-based detection of areas with copper bearing minerals. A combined vehicular and pedestrian approach was utilized in which areas with tombs, architecture, and/or dense vegetation were specifically targeted.

Survey units were differentiated by landform categories as follows:

(1) Bedrock Slope – Greater than 15^o slope or cliff (sometimes partially covered in talus or scree) that often separates upland plateaus from other landform classes.

(2) Scree Slope – Angular clasts often on a low (<200º) gradient between bedrock slopes, terraces, and wadi sediments.

(3) Plateau – Upland bedrock surfaces above bedrock slopes and cliffs, primarily covered in small cobble size clasts.

(4) Gravel Terrace – Sub-rounded to rounded clasts often capping wadi silts located near wadi channels.

(5) Bedrock Terrace – Low angle (<50º) or horizontal bedrock surface adjacent to wadi sediments and/or scree slopes primarily covered in small cobble size clasts.

(6) Wadi Silts – Pinkish tan colored areas of very fine sand and silt above wadi channels, which often contain isolated lenses and scattered cover of gravel and/or scree.

(7) Wadi Channel – The lowest and most fluvially active area often demarcated by whitish grey rounded cobbles, boulders and more prevalent vegetation.

The following system was used to define different types of sites discovered during archaeological survey:

(1) Find Spots: Isolated small sites that when intensively examined yielded at least 15-20 artifacts (most commonly pottery sherds or lithics) within roughly 5 minutes. A Trimble GPS point that includes a six-digit site number as well as information on landform, photographs, estimated age, and bags of artifacts collected was taken at the center of each site.

(2) Artifact Scatters: Sites exhibiting higher artifact densities and a definable areal extent that is generally no more than 2 hectares. A Trimble GPS point that includes a six-digit site number as well as information on landform, photographs, estimated age, and bags

of artifacts collected was taken at the center of each site. The areal extent of the site was also mapped as a GPS polygon.

(3) Settlements: Sites (generally larger than 1 hectare) that exhibit high artifact densities, walls, hearths, metallurgical slag or other evidence of longer term or periodic occupation are designated settlements. A Trimble GPS point that includes a six-digit site number as well as information on landform, photographs, estimated age, and bags of artifacts collected was taken at the center of each site. The areal extent of the site was also mapped as a GPS polygon.

(4) Other Sites: Towers, Tombs, Structures, Water Management Features and Rockshelters: In addition to the aforementioned site types, these additional remains were designated as individual sites (sometimes within the areal extent of a larger settlement). A Trimble GPS point that includes a six-digit site number as well as information on landform, photographs, estimated age, and bags of artifacts collected was taken at the center of each site. If applicable, the linear or areal extent of the site was also mapped as a GPS line or polygon.

Artifacts including predominantly lithic stone tools and ceramics were collected, bagged and tagged according to survey unit number and site number. A sample of each ceramic ware as well as diagnostic sherds and lithics were collected. In addition to names solicited through inquiries with local people, sites are referred to according to their three-digit sector number followed by a three-digit site number that begins anew for each sector (e.g. Khadil 959-001).

The ArWHO Copper Survey – conducted as an offshoot of the ArWHO project, the copper survey included a targeted survey that combined information generated through traditional geologic research and through remote sensing. Beginning in 2012, the copper survey represented

an endeavor to collect dissertation data relating to the distribution of copper sources and archaeological sites with evidence of copper production. Assembling this information was achieved through ground-truthing of satellite imagery-derived copper prospectivity maps, archaeological survey, and geological reconnaissance.

Following the production of copper prospectivity maps (see section 4.3), the ArWHO Copper Survey team engaged in three seasons of ground-truthing (2013, 2015, and 2016). Ground-truthing entailed selecting from copper prospectivity maps areas that represent positive detections, navigating to the detected pixels, and examining the surrounding geology for readily distinguishable copper minerals, identified by their color, physical properties, and crystal habit. Sites identified through detection were in the Samail Nappe ophiolite sequence, in particular in the sheeted dyke, cumulate layered gabbro, and high-level gabbro complexes.

During the 2013 and 2015 seasons, areas were selected for ground-truthing based on accessibility, proximity to known smelting sites, and number of pixels detected. Conversely, the strategy employed during the 2016 field season also took into account information from geological maps (Béchennec 1992) and landforms that can host copper minerals were prioritized. The goal of this new tactic was to identify and map mineral-rich micro-regions within the larger potentially copper-bearing geologies, thereby streamlining prospection.

To determine the prevalence of false negatives, the ArWHO team also conducted a survey of a randomly selected area covered by a Hyperion scene that had been analyzed for the presence of copper-bearing minerals. Twenty transects, each measuring 500 by 500 meters, were surveyed by a two-person team.

Supplementing the ground-truthing expedition and the archaeological survey is the last component of the ArWHO copper survey: a judgmental geological survey that relied upon geological information acquired from traditional geological maps to re-locate previously identified copper sources (Béchennec 1992). Geological samples collected from these sources were subsequently geochemically analyzed with a portable X-Ray Fluorescence instrument in the field laboratory (see section 4.6.1).

4.4.2.1. ArWHO Ceramic Analysis

Ceramic analyses informed identification of the time periods represented at the sites under investigation in this study and were undertaken by Jennifer Swerida and Eli Dollarhide (New York University).

In the course of both systematic and opportunistic survey, all diagnostic ceramic sherds and at least one example of each fabric occurring at a site were collected. The subsequent ceramic interpretation was based on macrostylistic analysis of vessel form, ware, and surface decoration. All collected pottery was sorted according to general ware and form types, which were then, when possible, internally sorted into subclasses identifiable with specific archaeological periods. These criteria are used to estimate the period of origin and contribute to further interpretation of the sites in question.

4.5. Geochemical characterization of copper ore, slag, and obsidian using X-Ray Fluorescence

This study uses X-Ray Fluorescence as a non-destructive analytical technique to identify elemental compositions of samples. X-Ray beams with enough energy to interact with the electron

in the inner shells of an atom are used to displace these electrons from their orbits. Attendant upon this displacement is an element-specific burst of energy that is registered by a detector located inside the XRF instrument, and used to geochemically characterize the sample being analyzed (Shugar and Mass 2012).

Atoms are made up of a nucleus and one or more electrons that are bound to the nucleus, forming distinct orbital patterns. Electrons orbiting around the nucleus form shells (labeled, from the interior to the exterior: K, L, M, N, O, P, Q). The farther the shell from the nucleus, the higher the average energy of the electrons within it. The space that exists between shells is element-specific and can thus be used as a signature in the characterization process. Electrons orbiting the nucleus will generally occupy an outer shell if all other inner shell orbital positions have already been occupied by other electrons. Furthermore, each shell contains a fixed number of orbital positions. As such, electrons displaced from their atomic orbits by high energy X-Ray beams will leave unoccupied positions that temporarily destabilize an atom. This imbalance is urgently rectified with the voids being occupied by electrons from higher orbits that fall into the gaps left by displaced electrons from lower shells. Because the farther an electron is from the nucleus, the higher its binding energy, when it falls from a higher orbit to a lower one, the electron loses some energy. A falling electron loses energy corresponding to the difference in energy between the two shells, which is dictated by the element-specific distance between the shells. The amount of lost energy is recorded by the pXRF and used to determine the elemental composition of the sample.

Geochemical data was collected in both study areas using handheld or portable X-Ray Fluorescence instruments (pXRF). In Oman, a Thermo Niton XL3t GOLDD+ XRF analyzer was used to collect spectra from copper ore and from slag samples. The Thermo Niton measures relative elemental composition qualitatively – data which can be used to look for the presence or

absence of specific elemental features. When paired with instrument-specific calibration information and an understanding of the expected chemistry of a sample, spectra can be used to calculate empirical values of elemental concentrations (see below for details).

In Ethiopia, a Brucker Tracer III-V XRF analyzer was used to collect spectra from archaeological obsidian samples. The Brucker allows for both qualitative and so-called semi-quantitative processing. Qualitative processing consists of identifying which elements are present within a sample, while semi-quantitative processing allows one to calculate the relative quantities of each identified element, allowing one to compare rations of elements present in different samples.

According to Shugar, "successful XRF analysis is 10% collection and 90% inspection" (Shugar 2009: 8) and, as such, proper precautions must be taken to ensure that spectra collection is undertaken with the utmost care towards minimizing and understanding the deleterious effects of certain factors that can affect analysis.

To collect spectra properly, the right voltage, current, and filter must be selected to match the specifications appropriate for the part of the spectrum that the sample is thought to correspond to. A protocol for materials characterization must be developed and collection conditions must be standardized in accordance with industry specifications and the orthodoxy of the field, to allow comparison between similar groups of samples. Different types of samples necessitate different preparation procedures. In the case of the copper ore and slag analyses, samples were cleaved with a rock hammer and a freshly created edge was analyzed. This is done in an attempt to circumvent gathering weathering-related spectra. Where obsidian was concerned, the samples were cleaned thoroughly with water and left to dry before analysis was undertaken along the thickest edge of the sample. Thickness of sample is important because, while the majority of the return derives

from the surface and adjacent to surface areas, the X-Ray beam can nonetheless penetrate the sample and even pass through it.

Finally, an accurate interpretation of analysis results cannot exist in the absence of a modicum of knowledge of X-Ray physics, instrument-specific parameters, and comprehension of the expected chemistry of the sample.

As previously stated, photons and their recorded energies are used as signatures to identify the geochemical composition of materials during the fluorescence process. Copper (Cu), for instance, is characterized by three fluorescence emissions in the K shell (Kα1 at 8.04778 KeV, Kα2 at 8.02783 KeV, and Kβ1 at 8.90529 KeV) and three in the L shell (Lα1 at 0.9297 KeV, Lα2 at 0.9297 KeV, L at β1 0.9498 Kev). The strongest of these are Kα1 and Kβ1. With regards to obsidian, the X-Ray emission lines for Nb Kα, Zr Kα, Sr Kα, Rb Kα, Th Lα, and Pb Lβ are used to determine trace element composition. The intensity of Zr Kα, Sr Kα, and Rb Kα are of particular interest for differentiating between obsidian samples.

Factors that affect interpretations of the collected spectra include the issue of spectral emission line overlap. This problem occurs when the X-Ray emission lines for two different elements overlap. For instance, the emission line for Pb Lα is 10.5515 keV, which is similar to the emission line for As Kα – 10.54372 KeV. Issues such as this one should be kept in mind and can often be resolved through more considered XRF analysis that necessitate the interpretation of problematic peaks in context with the entirety of the data collected from the challenging sample and aided by resources such as the *X-Ray Data Booklet*, published by Lawrence Berkeley National Laboratory (http://xdb.lbl.gov/xdb.pdf). This resource is vital for aiding in the identification of the elements associated with recorded peaks and for resolving the problem of emission line overlaps. This latter

task is further assisted by means of the use of the *Spectral Emission Line Overlap Checker* (http://www.ucl.ac.uk/archmat/tools/emission.php).

Other factors that can potentially skew interpretation by producing artificial peaks include: Rayleigh scattering, Compton scattering, sum peaks/ double photon counting events, escape peaks, etc. (Jenkins 2012). *Rayleigh scattering* ensues following the failure of X-Ray beams to provoke energy loss in analysis samples. These X-Rays are then recorded by the instrument as originating from the sample and usually are derived from W, Rh, Mo, Ag, and Re (Shugar 2009: 9).

A second scattering process, *Compton scattering*, is produced when an X-Ray photon interacts with the loosely-bound electrons orbiting in the outer shells of an atom and in so doing imparts some of its energy to the electrons. Depending on the material that is being analyzed, Compton scattering can produce a peak that can be mistaken for the characteristic peak of an element.

Sum peaks or *double photon counting events* can occur when two photons arrive at the instrument at the same time and are recorded as one, with double the energy, resulting in the recording of a peak that is twice as large than the characteristic peak of the element. This becomes a problem when the value of the sum peak overlaps the value of another element. For instance, the emission line for Pb Lβ is 12.61 KeV, which means that the sum peak of Pb Lβ is 25.22 KeV, overlapping the emission line of Sn Kα This can potentially lead to the misidentification of Pb for Sn.

Escape peaks are artificial peaks that occur when Si atoms from the detector absorb some of the energy from an X-Ray. This results in the recording of a so-called escape peal located at 1.74 KeV, which represent the Si Kα emission line.

4.5.1. Geochemical Analyses of Copper Ore and Slag

Data collection began with the development of a protocol for materials characterization of copper ore and slag using in-field mineralogical examination and portable X-Ray Florescence (pXRF). These methods are intended, in the long-term, to help link ancient mining sites with locations of production and consumption. A Thermo Niton XL3t GOLDD+ was calibrated for the Mining Cu/Zn mode and measured the following elements: Cu, Fe, As, Sn, Pb, Fe, Zn, Co, Ni, Sb, Bi, Mn, Au, and Ag.

For each sample, a fresh surface was exposed and analyzed three times for a duration of 600 cumulative seconds. The samples analyzed were collected during the 2012, 2015, 2016, and 2017 seasons. In total, 112 samples of copper ore and 142 slag samples were analyzed. The analyzed slag assemblage contained samples that were collected from slag scatters and slag heaps from within the ArWHO survey area. Slags were dated by relative means largely through their affiliation with diagnostic material culture and fall into three categories: (1) tap slags, (2) bowl slag, and (3) furnace slag.

There are many advantages to using a pXRF for geochemical analysis, including that it can generate rapid in-field compositional measurements across different material types. This contrasts with large benchtop XRF analyzers, which are usually not removed from laboratories. These instruments have the ability to measure relative elemental compositions qualitatively and reveal the presence or absence of diagnostic elemental profiles. Where slag and ores are concerned, a pXRF can be used to identify relative concentrations of copper in ore groups and slag types as well as the presence of diagnostic elements, such as cobalt, nickel, antimony, and arsenic.

These qualitative spectral values can be converted into elemental concentrations in empirical values by combining knowledge of the expected chemistry of the analysis sample with information regarding the parameters of the pXRF instrument as well as a suite of complex calibration. Such quantitative analyses require that XRF spectra of field samples be compared to standards representing the known compositional ranges of the samples being analyzed. In contrast, semi-quantitative methods utilize the standard libraries built into the instruments as well as knowledge of the parameters of these instruments and forego the use of independent standards.

Data collection for this study was undertaken using semi-quantitative methods. Using the instrument's Mining Cu/Zn mode, this method was able to measure major, minor, and some trace concentrations of 26 elements. These were subsequently converted into their common oxides through stoichiometry (Table 4.1):[41]

Table 4.1 Elements and their oxides monitored for each sample.

SiO2	FeO	CaO	CoO	SeO2	Nb2O5	Ag2O
Al2O3	TiO2	SO3	Cl	Rb2O	BaO	MgO
P2O5	Cr2O3	CuO	V2O5	SrO	PbO	

Because these samples were not analyzed in ideal laboratory conditions (which improve the sensitivity of light elements), one must be cautious when analyzing results for these elements (e.g. Al, Ca, P, K, Mn, Mg, S).

[41] In field data collection was undertaken by Ioana A. Dumitru and conversion to oxides by Joseph W. Lehner (Faculty of Arts and Social Sciences, U. Sydney).

4.5.2. Geochemical Analyses of Obsidian

In Ethiopia, a Bruker Tracer III-V pXRF instrument was used to analyze the elemental composition of 328 pieces of archaeological obsidian collected through systematic survey and excavation by the SRSAH team over the course of four seasons (2011, 2012, 2015, and 2016). The Bruker Tracer III-V is a portable non-destructive instrument used for elemental analysis. Depending on one's obsidian analysis goal, this instrument is capable of undertaking two processing methods: quantitative processing (ppm) and semi-quantitative processing (photon count). The quantitative analysis method allows one to identify which elements are present in the obsidian sample, whereas the semi-quantitative analysis method, while not being able to provide absolute quantities of any element, can nonetheless provide relative quantities of each element, allowing one to compare ratios of elements present in different samples. Both elemental ppm and photon count data allows obsidian samples to be separated by elemental or chemical group, even when the specific source is not known.[42] Once source elemental data are known, they can be compared to the chemical groups determined during the analysis of artifact specimens.

Towards the reconstruction of obsidian groups, the Bruker Tracer III-V pXRF instrument was able to monitor for the presence and concentration of Rb, Sr, Yr, Zr, and Nb.

[42] In field data collection was undertaken by Ioana A. Dumitru and processing by Lucas R. Martindale Johnson (Far Western Anthropological Research Group, Inc.) under the guidance of Steve Brandt (University of Florida).

Chapter 5

Archaeological Survey Results in the Broader Research Areas

5.1. Introduction to ArWHO and SRSAH

A large portion of the data analyzed for this dissertation was collected by the Archaeological Water Histories of Oman (ArWHO) Project and by the Southern Red Sea Archaeological Histories (SRSAH) Project. These two NASA-funded projects focus on comparing the development of water histories in Oman and in Ethiopia. The data that will be presented in this chapter was collected in Oman between 2012 and 2018 and in Ethiopia between 2009 and 2016. With the exception of the excavation of the multi-period site of Beta Samati, whose occupation spans the entire period of interest for this dissertation, the majority of the data discussed in this chapter was collected through a combination of systematic and reconnaissance survey. The same systematic survey method was applied for both projects, ensuring the comparability of results and facilitating analysis of site distribution across two environmentally, culturally, and historically different regions. Fifty survey transects were chosen for stratified random survey in the Ad-Dhahirah Governorate of northern Oman and in the Tigray Region of northern Ethiopia. A total of 84 archaeological sites in Ethiopia and 225 archaeological sites in Oman were recorded primarily as a result of systematic survey efforts. These data were then combined with data collected through broader reconnaissance survey.

5.2. ArWHO Survey Research Results

Archaeologists have long identified irrigation as one of several primary factors involved in the origins of agriculture and in the rise of the worlds' earliest civilizations. The Archaeological Water

Histories of Oman (ArWHO) Project adapts archaeological survey, satellite imagery, and geospatial analysis to examine the role of water availability and irrigation in the long-term histories of ancient societies.

The ArWHO Project had three broad objectives:

(1) To investigate the capabilities of hyperspectral (Hyperion) imagery for detecting ancient settlements, irrigation impacted sediments, as well as copper and chlorite sources.
(2) To examine the capacities of radar satellite imagery of detecting and mapping ancient waterways, field systems and other remnants of irrigation agriculture and human activity.
(3) To compare archaeological survey data with satellite imagery-derived measures of wetness and evapotranspiration to evaluate spatial patterning of human activities relative to water.

The survey strategy in Oman has involved both systematic stratified random sampling and wider judgmental reconnaissance aimed at building an understanding of site distributions with respect to water sources and raw material resources. In addition to aiding in the discovery of new sites, this research allows us to determine which areas were specifically targeted by ancient populations for different purposes, such as hunting, camping, herding, farming, copper exploitation (mining and smelting), as well as establishing permanent settlements. Perhaps of equal significance is the information we gain regarding areas that were less frequently utilized. The strategy devised and implemented for the systematic surveys in both Oman and Ethiopia was that of a stratified random survey, which sampled 5% of the 100 km^2 research areas (Fig. 5.1).

A total of 224 sites were surveyed between 2012 and 2018 (Fig. 5.2 and Fig. 5.3). A system of archaeological site classification was used to characterize sites based on site size, artifact density, and perceived site function. The site classification includes: find spots, artifact scatters, settlements, and other sites.

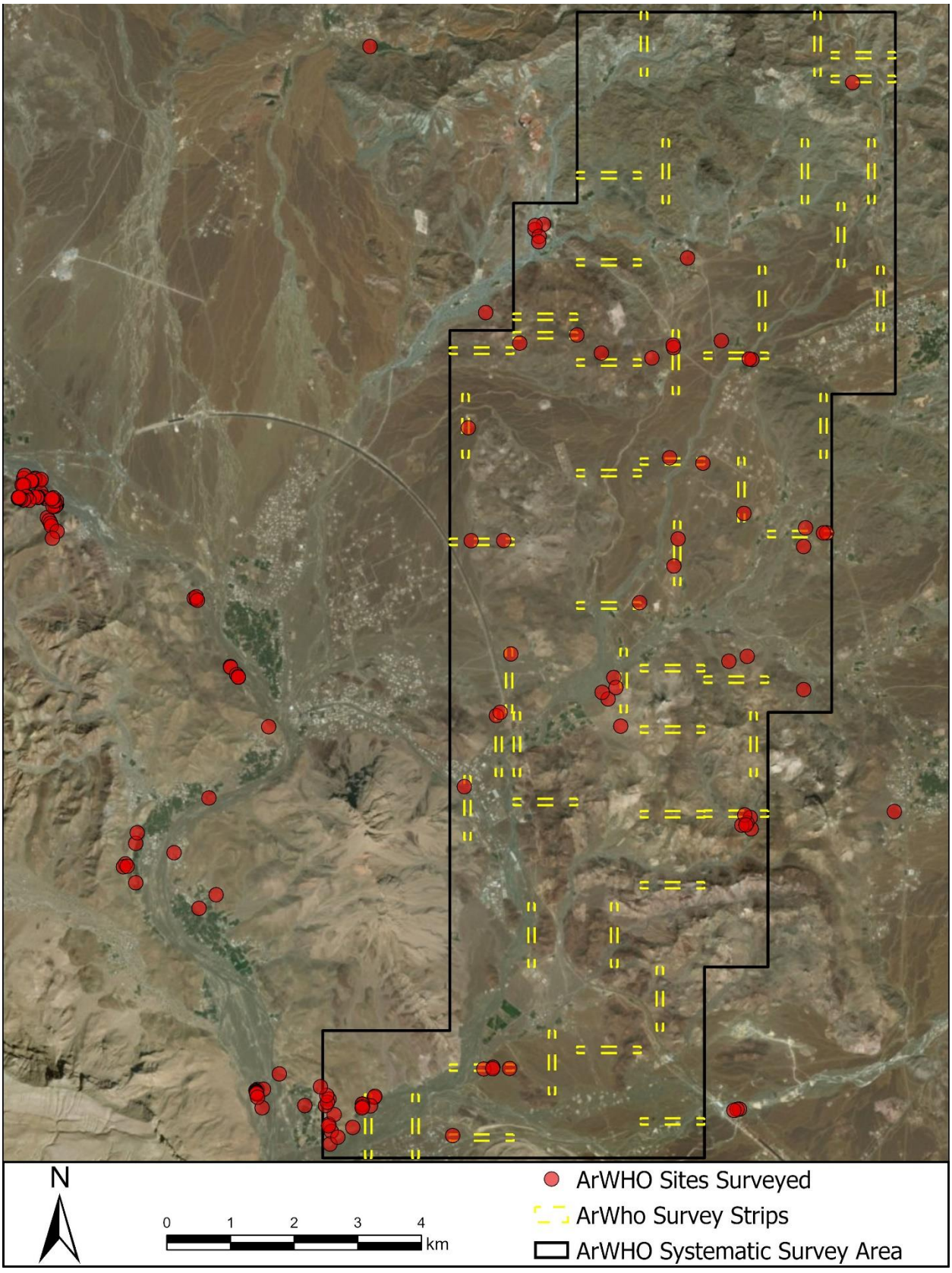

Figure 5.1 ArWHO Systematic Survey Area.

Of the total of 225 sites, 39 were identified as find spots. *Find Spots* are isolated small sites that yielded at least 15 – 20 artifacts (most commonly pottery sherds or lithics), upon intensive examination within the span of 5 minutes. A total of 20 sites were identified as *artifact scatters*. Artifact scatters are defined as sites exhibiting higher artifact densities (than find spots) and a definable areal extent that is generally no larger than 2 hectares. A total of 31 sites were identified as *settlements*. Settlements are sites that are generally larger than 1 hectare that exhibit high artifact densities, as well as evidence of archaeological features (such as walls, hearths, metallurgical slag, or other evidence of longer term or period occupation). A total of 105 sites were identified as *other sites*. Other sites include towers, tombs, isolated structures, water management features, and rockshelters. In addition to the aforementioned site types, these additional remains were designated as individual sites (sometimes within the areal extent of a larger settlement). Finally, a total of 30 sites were not identified by site type (Table 5.1).

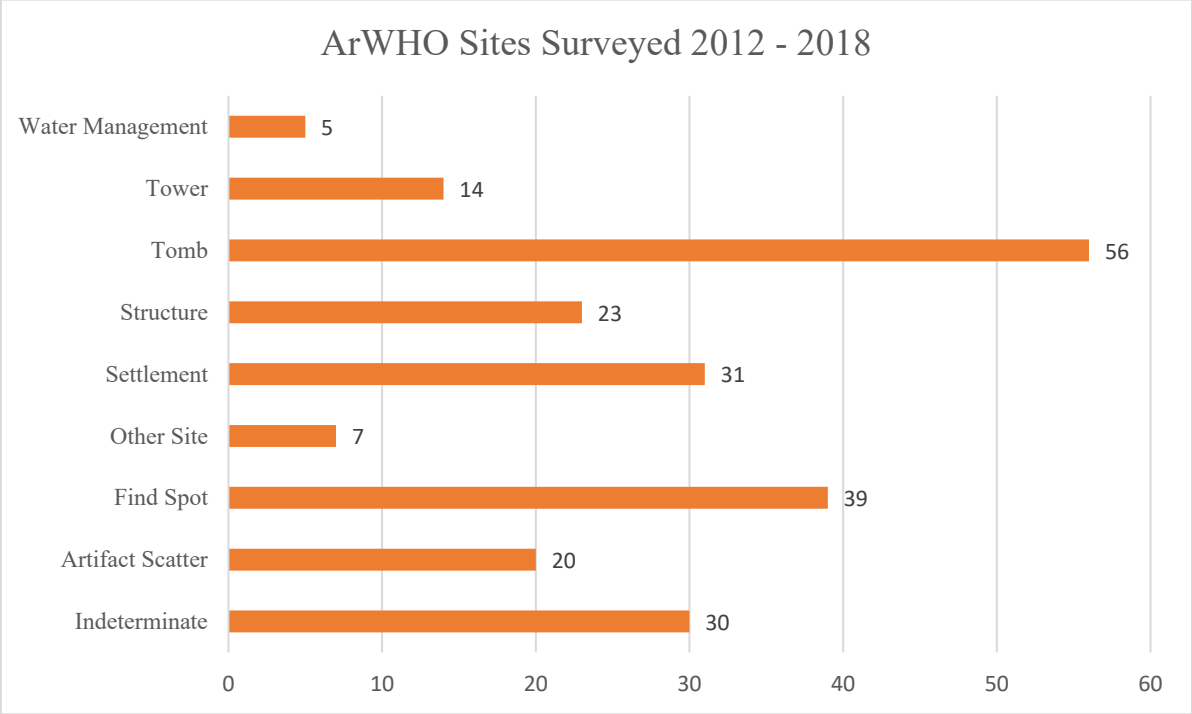

Figure 5.2 Breakdown of ArWHO site types.

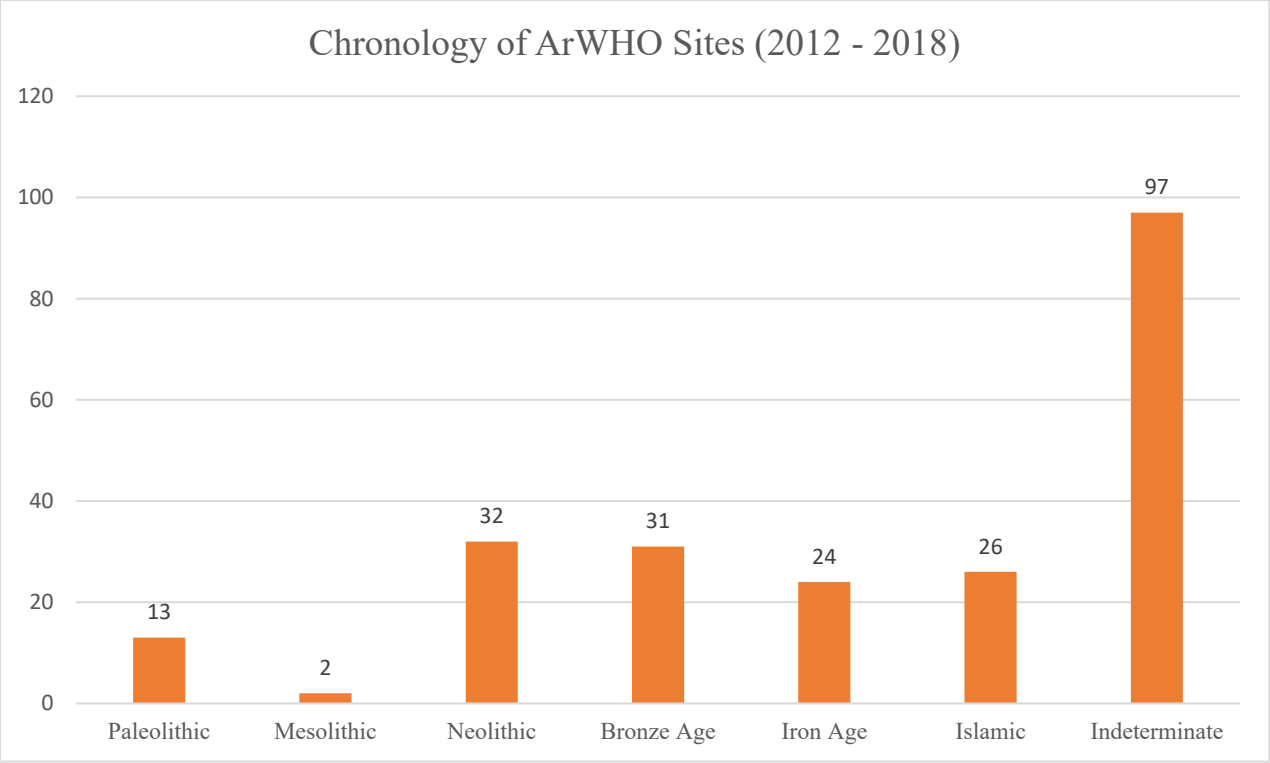

Figure 5.3 Breakdown of ArWHO sites by time period.

Table 5.1 Complete List of ArWHO Sites Surveyed 2012 - 2018.

	Site_Name	Site #	Age	Site_Type	UTM Northing	UTM Easting
0	Wim 1	988-001	Islamic	Settlement	2655848.998	459571
1	Wim 2	988-002	Bronze Age	Settlement	2656118.98	459710.17
2		985-001	Bronze Age	Settlement	2608948.562	456730.371
3	Husn Al-Khutam	999-001	Iron Age	Settlement	2608774.033	453151.993
4	Sayya	998-001	Islamic	Settlement	2619457.542	454744.554
5	Falaj As-Sidariyyin	996-002	Islamic	Settlement	2624054.886	450260.226
6	Al-Masarah	996-001	Islamic	Settlement	2632721.228	444230.11
7	Hayy Ukur	994-001	Bronze Age	Settlement	2632046.987	451426.85
8	Urukbana	995-002	Islamic	Settlement	2631394.126	451853.149
9	Abu Suwaih	997-003	Bronze Age	Settlement	2612630.235	449548.183
10	Aded Arshi 1	993-001	Islamic	Settlement	2631923.755	452904.165
11	Aded Arshi	993-002	Islamic	Settlement	2632267.858	453164.19
12	Abu Suwaih	997-008	Iron Age	Settlement	2612676.546	449479.484
13	Abu Suwaih	997-007	Iron Age	Settlement	2612657.761	449467.42

14	Abu Suwaih	997-010	Iron Age	Settlement	2612673.804	449299.972
15	Tawi Raki 1 - 3	984-001	Iron Age	Settlement	2616136.945	459734.317
16	Abu Suwaih	997-015	Paleolithic	Find Spot	2612447.521	449573.608
17	Falaj As-Sidariyyin	996-003	Indeterminate	Other Site	2623213.565	450277.595
18	Falaj As-Sidariyyin	996-004	Islamic	Other Site	2622973.354	450293.393
19	Abu Suwaih	997-001	Bronze Age	Tower	2612657.287	449575.24
20	Safri 4	990-001	Islamic	Structure	2606942.073	451062.822
21	Abu Suwaih	997-009	Bronze Age	Tower	2612720.036	449316.421
22	Abu Suwaih	997-012	Bronze Age	Structure	2612566.795	449277.966
23	Abu Suwaih	997-027	Indeterminate	Structure	2612261.114	449819.385
24	Abu Suwaih	997-004	Indeterminate	Tomb	2612629.604	449431.035
25	Abu Suwaih	997-005	Indeterminate	Tomb	2612631.217	449425.333
26	Abu Suwaih	997-006	Indeterminate	Tomb	2612633.843	449418.381
27	Abu Suwaih	997-011	Indeterminate	Tomb	2612565.494	449283.282
28	Abu Suwaih	997-013	Indeterminate	Tomb	2612571.324	449277.214
29	Abu Suwaih	997-014	Indeterminate	Tomb	2612571.701	449303.181
30	Abu Suwaih	997-016	Indeterminate	Tomb	2612358.561	449648.003
31	Abu Suwaih	997-017	Indeterminate	Tomb	2612382.767	449607.611
32	Abu Suwaih	997-018	Indeterminate	Tomb	2612378.335	449532.797
33	Abu Suwaih	997-019	Indeterminate	Tomb	2612372.583	449529.708
34	Abu Suwaih	997-020	Indeterminate	Tomb	2612375.25	449516.297
35	Abu Suwaih	997-021	Indeterminate	Tomb	2612376.144	449510.101
36	Abu Suwaih	997-022	Indeterminate	Tomb	2612385.662	449464.484
37	Abu Suwaih	997-023	Indeterminate	Tomb	2612390.444	449347.576
38	Abu Suwaih	997-024	Indeterminate	Tomb	2612387.021	449336.672
39	Abu Suwaih	997-025	Indeterminate	Tomb	2612329.157	449385.951
40	Abu Suwaih	987-001	Indeterminate	Tomb	2612057.662	449673.014
41	Abu Suwaih	987-002	Indeterminate	Tomb	2612010.477	449700.776
42	Abu Suwaih	987-003	Indeterminate	Tomb	2611968.552	449722.689
43	Abu Suwaih	987-004	Indeterminate	Tomb	2611927.426	449736.234
44	Abu Suwaih	987-005	Indeterminate	Tomb	2611842.523	449827.012
45	Abu Suwaih	987-006	Indeterminate	Tomb	2611734.856	449752.445

46	Abu Suwaih	986-001	Indeterminate	Tomb	2612335.475	449301.503
47	Abu Suwiah	986-002	Indeterminate	Tomb	2612339.053	449300.257
48	Abu Suwaih	986-003	Indeterminate	Tomb	2612359.071	449250.216
49	Abu Suwaih	986-004	Indeterminate	Tomb	2612362.455	449252.514
50	Abu Suwaih	986-005	Indeterminate	Tomb	2612365.784	449225.678
51	Abu Suwaih	986-006	Indeterminate	Tomb	2612365.027	449215.876
52	Abu Suwaih	986-007	Indeterminate	Tomb	2612376.429	449220.577
53	Abu Suwaih	986-008	Indeterminate	Tomb	2612375.642	449229.033
54	Abu Suwaih	997-002	Indeterminate	Tomb	2612273.532	449808.297
55	Abu Suwaih	997-026	Indeterminate	Tomb	2612257.665	449807.37
56	Abu Suwaih	997-028	Indeterminate	Tomb	2612236.34	449794.539
57	Abu Suwaih	997-029	Indeterminate	Tomb	2612235.794	449763.053
58	Abu Suwaih	997-030	Indeterminate	Tomb	2612327.655	449815.205
59	Abu Suwaih	997-031	Indeterminate	Tomb	2612318.226	449782.062
60	Abu Suwaih	997-032	Indeterminate	Tomb	2612371.196	449768.854
61	Abu Suwaih	997-033	Indeterminate	Tomb	2612355.344	449748.643
62	Abu Suwaih	997-034	Indeterminate	Tomb	2612355.609	449742.981
63	Safri 1	989-001	Indeterminate	Tower	2607108.16	451085.776
64	Safri 3	989-003	Indeterminate	Tower	2606619.204	450901.338
65		989-005	Indeterminate	Tomb	2606574.203	450869.207
66		989-004	Indeterminate	Tomb	2606582.73	450927.806
67	Safri 2	989-002	Indeterminate	Tower	0	0
68	Shaghy 1	976-001	Bronze Age	Artifact Scatter	2597970.73	455899.73
69	Shaghy 2	976-002	Bronze Age	Artifact Scatter	2598011.89	456068.5
70		972-001	Paleolithic	Artifact Scatter	2599173.77	455791.64
71		074-001	Paleolithic	Artifact Scatter	2607168.7	460734.95
72		074-002	Paleolithic	Artifact Scatter	2607347.38	460720.92
73		074-004	Paleolithic	Artifact Scatter	2607261.32	460667.5
74		095-001	Neolithic	Artifact Scatter	2602952.82	454811.4
75		091-001	Neolithic	Artifact Scatter	2603398.59	456532.35
76		091-002	Neolithic	Artifact Scatter	2603423.9	456676.2
77		091-004	Neolithic	Artifact Scatter	2603406.7	456937.79

78	Al-Muaydin 2	961-001	Iron Age	Artifact Scatter	2634099.22	438588.47
79	Khadil	959-001	Neolithic	Artifact Scatter	2596434.73	464975.76
80	Raki 2	981-001	Iron Age	Settlement	2616666.07	457470.78
81	Muwiyh	974-001	Neolithic	Settlement	2603075.29	452969.91
82	Wadi Hareem	973-001	Bronze Age	Settlement	2636540.01	435470.89
83	Qumaira	970-003	Indeterminate	Settlement	2640411.2	417478.49
84	Qumaira Safri	969-001	Islamic	Settlement	2647287.68	418433.24
85	A'Sayah	968-001	Islamic	Settlement	2647465.12	426868.93
86	Al Hail	967-001	Islamic	Settlement	2647461.16	423354.17
87	Bilt	966-001	Islamic	Settlement	2646991.78	421797.46
88	Fort Bilt	965-001	Islamic	Settlement	2646617.19	421802.82
89	Al-Muaydin	962-001	Iron Age	Settlement	2634511.09	437991.75
90	shell gas station	982-001	Paleolithic	Find Spot	2607832.41	456227.52
91		977-001	Bronze Age	Find Spot	2597731.81	456104.6
92		052-001	Bronze Age	Find Spot	2611604.95	461558.79
93		052-002	Iron Age	Find Spot	2611818.73	461919.82
94		052-003	Iron Age	Find Spot	2611818.02	461871.27
95		052-004	Paleolithic	Find Spot	2611897.26	461589.08
96		097-001	Iron Age	Find Spot	2602352.08	456043.59
97	Muwiyh	974-002	Bronze Age	Find Spot	2602787.96	453049.03
98	Muwiyh	974-003	Bronze Age	Find Spot	2603079.15	453070.97
99		972-002	Islamic	Find Spot	2598958.01	455603.66
100		074-005	Islamic	Find Spot	2607227.35	460588.31
101		074-006	Paleolithic	Find Spot	2607388.71	460634.21
102		095-002	Iron Age	Find Spot	2602968.3	454821.29
103		095-003	Iron Age	Find Spot	2602819.36	454752.07
104		091-003	Indeterminate	Find Spot	2603402.38	456671.84
105	Bayha	963-001	Iron Age	Find Spot	2639163.77	436291.99
106	Khadil	959-002	Bronze Age	Find Spot	2596444.31	464981.91
107		975-001	Iron Age	Other Site	2602823.43	430100.54
108	Wadi Hareem	973-006	Bronze Age	Structure	2636481.29	435491.1
109	Wadi Hareem	973-002	Bronze Age	Tower	2636548.1	435506.69

110	Wadi Hareem	973-003	Indeterminate	Structure	2636483.87	435448.48
111	Wadi Hareem	973-004	Bronze Age	Structure	2636474.76	435435.69
112	Wadi Hareem	973-007	Bronze Age	Structure	2636476.22	435557.57
113	Qumaira	970-001	Bronze Age	Tower	2640593.99	417348.63
114	Qumaira	970-002	Bronze Age	Tower	2640429.01	417457.19
115	Qumaira	970-004	Bronze Age	Tower	2640460.51	417276
116	Wadi Hareem	973-010	Bronze Age	Structure	2636464.46	435456.74
117	Al-Joghnah	960-001	Bronze Age	Tower	2606795.3	451665.09
118	Muwiyh	974-004	Neolithic	Structure	2603058.56	452950.57
119	Muwiyh	974-005	Neolithic	Structure	2603043.56	452958.15
120	Muwiyh	974-006	Neolithic	Structure	2603032.33	452961.76
121	Muwiyh	974-008	Neolithic	Structure	2603003.54	452964.91
122	Khadil	959-003	Neolithic	Structure	2596450.48	464955.41
123	Khadel Tower 2	971-002	Bronze Age	Tower	2595863.09	465104.22
124	Khadel Tower 3	971-003	Bronze Age	Tower	2595908.84	465405.75
125	Khadil	971-001	Bronze Age	Tower	2596178.02	465125.25
126	Yanqul Islamic Tower	980-001	Islamic	Structure	2607655.1	452212.7
127	Wadi Hareem	973-008	Indeterminate	Tomb	2636497.29	435682.05
128	Wadi Hareem	973-009	Indeterminate	Tomb	2636532.41	435705.43
129		074-003	Indeterminate	Tomb	2607231.78	460650.19
130	Muwiyh	974-007	Indeterminate	Tomb	2603017.25	452962.35
131	Muwiyh	974-009	Indeterminate	Tomb	2602953.68	452976.94
132	Khadel	971-004	Indeterminate	Tomb	2595926.22	465480.79
133	Khadel	971-005	Indeterminate	Tomb	2595937.44	465487.85
134		973-005	Indeterminate	Water Management	2636557.18	435439.34
135		044-002	Neolithic	Artifact Scatter	2612998.557	459453.3733
136	Al-Nuwyqat	063-002	Neolithic	Artifact Scatter	2609879.609	460672.3059
137	Wadi al-Lathli	061-001	Neolithic	Artifact Scatter	2609209.876	458486.0395
138	Wadi al-Raki 1	956-001	Neolithic	Artifact Scatter	2615280.279	456562.5917
139	Khorat Gadir 1	047-001	Paleolithic	Artifact Scatter	2611698.514	456845.8527
140	Khorat Gadir 2	047-002	Neolithic	Artifact Scatter	2611695.755	456334.532
141		095-004	Neolithic	Artifact Scatter	2602835.52	454624.2446

142	Dhahir	031-002	Neolithic	Artifact Scatter	2614729.007	459513.8571
143		958-001	Islamic	Settlement	2640423.484	420276.9637
144	Hayy Beni Kathir	957-001	Islamic	Settlement	2628235.122	465356.7986
145		010-001	Islamic	Settlement	2618891.545	462329.6733
146	Aqir Al-Shamoos	952-001	Iron Age	Settlement	2640365.235	434154.7382
147	Hayl Al-Arb	950-001	Islamic	Settlement	2640765.963	433735.2941
148	Hayy al-Nahza	985-002	Neolithic	Find Spot	2609000.1	456790.6133
149		050-001	Indeterminate	Find Spot	2611298.257	459519.9151
150		050-002	Indeterminate	Find Spot	2611724.177	459586.4941
151		044-001	Iron Age	Find Spot	2612913.394	459976.3167
152		063-001	Bronze Age	Find Spot	2609802.966	460384.3056
153		045-001	Neolithic	Find Spot	2612124.526	460621.2198
154		032-001	Neolithic	Find Spot	2614837.255	460265.6148
155		029-001	Neolithic	Find Spot	2614928.263	457996.6464
156		029-002	Neolithic	Find Spot	2614799.385	457097.3987
157		035-001	Neolithic	Find Spot	2613469.104	456288.8349
158		030-001	Paleolithic	Find Spot	2614643.836	458380.1835
159		031-001	Paleolithic	Find Spot	2614565.874	459174.7238
160		031-002	Neolithic	Find Spot	2614766.877	459507.3868
161	Hayl Al-Manathrah 1	955-001	Neolithic	Find Spot	2602530.317	454096.1147
162	Hayl Al-Manathrah 2	954-001	Islamic	Find Spot	2602823.986	453719.5345
163	Hayl Manathrah	953-006	Islamic	Find Spot	2602681.691	454181.3811
164		095-008	Neolithic	Find Spot	2602480.906	454473.0786
165		095-009	Paleolithic	Find Spot	2602417.561	454135.7228
166		095-010	Neolithic	Find Spot	2602219.173	454115.6584
167		061-001a	Neolithic	Find Spot	2609313.931	458392.0045
168	Mahyul 1	948-001	Neolithic	Find Spot	2607441.946	462984.9613
169		070-001	Neolithic	Other Site	2609356.991	461559.5828
170		055-001	Neolithic	Other Site	2610722.648	458981.3834
171	Tawi Zaba	951-001	Islamic	Other Site	2641390.64	433499.7823
172		954-002	Indeterminate	Water Management	2603320.939	453319.3846

173		953-003b	Indeterminate	Water Management	2602924.964	454099.5178
174		953-004	Indeterminate	Water Management	2602824.161	454045.0506
175		953-002a	Indeterminate	Water Management	2602874.982	454074.8961
176	Wadi Al-Lathli 2	061-002	Iron Age	Other Site	2609546.223	458575.0819
177	Raki 2	981-001	Indeterminate	Structure	2616583.305	457334.8299
178	Raki 2	981-001	Indeterminate	Structure	2616645.727	457340.3235
179	Raki 2	981-001	Indeterminate	Structure	2616475.856	457401.7153
180	Raki 2	981-001	Indeterminate	Structure	2616393.391	457394.5492
181		032-002	Islamic	Structure	2614541.807	460745.4865
182		032-003	Indeterminate	Structure	2614550.225	460705.58
183	Hayl Manathrah 1	955-002	Iron Age	Structure	2602505.473	454093.5516
184	Hayl Al-Manathrah 3	953-001	Iron Age	Structure	2602982.765	454064.7727
185	Hayl Manathrah 3	953-005	Iron Age	Structure	2603117.832	453965.9595
186		059-001a	Indeterminate	Tomb	2609917.102	456957.9062
187		095-005	Indeterminate	Tomb	2602849.132	454623.7745
188		095-006	Indeterminate	Tomb	2602806.593	454627.7478
189		095-007	Indeterminate	Tomb	2602786.914	454620.7966
190		095-011	Indeterminate	Tomb	2602327.058	454238.4934
191		947-001	Indeterminate	Tomb	2602766.84	460550.2585
192		947-002	Indeterminate	Tomb	2602763.309	460513.4066
193		947-002a	Indeterminate	Tomb	2602746.618	460463.0974
194	Ajran	000	Bronze Age	Tower	2657868.653	417393.247
195		943-001	Paleolithic	Indeterminate	2610781.01	452013.38
196	Shwaghy	939-001	Indeterminate	Indeterminate	2626959.26	446458.98
197	C105 Aqir Al-Shamoos 2	952-002	Indeterminate	Indeterminate	2640283	434286
198	C97 Zuha	~~933-001~~	Indeterminate	Indeterminate	2675685.24	451809.79
199	C98 Zuha	~~933-002~~	Indeterminate	Indeterminate	2675680.1	451898.9
200	C99 Zuha	~~933-003~~	Indeterminate	Indeterminate	2675684.46	451916.57
201	C101 Zuha	~~933-005~~	Indeterminate	Indeterminate	2675521.21	452203.56
202	C100 Zuha	~~933-004~~	Indeterminate	Indeterminate	2675553.34	452172.16

203	Al-Qaboura	945-001	Islamic	Indeterminate	2605921.62	452057.65
204	Waby al-Zady	937-001	Iron Age	Indeterminate	2641781.47	433588.37
205		927-001	Indeterminate	Indeterminate	2694705.73	439080.35
206	Tawi Zaba	951-001	Indeterminate	Indeterminate	2641383.15	433498.65
207	Hayl Al-Arb 2	950-002	Iron Age	Indeterminate	2640938.89	433702.14
208		938-001	Indeterminate	Indeterminate	2632852.42	438153.64
209	Wadi Fida	941-001	Iron Age	Indeterminate	2599286.17	446665.92
210	Wadi al-Lathli	067-001	Mesolithic	Indeterminate	2608782.8	458684.25
211	Wadi al-Lahli	061-003	Mesolithic	Indeterminate	2609389.68	458609.78
212		944-001	Bronze Age	Indeterminate	2609719.52	452549.54
213		944-002	Bronze Age	Indeterminate	2609706.98	452554.89
214		927-002	Indeterminate	Indeterminate	2694729.05	439109.52
215	Tawi Arja	930-001	Indeterminate	Indeterminate	2693270.11	441122.78
216	Tawi Arja	930-002	Indeterminate	Indeterminate	2693244.02	441080
217	As-Safah	940-001	Indeterminate	Indeterminate	2579649.54	382264.85
218	Al-Qaboura 2	945-002	Indeterminate	Indeterminate	2606134.72	452326.06
219		942-001	Indeterminate	Indeterminate	2609592.46	452648.66
220		942-002	Indeterminate	Indeterminate	2609560.69	452672.62
221		942-003	Indeterminate	Indeterminate	2609551.19	452676.53
222		943-001	Indeterminate	Indeterminate	2610792.46	451982.17
223		943-002	Indeterminate	Indeterminate	2610813.74	452013.3
224		943-003	Indeterminate	Indeterminate	2610760.72	452032.35

5.2.1. ArWHO Copper Survey: Archaeological Findings

The ArWHO copper project has generated information relating to the distribution of both copper sources and archaeological sites with evidence of copper production (Table 5.2). Data collection entailed ground-truthing of satellite imagery-derived copper prospectivity maps (which was begun in 2013), archaeological survey, and geological reconnaissance (Fig. 5.4). Results of prospectivity mapping and geological reconnaissance are discussed in Chapter 6. In total, 152

copper points were recorded. Out of these, 31 points are associated with copper deposits, 37 points are associated with slag, and 84 points are false positives.

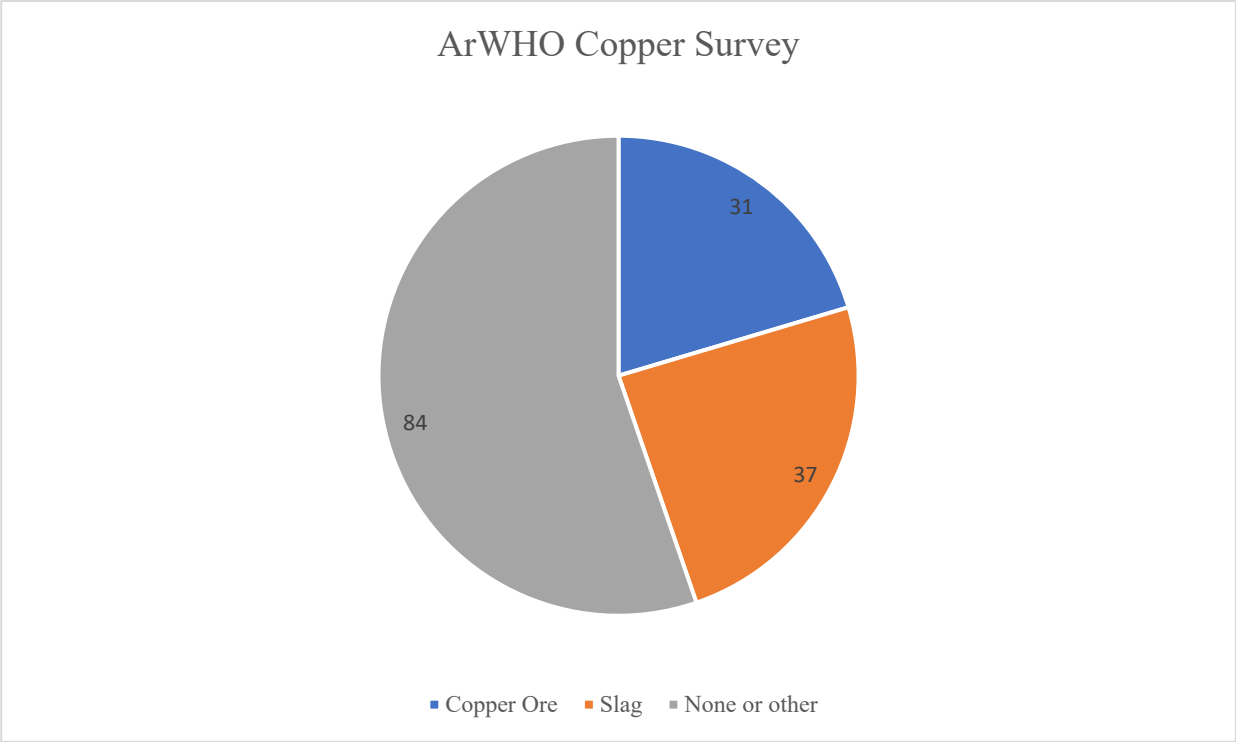

Figure 5.4 ArWHO Copper Survey by Recorded Artifact Type.

Table 5.2 Copper Survey Database.

#	C#	Site Number	Site Name	Artifact Type	Comments	Northing	Easting
1	C1	N/A	N/A	None	False Positive	2611911	457597
2	C2	N/A	N/A	None	False Positive	2597688	456218
3	C3	N/A	N/A	None	False Positive	2597988	455903
4	C4	989-001	Safri	Slag	Discovered near Safri 1 in association w crucible base	2607158	451029
5	C5	976-001	N/A		Discovered in 2013 near 976-001	2598350	456195
6	C6	N/A	N/A	None	False positive	2598435	455939
7	C7	N/A	N/A	None	False Positive	2598342	455974
8	C8	N/A	N/A	None	False Positive	2598256	455688
9	C9	N/A	N/A	None	False Positive	2599193	455828
10	C10	N/A	N/A	None	False Positive	2607122	460692

11	C11	N/A	N/A	None	False Positive	2608109	456997
12	C12	N/A	N/A	None	False Positive	2606264	461964
13	C13	N/A	N/A	None	False Positive	2588732	457421
14	C14	N/A	N/A	None	False Positive	2585774	457740
15	C15	N/A	N/A	None	False Positive	2589085	457536
16	C16	N/A	N/A	None	False Positive	2587342	457570
17	C17	971-001	Khadil	Slag	Discovered in 2013 near Khadil	2596510	464865
18	C18	N/A	N/A	None	False Positive	2594614	457510
19	C19	N/A	N/A	None	Potential Hawassina bedrock	2609527	459802
20	C20	N/A	N/A	None	Potential Hawassina bedrock	2609189	459817
21	C21	N/A	N/A	None	Potential Hawassina bedrock	2608940	459842
22	C22	N/A	N/A	None	Initially identified as exploitation holes	2608828	459841
23	C23	N/A	N/A	None	Initially identified as exploitation holes	2608273	459845
24	C24	N/A	N/A	None	Initially identified as exploitation holes	2607750	460887
25	C25	N/A	N/A	None	False Positive	2608729	460994
26	C26	N/A	N/A	None	Initially identified as exploitation holes	2608585	460989
27	C27	N/A	N/A	None	Initially identified as exploitation holes	2608457	460991
28	C28	N/A	N/A	None	False Positive	2612453	457327
29	C29	N/A	N/A	None	False Positive	2612268	457450
30	C30	N/A	N/A	None	False Positive	2612309	457580
31	C31	N/A	N/A	None	False Positive	2612304	457644
32	C32	N/A	N/A	None	False Positive	2611330	457403
33	C33	N/A	N/A	None	False Positive	2611380	457415
34	C34	N/A	N/A	None	False Positive	2611391	457470
35	C35	N/A	N/A	None	False Positive	2611381	457509
36	C36	N/A	N/A	None	False Positive	2611607	457609
37	C37	N/A	N/A	None	False Positive	2611597	457662

38	C38	N/A	N/A	None	False Positive	2612952	459059
39	C39	N/A	N/A	None	False Positive	2612893	459185
40	C40	N/A	N/A	None	False Positive	2612995	459299
41	C41	N/A	N/A	None	False Positive	2619055	462021
42	C42	N/A	N/A	None	False Positive	2617968	461646
43	C43	N/A	N/A	None	False Positive	2611729	456695
44	C44	N/A	N/A	None	False Positive	2607244	456072
45	C45	N/A	Muaydin	Slag	Smelting site near copper source	2634511	437991
46	C46	N/A	N/A	None	False Positive	2609894	456953
47	C47	981-001	Raki	Slag and ore	Smelting site	2616583	457334
48	C48	N/A	Raki modern mine	Copper Ore	geo samples - Cu in pillow lavas - former C#10	2618679	457362
49	C49	N/A	N/A	None	False Positive	2627865	432946
50	C50	N/A	N/A	None	False Positive	2609541	458594
51	C51	31	N/A	Slag	Small slag scatter in Dhahir	2614659	459547
52	C52	921-001	N/A	Slag	Single piece near formerly detected area	2612833	458807
53	C53	924-001	N/A	Slag	Slag scatter in wadi channel below mine	2619616	458462
54	C54	935-001	N/A	Slag	Copper mine (Iron Age & Islamic)	2619631	458502
55	C55	N/A	N/A	None	Small exploitation holes near big mine	2619648	458482
56	C56	N/A	N/A	None	Exploitation hole south of large mine	2619447	458263
57	C57	962-001	Muaydin	Copper Ore	Collection in detected pixel	2634617	438232
58	C58	962-001	Muaydin	None	False positive	2634518	438386
59	C59	962-001	Muaydin	Copper Ore	Chrysocolla, ephemeral malachite, sample collected	2634558	438259
60	C60	962-001	Muaydin	Copper Ore	copper ore washing down bedrock channel	2634557	438245
61	C61	962-001	Muaydin	Slag	slag heap	2634550	438240

62	C62	962-001	Muaydin	Copper Ore	ore source - in exploitation cut	2634680	438091
63	C63	N/A	N/A	None	False Positive	2637542	434791
64	C64	N/A	N/A	Copper Ore	disturbed area,sheeted dyke,gabbro,wadi	2637716	434713
65	C65	923-001	N/A	Slag	slag enclosed poss tower, near detected pixel	2637780	434647
66	C66	922-001	N/A	Slag	slag findspot	2637814	434613
67	C67	N/A	N/A	None	False positive - gabbro with desert varnish	2637907	434527
68	C68	925-001	N/A	Slag	single slag piece	2637861	434554
69	C69	N/A	N/A	Copper Ore	near pixel; cut by recent digging	2637653	434799
70	C70	920-001	N/A	Slag	on terrace in between wadi and mountain	2637617	435011
71	C71	984-001	N/A	Copper Ore & slag	gossan	2615902	459807
72	C72	936-001	N/A	Slag	smelting site near Raki mine	2618679	457508
73	C73	984-001	N/A	Copper Ore	copper in gossan	2615932	459856
74	C74	981-001	Raki modern mine	Copper Ore	azurite	2618698	457252
75	C75	984-001	N/A	Slag	slag heap	2616134	459749
76	C76	984-001	N/A	Slag	large slag heap	2616044	459720
77	C77	926-001	N/A	Copper Ore	ore washed down slope with pottery	2615892	459895
78	C78	984-001	N/A	Slag	on the slope near roaster	2616261	459862
79	C79	N/A	N/A	None	false positive near smelting site	2618686	457584
80	C80	N/A	N/A	Copper Ore	gossan in wadi channel being detected	2618342	457506
81	C81	N/A	N/A	None	False Positive	2630543	443627
82	C82	N/A	N/A	Other		2633728	446608
83	C83	N/A	N/A	Copper Ore	positive detection - 3 pix on ridge	2629021	443626

84	C84	N/A	N/A	Copper Ore	small copper smear found through survey	2630238	443585
85	C85	N/A	Sayyah	Copper Ore	copper deposit near large modern mine	2618751	453227
86	C86	N/A	N/A	None	False positive - radiolarian chert - 260 m from det pix	2615048	459920
87	C87	N/A	N/A	None	False positive	2615119	460072
88	C88	N/A	N/A	None	False positive	2614252	459865
89	C89	N/A	N/A	None	False positive	2614297	460118
90	C90	N/A	N/A	None	False positive near F. Sudayriyin	2621846	449927
91	C91	N/A	N/A	None	point on ridge close to inaccessible detection	2620339	448864
92	C92	N/A	N/A	None	point on ridge close to inaccessible detection	2620362	445988
93	C93	N/A	N/A	None	False positive	2620729	446159
94	C94	N/A	N/A	None	False positive	2622199	443124
95	C95	N/A	N/A	None	False positive	2625750	443230
96	C96	984-001	N/A	Copper Ore	gossan with chalcopyrite	2616180	459807
97	C97	N/A	N/A	None	False positive	2634726	446169
98	C98	~~933-002~~	Zuha	Copper Ore	potential sulfide ore in pillow basalt	2675678	451899
99	C99	~~933-003~~	Zuha	Copper Ore	ore in pillow basalt	2675683	451917
100	C100	~~933-004~~	Zuha	Copper Ore	ore body sharp contact w pillow basalt	2675552	452172
101	C101	~~933-005~~	Zuha	Copper Ore	modern mining pillow basalt with Cu on boundary	2675520	452204
102	C102	N/A	Greater Arja Area	Copper Ore	ore sample near modern Arja mine	2692991	440280
103	C103	N/A	Greater Arja Area	Copper Ore	copper ore in pillow basalt	2692855	441012
104	C104	N/A	Greater Arja Area	Copper Ore	ore in pillow basalt with possible struct to south	2692946	440931
105	C105	952-002	Aqir Al-Shamoos 2	Slag		2640283	434286

106	C106	N/A	near Tawi Hareem	None	False positive near known copper source	2637338	434142
107	C107	N/A	Tawi Hareem	Other	False positive near known copper source	2636115	434223
108	C108	N/A	Wadi Hareem	Copper Ore	Positive detection	2636206	435077
109	C109	N/A	Bayha	None	False positive over the town of Bayha	2638951	436594
110	C110	932-001	Lasail	Slag	slag from section	2684896	442660
111	C111	932-002	Lasail	Slag	Lasail general point	2684870	442661
112	C112	932-003	Lasail	Slag	slag around resmelt depression	2684837	442630
113	C113	932-004	Lasail	Slag	reddish slag from around depression	2684872	442619
114	C114	931-001	Bayda	Slag	Islamic architecture w slag and pottery	2694802	439957
115	C115	930-001	Tawi Arja	Slag	Slag scatter to south of "Ziggurat"	2693127	441033
116	C116	930-001	Tawi Arja	Ceramics	Possible roaster on slope	2693213	440881
117	C117	930-003	Tawi Arja	Copper Ore	Possible copper in pillow basalt above possible roaster	2693228	440874
118	C118	930-001	Tawi Arja	Slag	Slag scatter with architecture on slope	2693227	440940
119	C119	929-001	Arja	Slag	Slag scatter with architecture on slope	2693267	440993
120	C120	994-001	Hayy Ukur	Slag	Slag scatter at site of Hayy Ukur	2632061	451436
121	C121	N/A	N/A	None	Pillow basalts near detected pixels	2612525	462174
122	C122	Sector 268	N/A	None	SE corner of 268	2610807	454822
123	C123	Sector 286	N/A	None	SE corner of 286	2609947	454821
124	C124	Sector 374	N/A	None	SE corner of 374	2606274	459158
125	C125	Sector 39	N/A	None	SW corner of 39	2570999	450500
126	C126	Sector 78	N/A	None	SW corner of 78	2572001	453000
127	C127	Sector 358	N/A	None	SW corner of 358 - 90 m away	2580091	454001
128	C128	Sector 322	N/A	None	SW corner of 322	2578999	453501

129	C129	Sector 284	N/A	None	200 m from SW corner of 284	2577999	451687
130	C130	Sector 1038	N/A	None	SW corner of 1038 (1039 too steep)	2599500	458001
131	C131	Sector 433	N/A	None	SW corner of 433	2582500	448000
132	C132	Sector 1457	N/A	None	SW corner of 1457	2611997	454000
133	C133	918-001	N/A	Slag	slag scatter	2612501	454002
134	C134	N/A	N/A	Copper Ore	Possible copper ore in sheeted dyke	2614285	461544
135	C135	Sector 1540	N/A	None	200 m from SW corner of 1540	2614203	461503
136	C136	Sector 1513	N/A	None	SW corner of 1513	2613498	456501
137	C137	N/A	N/A	None	False positive in radiolar chert & carbonate	2613185	456760
138	C138	N/A	Tawi Salamah	Copper Ore	Layered gabbro	2632688	440473
139	C139	N/A	Tawi Salamah	Copper Ore	Second Tawi Salamah outcrop with visible copper	2632554	441017
140	C140	N/A	Tawi Harim	Copper Ore	From Tawi Harim point from geological map	2637314	433765
141	C141	N/A	N of Ghadhiya	Copper Ore	Copper point from geological map	2620941	438315
142	C142	N/A	N of Ghadhiya	Slag	Collection of slag, ore pieces, pottery, furnace pieces	2621197	438682
143	C143	952-001	Aqir Al-Shamoos	Slag	Slag scatter	2640365	434154
144	C144	Sector 1341	N/A	None	SW corner of 1341	2608500	456500
145	C145	934-001	Al Arid	Slag	Slag from Sabatino	2592382	463370
146	C146	985-002	Hayy al-Nahza	Slag		2608999	456791
147	C147	997-027	Abu Suwaih	Slag		2612261	449819
148	C148	984-001	Raki	Slag		2616044	459720
149	C149	944-001		Slag		2609719	452549
150	C150	N/A	Hala	Slag	Slag with architecture on slope	2578223	486879

151	C151	N/A	Yankul Mt.	None	False positive - detecting pink limestone in fault line	2607102	455127
152	C152	N/A	N/A	None	False positive - took sample	2633632	438187
153	C154	973-001	Wadi Harim	Slag		2636540	435470
154	C157	970-003	Qumaira	Slag		2640411	417478
155	C160	973-006	Wadi Harim	Slag		2636481	435491
156	C163	950-001	Hayl al-Arb	Slag		2640765	433735

5.3. SRSAH Survey Research Results

The SRSAH survey area is located in the general region surrounding the ancient site of Yeha, in the central zone of the Northern Tigray Region. The survey method employed for the SRSAH project was initially devised for the Eastern Tigrai Archaeological Project (ETAP) and, as with the ArWHO project, involves both systematic and judgmental reconnaissance sampling (Harrower and D'Andrea 2014). Methodological consistency with both the ETAP project and the ArWHO project ensures comparability of results and is helping to generate wider understanding of Pre – to Late-Aksumite societies in the region as well as a comparative dataset crucial to examining the role of water availability and irrigation in the long-term histories of ancient societies.

Systematic survey efforts, led by Dr. Michael Harrower and Dr. Catherine D'Andrea, initially began in 2009 when sites that had been identified by the previous surveys of Francis Anfray and Joseph Michels were re-identified. During this first season, some of the largest and most easily recognizable archaeological sites in the area were newly recorded. In 2011 further opportunistic work was undertaken in the region surrounding Yeha. In 2012, a 100 km^2 survey area was delineated in the greater Yeha region (Fig. 5.5). This survey area was demarcated to exclude inaccessible cliffs and mountains that would have otherwise made survey difficult or impossible. This area was divided into one hundred 1x1 km sectors and a program of systematic survey was

begun. This survey involved 5% stratified random sampling (50 transect strips) and was completed in 2015. The 2016 season concentrated on following up at a number of sites with indeterminate ages and/or incomplete information. In total, the archaeological survey from 2009 to 2016 recorded 84 sites including 29 settlements, 20 artifact scatters, 29 find spots, and 6 other sites (Fig. 5.6).

Four sites (Adi Abiselam 999-001 and Mai Omo 998-001, 998-002, 998-003) are located just outside our survey area boundary and therefore have not be collected or recorded. Similarly, the German team and thus have not been collected nor studied by SRSAH.

In similar fashion to the ArWHO survey methods, to maximize the discovery of important new settlement sites and gain a statistically representative understanding of the area, the SRSAH team employed both opportunistic and systematic survey. A combined vehicular and pedestrian approach specifically targeted areas with stone architectural debris that often demarcates ancient settlements.

When sites were discovered, artifacts such as lithic tools and ceramics were collected, bagged and tagged according to survey unit number and site number. A sample of each ceramic ware or lithic raw material as well as diagnostic sherds and lithics were collected. In addition to names solicited through inquiries with local people, sites are referred to according to their three-digit survey unit/sector number followed by a three-digit site number (e.g. Beta Samati 006-001 is the first site in Sector 6). In some circumstances archaeological material was found just outside the borders of our project survey area. When this happened, the team began a running count for the "sector number" counting down from 999 but otherwise following the same format as the rest of the sites.

Out of a total of 84 sites (Table 5.3), 15 sites are of indeterminate age – because of lack of diagnostic surface remains collected and analyzed by the SRSAH team. Eight of the indeterminate age sites are Find Spots – which are quite ephemeral and, at times, did not contain enough data to assign a firm date. Six of these sites are designated "Other Sites" which had no or very few remains visible on the surface.

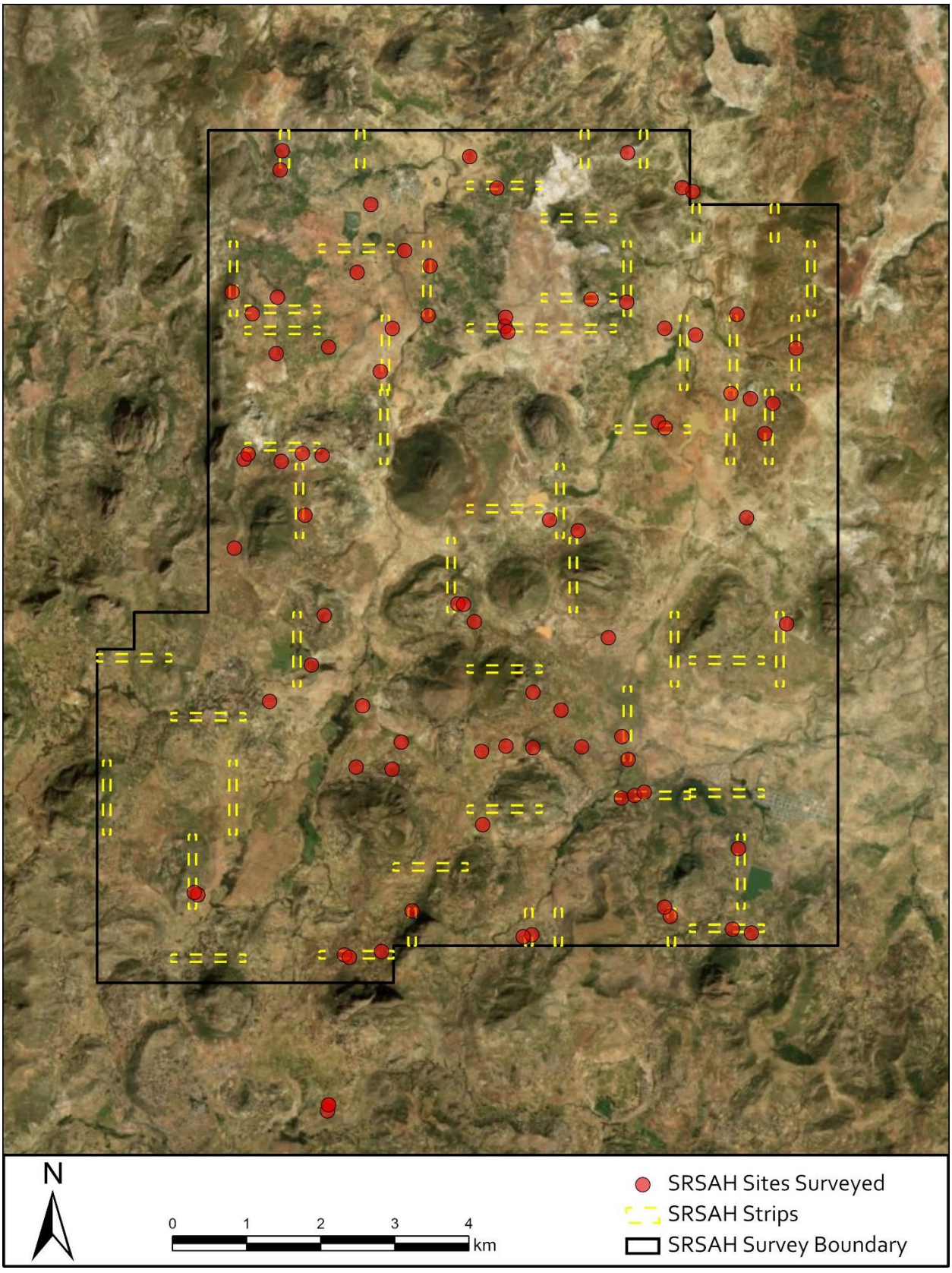

Figure 5.5 SRSAH Systematic Survey Area.

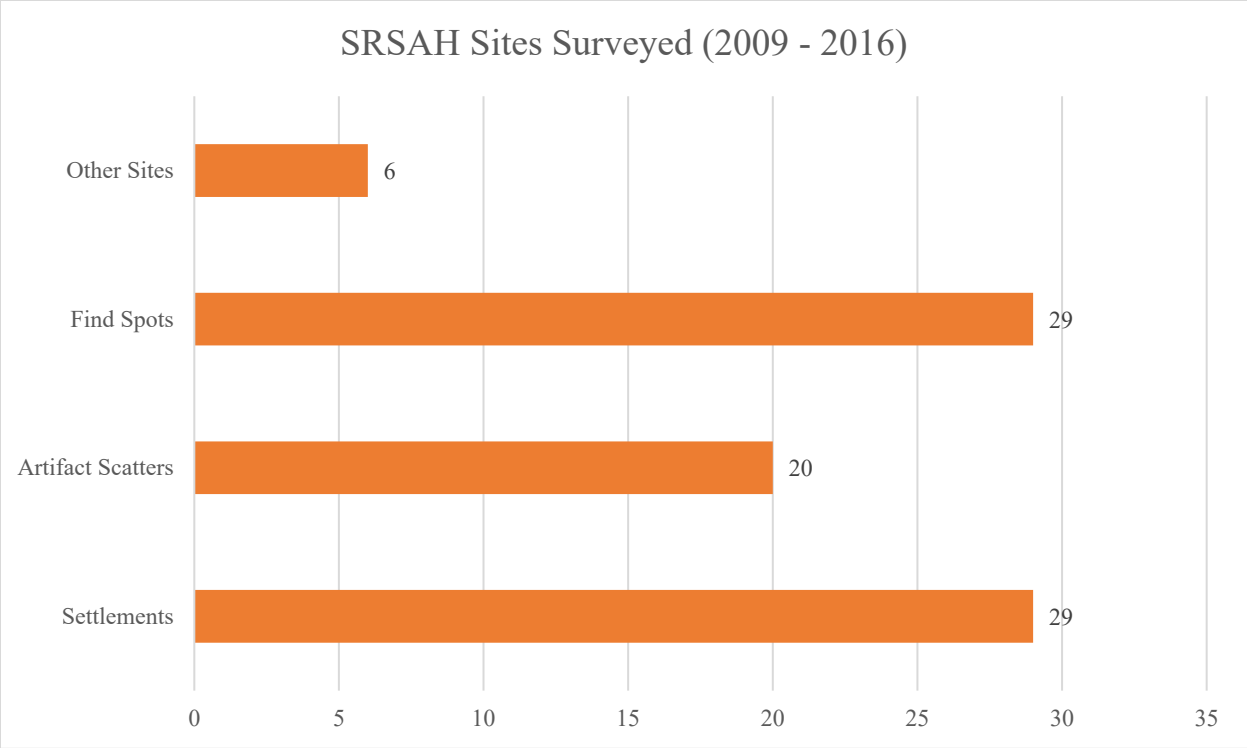

Figure 5.6 Breakdown of SRSAH Site Types (2009 - 2016).

Table 5.3. Complete List of SRSAH Sites Surveyed 2009 - 2016.

	Site Name	Site #	Size (ha)	Age	UTM Northing	UTM Easting	Year Found
	Settlements						
1	Beta Samati	006-001	20.28	Classic to Post-Aksumite	1585500	503694	2009
2	Enda Gally	057-001	8.69	Pre-Aksumite to Late Aksumite	1579957	503066	2009
3	Mes'hl	092-001	3.98	Early to Late Aksumite	1576809	508656	2015
4	Dungur	022-003	3.56	Pre-Aksumite to Late Aksumite	1583575	503124	2011
5	Sekoualou	044-001	3.24	Pre-Aksumite	1581273	508766	2009
6	Dergouah	060-001	3.24	Middle to Late Aksumite	1579655	506901	2009
7	Mai Fesasi	029-002	2.47	Middle to Post-Aksumite	1582035	502486	2015
8	Sefra Tourkui	027-001	2.4	Pre-Aksumite	1583740	508076	2009
9	Tigala 3	097-003	2.38	Classic to Late Aksumite	1575421	503837	2015
10	Mai Awa'ur	020-001	2.11	Middle Aksumite	1582065	501982	2015

11	Enda Giordis Mogu'o	042-002	1.97	Middle Aksumite	1581098	506492	2015
12	Dem Elal	013-001	1.88	Pre-Aksumite to Post-Aksumite	1584583	503509	2011
13	Da'ero Arat/St. Gabriel Church	079-001	1.66	Classic to Middle Aksumite	1577132	505203	2015
14	Sefra Aboun	071-001	1.4	Pre-Aksumite to Middle Aksumite	1578320	507081	2009
15	Enda Mariam Adekeras	100-002	1.28	Classic to Middle Aksumite	1575672	508831	2015
16	Enda Cha'atat	002-001	1.11	Classic to Middle Aksumite	1586146	505029	2015
17	Fedaga Aro	003-001	1.1	Classic to Late Aksumite	1586199	507159	2015
18	Enda Nuwutu	027-002	1.01	Classic to Middle Aksumite	1584017	508636	2009
19	Adi Wesak 2	034-002	0.9	Middle to Post-Aksumite	1582640	507620	2015
20	Tseratsur	069-001	0.9	Classic to Late Aksumite	1578919	505883	2015
21	Enda Mikeal	012-001	0.82	Pre-Aksumite to Post-Aksumite	1584249	502434	2012
22	Luhuts	077-001	0.66	Middle Aksumite	1577882	503980	2015
23	Enda Aboy Meles	022-002	0.62	Pre-Aksumite	1583828	503984	2009
24	Ser Ser Adi Keshi	037-001	0.56	Classic to Late Aksumite	1580864	501852	2009
25	Adi Kesho/Adi Hano	069-002	0.45	Early to Post-Aksumite	1578192	505517	2015
26	Adi Helafa	014-001	0.42	Post-Aksumite	1584877	504150	2011
27	Enda Balata Dista	022-001	0.42	Pre-Aksumite	1583248	503822	2009
28	Musa Metahen	056-001		Indeterminate	1579288	502891	2009
29	Min Gerger Abi Adi	066-001		Indeterminate	1578796	502327	2009
	Artifact Scatters						
1	N/A	005-001	1.01	Late Aksumite	1585965	502470	2012
2	Berik Gadm	035-002	0.95	Post-Aksumite	1582879	508817	2012

3	Hedar 2	048-001	0.82	Middle to Post-Aksumite	1580112	504869	2015
4	Mirai Abune Afsea	068-001	0.6	Pre-Aksumite	1578247	504106	2011
5	Hchen	026-001	0.54	Pre- to Early Aksumite	1583830	507659	2012
6	Endaba Hailu	017-001	0.44	Late to Post-Aksumite	1584182	507146	2012
7	Beloho	030-001	0.36	Classic to Middle Aksumite	1582116	503036	2015
8	Adi Abisalem	999-001	0.28	Middle Aksumite	1585674	508040	2015
9	Aoudi Welka	067-001	0.27	Pre-Aksumite to Early Aksumite*	1578737	503582	2011
10	N/A	024-002	0.25	Classic Aksumite	1583978	505512	2012
11	Gembes	024-001	0.24	Late to Post-Aksumite	1583855	505504	2012
12	Gobo Terer	028-001	0.24	Classic to Middle Aksumite	1583561	509433	2015
13	Enda Mariam Adekeras	100-001	0.18	Classic to Post-Aksumite	1575724	508575	2015
14	N/A	001-001	0.12	Classic to Post-Aksumite	1586224	502498	2012
15	Kawhi Aboi Haftom	069-004	0.1	Early Aksumite*	1578172	505880	2015
16	Adi Klte	085-001	0.1	Classic to Middle Aksumite	1576187	501359	2015
17	Enda Nebsay	012-002	0.09	Pre-Aksumite to Post-Aksumite	1584026	502094	2012
18	N/A	036-001	0.08	Pre-Aksumite	1582407	509011	2012
19	Mekebr Aslem	035-001	0.06	Post-Aksumite	1582951	508553	2012
20	Negasti Wolahu	070-001		Classic to Middle Aksumite	1578182	506540	2009
	Find Spots						
1	N/A	004-001		Middle Aksumite	1584319	501821	2012
2	N/A	008-001		Middle to Post-Aksumite	1585721	505394	2012
3	Adi Abisalem 2	010-001		Classic to Middle Aksumite	1585726	507894	2015
4	Adi Halefa	014-002		Proto to Early Aksumite	1584670	504493	2012
5	Gogoweyten	014-003		Pre- to Early Aksumite*	1584002	504469	2012
6	N/A	016-001		Post-Aksumite	1584222	506666	2012

7	Eda Felasi	021-001		Indeterminate	1583488	502416	2012
8	N/A	024-003		Classic Aksumite	1583780	505542	2012
9	Mai Awa'ur 2	029-001		Classic to Middle Aksumite	1582134	502038	2015
10	Zban Ma'ekune/Beloho	029-003		Indeterminate	1582141	502769	2015
11	Adi Wesak	034-001		Indeterminate	1582487	507664	2015
12	N/A	036-002		Post-Aksumite	1582816	509122	2012
13	Welaha/Dembi Arar	038-001		Middle Aksumite	1581307	502805	2015
14	N/A	042-001		Post-Aksumite	1581244	506106	2012
15	Hedar	048-002		Classic to Middle Aksumite	1580106	504946	2015
16	Ksadke’re	063-001		Early to Classic Aksumite	1579841	509305	2012
17	Kohama	069-003		ESA to Pre-Aksumite*	1578123	505188	2015
18	Tseratsur	070-002		Pre- to Middle Aksumite	1578678	506261	2015
19	Mai Eungug	071-002		Pre- to Classic Aksumite*	1578011	507166	2015
20	Mwal Sienom	077-002		Indeterminate	1577909	503495	2015
21	Adi Krumbe/Tahtay	081-001		Pre-Aksumite	1577493	507077	2015
22	Adi Krumbe/Tahtay 2	081-002		Classic to Middle Aksumite	1577527	507254	2015
23	Adi Krumbe/Tahtay 3	081-003		Classic to Middle Aksumite	1577572	507384	2015
24	Ak'akuh	091-001		Middle Aksumite	1575990	507697	2015
25	Tigala	097-001		Indeterminate	1575377	503339	2015
26	Tigala 2	097-002		Middle Aksumite	1575342	503404	2015
27	Mtkal Wocho 2	098-002		Classic to Late Aksumite	1575647	505868	2015
28	Mai Meteto	098-003		Indeterminate	1575970	504252	2015
29	Ak'akuh	099-001		Indeterminate	1575899	507736	2015
	Other Sites						
1	N/A	059-001		Indeterminate	1579871	505091	2015
2	Adi Klte 2	085-002		Indeterminate	1576218	501312	2015
3	Mtkal Wocho	098-001		Indeterminate	1575621	505750	2015
4	Mai Omo	998-001		Indeterminate	1573271	503109	2015

5	Mai Omo	998-002		Indeterminate	1573271	503109	2015
6	Mai Omo	998-003		Indeterminate	1573353	503124	2015
Sites with an asterisk (*) are dated solely by diagnostic lithic remains							
		All Sites are in UTM Zone 37 North Adindan					

Chapter 6

Creating Preliminary Exploratory Geological Resource Maps of Copper in Oman and Obsidian in Ethiopia

6.1. Introduction

The goal of this chapter is to present the process by which preliminary exploratory geological resource maps were created for the two study regions in Oman and Ethiopia. Creating these maps was undertaken with the dual objective of (1) gaining a general spatial understanding of the distribution of copper and obsidian sources and (2) assisting in the identification of production sites associated with sources. This method does not purport to link production sites to sources, but rather to map the spatial distribution of potential sources.

The second objective was achieved in Oman, where production sites are often located either in close proximity to or in the general vicinity of copper sources. Smelting sites recorded following ground-truthing of potential copper resource maps therefore became nodes in the copper production networks, which were subsequently analyzed using Social Network Analysis (SNA) methods.

In Ethiopia, on the other hand, the production landscape under investigation is located tens or hundreds of kilometers away from the volcanic environments that likely originated the obsidian sources. As such, satellite imagery for obsidian detection did not lead to the discovery of

production sites. Indeed, with one exception,[43] ground-truthing of potential obsidian sources was unachievable because these landscapes are remote and difficult to access.

Gaining a high-resolution understanding of the distribution of copper sources in Oman and of obsidian outcrops in Ethiopia was deemed unachievable merely with the aid of traditional geological maps. This is because many current geological maps, and certainly the ones available for Ethiopia and to a lesser extent for Oman, generally identify the locations of copper minerals and obsidian outcroppings with the larger geological units they are embedded into. However, the complexities of copper mineralization and obsidian formation result in the development of spatially heterogenous landscapes which are often characterized by granular and sporadic distributions of comingled rocks and minerals.

This circumstance created the need for high resolution spectral mapping which was undertaken through analysis of Hyperion hyperspectral satellite imagery. It is important to note that information gained through the consultation of traditional geological maps ultimately proved invaluable in the creation of the final resource maps and that, indeed, the best product will result from the combination of all available data streams.

Satellite imagery mapping allows the remote surveillance of large areas in relatively inexpensive and expeditious ways and facilitates the mapping of inaccessible landscapes, whether that inaccessibility is due to safety concerns or geographical remoteness. Hyperspectral satellite imagery has the potential to produce detailed and precise maps, which are particularly representative of the patchy distribution of many raw materials. To be clear, establishing accuracy,

[43] In 2014, Dumitru joined a research team led by Steve Brandt (University of Florida) which focused on an area near the modern town of Wolaita Sodo (in southern Ethiopia). This area represents the location of the prehistoric obsidian production site of Humbo Baantu. A survey of the surrounding geology of the site was conducted to map obsidian sources. Subsequent detection run on a Hyperion swath containing Humbo Baantu identified the location of potential obsidian sources surrounding the site (Dumitru and Harrower 2019a).

where this method is concerned, still depends upon ground-truthing. However, as the methodology improves and is better understood over time, confidence may be achieved with minimal highly targeted ground-truthing.

This chapter is divided into two parts. The first part details the process of creating a preliminary resource map of potential copper mineral distributions in the al-Hajar mountains of north-eastern Oman and begins with a brief introduction to the geology of Oman. The second section reviews the similar process by which preliminary resource maps of potential obsidian outcroppings were produced and begins with an introduction to volcanism in the northern Horn of Africa. Satellite images analyzed represent areas in the Danakil depression and in the Eastern Rift Valley, both of which were characterized by a series of intense volcanic events.

6.2. Geology of Oman

The environments and ecologies that arose in southeastern Arabia, as well as the lifeways humans developed to adapt to them, were in large part influenced by the al-Hajar mountain chain. Occupying the northeastern corner of Oman, the al-Hajar Mountains developed through a series of geological processes. Perhaps the most important of these processes, both for the geological evolution of the region as well as for its later economic and socio-cultural development was the emplacement of oceanic crust, or ophiolite, onto the continental margin of the Arabian Plate (Glennie 2005).

Being a cross-section of oceanic lithosphere, the Semail ophiolite unit is the second allochtonous unit to be emplaced onto the Arabian continental margin. This emplacement event followed a previous one which consisted of the emplacement of the so-called Hawasina nappes. Named after Wadi Hawasina, in the northern al-Hajar mountains, where portions of this

tectonostratigraphic unit were first identified, the Hawasina nappes formed concomitantly with the Arabian plate, between the Late Permian and the Late Cretaceous. The Hawasina unit is made up of Hawasina sequence continental rise sediments, Sumeini continental slope sediments, Haybi oceanic sediments, and Kawr group so-called "Oman Exotics" (Pillevuit et al. 1997), that formed in the Hawasina basin, at the southern margin of the Neotethys Ocean. The sediments that formed in the deepest parts of the basin, where calcium carbonate dissolves and where there is an absence of continental sediments, are made up of the silica-rich mineralized skeletal remains of radiolarian protozoa and are called radiolarian chert deposits.

The second allochtonous unit is made up of the Semail ophiolite[44] which is the source of most copper deposits in the al-Hajar. At a length of 500 km, a width ranging from 50 to 100 km, and a thickness of roughly 15 km, the Semail unit represents the largest intact ophiolite unit in the world (Glennie et al. 1974, Boudier and Nicolas 1995). This unit is made up of two types of magmatic rocks: (1) Triassic to Mid Cretaceous basalts and gabbros that developed at the spreading center of the Neotethys Ocean and (2) Mid Cretaceous basalts and andesites that developed in a supra-subduction zone (SSZ) and were later thrust into the basalt and gabbro layer (Goodenough et al. 2013). The process of obduction began roughly 80 Mya (Searle 2007) in the Late Cretaceous.

The al-Hajar mountains extend along a 700-km long arc that parallels the coast, beginning in the northwest near the Straits of Hormuz and ending in the southeast, towards the Arabian Sea. At

[44] Ophiolite sequences, representing an igneous cross section of the oceanic lithosphere, derive their name from the Greek words for snake (ὄφις) and stone (λίθος). The term undoubtedly is meant to emphasize the prevalence of green colors among the rocks that make up the ophiolite sequence. The term was coined by French mineralogist Alexandre Brongniart, and initially used in reference to green-colored serpentinites and diabase rocks observed in the Alps. In observing ophiolites in the Alps, the early twentieth century German geologist Gustav Steinmann altered this category of rocks to include serpentinites, pillow lavas, and chert (an assemblage of rocks that have subsequently been termed Steinmann's trinity). This term only gained traction in the early 1960s following the recognition that ophiolite assemblages characterize oceanic crust that formed through ocean floor spreading and was emplaced onto land. Indeed, this discovery was instrumental in refining the theory of plate tectonics, as ophiolites indicated the existence of now defunct ocean basins that had been subducted under continental plates.

their widest, the chain measures 120 km, with its narrowest portion measuring 40 km in width. Millennia of seasonal washes flowing over the mountains have produced wadis, or ravines, creating passes that connect the interior of the country with the Batinah coastal plain. In addition to the passes, the washes transported tons of alluvial sediment which, over the period of the Pleistocene and Early Holocene, contributed to the creation of large alluvial plains on both sides of the al-Hajar Mountains. Areas in which the alluvial deposition coincided with the availability of groundwater sources saw the development of horticultural and agricultural activities, primarily concentrating around date palm cultivation.

Their complicated orogenesis has made the al-Hajar Mountains an important source of sundry raw materials of economic significance. Historically, the most important resources seem to have been copper, for which there is evidence of exploitation as early as the Neolithic period (Weisgerber 1980, 1981; Weeks 1999, 2003), chlorite, most commonly used to shape vessels and exploited as early as the Umm an-Nar period (Harrower et al. 2016, David 2002), and different types of clay that were used across the millennia in the production of many successive ceramic industries. In the region surrounding the ArWHO research area previous geological studies have determined that copper, gold, chromite, iron, and manganese are important mineral resources that are being exploited to this day.

The research area that is under investigation surrounds the town of Yanqul, which is located 150 km west of Muscat in the eastern al-Hajar Mountains, in the ad-Dhahirah Governorate. Geologically, this area is characterized by four tectonostratigraphic units: (1) a pre-obduction

autochthonous unit,[45] (2) part of the Hawasina Nappes,[46] (3) a portion of the Semail Nappes, and (4) a post-nappe autochthonous unit[47] (Villey et al. 1986).

Copper mineralization largely occurs in the Semail Ophiolite Nappe which can be sub-divided into three subunits, all of which are represented in the research area. The lowest subunit is comprised of tectonites, the middle subunit contains a layered cumulate series, while the top-most subunit is characterized by high-level gabbros in a complex of volcanic and subvolcanic rocks. This primary suite was later intruded by magmatic rocks from a later volcanic event. In most areas the Semail unit rests on top of Hawasina Nappes; however, because of post-obduction thrusting and overturning, in some parts of the mountains, the tectonostratigraphic sequence is reversed. Most copper mineralization has been observed in particular in the sheeted dyke, cumulate layered gabbro, and high-level gabbro complexes, a pattern that has also been corroborated through ground-truthing of detection results.

[45] The pre-obduction autochthonous unit represents a portion of the Arabian plate, whose position was altered following the obduction event that thrust the Hawasina and Semail nappes onto the margin of the continent.

[46] The Hawasina Nappes overlie the pre-obduction autochthonous unit and are made up of three sequences of rocks. The lowest subunit, the so-called Hamrat Duru Group, is a sedimentary unit mainly comprised of turbidites. The Hamrat Duru Group originally formed between the Late Permian and the Late Cretaceous. The middle subunit is the so-called al-Aridh Group and is made up of slope deposits, while the top-most unit, the sedimentary Umar Basin Group contains micritic limestone and radiolarian chert. Post-obduction tectonics, involving secondary thrusting processes, overturning, and folding, have created a cross-section in which older subunits override and overlap with younger ones.

[47] The post-nappe autochthonous unit is made up of Late Cretaceous, Tertiary, and Quaternary rocks. The Late Cretaceous (Maastrichtian) and Tertiary rocks are sedimentary, overlie the Nappes, and are located to the southwest of Yanqul. The Quaternary deposits are comprised of alluvial sediments and scree and can be found around Yanqul and to the northeast, on the Batinah plain.

6.2.1. Creating a Preliminary Exploratory Geological Resource Map of Copper in Northeast Oman

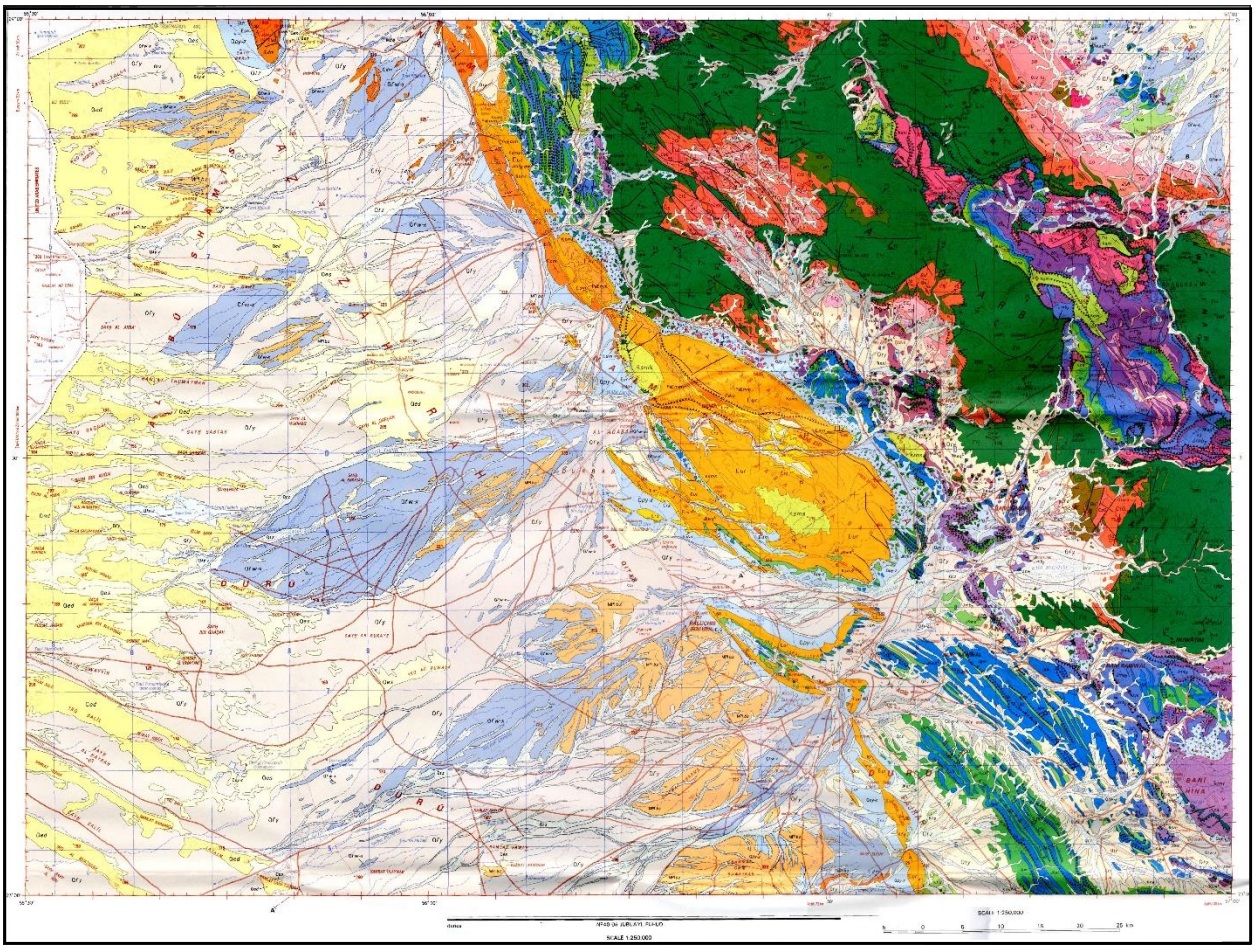

Figure 6.1 Ibri Geological Map (1:250,000) created by Béchennec et al. 1992.

Creating a resource map of copper distribution in north-eastern Oman has been a multistep process involving satellite imagery analysis, ground-truthing, and judgmental triage of results following the removal of areas with verified false positive detection, as well as the elimination of results from geological contexts that do not support copper mineralization. This last step would not have been possible in the absence of geological maps. The map used was at a scale of 1: 250,000 and centered around the Ibri area (Fig. 6.1) in the northwestern part of the central al-Hajar (Béchennec et al. 1992).

6.2.1.1. Detection Workflow

The layouts presented in this chapter are the result of a lengthy process. Initial detection was undertaken using ERDAS Imagine's Spectral Analysis module and the Orthogonal Subspace Projection (OSP). In 2012, detection layouts produced using this method were the first to be ground-truthed.

Figure 6.2 Total Hyperion Coverage in the ArWHO Survey Area.

Since this first round of ground-truthing, I slowly began transitioning from using ERDAS Imagine to ENVI for all remote sensing work. With few exceptions, most layouts included in this chapter were produced using ENVI 5.3's Target Detection Wizard.

The target detection workflow is a multistep process. The Hyperion imagery was ordered from the EarthExplorer (EE) online search tool developed by the United States Geological Survey (USGS). Hyperion provided near total coverage of the ArWHO survey area (Fig. 6.2). Many regions within this area had been collected more than once. When this was the case, the swath that was least impacted by cloud cover was selected. Because they are radiometrically and geometrically corrected, Hyperion L1G level products were selected for analysis. However, the available version of ENVI was unable to ingest the L1G data format (GeoTIFF). As such, it became necessary to download the Hyperion Tools plugin for ENVI.[48] Once brought into the program, the Hyperion swath was atmospherically corrected using ENVI's FLAASH tool which output scaled reflectance values. The ensuing reflectance image was analyzed using the Target Detection Wizard which output a shapefile that was used to create layouts in ArcGIS Pro.

Pre-processing of Satellite Imagery: atmospheric correction and data calibration – The amount and quality of information that can be extracted from satellite imagery is lessened by atmospheric effects, by coarse spatial, spectral, and temporal resolution (Warner et al. 2009: 47).

By the time electromagnetic energy is recorded by the sensor on board a satellite it will have passed through the atmosphere twice and been subjected to processes of absorption and scattering, thereby affecting the accuracy of the image. Atmospheric correction is, therefore, undertaken to remove the effects of scattering and absorption and produce an image representing surface reflectance. Used to atmospherically correct the Hyperion images analyzed for this project, ENVI's Fast Line-of-sight Atmospheric Analysis Hypercubes (FLAASH) tool works with

[48] Code for this tool was written by Devin White (Urban Dynamics Institute, Oak Ridge National Laboratory) and was made available on the Excelis VIS code library.

hyperspectral and multispectral data and corrects wavelengths from the visible range through the near-infrared and shortwave infrared ranges.

Before employing FLAASH, a radiance image is produced using ENVI's Radiometric Calibration tool. The resulting image is supported by the FLAASH tool and characterized by a band-interleaved-by-line (BIL) format, with a floating-point data type, and a scale factor of 0.1. This process scales the data to units supported by FLAASH: μW/ (cm2 * sr * nm). Before the data is analyzed, bad bands are removed (Table 6.1).

Table 6.1 Hyperion Bad Bands.

1 – 7	Not illuminated
58 – 78	Overlap Region
120 – 132	Water Vapor Absorption Band
165 – 182	Water Vapor Absorption Band
185 – 187	Identified by Hyperion Bad Band List
221 – 224	Water Vapor Absorption Band
225 – 242	Not illuminated

FLAASH necessitates several input parameters to be able to undertake atmospheric correction. These include: (1) scene center location (in latitude/ longitude), (2) sensor altitude (705 km), (3) mean ground elevation (km), pixel size (30 m), (4) flight date, (5) flight time, (6) atmospheric model (can be selected from a drop-down list of standard MODTRAN® model atmospheres), etc.[49]

[49] Note that the Tile Size (MB) is set to 100 by default. However, at this processing size, the atmospheric correction process is unsuccessful. As such, the tile size must be increased. This can be done through FLAASH's Advanced Settings. I increased tile size to 4700 MB.

Classification Methods – Once the image was converted to reflectance, target detection was undertaken using both ERDAS IMAGINE 2016 and 2018 Spectral Analysis Workstation[50] and ENVI 5.3. Target Detection Wizard. Selecting the Target Detection mode is appropriate when analyzing images for spectra (targets) that are thought to be present in low concentrations within the scene. ENVI's Target Detection Wizard leads the analyst through a workflow that contains ten steps (Table 6.2).

Table 6.2 ENVI Target Detection Wizard Workflow.

Step	Process
1	Input Scene
2	Atmospheric Correction (optional)
3	Select Target Spectra
4	Select Non-Target Spectra (optional)
5	Apply MNF Transform (optional)
6	Select Target Detection Methods
7	Load Rule Images and Preview Results
8	Filter Targets
9	Export Results
10	View Statistics and Report

Spectral signatures are required for target detection. A spectral signature is the information used to radiometrically classify a pixel. Targeted material signatures were imported from the ASTER Spectral Library, which can be accessed directly through the Target Detection Wizard. In

[50] Because results obtained using ERDAS' workflow are not presented in this chapter, I will only describe the process by which detection was undertaken in ENVI 5.3.

total, detection was run using 15 spectral signatures of 5 copper minerals. Two carbonate minerals (Fig. 6.3; azurite $Cu_3(CO_3)_2(OH)_2$ and malachite $Cu_2CO_3(OH)_2$) and three sulfide minerals (Fig. 6.4; chalcopyrite ($CuFeS_2$, chalcocite (Cu_2S), and bornite (Cu_5FeS_4) were selected for detection. Three different signatures were utilized for each mineral, each collected from a coarse, medium, or fine sample (Fig. 6.5).

Spectral Properties of Copper Minerals – The SWIR portion of the EM spectrum is particularly useful for mapping copper minerals. Studies have shown that spectral signatures of carbonates, sulfates, and ferric iron are more successfully extracted from SWIR-1 bands (1.57-1.65µm). SWIR-2 bands (2.08-2.35µm) are specifically useful for detecting mineral such as copper and sulfates.

According to the USGS Spectral Library Version 7, the sulfide mineral chalcopyrite ($CuFeS_2$)[51] is characterized by a fall-off in reflectivity towards the blue as well as by a weak band near 0.9µm. These spectral characteristics are determined by the iron within the mineral, with the copper also making a contribution to the absorption feature around 0.9µm (Kokaly et al. 2017).

Both azurite ($Cu_3(CO_3)_2(OH)_2$) and malachite ($Cu_2CO_3(OH)_2$)[52] are secondary carbonate minerals, characterized by an atypical carbonate ion spectrum. The spectral signature of these carbonate minerals is characterized by a broad 0.8µm band and a short wavelength fall-off below 0.52µm. Three other features can be noticed in the spectral curve near 2.29, 2.37 and 2.52µm and are likely determined by CO_3.

[51] Spectra for this sample were originally collected in Quebec and published in: Hunt, G.R., J.W. Salisbury, and C.J. Lenhoff, 1971, Visible and near-infrared spectra of minerals and rocks: IV. Sulfides and sulfates Modern Geology, v. 3, p. 1-14. This sample contained 95% chalcopyrite and 5% pyrrhotite.

[52] The original spectrum was published in: Hunt, G.R., J.W. Salisbury, 1971, Visible and near-infrared spectra of minerals and rocks: II. Carbonates. Modern Geology, v. 2, p. 23-30 and was collected in Bisbee, Arizona.

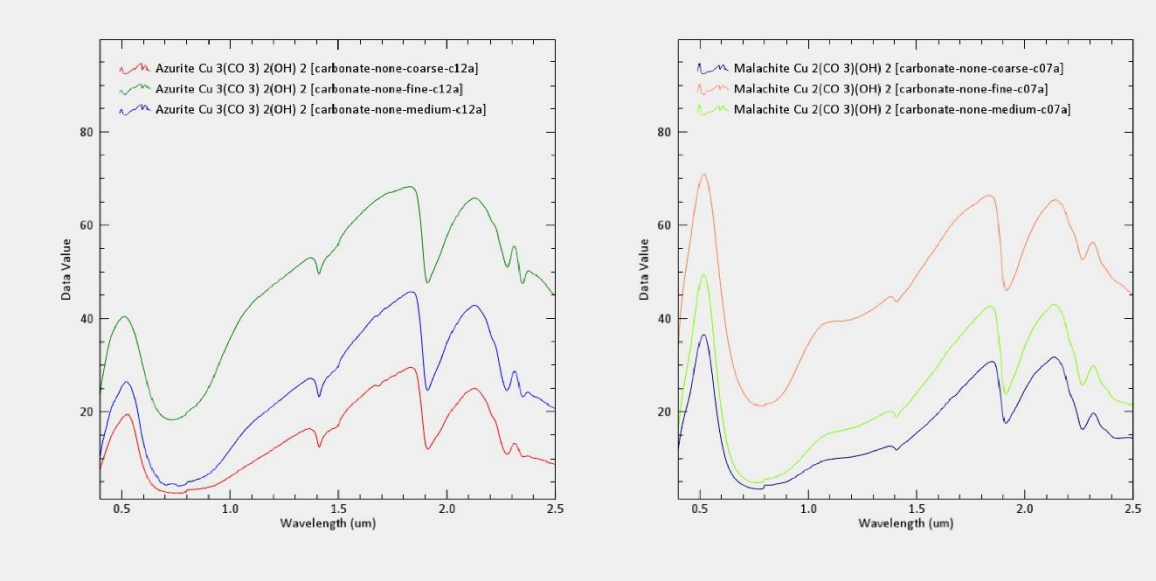

Figure 6.3 Carbonate Mineral Signatures.

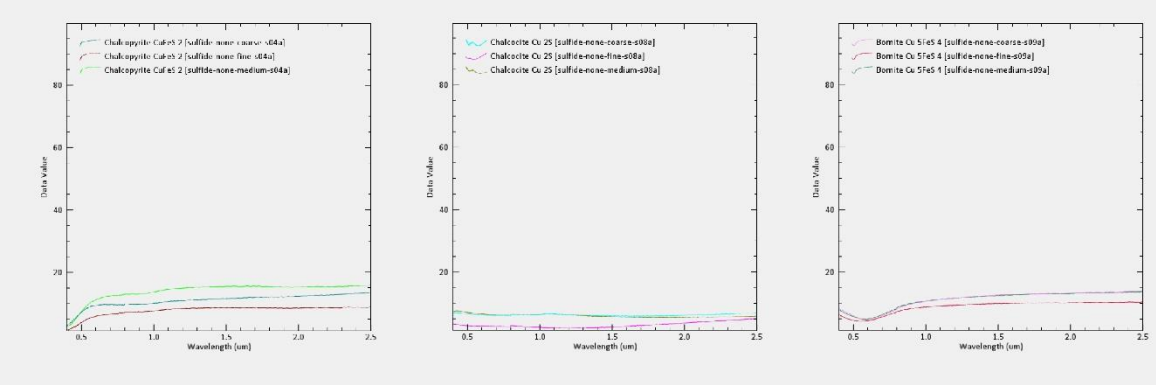

Figure 6.4 Sulfide Mineral Signatures.

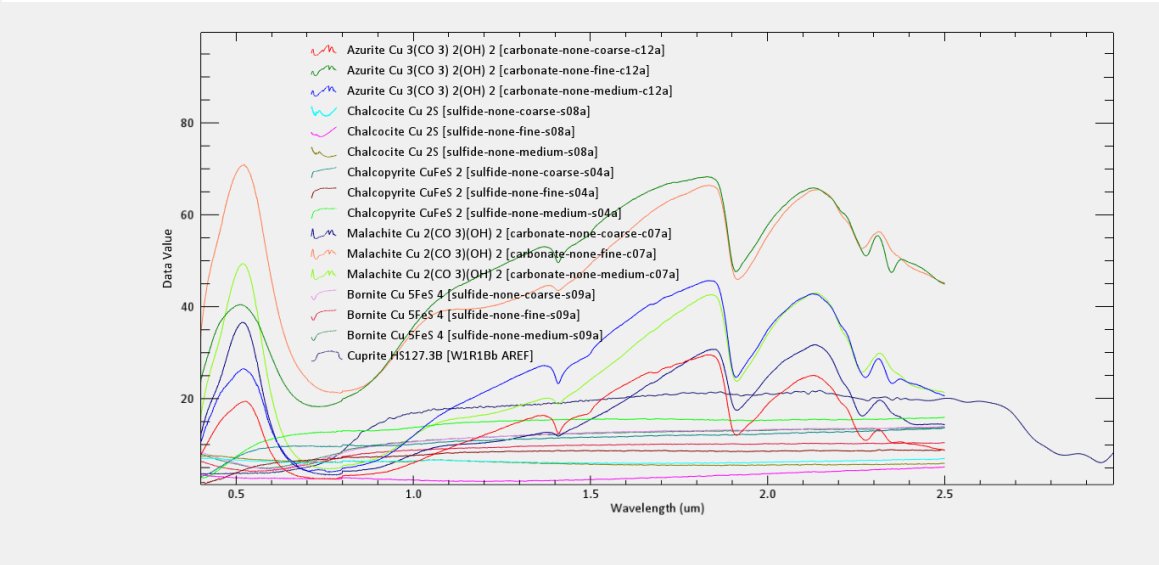

Figure 6.5 ASTER Spectral Signatures.

The target detection method selected was the Orthogonal Subspace Projection (OSP) algorithm. This classifier was created to differentiate between subpixel target component. In contrast to traditional linear spectral admixing methods (Lillesand and Kiefer 2000, Mundt et al. 2007), OSP aims to make pixel spectra and target spectra as similar as possible by reducing data dimensionality, suppressing background signal and minimizing the targeted spectra's signal to noise ratio. By designing an orthogonal subspace projector, the algorithm functions by eliminating non-targeted spectra from a pixel and then uses a matched filter to identify the targeted spectra.

The OSP hyperspectral imager classification technique was developed in 1994 by Harsanyi and Chang and is useful in facilitating linear unmixing.[53] This method was born out of a desire to utilize *a priori* knowledge of a scene and of a target when analyzing hundreds of contiguous hyperspectral bands. This method allows for the selection of target signatures that the analyst desires to locate and target signatures that the analyst wishes to ignore. The latter are target signatures that are believed to exist in the analysis scene, but not wanted in the final analysis map.

6.2.1.2. Ground-truthing

The ground-truthing aspect of this project included a survey whereby targeted pixels were observed on the ground to verify or refute their detection. Undertaken at the location of detection, a targeted pixel was verified through surface observations of visual properties. Information regarding its detection status (false positive vs. true positive) was recorded using a Trimble GeoXH GPS. Spatial data was subsequently imported into a GIS to aid in the elimination of false positives (Fig. 6.6). Thus, while the aim of ground-truthing is to eliminate errors of commission, the rate of

[53] J. C. Harsanyi, C.-I Chang, "Hyperspectral image classification and dimensionality reduction: An orthogonal subspace projection", IEEE Trans. Geosci. Remote Sens., vol. 32, no. 4, pp. 779-785, Jul. 1994.

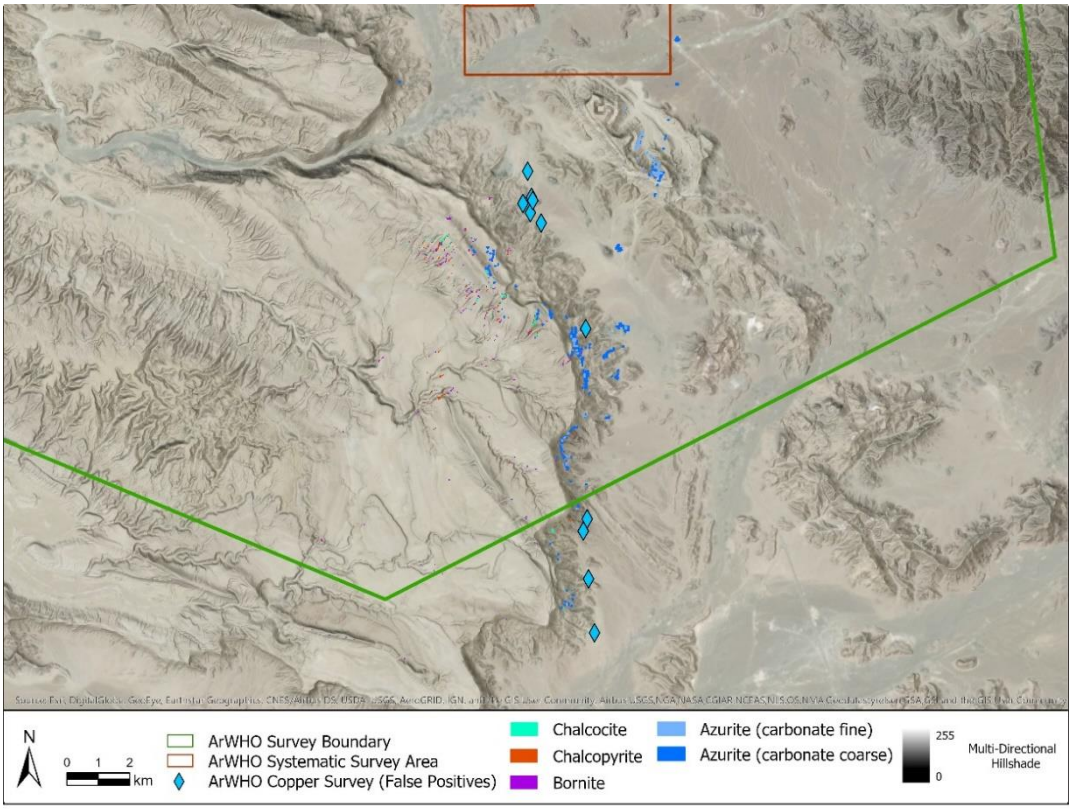

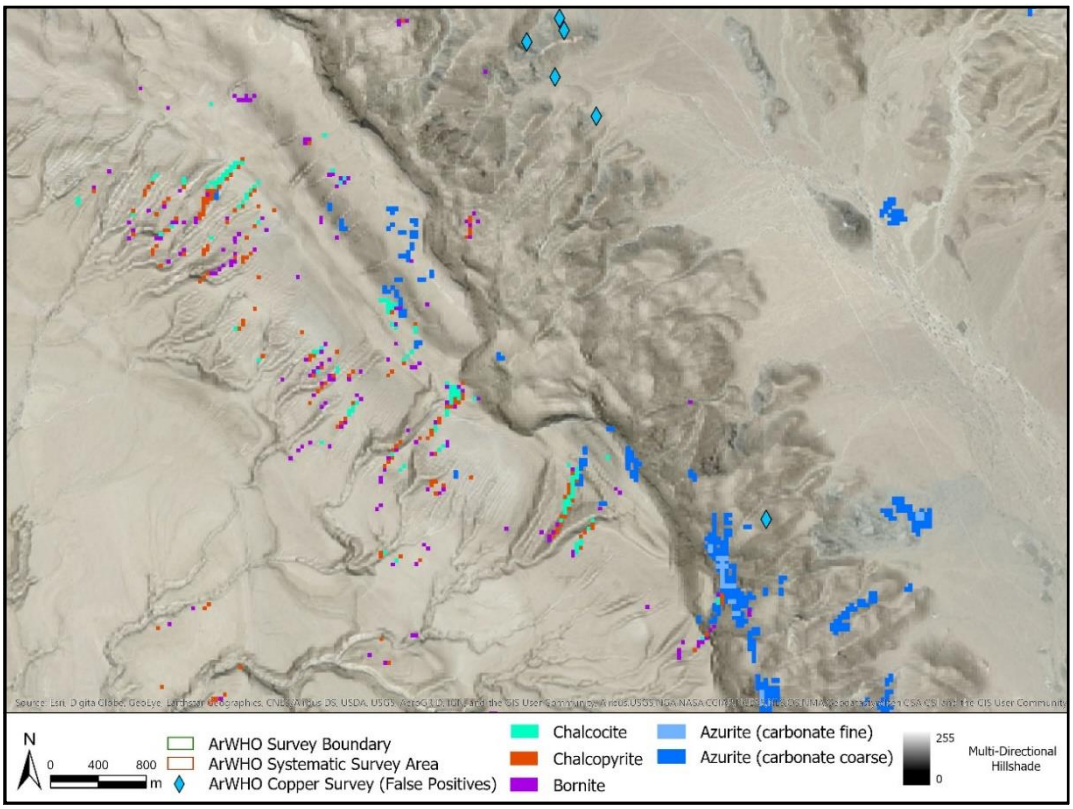

Figure 6.6 Positives identified through ground truthing.

errors of omission is established through a survey of randomly selected areas within the survey region.

ArWHO Copper Survey: Geological Results – As full-coverage survey was unfeasible, the selection of ground-truthing locations was determined by accessibility, proximity to known smelting sites, and geological formations that can host copper minerals. For geological information, the survey team relied on the *Geological Map of Ibri* commissioned by Oman's Ministry of Petroleum and Minerals, produced by a French team of surveyors, led by F. Béchennec, and published in 1992 by the Bureau de Recherches Géologiques et Minières. This process resulted

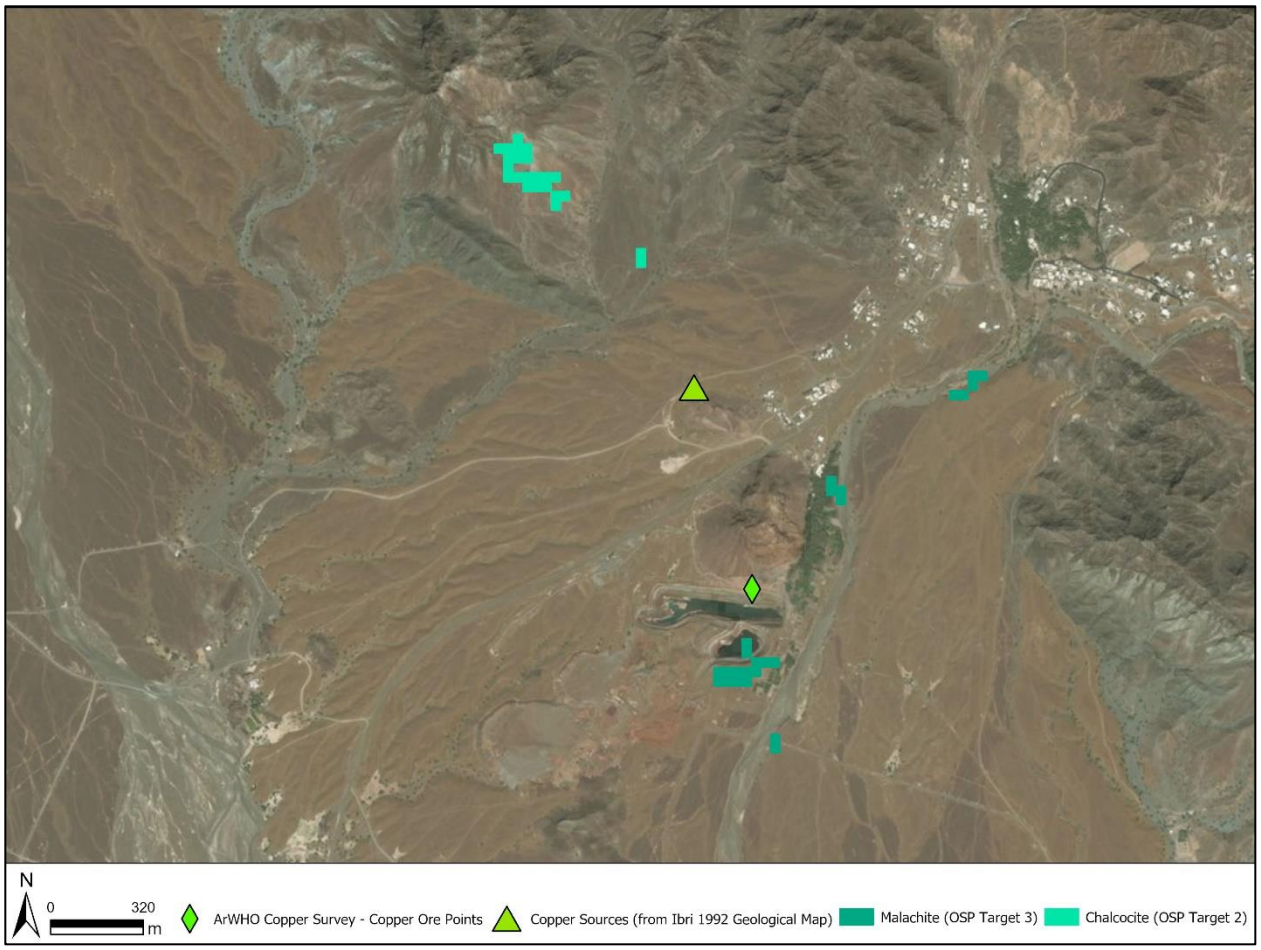

Figure 6.7 Chalcocite and malachite detection in the area surrounding Sayyah mine.

in the identification of mineral-rich micro-regions within the larger potentially copper-bearing geologies, thereby streamlining prospection.

Most of the sites that were confirmed or discovered through ground-truthing were characterized by easily identifiable copper minerals which were field identified based on color and crystalline habit.

Gossans, enriched with iron and manganese oxides, are typical of massive sulfide ore sources. These often co-occur with oxides, carbonates, and silicates of copper, including malachite and chrysocolla. It would appear that sulfides like chalcopyrite, chalcocite, and bornite are more commonly deeper in host rock. The entire sequence of commonly formed massive sulfides typical

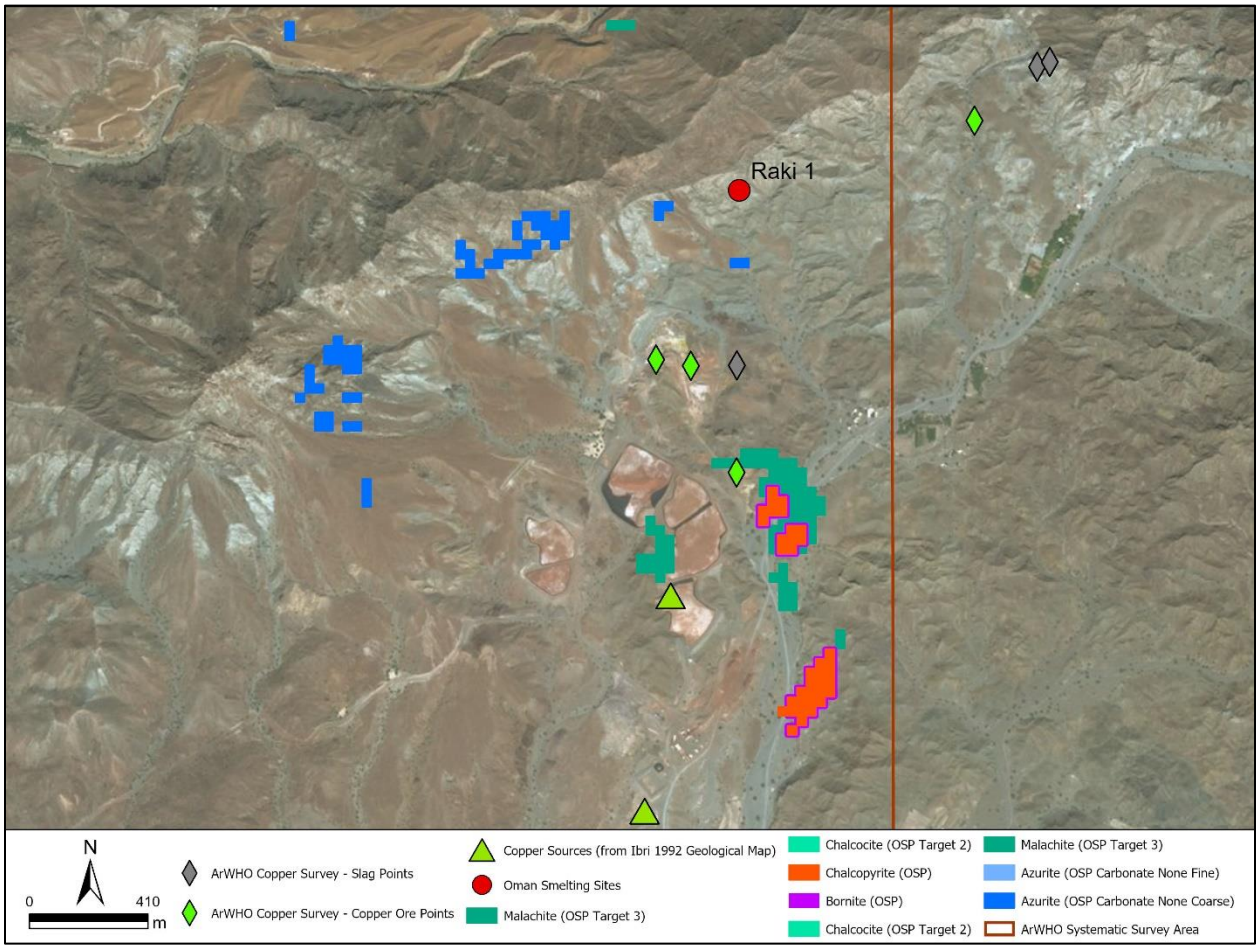

Figure 6.8 Detection of multiple sulfide and carbonate copper minerals in the area surrounding the Raki mine.

of ophiolitic environments globally was observed at larger modern mines (e.g. Sayyah, see Fig. 6.7, and Raki, see Fig. 6.8). This sequence was sampled and will be used for further analysis.

Many small deposits[54] appear to have been important to the ancient history of copper exploitation and production in Oman. One example of a notable small deposit originates near the smelting site of Muaydin. The small Muaydin deposit was discovered in an intact gossan. Cut by vertical water channels, the gossan reveals primary and secondary copper minerals (Fig. 6.9).

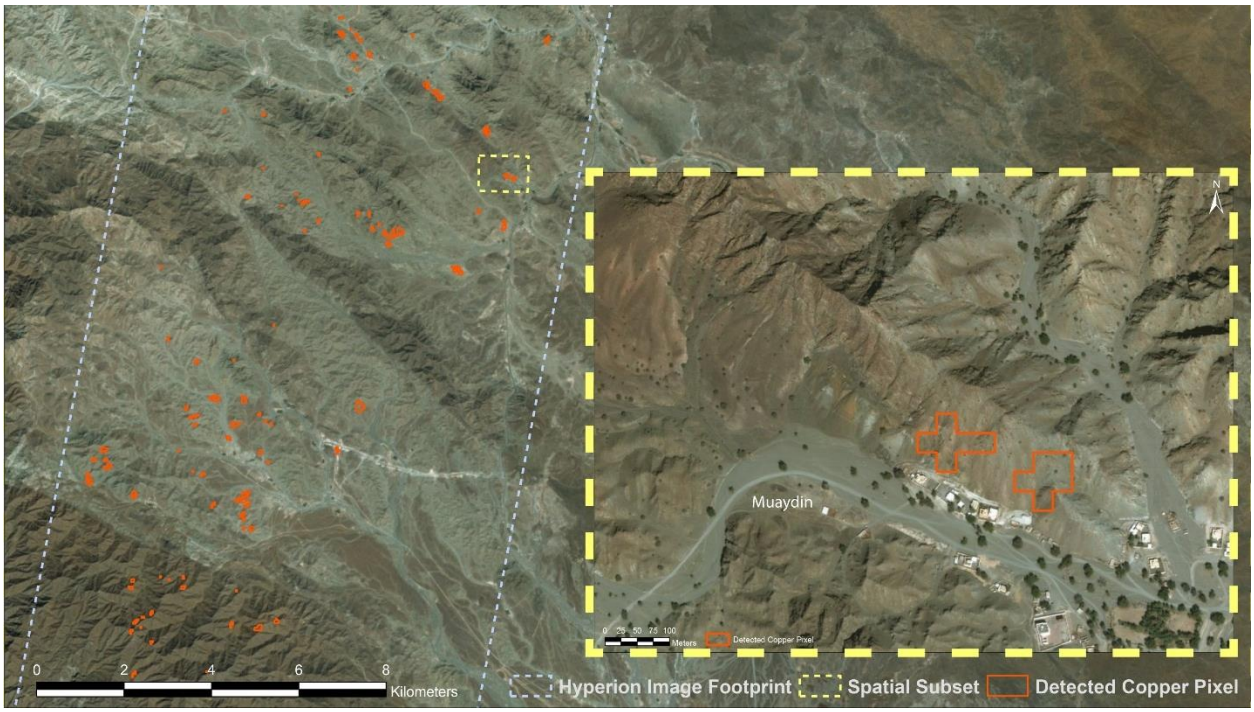

Figure 6.9 Map of Hyperion hyperspectral imagery target detection results for copper around the Iron Age metal working site of Muaydin rediscovered by the ArWHO Project in 2015 (inset imagery: Worldview-2 courtesy of Digital Globe; background imagery: Landsat-8 from USGS).

An interesting difference between the Muaydin deposit and the Raki deposit was noted in the field.[55] The Muaydin host rock of the copper ore were observed to be deeper in the ophiolite

[54] This is quantified in contrast to larger deposits associated with smelting sites that saw the production of thousands of pounds of copper.
[55] This observation was made by Dr. Joseph (Seppi) Lehner, Faculty of Arts and Social Sciences, Sydney University, and by field geologist, Alexander Sivitskis.

sequence than the Raki ore deposit. The Muaydin host rock includes blocks of sheeted dyke and possible lower units of harzburgite and dunite. This appears to be an uncommon occurrence in Oman, as such lower units usually do not contain evidence of copper mineralization. Highly fractured and faulted and likely forming in a hydrothermal environment, the Muaydin blocks may be the result of a different developmental history relative to the larger ore sources and could potentially be characterized by chemical and isotopic differences.

The Ibri map[56] records 11 copper deposits, 7 of which are located within the ArWHO Survey region (Fig. 6.10). Figure 10 reveals detection surrounding all 7 identified copper locations. Notably, most targeted spectra were detected in sheeted dyke, lower extrusive rock, basaltic pillow lavas, upper extrusive rocks, and cumulate layered gabbro.

When compared with the information recorded in the geological map, the usefulness of analyzing satellite imagery to remotely identify copper minerals becomes apparent, as it reveals the locations of previously unidentified copper sources. Noting, however, the high incidence of bornite detection which exceeds all expectations, it also becomes apparent that better methods are needed to more successfully eliminate errors of commission. Identifying and verifying such methods is presently outside of the scope of this dissertation. Ground-truthing of these areas revealed positive detections (Fig. 6.11a) as well as negative detections (Fig 6.11b).

This method has also been able to validate information gained through archaeometallurgical surveys (Weisgerber 1977, 1978, 1980) and has yielded detailed localized copper resource maps of significant ancient copper producing landscapes (see Fig. 6.12). Located in the northern stretches of the ArWHO systematic survey area lies a production landscape dotted with Iron Age

[56] Georeferencing of the *Geological Map of Ibri* was undertaken by Alexander Sivitskis.

and Islamic period smelting sites which have cumulatively produced approximately 150,000 tons of slag (Hauptmann 1985: 100). This landscape includes the sites of Raki 1, Raki 2, and Tawi Raki 1 – 3 (Fig. 6.12).

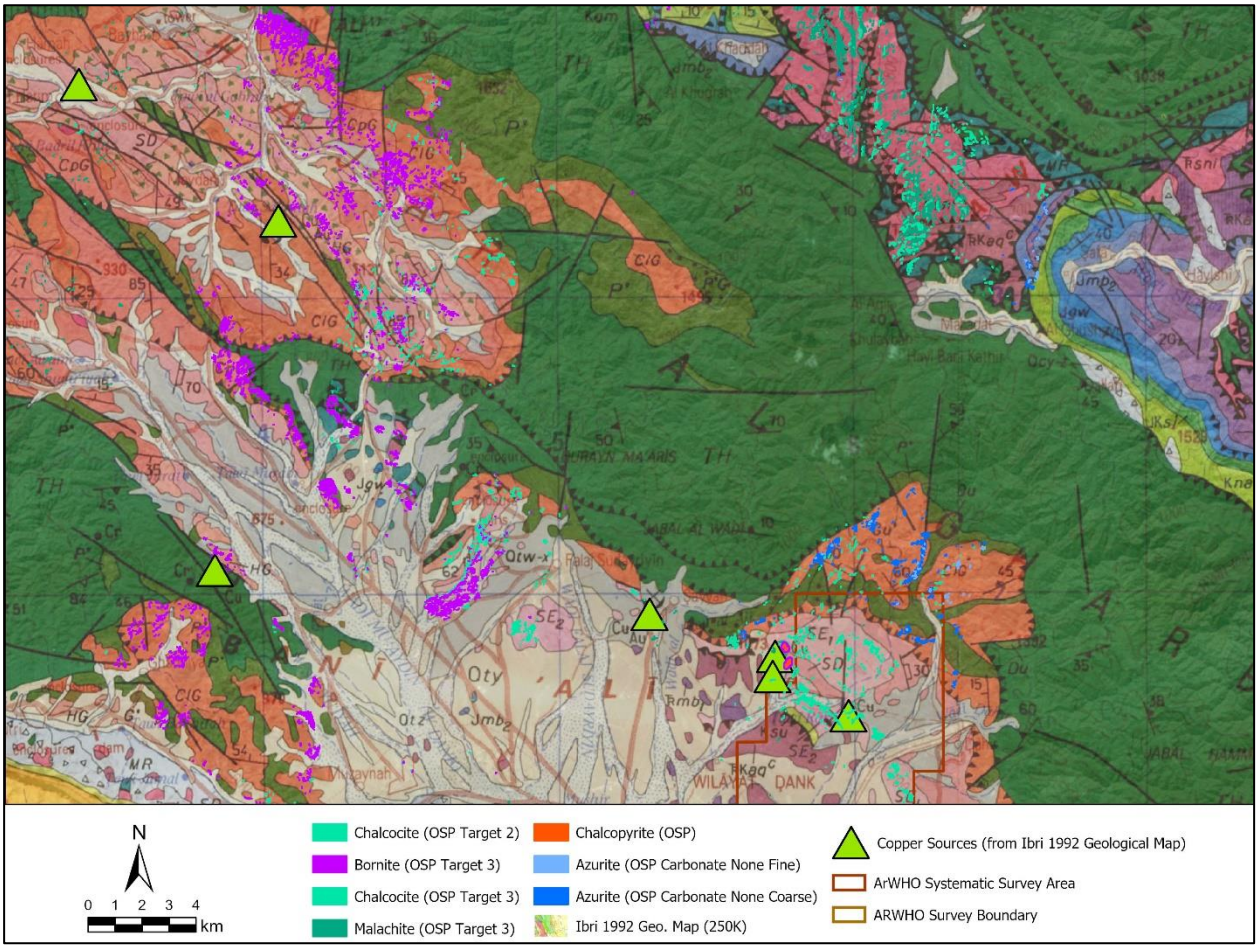

Figure 6.10 Detection around 7 copper deposits recorded in the 1992 Geological Map of Ibri (250K). Both detected spectra and the locations of the 7 copper deposits are overlaid on top of the georeferenced map.

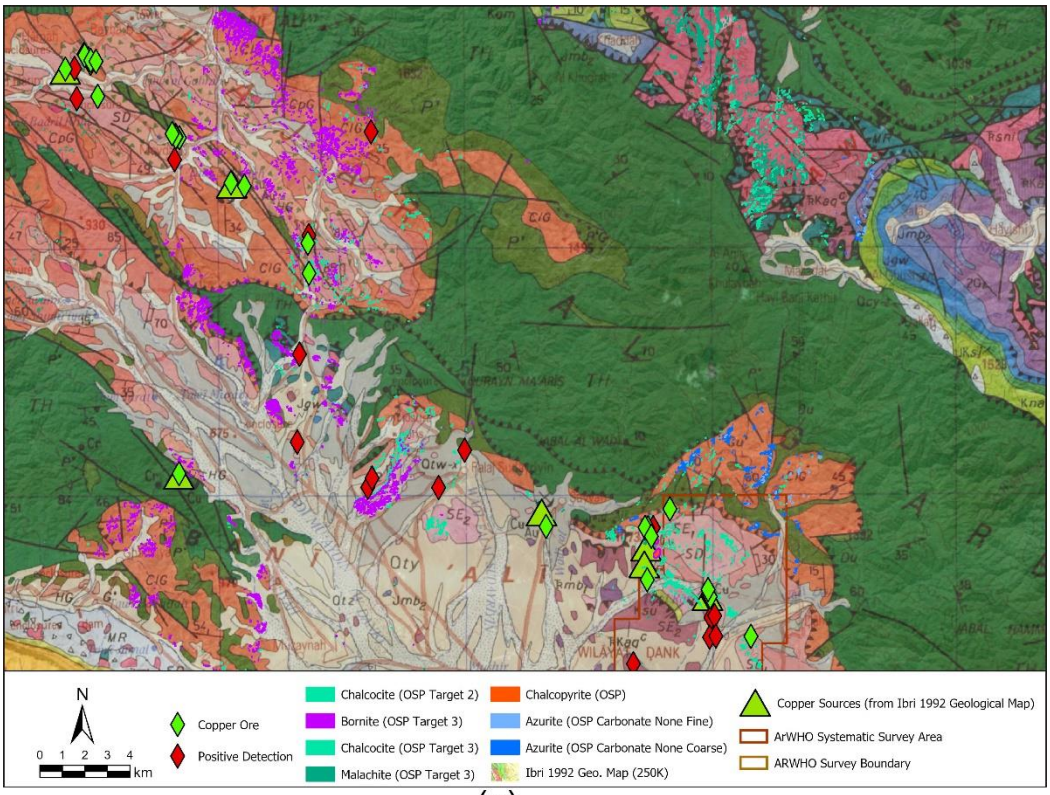

(a)

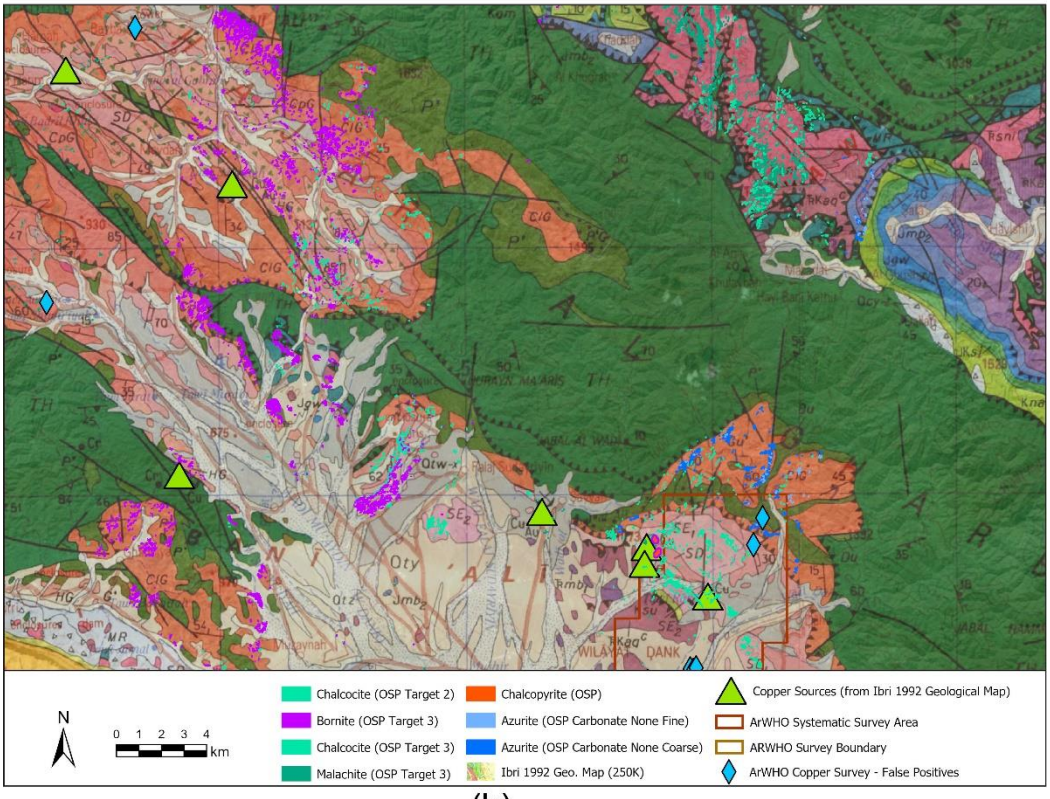

(b)

Figure 6.11 Detections around the 7 identified copper deposits with true positives (a) and false positives (b) represented.

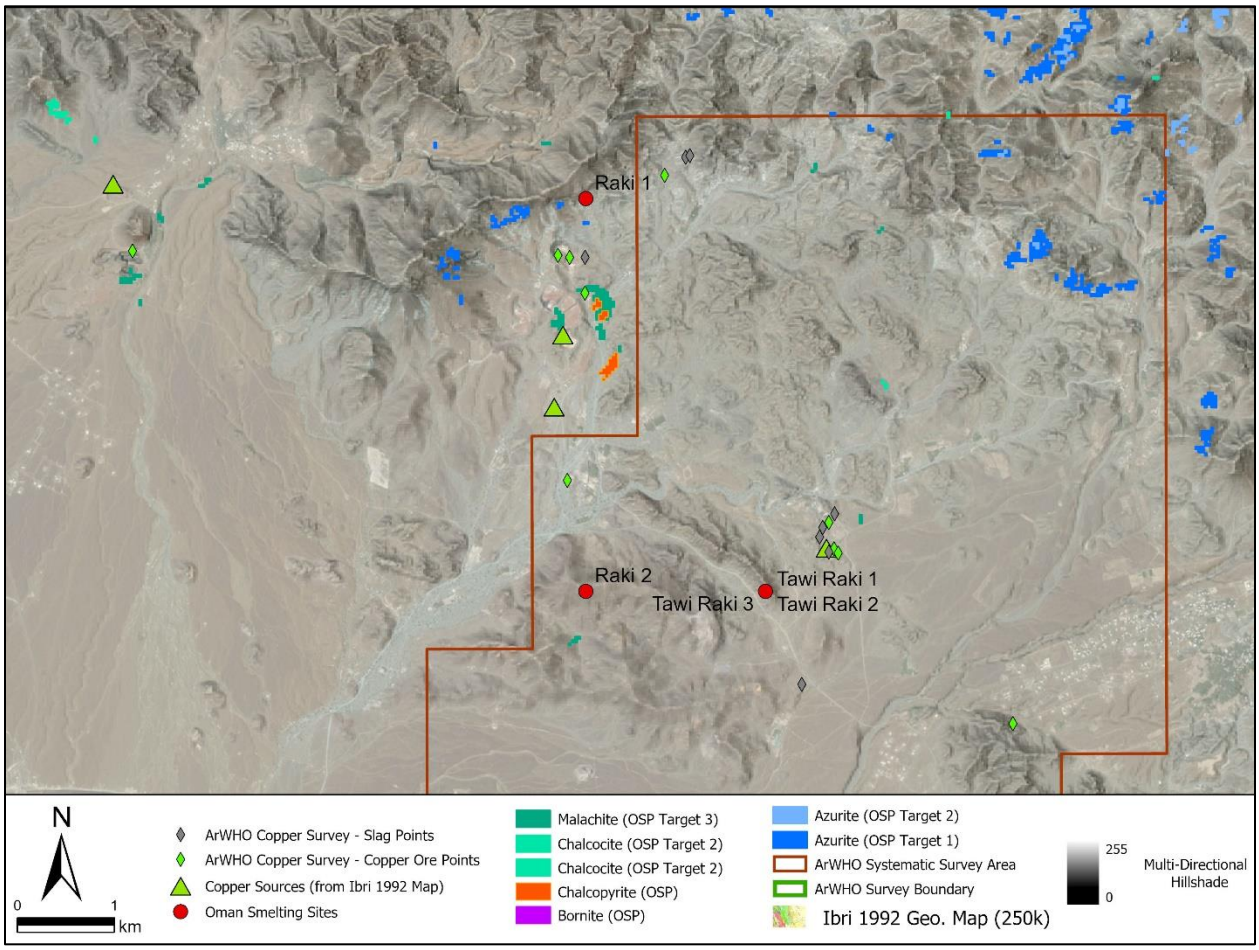

Figure 6.12 Cupriferous landscape surrounding Raki 1 - 2 and Tawi Raki 1 - 3, as revealed through target detection.

The mineral richness of the geology surrounding Raki 1 continues to be exploited to this day, though open-cast mining. Note that in Figure 6.8, in which the landscape surrounding Raki 1 is represented, the detected pixels appear to be slightly offset from the modern mine. This is owing to georeferencing issues that are still in the process of being resolved.

One other important ancient mining and smelting landscape was identified in the Greater Arja region of Wadi Jizzi, located in Al Batinah North (Hauptmann 1985). A cluster of sites, including Arja, Tawi Arja, Bayda, Arja Shemaal, and Umar West, have been recorded in this region whose cupriferous geology continues to be exploited to this day (Fig. 6.13).

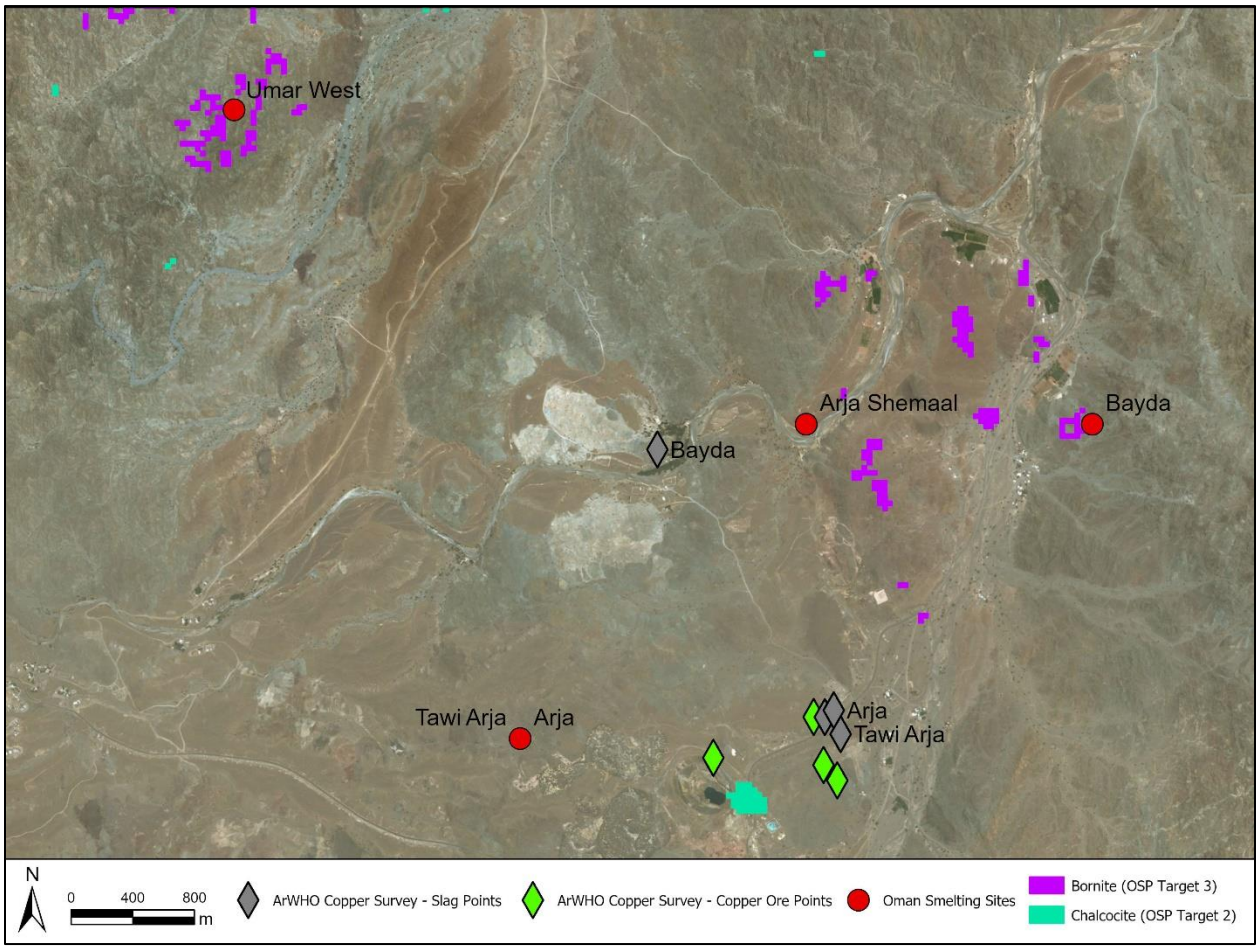

Figure 6.13 Cupriferous landscape of the Greater Arja region as revealed through target detection.

The sites certified through ground-truthing were characterized by readily distinguishable copper minerals, identified by their color, physical properties, and crystal habit. Sites identified through detection were in the Samail Nappe ophiolite sequence, in particular in the sheeted dyke, cumulate layered gabbro, and high-level gabbro complexes. In figure 6.14, the aggregate of ground-truthing data located in the ArWHO Systematic Survey region is represented.

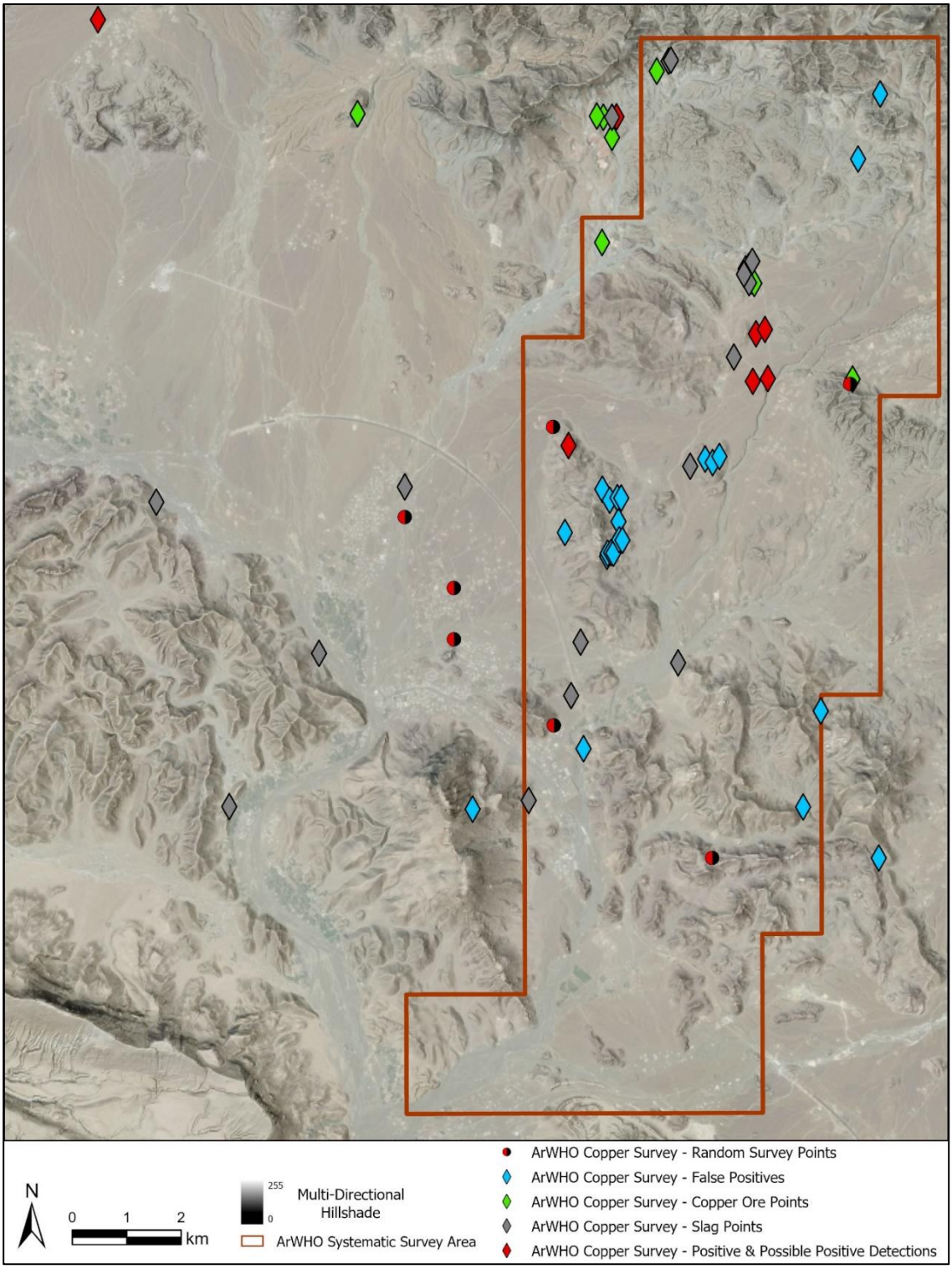

Figure 6.14 All ground truthed and surveyed locations in the ArWHO Systematic Survey region.

Figure 6.15 reveals the entirety of the spatial data collected through ground truthing and survey in the larger ArWHO region. Both layouts present data differentiated by type: false positives, true positives, locations of identified copper ore and slag, and points indicating random survey locations.

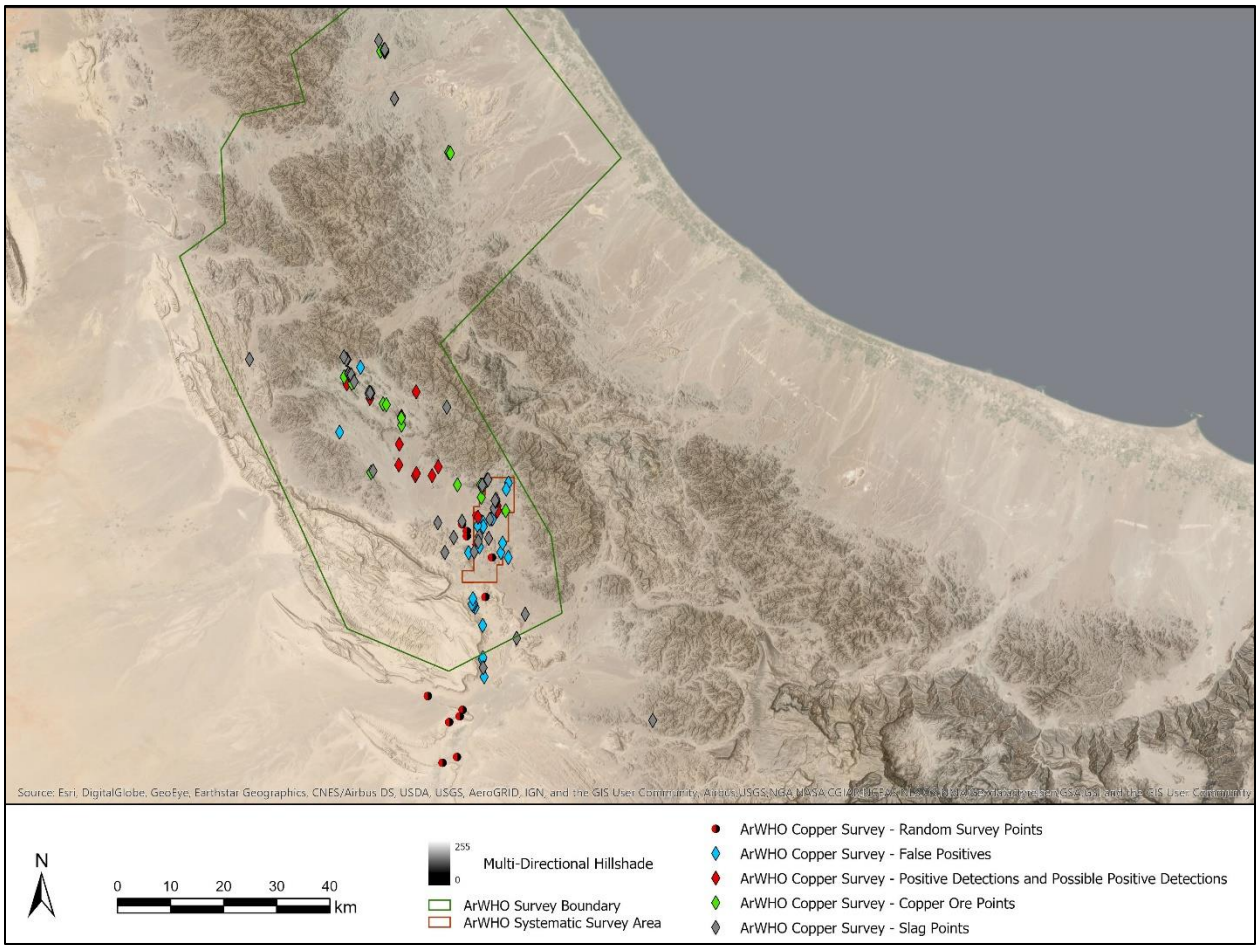

Figure 6.15 All ground truthed and surveyed locations in the larger ArWHO Survey region.

Random Survey – To determine the prevalence of false negatives, members of the ArWHO team[57] conducted a survey of randomly selected areas covered by Hyperion imagery that had been analyzed for the presence of copper-bearing minerals.

[57] The random survey was undertaken by Ioana A. Dumitru and Avary Taylor.

Twenty transects were selected for ground-truthing (Table 6.3). These were selected from within the boundaries of a 750 km^2 survey area, circumscribed by the boundaries of a Hyperion scene. A UTM grid divided into 500 by 500-meter sectors was overlaid on top of the area represented by the Hyperion scene. An online random number generator[58] was used to select the twenty sectors by generating 20 random numbers from 1 to 1179. This last number corresponds to the number of 500 by 500-meter sectors that make up the 750-square kilometer Hyperion scene.

To ensure adequate coverage, two field crew members standing about 125 meters apart walked lengthwise through each 500 x 500-meter sector. The initial positions for the surveyors were at 0 and 125 meters respectively. After a transect was walked lengthwise, the crew members would shift their positions until they were at the 250 and 375-meter marks. The transect would then be walked lengthwise once again in the opposite direction of the first walk-through. One crew member carried a Trimble GeoXH GPS and the other a handheld Garmin Etrex GPS, to ensure that the team remained within the designated transect boundaries. The Trimble GeoXH was also used to record the corner point at the beginning of the transect and was used to record any potential finds. These corner points were used to create the layout in Figure 6.16.

Of the twenty randomly selected sectors, six were inaccessible, being on top of Umm er-Radhuma Formation, the bioclastic, yellow marl, marly limestone, and limestone formation that divides Dhank from Yanqul. Undetected copper sources were not contained in any of the fourteen surveyed sectors. Undetected copper sources are also unlikely to be present in the four un-surveyed sectors, as these contained limestone geologies that are unlikely hosts of copper.

[58] www.graphpad.com/quickcalcs/randomN1

One sector (1457), located in a wadi within the boundary of the town of Yanqul, contained a large slag scatter (918-001), circumscribed by a ca. 360-meter perimeter. A single sherd was discovered amidst the smelting debris and on the basis of fabric has been tentatively dated to the Iron Age.

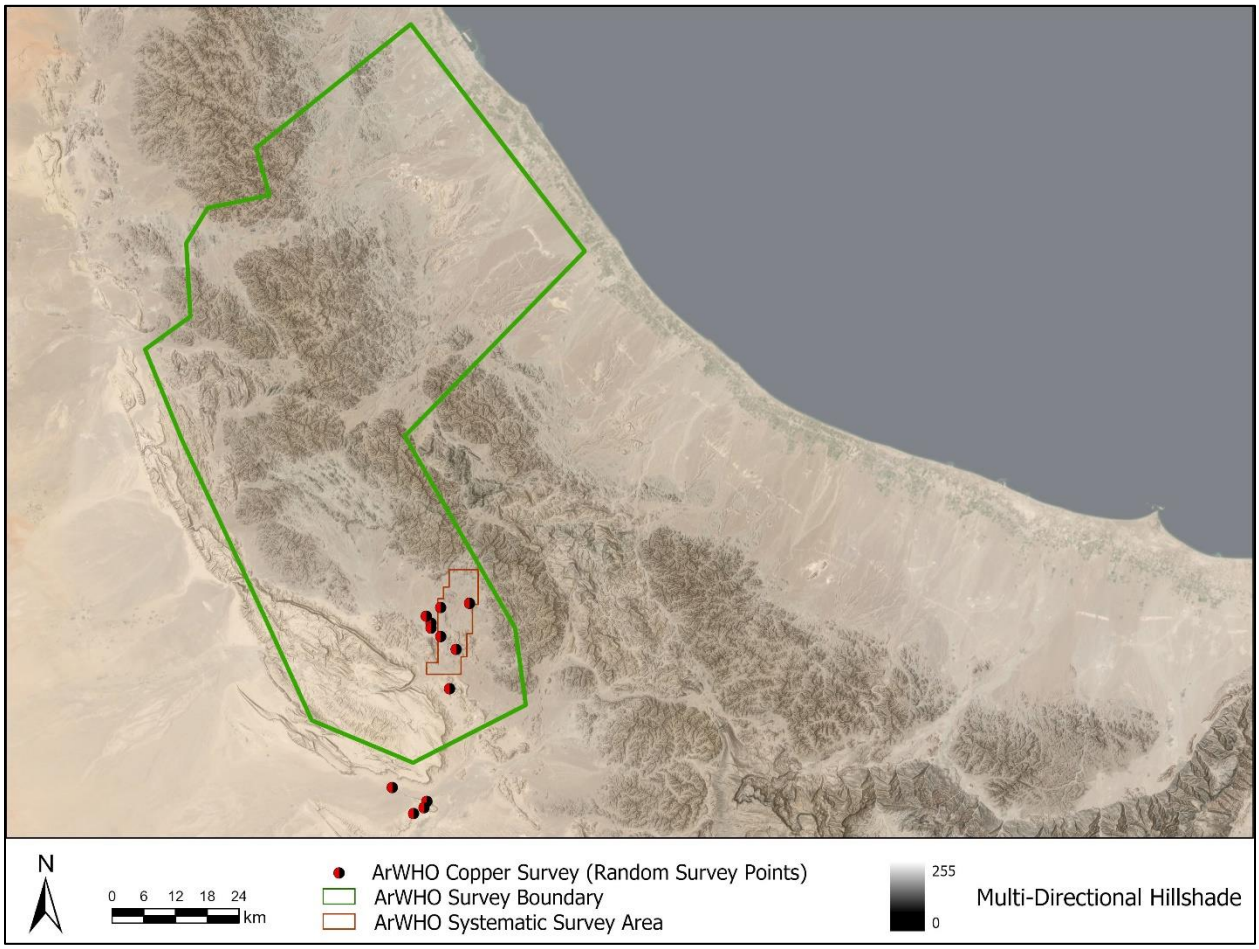

Figure 6.16 Random Survey Points.

Table 6.3: ArWHO Random Survey Sectors

#	Sector	C#	Date	E	N	False Negative	Notes
1	374	C124	11-Jan-17	459158	2606274	No	Rugged area to the south of town (SE corner) - these coordinates correspond to an initial grid
2	286	C123	11-Jan-17	454821	2609947	No	(SE corner) -- these coordinates correspond to an inital grid

3	268	C122	11-Jan-17	454822	2610807	No	Near Yanqul (SE corner) - - these coordinates correspond to an initial grid
4	205	N/A	11-Jan-17			No	Inaccessible (copper point not assigned)
5	39	C125	13-Jan-17	450500	2571000	No	SW corner
6	78	C126	13-Jan-17	453000	2572000	No	SW corner
7	284	C129	13-Jan-17	451500	2578000	No	SW corner
8	322	C128	13-Jan-17	453500	2579000	No	SW corner
9	358	C127	13-Jan-17	454000	2580000	No	SW corner
10	1038	C130	14-Jan-17	458000	2599500	No	SW corner inaccessible - coordinates shifted 500 m to the west - initial SW corners were 458500 (square 1039)
11	778	N/A	14-Jan-17	457500	2592500	No	Inaccessible - very close to limestone quarry (copper point not assigned)
12	433	C131	14-Jan-17	448000	448500	No	SW corner
13	1457	C132	14-Jan-17	454000	2612000	No	Slag scatter found at NW corner of 1457 (=C133)
14	1540	C135	14-Jan-17	461500	2614000	No	SW corner
15	1513	C136	15-Jan-17	456500	2613500	No	SW corner
16	555	N/A	16-Jan-17	449000	2586000	No	Inaccessible (copper point not assigned).
17	547	N/A	16-Jan-17	N/A	N/A	No	Inaccessible (copper point not assigned).
18	612	N/A	16-Jan-17	N/A	N/A	No	Inaccessible (copper point not assigned).
19	703	N/A	16-Jan-17	N/A	N/A	No	Inaccessible (copper point not assigned).
20	1341	C144	19-Jan-17	456500	2608500	No	SW corner

6.3. Volcanism in the Northern Horn of Africa

In terms of geological context, the northern Horn of Africa, an area which encompasses Ethiopia, Eritrea, Somalia, and Djibouti, consists of a variety of environmental zones, ranging from

the hyper-arid coastal plains of the Danakil Depression, to the volcanic landscape of the Rift Valley, to the lush highland areas of the Tigray Region. Geologically, the Tigrayan landscape is defined by basalt mountains (ambas), sandstone cliffs, and plateaus formed as a result of tectonic activity.

Intensive tectonic and volcanic activity in the southern Red Sea region led to obsidian sources being located on both sides of the southern Red Sea (Peate et al. 2005; Kabesh et al. 1980; Khalidi 2009). Because of its younger age and attendant reduced chance of devitrification, Ethiopian obsidian is considered to have been of better quality and, indeed, found its way to southwestern Arabia beginning in the sixth millennium BCE (Francaviglia 1990; Khalidi 2009).

The relief of the Red Sea region was formed through tectonic movements that resulted from the seafloor spreading of the Red Sea (Coleman 1993). Following the creation of a bathymetric chart of the Red Sea (Laughton et al. 1970), it was discovered that the main trough, located at the bottom of the sea, extends from Zubayr Island to the tip of the Sinai Peninsula. This trough is cut by an axial trough 5 to 30 km in width, that is characterized by high-temperature brine pools. This axial trough generates new oceanic crust and is characterized by active normal faulting. Indeed, the axial through is surrounded by fault terraces and is between 4 and 5 km wide at depths of around 2000 m. The extrusive zone characterizing the central part of the axial zone is defined by a string of young basalt volcanoes. These volcanoes have lava pipes that extrude magma. The floor of the trough is characterized by a sequence of silt-lava. Active extension can be seen throughout the zone.

There are four regions of volcanic activity within the Red Sea region. These are located: (1) at the northern termination of the East African rift system (an area that includes the Afar Depression transitional volcanics and the Ethiopian Plateau basalts), (2) on the Yemen volcanic plateau (an

area characterized by bimodal volcanics), (3) on the western Saudi Arabian Plateau (this region is characterized by basalts generated by separate volcanic centers, and (4) throughout the axial trough of the Red Sea (as a result of active seafloor spreading, leading to the formation of new oceanic crust in the median and southern Red Sea regions).

Detection was undertaken on scenes both from the Danakil and the Eastern Rift Valley (Fig. 6.17). Triangular in shape, the Afar Depression meets the Precambrian pan-African basement, which is overlain by a sequence of Ethiopian Plateau lavas (Mohr 1971, 1983, 1989), to the west. To the east, the Afar Depression meets the Danakil block. The Danakil block is made up of basement rocks, covered by Mesozoic marine sediments and, in parts, by Tertiary volcanics. Within the Depression, the volcanic and sedimentary sequences lay flat. Older stratigraphy is not exposed in this region.

The oldest sediments exposed in the Afar Depression are the so-called "Red Series". The "Red Series" is characterized by terrestrial alluvial deposits and by lacustrine and marine clays. K/Ar dating, undertaken on basalts that have been discovered interlayered with the sediments have produced dates ranging from 24 to 5.4 Ma. The geology of this area suggests changes in tectonism and volcanism occurring throughout the formation of the basin (Tierclelin et al. 1980). The Trap Series, composed of stratoid basalts, was formed when marginal fissures that were located parallel to the marginal fault system erupted (Mohr 1978). The eruption sequence began during the Late Oligocene and continued intermittently until the Late Miocene. The basalts in this series are transitional basalts, that were mostly made up of hawaiite-icelandite and were at times interlayered with trachytes and pantellerites. During the Quaternary, a series of volcanic eruptions occurred surrounding the axial ranges characterized by a northwest to southeast trend (Barberi et al. 1972, Tazieff et al. 1972).

6.3.1. Creating a Preliminary Exploratory Geological Resource Map of Obsidian in the Northern Horn of Africa

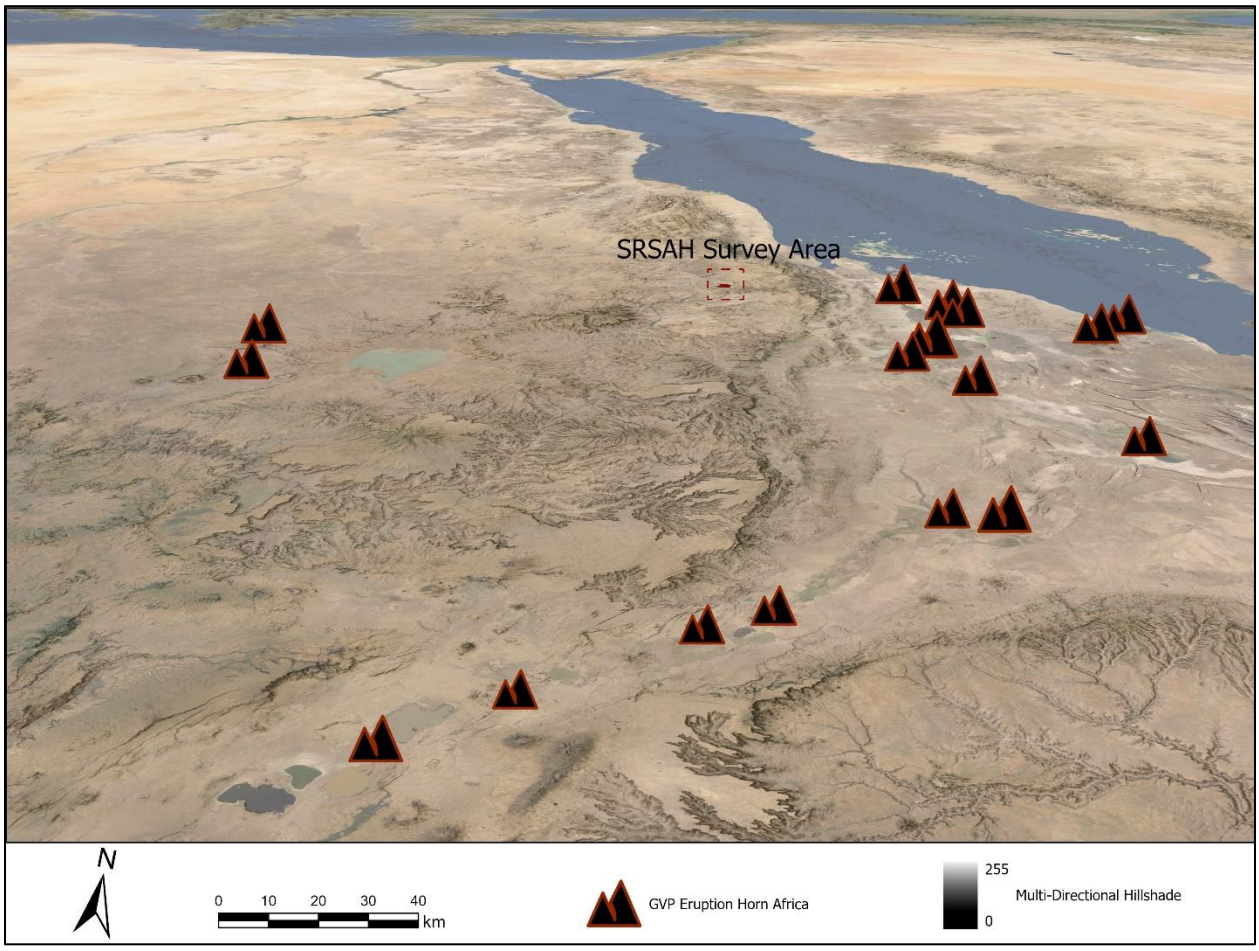

Figure 6.17 3D Scene of Volcanoes in the Danakil and the East Rift Valley with SRSAH Survey Area at the top and volcano locations as identified by the Global Volcanism Program.

The first step in creating an obsidian resource map is identifying the location of environments produced through volcanic activity. This is because obsidian, consisting mainly of SiO_2, is a volcanic glass which forms as an extrusive igneous rock as a result of felsic lava cooling rapidly and consequently producing minimal crystal growth. Obsidian does not form in a true crystalline fashion and, as such, is not classified as a mineral, being sometimes categorized as mineral-like or as a mineraloid. A felsic rock, obsidian co-occurs in the same volcanic environments as mafic

rocks like basalt. Their similarity in color and in spectral signatures makes distinguishing between the two in satellite imagery often problematic.

Spatial data relating to the location of volcanos in the Danakil and the East Rift Valley was downloaded from the Smithsonian's *Global Volcanism Program,*[59] (GVP) a database which records the location, physical characteristics, and eruption history of volcanoes. The Program's mission is to gain a better understanding of the Earth's active volcanoes as well as their eruption history during the last 10,000 years.

In addition to spatial information, the GVP provides information about known eruption start year, event type, and event remarks, when these are recorded (Table 6.4).

Table 6.4 Volcanoes in the Danakil and Eastern Rift Valley from the Global Volcanism Program.

Volcano Name	Eruption Number	Eruption Start Year	Event Number	Event Type
Dubbi	13937	1861	101789	Bombs
Dubbi	13937	1861	101790	Pyroclastic flow
Dubbi	13937	1861	101791	Lava flow(s)
Dubbi	13937	1861	101792	Property damage
Dubbi	13937	1861	101793	Fatalities
Dubbi	13937	1861	101794	Earthquakes (undefined)
Alayta	13940	1907	101799	Explosion
Alayta	13940	1907	101800	Lava flow(s)
Alayta	13940	1907	101801	Property damage
Alayta	13940	1907	101802	Fatalities
Alayta	13940	1907	101803	Earthquakes (undefined)
Alayta	13941	1915	101804	Explosion
Dabbahu	13942	2005	101806	Explosion
Dabbahu	13942	2005	101807	Ash
Dabbahu	13942	2005	101808	Lava dome formation
Dabbahu	13942	2005	101809	Evacuations
Dabbahu	13942	2005	101810	Volcanic tremor

[59] Data accessed at this website: https://volcano.si.edu/.

Dabbahu	13942	2005	101811	Earthquakes (undefined)
Dabbahu	13942	2005	101812	Earthquakes (undefined)
Dabbahu	13942	2005	101813	Earthquakes (undefined)
Manda Hararo	13943	2007	101815	Explosion
Manda Hararo	13943	2007	101816	Bombs
Manda Hararo	13943	2007	101817	Scoria
Manda Hararo	13943	2007	101818	Lava flow(s)
Manda Hararo	13943	2007	101819	Evacuations
Manda Hararo	13943	2007	101820	Earthquakes (undefined)
Tullu Moje	13955	1775	101823	Lava flow(s)
Tullu Moje	13956	1900	101825	Explosion
Tullu Moje	13956	1900	101826	Tephra
Tullu Moje	13956	1900	101827	Lava flow(s)
Tullu Moje	13956	1900	101828	Property damage
Alutu	13957	-50	101829	Explosion
Alutu	13957	-50	101830	Lava flow(s)
Alutu	13957	-50	101831	Lava flow(s) – obsidian observed
Alutu	13957	-50	101832	Pumice
Dallol	13926	1926	121024	Phreatic activity
Alu-Dalafilla	13927	2008	121026	Explosion
Alu-Dalafilla	13927	2008	121027	Lava flow(s)
Alu-Dalafilla	13927	2008	121028	Eruption cloud
Erta Ale	13931	1906	121033	Explosion
Erta Ale	13931	1906	121034	Lava flow(s)
Erta Ale	13931	1906	121035	Lava lake
Erta Ale	13933	1940	121039	Lava lake
Erta Ale	13934	1960	121042	Lava flow(s)
Erta Ale	13935	1967	121044	Lava flow(s)
Erta Ale	13935	1967	121045	Lava lake
Erta Ale	13935	1967	121046	Lava fountains
Dubbi	13936	1400	121049	Explosion
Dubbi	13936	1400	121050	Lava flow(s)
Dubbi	13936	1400	121051	Earthquakes (undefined)
Dubbi	13936	1400	121052	Lava flow(s)
Dubbi	13937	1861	121055	Explosion
Dubbi	13937	1861	121056	Ash
Manda Hararo	13944	2009	121057	Lava flow(s)
Manda Hararo	13944	2009	121058	Earthquakes (undefined)
Manda-Inakir	13945	1928	121060	Explosion
Manda-Inakir	13945	1928	121061	Lava flow(s)

Manda-Inakir	13945	1928	121062	Earthquakes (undefined)
Ardoukoba	13946	1978	121064	Explosion
Ardoukoba	13946	1978	121065	Bombs
Ardoukoba	13946	1978	121066	Scoria
Ardoukoba	13946	1978	121067	Lava flow(s)
Ardoukoba	13946	1978	121068	Lava lake
Ardoukoba	13946	1978	121069	Lava fountains
Ardoukoba	13946	1978	121070	Seismicity (volcanic)
Dama Ali	13947	1631	121071	Explosion
Dama Ali	13947	1631	121072	Loud audible noises
Dama Ali	13947	1631	121073	Earthquakes (undefined)
Dama Ali	13947	1631	121074	Earthquakes (undefined)
Dama Ali	13947	1631	121075	Earthquakes (undefined)
Fentale	13952	1250	121082	Lava flow(s)
Fentale	13952	1250	121083	Property damage
Fentale	13953	1820	121085	Lava flow(s)
Kone	13954	1820	121088	Explosion
Kone	13954	1820	121089	Lava flow(s)
Kone	13954	1820	121090	Cinder cone formation
Dama Ali	13947	1631	141521	Fatalities
Dallol	13926	1926	144366	VEI (Explosivity Index)
Alu-Dalafilla	13927	2008	144367	VEI (Explosivity Index)
Erta Ale	13931	1906	144371	VEI (Explosivity Index)
Erta Ale	13933	1940	144373	VEI (Explosivity Index)
Erta Ale	13934	1960	144374	VEI (Explosivity Index)
Erta Ale	13935	1967	144375	VEI (Explosivity Index)
Dubbi	13936	1400	144376	VEI (Explosivity Index)
Dubbi	13937	1861	144377	VEI (Explosivity Index)
Alayta	13940	1907	144379	VEI (Explosivity Index)
Alayta	13941	1915	144380	VEI (Explosivity Index)
Dabbahu	13942	2005	144381	VEI (Explosivity Index)
Manda Hararo	13943	2007	144382	VEI (Explosivity Index)
Manda Hararo	13944	2009	144383	VEI (Explosivity Index)

Manda-Inakir	13945	1928	144384	VEI (Explosivity Index)
Ardoukoba	13946	1978	144385	VEI (Explosivity Index)
Fentale	13953	1820	144390	VEI (Explosivity Index)
Kone	13954	1820	144391	VEI (Explosivity Index)
Nabro	20800	2011	150701	Thermal anomaly
Nabro	20800	2011	150702	Explosion
Nabro	20800	2011	150703	VEI (Explosivity Index)
Nabro	20800	2011	150704	Lava flow(s)
Nabro	20800	2011	150705	Fatalities
Dallol	20939	2011	151220	Phreatic activity
Dallol	20939	2011	151221	VEI (Explosivity Index)
Dabbahu	20944	-5850	151237	Lava flow(s)
Dabbahu	20945	-4450	151238	Lava flow(s)
Dabbahu	20946	-3450	151239	Lava flow(s)

6.3.1.1. Detection Workflow

The layouts presented in this chapter were created by analyzing Hyperion satellite imagery with ENVI 5.3's Target Detection Wizard using the Spectral Angle Mapper (SAM) algorithm. The total Hyperion coverage for the research area can be seen in Figure 6.18.

Classification Methods – The multistep process of target detection detailed in the first part of this chapter is replicated for obsidian detection with a few notable alterations which consist in the selection of non-target spectra alongside targeted spectra and the utilization of the Spectral Angle Mapper (SAM) classification method in lieu of the OSP method.

A single obsidian spectral signature is made available by the ASTER Spectral library for the wavelength range covered by the Hyperion hypercube (Fig. 6.19). Four basalt signatures were selected as non-target spectra (Fig. 6.20). Note the similarity between the spectral curves of the obsidian signature and the igneous mafic solid basalt sample.

The algorithm used for obsidian detection was Spectral Angle Mapper (SAM). An *n*-D angle is used to match pixels to targeted spectra. Spectra are treated as vectors in a space in which the dimensionality is determined by the number of bands. Similarity between spectra is calculated using the angle between them, with smaller angles revealing closer matches.

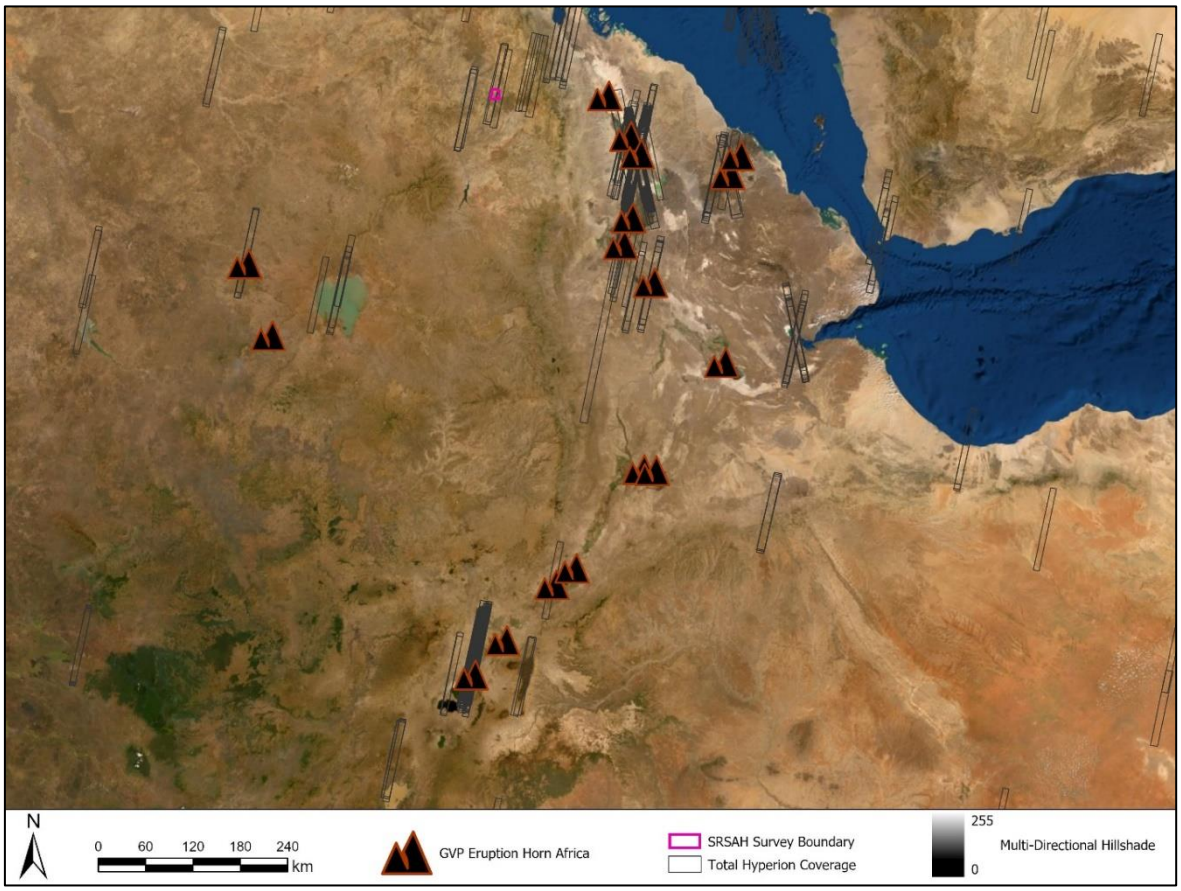

Figure 6.18 Total Hyperion Coverage in the Northern Horn of Africa.

Spectral Properties of Obsidian – Obsidian is a volcanic glass that is characterized by optical homogeneity and clarity. Optical homogeneity is determined by the absence of internal scatterers, suggesting that electromagnetic radiation interacts mostly with the first surface of the sample that it encounters (Yon and Pieters 1988).

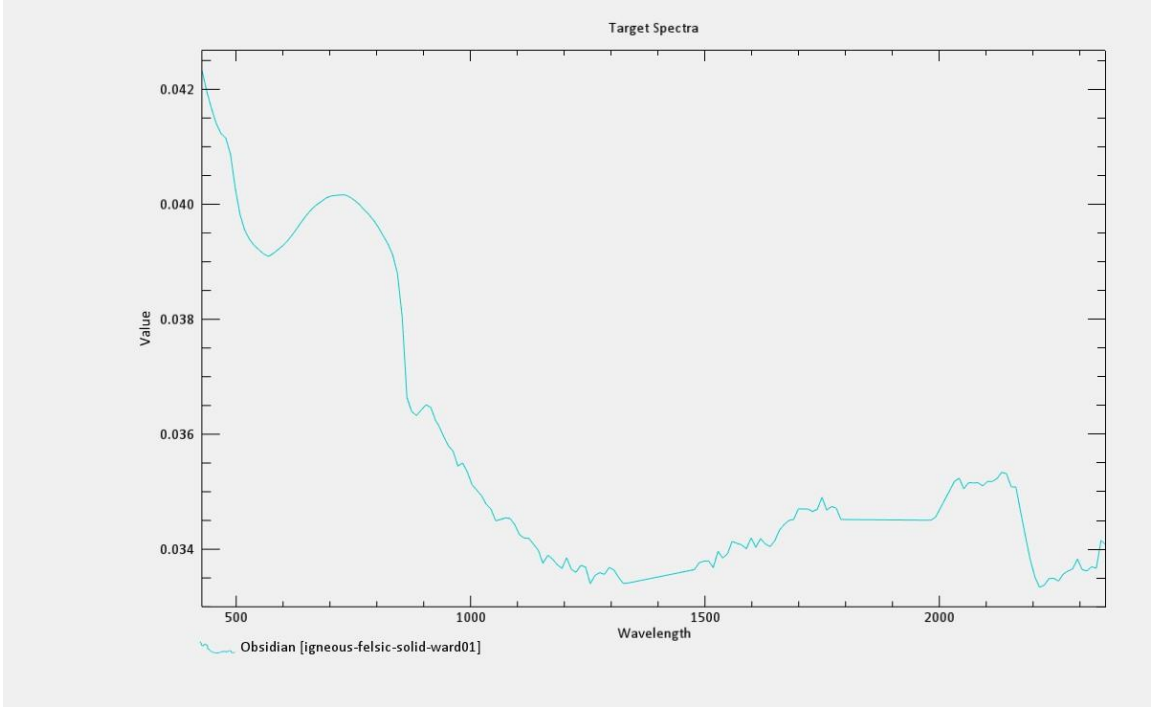

Figure 6.19 Obsidian Spectral Plot.

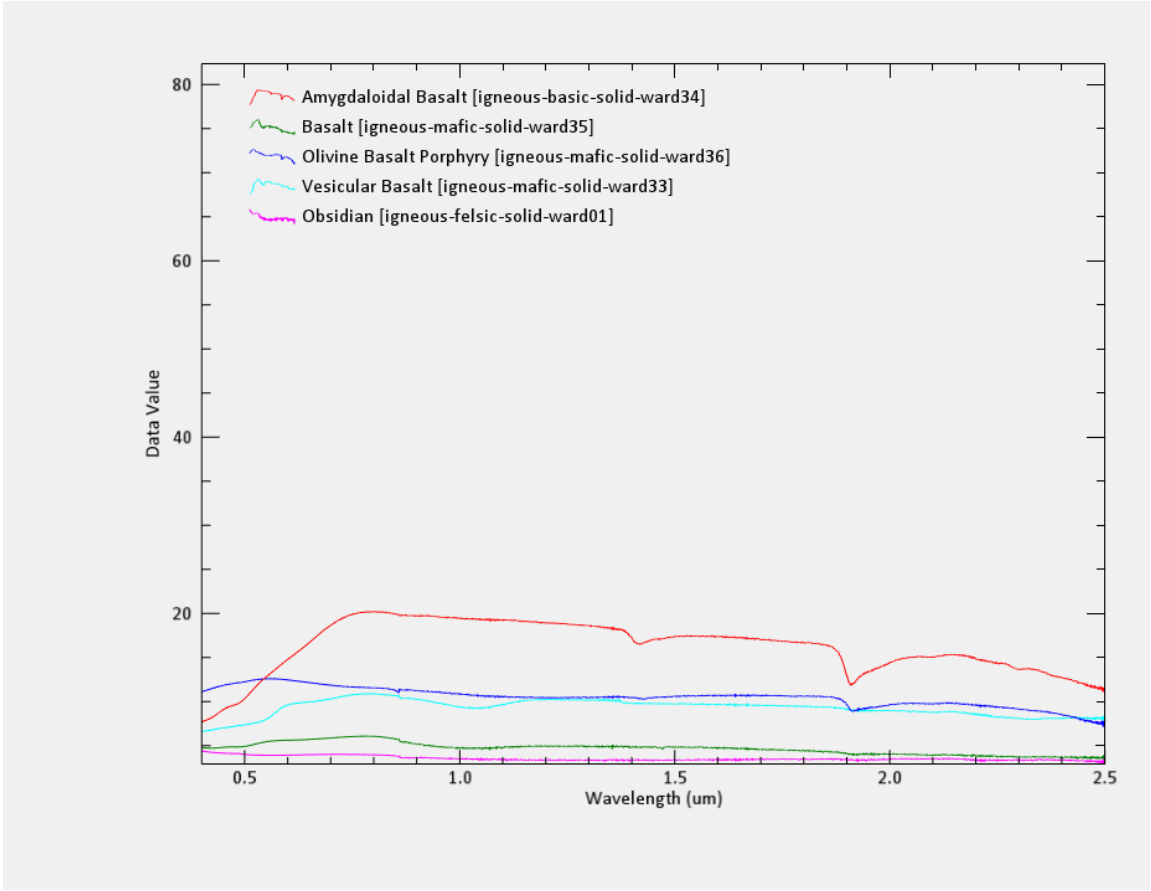

Figure 6.20 Obsidian and Basalt Spectral Signatures.

Because obsidian often lacks strong distinct absorption features in the VNIR and SWIR, a synergistic approach that combines VNIR/SWIR hyperspectral data with TIR data has often been adopted (Chen et al. 2007). As previously mentioned, the process of obsidian detection is confounded by its optical similarity with basalt and by their geologic co-occurrence (Fig. 6.19 and Fig. 6.20). Obsidian exhibits an absorption band near 1.14 μm as well as ultraviolet charge transfer absorption characteristics. The 1.14 μm absorption feature distinguishes obsidian signatures from basalt signatures. Basalt, on the other hand, is characterized by a pyroxene absorption band at ~1.03 μm, owing to electronic transitions in ferrous iron (Yon and Pieters 1988[60]).

6.3.1.2. Preliminary Results of Obsidian Detection

The obsidian detection results presented in this chapter are preliminary as these results have not yet been ground-truthed. Largely owing to the distance between the SRSAH survey area and the closest volcanic landscape (approximately 130 km), ground-truthing in Ethiopia has proven more difficult to undertake than ground-truthing in Oman.

The closest volcanos to the SRSAH Survey Area are Dallol, Alu-Dalafilla, and Erta Ale, located approximately 130 km, 170 km, and 190 km, respectively, to the south-east of the research area. Whereas there is no Hyperion coverage for Dallol, the area of Alu-Dalafilla and Erta Ale have been collected on many occasions (Fig. 6.21). Areas of potential detection have been identified to the north-east of Alu-Dalafilla, downslope from its caldera, as well as to the south-west of Erta Ale, downslope from its caldera.

[60] S.A. Yon, C.M. Pieters. Interactions of light with rough dielectric surfaces - Spectral reflectance and polarimetric properties. Lunar and Planetary Science Conference, 18th, Houston, TX, Mar. 16-20, 1987, Proceedings (A89-10851 01-91). Cambridge and New York/Houston, TX, Cambridge University Press/Lunar and Planetary Institute, 1988, p. 581-592.

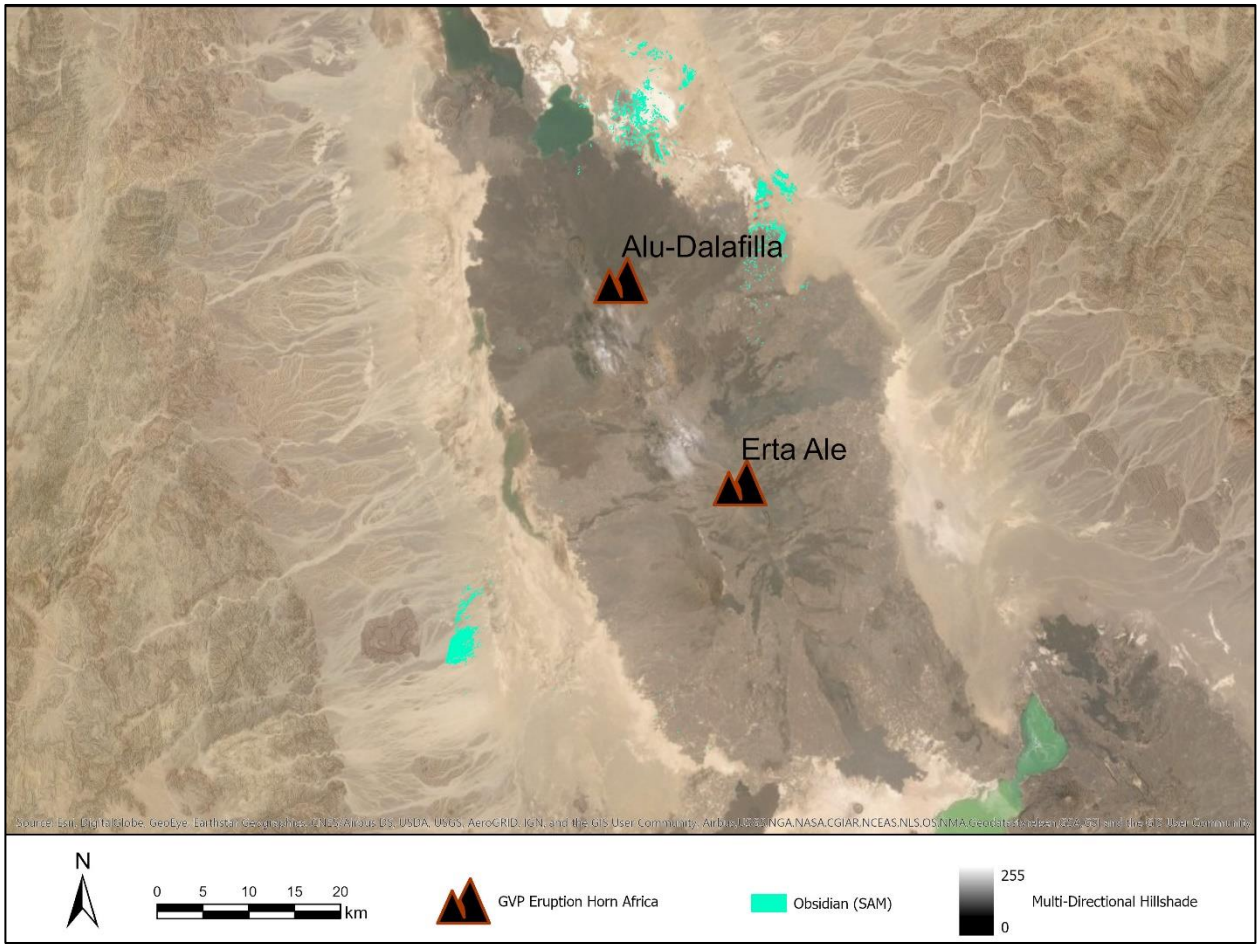

Figure 6.21 Potential obsidian detection located downslope from the Alu-Dalafilla and Erta Ale calderas.

Obsidian spectra were also detected to the south-east of the Erta Ale volcanic region, in a volcanic landscape containing the volcanoes Dubbi and Nabro. Located on the border between Ethiopia and Eritrea, Nabro is at approximately 307 km to the south-east of the SRSAH Survey region, while Dubbi finds itself 37 km to the north-east of Nabro in Eritrea proper (Fig. 6.22). A large area of potential obsidian detection has been identified in the caldera formed through the eruption of Nabro. Detected pixels associated with Dubbi, on the other hand, are located to the west of the volcano's caldera. Some pixels appear to follow what looks like a flow in satellite imagery. Caution must be employed when interpreting these results as the incidence of false

positives is likely high. The Dubbi detection reveals this potentiality, as one can also observe the effects of stripping.

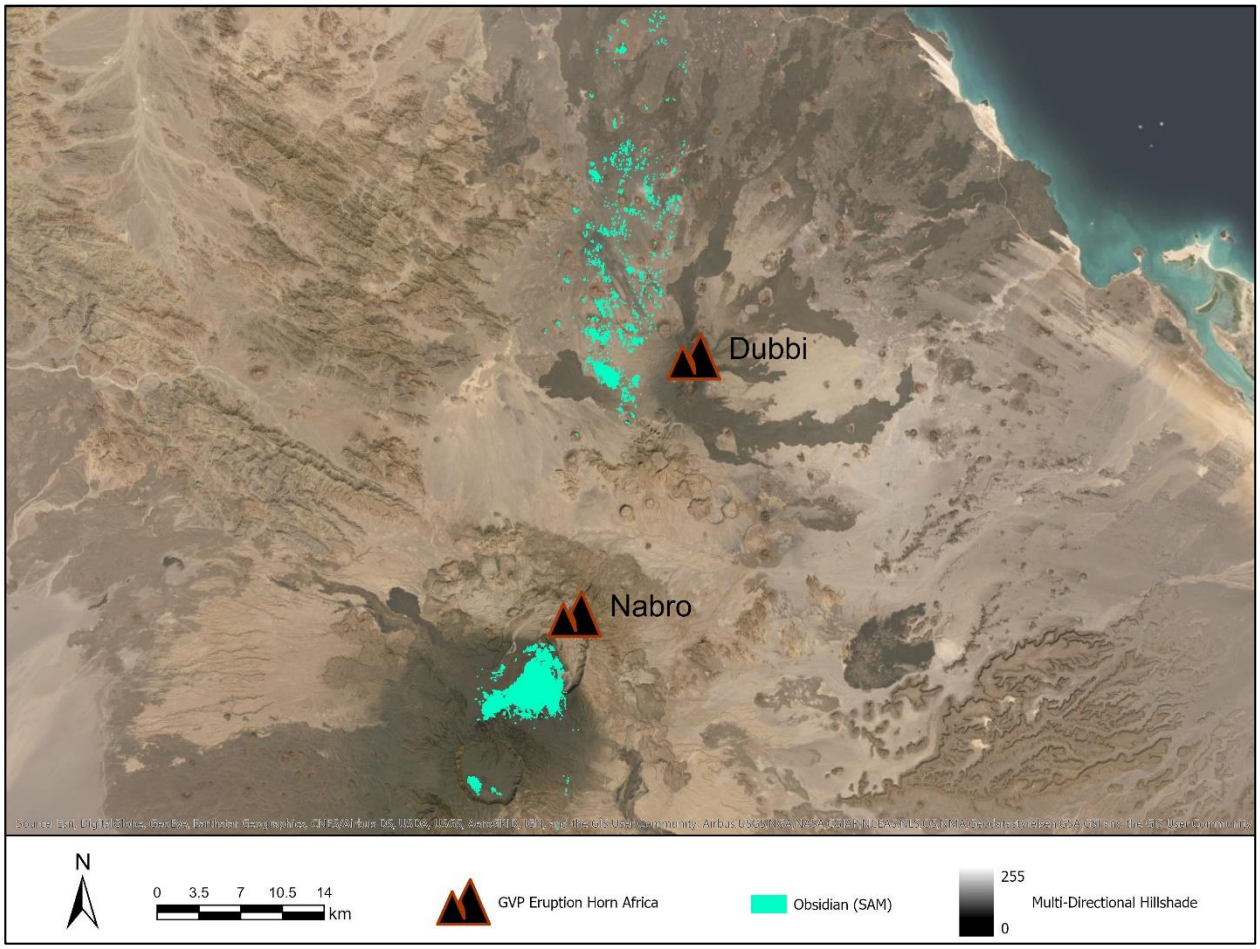

Figure 6.22 Potential obsidian detection located in the area surrounding the Nabro and Dubbi volcanos.

Another landscape that is potentially rich in obsidian outcrops is located approximately 220 km south-east from the SRSAH Survey Area and contains three volcanoes: Alatya, Dabbahu, and Manda Hararo (Fig. 6.23). Detection around Alatya (Fig. 6.23a), has been uncovered to the south-east of the volcano's caldera in what appears to be an area of lava flow. Obsidian spectra around Dabbahu (Fig. 6.23a) were primarily identified to the south-west, south-east, and east of

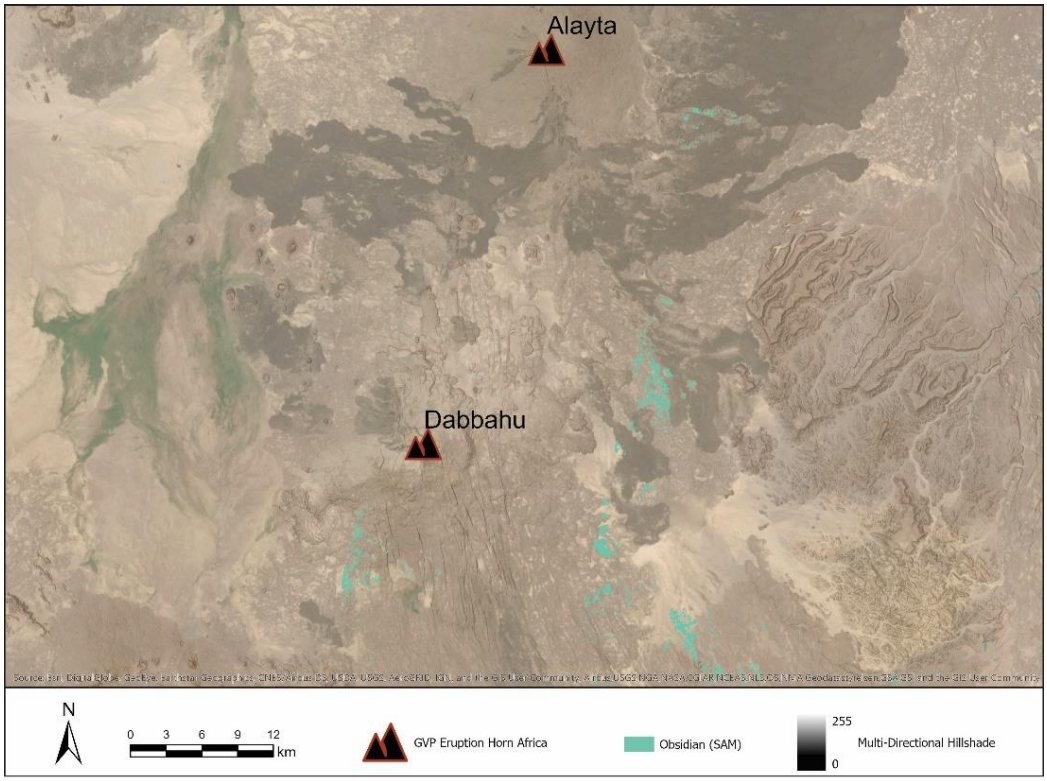

(a)

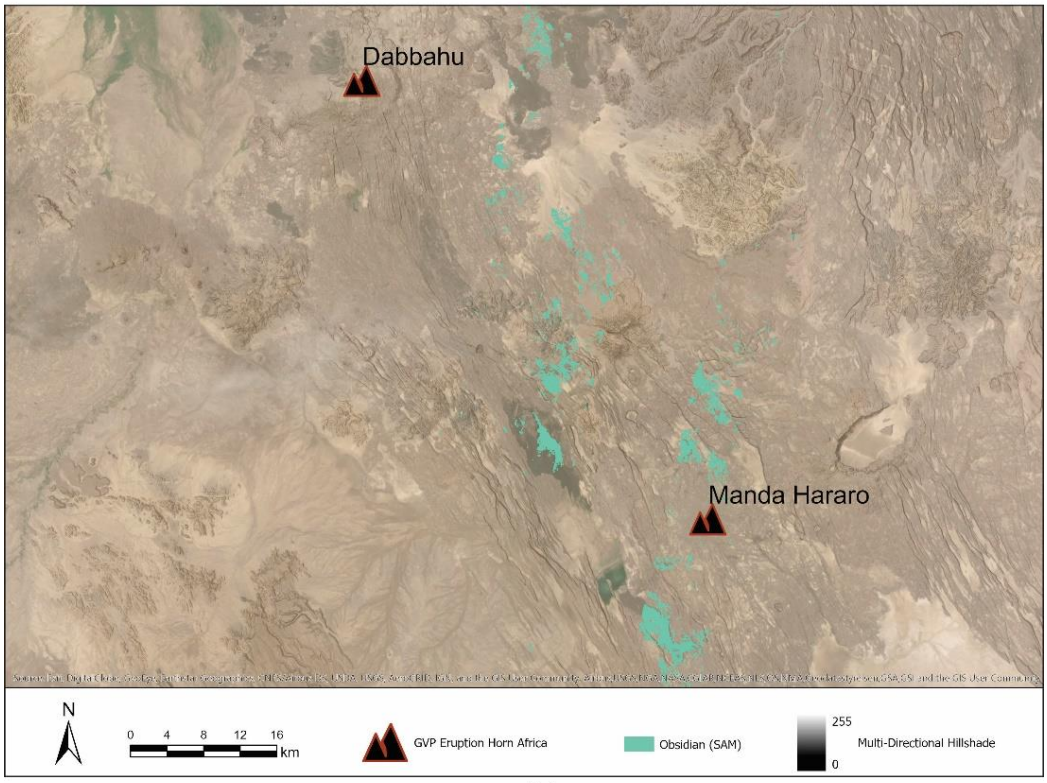

(b)

Figure 6.23 Potential obsidian detection between Alayta and Dabbahu (a) and Dabbahu and Manda Hararo (b).

Dabbahu with a few pixels detected to the north of the volcano's caldera. Eastern and south-eastern pixels seem to be located in areas of lava flow. Detection around Manda Hararo (Fig. 6.23b) appears to encircle the volcano's caldera. Particularly noteworthy is an area of detection to the south of the volcano's caldera which seems to entirely overlap a lava flow.

Further to the south, in the East Rift Valley, detection around the Kone volcanic complex has identified potential obsidian spectra particularly in association with silicic calderas and young basaltic cinder cones (Fig. 6.24). Similar patterns of detected pixels identified downslope from calderas were a welcome discovery as these findings cohere with known patterns of obsidian formation.

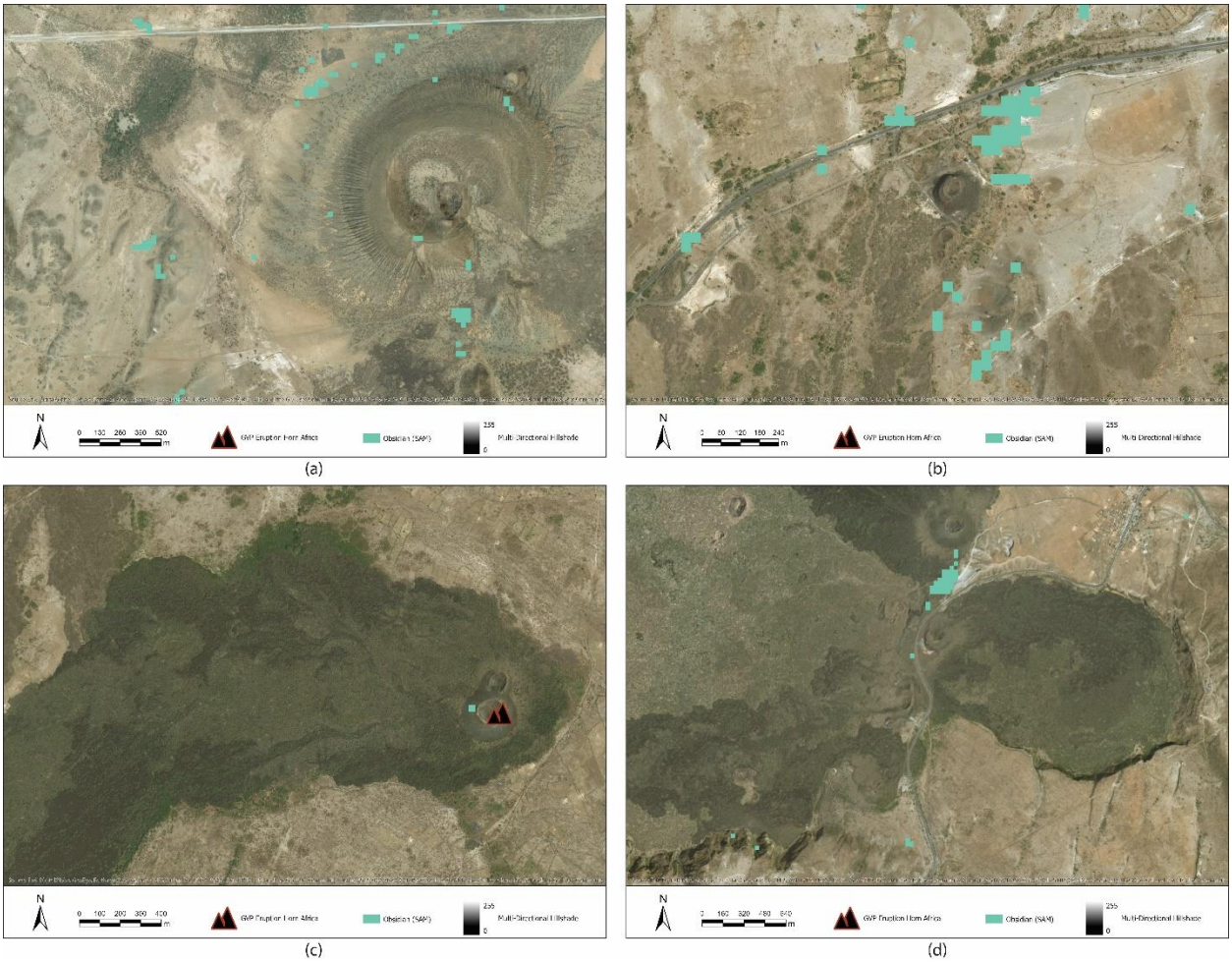

Figure 6.24 Potential obsidian detection in the Kone volcanic complex.

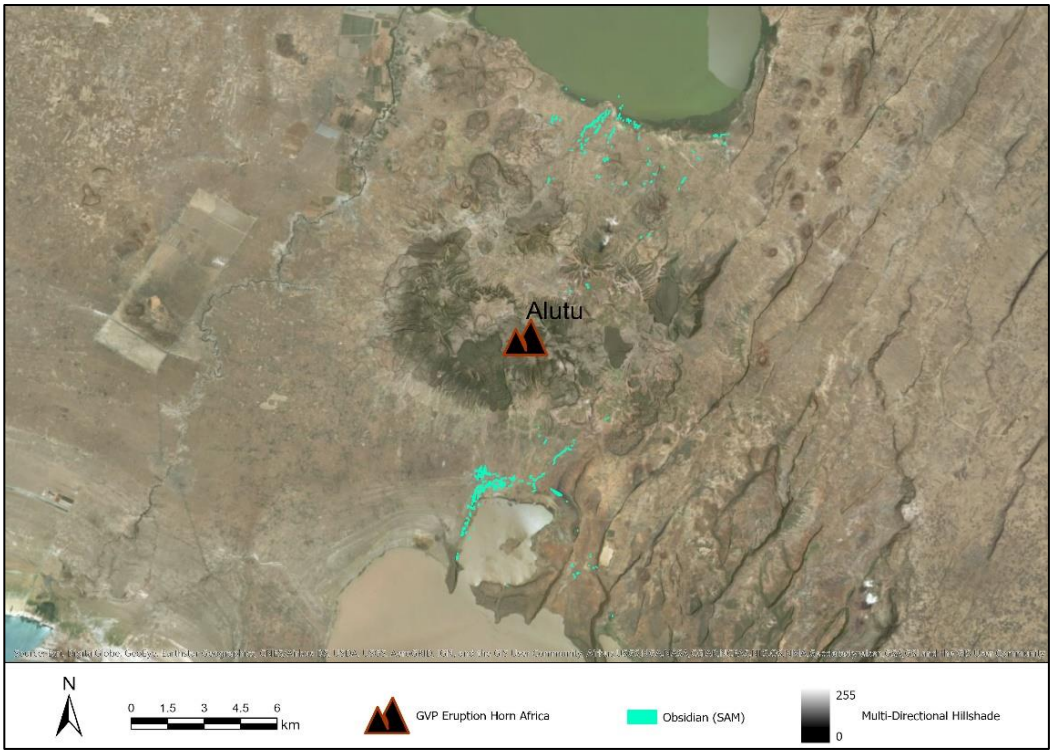

Figure 6.25 Potential obsidian detection in the environs surrounding Alutu volcano.

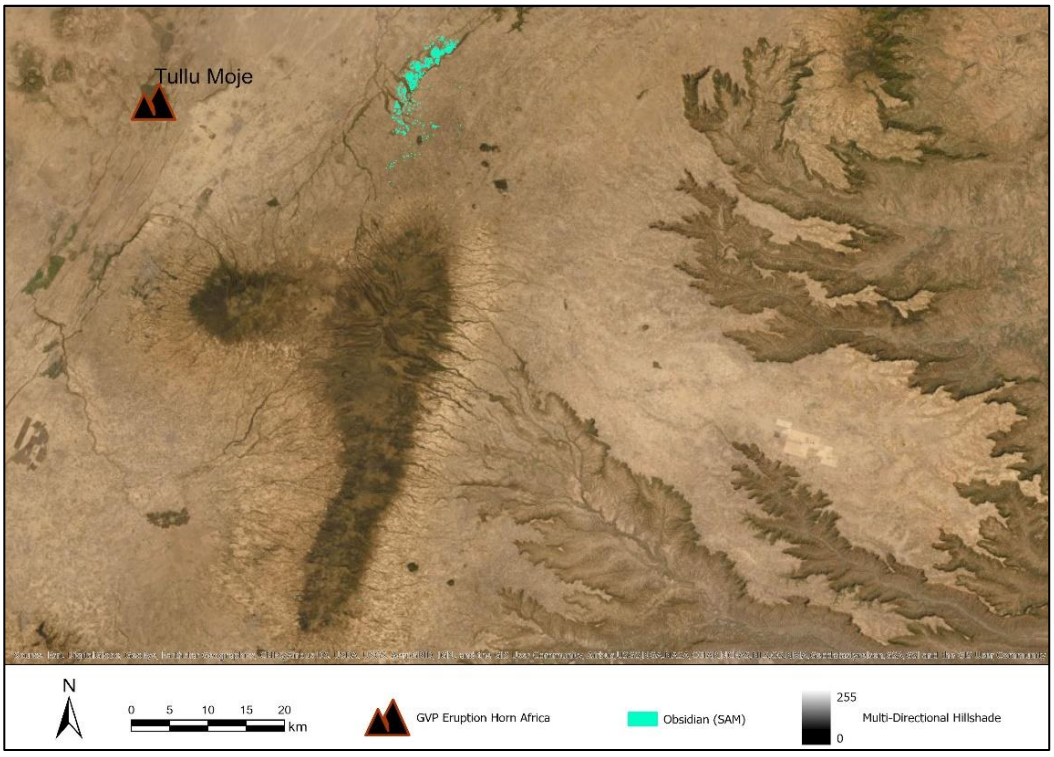

Figure 6.26 Potential obsidian detection to the east of Tullu Moje.

Finally, detection of several scenes was undertaken in the area that contains the volcanoes Alutu (Fig. 6.25) and Tullu Moje (Fig. 6.26). Analysis of the Alutu scene yielded detected spectra to the north and south of the Alutu volcano. Analysis of a scene located to the east of Tullu Moje also revealed potential obsidian detection. Available GVP information regarding Alutu indicates that the presence of obsidian has already been noted for this area.

6.4. Conclusion

This chapter describes the process of creating preliminary exploratory geological resource maps revealing the potential distribution of copper deposits in Oman and of obsidian sources in Ethiopia with the goal of gaining a better understanding of the geology of the two regions, as it relates to the supply networks being investigated. Future validation of results and calibration of the detection workflow is expected to improve the accuracy of the resource maps. Currently, these layouts represent useful preliminary tools for streamlining future geological surveys and for preliminarily modeling these raw material supply networks.

Chapter 7

Mapping and Modelling the Development of Copper Supply Networks in Oman and Obsidian Supply Networks in Ethiopia

7.1. Introduction

This chapter examines: (1) the structure of copper and obsidian supply networks and their diachronic developments in Oman and Ethiopia, respectively; (2) diachronic fluctuations in the position of individual nodes within each time period's network; and (3) changes in relationships between pairs of nodes. Where measures affecting network-level patterns are concerned, the focus will be on overall network centralization and connectedness.

Network *structure* is defined as the recurring patterns in relationships among active nodes within a network (cf. Wasserman and Faust 1994). The relationships analyzed in this chapter are economic in nature and the network structuring variables are represented by the strength of ties of similarity in material culture as proxied by copper slag in Oman and archaeological obsidian in Ethiopia. Links between nodes of interest were established based on typological and geochemical similarities of archaeological obsidian and slag. Nodes within these networks are represented by archaeological sites, where dyadic relationships between sites consist of pairs of artifacts belonging to the same chemical group.

7.1.1. Configuring the Archaeological Networks in Oman and Ethiopia

Creating an archaeological network for formal analysis necessitates the following: (1) the specification of parameters that determine network inclusion (boundary), (2) the definition of a set

of social actors (nodes), and (3) the designation of the relationship that exists between each pair of nodes within the established network (ties). Raw material production in Oman and Ethiopia is identified through material cultural proxies. In Oman, production is proxied by slag assemblages, the detritus that results from the smelting of copper ore. By reconstructing smelting practices from slag samples, I generated networks of settlements connected through similar implementation of shared technological knowledge. In Ethiopia, the production chain is proxied by obsidian assemblages largely made up of lithic debris (e.g. angular waste, flakes, flake fragments, etc.) with some evidence of formal tool types. By reconstructing different geochemically distinct obsidian groups, I produced networks of affiliation based on shared material culture.

While these networks form around a similar phenomenon, raw material production, they are arguably different in terms of what is being diffused through the network. Whereas in Ethiopia, the proxy is in effect the raw material itself (geochemically identified obsidian groups), in Oman, the proxy is the reconstructed technology. Although lithic traditions in northern Ethiopia are characterized by remarkable continuity across periods, obsidian assemblages are dated both typologically (when that identification can be made) and through association with other elements of material culture (such as pottery). Where slag detritus is concerned, contemporaneous assemblages were similarly dated by relative means largely through association with diagnostic material culture.

Boundaries – This project has taken a "nominalist" approach to defining the boundaries of the networks and employs an attribute-based strategy for defining nodes (Laumann et al. 1992, Peeples 2019). These are not total networks representing a social group (Borgatti and Halgin 2011), in the realist sense of the word, but rather analytical constructs developed for the purposes of understanding patterns of network flow and fluctuations in network positions.

To narrow down the boundaries of this network, I began with a database of 84 sites in Ethiopia and 225 sites in Oman. This database was compiled through systematic surveys of two 100 km^2 areas in northern Oman and northern Ethiopia. I then delimited two subsets of sites by selecting those characterized by slag detritus and obsidian debris, indicating copper and obsidian production, respectively. Because this is a longitudinal study, contemporaneity was considered when further subdividing the database into coeval production periods. Indeed, one of the limitations of this study is that networks contain both single and multi-period sites and, as such, network analyses generate models of potential structures, which cannot currently resolve uncertainties associated with the contemporaneity of multi-period sites.[61] As such, this research is intended to be a point of departure for the use of this methodology to analyze landscapes of production associated with copper in Oman and obsidian in Ethiopia. In the future, attempts will be made to gain more precise chronological controls of these datasets and interpretations will be refined accordingly.

Nodes and ties – This dissertation compares so-called one-mode networks, defined as networks in which all nodes belong to the same category, namely sites with evidence of production. Network ties, on the other hand, are based on similarities in technological practices (for copper producing sites in Oman) and on shared access to raw materials (for obsidian knapping sites in Oman). That is, the phenomenon studied in Oman is the diffusion of knowledge relating to copper smelting technologies. Conversely, in Ethiopia it is the diffusion of raw materials themselves that is under investigation. Of course, there is likely a great deal of overlap between networks of technology diffusion and networks through which copper ore and finished products circulate. Similarly, there is likely a great deal of overlap between obsidian raw material diffusion and networks in which

[61] The extent and manner in which interactions among non-production sites may have driven the development of this network structure is beyond the focus of this current study and cannot be further theorized.

knowledge of obsidian knapping is diffused. However, neither networks of knapping knowledge nor networks investigating the flow of copper ore and copper object are within the purview of this dissertation. This is because of the limiting factors inherent in the two datasets: obsidian geochemical analyses reconstruct categories of different materials (i.e. naturally occurring obsidian geochemical groups); geochemical analyses of slag, on the other hand, reconstruct smelting technologies (i.e. ideas and information). Despite their differences, both networks are proxies for understanding regional dynamics of production.

These networks are built by using artifact presence or absence as affiliation data. Nodes are connected when they share evidence of a specific category of object (see Mizoguchi 2009, 2013; Sindbæk 2007) and the strength of those connections is established by weighing ties based on the number of shared object types (see Blake 2013, 2014; Coward 2010, 2013).

Both affiliation networks are assumed to indicate potential social relations between the individuals associated with these communities of production that developed beyond the interactions that may have originated the proxy data (Borgatti and Halgin 2011a, Peeples 2019). In other words, the inherent assumption of affiliation networks is that social actors that are tied to each other through evidence of one form of interaction are also potentially tied together through other forms of interaction. However, where archaeological networks are concerned, these patterns should not be interpreted as revealing direct interactions between social actors but rather as evidence of repeated interactions over the course of long periods of time (Bernardini 2007, Mills 2016, Peeples 2019).

7.1.2. Contextualizing Centrality Measures, their Different Inherent Assumptions, and some Expectations for Networks in Oman and Ethiopia

The structural measures employed in this chapter can be divided into two types: node centrality and graph centralization[62] measures, on the one hand, and graph-theoretic measures of connectedness and cohesion. Centrality measures are used to generate centrality scores for individual nodes, thereby revealing their positions within the network and allowing for the identification of key sites for each time period. Centralization is used to generate a network-level measure. Measures of connectedness and cohesion, on the other hand, can be used to evaluate the structure and density of a network. While showcasing patterns in the overall structure of a network as well as in the embeddedness of individual nodes, network data is also investigated to reveal sub-structures and sub-groups of actors that are closer to each other than they are to other groups.

In addition to presenting and analyzing relational data, this chapter will integrate a geographic component by tracking diachronic changes in the spatial patterns of networks, thereby revealing fluctuations in regional patterns of interaction.

In this chapter I focus on several actor-level indices of centrality and power including: (1) degree centrality, (2) beta-centrality, (3) betweenness centrality, (4) flow betweenness, and (5) closeness centrality. The advantage of integrating multiple centrality methods hinges on the fact that each measure can reveal different nuances of network structure resulting from the different assumptions about mechanisms of flow that underlie each measure (Borgatti 2005).

Firstly, however, one must note that networks develop through the combination of two categories of attributes: (1) those relating to the mechanisms of transmission and (2) those relating

[62] In this chapter, the terms *centrality* and *centralization* are not used interchangeably: *centrality* is restricted to measures defining points or nodes, while *centralization* will be exclusively used to characterized properties relating to the network's structure as a whole.

to the kinds of trajectories that can be taken through the network. Each of these categories can in turn be subdivided.

There are three different mechanisms of transmission or diffusion between dyads. Two of these mechanisms are so-called *copy* mechanisms (parallel replication/ duplication and serial replication) and one is a so-called *move* mechanism (transfer). Parallel replication describes simultaneous transmission from one node to multiple nodes with that which is transmitted thereby existing in multiple places at the same time. Serial replication, on the other hand, is a type of copy mechanism that describes commodity flow from one node to another at the end of which each node has a copy of the initial commodity. A common example given to describe serial replication is an infection (Borgatti 2005: 58). Finally, transfer describes a commodity physically moving throw the network.

Mechanisms relating to the kinds of trajectories commodities can take through the network include geodesics, paths, trails, and walks. Each of these terms has a specific network definition: a *geodesic* is defined as the shortest path between two nodes; a *path* is a trajectory in which neither links nor nodes are repeated; a *trail* is a trajectory in which links are not repeated; and a *walk* is an unrestricted trajectory (Borgatti 2005).

Notably, different mechanisms of transmission can combine with different trajectories to form several network typologies and, as a result of their inherent assumptions, not all centrality measures will be usefully applied to all network typologies. Indeed, the mismatch between reconstructed flow process and centrality measure can lead to misleading or erroneous results (Borgatti 2005). As such, it becomes important to carefully consider what flow processes and trajectories are likely animating one's network in advance of selecting centrality measures.

When it comes to the question of dyadic diffusion and whether it is occurring through replication or transfer, my hypothesis is that where obsidian is concerned, the network is defined by a transfer mechanism; that is, obsidian physically moves between nodes. Slag technologies, on the other hand, more likely move according to parallel replication, although singular replication can, of course, also be surmised.[63] Where trajectories are concerned, it becomes more difficult to hypothesize whether geodesics would have been preferred over paths, trails, or walks.

Degree Centrality (Freeman Approach). This measure calculates the degree and normalized degree centrality for each node within a valued or weighted graph (Freeman 1979). The degree centrality for each node is calculated through the summation of the values of ties. The normalized degree centrality is calculated by dividing the degree by the maximum possible degree (which is expressed as a proportion).

For a network with vertices $v_1 \ldots v_n$, *group degree centralization* is calculated by dividing $\Sigma(c_{max} - c(v_i))$ by the maximum value possible, where $c(v_i)$ is the degree centrality of the vertex v_i and c_{max} is the maximum degree centrality (Freeman 1978: 229; Wasserman and Faust 1997: 180):

$$C_D = \frac{\sum_{i=1}^{g}[C_{D(n^*)} - C_{D(n_i)}]}{[(g-1)(g-2)]}$$

The maximum value of this measure is 1 and is attained when one actor chooses all other (g – 1) actors and conversely all other actors only interact with the one most central actor. The assumption

[63] To reiterate, knapping knowledge can, of course, be diffused through replication as is the case with slag technologies and the copper ore and copper objects can be diffused through transfer, as is the case for obsidian. However, when carefully considering the variables that characterize my respective databases, it becomes clear that, in Ethiopia, it is only the raw material that is being analyzed. In Oman, on the other hand, it is the reconstructed smelting technology itself that is being investigated.

inherent in this measure is that the most central actors will also be the most powerful because of their ability to influence other actors.

Borgatti argues that degree centrality is a method that measures immediate impacts (2005). When considering this aspect, it becomes clear that degree centrality is also useful when investigating a case of parallel duplication, as is potentially the case for Oman, as immediate access to as many social actors heightens the probability that information will reach a node.

In Ethiopia, where flow through transfer is concerned, degree centrality can be used to identify which actors are most likely to hold more power and influence. However, not all nodes with the same degree centrality measure have the same capacity for power and influence. Suppose a node is connected to several isolated actors, whereas a second node is connected to the same number of actors, except these actors are themselves well connected. Determining which of these two nodes is more powerful can prove challenging. One can argue that the second node is more powerful because it is connected to nodes that themselves are powerful. However, the opposite argument can also be made (Bonacich 1987): by being the best-connected node out of a set of fairly isolated nodes, this first node could potentially exert more influence than the second node, whose power can become diffuse in a network of other powerful actors (Hanneman and Riddle 2005).

Bonacich questioned the notion of correlating centrality with power and proposed a new measure to try to elucidate this dynamic: *beta-centrality* (or Bonacich's power, 1987). In this equation, the centrality of each vertex is computed by measuring the centrality of the vertices it is connected to:

$$ci = \Sigma Aij(\alpha + \beta cj)$$

The Bonacich centrality of vertex i (ci) is calculated using the above formula, where A is the adjacency matrix and α and β are parameters. The value of α is determined based on the normalization parameter, which is automatically selected, while the value of β is determined by the analyst. A negative β should be selected if the analyst believes that the power of a node increases by being connected to vertices with low power. On the other hand, a positive β should be selected if the power of a node increases by being connected to vertices with high power. The highest possible value for the β can be found by first computing the largest eigenvalue and then calculating a value that is 0.5% lower than the reciprocal of the largest eigenvalue.[64] Where transmission is concerned, beta-centrality assumes traffic over unrestricted walks and a parallel duplication mechanism and is aptly applied to the Omani network in particular.

Where the circulation of commodities or the spread of technologies is concerned, actors that lie on the paths between other actors may theoretically have strategic advantages, potentially having the ability to control commodity or information flows, therefore accruing more prestige and influence within a network (Bavelas 1948; Shaw 1954). These intermediaries are said to have higher betweenness centrality scores.

Betweenness centrality (Freeman Betweenness) determines which nodes are on the shortest paths between dyads. The underlying assumption is that more important nodes are on the shortest paths between many dyads because they are afforded more opportunities to mediate relations between pairs of nodes and control the flow of commodities and information. This measure is arrived at as follows: if the betweenness centrality of a node *k* is being measured, that centrality will be calculated by looking at the number of times node *i*, for instance, uses *k* as an intermediary

[64] In UCINET, this coefficient can be generated with the **Get Beta** function.

to reach a node *j* via the shortest path (Freeman 1979, Borgatti 2005). Thus, if g_{ij} represents the number of geodesic paths connecting *i* to *j*, and the number of geodesics that pass through *k* is g_{ikj} then the equation to calculate this measure would be:

$$\sum_i \sum_j \frac{g_{ikj}}{g_{ij}}, i \neq j \neq k$$

This equation in effect measures the degree to which node *k*'s position is exclusive, indicating how much of the network's flow is being controlled by *k*. Nodes with high betweenness measures are in potentially advantageous positions because of their ability to halt network flow at will (Borgatti 2005).

Borgatti (2005) suggests that this measure is most appropriate for networks of transfer whose trajectories are geodesics. In other words, this measure fits networks in which the commodity is indivisible and travels from node to node along the shortest path. This type of measure would seem to be applicable for the Ethiopian networks, if we can assume that access along shortest paths was important. Borgatti cautions that this measure would not be appropriate for understanding the flow of information within a network. Hanneman and Riddle (2005), on the other hand, have indicated that there is a place for analyzing networks of information with Freeman's betweenness and, as such, I have chosen to cautiously use this measure for studying the Omani network.

Flow Betweenness Centrality calculates the flow betweenness and normalized flow betweenness centrality of each vertex and gives the overall network betweenness centralization. Nodes with high flow betweenness scores can be interpreted as power brokers. Flow betweenness determines the contribution of a vertex to all possible maximum flows and is defined as follows: mjk is the amount of flow between vertex j and vertex k which must pass through i for any

maximum flow. The flow betweenness of vertex i is the sum of all mjk where i, j, and k are distinct and j < k (Freeman, Borgatti, and White 1991: 141 – 154, Hart et al. 2017).

In contrast with Freeman's betweenness, flow betweenness (Freeman et al. 1991) does not assume geodesics but does assume actual paths, where no node is visited more than once. In other words, this measure expands upon the previous betweenness calculation to take into consideration intermediaries that may be located on all paths. To compute the flow betweenness centrality for each node, this measure calculates that node's involvement in all flows between all other dyads. This measure is built upon some of the same assumptions that underlie Freeman's betweenness and will be applied to both the Ethiopian and the Omani networks.

Another way in which node centrality is measured is through *closeness* and relies on the geodesic distance from one actor to all other actors in a network. Centrality as it relates to distance hinges on the notion that it is inversely proportionate to distance. A central actor in a network is *close* inasmuch as it must undertake a minimum number of steps when interacting with other nodes (Hakimi 1965, Sabidussi 1966). Nodes with the shortest geodesics are revealed to be the most central. Unlike previous centrality measures, this type of centrality also accounts for indirect connections. Values range from a minimum of 0, when actors are not reachable from another node, to a maximum of $(g-1)^{-1}$ occurring when an actor is adjacent to all other actors. Because the maximum value of this index is reliant on g, comparing across networks of different sizes is problematic and values must be standardized.

Closeness is often interpreted as measuring the time it will take a commodity to flow to a particular node (Borgatti 1995). Thus, nodes with low closeness measures are assumed to receive a commodity sooner than nodes with higher closeness measures. This measure is applicable to networks in which flow occurs through parallel duplication (as has been suggested for Oman) or

through transfer (as has been suggested for Ethiopia). This is because the closest nodes are likely to be the best positioned to obtain information or objects sooner than other nodes.

Network closeness centralization attains maximum value when an actor choses all other actors. This central actor has a geodesic length of 1, with all other actors having a geodesic length of 2 to the remaining (g – 2) actors. The equation to calculate this measure is:

$$C_C = \frac{\sum_{i=1}^{g}[C'_C(n^*) - C'_C(n_i)]}{[(g-2)(g-1)/(2g-3)]}$$

Finally, *overall network density* is a measure that reveals group cohesion or *knittedness* (Bott 1957) and ranges between 0, in a so-called empty graph, and 1, in a complete graph, defined as a graph in which every dyad is connected by a unique edge. Density is calculated as the average standardized degree:

$$\Delta = \frac{\sum C_D(n_i)}{g(g-1)}$$

where $\frac{\sum C_D(n_i)}{g} = \bar{c}_D$ is the mean degree. This quantity varies between 0 and $g-1$, so to standardize it one must first divide by $g-1$. Caution must be employed when interpreting density measures as these can be misleading. Graphic theorists argue that network density decreases proportionate to the increase in network size, provided that actor degrees remain consistent. As such, density should always be considered in tandem with group size.

These methods provide tools that can be used to address an important and difficult to assess aspect of the structure of socio-economic networks, namely the sources and diffusion of power. Network theory assumes that the power of an actor is not a personal attribute, but rather emerges out of relations with other actors. Network analysis is also used to ascertain structural power

levels[65] as a result of variations in the patterns of ties among actors. These measures allow one to determine the degree of structural inequality or concentration of power.

Powerful actors gain their influence by occupying advantageous positions within relational networks. Advantages arise from positions of high degree, high closeness, or high betweenness. Whereas in simple network structures, these benefits generally covary, in more complex networks these advantages may not necessarily occur in the same network position; that is, an actor may hold one advantage (such as being in a position of high closeness), but may be disadvantaged in other ways (such as being in a position of low betweenness), etc. When such discrepancies occur, one must theorize about the particulars of one's case studies to effectively interpret results.

Finally, the underlying assumption of this research is that supply networks of raw material production will reflect group behavior and that the structure of this economic network can be used to illuminate aspects of interaction between social groups engaging in production and trade.

[65] These will be referred to as *tiers* throughout this chapter.

7.2. Modelling the Diachronic Development of Socio-Economic Networks of Copper Production in Oman

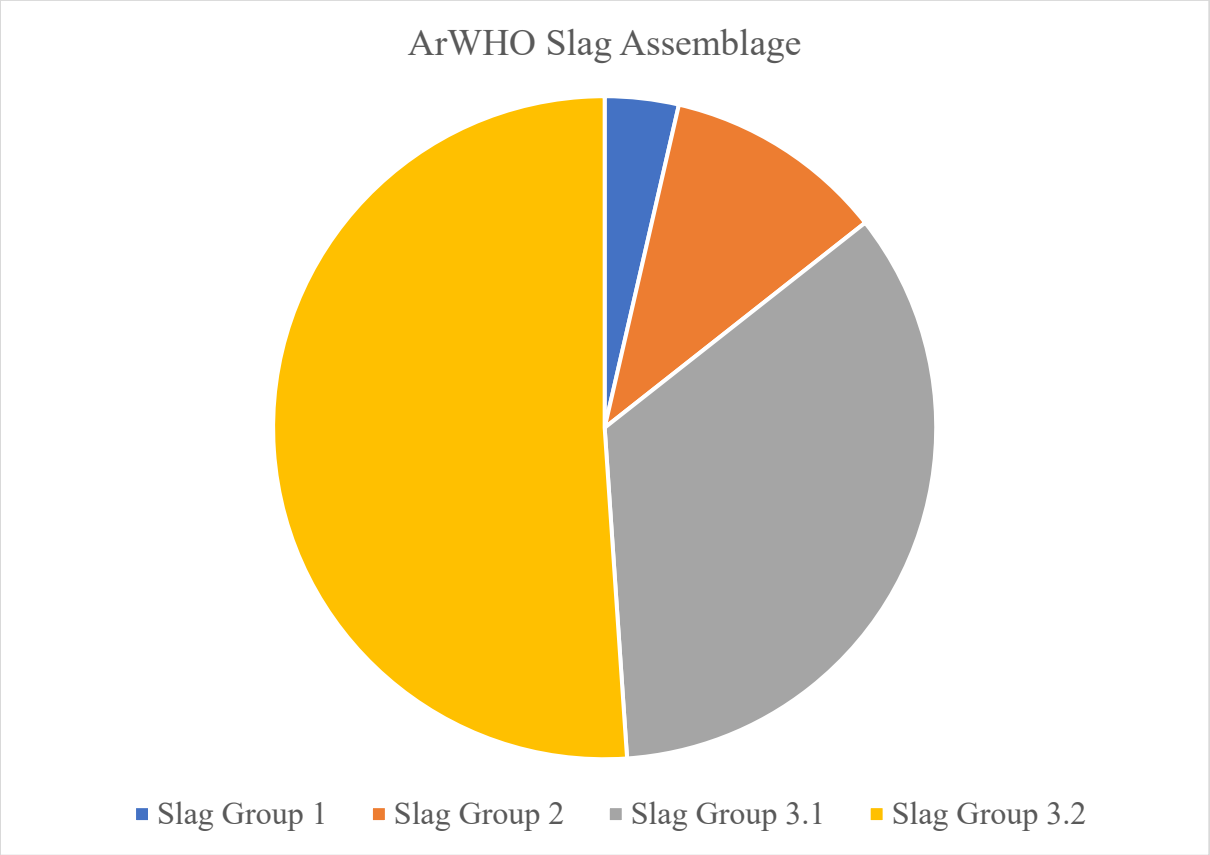

Figure 7.1 ArWHO Slag Assemblage (including slag groups 1, 2, 3.1, and 3.2).

The time period being investigated witnesses the development of the copper supply network in southeastern Arabia from the Bronze Age to the Late Islamic Period and is characterized by periods of economic expansion interwoven with periods of fragmentation (Appendix 1: Table 3). For each period of exploitation and production, a network comprised of coeval sites with evidence of copper production was analyzed to evaluate network cohesion, connectedness, centralization, and power, as well as the position of each node within it.

The longitudinal dataset analyzed for the purposes of this research comprises 142 samples[66] of slag (Fig. 7.1) that were collected as a result of systematic and reconnaissance survey from an area of ca. 5252 km^2 across 36 sites in northeastern Oman (see Fig. 7.7). Slag assemblages were dated through their association with diagnostic material culture. Typologically, slags fall into three categories: (1) tap slags, (2) bowl slag, and (3) furnace slag.

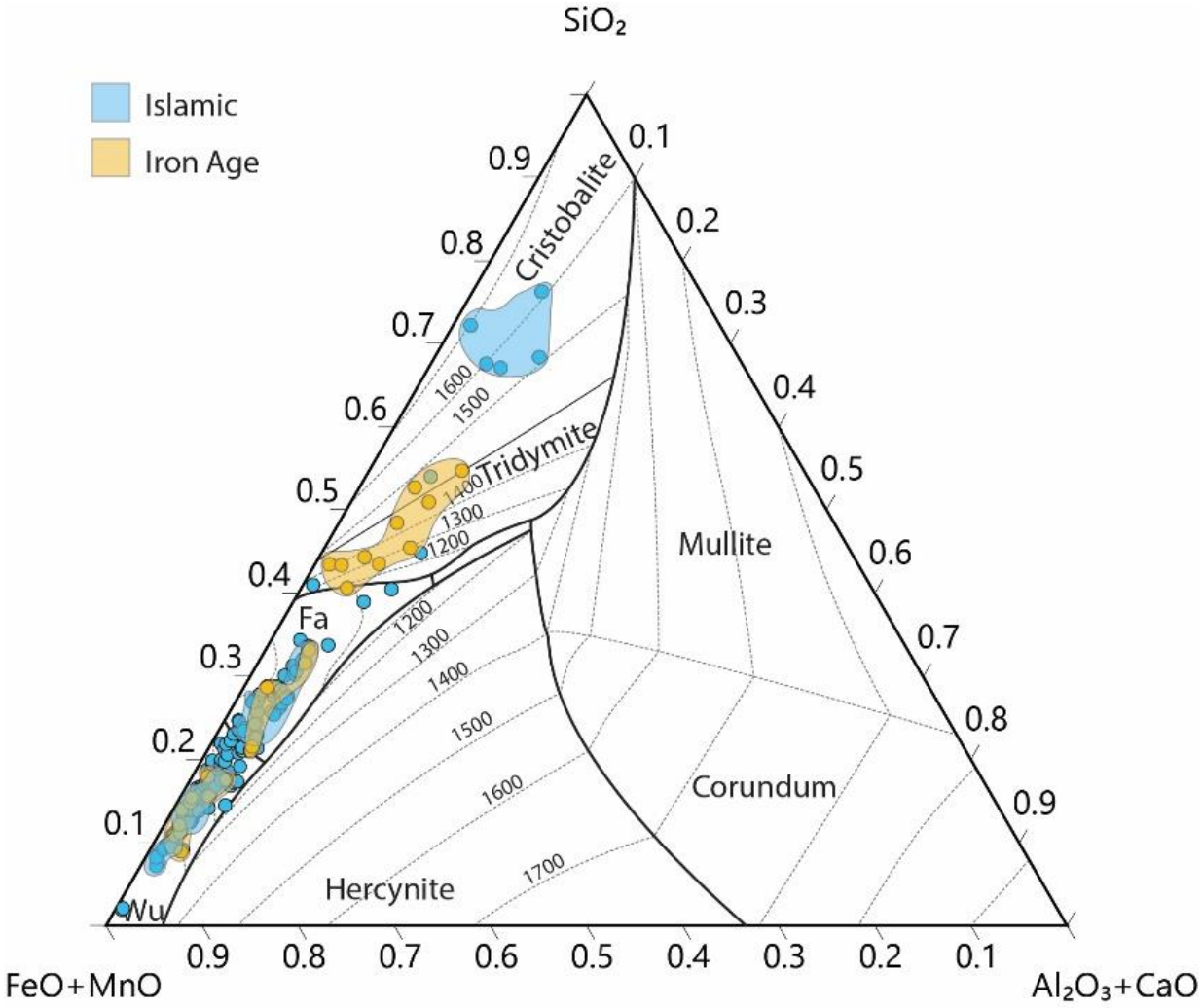

Figure 7.2 Phase Diagram for all Four Slag Groups (J. Lehner).

[66] Out of a total of 142 slag samples analyzed, 139 belong to slag groups 1, 2, 3.1, and 3.2. Three samples (from C71) belong to a fourth slag group, which will be disregarded for the purposes of this research. This is because the iron concentration measured for this samples are in the >90% range, a measure that is not possible for slags. This measure likely occurred as a result of: (1) surface impurities, (2) the points of analysis hitting extremely rich iron phases or possibly metallic iron, or (3) the quantifications getting skewed by extraneous peak data.

Analyses using a Thermo Niton XL3t GOLDD+ XRF analyzer establish the production of at least three slag groups, with the last being separated into two groups (3.1 and 3.2). Reconstruction of the archaeometallurgical process and the formulation of the four slag groups was conducted by J. Lehner (Fig. 7.2.; Appendix I: Table 1a and Table 1b).

Before proceeding to a summary detailing the composition of the slag groups, it is important to acknowledge several limitations to this dataset. First, slag samples have only been dated by association with known ceramic types, other material culture, or architectural features. A second complicating factor is the fact that Omani slag heaps are characterized by multi-period assemblages, spanning many production periods from the third and second millennia BCE to the first millennium CE and including evidence of modern production. Indeed, even in the case of slag samples that have been dated to a single period by association with material diagnostic to a single occupation, the possibility that the slag assemblage comprises samples dating to multiple periods must not be discounted. As such, each time period's network contains both single and multi-period sites with evidence of copper production and network analyses generate models of potential structures, which cannot, at the moment, resolve uncertainties around the contemporaneity of slag from multi-period sites.

Additionally, field conditions led to minimal sample preparation in advance of p-XRF analysis. As such, these measures retrieved surface analyses as opposed to bulk chemistry and must be understood as being incomplete and potentially overrepresenting certain elements while underrepresenting others. Finally, this research does not include analyses of known copper slag standards. As such, quantitative comparisons with analyses produced by previous researchers, like A. Hauptmann, cannot yet be undertaken in the absence of further analyses with more robust laboratory measures.

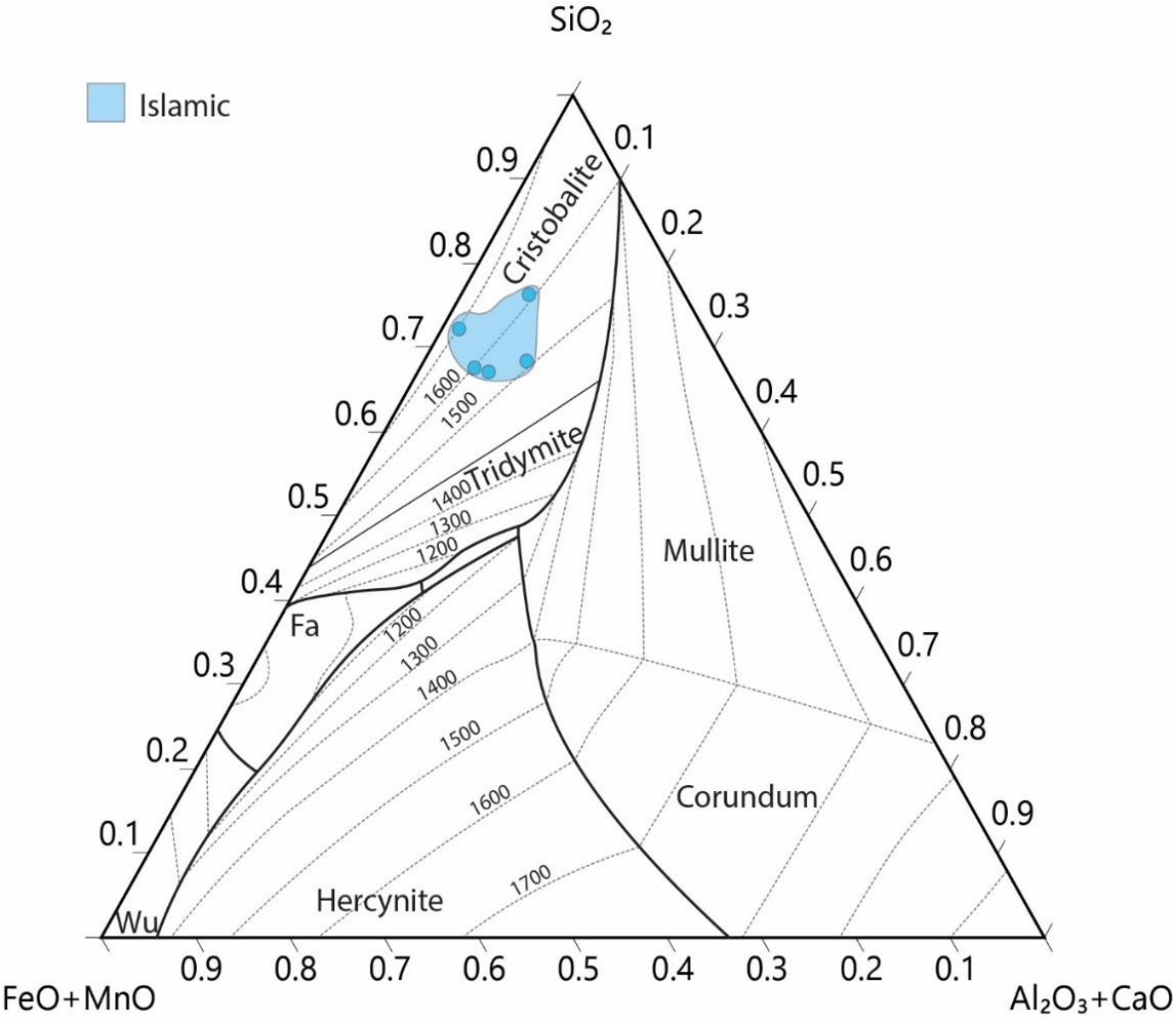

Figure 7.3 Phase Diagram Slag Group 1 (J. Lehner, I.A. Dumitru).

Slag Group 1 is limited to the Islamic period from the sites of Arja (C119) and Hayy al-Nahza (C146). Slags from group 1 have low copper oxide (CuO) content, demonstrating efficient copper extraction, and are characterized by low ferrous oxide and manganese oxide (FeO+MnO) contents and higher silicate contents (Fig. 7.3). The high silicate content can either point to high slag liquidus temperatures (of up to 1600 – 1700°C) or more likely to the intentional addition of silicates (such as sand) into the ore charge. This later suggestion has already been observed by

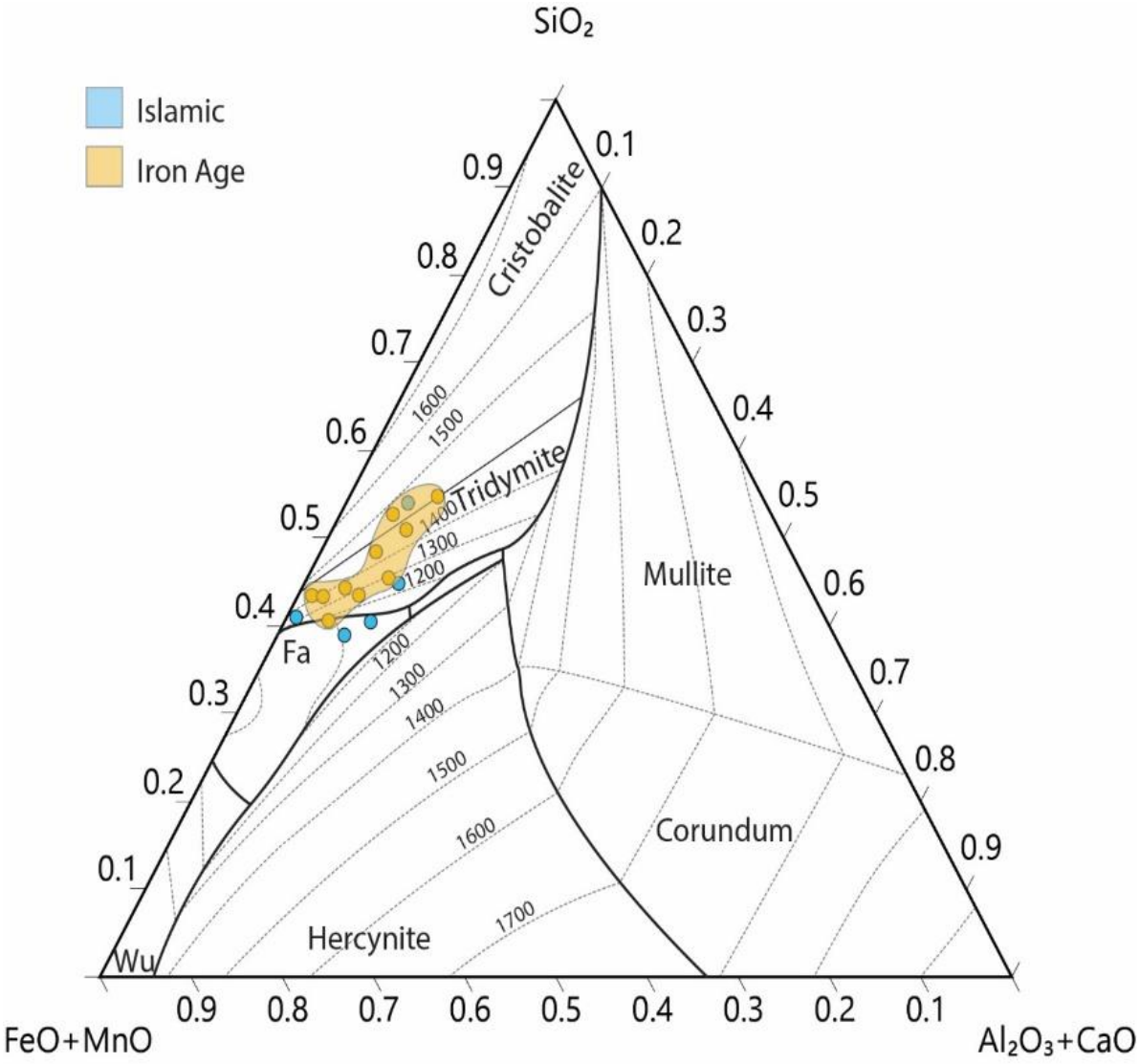

Figure 7.4 Phase Diagram Slag Group 2 (J. Lehner, I.A. Dumitru).

Hauptmann in the southern Levant. Containing 5 samples, this group represents 3.6% of the total slag assemblage (Appendix I: Table 2a and Table 2b).

Slag Group 2 is composed of slags primarily dating to the Iron Age, including locations at Tawi Arja, Raki 2, Safri 1, Aqir al-Shamoos, and Hayy Ukur. Group 2 contains 15 samples (10.79% of the total slag assemblage; Appendix I: Table 3a and Table 3b) and is also characterized by low ferrous oxide and manganese oxide (FeO+MnO) contents and higher silicate contents. Slags from this group demonstrate elevated concentrations of iron oxides, indicating that a more optimal zone of slag composition was approached. Varied copper (up to 16.2%) and sulfur (up to 14.1%) content show a range of extraction efficiencies and demonstrate the definite use of copper

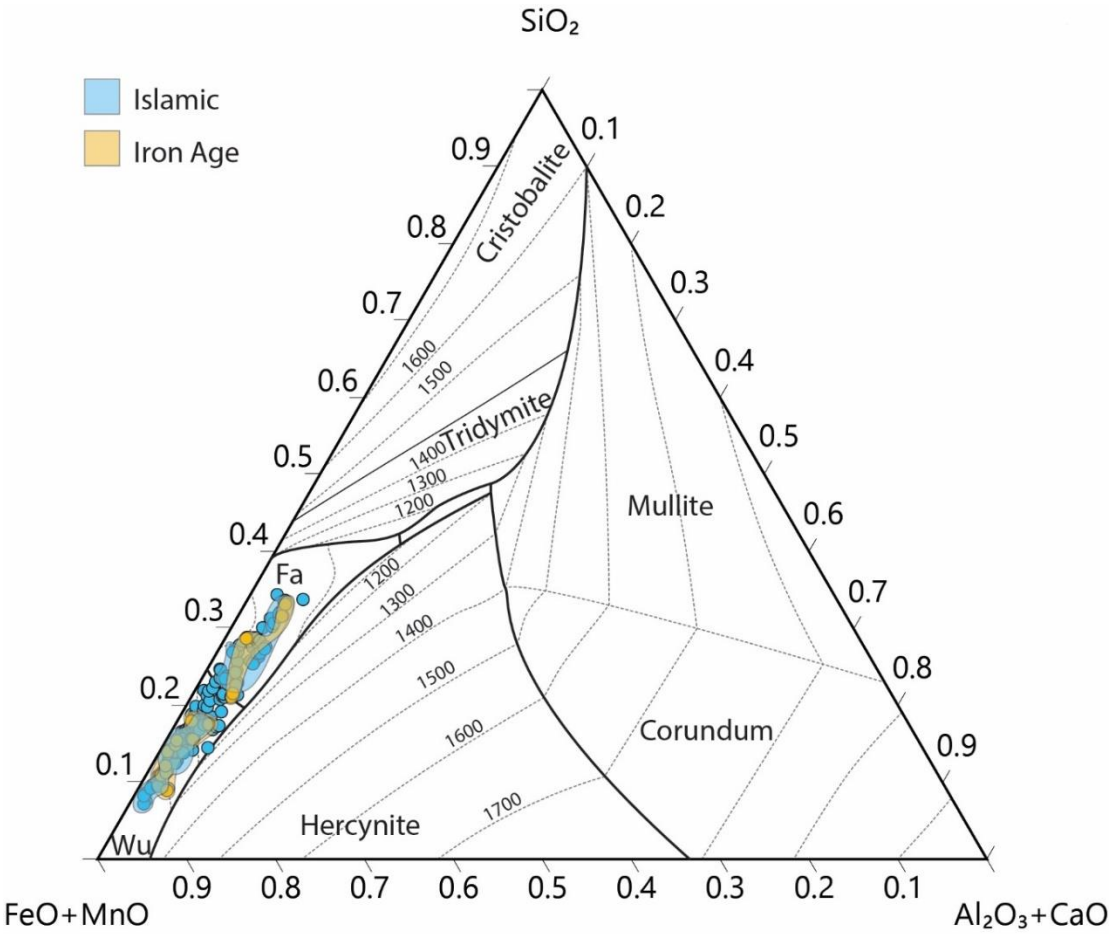

Figure 7.5 Phase Diagram Slag Group 3 (J. Lehner, I.A. Dumitru).

sulfides during this time period, thus confirming Hauptmann's hypothesis. These data cannot, however, confirm whether a separate matte production sequence was present during the Iron Age (Fig. 7.4).

Slag Group 3 (Fig. 7.5) is the most widely distributed slag group and is composed of a continuous sequence of high ferrous oxide and manganese oxide FeO(+MnO) to optimal ferrous oxide – manganese oxide – silica dioxide FeO(+MnO)-SiO2. The group is divided into two sub-groups, 3.1 and 3.2.

Group 3.1 (Fig. 7.6) represents an optimal range of slag composition within the region where fayalite is most stable around ca. 1200°C. Importantly, a group of Islamic period slags that fit within this range contain elevated concentrations of manganese oxide MnO (max 53% MnO). Such an elevated concentration is consistent with Hauptmann's findings both in Oman and in the southern Levant, where the intentional introduction of manganese-rich ores into the smelting mixture as a flux has been observed. In the case of Oman, Hauptmann believes that the manganese-rich materials were added to mitigate the production of deleterious copper-iron alloys in the smelting process. Group 3.1 contains 48 samples and represents 34.53% of the slag assemblage (Appendix6: Table 4a and Table 4b).

Group 3.2 (Fig. 7.6) is composed of high concentrations of ferrous oxide FeO and low concentrations of silicate. It is predicted these slags should show the presence of wustite. If wustite is present, then these slags would have formed at elevated temperatures (ca. 1400°C). Containing a total of 71 samples, this group represents 51.08% of the assemblage (Appendix I: Table 5a and Table 5b).

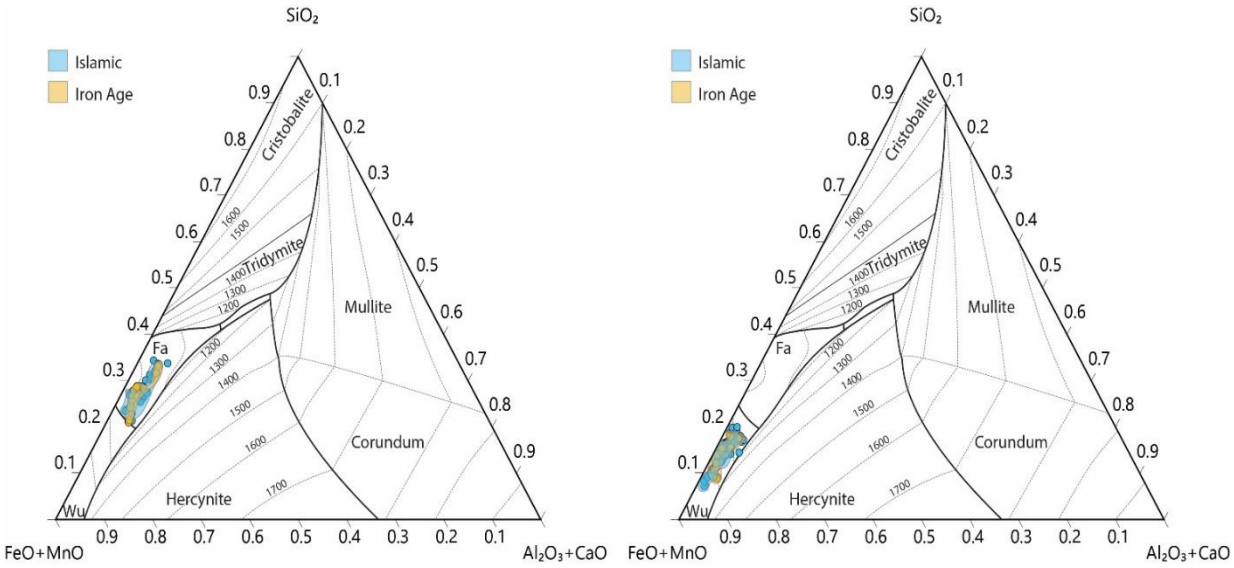

Figure 7.6 Phase Diagrams for Slag Group 3.1 (left) and Slag Group 3.2 (right) (J. Lehner, I.A. Dumitru).

This slag assemblage was accumulated through collections from 36 sites (Appendix I: Table 6; Fig. 7.7). Of these 36 sites, 14 are single period sites (Appendix I: Tables 12a and 13a), 16 are multi-period sites, and 6 have yet to be dated. Including multi-period sites, the Bronze Age network includes 5 sites (Appendix I: Table 11), the Iron Age network contains 20 sites (Appendix I: Table 12b), and the Islamic period network is comprised of 25 sites (Appendix I: Table 13b). It is important to note that with a sample size this small, a great deal of caution must be employed when interpreting results as patterns may change once the sample size is expanded. Limitations surrounding sample size are further compounded by the high incidence of multi-period site.

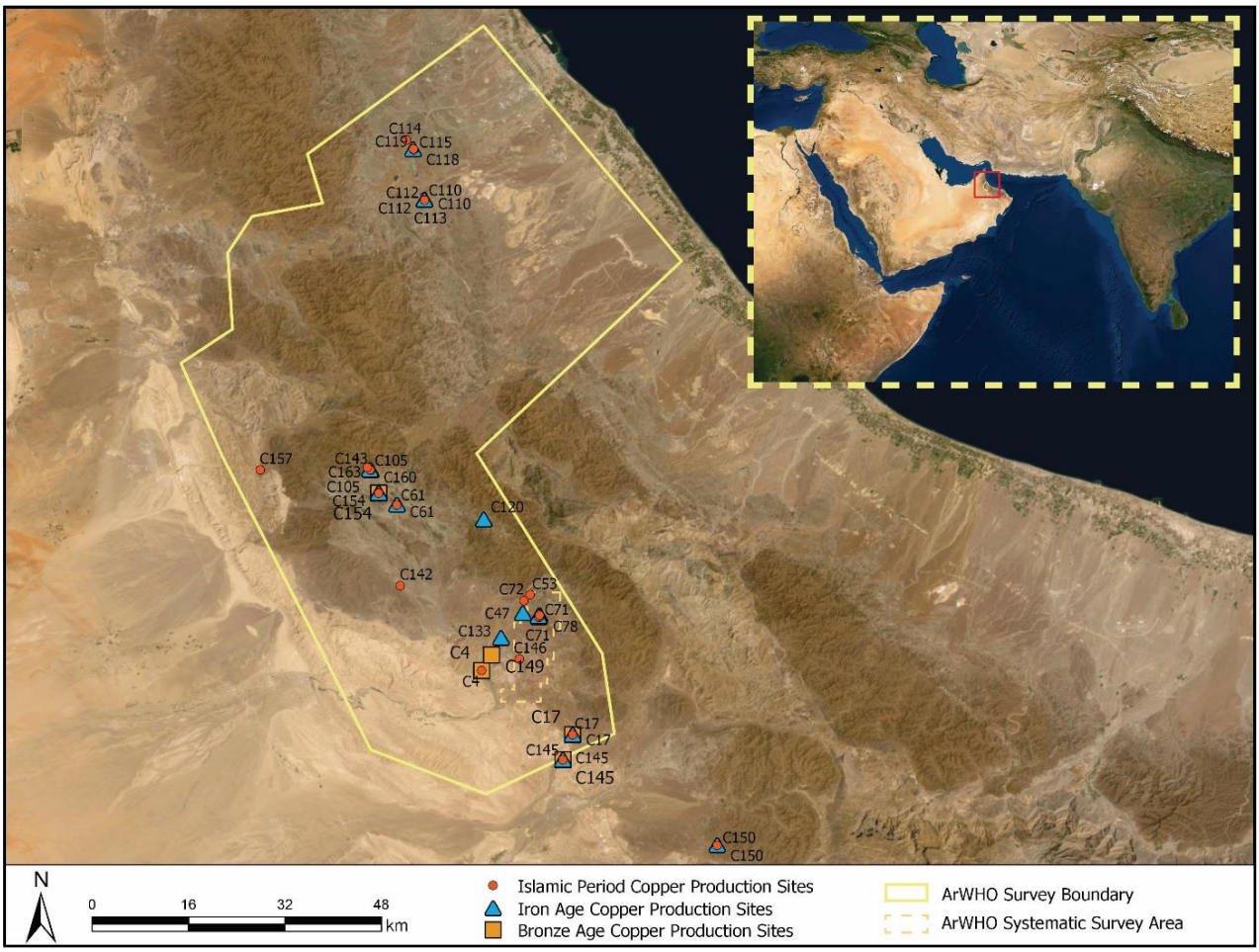

Figure 7.7 Copper Production Sites: All Time Periods.

7.2.1. The Copper Network during the Bronze Age (2500 – 1300 BCE)

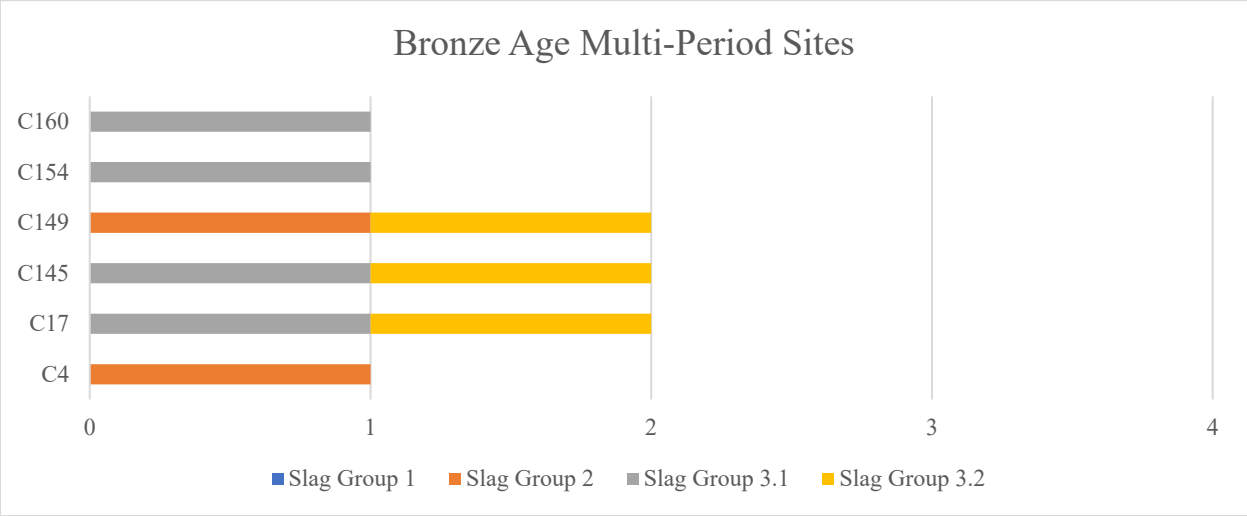

Figure 7.8 Bronze Age Multi-Period Sites and the Slag Groups they Shared.

The Bronze Age network contains 6 nodes that collectively share three slag groups (Fig. 7.8). Shared slag groups include slag group 2, slag group 3.1, and slag group 3.2. This network is entirely made up of 1 single period site (C149, 944-001; Appendix I: Table 11a) and 5 multi-period sites (Appendix I: Table 11b) and is characterized by 18 ties. As calculated using the Freeman Centralization approach, the overall group centralization is 0.2500 (25%). This measure indicates a relatively decentralized network, characterized by little variation in rank or power of individual nodes.

This network can be divided into three tiers (Table 7.1). With a degree centrality of 5, the best-connected sites are the tower site of Khadil (C17, 971-001) and the settlement of Al Arid (C145, 934-001). Represented by three sites, the second tier is characterized by a degree centrality of 3 and includes two settlements in Wadi Harim 973-001 (C154) and 973-006 (C160) and a single period habitation structure (C149, 944-001). Finally, the third tier consists of 1 tower site, Safri 1

(C4, 989-001), which is connected to the network through the intermediary of C149, which acts as a bridge (Fig. 7.9).

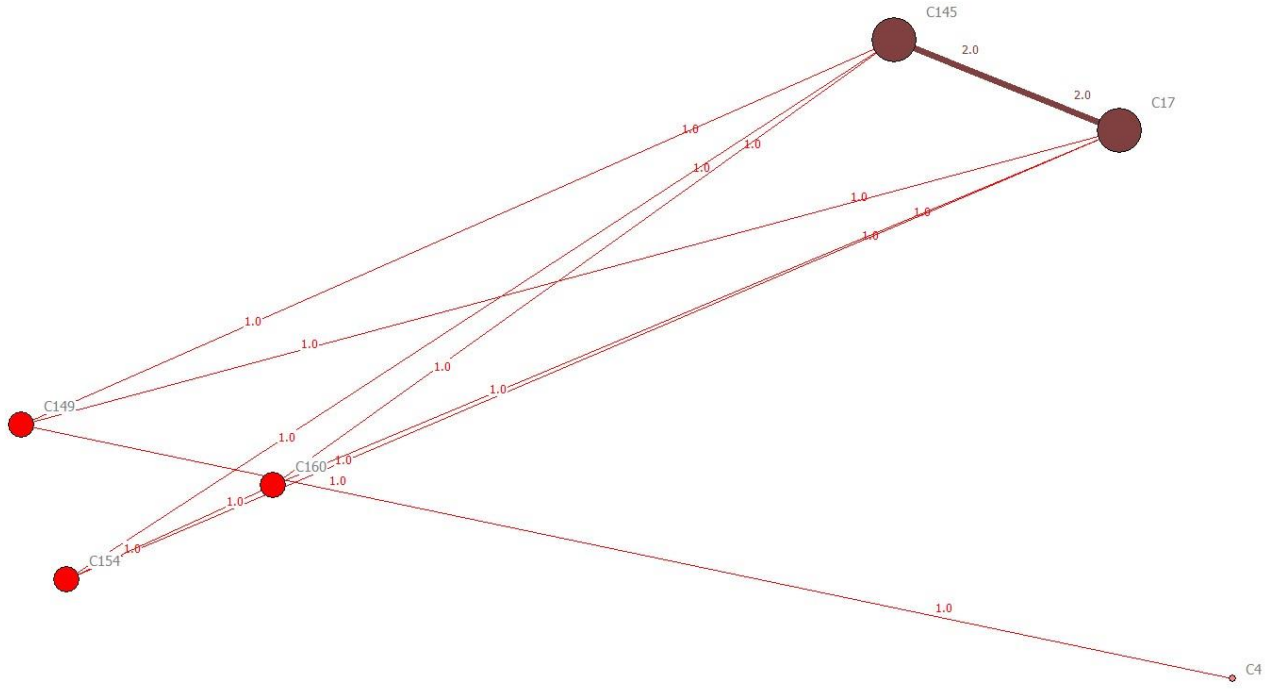

Figure 7.9 Bronze Age Network (Multi-Period Sites). Nodes Scaled by Degree Centrality.

To confirm this node order, a beta-centrality measure was calculated to reveal four tiers and a slightly different node order, with a first tier consisting of the same two sites revealed by the degree centrality measure (C17 and C145), a second tier containing sites C154 and C160, a third tier consisting of site C149, and a fourth tier consisting of site C4.

A Flow Betweenness Centrality was used to calculate a network centralization index of 28.53%. The most central site of the network in terms of flow betweenness is C149. With a flow betweenness measure of 5, the second tier of sites contains the two best connected sites in terms of degree centrality, C17 and C145. A third tier, consisting of sites C154 and C160, is characterized by a flow betweenness measure of 1.733. Finally, site C4 has a flow betweenness of 0.

Table 7.1 Weighted Adjacency Matrix with Degree Centrality Measure.

	C4	C17	C145	C149	C154	C160	Degree
C4		0	0	1	0	0	1
C17	0		2	1	1	1	5
C145	0	2		1	1	1	5
C149	1	1	1		0	0	3
C154	0	1	1	0		1	3
C160	0	1	1	0	1		3

Although the sample is small, many of the relationships revealed by the centrality measures correlated with spatial patterns (Fig. 7.10). The two sites with the highest degree centrality measure, C17 and C145, cluster spatially in the southern stretches of the greater ArWHO Survey Area, with C145 being located 4.39 km from C17. Two second tier sites (C154 and C160), characterized by a degree centrality of 3, also cluster together in the central region of the larger ArWHO Survey Area and are located at a distance of 63 meters from one another. Finally, C149, a site with a degree centrality of 3, clusters with C4, a site for which it acts as an intermediary to the rest of the network.

Additional centrality measures undertaken on the binarized dataset further indicate that a great deal of power is found with node C149. Freeman's Betweenness Centrality reveals a betweenness of 4 for C149, a betweenness of 2 for C17 and C145, measures of 0 for the rest of the sites of the Bronze Age Network and an overall Network Centralization Index of 32%. Additionally, Freeman's sum of geodesic distances indicates an overall Network Centralization of

41.15% and farness measures that reveal the following node order (from farthest to closest nodes): C4 (farness of 11), C154 and C160 (farness of 8), C149 (farness of 7), and C17 and C145 (farness of 6).

Several graph-theoretic measures of connectedness and cohesion were also run on the binarized dataset revealing a density of 0.600 (60%) and indicating a relatively porous network. Each site has a reachability of 1, indicating the absence of isolates within the network.

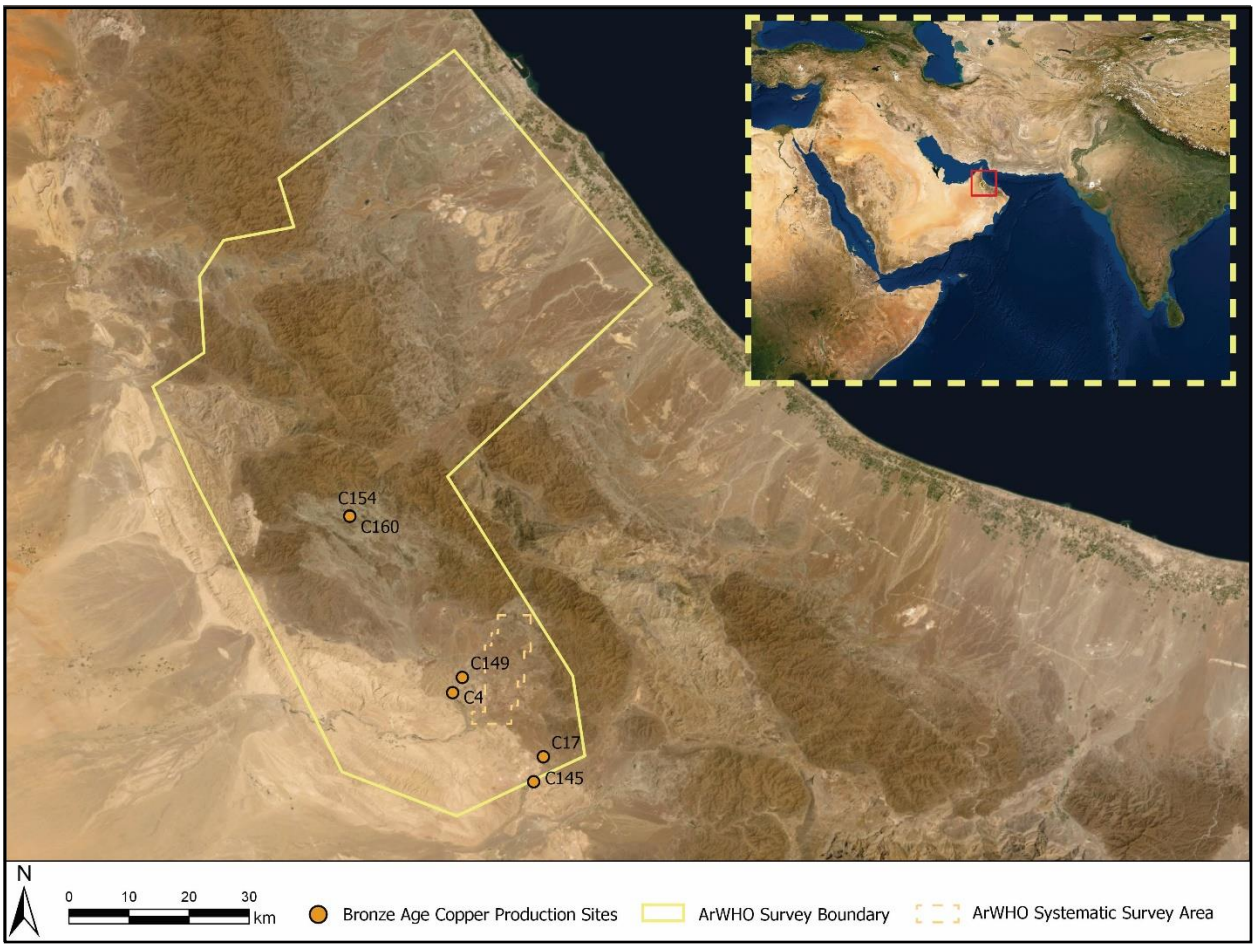

Figure 7.10 Bronze Age Network (including multi-period sites).

7.2.2. The Copper Network during the Iron Age (1300 – 300 BCE)

Figure 7.11 Iron Age Multi-Period Sites and the Slag Groups they share.

The Iron Age Copper Network contains 5 single period sites (Appendix I: Table 12a) and 15 multi-period sites (Appendix I: Table 12b) for a total of 20 nodes that collectively share slag from slag groups 2, 3.1, and 3.2 (Fig. 7.11). Network size represents an increase of 233.33% from the previous Bronze Age period. A total of 340 ties connecting the nodes of this network represents a 1788.89% increase in the number of ties from the previous period's network. With an overall graph

centralization of 0.1852 (18.52%), the Iron Age Network is the least centralized network out of the ones currently under investigation, observing a decrease in degree centralization of 25.92% from the previous period.

Based on the strength of their ties, each node can be divided into one of five tiers, as calculated using Freeman's Approach (Fig. 7.12; Table 7.2). With a degree centrality of 33, the first tier consists of three sites, the settlements of Raki 2 (C47, 981-001), Tawi Arja (C118, 930-001), and Aqir Al-Shamoos (C143, 952-001).

Characterized by 29 ties, the second most central position within the network includes 8 sites: Khadil, a tower site (C17, 971-001), 4 settlements and smelting sites, Muaydin (C61, 962-001), Tawi Raki (C71, 984-001), Al Arid (C145, 934-001), and Hala (C150), two locations within the large smelting site of Lasail (C110 and C112, 932-001 and 932-003, respectively), and one slag scatter, C133, 918-001.

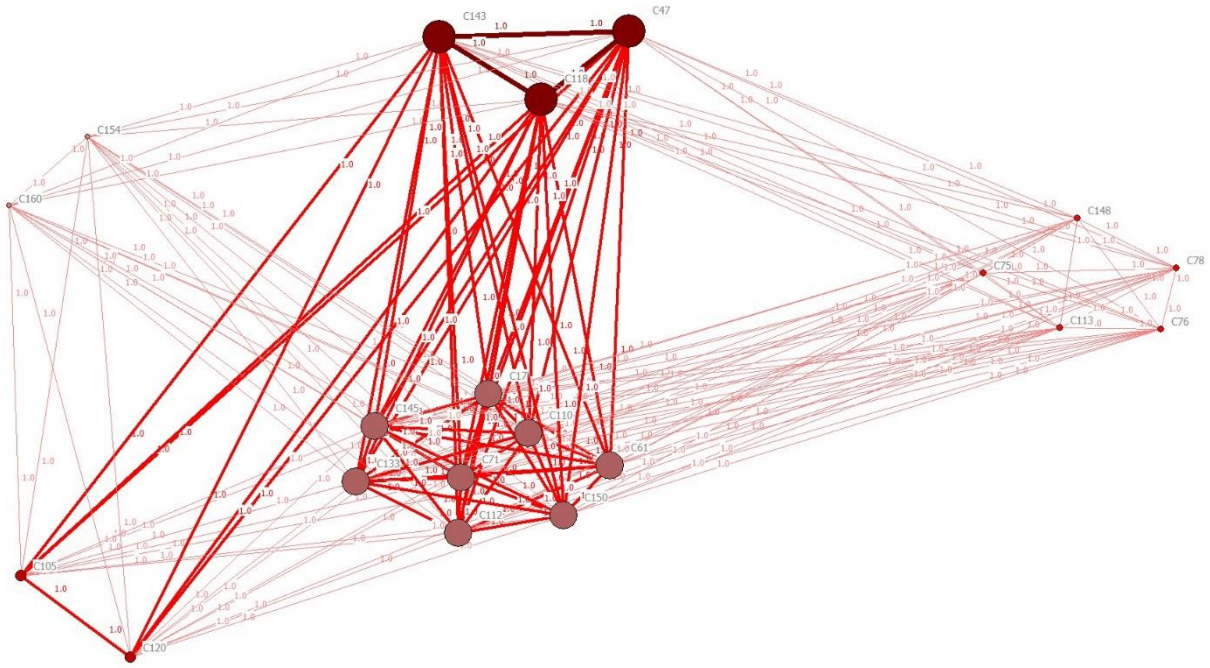

Figure 7.12 Iron Age Network (includes multi-period sites). Nodes Scaled by Degree Centrality.

Containing two sites, the third tier is characterized by a degree centrality of 18 and includes Aqir Al-Shamoos 2 (C105, 952-002), a site with architectural structures associated with a slag scatter and located across a ravine from the larger and better connected settlement of Aqir Al-Shamoos, and the settlement of Hayy Ukur (C120, 994-001).

The fourth tier is characterized by a degree centrality of 15 and contains 5 nodes, including four different locations at the large settlement and smelting site of Tawi Raki (C75, C76, C78, and C148, 984-001) and one node from the smelting site of Lasail (C113, 932-004). Finally, a fifth tier contains two nodes, both settlements located in Wadi Harim (C154, 973-001, and C160, 973-006) and is characterized by a degree centrality of 14.

Despite these differences in degree centrality, the overall centralization of the network indicates a relatively decentralized distribution of power within the Iron Age Network. A beta-centrality measure was used to reveal the same organization of nodes. Interestingly, a Flow Betweenness Centrality measure revealed the same node order for the first, second, and fifth tiers and different components for the third and fourth tiers. Indeed, third tier nodes (C75, C76, C78, C113, and C148) coincide with fourth tier nodes as indicated by the abovementioned degree centrality measure and, conversely, fourth tier nodes (C105 and C120) correspond with third tier nodes.

Table 7.2 Weighted Adjacency Matrix with Degree Centrality Measure.

	C17	**C47**	**C61**	**C71**	**C75**	**C76**	**C78**	**C105**	**C110**	**C112**	**C113**	**C118**	**C120**	**C133**	**C143**	**C145**	**C148**	**C150**	**C154**	**C160**	**Degree**
C17		2	2	2	1	1	1	1	2	2	1	2	1	2	2	2	1	2	1	1	29
C47	2		2	2	1	1	1	2	2	2	1	3	2	2	3	2	1	2	1	1	33
C61	2	2		2	1	1	1	1	2	2	1	2	1	2	2	2	1	2	1	1	29
C71	2	2	2		1	1	1	1	2	2	1	2	1	2	2	2	1	2	1	1	29
C75	1	1	1	1		1	1	0	1	1	1	1	0	1	1	1	1	1	0	0	15
C76	1	1	1	1	1		1	0	1	1	1	1	0	1	1	1	1	1	0	0	15
C78	1	1	1	1	1	1		0	1	1	1	1	0	1	1	1	1	1	0	0	15
C105	1	2	1	1	0	0	0		1	1	0	2	2	1	2	1	0	1	1	1	18

C110	2	2	2	2	1	1	1	1		2	1	2	1	2	2	2	1	2	1	1	29
C112	2	2	2	2	1	1	1	1	2		1	2	1	2	2	2	1	2	1	1	29
C113	1	1	1	1	1	1	1	0	1	1		1	0	1	1	1	1	1	0	0	15
C118	2	3	2	2	1	1	1	2	2	2	1		2	2	3	2	1	2	1	1	33
C120	1	2	1	1	0	0	0	2	1	1	0	2		1	2	1	0	1	1	1	18
C133	2	2	2	2	1	1	1	1	2	2	1	2	1		2	2	1	2	1	1	29
C143	2	3	2	2	1	1	1	2	2	2	1	3	2	2		2	1	2	1	1	33
C145	2	2	2	2	1	1	1	1	2	2	1	2	1	2	2		1	2	1	1	29
C148	1	1	1	1	1	1	1	0	1	1	1	1	0	1	1	1		1	0	0	15
C150	2	2	2	2	1	1	1	1	2	2	1	2	1	2	2	2	1		1	1	29
C154	1	1	1	1	0	0	0	1	1	1	0	1	1	1	1	1	0	1		1	14
C160	1	1	1	1	0	0	0	1	1	1	0	1	1	1	1	1	0	1	1		14

A Betweenness Centrality measure, run on the binarized matrix revealed that 55% of the nodes had a betweenness centrality of 1.818, with the rest having a betweenness centrality of 0 (Appendix I: XX). The nodes with a betweenness centrality of 1.818 are: C17, C47, C61, C71, C143, C145, C118, C150, C110, C112, and C133. These nodes are included in the top two tiers of the network, as revealed by the abovementioned degree centrality measure. Freeman's closeness centrality revealed three groups of nodes: (1) with a farness measure of 19, the best positioned group of nodes (in terms of closeness centrality) includes the same nodes that revealed a higher betweenness centrality measure; (2) a second group of nodes, characterized by a farness measure of 23, contains all of the nodes of the fourth tier of the network, in terms of degree centrality (C113, C75, C78, C148, C76); (3) the farthest nodes (C105, C120, C154, and C160), with a measure of 24, include nodes from the third and fifth tiers and characterized by degree centralities of 18 and 14 respectively.

Two graph-theoretic measures of connectedness and cohesion were also run on the dataset: density and reachability, revealing a network with a density of 89.5% and a reachability of 1 for each node.

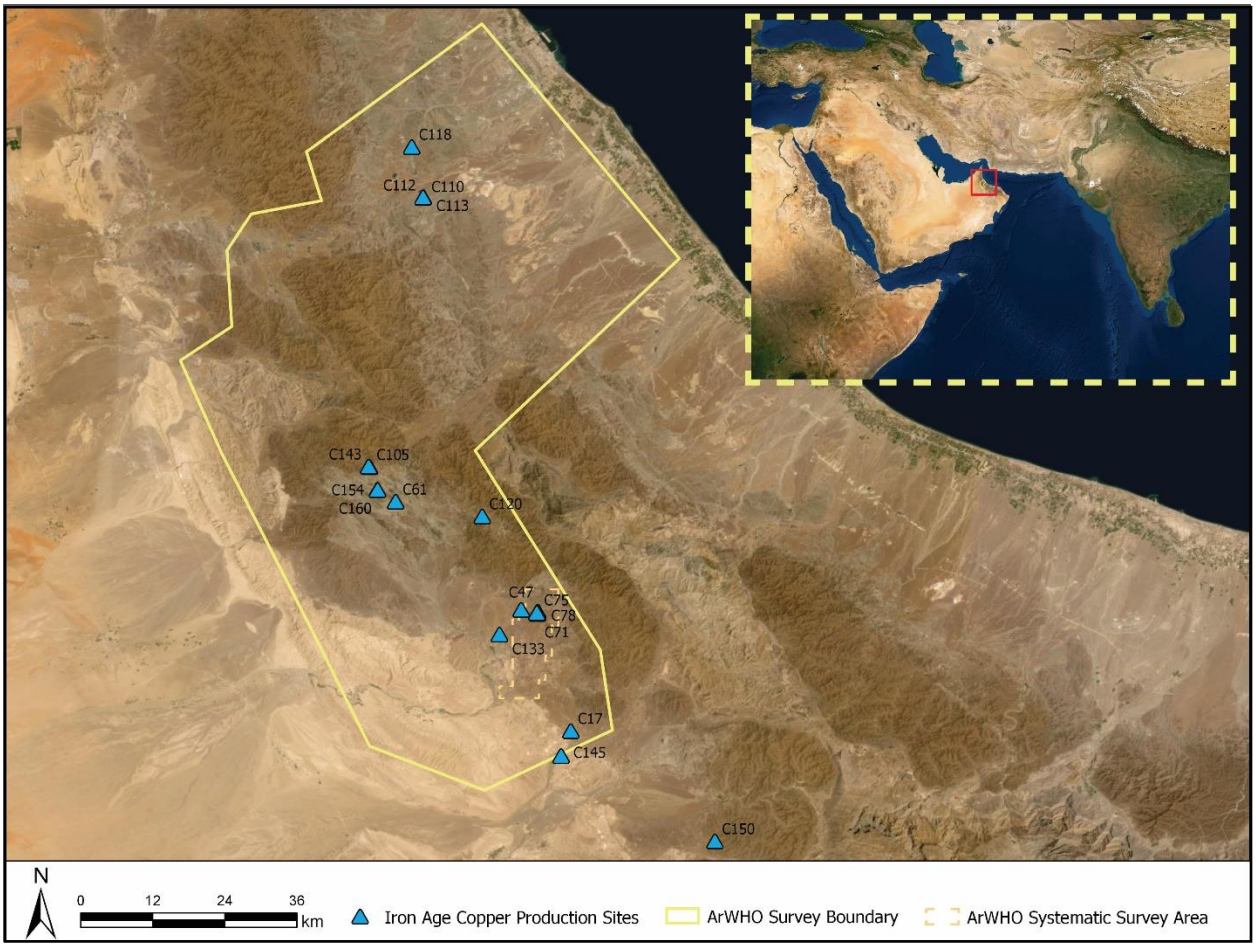

Figure 7.13 Iron Age Network (including multi-period sites).

The spatial pattern of sites reveals three cluster zones (Fig. 7.13): (1) one cluster (C110, C112, C113, C118) in Wadi Jizzi in the north of the larger ArWHO survey area, (2) one cluster close to the boundary between Ad Dhahirah, Al Buraymi (to the north-west), and Al Batinah (to the east), and (3) one towards the northern corner of the ArWHO Systematic Survey area. In addition to these clusters, the landscape of Iron Age copper production sites includes one pair of sites (C17 and C145), located towards the tip of the larger survey region, and two isolated sites, one located between the second and third clusters (C120) and another located 27.45 km south of the larger ArWHO survey area (C150).

When compared with the patterns indicated by the various network analyses, each cluster is revealed to contain at least one first tier node (degree centrality of 33), at least one second tier node (degree centrality of 29), and various different arrangements of third, fourth, and fifth tier nodes (Table 7.3). The pair containing C17 and C145 were both second tier sites and the two isolated nodes (C120 and C150) belonged to the third (degree centrality 18) and fifth (degree centrality 14) tiers, respectively.

Table 7.3 Iron Age Copper Production Sites: Spatial Clusters and Degree Centralities of Constitutive Nodes.

Wadi Jizzi Cluster	Middle Cluster	Southern Cluster	Pair	Isolates
C118 – DC 33	C143 – DC 33	C133 – DC 29	C17 – DC 29	C120 – DC 18
C110 – DC 29	C105 – DC 18	C47 – DC 33	C145 – DC 29	C150 – DC 14
C113 – DC 15	C154 – DC 14	C78 – DC 15		
C112 – DC 29	C160 – DC 14	C75 – DC 15		
	C61 – DC29	C76 – DC 15		
		C148 – DC 15		
		C71 – DC 29		

7.2.3. The Copper Network during the Islamic Period (635 – 1800 CE)

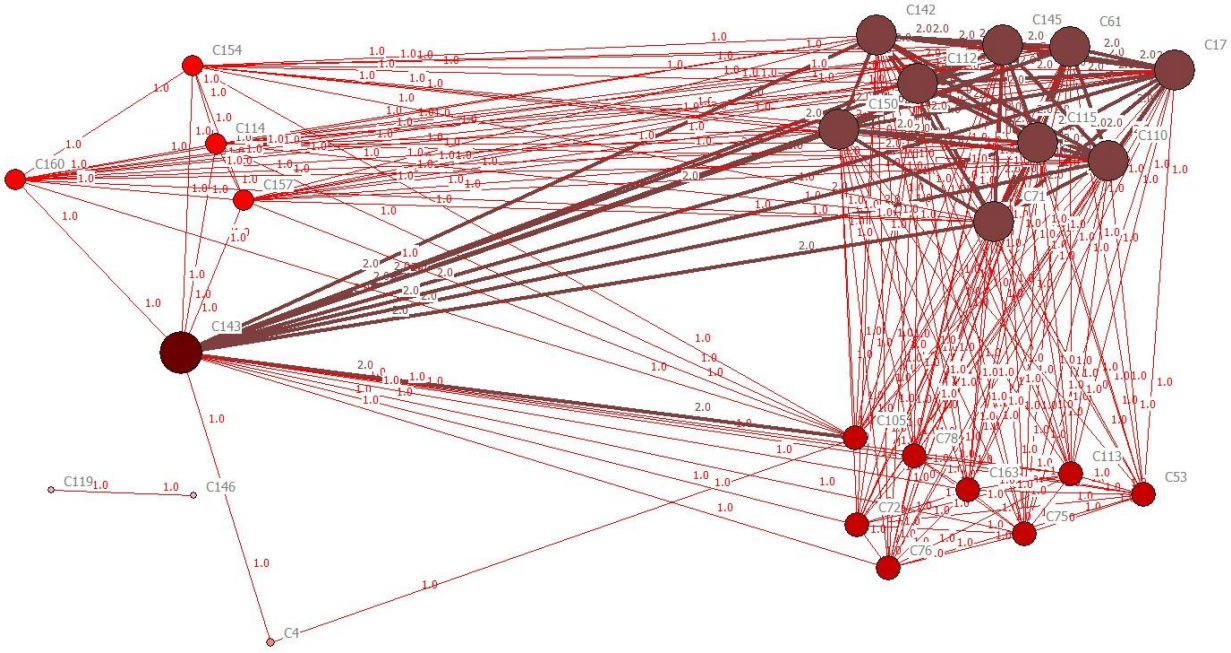

Figure 7.14 Islamic Period Network (including multi-period sites). Nodes Scaled by Degree Centrality.

The Islamic period network sees a 25% increase in node size, a 17.06% increase in number of ties, and a 51.62% increase in overall network centralization. This network contains 25 nodes, 398 ties, and a graph centralization of 28.08% (Fig. 7.14), as calculated using the Freeman Centralization approach. Islamic period sites share evidence of slag from all four slag groups (Fig. 7.15). This network contains 9 single period sites (Appendix I: Table 13a) and 16 multi-period sites (Appendix I: Table 13b).

Based on the strength of their ties, each node can be divided into 6 tiers. The first tier contains a single node, the settlement and smelting site of Aqir Al-Shamoos (C143, 952-001), the only remaining site of the triad of first tier sites from the previous period's network. This node is characterized by a degree centrality of 32.

With a degree centrality measure of 30, the second tier contains 36% of the total number of Islamic period sites and overlaps with 87.5% of the previous network's second tier nodes. This group includes one tower site, Khadil (C17, 971-001), 5 settlements and smelting sites, Muaydin (C61, 962-001), Tawi Raki (C71, 984-001), Tawi Arja (C115, 930-001), Al Arid (C145, 934-001), and Hala (C150), two locations within the large smelting site of Lasail (C110, 932-001, and C112, 932-003), and one slag scatter C142 (919-001).

With a degree centrality of 16, the third tier contains the second largest number of nodes (32%) and is characterized by a degree centrality index indicating that nodes found in tertiary positions of degree centrality have 53.33% fewer ties than second tier nodes. Sites contained by this group include the settlements and smelting sites of Raki 1 (C72, 936-001) and Tawi Raki (with three locations being represented therein C75, C76, C78), the settlement of Hayl al-Arb (C163, 950-001), the smelting site of Lasail (C113, 932-004), a site with architectural structures associated with a slag scatter Aqir Al-Shamoos 2 (C105, 952-002), and the slag scatter of 924-001 (C53).

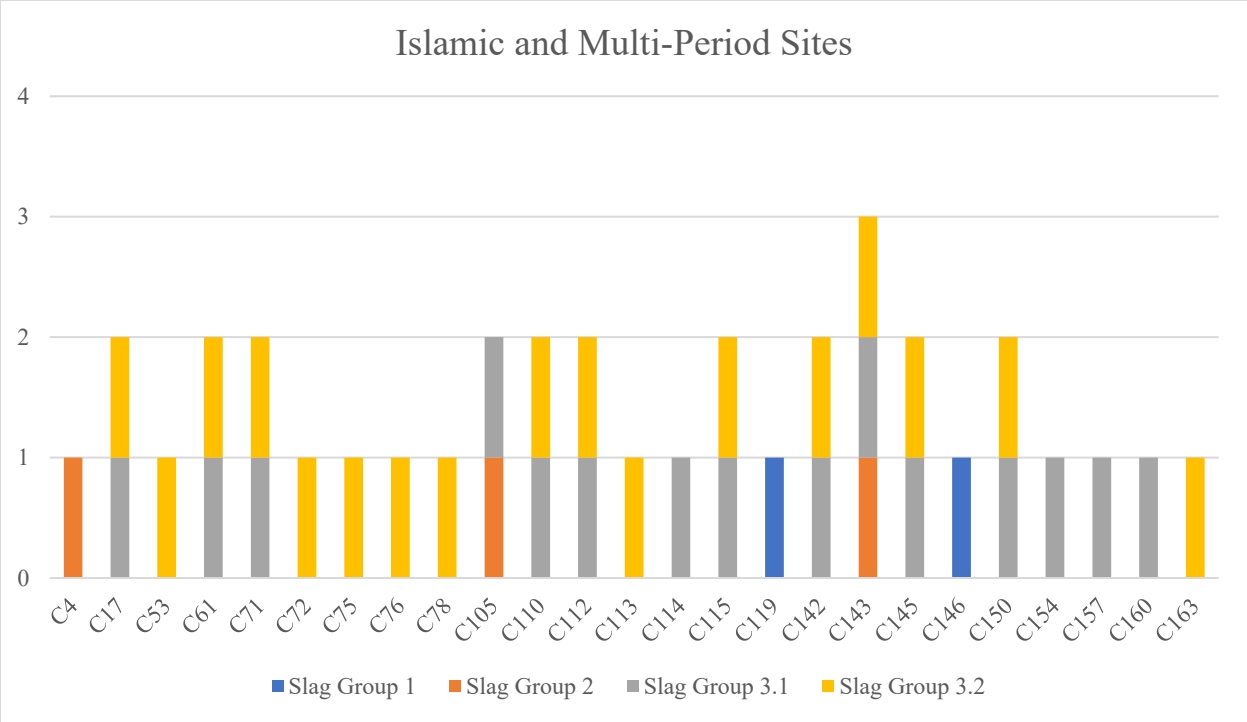

Figure 7.15 Islamic Period Multi-Period Sites and the Slag Groups they share.

The fourth tier contains four nodes, characterized by a degree centrality of 14 and includes the settlements of Bayda (C114, 931-001), Qumaira (C157, 970-003), and Wadi Harim (C154, 973-001), and another habitation structure associated with a slag scatter in Wadi Harim (C160, 973-006). With a degree centrality of 2, the fifth tier includes a single node: the tower site of Safri 1 (C4, 989-001). Finally, the sixth tier includes 2 nodes, the settlement and smelting site of Arja (C119, 929-001) and the find spot of Hayy al-Nahza (C146, 985-002).

Despite being the most centralized out of the three networks under investigation, the Islamic Period network, nonetheless, reveals the overall continuation of a relatively decentralized distribution of power, an aspect which was further confirmed with a Flow Betweenness Centrality Measure.

Interestingly, a beta-centrality measure revealed a slightly different node order than the one indicated by the degree centrality calculation and exposed the existence of 7 tiers. The first tier as

revealed by the beta-centrality measure coincides with the first tier indicated by the degree centrality measure: Aqir Al-Shamoos (C143, 952-001). Containing 9 nodes, the second tier overlaps entirely with the second tier nodes revealed through the degree centrality calculation. Third tier sites overlap with all but a single node of the second tier revealed through the degree centrality calculation. That single node, Aqir Al-Shamoos 2 (C105, 952-002) is characterized by a slightly lower Bonacich centrality measure and has been consigned to the fourth tier. Finally, fifth, sixth, and seventh tier nodes correspond with the fourth, fifth, and sixth tiers indicated by the degree centrality measure.

A Flow Betweenness Centrality measure illuminates a different node order, which, when compared to the patterns showcased by the previous centrality measures, revealed a complex network where power shifted between nodes when different traits where foregrounded. The first tier coincides with the first tier revealed by all other centrality measures, Aqir Al-Shamoos (C143), and is characterized by a flow betweenness measure of 52.871. With a flow betweenness measure of 34.571, the second tier comprises of a single node, Aqir Al-Shamoos 2 (C105), a node that had previously been part of the third tier of nodes as revealed by the degree centrality measure. Characterized by a flow betweenness of 27.871, the third tier overlaps entirely with the second tier revealed by the degree centrality measure. With a flow betweenness of 13.268, the fourth tier coincides with the fourth tier revealed by the degree centrality measure. With a similar flow betweenness of 13.125, the fifth tier overlaps with 87.5% of the nodes of the third tier revealed by the degree centrality measure. The sixth tier includes a single node and coincides with the fifth tier indicated by the degree centrality measure. Finally, the seventh tier consists of nodes C119 and C146. Characterized by no flow betweenness, these nodes overlap entirely with the sixth tier revealed by the degree centrality measure.

Table 7.4 Weighted Adjacency Matrix with Degree Centrality Measure.

	C4	C17	C53	C61	C71	C72	C75	C76	C78	C105	C110	C112	C113	C114	C115	C119	C142	C143	C145	C146	C150	C154	C157	C160	C163	Degree
C4		0	0	0	0	0	0	0	0	1	0	0	0	0	0	0	0	1	0	0	0	0	0	0	0	2
C17	0		1	2	2	1	1	1	1	1	2	2	1	1	2	0	2	2	2	0	2	1	1	1	1	30
C53	0	1		1	1	1	1	1	1	0	1	1	1	0	1	0	1	1	1	0	1	0	0	0	1	16
C61	0	2	1		2	1	1	1	1	1	2	2	1	1	2	0	2	2	2	0	2	1	1	1	1	30
C71	0	2	1	2		1	1	1	1	1	2	2	1	1	2	0	2	2	2	0	2	1	1	1	1	30
C72	0	1	1	1	1		1	1	1	0	1	1	1	0	1	0	1	1	1	0	1	0	0	0	1	16
C75	0	1	1	1	1	1		1	1	0	1	1	1	0	1	0	1	1	1	0	1	0	0	0	1	16
C76	0	1	1	1	1	1	1		1	0	1	1	1	0	1	0	1	1	1	0	1	0	0	0	1	16
C78	0	1	1	1	1	1	1	1		0	1	1	1	0	1	0	1	1	1	0	1	0	0	0	1	16
C105	1	1	0	1	1	0	0	0	0		1	1	0	1	1	0	1	2	1	0	1	1	1	1	0	16
C110	0	2	1	2	2	1	1	1	1	1		2	1	1	2	0	2	2	2	0	2	1	1	1	1	30
C112	0	2	1	2	2	1	1	1	1	1	2		1	1	2	0	2	2	2	0	2	1	1	1	1	30
C113	0	1	1	1	1	1	1	1	1	0	1	1		0	1	0	1	1	1	0	1	0	0	0	1	16
C114	0	1	0	1	1	0	0	0	0	1	1	1	0		1	0	1	1	1	0	1	1	1	1	0	14
C115	0	2	1	2	2	1	1	1	1	1	2	2	1	1		0	2	2	2	0	2	1	1	1	1	30
C119	0	0	0	0	0	0	0	0	0	0	0	0	0	0	0		0	0	0	1	0	0	0	0	0	1
C142	0	2	1	2	2	1	1	1	1	1	2	2	1	1	2	0		2	2	0	2	1	1	1	1	30
C143	1	2	1	2	2	1	1	1	1	2	2	2	1	1	2	0	2		2	0	2	1	1	1	1	32
C145	0	2	1	2	2	1	1	1	1	1	2	2	1	1	2	0	2	2		0	2	1	1	1	1	30
C146	0	0	0	0	0	0	0	0	0	0	0	0	0	0	0	1	0	0	0		0	0	0	0	0	1
C150	0	2	1	2	2	1	1	1	1	1	2	2	1	1	2	0	2	2	2	0		1	1	1	1	30
C154	0	1	0	1	1	0	0	0	0	1	1	1	0	1	1	0	1	1	1	0	1		1	1	0	14
C157	0	1	0	1	1	0	0	0	0	1	1	1	0	1	1	0	1	1	1	0	1	1		1	0	14
C160	0	1	0	1	1	0	0	0	0	1	1	1	0	1	1	0	1	1	1	0	1	1	1		0	14
C163	0	1	1	1	1	1	1	1	1	0	1	1	1	0	1	0	1	1	1	0	1	0	0	0		16

An additional centrality measure, run on a binarized version of the dataset (Table 7.4), further complicate the existing patterns revealed by the previous calculations. Freeman's betweenness measure reveals the existence of four groups. Containing 14 nodes, the bottom 56% is characterized by a betweenness centrality of 0 and overlaps with nearly the entire set of nodes from tiers three, four, five, and six, as revealed by the degree centrality calculation. One third tier node, Aqir Al-Shamoos 2 (C105), occupies the sole second tier position as indicated by this betweenness centrality measure and is characterized by a betweenness score of 6.5. The top tier position is once again occupied by Aqir Al-Shamoos (C143), which is characterized by a betweenness score of 17. Finally, the third group is comprised entirely of second tier nodes, as revealed by the degree centrality measure, and characterized by a betweenness score of 3.5. When

compared with the Flow Betweenness Centrality measure one can observe overlap in terms of the first three tiers. A divergent pattern is revealed where nodes from the bottom four tiers revealed by the Flow Betweenness Centrality are concerned. Whereas in the calculation run on the weighted dataset, these nodes show flow betweenness scores of 13.268, 13.125, 2.125, and 0, the calculation run on the binarized dataset illuminates scores of 0 for all of these nodes.

To undertake a closeness centrality calculation on the Islamic period network, the pair of outliers, C119 and C146, was removed. Freeman's sum of geodesic distances revealed 6 groups defined by farness scores. This pattern closely resembles the one revealed by the degree centrality calculation, with the farthest nodes also having the lowest degree centrality scores. Once again,

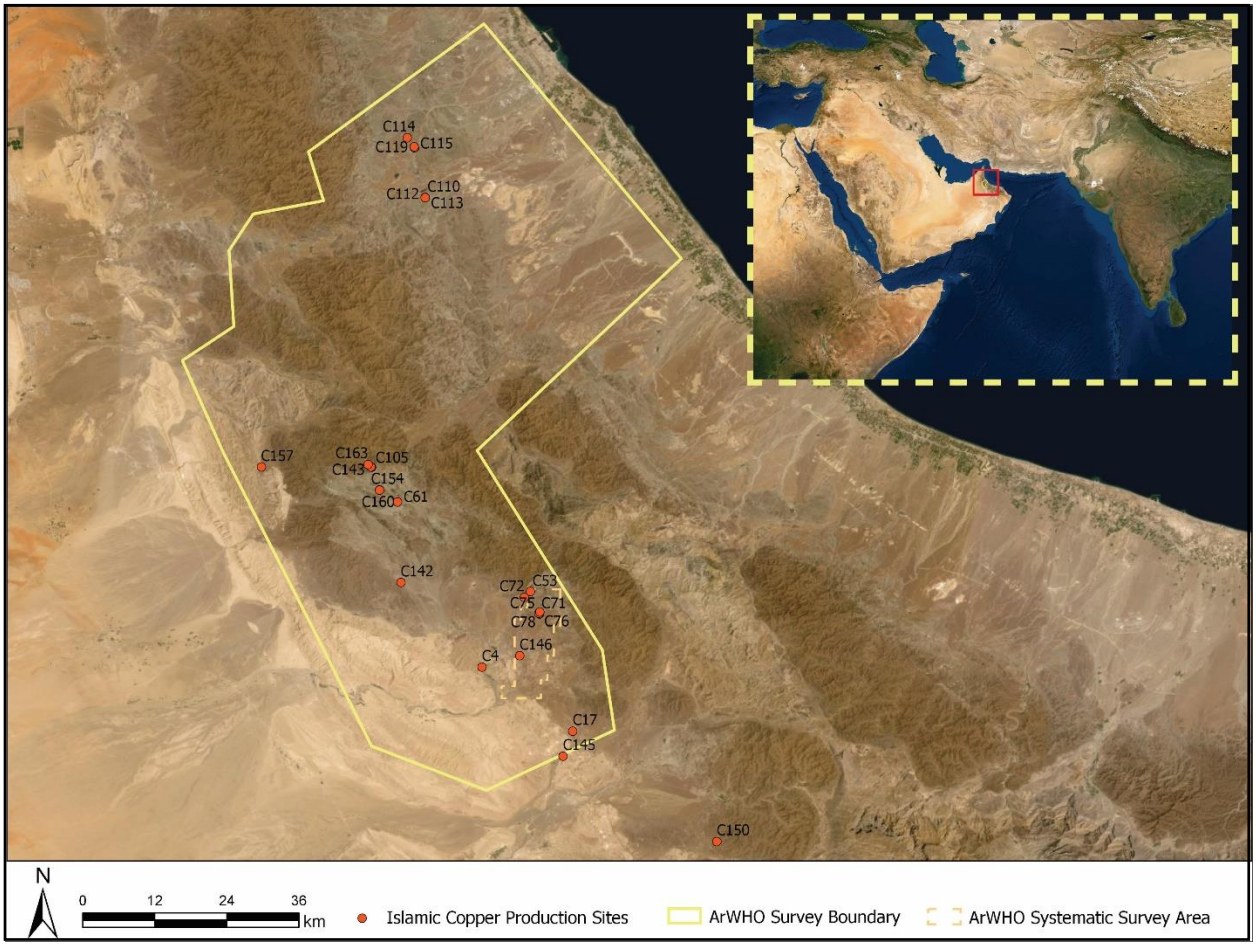

Figure 7.16 Islamic Period Network (including multi-period sites).

node C105, deviates from this norm, defining the third farthest group (with a farness score of 29), despite being in the third tier of sites defined by degree centrality. Indeed, the rest of the third tier sites comprise the fourth farthest group and are characterized by a lower farness score of 28.

The network's connectedness and cohesion were evaluated using two graph-theoretic measures: density and reachability. The overall density of the network is 66.3%. With the exception of the pair of isolated nodes, C119 and C146, each node has a reachability score of 1.

There is a great deal of continuity in terms of the spatial distribution of sites between the Iron Age and the Islamic period copper production landscape (Fig. 7.16, Table 7.5), with the maintenance of the same three clusters of sites: in Wadi Jizzi, in the middle of the larger ArWHO survey area, and in the southern reaches of the larger ArWHO survey area. In addition to these three clusters, the same pair of nodes endures at the southern tip of the larger survey area. The composition of these clusters, however, is slightly different. The Wadi Jizzi cluster contains six sites, three of which continued in use from the Iron Age period, C110, C112, and C113. These three nodes were locations from the larger smelting site of Lasail. The other three sites were the Islamic single period settlements and smelting sites of Bayda (C114, 931-001), Tawi Arja (C115, 930-001), and Arja (C119, 929-001). The middle cluster also consists of six nodes, five of which continued in use from the Iron Age period (C143, C105, C154, C160, and C61). Hayl al-Arb (C163, 950-001), a single-occupation Islamic period settlement represents the new addition to the cluster. With a total of 8 nodes, the southern cluster contains four sites that continued in use from the Iron Age period. These are the four nodes contained by the large smelting site of Tawi Raki (C71, C75, C76, and C78). New additions to the cluster include the tower site of Safri 1 (C4, 989-001), the slag scatter at 924-001 (C53), the smelting settlement of Raki 1 (C72, 936-001), and the

find spot of Hayy al-Nahza (C146, 985-002). Two additional isolates occur in this time period, including the slag scatter C142 (919-001) and the settlement of Qumaira (C157, 970-003).

Table 7.5 Islamic Period Copper Production Sites: Spatial Clusters and Degree Centralities of Constitutive Nodes.

Wadi Jizzi Cluster	Middle Cluster	Southern Cluster	Pair	Isolates
C114 – DC 14	C163 – DC 16	C53 – DC 16	C17 – DC 30	C157 – DC 14
C115 – DC 30	C143 – DC 32	C72 – DC 16	C145 – DC 30	C142 – DC 30
C119 – DC 1	C105 – DC 16	C78 – DC 16		C150 – DC 30
C110 – DC 30	C154 – DC 14	C75 – DC 16		
C113 – DC 16	C160 – DC 14	C76 – DC 16		
C112 – DC 30	C61 – DC 30	C71 – DC 30		
		C4 – DC 2		
		C146 – DC 1		

Within each cluster, a pattern similar to the one observed for the Iron Age network emerges in terms of the centrality scores of constituent nodes. Because there is only one first tier node (in the middle cluster), each Islamic period cluster is revealed to contain at least one second tier node (degree centrality of 30), and at least on third tier node (degree centrality of 16). The pair containing C17 and C145 continue to be second tier sites. Two of the isolated nodes (C142 and C150) are second tier sites, whereas the third (C157) is a fourth tier site.

7.2.4. Longitudinal Overview of the Copper Supply Network from the Bronze Age to the Islamic Period

Providing a longitudinal overview of the networks corresponding to the different periods of copper production in Oman (Fig. 7.17; Table 7.6), this section will begin by discussing group-level calculations, and will continue with an interpretation of actor-level patterns.

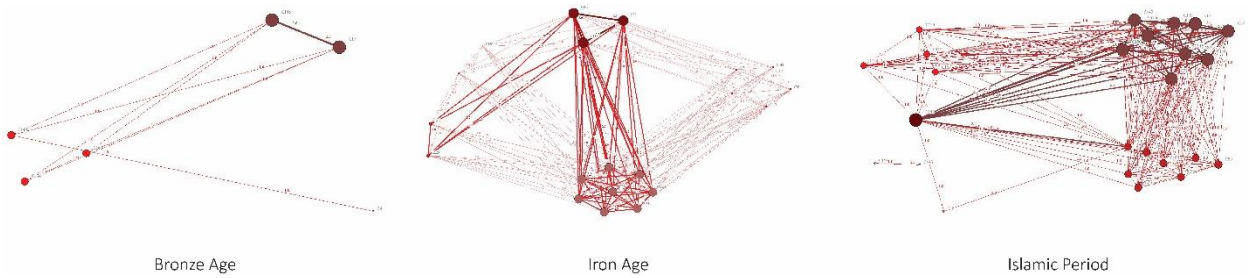

Figure 7.17 Oman Network Graphs: All Periods. Nodes Scaled by Degree Centrality.

While centralization indices suggest that the copper supply networks were largely decentralized and characterized by moderately prominent actors, analyses of sub-groups reveal a trajectory towards increased structural complexity.

Comprising of six nodes, the Bronze Age network has a group degree centralization of 25% revealing that the degree of inequality and concentration of power within the network had not been achieved by one node. Compared to the following two networks, the Bronze Age network is characterized by the second largest group centralization index. Divided into three tiers of prominence, the second tier is characterized by a 40% decrease in the number of ties incident upon a node, and the third tier by an 80% decrease in the number of ties.

Calculated at 28.533%, 32%, and 41.150%, respectively, two group betweenness indices and one group closeness centralization measure reveal that the Bronze Age network has the highest betweenness and closeness. The betweenness indices suggest that the Bronze Age network has the most intermediaries, or actors placed in strategic positions, out of the three networks. This network also has the highest closeness centralization of the three networks.

Characterized by a density index of 0.6, the Bronze Age network is the least cohesive of all the networks, being however comparable in density with the much larger Islamic period network which sees a negligible increase in density of 10.5%, for a measure of 0.663.

Table 7.6 Group Centralization Measures. [67]

	Bronze Age	Iron Age	Islamic Period
Nodes	6	20	25
Ties	18	340	398
DC	25%	18.52%	28.08%
DC (# of tiers)	3	5	6
DC First Tier	5	33	32
DC Second Tier	3	29	30
DC Third Tier	1	18	16
DC Fourth Tier	N/A	15	14
DC Fifth Tier	N/A	14	2
DC Sixth Tier	N/A	N/A	1
FBC	28.533%	2.2870%	6.3140%
BCFP	32.000%	0.5000%	5.5900%
CCSG	41.150%	18.4200%	34.2100%
Density	0.6	0.895	0.663

Compared to the previous period, the Iron Age network is characterized by an approximate 26% decrease in the overall group centralization index. Indeed, this period's network witnesses the lowest group degree centralization measure of the three networks, as well as the lowest group betweenness, and closeness centralization measures. These results further solidify the interpretation of a relatively decentralized structure, which is almost entirely devoid of power.

When we look at graph cohesion, however, this network is the closest to approach maximum group cohesion (0.895). Caution must, however, be employed when interpreting this measure and

[67] DC = degree centrality; FBC = flow betweenness centrality; BCFP = Betweenness Centrality Freeman (point) Betweenness; CCSG = Closeness Centrality Sum of Geodesic Distances (Freeman).

when comparing it to the previous period's network, as the size of the Iron Age network witnessed an increase of 233.33% as compared to the previous period's network. Attendant upon this significant increase in network size is a 1788.89% increase in the number of ties and a 66.67% increase in the number of tiers (5).

The largest and most centralized copper supply network is associated with the Islamic period, during which time network size increased by 25% from the previous period and the number of ties by 17.06%. This network is 51.62% more centralized than the Iron Age Network. With relatively low betweenness indices and a higher closeness centralization measure, this network appears to have few power brokers. Despite differences in size, the density of this network is comparable to the one associated with the Bronze Age period.

Despite the existence of relatively decentralized systems, a number of actors can be described as achieving a moderate level of prominence (Fig. 7.18). In what follows, I will summarize patterns in the network positions of actors across the three networks. The three actor-level indices used to identify the most central and powerful actors are degree, betweenness, and closeness (Appendix I: Table AI. 14).

For the Bronze Age period, the most central nodes with respect to degree are not also the most central with respect to betweenness and closeness. Two degree centrality measures, Freeman's approach (Freeman 1979) and Bonacich's "Power" or beta-centrality (Bonacich 1987) reveal the

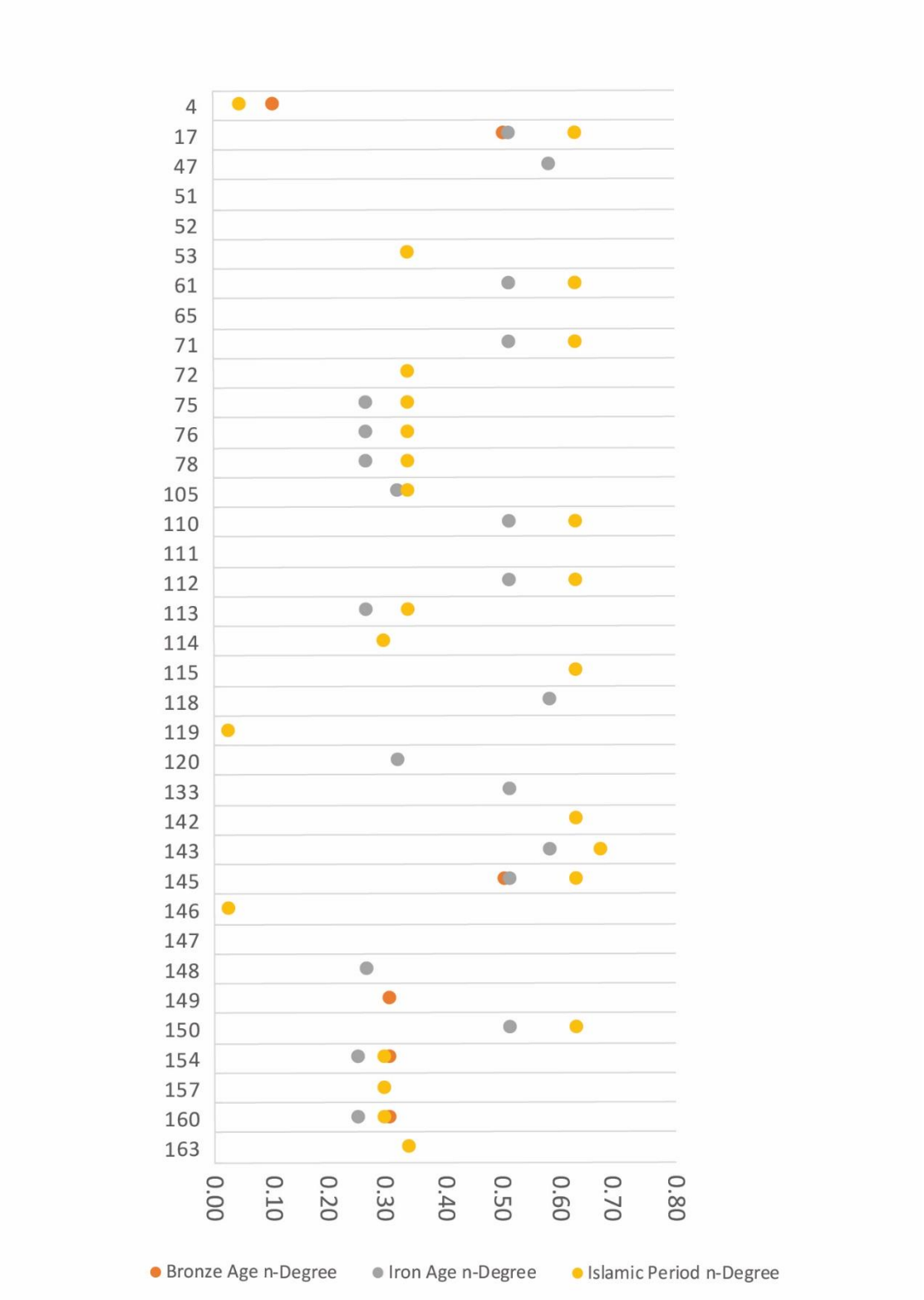

Figure 7.18 Diachronic Fluctuations in Degree Centrality (Normalized Degree) for all nodes from the Bronze Age to the Islamic Period.

same two nodes as occupying the most central position in the network. These nodes are C17 (971-001, Khadil) and C145 (934-001, Al Arid). The former is a slag scatter in the wadi channel surrounding the Bronze Age tower of Khadil, whereas the latter is a settlement located approximately 4 km to the southwest of C17. The prominence of these sites does not seem to be a function of sample size; the analyzed slag assemblage collected at C17 contains 3 pieces (2.11% of the total assemblage), whereas the assemblage from C149 contains 2 slag samples (1.41% of the total assemblage). The slag groups represented at these sites include 3.1 and 3.2. Linked by a tie with a strength of 2, these two nodes also have the strongest relationship within the network. Second tier sites include C149 (944-001), C154 (973-001, Wadi Harim), and C160 (973-006, Wadi Harim). Whereas C149 is a slag scatter, discovered approximately 3.5 km west of the ArWHO systematic survey area, C154 is a settlement located 0.6 km away from the structure of C160. Indeed, whereas the spatially adjacent nodes of C154 and C160 are adjacent within the network, sharing a tie with a strength of 1, C149 is not connected to either node with which it shares a degree centrality index. The second degree centrality measure (Bonacich "Power") reveals a slightly different node order, with C149 occupying a tertiary, rather than secondary position within the network.

Originally developed to measure information control and information flow, respectively, Freeman's Betweenness Centrality (Freeman 1979) and the Flow Betweenness Centrality (Freeman, Borgatti, and White 1991) measure have been adapted for the purposes of this research to measure the capacity for the flow of goods between nodes. By this measure, a single node emerges as the most central, C149, whose higher flow betweenness measure may be related to the fact that it may have been translating its advantageous position (of controlling the interaction of C4 with the rest of the network) into power. Second tier nodes, C17 and C145, correspond with

first tier nodes as related to degree centrality, while third tier nodes overlap with second tier nodes as revealed by the previous measures. The only node with a betweenness centrality index of 0 is C4.

The advantageous position of C149 revealed by the previous betweenness measure is further attested by Freeman's Betweenness Centrality approach, which was calculated using the binarized version of this dataset. Rather than assuming that nodes will use all paths that connect them, Freeman's approach to the study of betweenness theorizes that a node occupies a favorable position if it falls on the geodesic paths between other nodes. This is because such a strategically positioned node would have the opportunity to control the interactions it is intermediating. When analyzed with a focus on geodesics, the network reveals that C154 and C160 have a betweenness index of 0. The node order identified by the flow betweenness centrality measure is sustained by both the all paths and the geodesic distances closeness centrality measures. Node C4 (989-001, Safri 1) is the least powerful, least connected, and most distant actor in the network, being only adjacent to C149, to which it is also spatially proximate. Indeed, spatial distances seem to be a factor determining both network position and network adjacency.

Like the Bronze Age network before it, the Iron Age network reveals a changing array of prominent sites when comparing degree centrality, betweenness centrality, and closeness centrality. Two degree centrality measures (Freeman's approach and Bonacich's "Power" centrality) illuminate the same node order.

Three sites occupy the most central position within the network. With a degree centrality of 33 these are C47, C118, and C143. The tie strength of the edges connecting these three sites to each other is 3. All three actors are settlements and smelting sites and each one is located in one of the three cluster zones discussed earlier in this chapter. Located in Wadi Jizzi, in the northern stretches

of the larger ArWHO survey area, C118 (930-001, Tawi Arja) is a single period Iron Age site with evidence of three slag groups (2, 3.1, and 3.2) as identified through the analysis of 6 sample (representing 4.23% of the total assemblage). Sample size does not seem to have been a factor contributing to the prominence of these sites. Located in the center of the larger survey region, Aqir al-Shamoos (C143), is an Iron Age and Islamic multi-occupation site with evidence of the same three slag groups, identified through the analysis of 5 samples (3.52%). Finally, located within the boundary of the ArWHO systematic survey area, the final first tier site, C47 (981-001, Raki 2) is a single period site with evidence of slag groups 2, 3.1, and 3.2, as ascertained through the analysis of 3 slag samples (2.11%).

With a degree centrality of 29, the second tier consists of a total of 8 actors, two of which (C17 and C145) occupied the most prominent positions within the previous Bronze Age network. The remaining six contain two settlements (C61, 962-001, Muaydin and C150, Hala), both of which are characterized by an analyzed slag assemblage of 3 samples (2.11% of the total) and contain evidence of slag groups 3.1 and 3.2, groups that are shared by all second tier sites. This group also includes 2 slag scatters, one collected at the site of Tawi Raki (C71, 984-001) and another (C133, 918-001) 6.73 km to the southwest of C71. Nine samples were analyzed from C71 (representing 6.34% of the total assemblage), whereas only 4 samples were analyzed from C133 (2.28%). The last two actors both originate at the large multi-period smelting site of Lasail (C110 and C112) and are both characterized by a slag assemblage of 8 (5.63%) and 9 (6.34%) analyzed slag pieces, respectively.

With two constituent nodes, the third tier is characterized by a degree centrality of 18. One actor (C105, Aqir al-Shamoos 2), is located across a ravine from the most central site of Aqir al-Shamoos and shows evidence of Iron Age and Islamic occupation. Two slag groups (2. And 3.1)

have been identified at the site through the analysis of 2 samples (1.41%). In addition to the shared slag groups, the second node of this tier, Hayy Ukur (C120, 994-001) was also located deep within the al-Hajar mountains, approximately 20 km to the southeast of Aqir al-Shamoos 2. Whereas the latter node spatially clusters in the center of the larger ArWHO survey area, the former is spatially isolated. A determination of its access to different smelting technologies relied on the analysis of 7 samples (4.93%).

Containing five nodes, the fourth tier is characterized by a degree centrality of 15 and includes C75, C76, C78, C148, C113, the first four of which represent different collections from the large settlement and smelting site of Tawi Raki. All sites had evidence of slag group 3.2. Assemblages from the Tawi Raki sites were identified based on the analysis of 3 – 5 slag samples. The final node originated in Lasail (932-004) and was also identified based on the analysis of 5 samples.

Finally, the fifth tier of the network is populated by sites C154 and C160, both of which occupied more prominent positions in the previous Bronze Age network. This node order was further reinforced through Bonacich's approach.

Slight differences in network prominence are indicated by the two betweenness centrality measures. A flow betweenness centrality calculation reveals the same components occupying the top two as well as the bottom tier of prominence within the network. Prominence changes with the third and fourth tiers, whose centrality is flipped in between the time periods. That is, third tier sites as it relates to flow betweenness have higher betweenness indices, but lower degree centralities; conversely, fourth tier sites have lower betweenness and higher degree centrality.

Freeman's betweenness centrality, on the other hand, reveals the existence of two tiers within the network. Whereas the previous measure focused on flow capacity, this betweenness measure

reveals nodes placed in advantageous positions that allow them to intermediate between other nodes and can provide the broker with the opportunity to control the interactions. With a total of 11 nodes, the first tier of sites includes C17, C47, C61, C71, C110, C112, C118, C133, C145, and C150. In addition to having high betweenness centralities, all of these actors also have high degree centralities.

The two tiers identified by Freeman's betweenness centrality become three tiers as calculated by the sum of geodesic distances closeness centrality measure. Having identical first tier components, the differences rest on the composition of the second and third tiers. With an overlap of 55.55%, the second tier includes the five nodes associated with Tawi Raki (C75, C76, C78, C113, and C148). With the highest sum of geodesic distances, the remaining four nodes (C105, C120, C154, and C160) coincide with the bottom two tiers identified through the flow betweenness centrality. Whereas flow betweenness indexes flow capacity and Freeman's betweenness approach measures control, the sum of geodesic distances closeness centrality calculates an index of the expected time-until-arrival for commodities flowing through the network via optimal paths. As such, the discrepancies in centrality indices between these three measures suggests that the same 11 nodes that are located in strategic positions of control also have the shortest time-until-arrival for commodities flowing through the network; however, it is only the three nodes that are also central in terms of degree (C47, C118, and C143) that have the highest flow capacities.

With a total of 25 constitutive nodes, the Islamic Period network witnesses a 25% increase in network size. Out of the total number of nodes, 15 (60%) of these have co-membership in the Iron Age network: C17, C61, C71, C75, C76, C78, C105, C110, C112, C113, C143, C145, C150, C154, C160). Unlike the situation of the Bronze and Iron Age networks, degree centrality reveals the existence of a single node in top position, Aqir al-Shamoos (C143), the only remaining top tier

node of the Iron Age period. This settlement's prominence is reinforced through betweenness and closeness centralities, indicating that when compared to other sites C143 takes part in most of the activities in the network, has the highest flow capacity, is best positioned as an intermediary to control interactions between other sites, and has the shortest time-until-arrival.

The second tier of the network is populated by all of the multi-period sites from the Iron Age network that are still occupied during this time period (C17, C61, C71, C110, C112, C145, C150) along with two additional single occupation sites (C115 and C142). The first of these two new sites is located in the larger Tawi Arja region (930-001) and has been attributed to the Islamic period on the basis of corresponding material culture uncovered in association with the slag scatter. A total of 12 samples (8.45%) were analyzed to reveal the production of slag from groups 3.1 and 3.2. The second site is an artifact scatter, located in a spatially isolated position north of the identified copper source of Ghadhiya, to the northwest of the ArWHO systematic survey area. This site's production of slag from groups 3.1 and 3.2 was determined based on the analysis of 2 slag samples (1.41%). The secondary position of these nodes was further revealed through a Bonacich "Power" centrality measure. Betweenness and closeness centrality measures, on the other hand, reveal slightly different patterns where these nodes are concerned.

Comprising a total of 8 nodes, the third tier witnesses Aqir al-Shamoos 2 (C105) maintaining the tertiary position it had achieved during the Iron Age period. This tier also overlaps with 80% of the fourth tier sites identified through degree centrality for the Iron Age; these include all by one of the Tawi Raki nodes (C75, C76, and C78) and one site located at Lasail (C113). Three single-occupation Islamic period nodes (C53, C72, and C163) also occupy tertiary positions. The first of these, C53 (924-001) is an artifact scatter with evidence of production of slag from group 3.2, as revealed through the analysis of 6 samples (4.23%). The second, C72 (936-001) has been

recorded at the settlement and smelting site of Raki 1, located in the vicinity of the modern copper mine of Raki. Associated with a material assemblage dated to the Islamic period, slag from group 3.2 was produced at the site, as revealed through the analysis of 4 samples (2.82%). Finally, slag from group 3.2 was uncovered at the settlement of Hayl al-Arb (C163, 950-001), following the analysis of a single slag sample (0.7%). As shall be discussed in what follows, the position of these nodes does not remain constant across betweenness and closeness measurements.

Composed of four nodes characterized by a degree centrality of 14, the fourth tier includes two nodes which occupied similarly unimportant positions within the Iron Age Network, C154 and C160. The remaining two nodes are single-occupation Islamic periods settlements. The first, C114 (Bayda, 931-001), is located in Wadi Jizzi in the vicinity of the smelting site of Tawi Arja. Two samples were analyzed to reveal the production of slag from group 3.1 (1.41%). The second settlement, Qumaira (970-003), also shared in the production of slag from group 3.1 as indicated by the analysis of 1 slag sample (0.7%).

With a degree centrality of 2, site C4 occupies the fifth tier of the Islamic network, having maintained its low network position since the Bronze Age. Despite a seeming interruption in production during the Iron Age, the site appears to have maintained its lack of power within the network. Finally, the sixth node contains the only instance of an isolated dyad (C119, C146) within the three copper supply networks. These sites are the only ones with evidence of production of slag group 1. The former, C119 (929-001, Arja) represents a collection from the settlement and smelting site located in Wadi Jizzi. This slag group was identified through the analysis of four samples (2.82%) from C119 and 1 sample (0.7%) from the find spot of Hayy al-Nahza (985-002). This dyad's lack of centrality and connection with the rest of the network is reflected in all other centrality measures.

A flow betweenness centrality measure reveals the existence of a slightly different pattern. While C143 maintains top position, the second most central site with respect to flow capacity is Aqir al-Shamoos 2 (C105). The third and fourth tiers are comprised entirely of nodes with secondary and tertiary network positions in terms of degree. Excluding C105, the fifth tier is comprised on nodes that are co-members in the third tier as defined by degree. Excluding the isolated dyad, the lowest flow betweenness index within the network characterizes the least centralized node as pertains to degree, C4. Freeman's betweenness centrality also demonstrates the centrality of C105, which occupies a secondary position as revealed by this measure. It is worth nothing that during the Iron Age period, this node had a flow betweenness of 0 as well as the second lowest betweenness index. All third tier sites overlap entirely with the second tier sites by degree. More than half of this network (56%) is represented by nodes with no occasion to intermediate between other nodes or to control their interactions. Six out of this total of 14 nodes maintained a betweenness of 0 during the Iron Age period.

The closeness centrality as revealed by calculating the sum of geodesic distances for each vertex illuminates similar patterns as the ones indicated by the two betweenness centralities. A key difference rests once again with the position of Aqir al-Shamoos 2 (C105), which occupies a slightly less central position (fourth tier) than its counterparts with which it shared tertiary position in terms of degree. These three sets of measures reveal that despite not being central as relates to degree, and having high flow capacity, Aqir al-Shamoos 2 (C105) had a comparably long time-until-arrival index.

7.3. Modelling the Diachronic Development of Socio-Economic Networks of Obsidian Exploitation, Production, and Trade in Ethiopia

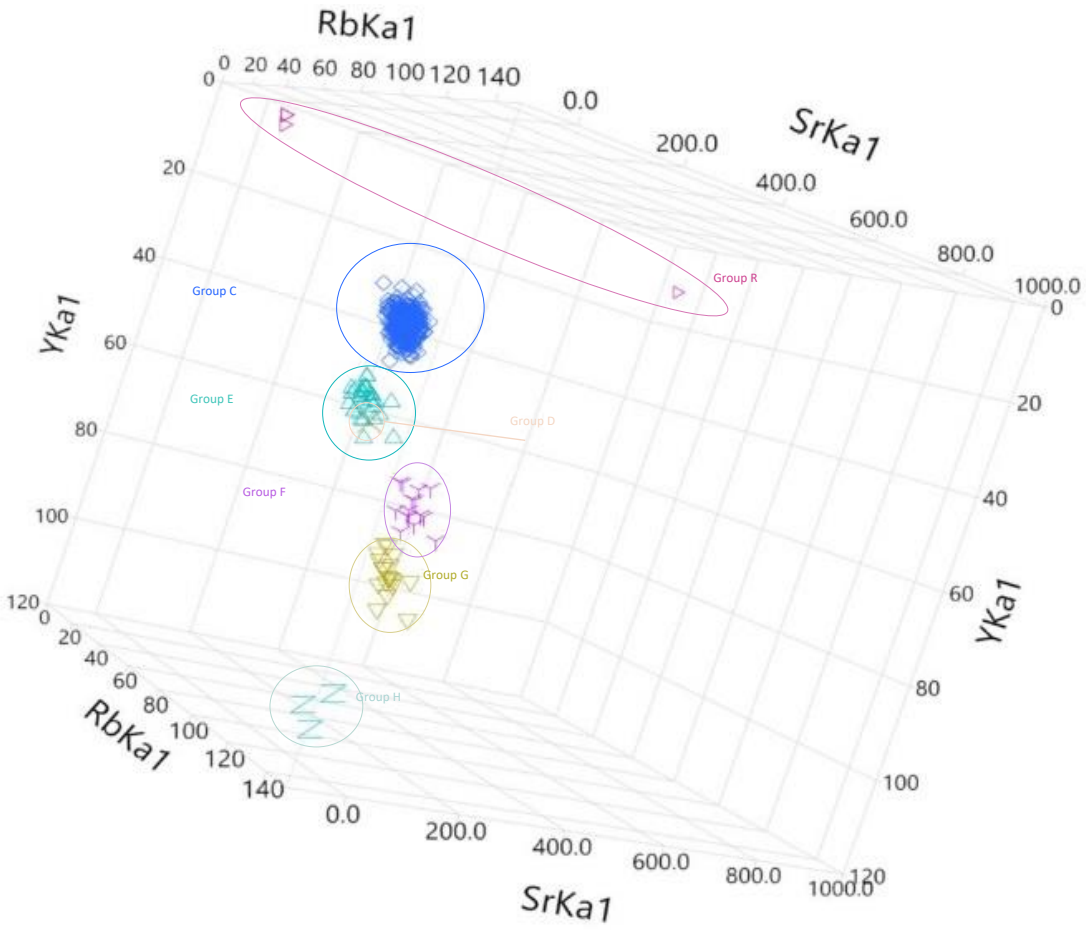

Figure 7.19 3-D Scatterplot of Obsidian Cluster Groups.

The period under investigation coincides with the rise and subsequent fall of the Aksumite Empire in northern Ethiopia and with its local pre-cursor, the Pre-Aksumite polity, and spans the early first millennium BCE to the late first millennium CE. This time range has been divided into six sub-periods (Appendix 1: Table 2). For each sub-period, a network comprised of coeval sites with evidence of obsidian production was analyzed to understand network density, cohesion, and centralization as well as the position of each node within it.

Before proceeding to interpret the structure and diachronic progression of networks, I will briefly summarize and describe the parameters that structured these networks. In Ethiopia, the analyzed dataset includes 324 pieces of archaeological obsidian[68] that were collected through survey and excavation from an area of ca. 100 km^2 and subsequently analyzed with a Brucker Tracer III-V p-XRF to identify a total of 6 cluster groups (Fig. 7.19).[69] This dataset represents 20% of the total pieces of obsidian recorded by the SRSAH project.

Over the course of four seasons (2011, 2012, 2015, and 2016), a total of 2380 lithics were recorded by the SRSAH project, 1705 (or 72%) of which were made from obsidian. Other utilized

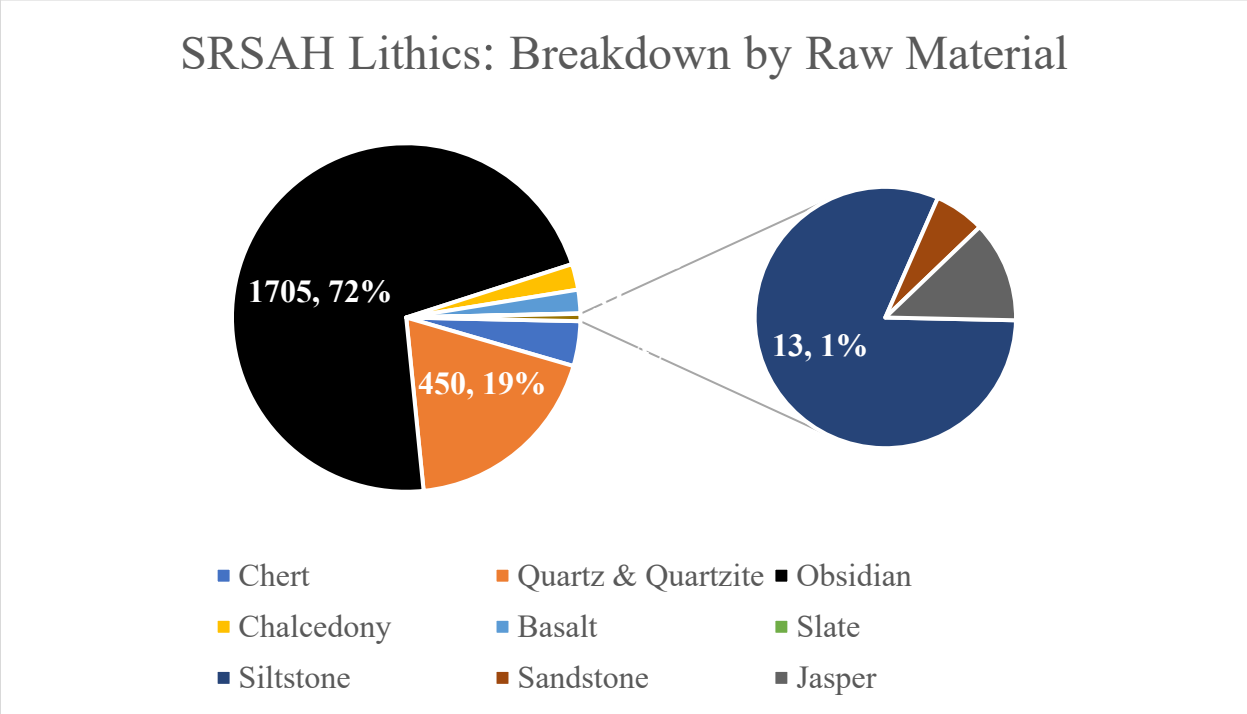

Figure 7.20 Lithics recorded by the SRSAH project (2011, 2012, 2015, 2016).

[68] A total of 328 lithics were analyzed using a Brucker Tracer III-V p-XRF, four of which were mistakenly identified as obsidian (cluster R), one of which is more likely a piece of burnt chert. These four have been removed from the analyses.

[69] Obsidian from cluster groups C, D, E, F, G, and H can be found in the SRSAH survey area. Five additional obsidian cluster groups were identified in the lithic assemblage recorded by the ETAP project in Eastern Tigray, for a total of 11 obsidian groups recognized in this area.

raw materials include chert, quartz and quartzite, chalcedony, basalt, slate, siltstone, sandstone, and jasper (Fig. 7.20).

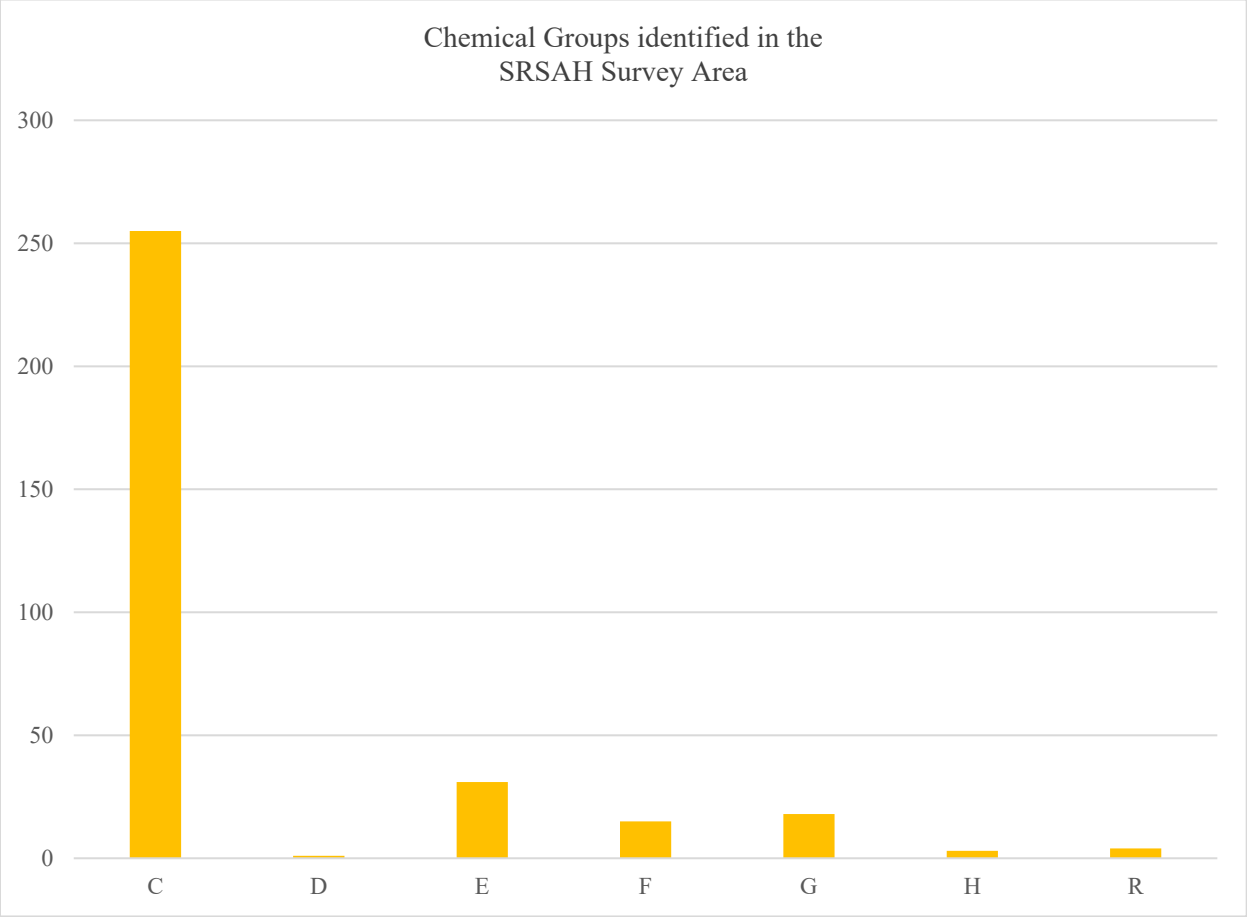

Figure 7.21 Breakdown of obsidian chemical groups identified in the SRSAH Survey Area.

Morphological analysis of SRSAH lithics was conducted during the 2016 archaeological field season by E.A. Peterson following the morphological typology established by S. Brandt for the Eastern Tigrai Archaeological Project (ETAP) directed by C. D'Andrea. This typology focuses on identifying and dating different types of shaped tools (backed pieces, scrapers, points/unifaces/bifaces), cores (bipolar, single platform, multiple platform, pyramidal etc.), and debitage/angular waste (flakes, bipolar flakes, flake fragments, angular waste etc.) based upon a

series of attributes (i.e. presence and location of retouch, presence/absence of striking platforms etc.).

Access to obsidian from each individual cluster group was not evenly distributed (Fig. 7.21). Obsidian from cluster group C is greatly overrepresented within the SRSAH lithic assemblage with a total of 256 pieces (or 79.1 %) being attributed to this group. The next best represented cluster is group E, containing 31 analyzed pieces (or 9.57%), followed by group G, containing 18 pieces (or 5.56%), group F, containing 15 pieces (or 4.63%), group H, containing 3 pieces (or 0.93%), and group D, containing a single analyzed obsidian piece (Appendix II: Table 53).

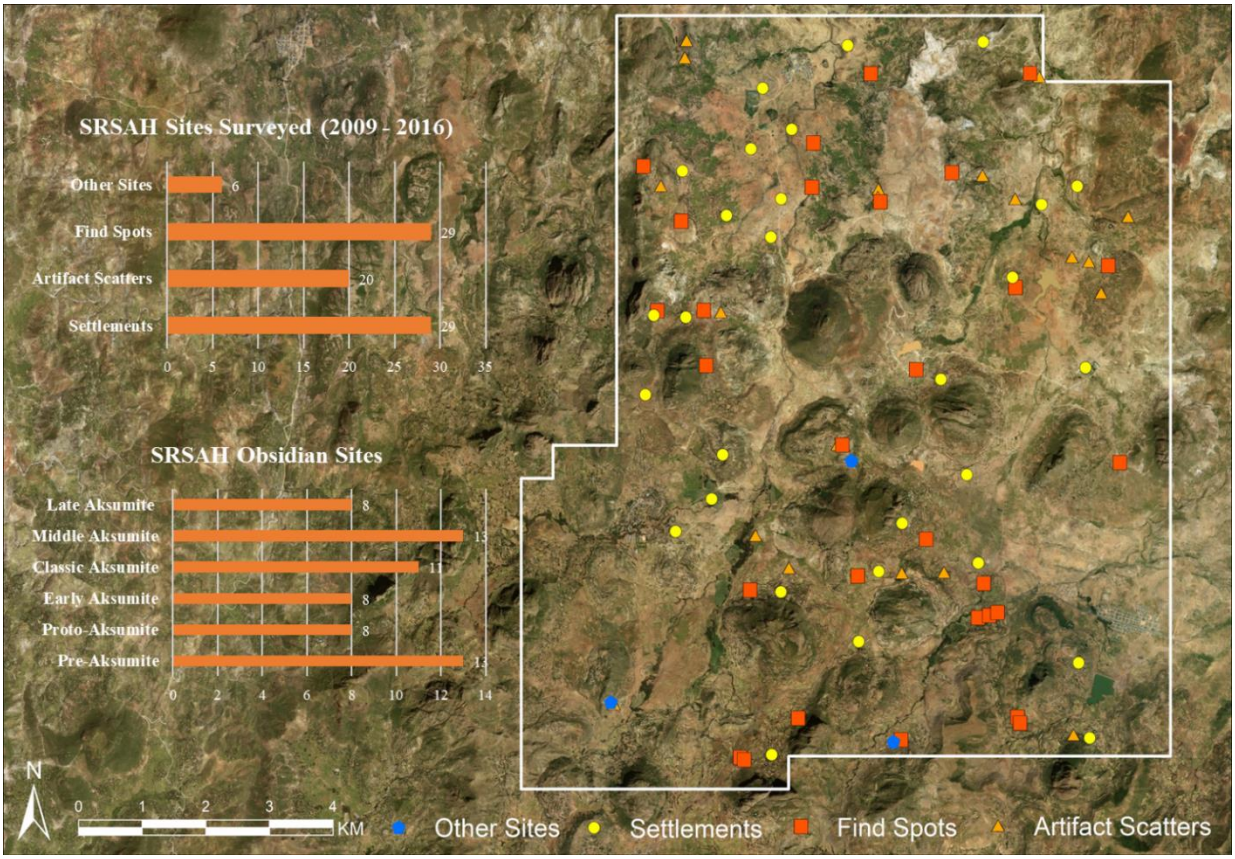

Figure 7.22 Breakdown of sites by types and of obsidian sites by time period (includes multi-period sites).

The artifacts analyzed to produce the obsidian cluster groups come from 30 sites and 14 survey units. Of the 30 sites, 14 are single period sites and 16 are multi-period sites. The survey unit

collections of indeterminate age were excluded from the initial round of analyses (Fig. 7.22). Including multi-period sites, the Pre-Aksumite network of obsidian sites includes 13 sites, the Proto-Aksumite network of obsidian sites includes 8 sites, the Early Aksumite network of obsidian sites includes 8 sites, the Classic Aksumite network includes 11 sites, the Middle Aksumite network includes 12 sites, and the Late Aksumite network includes 8 sites (Appendix II: Table 64).

7.3.1. The Obsidian Network during the Pre-Aksumite period (800 – 360 BCE)

The Pre-Aksumite period network contains 13 nodes that collectively share obsidian from 4 obsidian groups (Fig. 7.24). The obsidian groups represented are groups C, E, F, G, and H, with the latter only being consumed at a single site. This network contains 6 single period sites (Appendix II: Table 54a), 7 multi-period sites (Appendix II: Table 55a), and is characterized by 156 ties. The overall network centralization is 0.1496 (14.96%), as calculated using the Freeman Centralization approach. This measure indicates a relatively decentralized network with low degrees of overall centralization, characterized by little variation in rank or power of individual nodes. As will be revealed in comparison with later period networks, the Pre-Aksumite supply network is the second least centralized network of the networks under investigation.

Based on the strength of their ties, each node can be divided into one of five tiers. These tiers represent the degree centrality of each node, which was calculated using Freeman's Approach. With a degree centrality of 21, the most powerful and best-connected sites are the multi-period settlements of Sefra Aboun (071-001) and Beta Samati (006-001). Even though Beta Samati has access to five sources while Sefra Aboun only to four, these two settlements are both connected through 21 ties each with other Pre-Aksumite sites. This is because Beta Samati is the only site

within the Central Tigrayan region to have access to obsidian from cluster group H during the Pre-Aksumite period and, as such, its presence at the site does not increase Beta Samati's degree centrality.

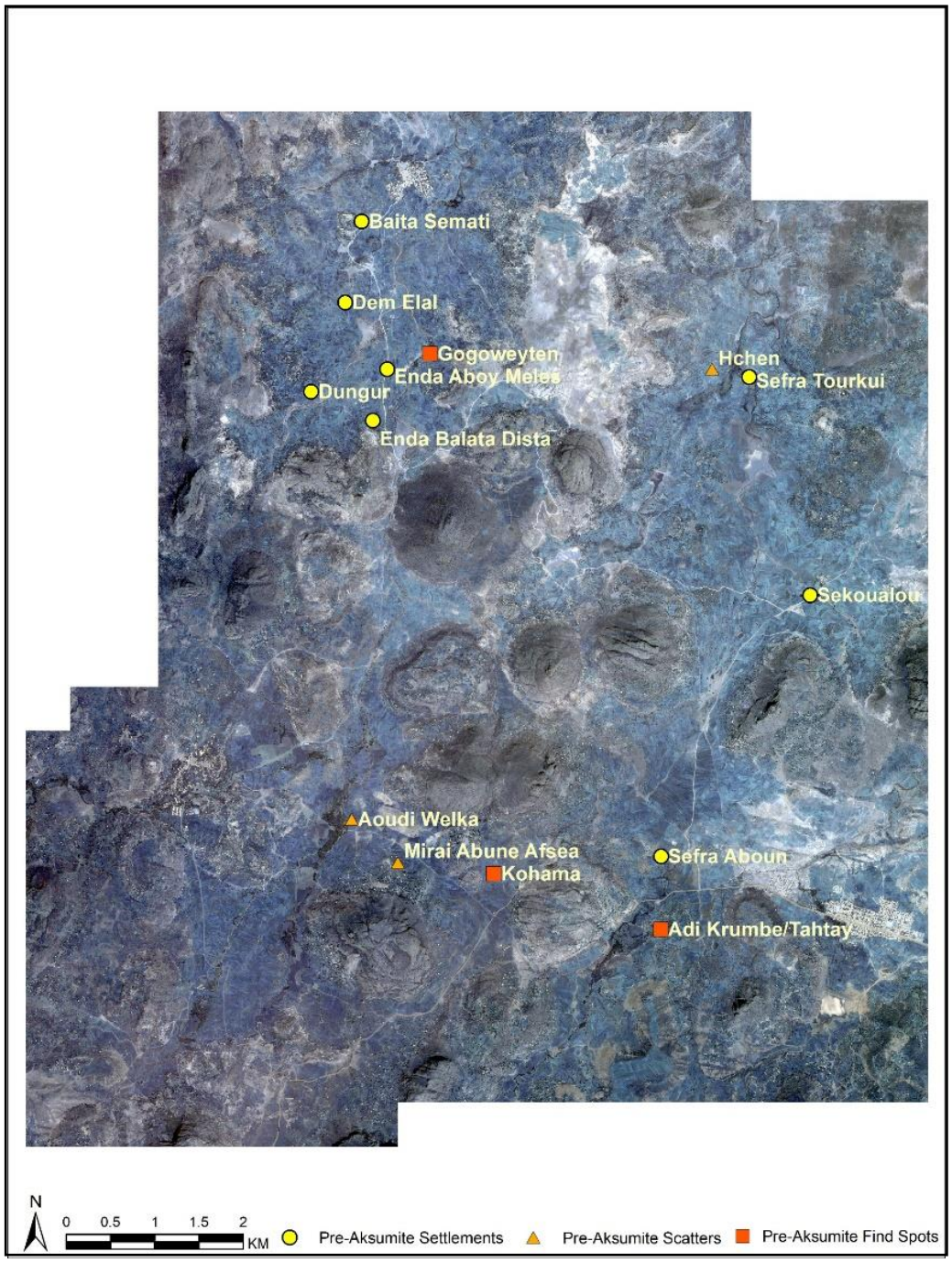

Figure 7.23 Pre-Aksumite Network (including multi-period sites).

The two most powerful sites are not located in geographically adjacent areas of the SRSAH survey region (Fig. 7.23), with Beta Samati being located in the northwestern quadrant of the region and Sefra Aboun in the southeastern quadrant.

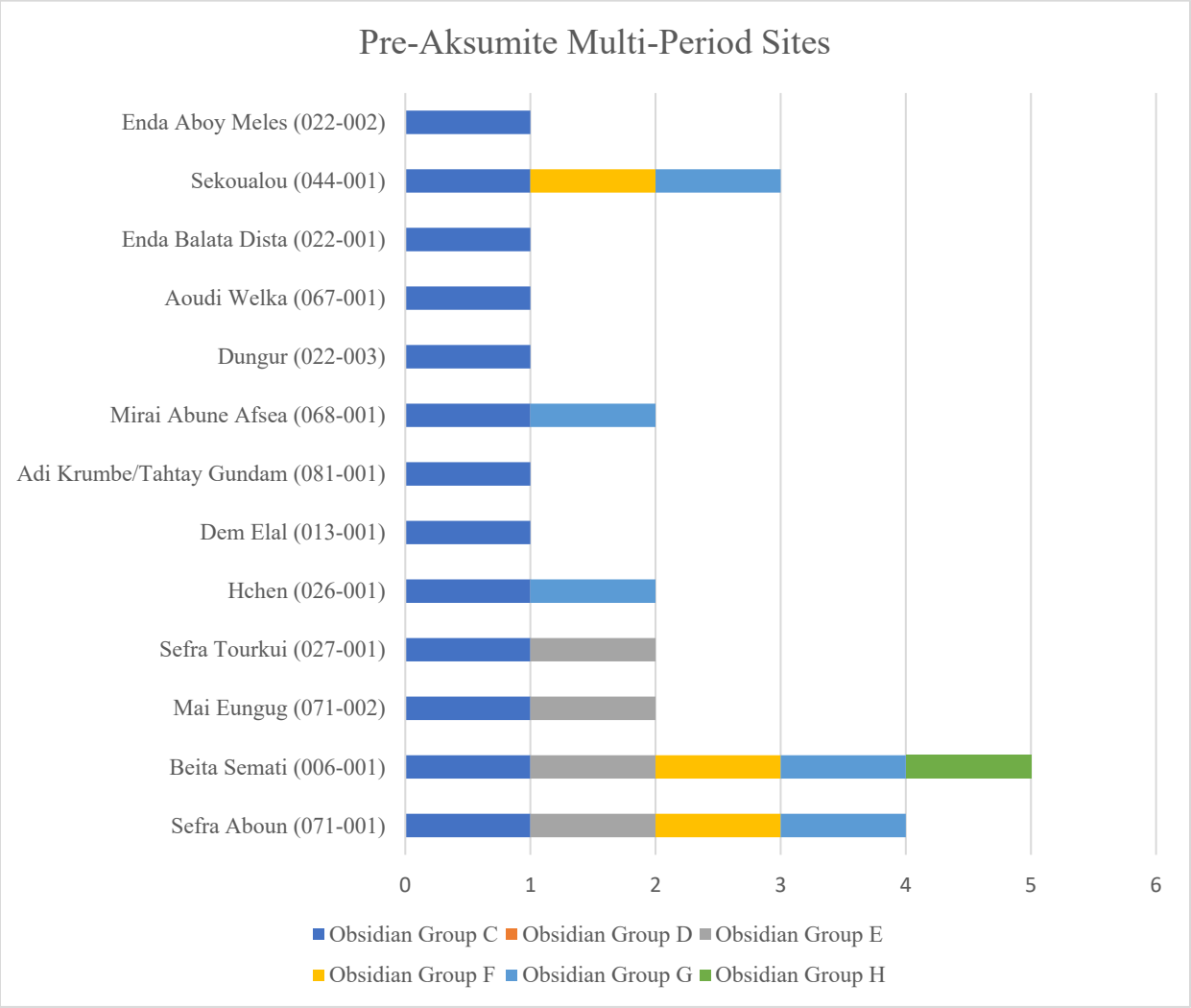

Figure 7.24 Pre-Aksumite Multi-Period Sites and the obsidian geochemical groups they have access to.

A single site occupies the second most central position within the network. With a degree centrality of 18, the settlement of Sekoualou (044-001) had access to three sources (C, F, and G). Sekoualou, a single occupation settlement, clusters spatially with neither of the two top tier sites and is located in the eastern stretches of the survey area.

There are two third tier sites, characterized by 16 ties each. These are two artifact scatters, Hchen (026-001) and Mirai Abune Afsea (068-001), the latter of which is a single-period Pre-Aksumite site, whereas the former has evidence of Early Aksumite occupation. Both sites share evidence of consumption of obsidian sources C and G.

Characterized by a degree centrality measure of 15, two sites occupy the fourth most powerful position within the Pre-Aksumite network; these are the find spot of Mai Eungug (071-002) and the single period settlement of Sefra Tourkui (027-001), both of which have evidence of obsidian groups C and E.

The last tier, characterized by a degree centrality of 12, contains nearly half of the nodes of the network. These are the multi-period settlement of Dem Elal (013-001), the Pre-Aksumite find spot of Adi Krumbe/ Tahtay Gundam (081-001), the Pre-Aksumite settlements of Enda Balata Dista (022-001) and Enda Aboy Meles (022-002), the multi-period settlement of Dungur (022-003), and the artifact scatter of Aoudi Welka (067-001).

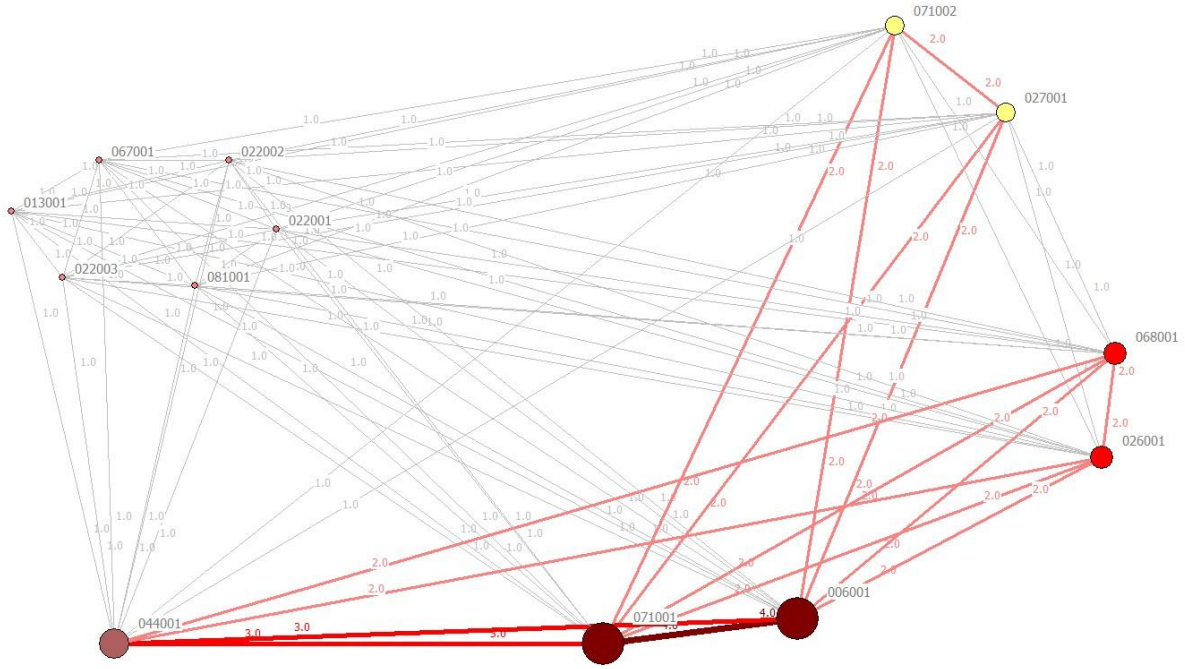

Figure 7.25 Pre-Aksumite Period Network (includes multi-period sites). Nodes Scaled by Degree Centrality.

Despite these slight differences in tie strength, the Freeman centralization score (mentioned above) suggests that positional advantages are relatively equally distributed within the Pre-Aksumite network (Fig. 7.25). These findings were further confirmed with a Bonacich's "Power" Centrality measure (Beta centrality), which revealed the same node order.

A Flow Betweenness Centrality likewise confirmed the same network position for the nodes, revealing a degree of equality and a lack of concentration in the distribution of flow betweenness centralities.

Table 7.7 Weighted Adjacency Matrix with Degree Centrality Measure.

Site	071001	006001	071002	027001	026001	013001	081001	068001	022003	067001	022001	044001	022002	Degree
071001		4	2	2	2	1	1	2	1	1	1	3	1	21
006001	4		2	2	2	1	1	2	1	1	1	3	1	21
071002	2	2		2	1	1	1	1	1	1	1	1	1	15
027001	2	2	2		1	1	1	1	1	1	1	1	1	15
026001	2	2	1	1		1	1	2	1	1	1	2	1	16
013001	1	1	1	1	1		1	1	1	1	1	1	1	12
081001	1	1	1	1	1	1		1	1	1	1	1	1	12
068001	2	2	1	1	2	1	1		1	1	1	2	1	16
022003	1	1	1	1	1	1	1	1		1	1	1	1	12
067001	1	1	1	1	1	1	1	1	1		1	1	1	12
022001	1	1	1	1	1	1	1	1	1	1		1	1	12
044001	3	3	1	1	2	1	1	2	1	1	1		1	18
022002	1	1	1	1	1	1	1	1	1	1	1	1		12

Two additional centrality measures, run on a binarized version of this dataset (Table 7.7), further solidify the interpretation that power is diffuse within this network. A Betweenness Centrality measure, which reveals nodes that are on the shortest geodesic paths between pairs of other nodes, produced betweenness centralities of 0 for each node and a network centralization index of 0.00%. This indicates a complete lack of power brokers and the absence of actors with opportunities to intermediate in relations between other actors and to control the flow of goods or information. In a network structural sense, these measures indicate a complete lack of power within the Pre-Aksumite obsidian supply network.

Several *cohesion measures* were also run on the binarized dataset. As was also revealed through the Betweenness Centrality measure, a density of 1 (100%) was calculated for the network,

further showcasing that all possible ties between nodes are being actualized. Consequently, each node has a distance of 1 and a reachability of 1, indicating that each node is directly reachable from all other nodes and that the cost of reaching a node is equal to the cost of reaching any of the other nodes. These measures suggest a lack of differentiation or stratification within the Pre-Aksumite obsidian supply network and reveal the absence of actors who, by virtue of being closer to more other actors, would have been able to exert more power than those who are more distant. Another measure of cohesion that was run to reveal the same patterns was Point Connectivity.

7.3.2. The Obsidian Network during the Proto-Aksumite period (360 – 80 BCE)

The Proto-Aksumite period network contains 8 nodes that collectively share obsidian from 4 groups. As was the case for the Pre-Aksumite network, obsidian from a fifth source (group H) is present only at the site of Beta Samati and, as such, does not increase the site's degree centrality. Shared obsidian groups represented include groups C, E, F, and G (Fig. 7.26).

Along with the Late Aksumite period network, this network is the smallest one and is entirely made up of multi-period sites (Appendix II: 56a) that are connected by a total of 56 ties. While the number of total ties decreased by approximately 64% from the previous period, it was accompanied by an attendant increase in the overall network centralization of approximately 3.48%. This score was calculated using a Freeman Centralization approach to be at 15.48%. As seems to have been the case for the previous network, a decentralized system of organization continued into the Proto-Aksumite period.

Freeman's Centralization Approach was also used to calculate degree centrality for each node as a result of which three tiers have been identified (Table 7.8). Characterized by 12 ties, the first tier contains the sites of Sefra Aboun (071-001) and Beta Samati (006-001), the two best connected sites of the Proto-Aksumite networks, which continue to share access to sources C, E, F, and G.

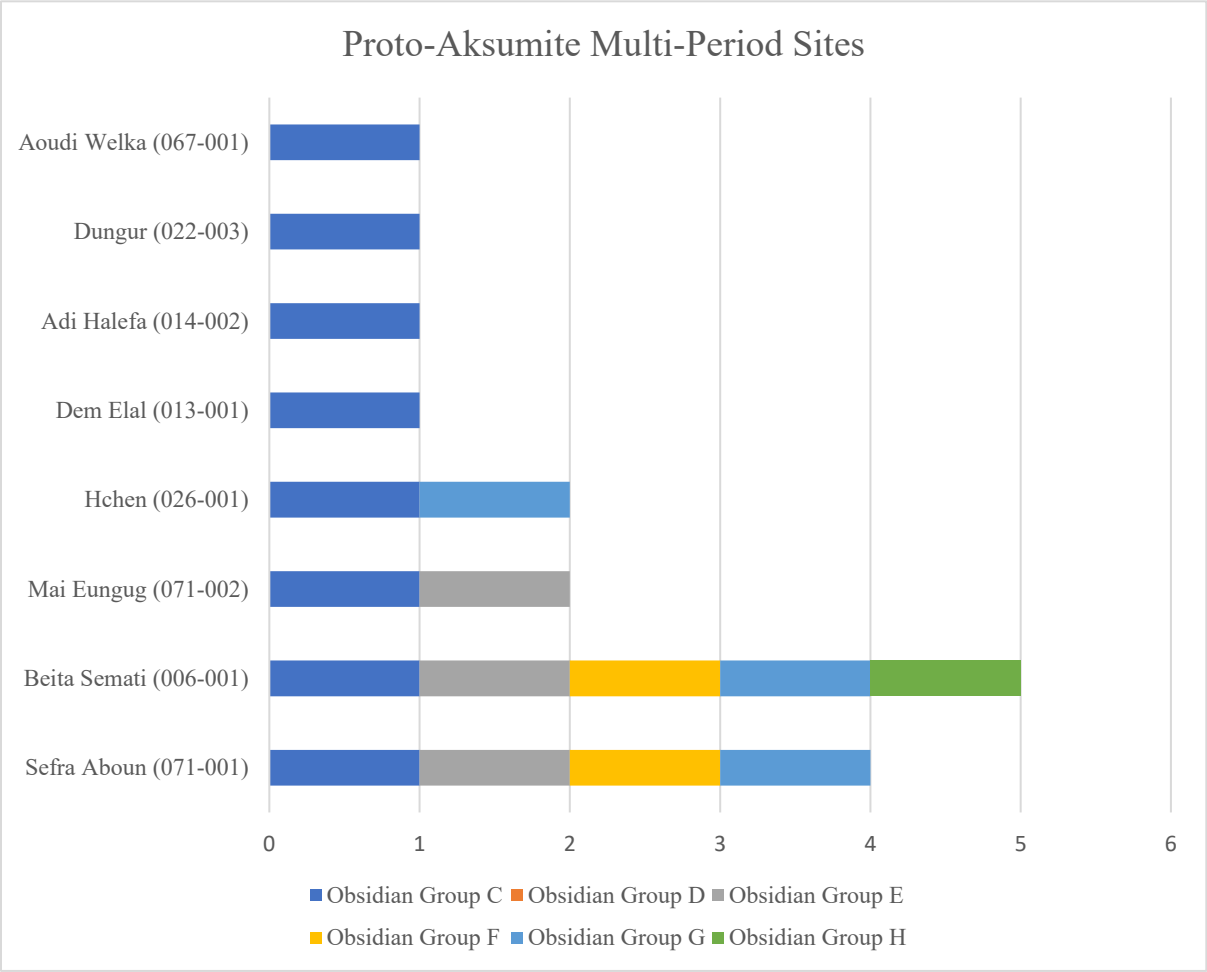

Figure 7.26 Proto-Aksumite Multi-Period Sites and the obsidian geochemical groups they have access to.

With a degree centrality of 9 ties, second tier sites include Mai Eungug (071-002) and Hchen (026-001). These two sites have evidence of access to two obsidian groups, sharing access of group C obsidian, but differing on the second group, with Mai Eungug being characterized by the use of group E obsidian and Hchen by the use of obsidian from group G (Fig. 7.27). Mai Eungug, a multi-

period find spot, clusters spatially with Sefra Aboun, being located ca. 2 km away from the site, while Hchen, a multi-period artifact scatter, is located ca. X km to the north-west of the site of Sefra Tourkui (027-001), a single-period settlement that was abandoned after the Pre-Aksumite period.

Finally, sites from the bottom 50% of the Proto-Aksumite obsidian supply network belong to the third tier and are characterized by a degree centrality of 7. This group of sites includes two multi-period settlements, Dem Elal (013-001) and Dungur (022-003), one multi-period artifact scatter, Aoudi Welka (067-001), and one multi-period find spot, Adi Halefa (014-002). All third-tier sites have access to a single obsidian group, group C.

To confirm this node order, a Bonacich "Power" Centrality measure as well as a Flow Betweenness Centrality measure were used. Put together with the overall network centralization score of 15.48%, these measures reveal the continuation of a decentralized network structure. Furthermore, Freeman's (point) Betweenness Centrality measure suggests that power brokers, or actors with opportunities to intermediate between other actors and to control the flow of commodities, did not emerge during this time period either. When compared with the Pre-Aksumite network, sites of this period are characterized by weaker relationships, or tie strengths, with percent decreases of approximately 43% between first tier sites, 50% between second tier sites, and 56% between third tier sites.

Table 7.8 Weighted Adjacency Matrix with Degree Centrality Measure.

	Sefra Aboun (071-001)	**Beta Samati (006-001)**	**Mai Eungug (071-002)**	**Hchen (026-001)**	**Dem Elal (013-001)**	**Adi Halefa (014-002)**	**Dungur (022-003)**	**Aoudi Welka (067-001)**	**Degree**
Sefra Aboun (071-001)		4	2	2	1	1	1	1	12
Beta Samati (006-001)	4		2	2	1	1	1	1	12
Mai Eungug (071-002)	2	2		1	1	1	1	1	9
Hchen (026-001)	2	2	1		1	1	1	1	9

Dem Elal (013-001)	1	1	1	1		1	1	1	7
Adi Halefa (014-002)	1	1	1	1	1		1	1	7
Dungur (022-003)	1	1	1	1	1	1		1	7
Aoudi Welka (067-001)	1	1	1	1	1	1	1		7

Regionally (Fig. 7.28), the spatial distribution of these sites observes a similar, albeit necessarily less dense, site pattern with some key differences. While the two core areas of the Pre-Aksumite network can be perceived in the northwestern quadrant and the southern stretches of the research areas, the northeastern cluster of sites now emerges as one isolated artifact scatter, following the abandonment of Sefra Tourkui after the Pre-Aksumite period.

Graph theoretic measures of connectedness and cohesion further showcase that the network is 100% dense, with all nodes being directly reachable from all other nodes by means of a path with the length of 1. These results suggest that the obsidian supply network remained unstratified with a complete lack of actors capable of exerting more power on other actors by virtue of proximity.

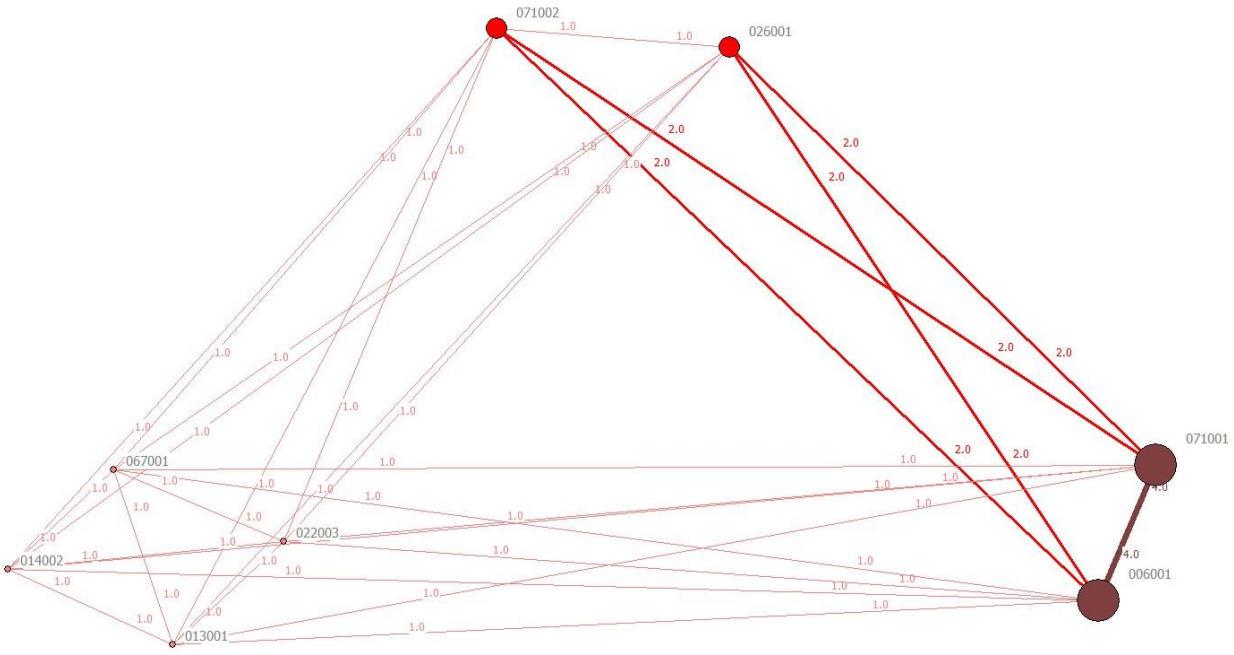

Figure 7.27 Proto-Aksumite Period Network (includes multi-period sites). Nodes Scaled by Degree Centrality.

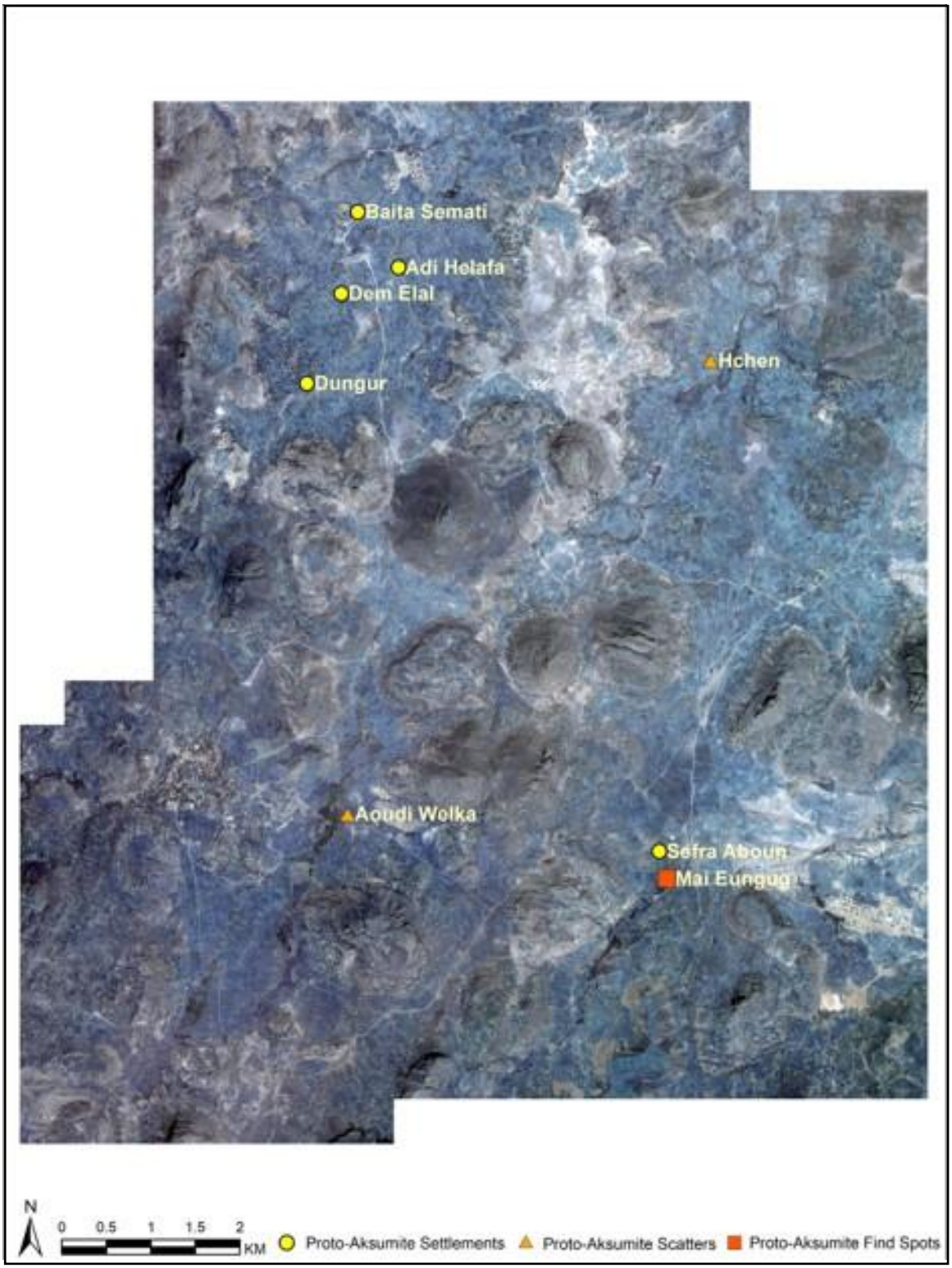

Figure 7.28 Proto-Aksumite Network (including multi-period sites).

7.3.3. The Obsidian Network during the Early Aksumite period (80 BCE – 160 CE)

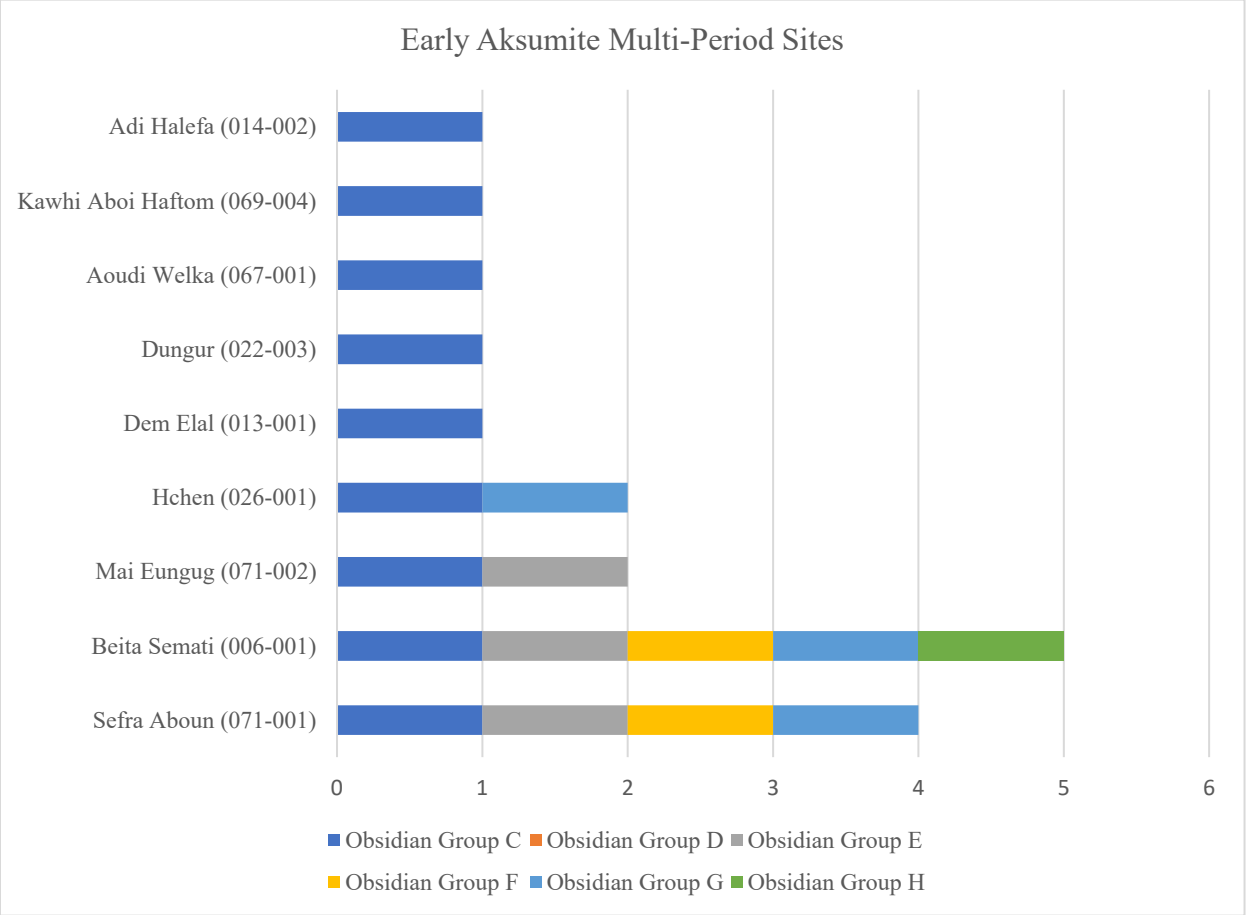

Figure 7.29 Early Aksumite Multi-Period Sites and the obsidian geochemical groups they have access to.

The Early Aksumite period network contains 9 nodes that collectively share obsidian from groups C, E, F, and G (Fig. 7.29). This network contains one single period site, Kawhi Aboi Haftom (069-004; Appendix II: Table 57a), and eight multi-period sites (Appendix II: Table 58a) and is characterized by 72 ties. While the number of ties increased by approximately 29%, the overall network centralization of 13.84% represents a 10.57% decrease from that of the previous period's network. This measure was calculated using the Freeman Centralization approach and suggests the maintenance of a decentralized system characterized by little variation in the rank or

power of individual nodes. Despite the low degrees of overall centralization, this network is also characterized by three tiers established by calculating degree centrality for each node (Table 7.9).

Characterized by 13 ties, the first tier of sites contains the two best connected sites of the previous two networks, the multi-period settlements of Sefra Aboun (071-001) and Beta Samati (006-001), which continue to share access to sources C, E, F, and G.

Table 7.9 Weighted Early Aksumite Adjacency Matrix with Degree Centrality Measure.

	Sefra Aboun (071-001)	Beta Samati (006-001)	Mai Eungug (071-002)	Hchen (026-001)	Dem Elal (013-001)	Dungur (022-003)	Aoudi Welka (067-001)	K. Aboi Haftom (069-004)	Adi Halefa (014-002)	Degree
Sefra Aboun (071-001)		4	2	2	1	1	1	1	1	13
Beta Samati (006-001)	4		2	2	1	1	1	1	1	13
Mai Eungug (071-002)	2	2		1	1	1	1	1	1	10
Hchen (026-001)	2	2	1		1	1	1	1	1	10
Dem Elal (013-001)	1	1	1	1		1	1	1	1	8
Dungur (022-003)	1	1	1	1	1		1	1	1	8
Aoudi Welka (067-001)	1	1	1	1	1	1		1	1	8
Kawhi Aboi Haftom (069-004)	1	1	1	1	1	1	1		1	8
Adi Halefa (014-002)	1	1	1	1	1	1	1	1		8

The second tier of sites coincides with the second tier of the previous Proto-Aksumite period, containing the multi-period find spot of Mai Eungug and the multi-period artifact scatter of Hchen. The number of links incident upon these nodes is 10.

With a degree centrality of 8, the bottom 56% percent of sites belong to the third tier. This category includes all the third-tier sites from the previous period's network along with an

additional single period artifact scatter, Kawhi Aboi Haftom (069-004), which also has access to a single obsidian group, group C.

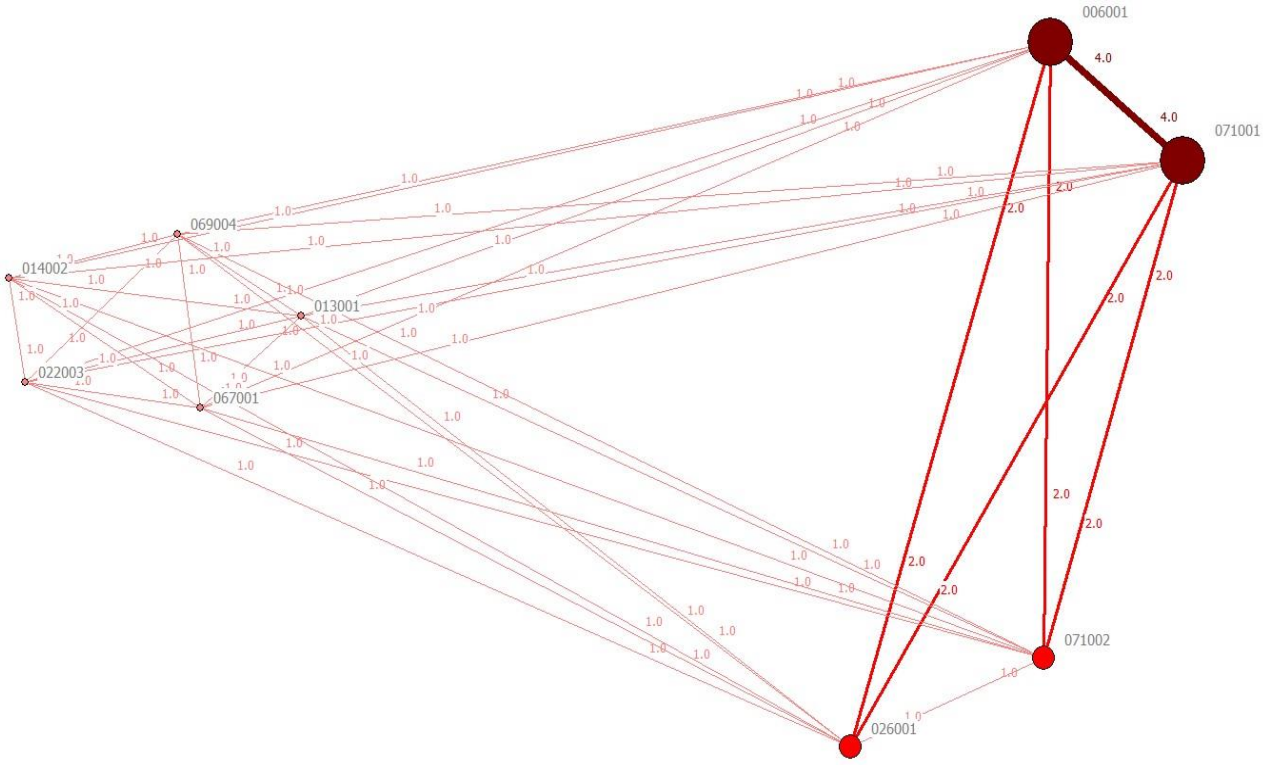

Figure 7.30 Early Aksumite Period Network (includes multi-period sites). Nodes Scaled by Degree Centrality.

This node order was further confirmed with a Bonacich's "Power" Centrality measure (Beta centrality) and with a Flow Betweenness Centrality Measure, both of which reveal a degree of equality and a lack of concentration in the distribution of flow betweenness centralities (Fig. 7.30). As in the previous two networks, the density of the Early Aksumite network is revealed to be 100%, with each node having a distance of 1 and a reachability of 1, indicating that each node is directly reachable from all other nodes and that the cost of reaching a node is equal to the cost of reaching any of the other nodes.

Additionally, Freeman's (point) Betweenness, calculated on binary data, indicates a complete lack of "betweenness" in a network where all nodes are in the same position, with none falling on the geodesic paths between other pairs of actors. That is, no node reveals itself to accrue power by acting like an intermediary between other nodes.

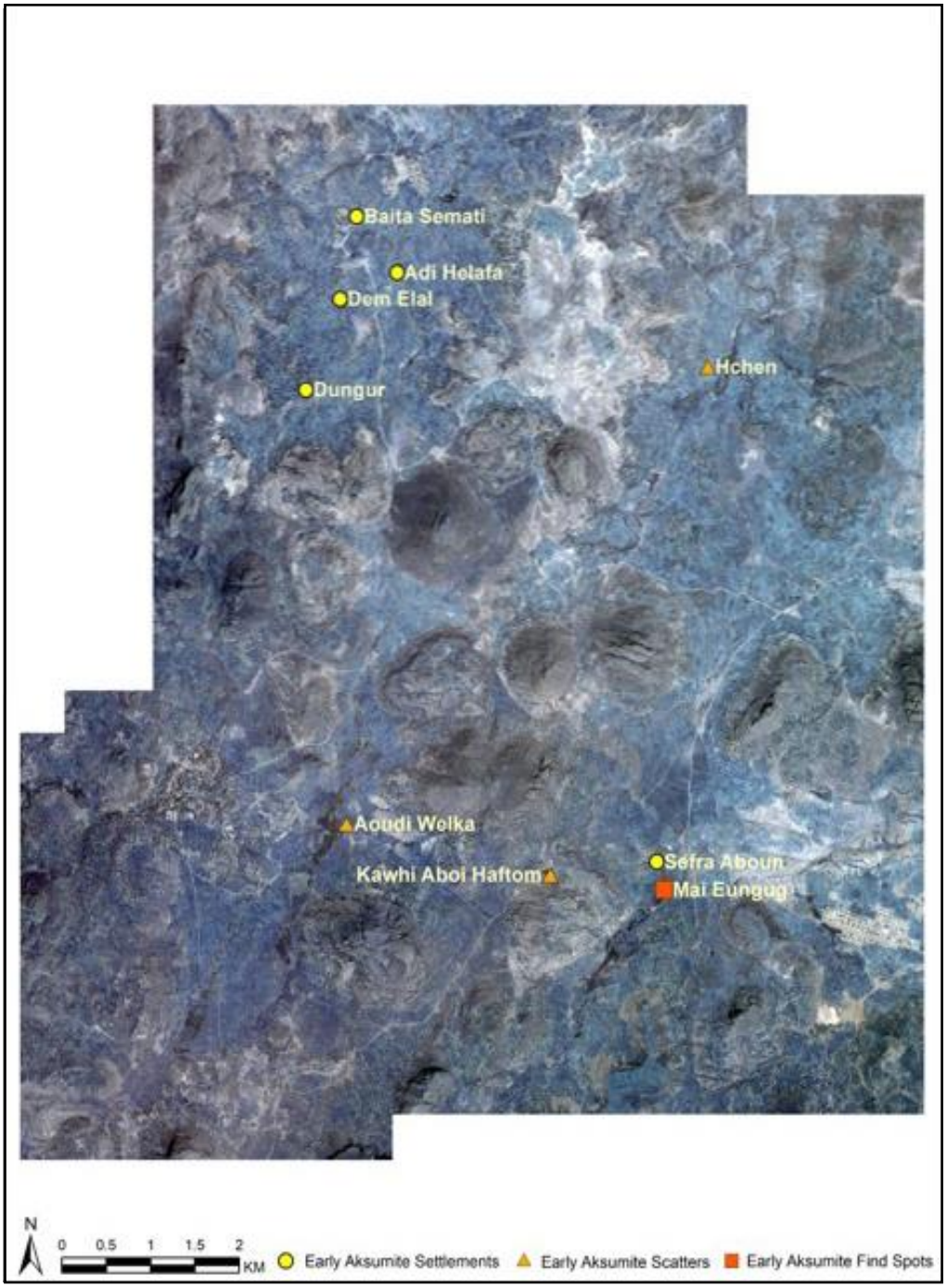

Figure 7.31 Early Aksumite Network (including multi-period sites).

Where the regional spatial distribution of sites is concerned, a similar pattern can be observed, with two core areas continuing to exist in the northwestern quadrant and in the southern stretches of the research areas and with an isolated artifact scatter, Hchen, in the northeastern quadrant (Fig. 7.31).

7.3.4. The Obsidian Network during the Classic Aksumite period (160 – 380 CE)

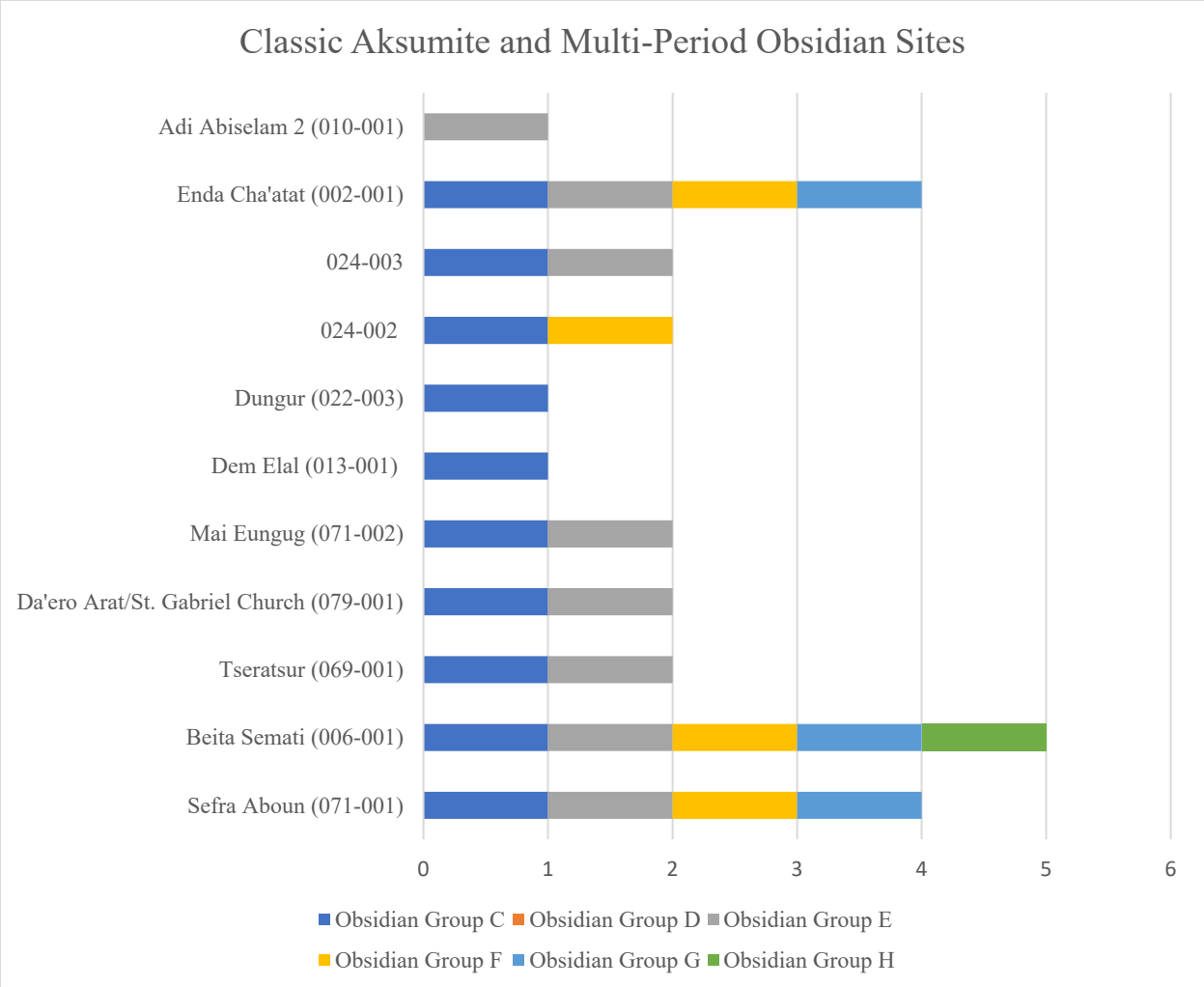

Figure 7.32 Classic Aksumite period sites and the obsidian geochemical groups they have access to.

The Classic Aksumite period network contains 11 nodes, tied by a total of 104 relationships revolving around the shared use of the same 4 obsidian groups (C, E, F, and G) that have characterized the previous three networks (Fig. 7.32). This network (Appendix II: Table 60a) contains 2 single period sites, the artifact scatter 024-002 (which has access to obsidian groups C and F) and the find spot 024-003 (which has access to obsidian groups C and E). The remaining 9 nodes are multi-period sites including 7 settlements (Enda Cha'atat, Dungur, Dem Elal, Da'ero Arat/St. Gabriel Church, Tseratsur, Beta Samati, and Sefra Aboun) and 2 find spots (Adi Abisalem 2 and Mai Eungug). The number of ties increased by 44.44% from the previous network and the overall network centralization by a notable 34.47%. Calculated using Freeman's Centralization approach to be approximately 18.61%, this measure suggests incremental levels of moderate hierarchization.

This network's 11 nodes are divided into 5 tiers (Table 7.10). The first tier includes three settlements: the two multi-period settlements, Sefra Aboun and Beta Samati, which have occupied the top network position since the Pre-Aksumite period and the multi-period settlement of Enda Cha'atat (002-001), a site that begins to be occupied during this time period. All three settlements share access to groups C, E, F, and G, with Beta Samati being the only settlement of the network to have access to obsidian from group H. [70] The number of ties incident upon these nodes is 21.

The second tier, characterized by a total of 16 ties, includes a total of four sites: two multi-period settlements, Tseratsur and Da'ero Arat/St. Gabriel Church, one multi-period find spot, Mai

[70] Obsidian from group H has also been found in Survey Unit 079a. This transect contains the Classic to Middle Aksumite settlement Da'ero Arat/St. Gabriel Church (079-001). Because of the spatial proximity of this survey unit obsidian to the settlement of Da'ero Arat, in section XX below I will integrate SU 079a obsidian with the data from 079-001 to produce a model network representative of the totality of the lithic assemblage.

Eungug, and one single period find spot, 024-003. All four sites shared access to obsidian groups C and E.

Table 7.10 Weighted Classic Aksumite Adjacency Matrix with Degree Centrality Measure.

	Sefra Aboun (071-001)	Beta Samati (006-001)	Tseratsur (069-001)	Da'ero Arat (079-001)	Mai Eungug (071-002)	Dem Elal (013-001)	Dungur (022-003)	024-002	024-003	Enda Cha'atat (002-001)	Adi Abiselam 2 (010-001)	Degree
Sefra Aboun (071-001)		4	2	2	2	1	1	2	2	4	1	21
Beta Samati (006-001)	4		2	2	2	1	1	2	2	4	1	21
Tseratsur (069-001)	2	2		2	2	1	1	1	2	2	1	16

A single site, the single-period artifact scatter 024-002, occupies the third-tier position, having 12 ties incident upon it. This site has access to obsidian groups C and F. The fourth tier is comprised of the multi-period settlements, Dem Elal and Dungur, both of which are characterized by the 9 ties and by shared access to obsidian from group C. Finally, the fifth tier is comprised of a single site, the multi-period find spot, Adi Abisalem 2, a site with 7 ties incident upon it, which is characterized by access to obsidian from group E (Fig. 7.33). This node order was further

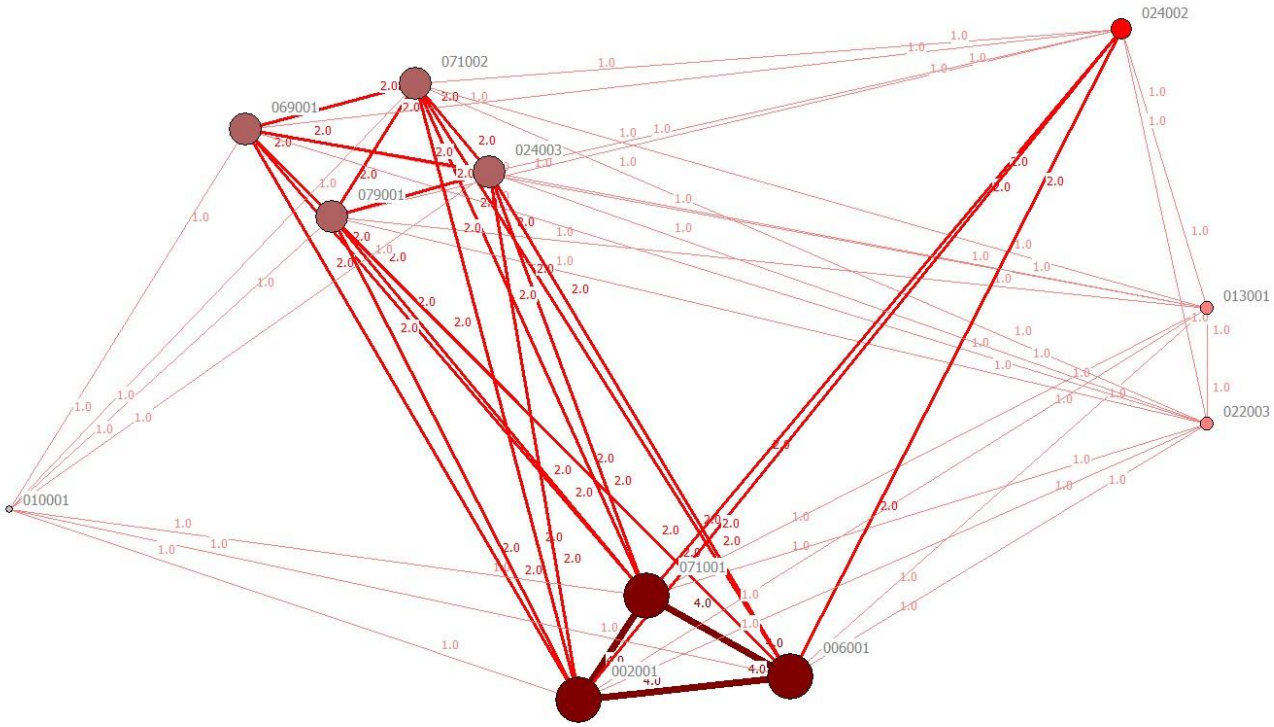

Figure 7.33 Classic Aksumite Period Network (includes multi-period sites). Nodes Scaled by Degree Centrality.

confirmed with a Bonacich's "Power" Centrality measure (Beta centrality) and with a Flow Betweenness Centrality measure.

Centrality measures run on the binarized dataset reveal higher levels of betweenness centralization than have been reconstructed for the networks of the previous periods. Freeman's (point) Betweenness Centrality reveals that 7 nodes have a betweenness centrality of 0.429, while the rest have a betweenness centrality of 0. The former category includes: 071-001, 006-001, 002-001, 069-001, 079-001,071-002, and 024-003. The nodes with higher betweenness measures constitute the two top tier nodes in terms of degree centrality. These betweenness centrality measures suggest that the two top tiers of the network are also power brokers, with greater degrees of power and control over the interactions between the rest of the nodes.

Other network centrality measures run on the binarized dataset include two closeness centrality measures: all paths and sum of geodesic distances (Freeman). The All paths measure revealed three categories of nodes related to farness. With a measure of 88.841, the nearest sites are 071-001, 006-001, 002-001, 069-001, 079-001,071-002, and 024-003. The second farthest nodes are 013-001, 022-003, and 024-002. These nodes have a farness measure of 89.254. Finally, the farthest site is 010-001 and has a farness measure of. The network centralization that emerged as a result of applying the all paths measure is 0.06%. Freeman's geodesic distances measure reveals the same node order, with the seven closest nodes being characterized by a farness measure of 10, the next three closest nodes by a farness measure of 11, and the farthest node by a farness measure of 13. The overall network centralization according to this measure is 10.63%

A number of graph-theoretic measures of connectedness and cohesion reinforce the unique aspects of this network, as compared to its predecessors. The Classic Aksumite period network also emerges as the least dense of the networks up to date, with an overall density of 94.5%. The

holes in the network occur as a result of the lack of a relationship between the multi-period find spot Adi Abiselam 2 (010-001) and the multi-period settlements of Dem Elal (013-001) and Dungur (022-003), and the single period artifact scatter of 024-002 (Table 7.11).

Table 7.9 Binary Classic Aksumite Adjacency Matrix.

	071001	**006001**	**069001**	**079001**	**071002**	**013001**	**022003**	**024002**	**024003**	**002001**	**010001**
071001		1	1	1	1	1	1	1	1	1	1
006001	1		1	1	1	1	1	1	1	1	1
069001	1	1		1	1	1	1	1	1	1	1
079001	1	1	1		1	1	1	1	1	1	1
071002	1	1	1	1		1	1	1	1	1	1
013001	1	1	1	1	1		1	1	1	1	0
022003	1	1	1	1	1	1		1	1	1	0
024002	1	1	1	1	1	1	1		1	1	0
024003	1	1	1	1	1	1	1	1		1	1
002001	1	1	1	1	1	1	1	1	1		1
010001	1	1	1	1	1	0	0	0	1	1	

Despite a lower overall density, this network contains no isolates, as determined by its reachability measure.

Spatially, the southern core of sites appears to cluster more noticeably in the southeastern quadrant, following the disappearance of multi-period artifact scatters from the central region of the southern half of the research area. In the northwestern quadrant, site density increases (Fig.7.34).

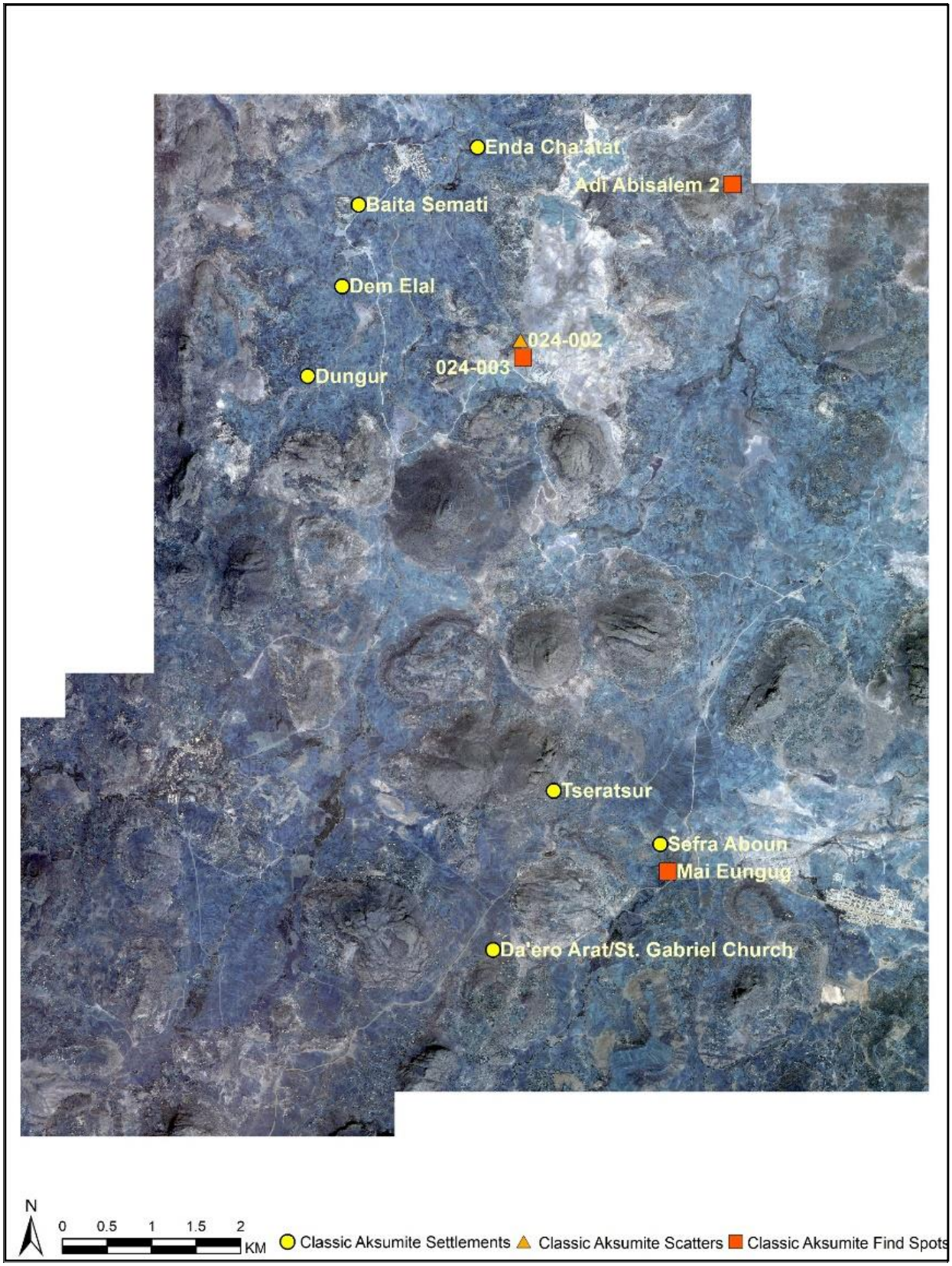

Figure 7.34 Classic Aksumite Network (including multi-period sites).

7.3.5. The Obsidian Network during the Middle Aksumite period (380 – 580 CE)

With a total of 12 constitutive nodes, the Middle Aksumite period network is the second largest and the most centralized out of all the obsidian supply networks being investigated. Tied by a total of 116 relationships revolving around the shared use of the same 4 obsidian groups (C, E, F, and G; Fig. 7.35),[71] this network contains 2 single period sites and 10 multi-period sites (Appendix II: Table 62a). In terms of the breakdown of site types, this network includes 9 settlements (Enda Giordis Mogu'o, Enda Cha'atat, Mai Fesasi, Dungur, Dem Elal, Da'ero Arat/St. Gabriel Church, Tseratsur, Beta Samati, and Sefra Aboun), 1 artifact scatter (Adi Abiselam), and 2 find spots (Adi Abisalem 2, 008-001).

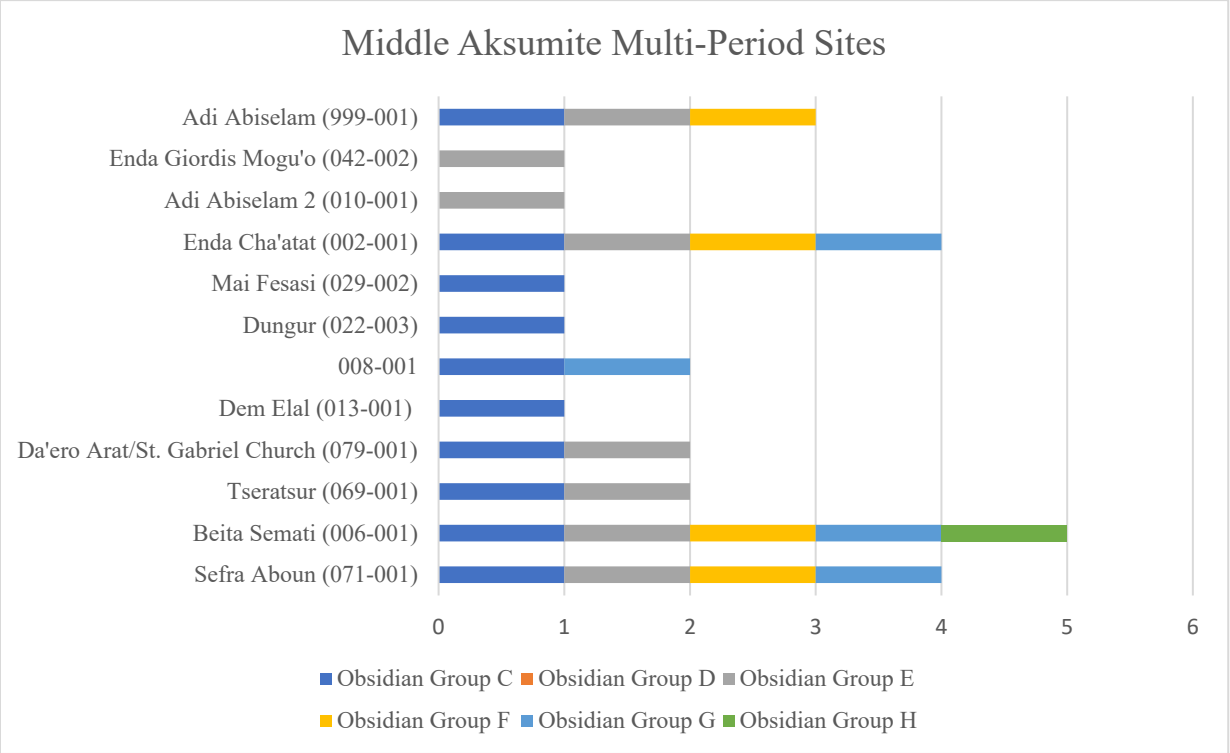

Figure 7.35 Middle Aksumite period sites and the obsidian geochemical groups they have access to.

[71] Lithics from obsidian group H were discovered in the environs of Luhuts (077-001), a Middle Aksumite single period settlement (0.66 ha) discovered within Survey Unit 077a. Survey collections from 077a revealed obsidian from group H. Because of the spatial proximity of this survey unit obsidian to the settlement of Luhuts, in section XX below I will integrate SU 077a obsidian with the data from 077-001 to produce a model network representative of the totality of the lithic assemblage.

This network sees an increase in the number of ties of 11.54% from the past period's supply network and an attendant increase in network centralization of 14.78%. Calculated using Freeman's Centralization approach to be approximately 21.36%, this measure suggests a continuation in the pattern of moderate and incremental hierarchization.

The supply network's 12 nodes are divided into six tiers (Table 7.12). Approaching this data longitudinally, first tier sites of the Middle Aksumite network have the highest degree centrality as compared to all preceding and following networks. Characterized by a total of 22 ties incident upon each node, this tier consists of three settlements: Sefra Aboun, Beta Samati, and Enda Cha'atat, all of which share access to all four obsidian groups.

Table 7.12 Weighted Middle Aksumite Adjacency Matrix with Degree Centrality Measure.

	Sefra Aboun (071-001)	Beta Samati (006-001)	Tseratsur (069-001)	Da'ero Arat (079-001)	Dem Elal (013-001)	008-001	Dungur (022-003)	Mai Fesasi (029-002)	Enda Cha'atat (002-001)	Adi Abiselam 2 (010-001)	Enda Giordis Mogu'o (042-002)	Adi Abiselam (999-001)	Degree
Sefra Aboun (071-001)		4	2	2	1	2	1	1	4	1	1	3	22
Beta Samati (006-001)	4		2	2	1	2	1	1	4	1	1	3	22
Tseratsur (069-001)	2	2		2	1	1	1	1	2	1	1	2	16
Da'ero Arat (079-001)	2	2	2		1	1	1	1	2	1	1	2	16
Dem Elal (013-001)	1	1	1	1		1	1	1	1			1	9
008-001	2	2	1	1	1		1	1	2			1	12
Dungur (022-003)	1	1	1	1	1	1		1	1			1	9
Mai Fesasi (029-002)	1	1	1	1	1	1	1		1			1	9
Enda Cha'atat (002-001)	4	4	2	2	1	2	1	1		1	1	3	22
Adi Abiselam 2 (010-001)	1	1	1	1					1		1	1	7
Enda Giordis Mogu'o (042-002)	1	1	1	1					1	1		1	7
Adi Abiselam (999-001)	3	3	2	2	1	1	1	1	3	1	1		19

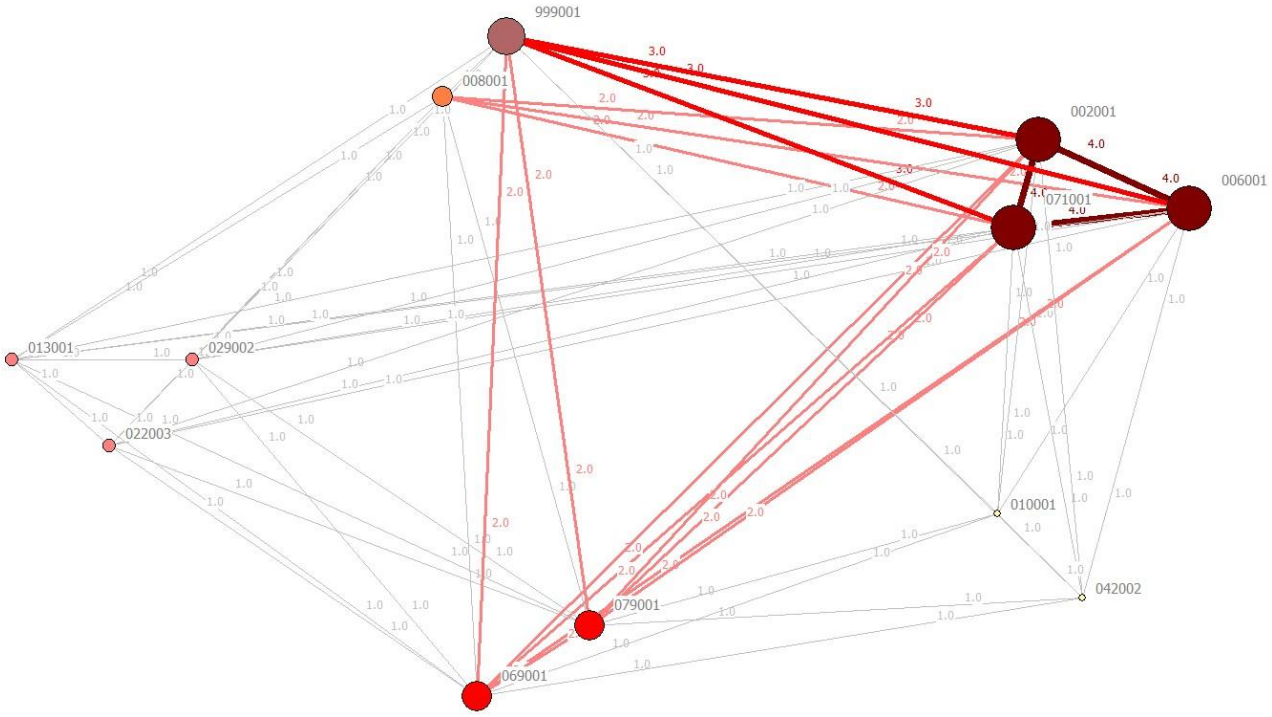

Figure 7.36 Middle Aksumite Period Network (includes multi-period sites). Nodes Scaled by Degree Centrality.

The second tier, characterized by 19 ties, includes a single site, a Middle Aksumite artifact scatter, Adi Abiselam (999-001), with access to obsidian groups C and F. Third tier sites, Tseratsur and Da'ero Arat, have 16 ties incident upon them and share access to groups C and E. With access to obsidian from group G, the fourth tier also consists of a single node: the multi-period find spot 008-001. This site has a degree centrality of 12. The fifth tier is characterized by a degree centrality of 9 and consists of three multi-period settlements, Dem Elal, Dungur, and Mai Fesasi, all of which have access to group C. Finally, the sixth tier consists of the Middle Aksumite settlement Enda Giordis Mogu'o and the multi-period find spot Adi Abisalem 2, both of which share access to obsidian source E and are characterized by a degree centrality of 7 (Fig. 7.36).

This node order was further confirmed with a Bonacich's "Power" Centrality measure (Beta centrality) and with a Flow Betweenness Centrality measure. The network centralization index calculated with the Flow Betweenness Centrality measure was 4.704%.

A Freeman (point) Betweenness Centrality run on the binarized dataset (Table 7.13) reveals a betweenness measure of 1.33 for half of the nodes of this network: 071-001, 006-001, 069-001, 079-001, 999-001, and 002-001 and an overall network centralization index of 1.32%. This measure reveals that first, second, and third tier sites have the same betweenness. The remaining 6 nodes have a betweenness of 0.

An All Paths closeness centrality revealed three farness levels, with sites from the sixth tier (010-001 and 042-002) having the highest farness measure (108.361), sites from the fourth (008-001) and fifth tiers (013-001, 022-003, and 029-003) having the second highest farness measure (107.583), and sites from the top three tiers (071-001, 006-001, 002-001, 999-001, 069-001, 079-001) having the lowest farness measure (106.689). The overall network centralization, as revealed by this measure, is 0.13%. Freeman's sum of geodesic distances measure reveals the same order of nodes and a network centralization of 21.93%.

Table 7.13 Binary Middle Aksumite Adjacency Matrix.

	Sefra Aboun (071-001)	Beta Samati (006-001)	Tseratsur (069-001)	Da'ero Arat/St. Gabriel Church (079-001)	Dem Elal (013-001)	008-001	Dungur (022-003)	Mai Fesasi (029-002)	Enda Cha'atat (002-001)	Adi Abiselam 2 (010-001)	Enda Giordis Mogu'o (042-002)	Adi Abiselam (999-001)
Sefra Aboun (071-001)		1	1	1	1	1	1	1	1	1	1	1
Beta Samati (006-001)	1		1	1	1	1	1	1	1	1	1	1
Tseratsur (069-001)	1	1		1	1	1	1	1	1	1	1	1
Da'ero Arat/St. Gabriel Church (079-001)	1	1	1		1	1	1	1	1	1	1	1
Dem Elal (013-001)	1	1	1	1		1	1	1	1			1
008-001	1	1	1	1	1		1	1	1			1
Dungur (022-003)	1	1	1	1	1	1		1	1			1
Mai Fesasi (029-002)	1	1	1	1	1	1	1		1			1
Enda Cha'atat (002-001)	1	1	1	1	1	1	1	1		1	1	1

Adi Abiselam 2 (010-001)	1	1	1	1					1		1	1
Enda Giordis Mogu'o (042-002)	1	1	1	1					1	1		1
Adi Abiselam (999-001)	1	1	1	1	1	1	1	1	1	1	1	

Regionally, a more diffuse pattern of sites can be observed within this time period (Fig. 7.37). While the same two core areas can be discerned, in the southeastern and northwestern quadrants, two settlements arise during this period that occupy the central region of the survey area. While the site of Enda Giordis Mogu'o is a single-period settlement that is abandoned following the Middle Aksumite period, Mai Fesasi continues to be used into the Post-Aksumite period. Interestingly, while the latter has evidence of access to obsidian from group C, the former is characterized by the use of obsidian from the lesser represented group E.

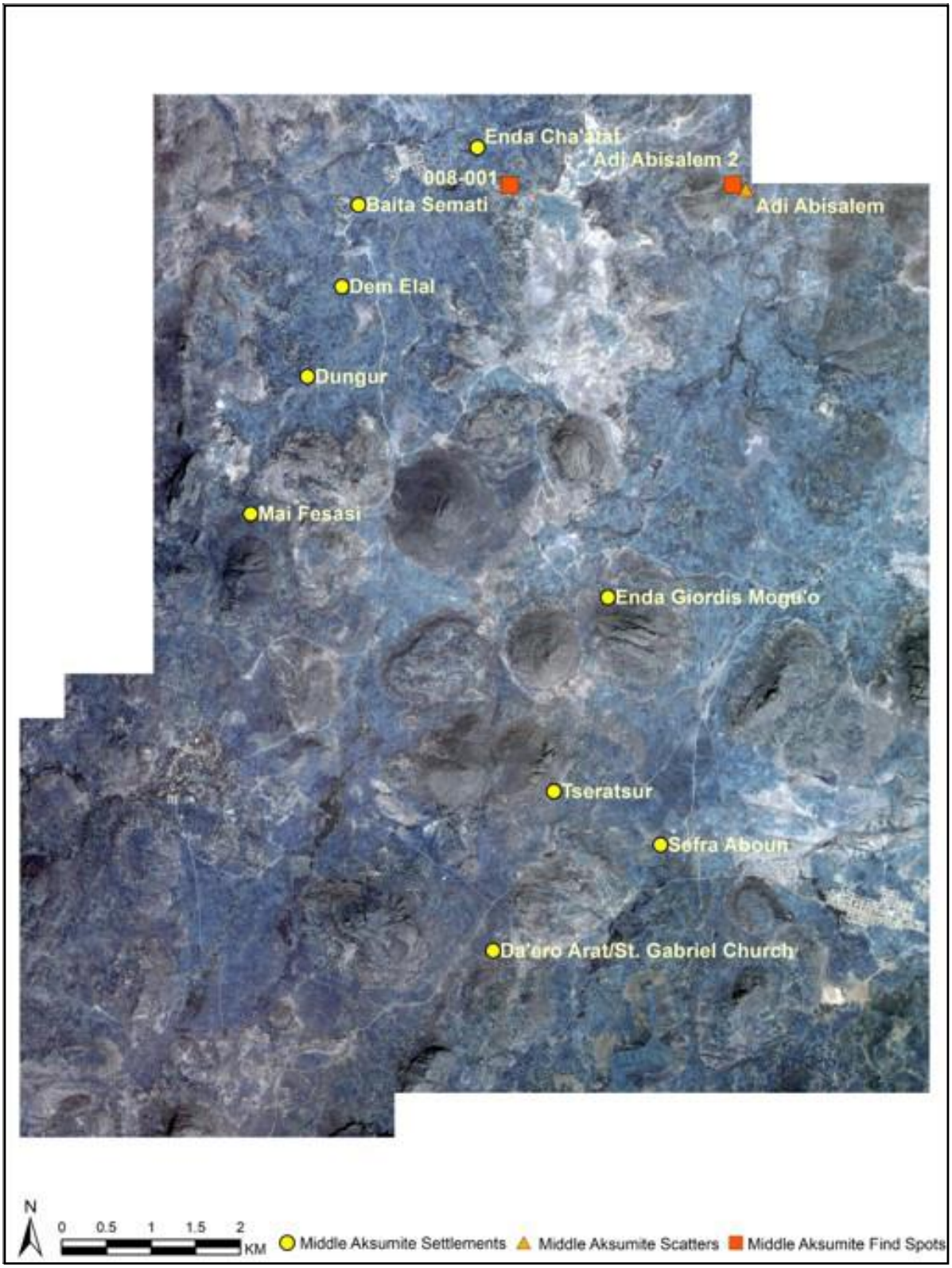

Figure 7.37 Middle Aksumite Network (including multi-period sites).

7.3.6. The Obsidian Network during the Late Aksumite period (580 – 825 CE)

With a total of 8 nodes and 56 ties, the Late Aksumite period contains the smallest[72] obsidian supply network. Compared to the previous period's network, the Late Aksumite obsidian supply network is characterized by a node decrease of 33.33% and an attendant decrease in ties of 51.72%. Unlike networks of the previous periods, three obsidian groups (Fig. 7.38) are shared among the 8 constitutive nodes: C, E, and G (with obsidian from groups F and H only being accessible to Beta Samati). All the Late Aksumite supply network sites are multi-period sites, including 5 settlements (Beta Samati, Tseratsur, Dem Elal, Dungur, Mai Fesasi), 2 artifact scatters (Endaba Hailu, Gembes), and 1 find spot (008-001).

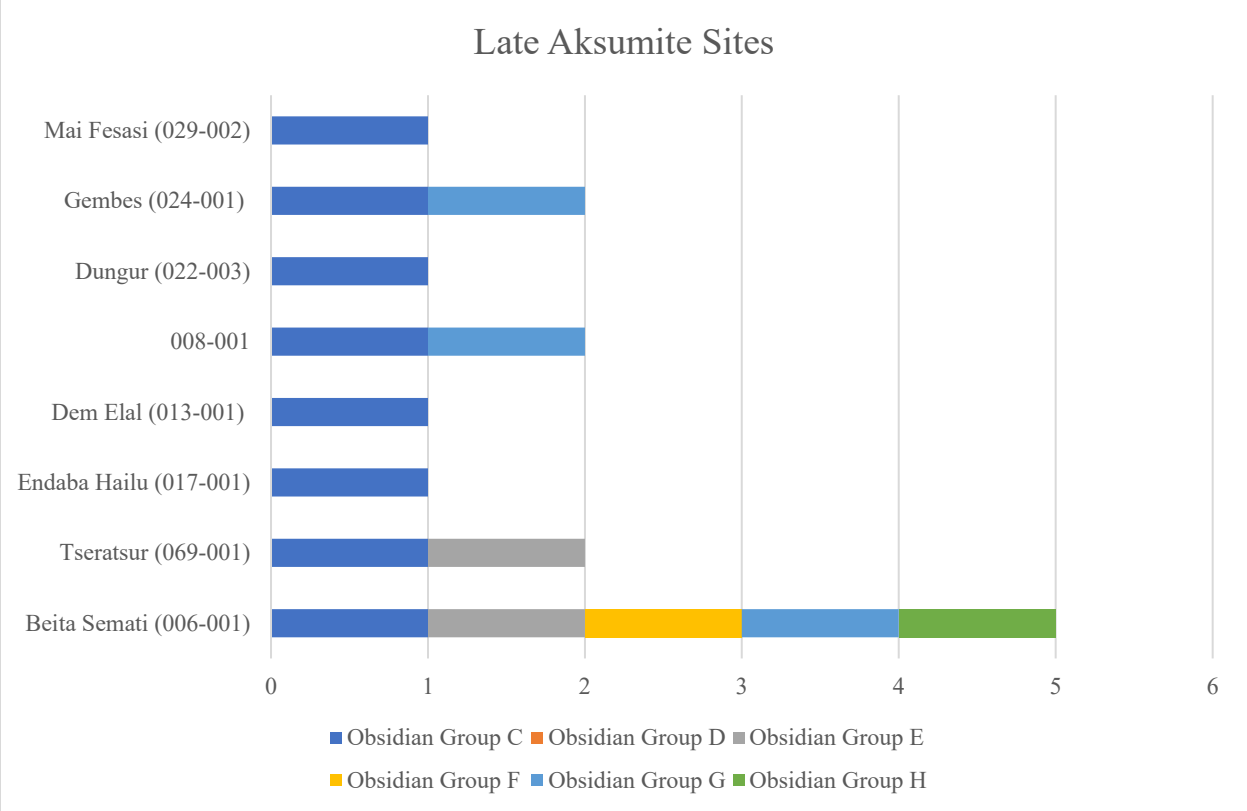

Figure 7.38 Late Aksumite period sites and the obsidian geochemical groups they have access to.

[72] This position is shared with the Proto-Aksumite supply network.

Despite its size, this network is the second most centralized network of the Pre-Aksumite and Aksumite periods, with an overall centralization index of 19.05% and is divided into 4 tiers (Table 7.14; Fig. 7.39). The first tier, characterized by 10 ties, contains a single site, the settlement Beta Samati, with access to three shared sources (C, E, and G). Characterized by 9 ties, the second tier consists of one find spot (008-001) and one artifact scatter (Gembes), both of which have access to groups C and G. The third tier, characterized by 8 ties, consists of 1 site, the settlement of Tseratsur, which had access to groups C and E. Finally, the fourth tier contains 4 sites with 7 ties incident upon them, including three settlements, Dem Elal (013-001), Dungur (022-003), and Mai Fesasi (029-002), and one artifact scatter, Endaba Hailu (017-001). These sites have access to group C obsidian.

Table 7.14 Weighted Late Aksumite Adjacency Matrix with Degree Centrality Measure.

	Beta Samati (006-001)	**Tseratsur (069-001)**	**Endaba Hailu (017-001)**	**Dem Elal (013-001)**	**008-001**	**Dungur (022-003)**	**Gembes (024-001)**	**Mai Fesasi (029-002)**	**Degree**
Beta Samati (006-001)		2	1	1	2	1	2	1	10
Tseratsur (069-001)	2		1	1	1	1	1	1	8
Endaba Hailu (017-001)	1	1		1	1	1	1	1	7
Dem Elal (013-001)	1	1	1		1	1	1	1	7
008-001	2	1	1	1		1	2	1	9
Dungur (022-003)	1	1	1	1	1		1	1	7
Gembes (024-001)	2	1	1	1	2	1		1	9
Mai Fesasi (029-002)	1	1	1	1	1	1	1		7

This node order was further confirmed with a Bonacich's "Power" Centrality measure (Beta centrality) and with a Flow Betweenness Centrality measure. Calculated with this measure, the network centralization index is 1.809%.

A Freeman (point) Betweenness Centrality run on the binarized dataset reveals betweenness measures of 0 for each node, indicating the lack of power brokers. Closeness Centrality measures (cf. All Paths and Freeman's Sum of geodesic distances) reveal that all nodes are at equal distances within the network.

In terms of network connectedness, density, reachability, and point connectivity measures all reveal a highly cohesive network with a density measure of 100%, with each node having a distance of 1 and a reachability of 1, indicating that each node is directly reachable from all other nodes and that the cost of reaching a node is equal to the cost of reaching any of the other nodes. In terms of the spatial patterning of the obsidian supply network, the southern stretches of the survey area become almost entirely devoid of sites, with the multi-period settlement Tseratsur being the only remaining obsidian site in the region (Fig. 7.40). The remainder of the activities appear to move into the northwestern quadrant of the survey area. This pattern can be indicative of a number of processes, including the centralization of activities at Tseratsur or an attendant shift of activities towards the north.

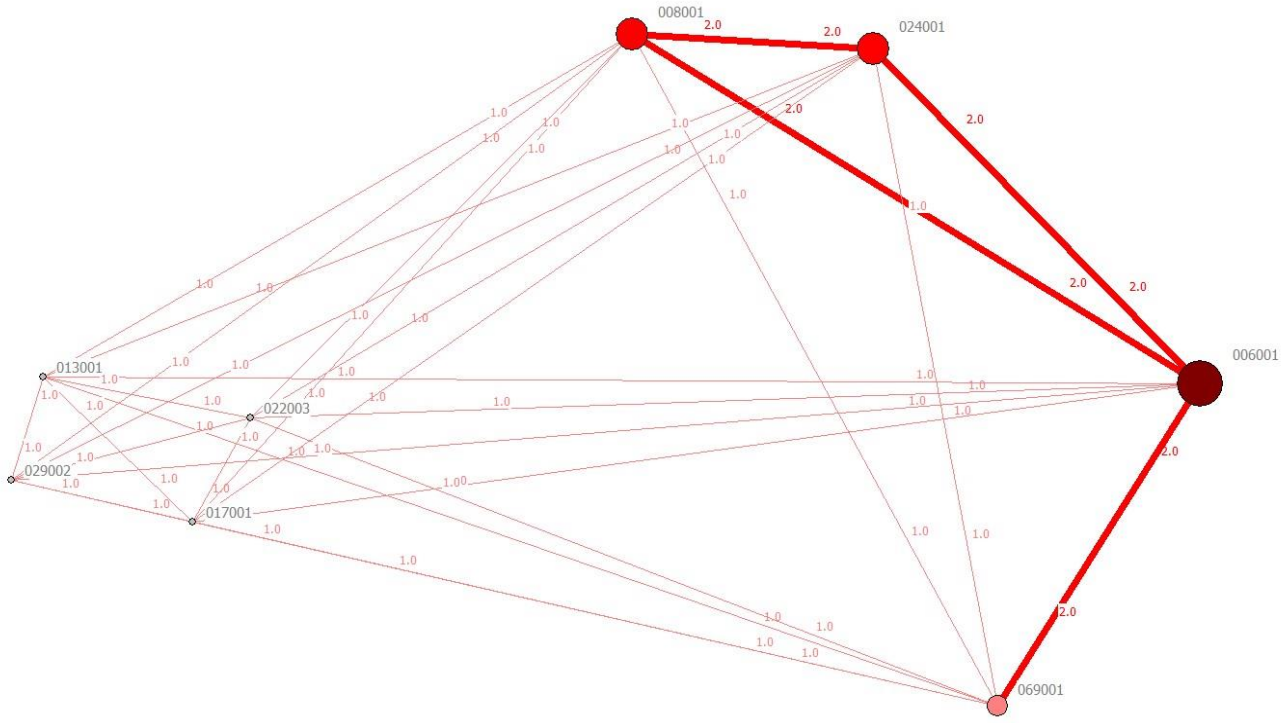

Figure 7.39 Late Aksumite Period Network (includes multi-period sites). Nodes Scaled by Degree Centrality.

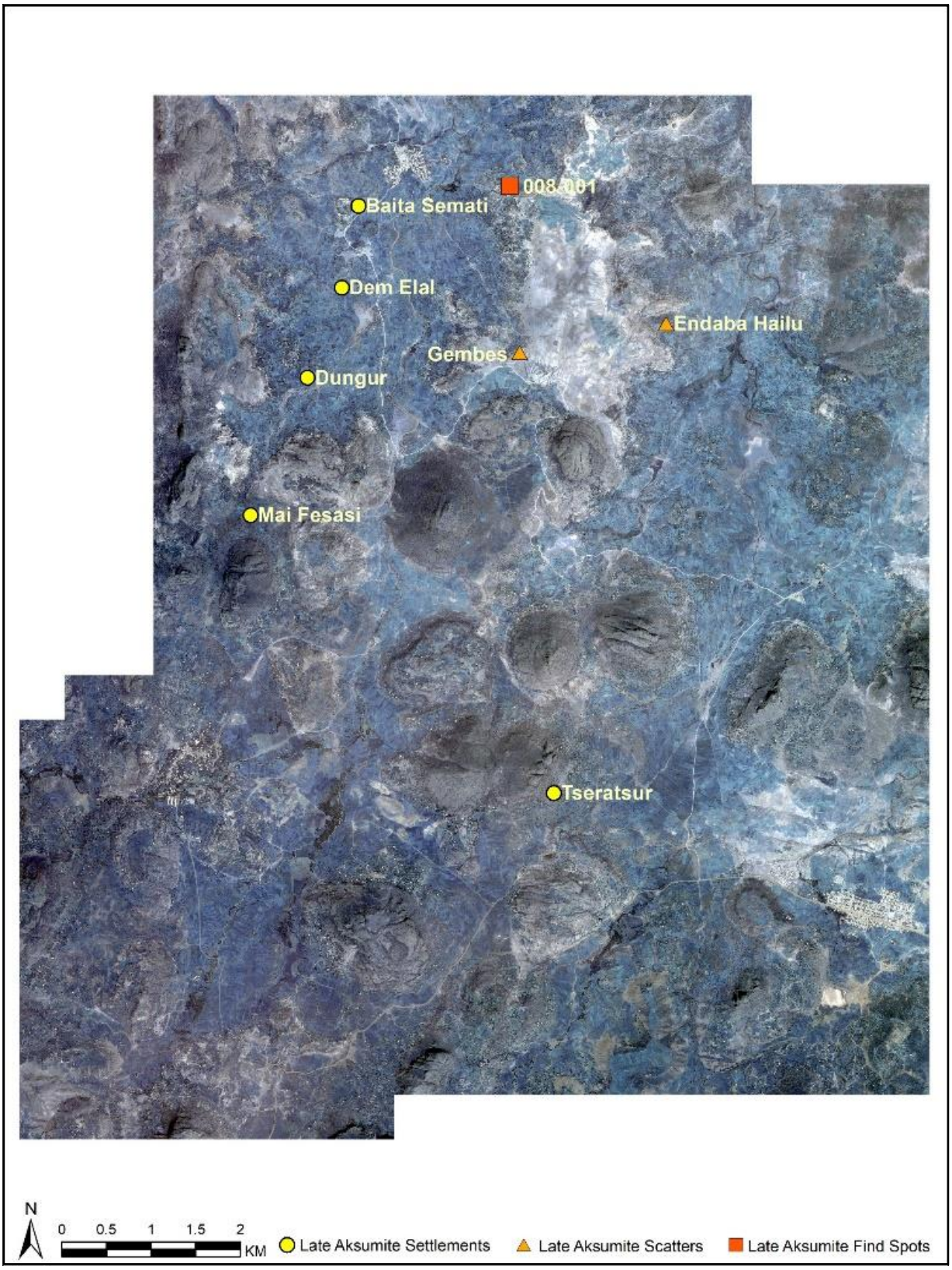

Figure 7.40 Late Aksumite Network (including multi-period sites).

7.3.7. Longitudinal Overview of the Obsidian Supply Network from the Pre-Aksumite to the Late Aksumite Period

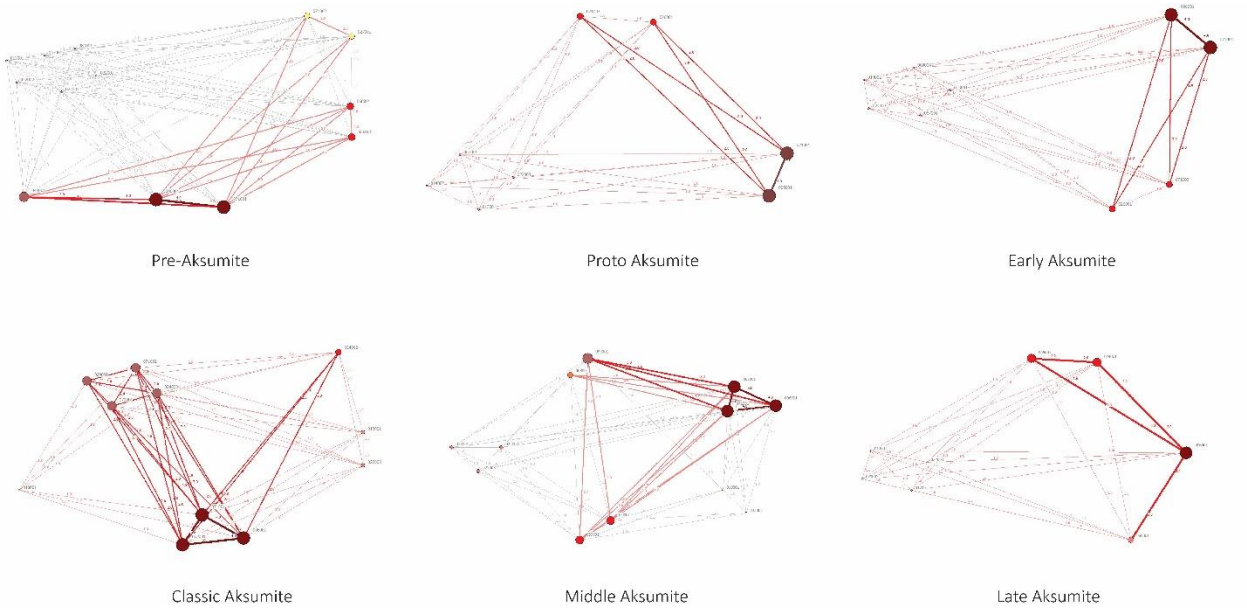

Figure 7.41 Ethiopia Network Graphs: All Periods. Nodes Scaled by Degree Centrality.

Beginning with an overview of network-level patterns of centralization and continuing with an interpretation of patterns observed at the level of nodes and cliques, this section provides a longitudinal overview of the networks corresponding to the six periods of obsidian exploitation and consumption (Fig. 7.41; Table 7.15; Appendix II: Table II.67a and Table II.67b).

Where network cohesion is concerned, social network analysis reveals high overall densities. With the exception of the network that developed during the Classic Aksumite period, which is characterized by a slightly lower density of 0.94, all other networks had a density of 1, revealing that 83% of the time, the maximum number of potential relationships were actualized.

Overall, network centralization indices reveal decentralized systems with fluctuations between periods. The pattern of centralization during the Pre-Aksumite and Aksumite periods, reveals slight increases in centralization between the first two periods, a decrease in centralization

during the third period, a renewed increase in centralization between the fourth and fifth periods, and a final period which witnesses a decrease in centralization.

This longitudinal pattern of network degree centralization is largely paralleled in the flow betweenness centralization data, with one key difference; whereas the Late Aksumite network is more centralized than the Classic Aksumite network (as this relates to degree), the Classic Aksumite network is more centralized than the Late Aksumite network in terms of flow betweenness centrality.

Comprising of 13 nodes, the Pre-Aksumite network has a group degree centralization of 14.96%, revealing a relatively decentralized distribution of power. The Pre-Aksumite network, is the second least centralized network, being 29.96% less centralized than the most centralized network, which developed during the Middle Aksumite period. This period's network also has the second lowest flow betweenness centrality index (1.3%).

Compared to the previous period, the Proto-Aksumite network sees a negligible 3.48% increase in group centralization, for a centralization index of 15.48%, and more significant 23.85% increase in flow betweenness, for a flow betweenness centralization index of 1.62%. Despite these slight changes, both periods are characterized by comparatively decentralized networks.

The Early Aksumite network is characterized by a decrease in both degree centralization and flow betweenness centralization, being 10.59% less centralized, as relates to degree, and 31.6% less centralized in terms of flow betweenness than the previous period's network.

The largest increase in centralization is seen between the Early Aksumite and Classic Aksumite periods. With a degree centralization of 18.61%, the Classic Aksumite period is 34.47%

more centralized than the Early Aksumite period and 228.25% more centralized in terms of flow betweenness centralization (3.63%).

The most centralized network develops during the Middle Aksumite period (21.36%), seeing a 14.78% increase in degree centralization from the previous period and a 29.34% increase in flow betweenness.

Finally, the Late Aksumite network witnessed the largest decrease in overall centralization with a 10.81% decrease in degree centralization (19.05%) and a 61.54% decrease in flow betweenness centrality (1.8%).

Table 7.15 Group Centralization Measures.

	Pre-Aksumite	**Proto Aksumite**	**Early Aksumite**	**Classic Aksumite**	**Middle Aksumite**	**Late Aksumite**
Nodes	13	8	9	11	12	8
Ties	156	56	72	104	116	56
DC	14.9600%	15.4800%	13.8400%	18.6100%	21.3600%	19.0500%
DC (Tiers)	5	3	3	5	6	4
DC (1st)	21	12	13	21	22	10
DC (2nd)	18	9	10	16	19	9
DC (3rd)	16	7	8	12	16	8
DC (4th)	15	N/A	N/A	9	12	7
DC (5th)	12	N/A	N/A	7	9	N/A
DC (6th)	N/A	N/A	N/A	N/A	7	N/A
FBC	1.3080%	1.6200%	1.1080%	3.6370%	4.7040%	1.8090%
BCFP	0.0000%	0.0000%	0.0000%	0.3800%	1.3200%	0.0000%
CCAp		0.0000%	0.0000%	0.0600%	0.1300%	0.0000%
CCSG		0.0000%	0.0000%	10.6300%	21.9300%	0.0000%
Density	1	1	1	0.945	1	1

Within these relatively decentralized systems, a number of actors achieved moderate levels of prominence. In what follows, I will trace patterns in the positions of actors within the six networks, with respect to degree centrality, betweenness centrality, and closeness centrality (Fig. 7.42, Appendix II: Table II.67a and Table II.67b).

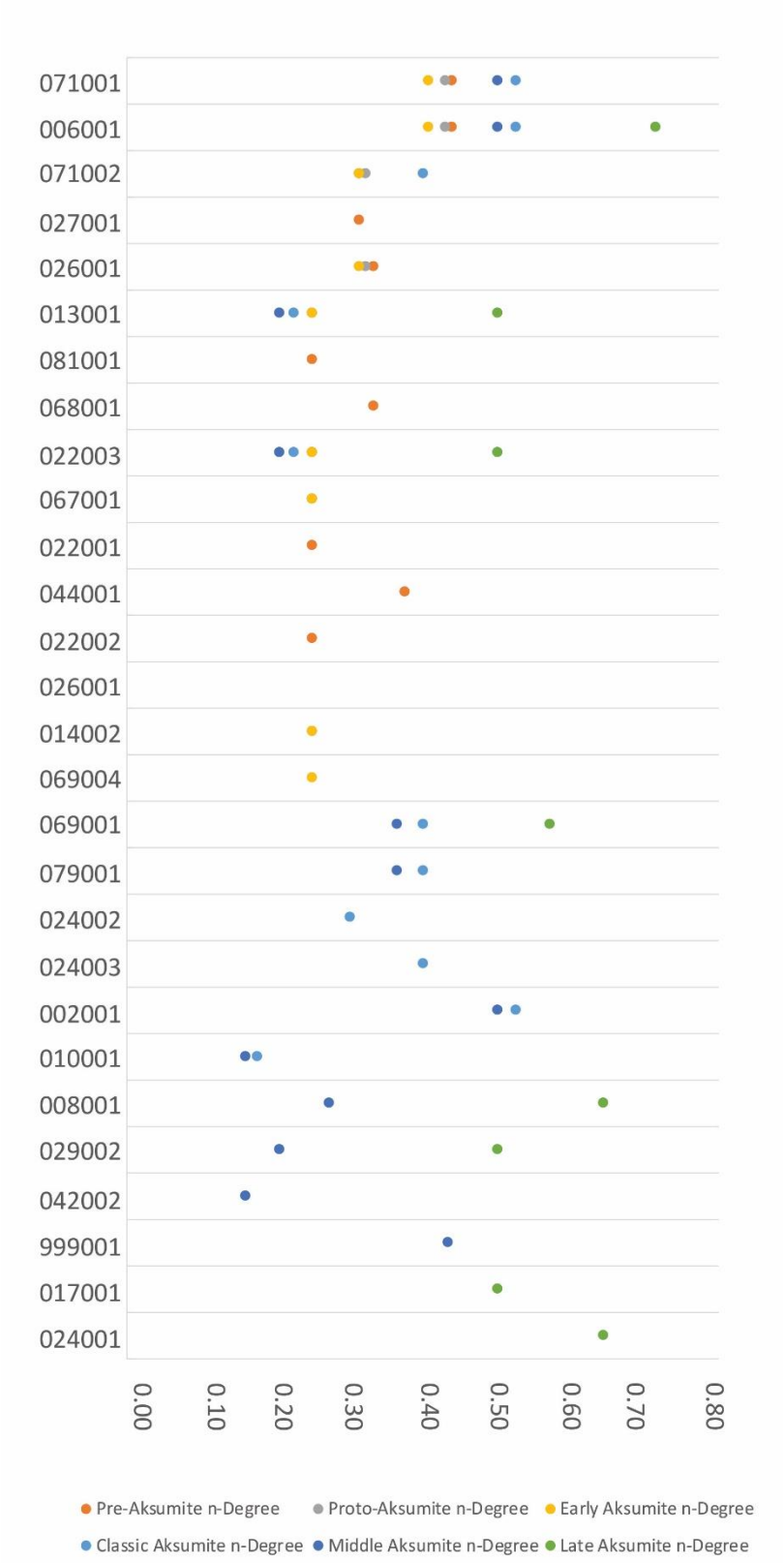

Figure 7.42 Diachronic Fluctuations in Degree Centrality (Normalized Degree) for all nodes from the Pre-Aksumite to Late Aksumite periods.

For the Pre-Aksumite period, the most central nodes with respect to degree do not overlap entirely with the most central nodes with respect to betweenness. Two degree centrality measures, Freeman's approach (Freeman 1979) and Bonacich's "Power" or beta-centrality (Bonacich 1987) reveal five tiers of prominence with nodes arranged in the same order. Sharing a degree centrality of 21, the most central nodes of the Pre-Aksumite period are the multi-period settlements of Sefra Aboun (071-001) and Beta Samati (006-001). These two nodes maintain the same network position throughout their respective periods of occupation, with Beta Samati occupying a top tier position until the Late Aksumite period and Sefra Aboun until the Middle Aksumite period, when it ceased to be occupied. Linked by a tie with strength 4, these two nodes shared obsidian groups C, E, F, and G.

A single node, the single period settlement of Sekoualou (044-001), occupies a secondary position within the Pre-Aksumite network, being characterized by a degree centrality of 18. This node has the strongest relationship with the two top tier nodes, sharing obsidian from groups C, F, and G with Beta Samati and Sefra Aboun.

Whereas three settlements occupy primary and secondary positions within the Pre-Aksumite network, the third tier of prominence is occupied by two artifact scatters, Hchen (026-001) and Mirai Abune Afsea (068-001), both characterized by a degree centrality of 16 and by the shared use of obsidian from groups C and G. While the former continues to be occupied until the Early Aksumite period, indeed occupying a more powerful secondary tier in the following two networks, the latter is a single occupation site, which is abandoned after this period.

The fourth tier includes one multi-period find spot, Mai Eungug (071-002) and one single-period Pre-Aksumite settlement, Sefra Tourkui (027-001). Linked by a tie with a strength of two,

these nodes share access to obsidian groups C and E and are characterized by a degree centrality of 15.

Finally, the fifth tier consist of 6 nodes, representing 46.1% of the Pre-Aksumite network. Characterized by shared access to obsidian from group C and by a degree centrality of 12, this tier contains four settlements, Dem Elal (013-001), Dungur (022-003), Enda Balata Dista (022-001), and Enda Aboy Meles (022-002), one artifact scatter, Aoudi Welka (067-001), and one find spot, Adi Krumbe/ Tahtay Gundam (081-001).

Despite relatively low amounts of variation in terms of flow betweenness among actors, this centrality measure reveals a slightly different node order than that revealed by the degree centrality calculation. The same three sites (Beta Samati, Sefra Aboun, and Sekoualou) have the highest flow betweenness indices. A difference in the order of sites is observed where third tier nodes are concerned, however; whereas in terms of degree centrality Hchen and Mirai Abune Afsea occupy a tertiary network position, in terms of flow betweenness it is Mai Eungug and Sefra Tourkui that are revealed to be more important power brokers. By comparison, Freeman's Betweenness Centrality reveals a complete lack of betweenness for all nodes, indicating that while there are slight differences in terms of flow capacity, these do not translate to positions that are advantageous enough to afford an opportunity to control the interactions that are being.

When analyzed with a view towards evaluating centrality as pertains to closeness, a lack of differentiation is observed within the Pre-Aksumite network, with all nodes being equidistant from each other.

Unlike the Pre-Aksumite network before it, the Proto-Aksumite network reveals an array of nodes whose prominence remains constant across degree, betweenness, and closeness measures

alike. Beta Samati and Sefra Aboun remain the most prominent nodes of the Proto-Aksumite period, being characterized by 12 ties.

With a degree centrality of 9, the secondary position in the Proto-Aksumite network is occupied by the artifact scatter of Hchen and the find spot of Mai Eungug, both of which witness increases in centrality from the previous period during which they occupied a tertiary and a quaternary position, respectively.

Finally, characterized by seven ties, the Proto-Aksumite network's third tier includes 50% of the period's actors, three of which also occupied the last tier of the Pre-Aksumite network: the settlements of Dem Elal and Dungur and the artifact scatter of Aoudi Welka. A final actor belonging to this tier, the find spot of Adi Halefa (014-002), is initially occupied during this time period and shares access to group C with the other nodes constituting this tier.

The Early Aksumite network parallels the Proto-Aksumite network's node order and network structure, overlapping almost entirely with it. The single difference between the two, consists in the presence of an additional single-period artifact scatter (Kawhi Aboi Haftom, 069-004) in tertiary position within the network.

During the Classic Aksumite period, the structure of the obsidian supply network becomes more complex. As revealed by two degree centrality measures, Freeman's approach and Bonacich's "Power" Centrality, five tiers of prominence comprise the period's network.

Beta Samati and Sefra Aboun continue to hold primary positions within the network. This first tier is characterized by 21 ties and, for the first time during this period, contains a third node, the multi-period settlement of Enda Cha'atat, which was occupied for the first time during the

Classic Aksumite period and continued to be in use during the Middle Aksumite period, sharing access to four obsidian groups (C, E, F, and G) with the other two most central nodes.

Four nodes occupy a secondary position within the network. The find spot of Mai Eungug maintains its second tier position and is joined by three sites that begin to be occupied during this period: the settlements of Tseratsur (069-001) and Da'ero Arat/ St. Gabriel's Church (079-001) and the find spot of 024-003. All four have a degree centrality of 16 and are characterized by the shared use of obsidian from groups C and E.

Also characterized by the use of two obsidian groups (C and F), the single period artifact scatter of 024-002 is characterized by 12 ties and occupies this network position alone.

The settlements of Dem Elal and Dungur, which were the least centralized nodes within the Pre-Aksumite, Proto-Aksumite, and Early Aksumite networks, now occupy a slightly more centralized fourth tier position within the network and are characterized by 9 ties.

The network's fifth and final tier is comprised of a single node, the multi-period find spot of Abi Adisalem 2 (010-001). Characterized by a degree centrality of 7, this node has access to a single obsidian group (E).

This same node order is revealed by a Flow Betweenness centrality calculation, which indicates a relatively high amount of variation, with the most central nodes being characterized by a flow betweenness of 11.7 and the least centralized by a flow betweenness of 2.5.

Freeman's betweenness centrality reveals two tiers. Nodes that occupy primary and secondary positions with respect to degree also have a higher betweenness centrality, indicating that these actors are in a position to control the interactions they are intermediating. The remaining nodes,

which occupy the third, fourth, and fifth tiers of the network in terms of degree, are not in a position to mediate any interactions within the network, being characterized by a betweenness of 0.

Closeness centrality measures reveal three tiers of prominence. The closest nodes are also the most centralized in terms of degree and betweenness, overlapping with the first and second tiers as relates to degree. The second closest sites contain third and fourth tier nodes, in terms of degree and flow betweenness. The farthest site of the network, Adi Abiselam 2, is also the least connected in terms of degree.

The Middle Aksumite network is divided into six tiers. With a degree centrality of 22, the best-connected nodes remain the multi-period settlements of Beta Samati, Sefra Aboun, and Enda Cha'atat.

Characterized by a degree centrality of 19 and by access to obsidian from sources C and F, a single node, the single period artifact scatter of Adi Abiselam (999-001), occupies the second tier of the Middle Aksumite network.

With a degree centrality of 16, two nodes occupy a tertiary position within the network. These are Tseratsur and Da'ero Arat, nodes that had occupied a secondary position in the previous network. The fourth tier of the network contains the find spot of 008-001. Characterized by a degree centrality of 12, this find spot demonstrates access to obsidian from groups C and G. The fifth tier of the network contains three nodes, two of which had also occupied the penultimate tier in the Classic Aksumite network (Dem Elal and Dungur). The third node is the multi-period settlement of Mai Fesasi, which begins to be occupied during this period. All three sites share access to obsidian from group C.

Finally, the sixth tier of the network is characterized by a degree centrality of 7 and contains the least centralized node of the Classic Aksumite period, the find spot of Adi Abisalem 2 (010-001), along with the newly occupied settlement of Enda Gordis Mogu'o, both of which share access to obsidian from group E.

A flow betweenness centrality measure confirmed the node order revealed by the degree centrality measures, showcasing the relative variability in the flow betweenness of actors, with the most centralized nodes being characterized by a betweenness of 14.5 and the least centralized by a betweenness of 4.5.

Freeman's betweenness centrality, on the other hand, reveals the existence of two tiers within the network. Nodes occupying primary, secondary, and tertiary positions with regards to degree have a betweenness index of 1.3, while fourth, fifth, and sixth tier nodes are not in a position to mediate network relationships.

The advantageous position of first, second, and third tier nodes is further confirmed through two measures of closeness centrality, which reveal that nodes occupying these positions are also the closest.

The Late Aksumite network witnesses a return to a less complex network structure. Following the abandonment of Sefra Aboun and Enda Cha'atat during the Middle Aksumite period, Beta Samati is the only remaining site within the network to occupy the primary position and does so with a degree centrality of 10.

Two sites occupy this network's second tier: the find spot of 008-001, which occupied a less centralized position in the Middle Aksumite network, and the artifact scatter of Gembes (024-001), with material culture dating to the Late and Post-Aksumite periods. These sites share access to

obsidian from groups C and G. The settlement of Tseratsur remains in tertiary network position. Characterized by a degree centrality of 8, this site occupies its position alone.

Finally, the least connected tier of the network contains four nodes, three of which occupied the penultimate tier in the Middle Aksumite network: the settlements of Dem Elal, Dungur, and Mai Fesasi. This tier also contains one new artifact scatter, which appeared during this period, Endaba Hailu (017-001). These nodes share access to obsidian from group C.

This node order is confirmed by a Bonacich "Power" Centrality and by a flow betweenness centrality, both of which reveal a relatively low amount of variation.

7.4. Discussion

Social Network Analysis methods have been used in this chapter to identify the sources and distribution of power within each phase in the development of raw material supply networks in Oman and Ethiopia. The power of a node is revealed through its interactions with other actors and the patterns that emerge from an analysis of these interactions illuminate structural power levels within each network. These measures expose the degree of structural inequality or concentration of power.

Although characterized by some diachronic fluctuations, all supply networks investigated in both Oman and Ethiopia reveal relatively low levels of network centralization, which in turn indicate relatively low amounts of inequality or concentration of power (Fig. 7.43). These measures suggest that both the exploitation and production of copper in Oman and of obsidian in Ethiopia were conducted within economic systems characterized by mechanisms of integration

which were embedded in supporting structures that were decentralized, likely not under elite control, and that served to regulate economic behavior.

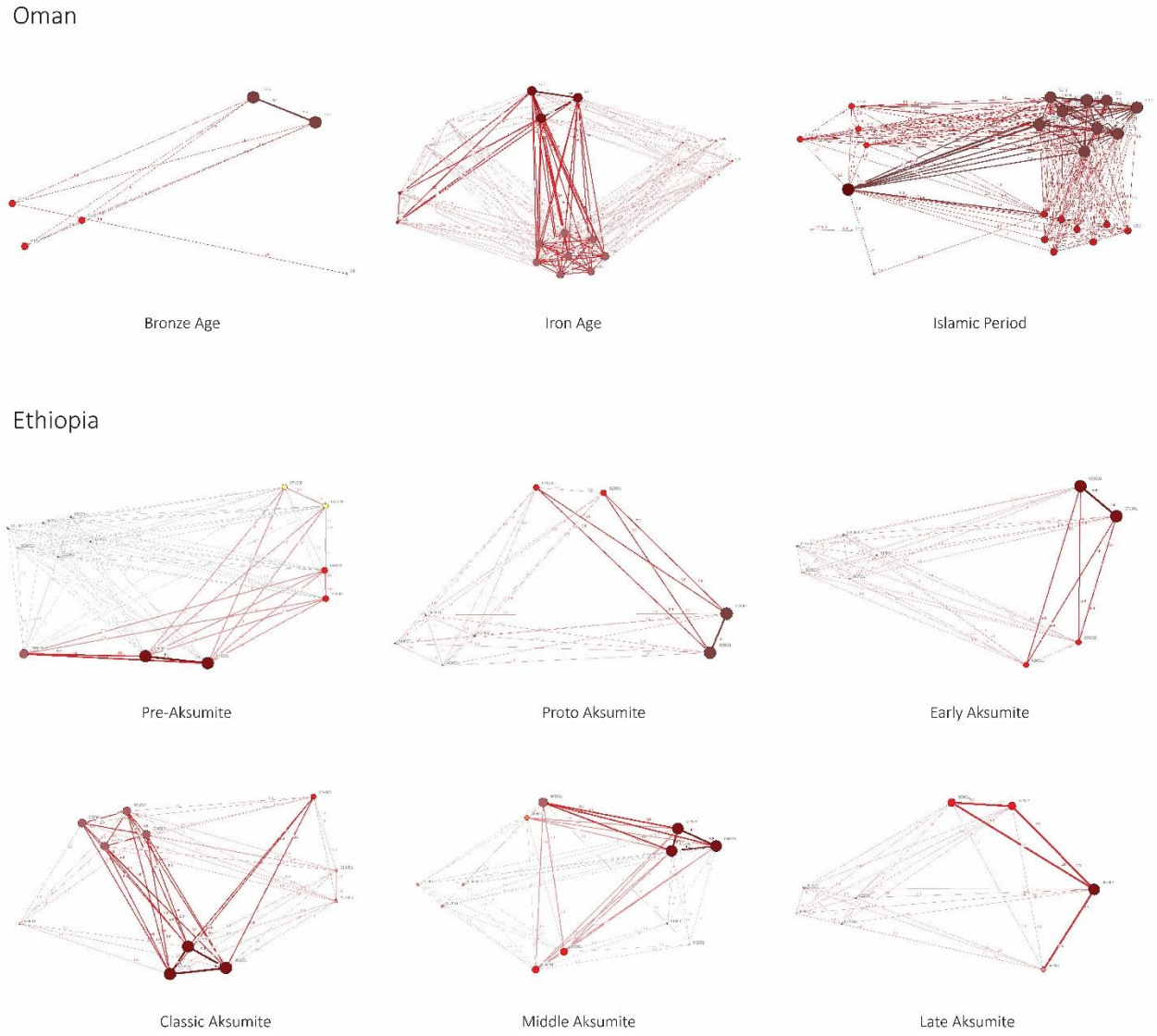

Figure 7.43 Oman and Ethiopia Network Graphs - All Periods. Nodes Scaled by Degree Centrality.

In Oman, the size of the Bronze Age network prevents us from drawing all but a few preliminary conclusions. The relatively decentralized nature of this period's network would not support the notion that early copper production was controlled by Mesopotamian political

authorities; rather, the picture that emerges is one of small-scale, decentralized production, embedded into local social relationships.

Unlike evidence relating to socio-political complexity, network findings do not indicate a steady trajectory towards increased centralization, as the Iron Age network witnessed a marked decrease in centralization as compared to the previous Bronze Age network. This is followed by an Islamic period network that is both larger in scale and 51% more centralized than the network that developed during the Iron Age.

Despite relatively low variations in centrality between nodes, certain actors are revealed as being relatively more central. The position of some of these central nodes appears to be a constant across multiple networks, indicating stability over time. There does not seem to be a relationship between site type or site size and position within a network.

Overall, the Ethiopian networks witness even less centralization than the Omani networks. This pattern likewise suggests a lack of elite control of the obsidian supply network. Instead, a decentralized system with a diluted distribution of power appears to have developed.

Characterized by the second lowest levels of centralization, the pattern observed within the Pre-Aksumite obsidian supply network indicates a lack of elite control of this sector of the economy, whether that control is theorized to have originated with a so-called South Arabian Ethio-Sabaean colony or with autochthonous elites.

Relatively higher levels of centralization were achieved incrementally during the Classic, Middle, and Late Aksumite networks in particular. These patterns in centralization appear to parallel a pattern observed within lithic assemblages of this period. A pattern from generalized to specialized lithic production begins to be revealed during the Early and Classic Aksumite periods.

This pattern towards increased specialization is characterized by the appearance of small specialized workshops (e.g. Mai Agam on Bieta Giyorgis), an increase in uniformity both within a tool type category and between lithic assemblages, and more intensive exploitation of specific quarry sites. The trend towards standardization reaches its peak during the Middle Aksumite period and has been defined through the presence of highly uniform lithics. It has been suggested that this pattern reveals a trend towards hyper-specialization and commoditization of the economy.

Chapter 8

Conclusions

This dissertation sets out to accomplish four interrelated tasks: (1) to examine the structure of copper and obsidian supply networks and outline their diachronic developments in Oman (ca. 2500 BCE – 1800 CE) and Ethiopia (ca. 800 BCE – 825 CE), (2) to undertake cross-cultural comparison of networks, (3) to explore the validity of employing a social network approach as an alternative to traditional Neoclassical and substantivist theories of economic interaction, and (4) to create preliminary exploratory geological resource maps of copper in Oman and obsidian in Ethiopia. In this chapter, I will briefly summarize findings related to each of these tasks.

Where the investigation of network structure is concerned, research findings are presented according to the following parameters: centralization, diachronic patterns in network stability, spatio-relational correlations, and diachronic patterns in the use of specific obsidian groups and of different smelting technologies.

Centralization in the Omani Networks – A centralized network concentrates power in one or a small number of nodes that wield outsized influence on the rest of the network. By contrast, a decentralized network dissipates power among all nodes of the network, preventing any one node from consolidating power.

In this dissertation, network analysis is used to determine powerful actors on the basis of advantageous network positions they occupy in relation to other actors. Network position and overall centralization is revealed through four centrality measures: degree centrality (Freeman approach), beta-centrality (Bonacich's "Power"), betweenness centrality (Freeman approach),

flow betweenness centrality, and closeness. Each measure exposes different nuances of network structure and different aspects of node centrality, as these result from contrasting assumptions about mechanisms of flow (Borgatti 2005).

The application of centrality measures to the Bronze Age network in Oman reveals a relatively decentralized network (25%), in terms of degree centrality, characterized by little variation in rank or power of individual nodes. This degree centralization measure is largely matched by the flow betweenness centralization index (28.58%) suggesting that few power brokers existed within the network. Where Freeman's betweenness is concerned, a centralization measure of 32%, matches previous measures, indicating however that there are a significant number of nodes that lie on the shortest paths between dyads, which afford more opportunities to mediate interactions between pairs of nodes and control the flow of information. Finally, this network's closeness centrality of 41% reveals a number of social actors in positions of high geodesic closeness. In such situations, power can derive from the fact that the closest nodes are likelier to obtain information or objects sooner than other nodes. When compared to the networks that develop in later periods, it is revealed that the Bronze Age network is characterized by the most intermediaries and by the highest closeness centralization out of the three networks.

The same centrality measures were used to analyze the Iron Age network. This period's network is characterized by the lowest degree centralization index out of the three Omani networks. Indeed, the Iron Age network appears to be 26% less centralized according to degree than the Bronze Age network and is further characterized by the lowest group betweenness and closeness centralization. These results solidify the interpretation of a relatively decentralized structure to the copper supply network.

While it may be tempting to suggest that a pattern towards decentralization is being observed diachronically, such a proposal must be made cautiously because of limitations in sample size and the high incidence of multi-period sites in both networks, but particularly in the Bronze Age network. It warrants mentioning, however, that if such a pattern is validated through future research, it would be depicting an economic trend that was at odds with the socio-political trend towards increased complexity.

The Islamic period network is the largest and most centralized of the three networks, being 51.6% more centralized than the Iron Age network. Like the Iron Age network that preceded it, the Islamic period network was characterized by low betweenness centrality; unlike the previous period's network, however, the Islamic period network is characterized by higher closeness centralization measures. In other words, despite the fact that the network has nodes in positions of high closeness that are poised to take a minimum number of steps when interacting with other social actors, these well positioned nodes do not take advantage of their positions to mediate interactions between dyads. It follows, therefore, that the flow of smelting technologies is not being controlled.

The network approach also provides independent evaluation for accepted archaeological narratives relating to copper production. The cultural context of the Bronze Age network is characterized by low levels of exploitation and by a relatively small amount of estimated copper production (2,000 – 4,000 tons) (Hauptmann 1985). Reconciling between traditional archaeological narratives of Bronze Age production, on the one hand, and network analysis findings, on the other hand¸ has proven difficult because the small sample size of the Bronze Age network warrants caution. Network data do, however, nuance current understandings regarding Bronze Age production. Using the overall low centralization indices as indicators of power within

the network reveals a decentralized system of production. This finding can tentatively be used to argue against the notion of elite control over production. Once could, thereby, suggest that if Sumer had an impact on the early development of large-scale copper production in the Southeast Arabia, that influence did not amount to direct control nor did it engender local structures of control.

Similarly, the pattern observed in the Iron Age network can be used to both nuance and support current archaeological narratives. Network data support the notion of a resurgence in production. Counter traditional archaeological narratives, however, network data do not provide evidence of an increase in economic complexity to parallel the purported increase in socio-political complexity that has been theorized for this period. This is because the Iron Age network is the least centralized of the three networks under investigation.

The largest and most centralized copper supply network is associated with the Islamic period. Network evidence upholds archaeological narratives related to the Islamic period, with the increase in scale of production being matched by an increase in the complexity of the economic system. However, despite being 51.6% more centralized than the Iron Age network, the Islamic period network is nonetheless characterized by an overall decentralized diffusion of power.

Diachronic Level of Stability – Understanding power centralization can provide a proxy for investigating social tensions within a network, which in turn can be indicative of network stability. The abovementioned measures provide a tiered node order that is characterized by remarkable continuity between the Iron Age and the Islamic periods. For instance, the Islamic period network contains a single site in top tier position, Aqir al-Shamoos; this site was one of three Iron Age sites to occupy that network's top tier. Similarly, 36% of second tier Islamic period nodes overlap with 87% of second tier Iron Age nodes, with some overlap existing between third tier sites in both networks as well.

This pattern suggests remarkable continuity both at the level of the network and in terms of node positions. This level of stability is certainly thought-provoking, considering the cyclicity of copper production itself and future research will aim to understand the phenomena that generated this pattern.

Spatio-relational correlation – During the Bronze Age, the patterns revealed by the centrality measures correlate with spatial patterns as well. The two best connected sites of the Bronze Age cluster spatially in the southern stretches of the greater survey area; similar spatial clustering is observed for the two second tier sites located in the central region of the larger survey area; additionally, the site with the lowest degree centrality clusters together with the site that intermediates its connection with the rest of the network. While intriguing, Bronze Age patterns must be interpreted with caution because of small sample size.

Similar spatio-relational clustering is also observed for the Iron Age period. This period is characterized by the presence of three cluster zones and two isolated nodes: Hayy Ukur, a remote settlement in the al-Hajar mountains, and Hala, a site whose surrounding area has not been adequately surveyed and, as such, may in fact not be an isolate. Each cluster has been revealed to contain at least one first tier node, at least one second tier node, and various different arrangements of third, fourth, and fifth tier nodes. The existence of what appear to be small spatial sub-groups, characterized by some degree of local power differentiation is a pattern that warrants more research.

The Islamic period landscape of production is characterized by a great deal of continuity with the Iron Age copper production landscape, with the same three clusters of sites being revealed in Wadi Jizzi, in the middle of the larger ArWHO survey area, and in its southern reaches. Unlike the previous period, however, the composition of these clusters is slightly different. Within each

cluster, a pattern similar to the one observed for the Iron Age network emerges in terms of the centrality scores of constituent nodes. Because there is only one first tier node, each Islamic period cluster is revealed to contain at least one second tier node, and at least on third tier node.

Diachronic patterns in the use of smelting technologies – Where the diachronic diffusion of slag technologies is concerned, the Bronze Age network is defined by shared smelting technologies resulting in the production of slag groups 2, 3.1, and 3.2. The same three smelting technologies are proxied by Iron Age slag assemblages. The Islamic period observes continuity in smelting traditions that produce slag groups 2, 3.1, and 3.2. and witnesses the introduction of slag group 1. Evidence of this smelting tradition has, so far, only been discovered at two isolated, spatially distinct nodes (Arja and Hayy al-Nahza). The pattern that emerges also demonstrates continuity in large-scale smelting practices across the millennia, with some evidence of small-scale, localized innovation occurring in the Islamic period alone.

Centralization in the Ethiopian Networks – The application of centrality measures to the Pre-Aksumite and Aksumite networks in Ethiopia reveals an interesting pattern. Overall, network centralization indices across all six sub-periods reveal low levels of centralization with some fluctuations between periods. Centralization increases slightly (by 3.48%) between the Pre-Aksumite and Proto Aksumite networks only to decrease again (by 10.59%) between the Proto Aksumite and the Early Aksumite networks. Additionally, in terms of flow betweenness, the Early Aksumite period sees a 31.6% decrease from the previous period's network.

The largest increase in centralization is seen between the Early Aksumite and Classic Aksumite periods. With a degree centralization of 18.61%, the Classic Aksumite period is 34.47% more centralized than the Early Aksumite period and 228.25% more centralized in terms of flow betweenness centralization (3.63%).

The most centralized network develops during the Middle Aksumite period (21.36%), seeing a 14.78% increase in degree centralization from the previous period and a 29.34% increase in flow betweenness.

Finally, the Late Aksumite network witnesses the largest decrease in overall centralization with a 10.81% decrease in degree centralization (19.05%) and a 61.54% decrease in flow betweenness centrality (1.8%).

Accepted archaeological narratives about the development of lithic production in northern Tigray are evaluated according to network patterns to reveal interesting similarities. Attempts to differentiate between Pre- and Proto-Aksumite lithic assemblages have proven difficult, as this socio-political shift does not appear to have been accompanied by marked changes in material culture or by broader economic changes. In this respect, these network analyses are currently unable to shed light on potential differences between periods as both are characterized by relatively decentralized networks.

A similar situation is observed between Early and Classic Aksumite lithic assemblages, which cannot be differentiated on the basis of lithics alone. Evidence revealed through analysis of the Classic Aksumite network, on the other hand, indicates marked differences from the previous period's network, with the Classic Aksumite network being characterized by a significant increase in centralization (34.47%). This pattern validates the archaeological narrative according to which the Classic Aksumite period witnessed increased specialization in lithic production and an increase in small specialized workshops (L. Phillipson 2009b).

The professionalization of lithic manufacturing is theorized to have reached its peak during the Middle Aksumite period and to have continued into the Late Aksumite period. Lithic production

during these periods has been discovered at a number of specialized sites, each focused on producing one increasingly standardized tool type. Once again, this archaeological pattern appears to be independently supported by the network results, with the Middle Aksumite network being characterized by the highest centralization index (21%) and the Late Aksumite network by the second highest centralization index (19%).

Diachronic patterns in network stability – Overall, only top tier nodes appear to maintain their position through time. Indeed, there is complete overlap in terms of top tier nodes between the Pre-Aksumite and the Early Aksumite periods and 66% overlap between Classic and Middle Aksumite networks. Beta Samati and Sefra Aboun are consistently the most central sites of the network, with the former occupying top tier position throughout the time span under investigation and the latter maintaining top tier position from the Pre-Aksumite to the Middle Aksumite, when the site was abandoned. The find spot of Mai Eungug is the only node to recur in second tier position (Proto-Aksumite – Classic Aksumite). Where third tier nodes are concerned, there is 100% overlap between the Proto- and Early Aksumite periods and no discernible patterns between other periods.

With the exception of a recurring set of first tier nodes, the Ethiopian networks are characterized by more variability in terms of the network position of nodes through time. This pattern presents interesting interpretive possibilities that will be addressed through future research.

Spatio-relational correlations – In Ethiopia, relational clusters do not appear to overlap with spatial clusters. The two top tier nodes, Beta Samati and Sefra Aboun, are located in separate quadrants of the research area, with the former being located in the northwest and the latter in the southeast. Enda Cha'atat surfaces as a top tier in the Classic Aksumite network and is located approximately 1.5 km northeast of Beta Samati.

Second tier sites are also spatially dispersed. A tendency towards clustering around first tier nodes is, however, observed. A pattern beginning in the Early Aksumite period around Sefra Aboun intensifies during the Classic Aksumite period when Tseratsur, Mai Eungug, and Da'ero Arat all cluster around the site.

This southeast group persists into the Middle Aksumite period. However, during this period, sites that cluster around Sefra Aboun occupy third tier positions. Indeed, the second tier of the Middle Aksumite network is occupied by a single site, Adi Abisalem, located approximately 4 km west of Beta Samati.

By the Late Aksumite period, the southeast quadrant of the research area becomes almost entirely devoid of obsidian production sites, with the multi-period settlement of Tseratsur, which occupies a tertiary position in the Late Aksumite network, being the only remaining site in the region. Activities relating to obsidian production appear to move into the northwest quadrant, clustering around the first tier node of Beta Samati. In addition to this first tier node, the northwestern group contains all second and fourth tier nodes.

Diachronic patterns in the use of obsidian groups – Where the diachronic diffusion of obsidian groups is concerned, obsidian from groups C, E, F, and G is used for lithic production from the Pre-Aksumite to the Middle Aksumite periods. During the Late Aksumite network, only the site of Beta Samati appears to have access to obsidian from group F. With the exception of a few samples recorded in systematic survey transects (but not associated with any sites), obsidian from group H is only found at Beta Samati throughout the entire period under review. In addition to being a top tier node, it would appear that Beta Samati also shows evidence of resource centralization. Whether there is a correlation between the resource diversification that

characterizes the site and its endurance following the abandonment of Sefra Aboun remains the subject of future research.

Cross-cultural comparison – Supply networks developing in both regions are remarkably decentralized. Emerging patterns suggest that productive resources were diffuse and that economic interactions associated with the exploitation and production of raw materials did not engender many occasions for social actors to amass power and influence. Indeed, while certain nodes were revealed to have been slightly better positioned than other nodes, differences in centrality were minimal and overall network centralization indices remained low.

This pattern is particularly intriguing considering the fact that socio-political centralization is evident in Ethiopia throughout the entire period under investigation and in Oman begins to be observed at the end of the second millennium BCE. Could this sector of the economy have been outside of the bounds of elite control and, if so, are these industries representative of the economic systems overall or are there circumstances specific to production in these types of contexts that would have engendered this pattern? Such questions remain the subject of future research.

Evidence of complexity is often sought after and amplified through archaeological research, yet on a regional scale, economic processes likely developed incrementally, being influenced by local practices (Dumitru and Harrower 2018b, Kristiansen 2010).

Social networks as models for explaining economic interaction – In the absence of evidence of elite control of this economic sector, what mechanisms were in place to engender the trust necessary for economic interaction to be undertaken and to ensure the maintenance of social order and the reproduction of the system? Notwithstanding phase-related fluctuations in the network positions of lower nodes (particularly in Ethiopia), the networks that developed from period to

period showed remarkable stability. This is particularly unexpected in Oman, where the history of copper exploitation is defined by notable cyclicity, with periods of fluorescence, followed by periods of almost complete collapse. Yet despite this broad pattern, there is significant overlap between periods in terms of which nodes occupied which positions.

This dissertation turns to social networks and social relationships, themselves, as the mechanisms that integrated economic interactions bringing about social order and maintaining stability. Social networks have lately been proposed as an alternative to theories of market exchange (Collins 1988, Bandyopadhyay et al. 2011). This development follows from the publications of new economic sociologist Mark Granovetter (1985). Granovetter argues against both under-socialized models of the economy (e.g. theories of market exchange) and over-socialized models (e.g. Polanyi's substantivism). Counter to the substantivists, he suggests that the degree to which economic activities were embedded in non-market societies is lower than currently theorized. Similarly, he places himself in opposition to formalist and Neoclassical economists by suggesting that embeddedness plays a more substantial role in contemporary economies than has been previously theorized. Granovetter points out that both over- and under-socialized conceptions of economic behavior understand social actors to be making decisions in a so-called "atomized" manner (Granovetter 1985: 485), with the former tapping into internalized patterns of behavior (for which change as a result of social interactions is not taken into consideration) and the latter being driven by an egocentric pursuit for utility maximization.

In recent years, however, more attention has been paid by economists to "imperfectly competitive markets" (Granovetter 1985: 488), defined as relatively small groups of economic partners. In such contexts, the notion of competition as the mechanism that explains how

malfeasance is avoided and social order maintained cannot be applied (because there is a limit to the number of competitors one can turn to).

Such an example has been an intuition-pump for economists attempting to understand economic behavior in such systems. New institutional economists adopt a Neoclassical perspective and suggest, in a manner reminiscent of structural-functionalism, that institutions develop as a response to particular problems within the economy (Alchian and Demsetz 1973; Lazear 1979; Rosen 1982; Williamson 1975, 1979, 1981; Williamson and Ouchi 1981). Thus, instances of repeated social disorder will engender an institutional solution that will operate in lieu of the existence of trust. Opponents of this notion, however, point out that in the total absence of trust, individuals would discover ways to deceive these institutions, thereby leading to social instability. Therefore, some level of trust must exist in order for economic systems to perpetuate themselves (Arrow 1974).

The question then becomes identifying the origins of the trust. Granovetter and other sociologists and new economic sociologists (Collins 1988, Bandyopadhyay et al. 2011) suggest that trust derives from being embedded in networks of relationships, where a predilection towards engaging in economic interaction with social actors of known reputation is actualized. This theory of embeddedness represents a departure from theories that focus solely on strict economic gains, arguing instead that economic partners are likewise desirous to accrue social gains (e.g. a good reputation). These social gains are described as deterrents against malfeasance.

Such a model certainly applies to economic systems in the past and, in particular, to the decentralized, seemingly stable and necessarily imperfectly competitive economic networks that developed in Oman and Ethiopia. Indeed, echoes of this economic theory of embeddedness predate its contemporary formulation by approximately 600 years and can be found in the work of Arab

historian Ibn Khaldun, who proposed the theory of '*aṣabîyah* (or 'group feeling') as an explanation of cooperation and solidarity. This notion has already been applied to interpret social developments in the ancient Near East in general and in Oman in particular (Cleuziou and Tosi 2007, Magee 2014, McCorriston 2011).

Create a preliminary exploratory geological resource map of copper in Oman and obsidian in Ethiopia – A final goal that this dissertation set out to accomplish was to gain an understanding of the spatial distribution of raw materials to understand the origin point in the respective supply chains of copper exploitation in Oman and obsidian exploitation in Ethiopia. Acquiring a high-resolution appreciation of the distribution of these resources was unattainable using traditional maps alone. As such, spectral mapping through Hyperion hyperspectral satellite imagery was employed in the creation of resource maps, whose validity was tested through ground-truthing in Oman. The maps produced through this method will prove useful for identifying prospective locations for future sourcing projects.

Appendix I: Copper Supply Network Dataset

Table AI.1a: Chemical Composition ArWHO Survey Area Slag.

Sample	Slag Group	Period	SiO_2	Al_2O_3	P_2O_5	K_2O	FeO	TiO_2	Cr_2O_3	MnO
C78_004	3.2	IA & Isl.	11.04		0.13	3.50	76.25	0.11	0.08	0.04
C78_003	3.2	IA & Isl.	11.36		0.09	3.92	75.86	0.10	0.07	0.04
C78_002	3.2	IA & Isl.	17.95		0.14	5.83	71.24	0.11	0.08	0.06
C76_003	3.2	IA & Isl.	12.17		0.18	3.70	76.19	0.12	0.09	0.04
C76_002	3.2	IA & Isl.	12.60	0.85		3.44	74.61	0.10	0.08	0.03
C76_001	3.2	IA & Isl.	13.14	1.99		3.76	59.87	0.18	0.06	0.06
C75_003	3.2	IA & Isl.	11.85		0.09	3.86	77.21	0.10	0.07	0.04
C75_002	3.2	IA & Isl.	9.54			2.67	78.99	0.14	0.08	
C75_001	3.2	IA & Isl.	12.69	1.18	0.16	3.01	74.11	0.11	0.07	0.04
C72_004	3.2	Isl.	5.82			26.51	62.52	0.05	0.05	0.18
C72_003	3.2	Isl.	10.92		0.13	3.30	73.50	0.08	0.07	0.06
C72_002	3.2	Isl.	14.40			3.61	75.64	0.10	0.08	0.05
C72_001	3.2	Isl.	7.92			11.95	75.45	0.07	0.07	0.07
C71_005	3.2	IA & Isl.	12.95			2.89	75.43	0.13	0.07	0.04
C71_004	3.2	IA & Isl.	14.88			2.97	74.09	0.12	0.06	0.06
C71_003	3.2	IA & Isl.	11.32			11.82	71.28	0.53	0.09	0.06
C71_002	3.2	IA & Isl.	15.16	2.39	0.14	5.28	72.07	0.12	0.07	0.09
C71_001	3.2	IA & Isl.	12.32	0.80		3.32	77.64	0.17	0.07	0.07
C61_002	3.2	IA & Isl.	16.36	1.17	0.29	6.85	71.41	0.19	0.33	0.06
C53_006	3.2	Isl.	12.41		0.18	5.32	73.89	0.11	0.10	0.10
C53_005	3.2	Isl.	10.95		0.14	6.30	68.26	0.14	0.09	0.07
C53_004	3.2	Isl.	9.94		0.14	5.21	78.53	0.09	0.08	0.07
C53_003	3.2	Isl.	12.21			5.36	73.48	0.14	0.10	0.10
C53_002	3.2	Isl.	10.47	0.87		3.81	62.63	0.10	0.16	0.06
C53_001	3.2	Isl.	5.73			8.20	70.53	0.10	0.10	0.08
C51_003	3.2	N/A	12.35		0.14	5.22	76.35	0.14	0.09	0.07
C51_002	3.2	N/A	11.53		0.11	5.82	75.70	0.16	0.08	0.06
C51_001	3.2	N/A	13.68	0.44	0.07	7.06	73.01	0.18	0.10	0.07
C47_001	3.2	IA	13.37			4.15	75.64	0.25	0.13	0.09
C17_002	3.2	BA, IA, Isl.	8.69		0.14	27.47	52.59	0.17	0.46	0.10
C17_001	3.2	BA, IA, Isl.	12.35		0.25	24.01	53.12	0.16	0.64	0.29
C163_001	3.2	Isl.	16.03	2.18		3.87	70.73	0.19	0.13	0.19
C150_009	3.2	IA & Isl.	16.00		0.22	8.72	68.31	0.06	0.61	0.25
C149_002	3.2	N/A	9.43			2.71	38.22	0.07	0.11	

C148_005	3.2	IA	7.67		0.14	0.66	75.02	0.07	0.06	0.04
C148_004	3.2	IA	15.81	0.98	0.18	5.59	71.20	0.15	0.08	0.09
C148_003	3.2	IA	8.50			4.46	68.09	0.11	0.07	0.03
C148_002	3.2	IA	11.01		0.14	1.34	78.27	0.12	0.08	0.03
C148_001	3.2	IA	14.26		0.14	2.90	77.30	0.11	0.07	0.04
C145_002	3.2	BA, IA, Isl.	10.23		0.18	8.33	42.45	0.15	0.11	0.14
C143_003	3.2	IA & Isl.	9.97		0.22	5.39	66.17	0.13	0.86	
C142_007	3.2	Isl.	13.15		0.17	7.51	73.50	0.14	0.26	0.04
C133_004	3.2	IA	12.47			2.75	76.09	0.19	0.16	0.05
C133_002	3.2	IA	10.63	1.06		2.16	81.99	0.30	0.15	0.06
C133_001	3.2	IA	14.93	1.57	0.10	0.96	78.30	0.16	0.11	0.03
C118_003	3.2	IA	16.06			6.08	72.20	0.28	0.10	0.06
C115_012	3.2	Isl.	12.91		0.19	3.59	67.07	0.32	0.07	0.04
C115_011	3.2	Isl.	7.94			2.15	72.75	0.17	0.07	0.04
C115_006	3.2	Isl.	9.60			10.60	17.25	0.36	0.08	39.84
C115_004	3.2	Isl.	15.49	1.01	0.15	7.05	69.88	0.39	0.10	0.09
C115_003	3.2	Isl.	14.98	0.87	0.15	6.89	70.64	0.36	0.13	0.09
C115_002	3.2	Isl.	15.00	0.54	0.10	7.05	70.80	0.38	0.11	0.09
C113_005	3.2	IA & Isl.	13.36		0.22	3.41	65.85	0.11	0.06	0.05
C113_004	3.2	IA & Isl.	10.07	1.76	0.13	17.19	44.82	0.16	0.04	1.72
C113_003	3.2	IA & Isl.	15.71		0.22	4.42	73.05	0.15	0.08	0.04
C113_002	3.2	IA & Isl.	16.18	1.07	0.24	6.71	69.41	0.14	0.08	0.06
C113_001	3.2	IA & Isl.	16.38	2.30	0.16	5.08	66.50	0.12	0.08	0.07
C112_009	3.2	IA & Isl.	10.44	2.68	0.21	12.67	59.03	0.10	0.06	0.10
C112_008	3.2	IA & Isl.	15.61		0.28	4.02	74.17	0.09	0.06	0.05
C112_007	3.2	IA & Isl.	9.33		0.23	14.41	71.26	0.09	0.07	0.03
C112_006	3.2	IA & Isl.	15.10		0.29	4.58	73.85	0.11	0.07	
C112_005	3.2	IA & Isl.	15.41		0.24	5.45	71.65	0.08	0.07	0.08
C112_004	3.2	IA & Isl.	14.96		0.28	4.91	73.34	0.09	0.07	0.08
C112_001	3.2	IA & Isl.	17.75	0.75	0.23	3.86	70.92	0.11	0.07	0.06
C111_004	3.2	N/A	11.05		0.15	2.26	55.75	0.05	0.05	0.04
C111_003	3.2	N/A	16.62		0.19	4.10	72.65	0.09	0.07	0.04
C110_008	3.2	IA. & Isl.	14.95		0.44	6.04	73.43	0.11	0.08	0.07
C110_006	3.2	IA. & Isl.	15.11		0.44	16.42	64.44	0.16	0.08	0.13
C110_003	3.2	IA. & Isl.	14.68		0.41	8.40	70.10	0.22	0.09	0.44
C110_002	3.2	IA. & Isl.	16.49		0.30	7.87	67.89	0.24	0.07	0.20
C71_009	3.1	IA. & Isl.	19.73		0.21	2.94	70.54	0.30	0.06	

C65_008	3.1	N/A	21.25	1.24	0.28	20.40	51.09	0.31	0.49	0.15
C65_007	3.1	N/A	21.45	2.19	0.15	17.59	52.75	0.31	0.44	0.14
C65_006	3.1	N/A	17.41			20.80	53.04	0.31	0.30	0.15
C65_005	3.1	N/A	26.82	1.13	0.23	17.68	49.49	0.28	0.31	0.16
C65_004	3.1	N/A	23.57	1.95	0.42	17.77	52.45	0.43	0.31	0.39
C65_003	3.1	N/A	24.09	1.77		18.85	50.61	0.41	0.39	0.18
C65_002	3.1	N/A	21.86	1.12		18.75	52.30	0.29	0.40	0.17
C65_001	3.1	N/A	21.65	2.01	0.20	18.33	52.15	0.29	0.30	0.14
C61_003	3.1	IA & Isl.	18.08	1.57	0.25	7.47	67.02	0.25	0.59	0.08
C61_001	3.1	IA & Isl.	18.69	1.35	0.22	6.36	67.68	0.16	0.33	0.06
C52_001	3.1	N/A	26.74	3.30	0.22	15.73	4.90	0.75	0.04	43.43
C47_003	3.1	IA	19.26	2.27	0.14	6.66	66.56	0.24	0.13	0.09
C17_003	3.1	BA, IA, Isl.	20.60		0.30	8.69	62.31	0.22	1.04	0.32
C160_001	3.1	BA, IA, Isl.	21.87	1.66		16.30	55.33	0.32	0.33	0.16
C157_001	3.1	Isl.	19.21			25.99	50.97	0.20	0.26	0.08
C154_004	3.1	BA, IA, Isl.	24.41	2.32	0.20	18.53	50.24	0.31	0.41	0.14
C154_003	3.1	BA, IA, Isl.	24.10	2.13	0.27	17.91	51.66	0.31	0.33	0.15
C154_002	3.1	BA, IA, Isl.	22.50	1.42	0.25	17.13	53.54	0.34	0.53	0.15
C150_011	3.1	IA & Isl.	20.10		0.25	5.79	66.33	0.07	0.19	0.33
C150_010	3.1	IA & Isl.	24.85		0.32	6.49	63.44	0.09	0.22	0.25
C147_002	3.1	N/A	18.35	2.17	0.16	9.58	64.21	0.33	0.15	0.10
C147_001	3.1	N/A	22.09	1.69	0.28	10.51	60.86	0.42	0.17	0.09
C145_001	3.1	BA, IA, Isl.	21.21	0.98		12.41	59.76	0.29	0.33	0.13
C143_005	3.1	IA & Isl.	23.65	3.13	0.12	4.33	61.92	0.23	0.14	0.19
C143_001	3.1	IA & Isl.	25.00	2.56	0.37	9.50	54.56	0.33	0.15	0.23
C142_006	3.1	Isl.	20.08	0.72	0.26	11.10	63.19	0.16	0.70	0.05
C133_003	3.1	IA	18.91	2.27	0.15	4.16	67.03	0.34	0.14	0.16
C120_002	3.1	IA	22.53	0.97	0.22	9.48	54.32	0.14	0.17	0.30
C118_004	3.1	IA	26.66	1.63		12.96	50.33	0.54	0.11	0.39
C118_001	3.1	IA	23.58	1.79		22.45	47.50	0.40	0.13	0.41
C115_010	3.1	Isl.	21.32	2.31	0.38	11.94	4.98	0.38	0.10	53.75
C115_009	3.1	Isl.	24.23	1.74	0.35	14.54	8.89	0.57	0.09	39.67
C115_008	3.1	Isl.	26.27	1.28	0.33	17.53	4.74	0.53	0.11	44.51
C115_007	3.1	Isl.	21.87	2.35	0.18	12.32	4.66	0.53	0.08	51.21
C115_005	3.1	Isl.	20.16	1.37	0.24	12.10	8.04	0.45	0.06	52.13
C115_001	3.1	Isl.	21.59	2.10	0.24	12.60	4.57	0.54	0.09	51.01

C114_002	3.1	Isl.	20.21	2.10		16.02	4.17	1.52	0.06	45.90
C114_001	3.1	Isl.	16.62	1.53	0.15	16.48	11.21	1.43	0.06	42.48
C112_003	3.1	IA & Isl.	19.53		0.37	4.48	67.74	0.08	0.08	0.09
C112_002	3.1	IA & Isl.	19.81		0.32	3.84	70.52	0.11	0.08	0.05
C111_002	3.1	N/A	18.72	1.26	0.40	5.94	67.89	0.19	0.09	0.15
C111_001	3.1	N/A	18.90		0.33	5.64	69.62	0.14	0.07	0.06
C110_007	3.1	IA & Isl.	21.18		0.43	5.77	67.91	0.18	0.08	0.12
C110_005	3.1	IA & Isl.	24.15		0.48	6.79	64.04	0.22	0.09	0.12
C110_004	3.1	IA & Isl.	20.44	0.89	0.41	5.85	67.58	0.19	0.07	0.10
C110_001	3.1	IA & Isl.	18.97	1.26	0.25	5.79	67.45	0.21	0.09	0.10
C105_002	3.1	IA & Isl.	23.64	3.52	0.21	4.50	62.49	0.34	0.17	0.24
C47_002	2	IA	36.14	2.66	0.24	12.15	41.36	0.81	0.19	0.70
C4_001	2	BA & Isl.	43.33	2.74	0.40	14.16	31.67	0.55	0.28	0.40
C149_001	2	N/A	16.83			30.76	23.85	0.12	0.55	0.32
C143_004	2	IA & Isl.	31.46	4.93		11.37	43.83	0.24	0.37	0.25
C143_002	2	IA & Isl.	32.13	6.51	0.30	15.03	40.23	0.25	0.27	0.19
C120_007	2	IA	38.45	5.69		23.84	25.17	0.23	0.32	0.41
C120_006	2	IA	31.66	0.96		19.69	39.57	0.14	0.35	0.29
C120_005	2	IA	40.32	5.10		16.59	32.58	0.23	0.41	0.47
C120_004	2	IA	27.72			17.39	35.34	0.12	0.36	0.23
C120_003	2	IA	36.09	2.59		23.85	28.58	0.22	0.41	0.40
C120_001	2	IA	32.41	4.95		22.13	32.77	0.32	0.28	0.32
C118_006	2	IA	27.90	1.05	0.21	19.90	32.04	0.60	0.09	0.51
C118_005	2	IA	36.33	2.41		17.82	34.15	0.67	0.11	0.58
C118_002	2	IA	27.67	1.24		28.68	37.36	0.45	0.14	0.36
C105_001	2	IA & Isl.	30.72	6.09		24.76	31.02	0.19	0.30	0.23
C78_001	3.2	IA & Isl.	18.10		0.15	6.01	68.81	0.12	0.08	0.05
C146_001	1	Isl.	54.89	4.79	0.48	12.69	21.03	3.08	0.06	0.31
C119_004	1	Isl.	44.42	3.27		32.23	13.58	0.94	0.14	0.36
C119_003	1	Isl.	27.51			57.11	9.94	0.59	0.12	0.23
C119_002	1	Isl.	67.21	2.04	0.36	10.12	15.01	1.12	0.04	0.21
C119_001	1	Isl.	47.24	1.11		24.21	18.79	1.05	0.08	0.33

Table AI.1b Chemical Composition ArWHO Survey Area Slag.

Sample	CaO	SO_3	CuO	NiO (ppm)	CoO (ppm)	Cl (ppm)	V_2O_5 (ppm)	ZnO (ppm)	SeO_2 (ppm)	Rb_2O (ppm)	SrO (ppm)
C78_004	1.07	6.09	1.40	259.84		2186.09	445.20	285.99	40.26	4.96	418.69
C78_003	1.17	3.03	3.79	203.01		4177.67	421.29	378.69			441.81
C78_002	1.21	1.73	1.16	292.44		2998.77	489.82	485.58			803.52
C76_003	1.10	4.78	1.25	342.95		2187.46	505.90	460.67	38.02		445.81
C76_002	1.76	5.24	1.40	247.51		2509.55	557.24	557.83	57.59	4.84	462.52
C76_001	1.30	6.02	14.49	286.03		3037.97	463.80	381.97	344.28	8.94	377.32
C75_003	1.03	3.73	1.54	291.61		2953.95	510.87	602.17	29.81		509.06
C75_002	0.66	4.63	2.78	295.92		3269.50	472.09	445.09	32.53	4.75	377.49
C75_001	0.57	3.01	4.58	280.45		2469.18	547.76	509.72	37.65		470.97
C72_004	0.32	1.26	2.50		3154.05	2043.15	329.09	1111.90		3.09	552.59
C72_003	1.60	6.24	3.67	190.42		3198.82	431.31	571.06	36.17		362.23
C72_002	1.02	3.56	1.09	207.58		2416.75	489.65	503.40		3.14	569.50
C72_001	0.62	1.72	1.45		1405.35	2986.98	455.12	846.35			549.45
C71_005	0.91	5.08	1.95	371.16		2768.60	519.02	566.00		3.70	425.99
C71_004	0.72	3.28	3.36	311.20		2380.47	452.10	622.24		4.03	491.18
C71_003	1.15	2.77	0.92	213.65		2514.77	553.23	642.97		4.40	443.22
C71_002	1.10	1.47	1.77	220.57		2692.23	433.78	437.14	35.64	4.08	403.94
C71_001	0.54	2.80	2.29	258.26		3126.11	496.66	322.31	35.09	3.33	281.67
C61_002	0.92	1.01	1.54	615.75		3744.79	652.19	817.70			352.62
C53_006	0.94	5.13	1.40	450.19		2615.04	687.56	700.21		3.15	544.20
C53_005	0.54	4.75	8.33	551.87		2932.57	514.91	249.16	40.40	3.43	518.74
C53_004	0.84	2.93	1.67	284.09		3779.30	458.48	614.38			515.22
C53_003	1.00	4.54	2.62	251.83		2277.01	621.81	413.29			514.80
C53_002	0.69	8.41	12.73	217.74		2032.87	428.98	336.04	80.87		305.86
C53_001	0.75	2.94	10.13	399.52	5065.09	6519.17	487.95	996.60		4.01	397.26
C51_003	0.96	3.19	1.10	264.24		2089.98	703.95	285.53	59.80	3.73	505.81
C51_002	1.10	3.74	1.29	271.66		2144.60	752.21	334.44	97.25	5.22	650.55
C51_001	1.23	3.08	0.93	225.53		2449.35	722.44	295.94	38.11	4.14	688.54
C47_001	0.63	3.40	1.66	258.41		3027.87	604.72	2327.05		5.80	308.99
C17_002	0.39	0.61	7.18	843.55	1780.25	17194.74	570.43	753.67		9.12	841.38
C17_001	0.33	1.54	6.35	726.65	2799.12	3294.92	588.70	252.72		7.07	1092.92
C163_001	0.52	0.19	5.47	461.83		2694.96	1067.15	233.18			219.41
C150_009	0.78	1.34	3.16	1459.17		2623.56	497.11	783.01			515.37
C149_002	0.22	2.63	43.31	489.38	1191.89	28136.90	339.74	285.91	307.08	4.61	675.78
C148_005	2.29	12.23	1.52	346.86		2129.18	431.95	388.98	34.34		373.42
C148_004				382.82		2664.20	545.42	415.10	30.75	3.97	425.71

	1.78	3.33	1.03								
C148_003	0.84	14.08	3.34	326.36		2753.34	418.76	319.24	55.93	5.35	501.68
C148_002	0.85	6.94	0.92	247.72		2337.63	543.44	317.91	39.19		242.89
C148_001	0.53	2.75	1.47	298.88		2698.88	454.82	556.59		4.95	325.71
C145_002	0.43	0.30	31.47	626.34	1936.23	57238.67	630.53	473.85		8.79	556.45
C143_003	0.59	1.13	14.36	1186.04		9057.62	655.77	173.01		3.98	395.74
C142_007	0.82	0.54	3.08	1103.68	2467.85	2400.43	500.29	609.30		7.32	552.60
C133_004	0.22	4.88	2.51	228.65		3531.57	698.09	1780.41	36.27	5.70	180.60
C133_002	0.30	2.00	1.13	251.96		3081.17	831.61	891.83		4.16	264.08
C133_001	0.61	0.22	2.57		1128.40	2283.52	690.44	1254.17	34.70	6.88	35.26
C118_003	0.86	2.62	0.88	313.62		2628.75	1683.34	457.09		3.22	600.66
C115_012	1.67	8.96	3.93	395.40		3632.54	1807.30	530.75			877.84
C115_011	1.15	7.10	7.06	531.64		8431.48	1142.14	393.65		4.56	578.43
C115_006	0.73	5.77	13.07	2360.89	2921.74	14500.25	1271.82	2001.76		7.90	835.77
C115_004	1.28	3.41	0.85	300.57		3512.02	1798.80	400.90			723.60
C115_003	1.21	3.15	0.89	286.26		2972.12	1724.84	396.96		4.09	693.31
C115_002	1.26	3.27	0.86	258.03		3036.36	1840.64	393.70		5.30	695.05
C113_005	0.73	6.79	9.01	267.85		3415.16	404.98		42.79		383.36
C113_004	0.63	4.90	18.42	469.49	3436.27	2364.68	348.12	548.81		4.93	617.16
C113_003	1.04	3.83	0.95	309.81		3023.28	585.04	168.75			501.96
C113_002	1.43	3.64	0.99	246.50		5079.72	493.08	199.44			1044.82
C113_001	0.86	3.29	4.78	282.31		2804.86	607.17	219.03			569.77
C112_009	0.60	4.70	9.81	354.87		3083.48	410.04	217.44			596.63
C112_008	1.01	3.05	1.10	358.83		3674.51	439.52	261.94		3.83	573.17
C112_007	0.91	1.72	1.65	227.79		2650.37	412.54	270.66			726.76
C112_006	1.01	3.42	1.06	326.90		2976.19	453.36	252.86			650.72
C112_005	0.98	4.04	1.40	315.09		3833.65	426.56	278.17			731.89
C112_004	1.01	3.35	1.26	406.50		4287.23	407.20	258.65			717.32
C112_001	0.85	3.35	1.92	297.68		4480.66	506.28	237.75			413.75
C111_004	0.35	10.35	19.45	277.88	1052.59	2745.58	333.64	204.18	42.80	3.97	299.54
C111_003	0.85	3.56	1.33	192.16		3376.40	482.42	273.35			539.25
C110_008	0.77	1.66	1.82	495.97		4166.33	468.58	296.54		4.41	502.05
C110_006	0.98	0.93	0.81	438.94		2793.87	456.41	94.90		5.26	699.20
C110_003	1.23	1.72	1.98	349.19		4573.54	674.09	124.49		5.85	1044.41
C110_002	1.35	3.22	1.60	232.41		5021.94	564.27	202.99			1163.67
C71_009	0.30	5.37	0.03	313.04		3060.50	1135.13				427.69
C65_008	0.71	0.77	2.52	775.46	1005.14	3338.11	917.36	746.28		6.59	692.12
C65_007	0.45	1.19	2.59	813.79		4809.23	842.49	787.16		4.75	590.20

C65_006	0.63	0.65	5.63	944.60	1541.51	5356.35	830.80	788.67		7.81	686.58
C65_005	0.70	0.26	2.18	1591.87		3957.78	846.66	684.76		7.51	622.02
C65_004	0.31	0.81	0.84	1053.63		3506.08	1087.27	664.05			509.25
C65_003	0.64	0.37	1.91	849.17		3955.16	956.58	724.19		7.40	741.35
C65_002	0.83	0.60	3.21	1219.18		3899.66	822.84	802.58		9.22	853.81
C65_001	0.55	1.40	2.26	852.88	904.21	4386.51	851.97	767.93		6.32	717.77
C61_003	0.81	2.14	1.19	520.76		2803.60	759.87	645.81			385.36
C61_001	1.17	1.70	1.72	657.94		2821.63	676.02	789.97	34.07		355.31
C52_001	1.12	2.69	0.34	225.62		2635.13	1152.98	371.35		12.21	1827.89
C47_003	1.12	1.87	1.10	254.10		3098.15	737.56	1513.31			511.70
C17_003	0.63	0.27	4.49	3165.92	1086.11	4137.43	725.94	501.51		6.20	650.26
C160_001	0.76	0.39	2.11	984.35	1101.91	3246.56	910.86	846.26		7.45	739.08
C157_001	0.81	0.23	1.32	562.47		4826.31	664.65	1239.27		9.09	1151.63
C154_004	0.80	0.38	1.52	829.00		4236.79	865.05	800.91		6.31	707.30
C154_003	0.88	0.50	1.14	735.56		3261.38	896.58	705.23		6.73	733.55
C154_002	0.85	0.57	2.10	785.54		3842.45	877.84	808.73		6.05	745.64
C150_011	0.95	0.85	4.43	1536.86		2803.20	464.19	1138.66		5.02	632.44
C150_010	1.24	0.88	1.69	783.33		2583.98	516.49	392.10		4.56	577.96
C147_002	1.63	1.92	0.79	223.51		2756.99	762.01	938.40		10.17	1085.87
C147_001	1.44	1.58	0.94	187.77		3229.33	793.69	1236.80		10.36	756.69
C145_001	0.84	0.30	3.48	698.84	2246.83	3329.69	911.06	712.78		6.80	681.35
C143_005	0.46	0.15	5.10	400.92	894.85	2425.99	913.64	430.06			220.66
C143_001	0.63	0.54	5.45	480.16		3762.62	1268.06	342.34		5.32	419.67
C142_006	0.96	0.72	1.27	467.58	3930.31	3533.59	605.59	428.20		4.52	606.04
C133_003	1.14	1.64	1.26	211.31		3199.72	863.92	24005.66		7.42	342.75
C120_002	0.39	0.30	10.85	744.41		5205.94	1413.04	115.71		5.79	194.06
C118_004	1.51	2.25	2.38	350.67		4055.26	1655.34	1843.57		8.28	762.67
C118_001	1.39	0.48	0.85	304.96	723.00	2911.01	1361.56	2205.89		6.43	969.56
C115_010	1.12	2.06	0.92	249.39		2360.93	783.84	514.38		3.93	2256.74
C115_009	1.14	0.45	6.54	781.49		10345.63	1386.22	744.86		9.32	1273.76
C115_008	1.55	2.34	0.35			3790.31	938.88	268.36		9.05	2379.22
C115_007	1.09	4.39	0.42	191.53		2612.41	1830.85	558.22		7.36	954.31
C115_005	0.87	0.96	2.31	518.78	1490.22	4544.69	1539.15	413.81		10.28	1006.18
C115_001	1.09	4.78	0.42	175.42		2372.86	1775.87	565.41		7.30	933.74
C114_002	1.18	4.25	0.79	402.35		3144.80	7759.76	189.20		6.72	1958.24
C114_001	1.10	2.84	1.82	558.45	930.07	4342.00	7404.54	367.02		7.97	2264.98

C112_003	1.04	2.51	3.43	424.93		4307.80	480.81	185.10		3.54	700.38
C112_002	0.81	2.86	1.07	335.09		3391.84	491.90	203.97		4.03	490.83
C111_002	1.51	2.06	1.03	407.26		5430.09	582.07	196.45			643.24
C111_001	0.91	2.94	0.79	451.90		3805.05	488.98	177.23		3.69	578.64
C110_007	1.19	1.19	1.40	457.00		3160.94	528.33	143.29		3.33	688.29
C110_005	1.44	1.43	0.71	420.26		3037.71	543.75	101.00		5.82	719.50
C110_004	1.52	1.05	1.36	432.50		3074.48	488.55	125.77		4.92	708.82
C110_001	1.19	2.16	1.95	289.35		3405.78	595.11	174.93			799.47
C105_002	0.35	0.15	3.85	456.86		2459.21	1414.82	345.02			221.87
C47_002	2.30	0.54	1.74	271.73		3506.38	1937.73	6077.34		19.49	744.13
C4_001	2.17	0.32	2.86	366.34		4335.26	1123.69	5120.04		21.83	1053.69
C149_001	0.15	3.91	18.30	3254.28	6087.49	35647.24	391.54	126.99		6.54	1909.55
C143_004	0.47	0.24	6.12	1041.08	898.18	2912.95	1172.18	777.02		5.75	362.60
C143_002	0.48	0.12	3.87	881.06		3029.94	1072.41	284.44		4.77	433.25
C120_007	0.62	0.23	4.19	501.99		5358.04	1242.98	148.16			550.15
C120_006	0.62		6.31	1390.95		3451.48	871.09	434.27		5.83	529.17
C120_005	0.79	0.21	2.73	377.46		2981.56	1410.63	132.08			331.37
C120_004	0.56	0.42	16.20	2696.76		11424.35	756.77	529.94		5.21	713.20
C120_003	0.90	0.20	5.89	585.21		5465.54	1403.14	131.36		6.16	439.12
C120_001	0.93	0.19	4.96	493.00		4322.80	1322.70	276.63		8.55	322.82
C118_006	1.51	1.44	13.73	708.69		3537.08	1259.80	2568.51		12.76	918.75
C118_005	1.63	0.54	4.64	597.31		3024.44	1388.51	3086.20		11.73	780.56
C118_002	1.56	0.65	0.81	318.22		2578.60	1301.97	1609.23		11.07	2081.98
C105_001	0.53	0.58	4.73	496.57		4071.32	870.41	1602.95		6.11	928.44
C78_001	1.48	3.70	0.95	283.02		2834.85	503.81	492.45			996.24
C146_001	0.81	1.05	0.03			3594.01	1991.57	282.60		6.38	890.78
C119_004	3.36	0.88	0.03	726.22		2980.40	1060.25	168.14		33.14	1928.84
C119_003	0.45	3.19	0.06	566.37		3848.48	951.33	326.87		5.65	862.90
C119_002	3.71	0.86	0.03			4595.46	1003.96	166.82		41.09	193.98
C119_001	2.46	3.81	0.08	317.22		5249.15	1331.79	212.13		29.98	733.96

Table AI.1c Chemical Composition ArWHO Survey Area Slag.

Sample	ZrO_2 (ppm)	Nb_2O_5 (ppm)	BaO (ppm)	PbO (ppm)	As_2O_3 (ppm)	Ag_2O (ppm)	MgO	Total w/o normalization	FeO+MnO	$CaO+Al_2O_3$
C78_004	17.78		318.09			20.70		78.55	76.28	1.07
C78_003	17.94	7.97	376.48		12.63	19.03		72.47	75.89	1.17

C78_002	14.98		323.21		11.11	17.12		69.51	71.30	1.21
C76_003	20.44		308.99			18.79		77.59	76.23	1.10
C76_002	13.56		273.38			22.04		75.30	74.64	2.62
C76_001	31.15		410.43		28.13	48.15		67.17	59.93	3.29
C75_003			387.34			22.93		71.97	77.25	1.03
C75_002	33.02		334.24			19.90		75.37	78.99	0.66
C75_001	16.87		308.44			16.37		74.06	74.15	1.75
C72_004		7.66	573.83		30.74			74.92	62.71	0.32
C72_003	19.05		308.38		30.11	19.91		78.50	73.56	1.60
C72_002	19.98		358.62		22.30			73.16	75.70	1.02
C72_001	16.46	6.51	400.06		18.43	13.26		73.88	75.52	0.62
C71_005	14.91		312.31		16.25	19.34		73.75	75.47	0.91
C71_004	15.43		342.17		14.47	19.54		67.77	74.15	0.72
C71_003	14.56		284.61					74.60	71.34	1.15
C71_002	20.75		318.87			17.00		80.00	72.15	3.49
C71_001	25.61		317.16					71.08	77.71	1.34
C61_002	13.38		375.30		24.34	26.55		59.43	71.46	2.09
C53_006			419.92		14.83	20.42		75.76	73.98	0.94
C53_005	26.17		363.75		244.95			71.80	68.33	0.54
C53_004	15.66		364.69		26.72	24.30		69.52	78.59	0.84
C53_003	17.78		382.39		27.97	20.19		74.21	73.58	1.00
C53_002	15.51		209.44		99.95	21.41		80.49	62.69	1.56
C53_001	20.26		351.77		219.90	22.79		68.65	70.61	0.75
C51_003	23.23		399.91			17.40		74.50	76.42	0.96
C51_002	22.00	9.35	313.84		16.54			75.09	75.76	1.10
C51_001	29.38	7.97	387.03		13.18	16.57		70.99	73.08	1.67
C47_001	43.58	13.09	344.18		48.67			63.77	75.72	0.63
C17_002	48.88	9.66	562.92		97.45			60.39	52.70	0.39
C17_001	23.41	10.90	626.89		135.70			61.14	53.41	0.33
C163_001			346.45		18.68	16.15		67.50	70.92	2.71
C150_009	17.07		516.34		12.70	16.04		63.23	68.55	0.78
C149_002			318.55		1411.39			71.60	38.22	0.22
C148_005			260.11					78.31	75.06	2.29
C148_004	13.14		370.39		13.08	19.54		72.57	71.29	2.77
C148_003	19.01		324.15		15.04	19.29		79.88	68.12	0.84
C148_002	14.86		301.29			18.58		75.63	78.31	0.85
C148_001	21.66		366.26			19.67		70.48	77.35	0.53
C145_002	79.94		737.04	200.81	45.92			53.25	42.59	0.43
C143_003	21.44		410.06		38.07	20.84		65.96	66.17	0.59
C142_007	32.01	9.56	315.79		25.32			64.96	73.54	0.82
C133_004	36.92		317.29		3.72			67.51	76.14	0.22

C133_002	52.10		424.62		33.32			60.70	82.05	1.36
C133_001	39.78	11.30	309.65		19.62	16.75		68.76	78.33	2.18
C118_003	16.05		3009.84		16.42	15.75		69.36	72.26	0.86
C115_012			5816.67		225.02			68.21	67.11	1.67
C115_011			4485.78	30.43	230.96			56.57	72.79	1.15
C115_006	41.97	13.04	3044.25		56.35			57.53	57.08	0.73
C115_004	23.15	8.30	4060.93			14.58		71.00	69.97	2.28
C115_003	19.90		3750.41		13.96			69.93	70.72	2.08
C115_002	19.84	9.68	3703.42		12.12	14.81		70.55	70.88	1.80
C113_005	14.46		328.83			16.38		72.90	65.90	0.73
C113_004	24.26	11.30	358.97					68.84	46.55	2.40
C113_003	15.69		357.65			15.89		71.29	73.10	1.04
C113_002	25.51		395.12		10.80	24.79		70.53	69.47	2.50
C113_001	19.68		458.06		14.20	19.23		66.96	66.57	3.16
C112_009	17.72		432.80		13.23	20.16		66.65	59.12	3.28
C112_008			319.09			17.40		71.47	74.22	1.01
C112_007	15.36		328.08		15.27	21.44		72.10	71.29	0.91
C112_006	17.46		374.06			15.55		74.03	73.85	1.01
C112_005			393.96			18.93		74.84	71.73	0.98
C112_004			357.76		12.51			69.21	73.42	1.01
C112_001	16.87		354.72			19.18		72.08	70.98	1.60
C111_004			241.00		19.06	19.73		80.92	55.79	0.35
C111_003	16.27		306.87			18.04		72.54	72.69	0.85
C110_008	15.75		421.05			16.74		64.17	73.50	0.77
C110_006	26.40		524.61		11.01			61.90	64.57	0.98
C110_003	31.07	14.12	497.89		16.17			56.35	70.55	1.23
C110_002	25.96		508.14		13.58	18.41		58.29	68.09	1.35
C71_009	21.84		313.64		37.20			63.40	70.54	0.30
C65_008	44.37	9.41	510.36	27.02	44.51			54.21	51.24	1.95
C65_007	50.72	8.91	437.80		42.48			54.44	52.88	2.65
C65_006	55.01	13.34	539.06		70.28			47.52	53.19	0.63
C65_005	34.61		528.13		39.57			49.59	49.65	1.83
C65_004	65.35	6.75	558.75	21.59	47.74			52.37	52.84	2.26
C65_003	51.79	9.92	569.45		37.53			51.22	50.79	2.41
C65_002	47.16	9.03	591.21		56.89			46.99	52.47	1.96
C65_001	45.71	9.76	538.02		33.18			56.72	52.29	2.57
C61_003	13.27	8.37	401.93		17.32			62.20	67.11	2.38
C61_001			353.64		29.85			64.13	67.74	2.52
C52_001	99.16	19.29	2161.26			16.17		60.77	48.33	4.42
C47_003	24.99		375.71		55.51			62.34	66.66	3.39
C17_003	35.85		545.63		398.64			52.30	62.63	0.63
C160_001	52.94	11.03	540.15		36.96			53.41	55.49	2.41
C157_001	45.63	12.64	606.08	184.80				51.17	51.05	0.81

C154_004	46.16	10.21	507.41	31.63	35.28			55.63	50.38	3.12
C154_003	50.05	7.84	557.87		28.03			54.52	51.81	3.01
C154_002	54.58		560.00		52.18			51.98	53.70	2.27

Table AI.2a Slag Group 1 Chemical Composition.

Sample	Slag Group	Period	SiO_2	Al_2O_3	P_2O_5	K_2O	FeO	TiO_2	Cr_2O_3	MnO
C146_001	1	Isl.	54.89	4.79	0.48	12.69	21.03	3.08	0.06	0.31
C119_004	1	Isl.	44.42	3.27		32.23	13.58	0.94	0.14	0.36
C119_003	1	Isl.	27.51			57.11	9.94	0.59	0.12	0.23
C119_002	1	Isl.	67.21	2.04	0.36	10.12	15.01	1.12	0.04	0.21
C119_001	1	Isl.	47.24	1.11		24.21	18.79	1.05	0.08	0.33

Table AI.2b Slag Group 1 Chemical Composition.

Sample	CaO	SO_3	CuO	NiO (ppm)	CoO (ppm	Cl (ppm)	V_2O_5 (ppm)	ZnO (ppm)	SeO_2 (ppm)	Rb_2O (ppm)	SrO (ppm)	ZrO_2 (ppm)	Nb_2O_5 (ppm)
C146_001	0.81	1.05	0.03			3594.01	1991.57	282.60		6.38	890.78	456.65	59.28
C119_004	3.36	0.88	0.03	726.22		2980.40	1060.25	168.14		33.14	1928.84	217.41	27.89
C119_003	0.45	3.19	0.06	566.37		3848.48	951.33	326.87		5.65	862.90	209.59	20.55
C119_002	3.71	0.86	0.03			4595.46	1003.96	166.82		41.09	193.98	116.15	11.08
C119_001	2.46	3.81	0.08	317.22		5249.15	1331.79	212.13		29.98	733.96	191.49	20.81

Table AI.2c Slag Group 1 Chemical Composition.

Sample	BaO (ppm)	PbO (ppm)	As_2O_3 (ppm)	Ag_2O (ppm)	MgO	Total un-normalized	FeO+MnO	$CaO+Al_2O_3$
C146_001	551.43					39.35	21.35	5.60
C119_004	862.10					41.68	13.93	6.63
C119_003	1289.45		28.48			45.98	10.17	0.45
C119_002	466.22					30.73	15.22	5.76
C119_001	615.54					33.36	19.12	3.56

Table AI.3a Slag Group 2 Chemical Compositions.

Sample	Slag Group	Period	SiO2	Al2O3	P2O5	K2O	FeO	TiO2	Cr2O3	MnO	CaO
C47_002	2	IA	36.14	2.66	0.24	12.15	41.36	0.81	0.19	0.70	2.30
C4_001	2	BA, Isl.	43.33	2.74	0.40	14.16	31.67	0.55	0.28	0.40	2.17
C149_001	2	N/A	16.83			30.76	23.85	0.12	0.55	0.32	0.15
C143_004	2	IA, Isl.	31.46	4.93		11.37	43.83	0.24	0.37	0.25	0.47
C143_002	2	IA, Isl.	32.13	6.51	0.30	15.03	40.23	0.25	0.27	0.19	0.48

C120_007	2	IA	38.45	5.69		23.84	25.17	0.23	0.32	0.41	0.62
C120_006	2	IA	31.66	0.96		19.69	39.57	0.14	0.35	0.29	0.62
C120_005	2	IA	40.32	5.10		16.59	32.58	0.23	0.41	0.47	0.79
C120_004	2	IA	27.72			17.39	35.34	0.12	0.36	0.23	0.56
C120_003	2	IA	36.09	2.59		23.85	28.58	0.22	0.41	0.40	0.90
C120_001	2	IA	32.41	4.95		22.13	32.77	0.32	0.28	0.32	0.93
C118_006	2	IA	27.90	1.05	0.21	19.90	32.04	0.60	0.09	0.51	1.51
C118_005	2	IA	36.33	2.41		17.82	34.15	0.67	0.11	0.58	1.63
C118_002	2	IA	27.67	1.24		28.68	37.36	0.45	0.14	0.36	1.56
C105_001	2	IA, Isl.	30.72	6.09		24.76	31.02	0.19	0.30	0.23	0.53

Table AI.3b Slag Group 2 Chemical Compositions.

Sample	SO3	CuO	NiO (ppm)	CoO (ppm)	Cl (ppm)	V2O5 (ppm)	ZnO (ppm)	SeO2 (ppm)	Rb2O (ppm)	SrO (ppm)	ZrO2 (ppm)	Nb2O5 (ppm)
C47_002	0.54	1.74	271.73		3506.38	1937.73	6077.34		19.49	744.13	77.05	14.44
C4_001	0.32	2.86	366.34		4335.26	1123.69	5120.04		21.83	1053.69	60.24	11.62
C149_001	3.91	18.30	3254.28	6087.49	35647.24	391.54	126.99		6.54	1909.55		13.09
C143_004	0.24	6.12	1041.08	898.18	2912.95	1172.18	777.02		5.75	362.60	17.51	
C143_002	0.12	3.87	881.06		3029.94	1072.41	284.44		4.77	433.25	18.90	
C120_007	0.23	4.19	501.99		5358.04	1242.98	148.16			550.15	19.66	
C120_006		6.31	1390.95		3451.48	871.09	434.27		5.83	529.17	23.10	
C120_005	0.21	2.73	377.46		2981.56	1410.63	132.08			331.37	11.60	
C120_004	0.42	16.20	2696.76		11424.35	756.77	529.94		5.21	713.20	22.42	
C120_003	0.20	5.89	585.21		5465.54	1403.14	131.36		6.16	439.12	21.84	
C120_001	0.19	4.96	493.00		4322.80	1322.70	276.63		8.55	322.82	74.31	9.55
C118_006	1.44	13.73	708.69		3537.08	1259.80	2568.51		12.76	918.75	74.09	13.05
C118_005	0.54	4.64	597.31		3024.44	1388.51	3086.20		11.73	780.56	86.45	13.48
C118_002	0.65	0.81	318.22		2578.60	1301.97	1609.23		11.07	2081.98	103.00	11.83

C105_001	0.58	4.73	496.57		4071.32	870.41	1602.95		6.11	928.44	17.61	

Table AI.3c Slag Group 2 Chemical Compositions.

Sample	BaO (ppm)	PbO (ppm)	As2O3 (ppm)	Ag2O (ppm)	MgO	Total un-normalized	FeO+MnO	CaO+Al2O3
C47_002	626.24		100.29			43.63	42.06	4.96
C4_001	583.03		37.82			38.78	32.07	4.91
C149_001	482.35		4168.10			50.41	24.17	0.15
C143_004	489.01		67.15			50.85	44.09	5.40
C143_002	484.95		35.91			48.13	40.42	7.00
C120_007	743.22					38.87	25.58	6.31
C120_006	568.22		12.41			44.21	39.86	1.57
C120_005	547.76					39.78	33.04	5.89
C120_004	508.55		19.05			46.09	35.57	0.56
C120_003	654.22					38.56	28.98	3.50
C120_001	570.22					42.98	33.09	5.88
C118_006	2483.55		13.46			47.32	32.55	2.56
C118_005	2377.30					51.17	34.73	4.04
C118_002	2761.31					56.59	37.72	2.80
C105_001	568.62					41.53	31.25	6.62

Table AI.4a Slag Group 3.1 Chemical Composition.

Sample	Slag Group	Period	SiO2	Al2O3	P2O5	K2O	FeO	TiO2	Cr2O3	MnO	CaO
C71_009	3.1	IA, Isl.	19.73		0.21	2.94	70.54	0.30	0.06		0.30
C65_008	3.1	N/A	21.25	1.24	0.28	20.40	51.09	0.31	0.49	0.15	0.71
C65_007	3.1	N/A	21.45	2.19	0.15	17.59	52.75	0.31	0.44	0.14	0.45
C65_006	3.1	N/A	17.41			20.80	53.04	0.31	0.30	0.15	0.63
C65_005	3.1	N/A	26.82	1.13	0.23	17.68	49.49	0.28	0.31	0.16	0.70

C65_004	3.1	N/A	23.57	1.95	0.42	17.77	52.45	0.43	0.31	0.39	0.31
C65_003	3.1	N/A	24.09	1.77		18.85	50.61	0.41	0.39	0.18	0.64
C65_002	3.1	N/A	21.86	1.12		18.75	52.30	0.29	0.40	0.17	0.83
C65_001	3.1	N/A	21.65	2.01	0.20	18.33	52.15	0.29	0.30	0.14	0.55
C61_003	3.1	IA, Isl.	18.08	1.57	0.25	7.47	67.02	0.25	0.59	0.08	0.81
C61_001	3.1	IA, Isl.	18.69	1.35	0.22	6.36	67.68	0.16	0.33	0.06	1.17
C52_001	3.1	N/A	26.74	3.30	0.22	15.73	4.90	0.75	0.04	43.43	1.12
C47_003	3.1	IA	19.26	2.27	0.14	6.66	66.56	0.24	0.13	0.09	1.12
C17_003	3.1	BA, IA, Isl	20.60		0.30	8.69	62.31	0.22	1.04	0.32	0.63
C160_001	3.1	BA, IA, Isl	21.87	1.66		16.30	55.33	0.32	0.33	0.16	0.76
C157_001	3.1	Isl.	19.21			25.99	50.97	0.20	0.26	0.08	0.81
C154_004	3.1	BA, IA, Isl	24.41	2.32	0.20	18.53	50.24	0.31	0.41	0.14	0.80
C154_003	3.1	BA, IA, Isl	24.10	2.13	0.27	17.91	51.66	0.31	0.33	0.15	0.88
C154_002	3.1	BA, IA, Isl	22.50	1.42	0.25	17.13	53.54	0.34	0.53	0.15	0.85
C150_011	3.1	IA, Isl	20.10		0.25	5.79	66.33	0.07	0.19	0.33	0.95
C150_010	3.1	IA, Isl	24.85		0.32	6.49	63.44	0.09	0.22	0.25	1.24
C147_002	3.1	N/A	18.35	2.17	0.16	9.58	64.21	0.33	0.15	0.10	1.63
C147_001	3.1	N/A	22.09	1.69	0.28	10.51	60.86	0.42	0.17	0.09	1.44
C145_001	3.1	BA, IA, Isl	21.21	0.98		12.41	59.76	0.29	0.33	0.13	0.84
C143_005	3.1	IA, Isl	23.65	3.13	0.12	4.33	61.92	0.23	0.14	0.19	0.46
C143_001	3.1	IA, Isl	25.00	2.56	0.37	9.50	54.56	0.33	0.15	0.23	0.63
C142_006	3.1	Isl.	20.08	0.72	0.26	11.10	63.19	0.16	0.70	0.05	0.96
C133_003	3.1	IA	18.91	2.27	0.15	4.16	67.03	0.34	0.14	0.16	1.14
C120_002	3.1	IA	22.53	0.97	0.22	9.48	54.32	0.14	0.17	0.30	0.39
C118_004	3.1	IA	26.66	1.63		12.96	50.33	0.54	0.11	0.39	1.51
C118_001	3.1	IA	23.58	1.79		22.45	47.50	0.40	0.13	0.41	1.39
C115_010	3.1	Isl.	21.32	2.31	0.38	11.94	4.98	0.38	0.10	53.75	1.12
C115_009	3.1	Isl.	24.23	1.74	0.35	14.54	8.89	0.57	0.09	39.67	1.14
C115_008	3.1	Isl.	26.27	1.28	0.33	17.53	4.74	0.53	0.11	44.51	1.55
C115_007	3.1	Isl.	21.87	2.35	0.18	12.32	4.66	0.53	0.08	51.21	1.09
C115_005	3.1	Isl.	20.16	1.37	0.24	12.10	8.04	0.45	0.06	52.13	0.87

C115_001	3.1	Isl.	21.59	2.10	0.24	12.60	4.57	0.54	0.09	51.01	1.09
C114_002	3.1	Isl.	20.21	2.10		16.02	4.17	1.52	0.06	45.90	1.18
C114_001	3.1	Isl.	16.62	1.53	0.15	16.48	11.21	1.43	0.06	42.48	1.10
C112_003	3.1	IA, Isl	19.53		0.37	4.48	67.74	0.08	0.08	0.09	1.04
C112_002	3.1	IA, Isl	19.81		0.32	3.84	70.52	0.11	0.08	0.05	0.81
C111_002	3.1	N/A	18.72	1.26	0.40	5.94	67.89	0.19	0.09	0.15	1.51
C111_001	3.1	N/A	18.90		0.33	5.64	69.62	0.14	0.07	0.06	0.91
C110_007	3.1	IA, Isl.	21.18		0.43	5.77	67.91	0.18	0.08	0.12	1.19
C110_005	3.1	IA, Isl.	24.15		0.48	6.79	64.04	0.22	0.09	0.12	1.44
C110_004	3.1	IA, Isl.	20.44	0.89	0.41	5.85	67.58	0.19	0.07	0.10	1.52
C110_001	3.1	IA, Isl.	18.97	1.26	0.25	5.79	67.45	0.21	0.09	0.10	1.19
C105_002	3.1	IA, Isl.	23.64	3.52	0.21	4.50	62.49	0.34	0.17	0.24	0.35

Table AI.4b Slag Group 3.1 Chemical Compositions.

Sample	SO3	CuO	NiO (ppm)	CoO (ppm)	Cl (ppm)	V2O5 (ppm)	ZnO (ppm)	SeO2 (ppm)	Rb2O (ppm)	SrO (ppm)	ZrO2 (ppm)	Nb2O5 (ppm)
C71_009	5.37	0.03	313.04		3060.50	1135.13				427.69	21.84	
C65_008	0.77	2.52	775.46	1005.14	3338.11	917.36	746.28		6.59	692.12	44.37	9.41
C65_007	1.19	2.59	813.79		4809.23	842.49	787.16		4.75	590.20	50.72	8.91
C65_006	0.65	5.63	944.60	1541.51	5356.35	830.80	788.67		7.81	686.58	55.01	13.34
C65_005	0.26	2.18	1591.87		3957.78	846.66	684.76		7.51	622.02	34.61	
C65_004	0.81	0.84	1053.63		3506.08	1087.27	664.05			509.25	65.35	6.75
C65_003	0.37	1.91	849.17		3955.16	956.58	724.19		7.40	741.35	51.79	9.92
C65_002	0.60	3.21	1219.18		3899.66	822.84	802.58		9.22	853.81	47.16	9.03
C65_001	1.40	2.26	852.88	904.21	4386.51	851.97	767.93		6.32	717.77	45.71	9.76
C61_003	2.14	1.19	520.76		2803.60	759.87	645.81			385.36	13.27	8.37
C61_001	1.70	1.72	657.94		2821.63	676.02	789.97	34.07		355.31		
C52_001	2.69	0.34	225.62		2635.13	1152.98	371.35		12.21	1827.89	99.16	19.29
C47_003	1.87	1.10	254.10		3098.15	737.56	1513.31			511.70	24.99	
C17_003	0.27	4.49	3165.92	1086.11	4137.43	725.94	501.51		6.20	650.26	35.85	

C160_001	0.39	2.11	984.35	1101.91	3246.56	910.86	846.26		7.45	739.08	52.94	11.03
C157_001	0.23	1.32	562.47		4826.31	664.65	1239.27		9.09	1151.63	45.63	12.64
C154_004	0.38	1.52	829.00		4236.79	865.05	800.91		6.31	707.30	46.16	10.21
C154_003	0.50	1.14	735.56		3261.38	896.58	705.23		6.73	733.55	50.05	7.84
C154_002	0.57	2.10	785.54		3842.45	877.84	808.73		6.05	745.64	54.58	
C150_011	0.85	4.43	1536.86		2803.20	464.19	1138.66		5.02	632.44	14.73	
C150_010	0.88	1.69	783.33		2583.98	516.49	392.10		4.56	577.96	15.62	
C147_002	1.92	0.79	223.51		2756.99	762.01	938.40		10.17	1085.87	44.73	8.99
C147_001	1.58	0.94	187.77		3229.33	793.69	1236.80		10.36	756.69	50.16	11.68
C145_001	0.30	3.48	698.84	2246.83	3329.69	911.06	712.78		6.80	681.35	43.22	11.77
C143_005	0.15	5.10	400.92	894.85	2425.99	913.64	430.06			220.66	23.80	
C143_001	0.54	5.45	480.16		3762.62	1268.06	342.34		5.32	419.67	31.69	8.94
C142_006	0.72	1.27	467.58	3930.31	3533.59	605.59	428.20		4.52	606.04	37.51	9.55
C133_003	1.64	1.26	211.31		3199.72	863.92	#######		7.42	342.75	36.76	
C120_002	0.30	10.85	744.41		5205.94	1413.04	115.71		5.79	194.06	13.49	
C118_004	2.25	2.38	350.67		4055.26	1655.34	1843.57		8.28	762.67	60.59	10.15
C118_001	0.48	0.85	304.96	723.00	2911.01	1361.56	2205.89		6.43	969.56	31.74	13.73
C115_010	2.06	0.92	249.39		2360.93	783.84	514.38		3.93	2256.74	37.23	13.42
C115_009	0.45	6.54	781.49		10345.63	1386.22	744.86		9.32	1273.76	64.88	15.03
C115_008	2.34	0.35			3790.31	938.88	268.36		9.05	2379.22	68.71	14.55
C115_007	4.39	0.42	191.53		2612.41	1830.85	558.22		7.36	954.31	47.30	14.43
C115_005	0.96	2.31	518.78	1490.22	4544.69	1539.15	413.81		10.28	1006.18	53.95	11.27
C115_001	4.78	0.42	175.42		2372.86	1775.87	565.41		7.30	933.74	48.75	14.47
C114_002	4.25	0.79	402.35		3144.80	7759.76	189.20		6.72	1958.24	61.36	17.09
C114_001	2.84	1.82	558.45	930.07	4342.00	7404.54	367.02		7.97	2264.98	67.24	18.51

C112_003	2.51	3.43	424.93		4307.80	480.81	185.10		3.54	700.38	16.64	
C112_002	2.86	1.07	335.09		3391.84	491.90	203.97		4.03	490.83	17.46	
C111_002	2.06	1.03	407.26		5430.09	582.07	196.45			643.24	17.56	
C111_001	2.94	0.79	451.90		3805.05	488.98	177.23		3.69	578.64	23.52	
C110_007	1.19	1.40	457.00		3160.94	528.33	143.29		3.33	688.29	20.50	
C110_005	1.43	0.71	420.26		3037.71	543.75	101.00		5.82	719.50	23.21	
C110_004	1.05	1.36	432.50		3074.48	488.55	125.77		4.92	708.82	20.94	
C110_001	2.16	1.95	289.35		3405.78	595.11	174.93			799.47	29.19	
C105_002	0.15	3.85	456.86		2459.21	1414.82	345.02			221.87	13.04	

Table AI.4c Slag Group 3.1 Chemical Compositions.

Sample	BaO (ppm)	PbO (ppm)	As2O3 (ppm)	Ag2O (ppm)	MgO	Total un-normalized	FeO+MnO	CaO+Al2O3
C71_009	313.64		37.20			63.40	70.54	0.30
C65_008	510.36	27.02	44.51			54.21	51.24	1.95
C65_007	437.80		42.48			54.44	52.88	2.65
C65_006	539.06		70.28			47.52	53.19	0.63
C65_005	528.13		39.57			49.59	49.65	1.83
C65_004	558.75	21.59	47.74			52.37	52.84	2.26
C65_003	569.45		37.53			51.22	50.79	2.41
C65_002	591.21		56.89			46.99	52.47	1.96
C65_001	538.02		33.18			56.72	52.29	2.57
C61_003	401.93		17.32			62.20	67.11	2.38
C61_001	353.64		29.85			64.13	67.74	2.52
C52_001	2161.26			16.17		60.77	48.33	4.42
C47_003	375.71		55.51			62.34	66.66	3.39
C17_003	545.63		398.64			52.30	62.63	0.63

C160_001	540.15		36.96			53.41	55.49	2.41
C157_001	606.08	184.80				51.17	51.05	0.81
C154_004	507.41	31.63	35.28			55.63	50.38	3.12
C154_003	557.87		28.03			54.52	51.81	3.01
C154_002	560.00		52.18			51.98	53.70	2.27
C150_011	541.96					62.08	66.66	0.95
C150_010	535.89					58.60	63.68	1.24
C147_002	461.88		16.10	9.79		61.25	64.31	3.80
C147_001	449.58		122.52			56.91	60.95	3.13
C145_001	622.61		53.85			59.17	59.88	1.81
C143_005	387.05		51.70			65.49	62.11	3.59
C143_001	445.00		29.77			56.03	54.79	3.19
C142_006	407.27		112.91	17.22		58.82	63.24	1.68
C133_003	403.49	28.16	96.65			60.14	67.19	3.41
C120_002	480.07		15.90	20.67		48.74	54.62	1.36
C118_004	3738.26					55.86	50.73	3.13
C118_001	2119.74		16.15			55.10	47.91	3.19
C115_010	1268.79					66.49	58.72	3.43
C115_009	3239.52		21.97			54.36	48.56	2.88
C115_008	1307.22					50.94	49.25	2.83
C115_007	3933.15					65.52	55.87	3.44
C115_005	4293.83		22.43			59.93	60.17	2.24
C115_001	3932.21					62.89	55.58	3.19
C114_002	24631.98					61.14	50.07	3.28
C114_001	27434.25		15.10			60.42	53.69	2.64
	340.11			20.76		70.04	67.83	1.04
C112_002	384.20		16.35	16.40		70.81	70.57	0.81
C111_002	414.28			16.43		70.53	68.04	2.77

C111_001	542.18		11.37	18.21		66.41	69.69	0.91
C110_007	423.97					67.60	68.03	1.19
C110_005	407.95					60.77	64.16	1.44
C110_004	409.58		7.42	12.30		64.26	67.69	2.41
C110_001	448.73		14.20	16.73		68.63	67.55	2.45
C105_002	400.14		22.18			57.41	62.72	3.87

Table AI.5a Slag Group 3.2 Chemical Composition.

Sample	Slag Group	Period	SiO2	Al2O3	P2O5	K2O	FeO	TiO2	Cr2O3	MnO
C78_004	3.2	IA & Isl.	11.04		0.13	3.50	76.25	0.11	0.08	0.04
C78_003	3.2	IA & Isl.	11.36		0.09	3.92	75.86	0.10	0.07	0.04
C78_002	3.2	IA & Isl.	17.95		0.14	5.83	71.24	0.11	0.08	0.06
C76_003	3.2	IA & Isl.	12.17		0.18	3.70	76.19	0.12	0.09	0.04
C76_002	3.2	IA & Isl.	12.60	0.85		3.44	74.61	0.10	0.08	0.03
C76_001	3.2	IA & Isl.	13.14	1.99		3.76	59.87	0.18	0.06	0.06
C75_003	3.2	IA & Isl.	11.85		0.09	3.86	77.21	0.10	0.07	0.04
C75_002	3.2	IA & Isl.	9.54			2.67	78.99	0.14	0.08	
C75_001	3.2	IA & Isl.	12.69	1.18	0.16	3.01	74.11	0.11	0.07	0.04
C72_004	3.2	Isl.	5.82			26.51	62.52	0.05	0.05	0.18
C72_003	3.2	Isl.	10.92		0.13	3.30	73.50	0.08	0.07	0.06
C72_002	3.2	Isl.	14.40			3.61	75.64	0.10	0.08	0.05
C72_001	3.2	Isl.	7.92			11.95	75.45	0.07	0.07	0.07
C71_005	3.2	IA & Isl.	12.95			2.89	75.43	0.13	0.07	0.04
C71_004	3.2	IA & Isl.	14.88			2.97	74.09	0.12	0.06	0.06
C71_003	3.2	IA & Isl.	11.32			11.82	71.28	0.53	0.09	0.06
C71_002	3.2	IA & Isl.	15.16	2.39	0.14	5.28	72.07	0.12	0.07	0.09
C71_001	3.2	IA & Isl.	12.32	0.80		3.32	77.64	0.17	0.07	0.07
C61_002	3.2	IA & Isl.	16.36	1.17	0.29	6.85	71.41	0.19	0.33	0.06
C53_006	3.2	Isl.	12.41		0.18	5.32	73.89	0.11	0.10	0.10
C53_005	3.2	Isl.	10.95		0.14	6.30	68.26	0.14	0.09	0.07
C53_004	3.2	Isl.	9.94		0.14	5.21	78.53	0.09	0.08	0.07
C53_003	3.2	Isl.	12.21			5.36	73.48	0.14	0.10	0.10
C53_002	3.2	Isl.	10.47	0.87		3.81	62.63	0.10	0.16	0.06
C53_001	3.2	Isl.	5.73			8.20	70.53	0.10	0.10	0.08
C51_003	3.2	N/A	12.35		0.14	5.22	76.35	0.14	0.09	0.07
C51_002	3.2	N/A	11.53		0.11	5.82	75.70	0.16	0.08	0.06
C51_001	3.2	N/A	13.68	0.44	0.07	7.06	73.01	0.18	0.10	0.07

C47_001	3.2	IA	13.37			4.15	75.64	0.25	0.13	0.09
C17_002	3.2	BA, IA, Isl.	8.69		0.14	27.47	52.59	0.17	0.46	0.10
C17_001	3.2	BA, IA, Isl.	12.35		0.25	24.01	53.12	0.16	0.64	0.29
C163_001	3.2	Isl.	16.03	2.18		3.87	70.73	0.19	0.13	0.19
C150_009	3.2	IA & Isl.	16.00		0.22	8.72	68.31	0.06	0.61	0.25
C149_002	3.2	N/A	9.43			2.71	38.22	0.07	0.11	
C148_005	3.2	IA	7.67		0.14	0.66	75.02	0.07	0.06	0.04
C148_004	3.2	IA	15.81	0.98	0.18	5.59	71.20	0.15	0.08	0.09
C148_003	3.2	IA	8.50			4.46	68.09	0.11	0.07	0.03
C148_002	3.2	IA	11.01		0.14	1.34	78.27	0.12	0.08	0.03
C148_001	3.2	IA	14.26		0.14	2.90	77.30	0.11	0.07	0.04
C145_002	3.2	BA, IA, Isl.	10.23		0.18	8.33	42.45	0.15	0.11	0.14
C143_003	3.2	IA & Isl.	9.97		0.22	5.39	66.17	0.13	0.86	
C142_007	3.2	Isl.	13.15		0.17	7.51	73.50	0.14	0.26	0.04
C133_004	3.2	IA	12.47			2.75	76.09	0.19	0.16	0.05
C133_002	3.2	IA	10.63	1.06		2.16	81.99	0.30	0.15	0.06
C133_001	3.2	IA	14.93	1.57	0.10	0.96	78.30	0.16	0.11	0.03
C118_003	3.2	IA	16.06			6.08	72.20	0.28	0.10	0.06
C115_012	3.2	Isl.	12.91		0.19	3.59	67.07	0.32	0.07	0.04
C115_011	3.2	Isl.	7.94			2.15	72.75	0.17	0.07	0.04
C115_006	3.2	Isl.	9.60			10.60	17.25	0.36	0.08	39.84
C115_004	3.2	Isl.	15.49	1.01	0.15	7.05	69.88	0.39	0.10	0.09
C115_003	3.2	Isl.	14.98	0.87	0.15	6.89	70.64	0.36	0.13	0.09
C115_002	3.2	Isl.	15.00	0.54	0.10	7.05	70.80	0.38	0.11	0.09
C113_005	3.2	IA & Isl.	13.36		0.22	3.41	65.85	0.11	0.06	0.05
C113_004	3.2	IA & Isl.	10.07	1.76	0.13	17.19	44.82	0.16	0.04	1.72
C113_003	3.2	IA & Isl.	15.71		0.22	4.42	73.05	0.15	0.08	0.04
C113_002	3.2	IA & Isl.	16.18	1.07	0.24	6.71	69.41	0.14	0.08	0.06
C113_001	3.2	IA & Isl.	16.38	2.30	0.16	5.08	66.50	0.12	0.08	0.07
C112_009	3.2	IA & Isl.	10.44	2.68	0.21	12.67	59.03	0.10	0.06	0.10
C112_008	3.2	IA & Isl.	15.61		0.28	4.02	74.17	0.09	0.06	0.05
C112_007	3.2	IA & Isl.	9.33		0.23	14.41	71.26	0.09	0.07	0.03
C112_006	3.2	IA & Isl.	15.10		0.29	4.58	73.85	0.11	0.07	
C112_005	3.2	IA & Isl.	15.41		0.24	5.45	71.65	0.08	0.07	0.08
C112_004	3.2	IA & Isl.	14.96		0.28	4.91	73.34	0.09	0.07	0.08
C112_001	3.2	IA & Isl.	17.75	0.75	0.23	3.86	70.92	0.11	0.07	0.06
C111_004	3.2	N/A	11.05		0.15	2.26	55.75	0.05	0.05	0.04
C111_003	3.2	N/A	16.62		0.19	4.10	72.65	0.09	0.07	0.04
C110_008	3.2	IA. & Isl.	14.95		0.44	6.04	73.43	0.11	0.08	0.07
C110_006	3.2	IA. & Isl.	15.11		0.44	16.42	64.44	0.16	0.08	0.13
C110_003	3.2	IA. & Isl.	14.68		0.41	8.40	70.10	0.22	0.09	0.44
C110_002	3.2	IA. & Isl.	16.49		0.30	7.87	67.89	0.24	0.07	0.20

C78_001	3.2	IA & Isl.	18.10		0.15	6.01	68.81	0.12	0.08	0.05

Table AI.5b Slag Group 3.2 Chemical Composition.

Sample	CaO	SO3	CuO	NiO (ppm)	CoO (ppm)	Cl (ppm)	V2O5 (ppm)	ZnO (ppm)	SeO2 (ppm)
C78_004	1.07	6.09	1.40	259.84		2186.09	445.20	285.99	40.26
C78_003	1.17	3.03	3.79	203.01		4177.67	421.29	378.69	
C78_002	1.21	1.73	1.16	292.44		2998.77	489.82	485.58	
C76_003	1.10	4.78	1.25	342.95		2187.46	505.90	460.67	38.02
C76_002	1.76	5.24	1.40	247.51		2509.55	557.24	557.83	57.59
C76_001	1.30	6.02	14.49	286.03		3037.97	463.80	381.97	344.28
C75_003	1.03	3.73	1.54	291.61		2953.95	510.87	602.17	29.81
C75_002	0.66	4.63	2.78	295.92		3269.50	472.09	445.09	32.53
C75_001	0.57	3.01	4.58	280.45		2469.18	547.76	509.72	37.65
C72_004	0.32	1.26	2.50		3154.05	2043.15	329.09	1111.90	
C72_003	1.60	6.24	3.67	190.42		3198.82	431.31	571.06	36.17
C72_002	1.02	3.56	1.09	207.58		2416.75	489.65	503.40	
C72_001	0.62	1.72	1.45		1405.35	2986.98	455.12	846.35	
C71_005	0.91	5.08	1.95	371.16		2768.60	519.02	566.00	
C71_004	0.72	3.28	3.36	311.20		2380.47	452.10	622.24	
C71_003	1.15	2.77	0.92	213.65		2514.77	553.23	642.97	
C71_002	1.10	1.47	1.77	220.57		2692.23	433.78	437.14	35.64
C71_001	0.54	2.80	2.29	258.26		3126.11	496.66	322.31	35.09
C61_002	0.92	1.01	1.54	615.75		3744.79	652.19	817.70	
C53_006	0.94	5.13	1.40	450.19		2615.04	687.56	700.21	
C53_005	0.54	4.75	8.33	551.87		2932.57	514.91	249.16	40.40
C53_004	0.84	2.93	1.67	284.09		3779.30	458.48	614.38	
C53_003	1.00	4.54	2.62	251.83		2277.01	621.81	413.29	
C53_002	0.69	8.41	12.73	217.74		2032.87	428.98	336.04	80.87
C53_001	0.75	2.94	10.13	399.52	5065.09	6519.17	487.95	996.60	
C51_003	0.96	3.19	1.10	264.24		2089.98	703.95	285.53	59.80
C51_002	1.10	3.74	1.29	271.66		2144.60	752.21	334.44	97.25
C51_001	1.23	3.08	0.93	225.53		2449.35	722.44	295.94	38.11
C47_001	0.63	3.40	1.66	258.41		3027.87	604.72	2327.05	
C17_002	0.39	0.61	7.18	843.55	1780.25	17194.74	570.43	753.67	
C17_001	0.33	1.54	6.35	726.65	2799.12	3294.92	588.70	252.72	
C163_001	0.52	0.19	5.47	461.83		2694.96	1067.15	233.18	
C150_009	0.78	1.34	3.16	1459.17		2623.56	497.11	783.01	
C149_002	0.22	2.63	43.31	489.38	1191.89	28136.90	339.74	285.91	307.08
C148_005	2.29	12.23	1.52	346.86		2129.18	431.95	388.98	34.34
C148_004	1.78	3.33	1.03	382.82		2664.20	545.42	415.10	30.75
C148_003	0.84	14.08	3.34	326.36		2753.34	418.76	319.24	55.93

C148_002	0.85	6.94	0.92	247.72		2337.63	543.44	317.91	39.19
C148_001	0.53	2.75	1.47	298.88		2698.88	454.82	556.59	
C145_002	0.43	0.30	31.47	626.34	1936.23	57238.67	630.53	473.85	
C143_003	0.59	1.13	14.36	1186.04		9057.62	655.77	173.01	
C142_007	0.82	0.54	3.08	1103.68	2467.85	2400.43	500.29	609.30	
C133_004	0.22	4.88	2.51	228.65		3531.57	698.09	1780.41	36.27
C133_002	0.30	2.00	1.13	251.96		3081.17	831.61	891.83	
C133_001	0.61	0.22	2.57		1128.40	2283.52	690.44	1254.17	34.70
C118_003	0.86	2.62	0.88	313.62		2628.75	1683.34	457.09	
C115_012	1.67	8.96	3.93	395.40		3632.54	1807.30	530.75	
C115_011	1.15	7.10	7.06	531.64		8431.48	1142.14	393.65	
C115_006	0.73	5.77	13.07	2360.89	2921.74	14500.25	1271.82	2001.76	
C115_004	1.28	3.41	0.85	300.57		3512.02	1798.80	400.90	
C115_003	1.21	3.15	0.89	286.26		2972.12	1724.84	396.96	
C115_002	1.26	3.27	0.86	258.03		3036.36	1840.64	393.70	
C113_005	0.73	6.79	9.01	267.85		3415.16	404.98		42.79
C113_004	0.63	4.90	18.42	469.49	3436.27	2364.68	348.12	548.81	
C113_003	1.04	3.83	0.95	309.81		3023.28	585.04	168.75	
C113_002	1.43	3.64	0.99	246.50		5079.72	493.08	199.44	
C113_001	0.86	3.29	4.78	282.31		2804.86	607.17	219.03	
C112_009	0.60	4.70	9.81	354.87		3083.48	410.04	217.44	
C112_008	1.01	3.05	1.10	358.83		3674.51	439.52	261.94	
C112_007	0.91	1.72	1.65	227.79		2650.37	412.54	270.66	
C112_006	1.01	3.42	1.06	326.90		2976.19	453.36	252.86	
C112_005	0.98	4.04	1.40	315.09		3833.65	426.56	278.17	
C112_004	1.01	3.35	1.26	406.50		4287.23	407.20	258.65	
C112_001	0.85	3.35	1.92	297.68		4480.66	506.28	237.75	
C111_004	0.35	10.35	19.45	277.88	1052.59	2745.58	333.64	204.18	42.80
C111_003	0.85	3.56	1.33	192.16		3376.40	482.42	273.35	
C110_008	0.77	1.66	1.82	495.97		4166.33	468.58	296.54	
C110_006	0.98	0.93	0.81	438.94		2793.87	456.41	94.90	
C110_003	1.23	1.72	1.98	349.19		4573.54	674.09	124.49	
C110_002	1.35	3.22	1.60	232.41		5021.94	564.27	202.99	
C78_001	1.48	3.70	0.95	283.02		2834.85	503.81	492.45	

Table AI.5c Slag Group 3.2 Chemical Composition.

Sample	Rb2O (ppm)	SrO (ppm)	ZrO2 (ppm)	Nb2O5 (ppm)	BaO (ppm)	PbO (ppm)
C78_004	4.96	418.69	17.78		318.09	
C78_003		441.81	17.94	7.97	376.48	
C78_002		803.52	14.98		323.21	
C76_003		445.81	20.44		308.99	

C76_002	4.84	462.52	13.56		273.38	
C76_001	8.94	377.32	31.15		410.43	
C75_003		509.06			387.34	
C75_002	4.75	377.49	33.02		334.24	
C75_001		470.97	16.87		308.44	
C72_004	3.09	552.59		7.66	573.83	
C72_003		362.23	19.05		308.38	
C72_002	3.14	569.50	19.98		358.62	
C72_001		549.45	16.46	6.51	400.06	
C71_005	3.70	425.99	14.91		312.31	
C71_004	4.03	491.18	15.43		342.17	
C71_003	4.40	443.22	14.56		284.61	
C71_002	4.08	403.94	20.75		318.87	
C71_001	3.33	281.67	25.61		317.16	
C61_002		352.62	13.38		375.30	
C53_006	3.15	544.20			419.92	
C53_005	3.43	518.74	26.17		363.75	
C53_004		515.22	15.66		364.69	
C53_003		514.80	17.78		382.39	
C53_002		305.86	15.51		209.44	
C53_001	4.01	397.26	20.26		351.77	
C51_003	3.73	505.81	23.23		399.91	
C51_002	5.22	650.55	22.00	9.35	313.84	
C51_001	4.14	688.54	29.38	7.97	387.03	
C47_001	5.80	308.99	43.58	13.09	344.18	
C17_002	9.12	841.38	48.88	9.66	562.92	
C17_001	7.07	1092.92	23.41	10.90	626.89	
C163_001		219.41			346.45	
C150_009		515.37	17.07		516.34	
C149_002	4.61	675.78			318.55	
C148_005		373.42			260.11	
C148_004	3.97	425.71	13.14		370.39	
C148_003	5.35	501.68	19.01		324.15	
C148_002		242.89	14.86		301.29	
C148_001	4.95	325.71	21.66		366.26	
C145_002	8.79	556.45	79.94		737.04	200.81
C143_003	3.98	395.74	21.44		410.06	
C142_007	7.32	552.60	32.01	9.56	315.79	
C133_004	5.70	180.60	36.92		317.29	
C133_002	4.16	264.08	52.10		424.62	
C133_001	6.88	35.26	39.78	11.30	309.65	
C118_003	3.22	600.66	16.05		3009.84	
C115_012		877.84			5816.67	
C115_011	4.56	578.43			4485.78	30.43

C115_006	7.90	835.77	41.97	13.04	3044.25	
C115_004		723.60	23.15	8.30	4060.93	
C115_003	4.09	693.31	19.90		3750.41	
C115_002	5.30	695.05	19.84	9.68	3703.42	
C113_005		383.36	14.46		328.83	
C113_004	4.93	617.16	24.26	11.30	358.97	
C113_003		501.96	15.69		357.65	
C113_002		1044.82	25.51		395.12	
C113_001		569.77	19.68		458.06	
C112_009		596.63	17.72		432.80	
C112_008	3.83	573.17			319.09	
C112_007		726.76	15.36		328.08	
C112_006		650.72	17.46		374.06	
C112_005		731.89			393.96	
C112_004		717.32			357.76	
C112_001		413.75	16.87		354.72	
C111_004	3.97	299.54			241.00	
C111_003		539.25	16.27		306.87	
C110_008	4.41	502.05	15.75		421.05	
C110_006	5.26	699.20	26.40		524.61	
C110_003	5.85	1044.41	31.07	14.12	497.89	
C110_002		1163.67	25.96		508.14	
C78_001		996.24	14.89		383.15	

Table AI.5d Slag Group 3.2 Chemical Composition.

Sample	As2O3 (ppm)	Ag2O (ppm)	MgO	Total un- normalized	FeO+MnO	CaO+Al2O3
C78_004		20.70		78.55	76.28	1.07
C78_003	12.63	19.03		72.47	75.89	1.17
C78_002	11.11	17.12		69.51	71.30	1.21
C76_003		18.79		77.59	76.23	1.10
C76_002		22.04		75.30	74.64	2.62
C76_001	28.13	48.15		67.17	59.93	3.29
C75_003		22.93		71.97	77.25	1.03
C75_002		19.90		75.37	78.99	0.66
C75_001		16.37		74.06	74.15	1.75
C72_004	30.74			74.92	62.71	0.32
C72_003	30.11	19.91		78.50	73.56	1.60
C72_002	22.30			73.16	75.70	1.02
C72_001	18.43	13.26		73.88	75.52	0.62
C71_005	16.25	19.34		73.75	75.47	0.91
C71_004	14.47	19.54		67.77	74.15	0.72
C71_003				74.60	71.34	1.15
C71_002		17.00		80.00	72.15	3.49

C71_001				71.08	77.71	1.34
C61_002	24.34	26.55		59.43	71.46	2.09
C53_006	14.83	20.42		75.76	73.98	0.94
C53_005	244.95			71.80	68.33	0.54
C53_004	26.72	24.30		69.52	78.59	0.84
C53_003	27.97	20.19		74.21	73.58	1.00
C53_002	99.95	21.41		80.49	62.69	1.56
C53_001	219.90	22.79		68.65	70.61	0.75
C51_003		17.40		74.50	76.42	0.96
C51_002	16.54			75.09	75.76	1.10
C51_001	13.18	16.57		70.99	73.08	1.67
C47_001	48.67			63.77	75.72	0.63
C17_002	97.45			60.39	52.70	0.39
C17_001	135.70			61.14	53.41	0.33
C163_001	18.68	16.15		67.50	70.92	2.71
C150_009	12.70	16.04		63.23	68.55	0.78
C149_002	1411.39			71.60	38.22	0.22
C148_005				78.31	75.06	2.29
C148_004	13.08	19.54		72.57	71.29	2.77
C148_003	15.04	19.29		79.88	68.12	0.84
C148_002		18.58		75.63	78.31	0.85
C148_001		19.67		70.48	77.35	0.53
C145_002	45.92			53.25	42.59	0.43
C143_003	38.07	20.84		65.96	66.17	0.59
C142_007	25.32			64.96	73.54	0.82
C133_004	43.72			67.51	76.14	0.22
C133_002	33.32			60.70	82.05	1.36
C133_001	19.62	16.75		68.76	78.33	2.18
C118_003	16.42	15.75		69.36	72.26	0.86
C115_012	225.02			68.21	67.11	1.67
C115_011	230.96			56.57	72.79	1.15
C115_006	56.35			57.53	57.08	0.73
C115_004		14.58		71.00	69.97	2.28
C115_003	13.96			69.93	70.72	2.08
C115_002	12.12	14.81		70.55	70.88	1.80
C113_005		16.38		72.90	65.90	0.73
C113_004				68.84	46.55	2.40
C113_003		15.89		71.29	73.10	1.04
C113_002	10.80	24.79		70.53	69.47	2.50
C113_001	14.20	19.23		66.96	66.57	3.16
C112_009	13.23	20.16		66.65	59.12	3.28
C112_008		17.40		71.47	74.22	1.01
C112_007	15.27	21.44		72.10	71.29	0.91
C112_006		15.55		74.03	73.85	1.01

C112_005		18.93		74.84	71.73	0.98
C112_004	12.51			69.21	73.42	1.01
C112_001		19.18		72.08	70.98	1.60
C111_004	19.06	19.73		80.92	55.79	0.35
C111_003		18.04		72.54	72.69	0.85
C110_008		16.74		64.17	73.50	0.77
C110_006	11.01			61.90	64.57	0.98
C110_003	16.17			56.35	70.55	1.23
C110_002	13.58	18.41		58.29	68.09	1.35
C78_001	10.91	13.45		70.01	68.85	1.48

Table AI.6 Number of Slag Samples Analyzed with Thermo Niton XL3t GOLDD+ XRF analyzer and Number of Slag Groups Revealed for Each Site

C Sites	Number of Samples Analyzed	% of Total	Slag Group 1	Slag Group 2	Slag Group 3.1	Slag Group 3.2	Number of Slag Groups by C Site	Periodization
C4	1	0.7	0	1	0	0	1	Bronze Age & Islamic
C17	3	2.11	0	0	1	1	2	Bronze Age, Iron Age, & Islamic
C47	3	2.11	0	1	1	1	3	Iron Age
C51	3	2.11	0	0	0	1	1	N/A
C52	1	0.7	0	0	1	0	1	N/A
C53	6	4.23	0	0	0	1	1	Islamic
C61	3	2.11	0	0	1	1	2	Iron Age & Islamic
C65	8	5.63	0	0	1	0	1	N/A
C71	9	6.34	0	0	1	1	3	Iron Age & Islamic
C72	4	2.82	0	0	0	1	1	Islamic
C75	3	2.11	0	0	0	1	1	Iron Age & Islamic
C76	3	2.11	0	0	0	1	1	Iron Age & Islamic
C78	4	2.82	0	0	0	1	1	Iron Age & Islamic
C105	2	1.41	0	1	1	0	2	Iron Age & Islamic
C110	8	5.63	0	0	1	1	2	Iron Age & Islamic
C111	4	2.82	0	0	1	1	2	N/A
C112	9	6.34	0	0	1	1	2	Iron Age & Islamic
C113	5	3.52	0	0	0	1	1	Iron Age & Islamic
C114	2	1.41	0	0	1	0	1	Islamic
C115	12	8.45	0	0	1	1	2	Islamic
C118	6	4.23	0	1	1	1	3	Iron Age
C119	4	2.82	1	0	0	0	1	Islamic
C120	7	4.93	0	1	1	0	2	Iron Age
C133	4	2.82	0	0	1	1	2	Iron Age
C142	2	1.41	0	0	1	1	2	Islamic

C143	5	3.52	0	1	1	1	3	Iron Age & Islamic
C145	2	1.41	0	0	1	1	2	Bronze Age, Iron Age, & Islamic
C146	1	0.7	1	0	0	0	1	Islamic
C147	2	1.41	0	0	1	0	1	N/A
C148	5	3.52	0	0	0	1	1	Iron Age
C149	2	1.41	0	1	0	1	2	N/A
C150	3	2.11	0	0	1	1	2	Iron Age & Islamic
C154	3	2.11	0	0	1	0	1	Bronze Age, Iron Age, & Islamic
C157	1	0.7	0	0	1	0	1	Islamic
C160	1	0.7	0	0	1	0	1	Bronze Age, Iron Age, & Islamic
C163	1	0.7	0	0	0	1	1	Islamic
Totals	**142**	**100**	**2**	**7**	**23**	**24**		

Table AI.7 Elements and their oxides monitored for each sample.

SiO_2	FeO	CaO	CoO	SeO_2	Nb_2O_5	Ag_2O
Al_2O_3	TiO_2	SO_3	Cl	Rb_2O	BaO	MgO
P_2O_5	Cr_2O_3	CuO	V_2O_5	SrO	PbO	

Table AI.8 Summary Statistics of Important Reducing and Non-Reducing Compounds for Slags and Ores Analyzed for this Study.

		MATERIAL				**MATERIAL**	
Compound	**Statistic**	**Ore**	**Slag**	**Compound**	**Statistic**	**Ore**	**Slag**
SiO2	Mean	36.8	18.9	NiO (ppm)	Mean	3441	549
	Std Dev	17.9	9.7		Std Dev	5948	502
	Quantile-9	58	31.2		Quantile-9	14160	1001
Al2O3	Mean	2.9	2	CoO (ppm)	Mean	2825	2047
	Std Dev	1.6	1.3		Std Dev	3207	1402
	Quantile-9	4.8	4.2		Quantile-9	9523	4384
P2O5	Mean	0.4	0.2	As2O3 (ppm	Mean	264	114
	Std Dev	0.5	0.1		Std Dev	692	452
	Quantile-9	0.6	0.4		Quantile-9	577	223
K2O	Mean	12.4	10.4	Ag2O (ppm)	Mean	51	19
	Std Dev	11.8	8.3		Std Dev	48	5
	Quantile-9	30.2	21.7		Quantile-9	121	24
FeO	Mean	24.6	57.6				
	Std Dev	16.9	21.5				
	Quantile-9	48.6	76.2				
Cr2O3	Mean	0.2	0.2				
	Std Dev	0.2	0.2				
	Quantile-9	0.7	0.4				

MnO	Mean	0.7	3.6				
	Std Dev	1.1	12.3				
	Quantile-9	1.2	0.5				
CaO	Mean	0.7	1				
	Std Dev	1	0.5				
	Quantile-9	1.6	1.5				
SO3	Mean	5.2	2.6				
	Std Dev	10.4	2.4				
	Quantile-9	11.7	5.2				
CuO	Mean	16	3.8				
	Std Dev	18.9	5.7				
	Quantile-9	45.6	9.6				

Table AI.9 Copper Survey Database.

#	C#	Site Type	Site Number	Site Name	Artifact Type	Comments	Northing	Easting
1	C1	Detected location	N/A	N/A	None	False Positive	2611911	457597
2	C2	Detected location	N/A	N/A	None	False Positive	2597688	456218
3	C3	Detected location	N/A	N/A	None	False Positive	2597988	455903
4	C4	Tower	989-001	Safri 1	Slag	Discovered near Safri 1 in association w crucible base	2607158	451029
5	C5		976-001	N/A		Discovered in 2013 near 976-001	2598350	456195
6	C6	Detected location	N/A	N/A	None	False positive	2598435	455939
7	C7	Detected location	N/A	N/A	None	False Positive	2598342	455974
8	C8	Detected location	N/A	N/A	None	False Positive	2598256	455688
9	C9	Detected location	N/A	N/A	None	False Positive	2599193	455828
10	C10	Detected location	N/A	N/A	None	False Positive	2607122	460692
11	C11	Detected location	N/A	N/A	None	False Positive	2608109	456997
12	C12	Detected location	N/A	N/A	None	False Positive	2606264	461964
13	C13	Detected location	N/A	N/A	None	False Positive	2588732	457421
14	C14	Detected location	N/A	N/A	None	False Positive	2585774	457740
15	C15	Detected location	N/A	N/A	None	False Positive	2589085	457536
16	C16	Detected location	N/A	N/A	None	False Positive	2587342	457570
	C17	Tower				Discovered in 2013 near Khadil	2596510	464865

17			971-001	Khadil	Slag			
18	C18	Detected location	N/A	N/A	None	False Positive	2594614	457510
19	C19	Geologic Point	N/A	N/A	None	Potential Hawassina bedrock	2609527	459802
20	C20	Geologic Point	N/A	N/A	None	Potential Hawassina bedrock	2609189	459817
21	C21	Geologic Point	N/A	N/A	None	Potential Hawassina bedrock	2608940	459842
22	C22	Geologic Point	N/A	N/A	None	Initially identified as exploitation holes	2608828	459841
23	C23	Geologic Point	N/A	N/A	None	Initially identified as exploitation holes	2608273	459845
24	C24	Geologic Point	N/A	N/A	None	Initially identified as exploitation holes	2607750	460887
25	C25	Detected location	N/A	N/A	None	False Positive	2608729	460994
26	C26	Geologic Point	N/A	N/A	None	Initially identified as exploitation holes	2608585	460989
27	C27	Geologic Point	N/A	N/A	None	Initially identified as exploitation holes	2608457	460991
28	C28	Detected location	N/A	N/A	None	False Positive	2612453	457327
29	C29	Detected location	N/A	N/A	None	False Positive	2612268	457450
30	C30	Detected location	N/A	N/A	None	False Positive	2612309	457580
31	C31	Detected location	N/A	N/A	None	False Positive	2612304	457644
32	C32	Detected location	N/A	N/A	None	False Positive	2611330	457403
33	C33	Detected location	N/A	N/A	None	False Positive	2611380	457415
34	C34	Detected location	N/A	N/A	None	False Positive	2611391	457470
35	C35	Detected location	N/A	N/A	None	False Positive	2611381	457509
36	C36	Detected location	N/A	N/A	None	False Positive	2611607	457609
37	C37	Detected location	N/A	N/A	None	False Positive	2611597	457662
38	C38	Detected location	N/A	N/A	None	False Positive	2612952	459059
39	C39	Detected location	N/A	N/A	None	False Positive	2612893	459185
40	C40	Detected location	N/A	N/A	None	False Positive	2612995	459299
41	C41	Detected location	N/A	N/A	None	False Positive	2619055	462021
42	C42	Detected location	N/A	N/A	None	False Positive	2617968	461646
43	C43	Detected	N/A	N/A	None	False Positive	2611729	456695

		location						
44	C44	Detected location	N/A	N/A	None	False Positive	2607244	456072
45	C45	Settlement	962-001	Muaydin	Slag	Smelting site near copper source	2634511	437991
46	C46	Detected location	N/A	N/A	None	False Positive	2609894	456953
47	C47	Settlement	981-001	Raki 2	Slag and ore	Smelting site	2616583	457334
48	C48	Geologic Point	N/A	Raki modern mine	Copper Ore	geo samples - Cu in pil lav - fomer C#10	2618678	457362
49	C49	Detected location	N/A	N/A	None	False Positive	2627865	432946
50	C50	Detected location	N/A	N/A	None	False Positive	2609541	458594
51	C51	Artifact Scatter	31	N/A	Slag	Small slag scatter in Dhahir	2614659	459547
52	C52	Find Spot	921-001	N/A	Slag	Single piece near formerly detected area	2612833	458807
53	C53	Artifact Scatter	924-001	N/A	Slag	Slag scatter in wadi channel below mine	2619616	458462
54	C54	Mine	935-001	N/A	Slag	Copper mine (Iron Age & Islamic)	2619631	458502
55	C55	Exploitation Hole	N/A	N/A	None	Small exploitation holes near big mine	2619648	458482
56	C56	Exploitation Hole	N/A	N/A	None	Exploitation hole south of large mine	2619447	458263
57	C57	Detected location	962-001	Muaydin	Copper Ore	Collection in detected pixel	2634617	438232
58	C58	Detected location	962-001	Muaydin	None	False positive	2634518	438386
59	C59	Detected location	962-001	Muaydin	Copper Ore	Chrysocolla, ephemeral malachite, sample collected	2634558	438259
60	C60	Geologic Point	962-001	Muaydin	Copper Ore	copper ore washing down bedrock channel	2634557	438245
61	C61	Settlement	962-001	Muaydin	Slag	slag heap	2634550	438240
62	C62	Geologic Point	962-001	Muaydin	Copper Ore	ore source - in exploitation cut	2634680	438091
63	C63	Detected location	N/A	N/A	None	False Positive	2637542	434791
64	C64	Geologic Point	N/A	N/A	Copper Ore	disturbed area, sheeted dyke, gabbro, wadi	2637716	434713
65	C65	Artifact Scatter	923-001	N/A	Slag	slag enclosed poss tower, near detected pixel	2637780	434647
66	C66	Find Spot	922-001	N/A	Slag	slag findspot	2637814	434613

67	C67	Detected location	N/A	N/A	None	False positive - gabbro with desert varnish	2637907	434527
68	C68	Find Spot	925-001	N/A	Slag	single slag piece	2637861	434554
69	C69	Detected location	N/A	N/A	Copper Ore	near pixel; cut by recent digging	2637653	434799
70	C70	Artifact Scatter	920-001	N/A	Slag	on terrace in between wadi and mountain	2637617	435011
71	C71	Artifact Scatter	984-001	N/A	Copper Ore & slag	gossan	2615902	459807
72	C72	Settlement	936-001	Raki 1	Slag	smelting site near Raki mine	2618679	457508
73	C73	Geologic Point	984-001	N/A	Copper Ore	copper in gossan	2615932	459856
74	C74	Geologic Point	981-001	Raki modern mine	Copper Ore	azurite	2618698	457252
75	C75	Settlement and smelting site	984-001	Tawi Raki	Slag	slag heap	2616134	459749
76	C76	Settlement and smelting site	984-001	Tawi Raki	Slag	large slag heap	2616044	459720
77	C77	Artifact Scatter	926-001	N/A	Copper Ore	ore washed down slope with pottery	2615892	459895
78	C78	Settlement	984-001	Tawi Raki	Slag	on the slope near roaster	2616261	459862
79	C79	Detected location	N/A	N/A	None	false positive near smelting site	2618686	457584
80	C80	Detected location	N/A	N/A	Copper Ore	gossan in wadi channel being detected	2618342	457506
81	C81	Detected location	N/A	N/A	None	False Positive	2630543	443627
82	C82		N/A	N/A	Other		2633728	446608
83	C83	Detected location	N/A	N/A	Copper Ore	positive detection - 3 pix on ridge	2629021	443626
84	C84	Geologic Point	N/A	N/A	Copper Ore	small copper smear found through survey	2630238	443585
85	C85	Geologic Point	N/A	Sayyah	Copper Ore	copper deposit near large modern mine	2618751	453227
86	C86	Detected location	N/A	N/A	None	False positive - radiolarian chert - 260 m from det pix	2615048	459920
87	C87	Detected location	N/A	N/A	None	False positive	2615119	460072
88	C88	Detected location	N/A	N/A	None	False positive	2614252	459865
89	C89	Detected location	N/A	N/A	None	False positive	2614297	460118

90	C90	Detected location	N/A	N/A	None	False positive near F. Sudayriyin	2621846	449927
91	C91	Detected location	N/A	N/A	None	point on ridge close to inaccessible detection	2620339	448864
92	C92	Detected location	N/A	N/A	None	point on ridge close to inaccessible detection	2620362	445988
93	C93	Detected location	N/A	N/A	None	False positive	2620729	446159
94	C94	Detected location	N/A	N/A	None	False positive	2622199	443124
95	C95	Detected location	N/A	N/A	None	False positive	2625750	443230
96	C96	Geologic Point	984-001	N/A	Copper Ore	gossan with chalcopyrite	2616180	459807
97	C97	Detected location	N/A	N/A	None	False positive	2634726	446169
98	C98	Geologic Point	933-002	Zuha	Copper Ore	potential sulfide ore in pillow basalt	2675678	451899
99	C99	Geologic Point	933-003	Zuha	Copper Ore	ore in pillow basalt	2675683	451917
100	C100	Geologic Point	933-004	Zuha	Copper Ore	ore body sharp contact w pillow basalt	2675552	452172
101	C101	Geologic Point	933-005	Zuha	Copper Ore	modern mining pillow basalt with Cu on boundary	2675520	452204
102	C102	Geologic Point	N/A	Greater Arja Area	Copper Ore	ore sample near modern Arja mine	2692991	440280
103	C103	Geologic Point	N/A	Greater Arja Area	Copper Ore	copper ore in pillow basalt	2692855	441012
104	C104	Geologic Point	N/A	Greater Arja Area	Copper Ore	ore in pillow basalt with possible struct to south	2692946	440931
105	C105	Architectural Structure	952-002	Aqir Al-Shamoos 2	Slag	Slag scatter associated with architectural structure	2640283	434286
106	C106	Detected location	N/A	near Tawi Hareem	None	False positive near known copper source	2637338	434142
107	C107	Detected location	N/A	Tawi Hareem	Other	False positive near known copper source	2636115	434223
108	C108	Detected location	N/A	Wadi Hareem	Copper Ore	Positive detection	2636206	435077
109	C109	Detected location	N/A	Bayha	None	False positive over the town of Bayha	2638951	436594
110	C110	Smelting Site	932-001	Lasail	Slag	slag from section	2684896	442660
111	C111	Smelting Site	932-002	Lasail	Slag	Lasail general point	2684870	442661
112	C112	Smelting Site	932-003	Lasail	Slag	slag around resmelt depression	2684837	442630

113	C113	Smelting Site	932-004	Lasail	Slag	reddish slag from around depression	2684872	442619
114	C114	Settlement	931-001	Bayda	Slag	Islamic architecture w slag and pottery	2694802	439957
115	C115	Settlement	930-001	Tawi Arja	Slag	Slag scatter to south of "Ziggurat"	2693127	441033
116	C116	Settlement	930-001	Tawi Arja	Ceramics	Possible roaster on slope	2693213	440881
117	C117	Geologic Point	930-003	Tawi Arja	Copper Ore	Possible copper in pillow basalt above possible roaster	2693228	440874
118	C118	Settlement	930-001	Tawi Arja	Slag	Slag scatter with architecture on slope	2693227	440940
119	C119	Settlement	929-001	Arja	Slag	Slag scatter with architecture on slope	2693267	440993
120	C120	Settlement	994-001	Hayy Ukur	Slag	Slag scatter at site of Hayy Ukur	2632061	451436
121	C121	Geologic Point	N/A	N/A	None	Pillow basalts near detected pixels	2612525	462174
122	C122	Random Survey	Sector 268	N/A	None	SE corner of 268	2610807	454822
123	C123	Random Survey	Sector 286	N/A	None	SE corner of 286	2609947	454821
124	C124	Random Survey	Sector 374	N/A	None	SE corner of 374	2606274	459158
125	C125	Random Survey	Sector 39	N/A	None	SW corner of 39	2570999	450500
126	C126	Random Survey	Sector 78	N/A	None	SW corner of 78	2572001	453000
127	C127	Random Survey	Sector 358	N/A	None	SW corner of 358 - 90 m away	2580091	454001
128	C128	Random Survey	Sector 322	N/A	None	SW corner of 322	2578999	453501
129	C129	Random Survey	Sector 284	N/A	None	200 m from SW corner of 284	2577999	451687
130	C130	Random Survey	Sector 1038	N/A	None	SW corner of 1038 (1039 too steep)	2599500	458001
131	C131	Random Survey	Sector 433	N/A	None	SW corner of 433	2582500	448000
132	C132	Random Survey	Sector 1457	N/A	None	SW corner of 1457	2611997	454000
133	C133	Artifact Scatter	918-001	N/A	Slag	slag scatter	2612501	454002
134	C134	Geologic Point	N/A	N/A	Copper Ore	Possible copper ore in sheeted dyke	2614285	461544
135	C135	Random Survey	Sector 1540	N/A	None	200 m from SW corner of 1540	2614203	461503

136	C136	Random Survey	Sector 1513	N/A	None	SW corner of 1513	2613498	456501
137	C137	Detected location	N/A	N/A	None	False positive in radiolar chert & carbonate	2613185	456760
138	C138	Geologic location	N/A	Tawi Salamah	Copper Ore	Layered gabbro	2632688	440473
139	C139	Geologic location	N/A	Tawi Salamah	Copper Ore	Second Tawi Salamah outcrop with visible copper	2632554	441017
140	C140	Geologic location	N/A	Tawi Harim	Copper Ore	From Tawi Harim point from geological map	2637314	433765
141	C141	Geologic location	N/A	N of Ghadhiya	Copper Ore	Copper point from geological map	2620941	438315
142	C142	Artifact scatter	919-001	N of Ghadhiya	Slag	Collection of slag, ore pieces, pottery, furnace pieces	2621197	438682
143	C143	Settlement	952-001	Aqir Al-Shamoos	Slag	Slag scatter	2640365	434154
144	C144	Random Survey	Sector 1341	N/A	None	SW corner of 1341	2608500	456500
145	C145	Settlement	934-001	Al Arid	Slag	Slag from Sabatino	2592382	463370
146	C146	Find Spot	985-002	Hayy al-Nahza	Slag		2608999	456791
147	C147	Structure	997-027	Abu Suwaih	Slag		2612261	449819
148	C148	Settlement	984-001	Tawi Raki	Slag		2616044	459720
149	C149	Artifact Scatter	944-001		Slag		2609719	452549
150	C150	Settlement	N/A	Hala	Slag	Slag with architecture on slope	2578223	486879
151	C151	Detected location	N/A	Yankul Mt.	None	False positive - detecting pink limestone in fault line	2607102	455127
152	C152	Detected location	N/A	N/A	None	False positive - took sample	2633632	438187
153	C154	Settlement	973-001	Wadi Harim	Slag		2636540	435470
154	C157	Settlement	970-003	Qumaira	Slag		2640411	417478
155	C160	Structure	973-006	Wadi Harim	Slag		2636481	435491
156	C163	Settlement	950-001	Hayl al-Arb	Slag		2640765	433735

Table AI.10 Slag Groups by Period.

Slag Group	Bronze Age	Iron Age	Islamic Period	Indeterminate
Slag Group 1	0	0	2	0
Slag Group 2	0	5	2	1
Slag Group 3.1	4	15	15	2

Slag Group 3.2	2	17	17	4

Table AI.11 Slag Group at Bronze Age and Multi-period Sites.

Site	Slag Group 1	Slag Group 2	Slag Group 3.1	Slag Group 3.2	Total
C4	0	1	0	0	1
C17	0	0	1	1	2
C145	0	0	1	1	2
C154	0	0	1	0	1
C160	0	0	1	0	1

Table AI.12a Slag Groups at Iron Age Single Period Sites.

Site	Slag Group 1	Slag Group 2	Slag Group 3.1	Slag Group 3.2	Total
C47	0	1	1	1	3
C118	0	1	1	1	3
C120	0	1	1	0	2
C133	0	0	1	1	2
C148	0	0	0	1	1

Table AI.12b Slag Groups at Iron Age Multi-Period Sites.

Site	Slag Group 1	Slag Group 2	Slag Group 3.1	Slag Group 3.2	Total
C17	0	0	1	1	2
C47	0	1	1	1	3
C61	0	0	1	1	2
C71	0	0	1	1	2
C75	0	0	0	1	1
C76	0	0	0	1	1
C78	0	0	0	1	1
C105	0	1	1	0	2
C110	0	0	1	1	2
C112	0	0	1	1	2
C113	0	0	0	1	1
C118	0	1	1	1	3
C120	0	1	1	0	2
C133	0	0	1	1	2
C143	0	1	1	1	3
C145	0	0	1	1	2
C148	0	0	0	1	1
C150	0	0	1	1	2
C154	0	0	1	0	1
C160	0	0	1	0	1

Table AI.133a Slag Groups at Islamic Single Period Sites

Site	Slag Group 1	Slag Group 2	Slag Group 3.1	Slag Group 3.2	Total
C53	0	0	0	1	1
C72	0	0	0	1	1
C114	0	0	1	0	1
C115	0	0	1	1	2
C119	1	0	0	0	1
C142	0	0	1	1	2
C146	1	0	0	0	1
C157	0	0	1	0	1
C163	0	0	0	1	1

Table AI.13b Slag Groups at Islamic Multi-Period Sites.

Site	Slag Group 1	Slag Group 2	Slag Group 3.1	Slag Group 3.2	Total
C4	0	1	0	0	1
C17	0	0	1	1	2
C53	0	0	0	1	1
C61	0	0	1	1	2
C71	0	0	1	1	2
C72	0	0	0	1	1
C75	0	0	0	1	1
C76	0	0	0	1	1
C78	0	0	0	1	1
C105	0	1	1	0	2
C110	0	0	1	1	2
C112	0	0	1	1	2
C113	0	0	0	1	1
C114	0	0	1	0	1
C115	0	0	1	1	2
C119	1	0	0	0	1
C142	0	0	1	1	2
C143	0	1	1	1	3
C145	0	0	1	1	2
C146	1	0	0	0	1
C150	0	0	1	1	2
C154	0	0	1	0	1
C157	0	0	1	0	1
C160	0	0	1	0	1
C163	0	0	0	1	1

Table AI. 14 Longitudinal Overview of Centrality Measures by Node.

	Bronze Age						Iron Age					Islamic Period				
C	DC	BP	FBC	BCFP	CCAp	CCSG	DC	BP	FBC	BCFP	CCSG	DC	BP	FBC	BCFP	CCSG
4	1	136.467	0	0	17.067	11	N/A	N/A	N/A	N/A	N/A	2	382.375	2.125	0	42
17	5	975.71	5	2	13.976	6	29	5768.846	22.823	1.818	19	30	5974.359	27.871	3.5	23
47	N/A	N/A	N/A	N/A	N/A	N/A	33	6515.142	25.251	1.818	19	N/A	N/A	N/A	N/A	N/A
51	N/A	N/A	N/A	N/A	N/A	N/A	N/A	N/A	N/A	N/A	N/A	N/A	N/A	N/A	N/A	N/A
52	N/A	N/A	N/A	N/A	N/A	N/A	N/A	N/A	N/A	N/A	N/A	N/A	N/A	N/A	N/A	N/A
53	N/A	N/A	N/A	N/A	N/A	N/A	N/A	N/A	N/A	N/A	N/A	16	3258.213	13.125	0	28
61	N/A	N/A	N/A	N/A	N/A	N/A	29	5768.846	22.823	1.818	19	30	5974.359	27.871	3.5	23
65	N/A	N/A	N/A	N/A	N/A	N/A	N/A	N/A	N/A	N/A	N/A	N/A	N/A	N/A	N/A	N/A
71	N/A	N/A	N/A	N/A	N/A	N/A	29	5768.846	22.823	1.818	19	30	5974.359	27.871	3.5	23
72	N/A	N/A	N/A	N/A	N/A	N/A	N/A	N/A	N/A	N/A	N/A	16	3258.213	13.125	0	28
75	N/A	N/A	N/A	N/A	N/A	N/A	15	3020.101	11.501	0	23	16	3258.213	13.125	0	28
76	N/A	N/A	N/A	N/A	N/A	N/A	15	3020.101	11.501	0	23	16	3258.213	13.125	0	28
78	N/A	N/A	N/A	N/A	N/A	N/A	15	3020.101	11.501	0	23	16	3258.213	13.125	0	28
105	N/A	N/A	N/A	N/A	N/A	N/A	18	3837.032	11.394	0	24	16	3207.049	34.571	6.5	29
110	N/A	N/A	N/A	N/A	N/A	N/A	29	5768.846	22.823	1.818	19	30	5974.359	27.871	3.5	23

111	N/A	N/A	N/A	N/A	N/A	N/A	N/A	N/A	N/A	N/A	N/A	N/A	N/A	N/A	N/A	N/A
112	N/A	N/A	N/A	N/A	N/A	N/A	29	5768.846	22.823	1.818	19	30	5974.359	27.871	3.5	23
113	N/A	N/A	N/A	N/A	N/A	N/A	15	3020.101	11.501	0	23	16	3258.213	13.125	0	28
114	N/A	N/A	N/A	N/A	N/A	N/A	N/A	N/A	N/A	N/A	N/A	14	2950.447	13.268	0	30
115	N/A	N/A	N/A	N/A	N/A	N/A	N/A	N/A	N/A	N/A	N/A	30	5974.359	27.871	3.5	23
118	N/A	N/A	N/A	N/A	N/A	N/A	33	6515.142	25.251	1.818	19	N/A	N/A	N/A	N/A	N/A
119	N/A	N/A	N/A	N/A	N/A	N/A	N/A	N/A	N/A	N/A	N/A	1	1.043	0	0	Exc.
120	N/A	N/A	N/A	N/A	N/A	N/A	18	3837.032	11.394	0	24	N/A	N/A	N/A	N/A	N/A
133	N/A	N/A	N/A	N/A	N/A	N/A	29	5768.846	22.823	1.818	19	N/A	N/A	N/A	N/A	N/A
142	N/A	N/A	N/A	N/A	N/A	N/A	N/A	N/A	N/A	N/A	N/A	30	5974.359	27.871	3.5	23
143	N/A	N/A	N/A	N/A	N/A	N/A	33	6515.142	25.251	1.818	19	32	6111.665	52.871	17	22
145	5	975.71	5	2	13.976	6	29	5768.846	22.823	1.818	19	30	5974.359	27.871	3.5	23
146	N/A	N/A	N/A	N/A	N/A	N/A	N/A	N/A	N/A	N/A	N/A	1	1.043	0	0	Exc.
147	N/A	N/A	N/A	N/A	N/A	N/A	N/A	N/A	N/A	N/A	N/A	N/A	N/A	N/A	N/A	N/A
148	N/A	N/A	N/A	N/A	N/A	N/A	15	3020.101	11.501	0	23	N/A	N/A	N/A	N/A	N/A
149	3	533.328	8.4	4	13.067	7	N/A	N/A	N/A	N/A	N/A	N/A	N/A	N/A	N/A	N/A
150	N/A	N/A	N/A	N/A	N/A	N/A	29	5768.846	22.823	1.818	19	30	5974.359	27.871	3.5	23

154	3	668.454	1.733	0	15.257	8	14	2963.347	8.895	0	24	14	2950.447	13.268	0	30
157	N/A	N/A	N/A	N/A	N/A	N/A	N/A	N/A	N/A	N/A	N/A	14	2950.447	13.268	0	30
160	3	668.454	1.733	0	15.257	8	14	2963.347	8.895	0	24	14	N/A	13.268	0	30
163	N/A	N/A	N/A	N/A	N/A	N/A	N/A	N/A	N/A	N/A	N/A	16	N/A	13.125	0	28

Appendix II: Obsidian Supply Network Dataset

Table II. 1 Cluster Stats for SRSAH Survey Area Obsidian.

		Rb	Rb	Rb	Sr	Sr	Sr	Y	Y	Y	Zr	Zr	Zr	Nb	Nb	Nb
Chemical Group	N =	Mean	Std Dev	CoV	Mean	Std Dev	CoV	Mean	Std Dev	CoV	Mean	Std Dev	CoV	Mean	Std Dev	CoV
C	256	99	5	5	49	3	7	41	3	6	250	9	4	75	4	5
D	1	122	8	7	59	5	8	48	3	7	311	13	4	89	4	5
E	31	102	8	8	13	4	32	57	3	5	379	14	4	116	6	5
F	15	134	7	5	16	2	14	70	3	4	486	19	4	105	9	9
G	18	141	17	12	9	8	86	84	4	5	576	27	5	125	23	18
H	3	161	27	17	6	2	35	109	6	6	762	44	6	133	19	14

Table II. 2 Group C Chemical Composition.

Specimen	MnKa1	FeKa1	ZnKa1	GaKa1	ThLa1	RbKa1	SrKa1	YKa1	ZrKa1	NbKa1	Chemical Group
s_93_071_001-b3-001	334	13648	58	22	11	99	51	41	256	77	C
s1_006-001-B45-L60-l1-b3	233	13123	56	23	15	93	46	39	260	74	C
s100_071-001-b3-001	372	14048	42	21	15	97	51	44	263	73	C
s101_071-001-b3-001	338	13547	46	23	13	104	48	41	259	78	C
s103_071-001-b3-001	344	13967	53	18	12	99	46	41	260	78	C
s104_071-001-b3-001	261	13572	52	23	10	100	49	42	257	72	C
s105_071-001-b3-001	193	13551	49	23	10	103	47	43	253	72	C
s108_071-001-b3-001	216	14217	61	20	14	98	50	41	254	72	C
s109_071-001-b3-001	342	14095	50	22	10	95	48	40	266	73	C
s11_006-001-B45-L64-l1-b7	246	13116	49	15	13	93	49	41	252	73	C
s110_071-001-b3-001	289	13713	58	19	13	100	50	39	262	76	C
s111_071-001-b3-001	362	13541	45	20	11	100	48	38	251	73	C
s112_071-001-b3-001	227	13550	54	18	11	102	48	39	244	73	C
s115_071-001-b3-001	272	13131	53	22	9	96	48	37	240	68	C
s116_071-001-b3-001	317	13870	54	22	12	103	47	42	260	71	C
s117_071-001-b3-001	230	13162	59	18	13	88	45	39	244	74	C
s118_071-001-b3-001	288	13048	39	21	9	95	45	40	237	71	C
s119_071-001-b3-001	77	12475	40	18	11	98	47	37	245	71	C
s12_006-001-B28-L62-l2-b4	176	12815	54	19	9	95	47	37	240	70	C
s121_071-001-b3-001	262	13776	55	20	11	104	50	43	256	75	C

s122_071-001-b3-001	290	13323	45	20	14	97	50	37	261	73	C
s123_071-001-b3-001	307	13360	51	19	12	100	48	37	246	70	C
s124_071-001-b3	290	13128	50	20	10	101	48	38	247	71	C
s125_069_001-b2-001	177	13501	40	22	11	102	49	44	258	77	C
s127_069_001-b2-001	208	12472	36	21	10	92	45	38	234	72	C
s128_069_001-b2-001	285	13431	47	20	11	98	47	40	254	75	C
s13_006-001-B28-L62-l2-b4	140	14102	57	21	12	101	46	43	256	71	C
s130_069_001-b2-001	196	13828	63	21	12	98	47	40	255	75	C
s131_069_001-b2-001	341	13296	59	21	10	102	49	38	251	76	C
s133_071_001-b2-001	238	12761	51	18	11	96	48	43	245	72	C
s134_071_001-b2-001	201	13979	47	20	13	98	46	45	263	75	C
s135_071_001-b2-001	238	13144	45	21	12	97	47	40	263	77	C
s14_006-001-B45-L64-l2-b15	165	12330	57	18	13	88	45	37	235	68	C
s140_071_001-b2-001	200	14052	52	23	11	99	53	36	259	76	C
s141_071_001-b2-001	371	13509	43	21	14	105	48	39	259	73	C
s142_079_001-b2-001	307	13376	55	18	13	103	49	39	257	75	C
s143_079_001-b2-001	246	13160	55	20	11	96	44	40	250	69	C
s145_079_001-b2-001	235	13316	44	21	13	99	48	38	250	73	C
s146_079_001-b2-001	199	13965	52	21	13	98	47	42	262	71	C
s147_079_001-b2-001	400	12789	53	19	12	93	46	39	245	71	C
s149_071_002-b1-001	252	13483	43	21	13	100	50	41	251	75	C
s15_006-001-B35-L68-l1-b5	207	13605	50	19	12	104	51	41	248	70	C
s150_071_002-b1-001	175	12717	38	20	13	94	48	40	252	72	C
s153_052-b2-001	283	13491	54	20	14	101	46	37	260	76	C
s154_027_001-b2-001	264	13457	42	21	10	96	47	41	255	75	C
s155_027_001-b2-001	231	12410	55	17	9	95	45	38	240	65	C
s156_027_001-b2-001	196	14320	47	19	13	97	50	40	249	73	C
s157_027_001-b2-001	139	13002	43	19	7	97	46	40	239	70	C
s158_027_001-b2-001	262	12880	47	18	11	94	48	38	253	69	C
s159_027_001-b2-001	177	12250	42	20	11	90	44	36	224	64	C
s16_006-001-B35-L68-l1-b5	137	13128	55	23	10	101	48	39	257	74	C
s160_027_001-b2-001	180	12991	42	23	13	102	47	36	253	73	C
s161_027_001-b2-001	185	13187	60	22	11	98	47	40	256	74	C
s162_027_001-b2-001	272	13454	52	18	9	97	49	41	252	79	C

s163_027_001-b2-001	181	12610	55	18	10	92	46	38	235	69	C
s164_027_001-b2-001	215	13117	45	19	11	99	47	36	253	76	C
s165_027_001-b2-001	420	14194	50	20	11	102	51	42	261	77	C
s166_027_001-b2-001	217	13320	50	19	11	96	47	42	245	66	C
s167_027_001-b2-001	253	13243	51	19	10	98	48	41	243	69	C
s168_027_001-b2-001	367	13595	48	20	9	102	46	37	251	72	C
s169_027_001-b2-001	181	13608	44	20	11	97	46	40	258	75	C
s17_006-001-B45-L64-l2-b3	295	13082	53	18	10	96	43	41	242	72	C
s170_027_001-b2-001	237	13113	50	18	10	96	49	38	246	75	C
s171_027-001-b2-001	387	13614	62	18	12	100	48	39	245	70	C
s172_027-001-b2-001	146	11899	48	19	11	89	42	38	239	68	C
s173_027-001-b2-001	292	14420	62	21	11	95	43	39	249	71	C
s174_027-001-b2-001	192	12470	49	19	12	89	47	36	235	72	C
s175_027-001-b2-001	136	12966	44	19	10	98	47	37	245	72	C
s176_027-001-b2-001	211	13251	51	20	10	105	47	44	261	75	C
s177_027-001-b2-001	367	13302	49	21	15	99	50	39	265	78	C
s178_027-001-b2-001	176	14215	58	19	14	104	50	45	259	74	C
s179_027-001-b2-001	262	13244	44	21	12	94	47	40	246	72	C
s18_006-001-B38-L62-l1-b7	338	13584	57	21	11	104	50	40	259	77	C
s180_027-001-b2-001	302	13365	62	21	12	100	47	42	247	71	C
s181_027-001-b2-001	262	13881	57	18	12	98	48	41	251	72	C
s182_027-001-b2-001	262	13018	48	22	9	94	46	38	244	73	C
s183_027-001-b2-001	278	13547	54	20	10	99	49	40	249	74	C
s184_027-001-b2-001	195	12676	40	20	10	93	50	41	243	67	C
s185_027-001-b2-001	318	12358	60	19	8	88	42	37	226	64	C
s186_027-001-b2-001	281	12934	45	20	12	93	51	37	248	72	C
s187_027-001-b2-001	287	13637	59	20	12	99	50	43	256	75	C
s188_027-001-b2-001	294	13877	64	21	10	95	49	42	248	75	C
s189_027-001-b2-001	193	13129	53	19	14	98	48	39	245	75	C
s19_006-001-B38-L62-l1-b7	225	13056	62	19	10	106	50	40	254	73	C
s190_027-001-b2-001	231	13625	52	20	11	99	47	44	249	72	C
s191_027-001-b2-001	281	14206	41	21	12	96	47	40	256	75	C
s192_027-001-b2-001	247	13409	53	20	12	99	45	40	255	68	C
s193_027-001-b2-001	319	14210	59	20	13	97	51	40	250	79	C

s194_027-001-b2-001	186	11888	47	20	6	91	43	36	236	69	C
s195_027-001-b2-001	347	13305	59	21	14	96	49	38	248	71	C
s196_027-001-b2-001	294	13281	65	19	11	99	46	40	250	74	C
s197_027-001-b2-001	241	12970	40	19	10	95	46	40	245	71	C
s198_027-001-b2-001	242	12351	47	16	9	91	43	35	227	65	C
s199_027-001-b2-001	261	13805	46	22	10	95	51	40	249	71	C
s2_006-001-B35-L61-l1-b5	299	13868	64	19	12	102	51	38	256	77	C
s20_071-001-b3-001	453	13310	52	20	11	97	50	44	249	74	C
s200_016-001-b2-001	323	13394	52	22	10	102	46	38	257	72	C
s201_016-001-b2-001	307	13082	53	21	9	95	49	41	246	73	C
s202_016-001-b2-001	226	11783	44	20	13	91	42	38	239	67	C
s203_017-001-b2-001	221	13715	56	20	12	103	48	36	257	75	C
s204_026-001-b3-001	222	13143	47	17	8	92	46	42	245	71	C
s205_042-001-b1-001	167	12636	53	18	9	91	45	33	224	63	C
s208_009a-b2-001	262	12037	40	16	9	88	45	38	228	66	C
s210_008A-b1-001	299	13364	50	17	12	100	50	42	246	72	C
s214_027-001-b2-001	181	13248	34	19	11	98	51	38	249	72	C
s216_027-001-b2-001	206	13700	42	16	10	101	48	41	250	74	C
s217_61A-b1-001	292	13194	46	19	13	98	46	39	243	72	C
s219_25A-b2-001	160	12858	42	21	10	95	47	36	244	71	C
s22_006-001-B45-L60-l2-b6	229	14570	64	18	13	103	54	45	260	74	C
s220_014-002-b2-001	340	13169	51	23	13	95	46	42	251	74	C
s221_014-002-b2-001	130	13291	52	20	10	98	49	40	261	70	C
s222_068-001-b2-001	141	12626	49	21	13	98	46	36	248	69	C
s223_068-001-b2-001	263	13291	44	21	12	97	48	42	252	77	C
s224_068-001-b2-001	294	13860	55	19	12	96	51	36	246	73	C
s226_022-003-b2-001	273	12277	40	21	12	108	45	38	246	71	C
s228_24B-b1-001	222	13271	57	17	14	92	45	39	239	72	C
s229_014-002-b2-001	292	14801	61	21	10	98	51	43	253	76	C
s230_014-002-b2-001	247	13136	46	19	11	94	51	40	255	71	C
s231_024-001-b2-001	322	13306	43	21	10	96	47	36	249	75	C
s233_024-001-b2-001	243	12679	61	17	12	91	47	40	239	69	C
s234_024-021-b2-001	213	13623	46	19	14	98	49	41	251	73	C
s235_024-021-b2-001	253	14438	77	20	12	104	49	42	256	76	C

s236_024-021-b2-001	184	13570	49	23	7	93	47	38	250	74	C
s237_014-001-b2-001	175	13352	47	20	13	97	45	41	250	75	C
s238_014-001-b2-001	186	13424	57	20	10	95	45	40	242	75	C
s239_014-001-b2-001	331	13374	54	20	10	100	49	38	251	73	C
s24_006-001-B35-L70-l1-b1	325	13095	46	20	10	99	48	39	260	75	C
s240_014-001-b2-001	243	12927	46	18	15	98	46	39	249	74	C
s241_014-001-b2-001	234	13571	44	20	13	100	50	43	253	77	C
s242_067-001-b2-001	245	13492	49	22	11	99	46	41	252	75	C
s243_067-001-b2-001	230	12509	42	18	8	99	48	39	234	73	C
s244_067-001-b2-001	254	13824	57	20	12	102	52	43	256	73	C
s245_067-001-b2-001	107	13267	50	21	11	101	48	39	248	73	C
s246_067-001-b2-001	216	12834	54	18	8	100	45	42	247	74	C
s247_026-001-b2-001	215	12718	44	22	12	98	46	38	242	67	C
s248_026-001-b2-001	199	12860	51	17	13	93	46	39	241	69	C
s250_026-001-b2-001	224	12625	63	18	12	98	46	40	252	69	C
s251_071-001-b1-001	242	13391	42	20	13	105	45	38	244	74	C
s252_071-001-b1-001	234	13480	54	18	7	89	45	38	234	73	C
s253_071-001-b1-001	359	13057	45	19	12	98	45	33	240	73	C
s254_071-001-b1-001	116	12832	48	20	12	95	47	40	240	64	C
s255_071-001-b1-001	289	13273	47	21	12	100	49	40	258	76	C
s256_022-001-b2-001	277	13340	48	19	14	97	46	37	249	74	C
s257_022-001-b2-001	208	11870	52	21	8	93	44	37	237	68	C
s258_022-001-b2-001	267	12471	54	21	12	94	44	42	258	73	C
s26_006-001-B48-L67-l2-b3	195	13292	56	22	15	99	49	40	258	71	C
s260_022-002-b2-001	223	11508	60	17	10	83	41	33	206	58	C
s261_022-002-b2-001	281	13682	46	20	12	98	49	39	255	77	C
s262_022-002-b2-001	221	12987	39	21	10	97	47	40	247	74	C
s263_022-002-b2-001	311	13136	51	17	12	97	48	38	242	69	C
s264_024-003-b2-001	306	13171	61	17	12	100	46	40	252	73	C
s265_024-003-b2-001	232	13034	53	20	14	96	45	37	249	70	C
s267_024_003-b2-001	191	13236	57	20	10	98	45	40	245	74	C
s27_006-001-B25-L80-l1-b5	258	12652	62	19	12	97	47	41	243	73	C
s271_044-001-b2-001	248	12667	56	19	8	100	44	38	242	71	C
s272_044-001-b2-001	255	13337	51	20	14	102	50	38	257	71	C

s273_044-001-b2-001	355	13311	50	19	12	93	48	41	248	69	C
s275_044-001-b2-001	211	12421	39	18	9	97	48	34	232	70	C
s276_024-002-b3-001	266	13016	33	16	10	92	45	38	224	68	C
s281_013-001-b2-001	274	12267	38	19	10	95	44	39	232	65	C
s282_013-001-b2-001	313	13383	58	20	12	97	48	44	248	73	C
s283_013-001-b2-001	296	13542	49	22	13	96	47	41	246	71	C
s284_013-001-b2-001	231	13180	53	18	11	95	46	35	245	68	C
s285_013-001-b2-001	219	13302	55	19	12	92	45	37	249	72	C
s286_013-001-b2-001	284	13045	57	21	10	99	48	41	257	74	C
s287_006-001-B25-L60-l2-b6-001	81	11909	52	17	10	93	43	40	242	69	C
s288_006-001-B26-L96-l1-b15-001	363	13698	41	21	11	101	47	41	254	75	C
s29_006-001-B26-L85-l1-b3-001	298	13020	46	19	14	96	47	42	258	77	C
s290_006-001-B25-L81-l1-b8-001	234	13648	52	18	12	100	51	39	252	71	C
s291_006-001-B26-L96-l1-b3-001	229	12602	50	20	10	98	43	39	237	67	C
s292_006_001-A76-L31-b3-001	302	13889	42	20	13	96	48	47	262	75	C
s293_006_001-A75-L64-b0-001	388	17985	53	17	10	93	48	40	244	74	C
s294_006_001-A76-L29-b1-001	388	16115	47	20	13	95	53	43	244	71	C
s295_006_001-A75-L66-b2-001	364	16007	59	19	11	102	54	41	248	73	C
s298_006_001-A65-47-b4-001	243	12877	48	22	10	93	45	38	244	69	C
s299_006_001-A76-L31-b5-001	264	12774	53	22	12	101	48	40	251	71	C
s30_006-001-B28-L62-l3-b17-001	271	13106	51	21	12	100	49	45	261	75	C
s300_006_001-A75-L64-b6-001	195	12370	47	19	10	90	46	38	233	74	C
s301_006_001-A76-L46-b4-001	390	19336	56	18	9	98	51	36	259	75	C
S302_044_001-B2-001	264	13318	41	21	13	100	49	38	247	71	C
S303_044_001-B2-001	197	14096	58	21	12	104	47	40	260	77	C
S304_044_001-B2-001	272	13297	56	19	11	103	48	43	252	68	C
s306_027_001-b2-001	234	13141	53	20	10	100	49	35	245	73	C
s307_027_001-b2-001	382	13815	56	19	10	100	49	41	247	76	C
s308_027_001-b2-001	330	13416	48	19	11	98	49	41	249	73	C
s309_027_001-b2-001	293	14005	45	22	12	100	48	41	260	74	C
s31_029-002-b2-001	274	12865	59	17	11	93	49	43	249	73	C
s310_027_001-b2-001	336	13465	49	20	11	98	50	37	254	76	C
s311_027_001-b2-001	270	12913	54	17	9	97	44	36	241	72	C
s312_069_004-b2-001	351	13478	43	19	12	102	48	41	259	75	C

s313_069_004-b2-001	227	12705	53	18	11	93	47	41	239	72	C
s314_069_004-b2-001	225	12532	54	17	11	92	47	37	237	66	C
s315_071_002-b2-001	371	14029	52	20	9	106	43	40	259	72	C
s32_029-002-b2-001	250	13061	50	20	13	94	46	41	249	71	C
s321_002_001-b4-001	192	13124	41	20	10	95	46	37	244	73	C
s322_002_001-b4-001	350	13346	63	18	10	99	48	43	258	73	C
s323_002_001-b4-001	491	13249	48	21	8	100	45	37	244	75	C
s324_071_001-b2-001	357	13625	57	18	13	95	46	39	253	72	C
s325_071_001-b2-001	125	12442	50	19	10	87	44	36	231	71	C
s327_027-001-b2-001	241	12676	53	20	10	91	42	40	232	70	C
s33_029-002-b2-001	390	12915	46	23	12	96	49	44	253	75	C
s34_029-002-b2-001	306	12116	48	20	8	92	46	36	230	68	C
s35_029-002-b2-001	304	13917	50	20	13	104	49	40	259	77	C
s36_029-002-b2-001	265	13910	57	19	11	106	51	40	260	74	C
s37_029-002-b2-001	296	13698	57	21	11	101	53	42	262	76	C
s38_029-002-b2-001	260	14293	59	22	10	101	53	43	266	77	C
s39_029-002-b2-001	295	13989	47	21	16	101	53	40	259	73	C
s40_029-002-b2-001	299	13766	32	21	14	97	49	43	260	71	C
s41_029-002-b2-001	168	13338	52	21	13	94	47	41	251	77	C
s42_029-002-b2-001	324	14089	50	20	11	96	54	40	258	74	C
s43_029-002-b2-001	212	13357	41	23	9	104	48	41	264	76	C
s44_029-002-b2-001	241	13401	51	19	10	99	50	38	253	78	C
s45_029-002-b2-001	261	14622	54	24	13	104	50	41	259	75	C
s46_029-002-b2-001	235	13561	50	20	10	102	48	40	249	76	C
s47_029-002-b2-001	220	13850	53	21	12	103	49	43	261	74	C
s48_029-002-b2-001	357	13656	57	21	13	104	47	39	254	74	C
s49_029-002-b2-001	362	13636	43	19	11	96	45	41	244	71	C
s5_006-001-B48-L62-l1-b2	283	13978	59	20	13	103	50	45	262	74	C
s50_002-001-b2-001	220	13252	60	20	13	104	46	40	250	76	C
s52_002-001-b2-001	210	13129	49	21	10	94	48	40	246	71	C
s54_002-001-b2-001	362	13656	46	21	14	98	52	41	253	70	C
s55_002-001-b2-001	305	13387	43	23	13	99	51	40	260	75	C
s57_002-001-b2-001	204	13281	37	20	11	100	46	40	256	72	C
s59_002-001-b2-001	297	13603	68	22	13	102	47	40	266	77	C

s6_006-001-B48-L62-l1-b2	271	15555	81	24	15	106	51	44	277	77	C
s60_002-001-b2-001	310	14155	47	19	10	99	54	37	266	72	C
s61_002-001-b2-001	304	13477	34	21	11	92	45	42	264	68	C
s62_002-001-b2-001	204	13205	54	18	11	103	47	38	251	73	C
s63_002-001-b2-001	322	12603	57	18	12	93	40	36	226	65	C
s64_002-001-b2-001	280	12523	45	18	10	97	42	38	244	69	C
s65_002-001-b2-001	250	13667	56	20	14	101	47	39	264	74	C
s66_002-001-b2-001	287	13317	50	20	11	92	51	37	245	71	C
s67_002-001-b2-001	96	12504	57	19	11	90	44	37	242	66	C
s68_002-001-b2-001	256	12712	61	20	12	94	46	37	243	69	C
s69_002-001-b2-001	289	12155	55	20	9	94	44	38	237	69	C
s7_006-001-B35-L60-l1-b3	280	13191	55	22	9	97	50	39	250	75	C
s70_002-001-b2-001	298	13658	60	19	13	93	49	40	256	73	C
s71_078-b1-001	289	13493	64	20	11	104	46	39	252	75	C
s73_079A-b2-001	272	13680	54	20	9	97	46	39	246	73	C
s74_079A-b2-001	269	14033	45	20	12	100	48	40	251	75	C
s76_079A-b2-001	432	13920	56	20	10	101	50	42	260	68	C
s77_079A-b2-001	206	15230	63	19	11	101	51	37	255	71	C
s78_029-003-b2-001	326	13185	54	20	12	101	46	39	248	74	C
s82_097A-b1-001	324	13663	54	24	8	103	45	38	266	77	C
s83_007-001-b2-001	263	13141	45	21	11	95	49	41	249	70	C
s84_081-001-b2-001	223	13321	53	20	13	101	50	44	255	74	C
s85_081-001-b2-001	225	13442	60	19	12	99	49	38	256	73	C
s89_999-001-b2-001	184	13105	38	23	14	100	45	39	243	70	C
s9_006-001-B45-L60-l1-b22	259	14046	56	23	10	98	55	39	260	73	C
s90_999-001-b2-001	348	13333	48	19	11	98	44	38	250	74	C
s92_071-001-b3-001	368	13500	46	21	10	99	47	39	248	75	C
s95_071_001-b3-001	276	12783	40	19	9	102	47	40	249	74	C
s96_071_001-b3-001	166	12890	41	19	13	92	47	41	244	73	C
s97_071-001-b3-001	290	13544	59	20	11	99	46	39	245	74	C
s98_071-001-b3-001	153	13418	38	18	11	96	48	38	255	71	C
s99_071-001-b3-001	142	13280	60	22	11	95	48	37	252	70	C

Table II. 3 Group D Chemical Composition.

Specimen	MnKa 1	FeKa 1	ZnKa 1	GaKa 1	ThLa 1	RbKa 1	SrKa 1	YKa 1	ZrKa 1	NbKa 1	Obsidian Group
s207_13A-b1-001	385	15422	96	19	9	102	25	59	323	90	D

Table II. 4 Group E Chemical Composition.

Specimen	MnKa1	FeKa 1	ZnKa1	GaKa1	ThLa 1	RbKa1	SrKa 1	Y Ka1	ZrKa 1	NbKa1	Chemical Group
s10_006-001-B45-L64-l1-b7	363	17141	96	22	10	104	6	54	370	112	E
s102_071-001-b3-001	485	22833	122	20	12	108	8	58	362	126	E
s126_069_001-b2-001	440	18137	120	19	12	93	13	55	363	108	E
s129_069_001-b2-001	529	17477	91	22	9	97	15	55	387	113	E
s132_071_001-b2-001	386	16729	111	20	12	97	14	51	365	106	E
s136_071_001-b-001	504	17554	103	24	14	104	16	55	399	112	E
s144_079_001-b2-001	581	17204	84	20	16	97	16	54	387	113	E
s148_079_001-b2-001	550	15984	95	20	12	103	13	55	367	112	E
s151_071_002-b1-001	524	18212	101	20	10	93	14	57	356	108	E
s152_071_002-b1-001	524	17848	110	20	11	101	13	59	410	113	E
s206_13A-b1-001	480	18154	103	19	9	108	15	57	385	110	E
s207_13A-b1-001	385	15422	96	19	9	102	25	59	323	90	E
s209_009a-b2-001	605	17726	104	20	10	97	12	58	381	114	E
s211_081A-b1-001	523	16038	98	22	11	99	12	53	384	111	E
s212_009a-b2-001	321	16654	95	20	13	97	14	53	371	113	E
s215_027-001-b2-001	504	17676	97	21	10	99	15	56	383	114	E
s227_24B-b1-001	549	16622	111	20	9	92	13	54	354	111	E
s23_006-001-B38-L65-l1-b19	520	19186	101	23	14	120	3	60	411	125	E
s266_024_003-b2-001	552	17356	90	23	12	97	14	55	394	112	E
s268_024_003-b2-001	497	17123	103	19	9	94	13	54	370	112	E
s269_024_003-b2-001	586	17544	95	21	11	102	14	55	395	118	E
s270_024_003-b2-001	346	17440	104	21	15	104	15	56	380	117	E
s297_006_001-A65-47-b4-001	497	17130	106	22	14	99	14	58	400	116	E
s316_071_002-b2-001	447	18020	129	18	13	97	12	58	381	107	E
s320_002_001-b4-001	403	16764	83	20	10	98	14	53	368	114	E
s326_071-002-1-001	564	16860	91	19	11	97	13	51	366	110	E
s328_006-001-A76-L31-l1-b5-001	692	18658	99	20	12	114	3	54	386	117	E

s72_010-001-b3-001	618	23889	142	25	14	107	5	62	376	126	E
s79_069-b2-001	624	18906	101	22	13	97	13	54	377	116	E
s80_069-b2-001	483	19187	112	20	13	102	14	59	399	110	E
s81_097A-b1-001	499	18317	103	21	8	97	12	54	368	108	E
s86_042-002-b3-001	505	17829	115	19	11	101	14	54	377	108	E

Table II. 5 Group F Chemical Composition.

Specimen	MnKa1	FeKa1	ZnKa1	GaKa1	ThLa1	RbKa1	SrKa1	Y Ka1	ZrKa1	NbKa1	Chemical Group
s138_071_001-b2-001	239	14024	95	21	16	133	15	72	479	105	F
s213_009a-b2-001	275	14152	104	23	14	133	15	71	494	103	F
s259_044-001-b3-001	229	13526	100	21	15	133	14	69	487	101	F
s277_024-002-b3-001	185	13459	107	22	15	133	14	75	496	107	F
s278_024-002-b3-001	97	13634	103	21	15	139	13	66	478	98	F
s279_024-002-b3-001	259	12588	86	22	15	126	14	67	450	97	F
s280_024-002-b3-001	164	13329	78	19	15	128	15	72	484	103	F
s289_006-001-B26-L96-l1-b15-001	182	13958	95	24	16	138	16	71	501	103	F
s296_006_001-A75-L66-b1-001	264	14349	110	23	14	147	16	74	509	103	F
s318_071_001-b3-001	277	13942	111	22	14	134	15	72	481	98	F
s51_002-001-b2-001	235	14634	111	25	17	137	15	73	526	103	F
s53_002-001-b2-001	205	13320	103	20	11	134	16	67	470	101	F
s56_002-001-b2-001	201	13369	105	22	16	140	14	71	503	102	F
s87_999-001-b2-001	295	12880	106	23	16	127	15	67	457	98	F
s88_999-001-b2-001	177	13589	92	22	16	134	15	69	479	102	F

Table II. 6 Group G Chemical Composition.

Specimen	MnKa1	FeKa1	ZnKa1	GaKa1	ThLa1	RbKa1	SrKa1	Y Ka1	ZrKa1	NbKa1	Chemical Group
s_94_071_001-b3-001	438	19259	143	22	16	138	6	83	591	120	G
s106_071-001-b3-001	273	18764	161	23	15	129	6	80	548	112	G
s107_071-001-b3-001	341	18651	138	25	16	130	7	81	557	112	G
s113_071-001-b3-001	334	19320	135	22	18	136	7	83	584	118	G
s114_071-001-b3-001	246	18157	118	21	17	133	7	85	568	115	G
s137_071_001-b-001	324	18859	139	24	13	145	6	82	583	118	G
s139_071_001-b2-001	492	19695	127	21	14	137	6	83	549	114	G
s21_006-001-B45-L60-l1-b12	164	19704	133	22	18	136	6	89	582	121	G

s218_008-001-b2-001	412	19559	131	26	16	139	5	84	603	122	G
s225_068-001-b2-001	310	18400	114	24	15	135	7	79	534	110	G
s232_024-001-b2-001	413	18317	139	22	17	135	6	81	554	111	G
s249_026-001-b2-001	346	18666	140	22	15	133	7	82	554	113	G
s25_006-001-B35-L70-l1-b9	311	23052	157	26	17	149	5	88	612	118	G
s28_006-001-B47-L000-b4-001	423	18020	142	23	13	130	7	78	547	109	G
S305_044_001-B2-001	336	19027	125	24	18	133	5	82	578	117	G
s317_071_001-b3-001	295	19789	122	22	19	136	6	84	593	118	G
s319_071_001-b3-001	420	18264	119	22	15	132	5	78	554	117	G
s58_002-001-b2-001	209	19490	130	22	14	138	6	86	571	117	G

Table II. 7 Group H Chemical Composition.

Specimen	MnKa1	FeKa1	ZnKa1	GaKa1	ThLa1	RbKa1	SrKa1	Y Ka1	ZrKa1	NbKa1	Chemical Group
s75_079A-b2-001	296	20140	146	24	16	126	5	114	771	112	H
s8_006-001-B48-L62-l1-b18	413	18891	141	22	12	119	8	111	811	105	H
s91_077A-b2-001	316	22378	157	23	12	131	3	106	712	102	H

Table II. 8 Raw materials for SRSAH Lithics Total Counts.

Raw Material	Count
Chert	99
Quartz & Quartzite	450
Obsidian	1705
Chalcedony	57
Basalt	52
Slate	1
Siltstone	13
Sandstone	1
Jasper	2
Total	**2380**

Table II. 9 SRSAH Obsidian Types and Total Counts (analyzed by Dr. Elizabeth Peterson).

Date	Survey Unit	Site	Site Name	Area	Quad	Locus	Lot	Bag #	Season	Type	Raw Material	Count
04/08/2011	006	001	Beta Samati	A		11	1	8	2011	flake fragments distal	Obsidian	1
05/08/2011	006	001	Beta Samati	A		10	2	10	2011	bipolar flake	Obsidian	1
05/08/2011	006	001	Beta Samati	A		10	2	10	2011	flake fragments distal	Obsidian	1
05/08/2011	006	001	Beta Samati	A		10	2	10	2011	backed crescent	Obsidian	1

03/08/2011	006	001	Beta Samati	A		20	4	14	2012	bipolar flake fragment	Obsidian	1
03/08/2011	006	001	Beta Samati	A		20	4	14	2012	bipolar flake	Obsidian	2
23/07/11	006	001	Beta Samati	A		4	1	7	2011	flake	Obsidian	1
23/07/11	006	001	Beta Samati	A		4	1	7	2011	microflake	Obsidian	1
26/07/11	006	001	Beta Samati	A		4	1	12	2011	flake fragment	Obsidian	2
26/07/11	006	001	Beta Samati	A		4	1	12	2011	bipolar flake fragment	Obsidian	1
26/07/11	006	001	Beta Samati	A		4	1	12	2011	bipolar flake fragment	Obsidian	3
29/07/11	006	001	Beta Samati	A		10	1	5	2011	flake fragments medial	Obsidian	1
29/07/11	006	001	Beta Samati	A		10	1	5	2011	bipolar flake	Obsidian	1
29/07/11	006	001	Beta Samati	A		10	1	5	2011	flake	Obsidian	2
29/07/11	006	001	Beta Samati	A		10	1	5	2011	outil ecaill	Obsidian	1
27/07/11	006	001	Beta Samati	A		5	1	2	2011	bipolar flake	Obsidian	1
27/07/11	006	001	Beta Samati	A		4	1	20	2011	flake fragments distal	Obsidian	1
27/07/11	006	001	Beta Samati	A		4	1	20	2011	flake fragments medial	Obsidian	1
27/07/11	006	001	Beta Samati	A		4	1	20	2011	bipolar flake	Obsidian	2
27/07/11	006	001	Beta Samati	A		4	1	20	2011	flake	Obsidian	1
27/07/11	006	001	Beta Samati	A		4	1	20	2011	backed cresent	Obsidian	1
25/07/11	006	001	Beta Samati	A		3	1	8	2011	flake fragments distal	Obsidian	2
25/07/11	006	001	Beta Samati	A		3	1	8	2011	flake fragments medial	Obsidian	1
25/07/11	006	001	Beta Samati	A		3	1	8	2011	bipolar flake	Obsidian	2
20/07/11	006	001	Beta Samati	A		1	1	2	2011	bipolar flake	Obsidian	1
20/07/11	006	001	Beta Samati	A		1	1	2	2011	bipolar flake	Obsidian	1
05/08/2011	006	001	Beta Samati	A		14	1	2	2011	flake fragments proximal	Obsidian	1
10/08/2011	013	001	Dem Elal	N/A	N/A	N/A	N/A	2	2011	utilized flake	Obsidian	2
10/08/2011	013	001	Dem Elal	N/A	N/A	N/A	N/A	2	2011	bipolar core fragment	Obsidian	3
10/08/2011	013	001	Dem Elal	N/A	N/A	N/A	N/A	2	2011	bipolar core	Obsidian	15
10/08/2011	013	001	Dem Elal	N/A	N/A	N/A	N/A	2	2011	CTF	Obsidian	1
10/08/2011	013	001	Dem Elal	N/A	N/A	N/A	N/A	2	2011	prismatic core	Obsidian	1
10/08/2011	013	001	Dem Elal	N/A	N/A	N/A	N/A	2	2011	outil ecaille	Obsidian	5
10/08/2011	013	001	Dem Elal	N/A	N/A	N/A	N/A	2	2011	blade	Obsidian	2
10/08/2011	013	001	Dem Elal	N/A	N/A	N/A	N/A	2	2011	BIPOLAR FLAKE	Obsidian	10
10/08/2011	013	001	Dem Elal	N/A	N/A	N/A	N/A	2	2011	BIPOLAR FLAKE FRAGMENT	Obsidian	5
10/08/2011	013	001	Dem Elal	N/A	N/A	N/A	N/A	2	2011	FLAKE MEDIAL FRAGMENT	Obsidian	7
10/08/2011	013	001	Dem Elal	N/A	N/A	N/A	N/A	2	2011	FLAKE PROXMAL FRAGMENT	Obsidian	5

10/08/2011	013	001	Dem Elal	N/A	N/A	N/A	N/A	2	2011	FLAKE DISTAL FRAGMENT	Obsidian	8
10/08/2011	013	001	Dem Elal	N/A	N/A	N/A	N/A	2	2011	FLAKE	Obsidian	9
10/08/2011	013	001	Dem Elal	N/A	N/A	N/A	N/A	2	2011	NOTCHED SCRAPER FRAGMENTS	Obsidian	3
10/08/2011	013	001	Dem Elal	N/A	N/A	N/A	N/A	2	2011	denticulate scraper ON FLAKE	Obsidian	3
10/08/2011	013	001	Dem Elal	N/A	N/A	N/A	N/A	2	2011	END SCRAPER FLAKE	Obsidian	1
10/08/2011	013	001	Dem Elal	N/A	N/A	N/A	N/A	2	2011	UNIFACIAL POINT	Obsidian	1
04/08/2011	006	001	Beta Samati	A		10	2	5	2011	flake fragments distal	Obsidian	3
04/08/2011	006	001	Beta Samati	A		10	2	5	2011	flake fragments medial	Obsidian	1
04/08/2011	006	001	Beta Samati	A		10	2	5	2011	flake	Obsidian	1
20/06/12	006	001	Beta Samati	A		25	1	12	2012	backed cresent	Obsidian	1
20/06/12	006	001	Beta Samati	A		10	1	30	2011	utilized flake	Obsidian	1
10/08/2011	006	001	Beta Samati	B				2	2011	denticulate side scraper	Obsidian	1
10/08/2011	006	001	Beta Samati	B				2	2011	bipolar flake fragment	Obsidian	3
10/08/2011	006	001	Beta Samati	B				2	2011	blade	Obsidian	1
10/08/2011	006	001	Beta Samati	B				2	2011	bipolar flake	Obsidian	1
10/08/2011	006	001	Beta Samati	B				2	2011	flake	Obsidian	1
10/08/2011	071	001	Sefra-Aboun	N/A	N/A	N/A	N/A	1	2011	bipolar core	Obsidian	2
10/08/2011	071	001	Sefra-Aboun	N/A	N/A	N/A	N/A	1	2011	awl	Obsidian	1
10/08/2011	071	001	Sefra-Aboun	N/A	N/A	N/A	N/A	1	2011	flake fragments	Obsidian	12
10/08/2011	022	003	Dungur	N/A	N/A	N/A	N/A	2	2011	outil ecaille	Obsidian	1
10/08/2011	022	002	Enda Aboy Meles	N/A	N/A	N/A	N/A	2	2011	denticulate scraper	Obsidian	1
10/08/2011	022	002	Enda Aboy Meles	N/A	N/A	N/A	N/A	2	2011	angle burin	Obsidian	1
10/08/2011	022	002	Enda Aboy Meles	N/A	N/A	N/A	N/A	2	2011	side scraper	Obsidian	1
10/08/2011	022	002	Enda Aboy Meles	N/A	N/A	N/A	N/A	2	2011	bipolar flake	Obsidian	4
10/08/2011	022	002	Enda Aboy Meles	N/A	N/A	N/A	N/A	2	2011	flake fragments	Obsidian	36
10/08/2011	022	002	Enda Aboy Meles	N/A	N/A	N/A	N/A	2	2011	bipolar core	Obsidian	5
10/08/2011	022	002	Enda Aboy Meles	N/A	N/A	N/A	N/A	2	2011	single platform core	Obsidian	1
10/08/2011	022	002	Enda Aboy Meles	N/A	N/A	N/A	N/A	2	2011	backed fragment	Obsidian	1
10/08/2011	022	002	Enda Aboy Meles	N/A	N/A	N/A	N/A	2	2011	backed flake pice broken	Obsidian	1
10/08/2011	022	001	Enda Balata Dista	N/A	N/A	N/A	N/A	2	2011	flake	Obsidian	7
10/08/2011	022	001	Enda Balata Dista	N/A	N/A	N/A	N/A	2	2011	Bipolar flake	Obsidian	7
10/08/2011	022	001	Enda Balata Dista	N/A	N/A	N/A	N/A	2	2011	Backed crescent	Obsidian	1
10/08/2011	022	001	Enda Balata Dista	N/A	N/A	N/A	N/A	2	2011	Side scraper denticulated	Obsidian	1
10/08/2011	022	001	Enda Balata Dista	N/A	N/A	N/A	N/A	2	2011	Angular waste	Obsidian	9

10/08/2011	022	001	Enda Balata Dista	N/A	N/A	N/A	N/A	2	2011	Burin spaul	Obsidian	2
10/08/2011	022	001	Enda Balata Dista	N/A	N/A	N/A	N/A	2	2011	CTF	Obsidian	1
10/08/2011	022	001	Enda Balata Dista	N/A	N/A	N/A	N/A	2	2011	Bipolar core	Obsidian	3
10/08/2011	022	001	Enda Balata Dista	N/A	N/A	N/A	N/A	2	2011	flake proximal fragment	Obsidian	2
10/08/2011	022	001	Enda Balata Dista	N/A	N/A	N/A	N/A	2	2011	Flake distal fragment	Obsidian	3
10/08/2011	022	001	Enda Balata Dista	N/A	N/A	N/A	N/A	2	2011	Flake medial fragment	Obsidian	6
09/08/2011	067	001	Aoudi Welka	N/A	N/A	N/A	N/A	2	2011	blade	Obsidian	1
09/08/2011	067	001	Aoudi Welka	N/A	N/A	N/A	N/A	2	2011	flake	Obsidian	4
09/08/2011	067	001	Aoudi Welka	N/A	N/A	N/A	N/A	2	2011	Bipolar flake	Obsidian	3
09/08/2011	067	001	Aoudi Welka	N/A	N/A	N/A	N/A	2	2011	BIPOLAR CORE	Obsidian	2
09/08/2011	067	001	Aoudi Welka	N/A	N/A	N/A	N/A	2	2011	BURIN ANGULARE	Obsidian	1
09/08/2011	067	001	Aoudi Welka	N/A	N/A	N/A	N/A	2	2011	SIDE SCRAPER	Obsidian	1
09/08/2011	067	001	Aoudi Welka	N/A	N/A	N/A	N/A	2	2011	CTF	Obsidian	1
09/08/2011	067	001	Aoudi Welka	N/A	N/A	N/A	N/A	2	2011	OUTIL ECAILLE	Obsidian	1
09/08/2011	067	001	Aoudi Welka	N/A	N/A	N/A	N/A	2	2011	UTILIZED FLAKE	Obsidian	2
09/08/2011	067	001	Aoudi Welka	N/A	N/A	N/A	N/A	2	2011	FLAKE MEDIAL FRAGMENT	Obsidian	4
09/08/2011	067	001	Aoudi Welka	N/A	N/A	N/A	N/A	2	2011	FLAKE DISTAL FRAGMENT	Obsidian	5
19/06/12	006	001	Beta Samati	A		20	2	13	2012	flake	Obsidian	1
19/06/12	006	001	Beta Samati	A		20	2	13	2012	Angular waste	Obsidian	1
16/06/12	006	001	Beta Samati	B		6	1	88	2012	flake fragment	Obsidian	1
13/06/12	006	001	Beta Samati	B		6	1	49	2012	flake fragment	Obsidian	1
23/06/12	006	001	Beta Samati	A		20	4	14	2012	proximal flake fragment	Obsidian	1
23/06/12	006	001	Beta Samati	A		20	4	14	2012	FLAKE	Obsidian	2
21/06/12	006	001	Beta Samati	A		25	1	22	2012	utilized flake fragment	Obsidian	1
21/06/12	006	001	Beta Samati	A		25	1	22	2012	crecent backed	Obsidian	1
21/06/12	006	001	Beta Samati	A		25	1	22	2012	utilized flake fragment	Obsidian	1
21/06/12	006	001	Beta Samati	A		25	1	22	2012	bipolar core	Obsidian	1
06/06/2012	006	001	Beta Samati	A		15	1	2	2012	flake fragments proximal	Obsidian	2
06/06/2012	006	001	Beta Samati	A		15	1	2	2012	bipolar flake	Obsidian	1
26/06/12	006	001	Beta Samati	B		10	2	275	2012	bipolar flake	Obsidian	1
26/06/12	006	001	Beta Samati	B		10	2	275	2012	flake fragments distal	Obsidian	1
23/06/12	006	001	Beta Samati	B		10	2	228	2012	blade	Obsidian	1
23/06/12	006	001	Beta Samati	B		10	2	228	2012	partially backed	Obsidian	1
09/06/2012	006	001	Beta Samati	B		1	NA	10	2012	bipolar flake	Obsidian	1

24/06/12	006	001	Beta Samati	B		16	1	285	2012	backed flake pice broken	Obsidian	1
26/06/12	006	001	Beta Samati	B		14	1	282	2012	flake fragment	Obsidian	1
16/06/12	006	001	Beta Samati	A		20	2	4	2012	blade distal fragment	Obsidian	1
16/06/12	006	001	Beta Samati	A		20	2	4	2012	flake	Obsidian	1
16/06/12	006	001	Beta Samati	A		20	2	4	2012	bipolar flake	Obsidian	1
16/06/12	006	001	Beta Samati	A		20	2	4	2012	backed cresent	Obsidian	1
16/06/12	006	001	Beta Samati	A		20	2	4	2012	bipolar core	Obsidian	1
07/06/2012	006	001	Beta Samati	A		15	1	6	2012	bipolar flake	Obsidian	2
07/06/2012	006	001	Beta Samati	A		15	1	6	2012	flake fragments distal	Obsidian	1
23/06/12	006	001	Beta Samati	A		27	1	30	2012	bipolar flake fragment	Obsidian	2
16/06/12	006	001	Beta Samati	B		6	1	91	2012	CRF	Obsidian	1
27/06/12	006	001	Beta Samati	B		15	1	300	2012	bipolar flake	Obsidian	1
21/06/12	006	001	Beta Samati	B		11	2	139	2012	flake	Obsidian	1
21/06/12	006	001	Beta Samati	A		25	1	17	2012	flake	Obsidian	1
21/06/12	006	001	Beta Samati	A		25	1	17	2012	proximal flake fragment	Obsidian	1
21/06/12	006	001	Beta Samati	A		27	1	15	2012	MEDIAL BLADE FRAGMENT	Obsidian	1
21/06/12	006	001	Beta Samati	A		27	1	15	2012	proximal fragment	Obsidian	1
21/06/12	006	001	Beta Samati	A		27	1	15	2012	bipolar flake fragment	Obsidian	1
21/06/12	006	001	Beta Samati	B		12	1	138	2012	bipolar flake	Obsidian	1
20/06/12	006	001	Beta Samati	B		11	1	116	2012	bipolar flake	Obsidian	1
09/06/2012	024	001	NA		N/A			2	2012	bipolar flake fragment	Obsidian	5
09/06/2012	024	001	NA		N/A			2	2012	bipolar core	Obsidian	1
15/06/12	006	001	Beta Samati	B		7	1	67	2012	utilized flake fragment	Obsidian	1
22/06/12	006	001	Beta Samati	B		10	1	212	2012	flake fragments distal	Obsidian	1
22/06/12	006	001	Beta Samati	A		20	4	2	2012	flake	Obsidian	1
22/06/12	006	001	Beta Samati	A		20	4	2	2012	bipolar flake fragments	Obsidian	1
19/06/12	006	001	Beta Samati	A		20	3	5	2012	bipolar flake	Obsidian	2
19/06/12	006	001	Beta Samati	A		20	3	5	2012	blade	Obsidian	2
19/06/12	006	001	Beta Samati	A		20	3	5	2012	utilized blade	Obsidian	1
19/06/12	006	001	Beta Samati	A		20	3	5	2012	flake	Obsidian	1
19/06/12	006	001	Beta Samati	A		20	3	5	2012	bipolar core fragment	Obsidian	1
19/06/12	006	001	Beta Samati	A		20	3	5	2012	flake fragments medial	Obsidian	1
23/06/12	006	001	Beta Samati	A		25	2	10	2012	bipolar flake	Obsidian	1
23/06/12	006	001	Beta Samati	A		25	2	10	2012	bipolar flake fragment	Obsidian	3

09/06/2012	024	003	NA		N/A		2	2	2012	FLAKE	Obsidian	3
09/06/2012	024	003	NA		N/A		2	2	2012	BIPOLAR FLAKE	Obsidian	2
09/06/2012	024	003	NA		N/A		2	2	2012	Angular waste	Obsidian	3
09/06/2012	024	003	NA		N/A		2	2	2012	FLAKE PROXMAL FRAGMENT	Obsidian	1
09/06/2012	024	003	NA		N/A		2	2	2012	FLAKE DISTAL FRAGMENT	Obsidian	1
09/06/2012	024	003	NA		N/A		2	2	2012	FLAKE MEDIAL FRAGMENT	Obsidian	3
09/06/2012	024	003	NA		N/A		2	2	2012	bipolar core	Obsidian	2
09/06/2012	024	003	NA		N/A		2	2	2012	BIPOLAR CORE FRAGMENT	Obsidian	2
09/06/2012	24B				N/A			1	2012	OUTIL ECAILLE	Obsidian	1
09/06/2012	24B				N/A			1	2012	FLAKE PROXMAL FRAGMENT	Obsidian	1
09/06/2012	24B				N/A			1	2012	ALTERNATE EDGE POINT	Obsidian	1
09/06/2012	24B				N/A			1	2012	UTILIZED BIPOLAR FLAKE	Obsidian	1
07/06/2012	006	001	Beta Samati	B		1		5	2012	BURIN SPALL	Obsidian	1
07/06/2012	006	001	Beta Samati	B		1		5	2012	flake fragments proximal	Obsidian	14
07/06/2012	006	001	Beta Samati	B		1		5	2012	blade fragment proxmal end	Obsidian	1
07/06/2012	006	001	Beta Samati	B		1		5	2012	flake fragments medial	Obsidian	3
07/06/2012	006	001	Beta Samati	B		1		5	2012	bipolar flake fragments	Obsidian	2
07/06/2012	006	001	Beta Samati	B		1		5	2012	flake fragments distal	Obsidian	4
07/06/2012	006	001	Beta Samati	B		1		5	2012	flakes	Obsidian	13
07/06/2012	006	001	Beta Samati	B		1		5	2012	blade	Obsidian	2
07/06/2012	006	001	Beta Samati	B		1		5	2012	bipolar flake	Obsidian	2
07/06/2012	006	001	Beta Samati	B		1		5	2012	bipolar core	Obsidian	4
07/06/2012	006	001	Beta Samati	B		1		5	2012	CTF	Obsidian	1
07/06/2012	006	001	Beta Samati	B		1		5	2012	utilized blades	Obsidian	3
07/06/2012	006	001	Beta Samati	B		1		5	2012	backed crescent	Obsidian	5
07/06/2012	006	001	Beta Samati	B		1		5	2012	backed blade	Obsidian	1
07/06/2012	006	001	Beta Samati	B		1		5	2012	backed flake piece broken	Obsidian	3
07/06/2012	006	001	Beta Samati	B		1		5	2012	side scraper	Obsidian	1
07/06/2012	006	001	Beta Samati	B		1		5	2012	partially backed	Obsidian	1
16/06/12	006	001	Beta Samati	B		10	1	86	2012	flake fragment	Obsidian	1
04/07/2012	044	001	Sekoualou		N/A			3	2012	FLAKE DISTAL FRAGMENT	Obsidian	1
04/07/2012	044	001	Sekoualou		N/A			2	2012	BLADE	Obsidian	3
04/07/2012	044	001	Sekoualou		N/A			2	2012	END SCRAPER FLAKE	Obsidian	2
04/07/2012	044	001	Sekoualou		N/A			2	2012	BURIN SPALL	Obsidian	2

04/07/2012	044	001	Sekoualou		N/A			2	2012	OUTIL ECAILLE	Obsidian	1
04/07/2012	044	001	Sekoualou		N/A			2	2012	BIPOLAR CORE FRAGMENT	Obsidian	3
04/07/2012	044	001	Sekoualou		N/A			2	2012	BIPOLAR FLAKE FRAGMENT	Obsidian	3
04/07/2012	044	001	Sekoualou		N/A			2	2012	FLAKE PROXMAL FRAGMENT	Obsidian	4
04/07/2012	044	001	Sekoualou		N/A			2	2012	FLAKE MEDIAL FRAGMENT	Obsidian	4
04/07/2012	044	001	Sekoualou		N/A			2	2012	FLAKE DISTAL FRAGMENT	Obsidian	5
04/07/2012	044	001	Sekoualou		N/A			2	2012	bipolar flake	Obsidian	29
04/07/2012	044	001	Sekoualou		N/A			2	2012	BIPOLAR CORE	Obsidian	15
04/07/2012	044	001	Sekoualou		N/A			2	2012	FLAKE	Obsidian	20
04/07/2012	044	001	Sekoualou		N/A			2	2012	ANGULAR WASTE	Obsidian	8
04/07/2012	026	001	Hchen		N/A			2	2012	PARTIAL UNIFACE POINT	Obsidian	1
04/07/2012	026	001	Hchen		N/A			2	2012	ANGULAR WASTE	Obsidian	8
04/07/2012	026	001	Hchen		N/A			2	2012	UTILIZED FLAKE	Obsidian	1
04/07/2012	026	001	Hchen		N/A			2	2012	BACKED FRAGMENT	Obsidian	1
04/07/2012	026	001	Hchen		N/A			2	2012	BIPOLAR FLAKE	Obsidian	5
04/07/2012	026	001	Hchen		N/A			2	2012	FLAKE	Obsidian	3
04/07/2012	026	001	Hchen		N/A			2	2012	FLAKE MEDIAL FRAGMENT	Obsidian	3
09/06/2012	025A			A	N/A			2	2012	Angular waste	Obsidian	1
09/06/2012	025A			A	N/A			2	2012	flake	Obsidian	1
09/06/2012	025A			A	N/A			2	2012	burin	Obsidian	1
15/06/12	008	001	NA		N/A			2	2012	FLAKE DISTAL FRAGMENT	Obsidian	1
12/06/2012	082A			B	N/A			1	2012	flake	Obsidian	1
12/06/2012	082A			B	N/A			1	2012	flake fragment	Obsidian	1
08/06/2012	042	001	NA		N/A			1	2012	OUTIL ECAILLE	Obsidian	1
12/06/2012	061A				N/A			1	2012	BIPOLAR FLAKE	Obsidian	1
11/06/2012	016	001	NA		N/A			2	2012	ALTERNATE EDGE POINT	Obsidian	1
11/06/2012	016	001	NA		N/A			2	2012	BIPOLAR FLAKE	Obsidian	1
11/06/2012	016	001	NA		N/A			2	2012	BIPOLAR CORE	Obsidian	1
11/06/2012	081A				N/A			1	2012	FLAKE PROXMAL FRAGMENT	Obsidian	1
12/06/2012	014	002	Adi Halefa		N/A				2012	bipolar core	Obsidian	1
12/06/2012	014	002	Adi Halefa		N/A				2012	bipolar flake fragment	Obsidian	1
14/06/12	014	002	Adi Halefa		N/A			2	2012	BIPOLAR FLAKE	Obsidian	1
14/06/12	014	002	Adi Halefa		N/A			2	2012	FLAKE DISTAL FRAGMENT	Obsidian	1
13/06/12	006	001	Beta Samati	B	N/A	1	1	48	2012	bipolar flake fragment	Obsidian	1

04/07/2012	026	001	Hchen		N/A			3	2012	bipolar flake	Obsidian	1
15/06/12	009A				N/A			2	2012	bipolar flake fragment	Obsidian	3
15/06/12	014A				N/A			2	2012	BIPOLAR FLAKE FRAGMENT	Obsidian	1
15/06/12	008A				N/A			1	2012	BIPOLAR CORE FRAGMENT	Obsidian	1
13/06/12	013A				N/A			1	2012	flake fragment	Obsidian	1
13/06/12	013A				N/A			1	2012	flake	Obsidian	1
12/06/2012	017	001	Endaba Hailu		N/A			2	2012	BIPOLAR CORE FRAGMENT	Obsidian	1
11/06/2012	017	NONE SITE	Endaba Hailu	A	N/A			2	2012	flake fragment	Obsidian	1
20/06/12	006	001	Beta Samati	A	N/A	27	1	3	2012	flake fragment	Obsidian	1
20/06/12	006	001	Beta Samati	A	N/A	27	1	3	2012	bipolar flake fragment	Obsidian	1
20/06/12	006	001	Beta Samati	A	N/A	27	1	3	2012	CTF	Obsidian	1
09/06/2012	024	002	NA		N/A			3	2012	BURIN SPALL	Obsidian	1
09/06/2012	024	002	NA		N/A			3	2012	flake	Obsidian	1
09/06/2012	024	002	NA		N/A			3	2012	bipolar flake fragment	Obsidian	1
09/06/2012	024	002	NA		N/A			3	2012	double side scraper	Obsidian	1
09/06/2012	024	002	NA		N/A			3	2012	bipolar flake	Obsidian	1
09/06/2012	024	002	NA		N/A			3	2012	flake fragment	Obsidian	1
09/06/2012	024	002	NA		N/A			3	2012	bipolar flake fragment	Obsidian	1
02/07/2012	071	001	Sefra-Aboun		N/A			3	2012	FLAKE	Obsidian	20
02/07/2012	071	001	Sefra-Aboun		N/A			3	2012	bipolar flake	Obsidian	30
02/07/2012	071	001	Sefra-Aboun		N/A			3	2012	bipolar flake fragment	Obsidian	6
02/07/2012	071	001	Sefra-Aboun		N/A			3	2012	FLAKE PROXMAL FRAGMENT	Obsidian	2
02/07/2012	071	001	Sefra-Aboun		N/A			3	2012	FLAKE MEDIAL FRAGMENT	Obsidian	3
02/07/2012	071	001	Sefra-Aboun		N/A			3	2012	FLAKE DISTAL FRAGMENT	Obsidian	13
02/07/2012	071	001	Sefra-Aboun		N/A			3	2012	OUTIL ECAILLE	Obsidian	2
02/07/2012	071	001	Sefra-Aboun		N/A			3	2012	END AND SIDE SCRAPER	Obsidian	1
02/07/2012	071	001	Sefra-Aboun		N/A			3	2012	BIPOLAR CORE FRAGMENT	Obsidian	14
02/07/2012	071	001	Sefra-Aboun		N/A			3	2012	bipolar core	Obsidian	9
02/07/2012	071	001	Sefra-Aboun		N/A			3	2012	BACKED CRECENT	Obsidian	3
02/07/2012	071	001	Sefra-Aboun		N/A			3	2012	backed fragment	Obsidian	6
02/07/2012	071	001	Sefra-Aboun		N/A			3	2012	BURIN SPALL	Obsidian	2
02/07/2012	071	001	Sefra-Aboun		N/A			3	2012	Angular waste	Obsidian	44
09/08/2011	068	001	Mirai Abune Afsea		N/A			2	2011	FLAKE MEDIAL FRAGMENT	Obsidian	4
09/08/2011	068	001	Mirai Abune Afsea		N/A			2	2011	BIPOLAR FLAKE FRAGMENT	Obsidian	2

09/08/2011	068	001	Mirai Abune Afsea		N/A			2	2011	BIPOLAR FLAKE	Obsidian	2
09/08/2011	068	001	Mirai Abune Afsea		N/A			2	2011	BIPOLAR CORE FRAGMENT	Obsidian	1
09/08/2011	068	001	Mirai Abune Afsea		N/A			2	2011	UTILIZED FLAKE	Obsidian	2
05/08/2011	006	001	Beta Samati	A	N/A	11	2	5	2011	modified flake	Obsidian	1
05/08/2011	006	001	Beta Samati	A	N/A	11	2	5	2011	blade fragment	Obsidian	1
26/07/11	006	001	Beta Samati	A	N/A	3		15	2011	bipolar flake fragment	Obsidian	1
26/07/11	014	001	Adi Helafa		N/A			2	2011	FLAKE	Obsidian	3
10/08/2011	014	001	Adi Helafa		N/A			2	2011	bipolar flake	Obsidian	1
10/08/2011	014	001	Adi Helafa		N/A			2	2011	FLAKE PROXMAL FRAGMENT	Obsidian	2
10/08/2011	014	001	Adi Helafa		N/A			2	2011	bipolar flake fragment	Obsidian	5
10/08/2011	014	001	Adi Helafa		N/A			2	2011	NOTCHED	Obsidian	2
10/08/2011	014	001	Adi Helafa		N/A			2	2011	UNIFACE UNFINISHED	Obsidian	2
10/08/2011	014	001	Adi Helafa		N/A			2	2011	TRIANGULAR FLAKE	Obsidian	1
10/08/2011	014	001	Adi Helafa		N/A			2	2011	OUTIL ECAILLE	Obsidian	2
04/07/2012	027	001	Sefra Tourkui		N/A			2	2012	FLAKE	Obsidian	1
04/07/2012	027	001	Sefra Tourkui		N/A			2	2012	BLADE PROXMAL FRAGMENT	Obsidian	1
04/07/2012	027	001	Sefra Tourkui		N/A			2	2012	ANGULAR WASTE	Obsidian	1
04/07/2012	027	001	Sefra Tourkui		N/A			2	2012	ANGULAR WASTE	Obsidian	132
04/07/2012	027	001	Sefra Tourkui		N/A			2	2012	BIPOLAR FLAKE	Obsidian	74
04/07/2012	027	001	Sefra Tourkui		N/A			2	2012	BIPOLAR FLAKE FRAGMENT	Obsidian	31
04/07/2012	027	001	Sefra Tourkui		N/A			2	2012	UTILIZED FLAKE	Obsidian	8
04/07/2012	027	001	Sefra Tourkui		N/A			2	2012	CTF	Obsidian	3
04/07/2012	027	001	Sefra Tourkui		N/A			2	2012	modified flake	Obsidian	1
04/07/2012	027	001	Sefra Tourkui		N/A			2	2012	FLAKE PROXMAL FRAGMENT	Obsidian	19
04/07/2012	027	001	Sefra Tourkui		N/A			2	2012	FLAKE DISTAL FRAGMENT	Obsidian	34
04/07/2012	027	001	Sefra Tourkui		N/A			2	2012	FLAKE MEDIAL FRAGMENT	Obsidian	36
04/07/2012	027	001	Sefra Tourkui		N/A			2	2012	BLADE PROXMAL FRAGMENT	Obsidian	5
04/07/2012	027	001	Sefra Tourkui		N/A			2	2012	BLADE FRAGMENT DISTAL	Obsidian	5
04/07/2012	027	001	Sefra Tourkui		N/A			2	2012	BIPOLAR CORE FRAGMENT	Obsidian	24
04/07/2012	027	001	Sefra Tourkui		N/A			2	2012	BACKED FRAGMENT	Obsidian	9
04/07/2012	027	001	Sefra Tourkui		N/A			2	2012	BURIN SPALL	Obsidian	10
04/07/2012	027	001	Sefra Tourkui		N/A			2	2012	BLADE	Obsidian	5
04/07/2012	027	001	Sefra Tourkui		N/A			2	2012	bipolar core	Obsidian	13
04/07/2012	027	001	Sefra Tourkui		N/A			2	2012	OUTIL ECAILLE	Obsidian	8

04/07/2012	027	001	Sefra Tourkui		N/A			2	2012	SHATTER	Obsidian	123
04/07/2012	027	001	Sefra Tourkui		N/A			2	2012	FLAKE	Obsidian	62
04/07/2012	027	001	Sefra Tourkui		N/A			2	2012	SIDE SCRAPER	Obsidian	4
04/07/2012	027	001	Sefra Tourkui		N/A			2	2012	END SCRAPER FLAKE	Obsidian	1
04/07/2012	027	001	Sefra Tourkui		N/A			2	2012	DUBLE SIDE SCRAPER	Obsidian	1
04/07/2012	027	001	Sefra Tourkui		N/A			2	2012	STRAIGHT BACKED	Obsidian	1
04/07/2012	027	001	Sefra Tourkui		N/A			2	2012	PARTIAL UNIFACE POINT	Obsidian	3
04/07/2012	027	001	Sefra Tourkui		N/A			2	2012	BACKED CRECENT	Obsidian	11
07/06/2015	006	001	Beta Samati	A	?	64	1	6	2015	SIDE SCRAPER	Obsidian	1
23/05/15	006	001	Beta Samati	A	66	29	1	2	2015	BIPOLAR CORE	Obsidian	1
17/05/15	006	001	Beta Samati	A	75	29	1	7	2015	FLAKE MEDIAL FRAGMENT	Obsidian	1
17/05/15	006	001	Beta Samati	A	75	29	1	7	2015	FLAKE DISTAL FRAGMENT	Obsidian	1
17/05/15	006	001	Beta Samati	A	75	29	1	7	2015	ANGULAR WASTE	Obsidian	3
14/05/15	006	001	Beta Samati	A	76	29	1	1	2015	BIPOLAR FLAKE	Obsidian	1
14/05/15	006	001	Beta Samati	A	76	29	1	1	2015	FLAKE	Obsidian	1
20/05/15	006	001	Beta Samati	A	76	31	1	3	2015	BIPOLAR FLAKE	Obsidian	1
05/06/2015	006	001	Beta Samati	A	75	64	1	1	2015	FLAKE DISTAL FRAGMENT	Obsidian	2
05/06/2015	006	001	Beta Samati	A	75	64	1	1	2015	ANGULAR WASTE	Obsidian	1
20/05/15	006	001	Beta Samati	A	75	40	2	3	2015	FLAKE	Obsidian	1
23/05/15	006	001	Beta Samati	A	65	45	8	4	2015	FLAKE	Obsidian	1
23/05/15	006	001	Beta Samati	A	65	45	8	4	2015	FLAKE PROXMAL FRAGMENT	Obsidian	2
22/05/15	006	001	Beta Samati	A	75	37	1	3	2015	MEDIAL BLADE FRAGMENT	Obsidian	1
09/06/2015	006	001	Beta Samati	A	75	64	1	7	2015	LOUTIL ECAILLES	Obsidian	1
05/06/2015	006	001	Beta Samati	A	76	45	1	4	2015	FLAKE DISTAL FRAGMENT	Obsidian	1
05/06/2015	006	001	Beta Samati	A	76	45	1	4	2015	FLAKE MEDIAL FRAGMENT	Obsidian	1
05/06/2015	006	001	Beta Samati	A	76	45	1	4	2015	BIPOLAR FLAKE	Obsidian	1
25/05/15	006	001	Beta Samati	A	66	51	1	2	2015	SCRAPER FRAGMENT	Obsidian	1
25/05/15	006	001	Beta Samati	A	66	51	1	2	2015	BURIN SPAULL	Obsidian	1
25/05/15	006	001	Beta Samati	A	66	51	1	2	2015	BIPOLAR FLAKE	Obsidian	1
25/05/15	006	001	Beta Samati	A	76	31	1	5	2015	SCRAPER FRAGMENT	Obsidian	1
07/06/2015	006	001	Beta Samati	A	67	47	1	4	2015	FLAKE	Obsidian	2
07/06/2015	006	001	Beta Samati	A	67	47	1	4	2015	FLAKE DISTAL FRAGMENT	Obsidian	2
08/06/2015	006	001	Beta Samati	A	75	66	1	2	2015	FLAKE	Obsidian	2
08/06/2015	006	001	Beta Samati	A	75	66	1	2	2015	OUTIL ECAILLE	Obsidian	1

09/06/2015	006	001	Beta Samati	B	36	25	3	3	2015	OUTIL ECAILLE	Obsidian	1
07/06/2015	006	001	Beta Samati	B	36	24	1	11	2015	BIPOLAR CORE	Obsidian	1
07/06/2015	006	001	Beta Samati	B	36	24	1	11	2015	BIPOLAR FLAKE	Obsidian	1
25/05/15	006	001	Beta Samati	B	34	18	1	8	2015	FLAKE PROXMAL FRAGMENT	Obsidian	1
04/06/2015	006	001	Beta Samati	B	37	45	1	6	2015	END SCRAPER ON FLAKE	Obsidian	1
28/05/15	006	001	Beta Samati	B	37	25a	1	2	2015	FLAKE DISTAL FRAGMENT	Obsidian	1
08/06/2015	006	001	Beta Samati	B	37	45	2	15	2015	BACKED FRAGMENT	Obsidian	1
09/06/2015	006	001	Beta Samati	A	75	66	1	7	2015	FLAKE	Obsidian	1
10/06/2015	006	001	Beta Samati	A	73	63	3	8	2015	FLAKE	Obsidian	1
10/06/2015	006	001	Beta Samati	A	73	63	3	8	2015	BIPOLAR FLAKE	Obsidian	1
11/06/2015	006	001	Beta Samati	B	37	52	1	11	2015	FLAKE PROXMAL FRAGMENT	Obsidian	1
10/06/2015	006	001	Beta Samati	B	36	45	3	3	2015	BACKED CRESCENT	Obsidian	1
08/06/2015	006	001	Beta Samati	B	36	24	1	17	2015	BIPOLAR FLAKE	Obsidian	1
20/05/15	006	001	Beta Samati	B	36	24	1	3	2015	FLAKE	Obsidian	1
07/06/2015	006	001	Beta Samati	B	46	49	1	5	2015	FLAKE DISTAL FRAGMENT	Obsidian	1
10/06/2015	006	001	Beta Samati	B	37	50	1	3	2915	BIPOLAR FLAKE	Obsidian	2
12/06/2015	006	001	Beta Samati	B	37	51	1	14	2015	BIPOLAR FLAKE	Obsidian	1
12/06/2015	006	001	Beta Samati	B	37	44	2	6	2015	FLAKE	Obsidian	1
12/06/2015	006	001	Beta Samati	B	37	44	2	6	2015	FLAKE	Obsidian	1
11/06/2015	006	001	Beta Samati	A	75	53	1	1	2015	FLAKE DISTAL FRAGMENT	Obsidian	1
06/05/2015	010	001	Adi Abiselam 2	N/A	N/A	N/A	N/A	3	2015	BIPOLAR FLAKE	Obsidian	1
06/05/2015	010	001	Adi Abiselam 2	N/A	N/A	N/A	N/A	3	2015	FLAKE MEDIAL FRAGMENT	Obsidian	1
09/05/2015	051A	001	N/A	N/A	N/A	N/A	N/A	2	2015	BIPOLAR CORE	Obsidian	1
08/05/2015	069	001	Tseratsur	N/A	N/A	N/A	N/A	2	2015	FLAKE	Obsidian	2
20/05/15	081	001	Adi Krumbe/Tahtay Gundam	N/A	N/A	N/A	N/A	2	2015	FLAKE	Obsidian	1
20/05/15	081	001	Adi Krumbe/Tahtay Gundam	N/A	N/A	N/A	N/A	2	2015	bipolar core	Obsidian	1
28/05/15	029	003	Zban Ma'ekune/Beloho	N/A	N/A	N/A	N/A	2	2015	FLAKE DISTAL FRAGMENT	Obsidian	1
18/05/15	042	001	NA	N/A	N/A	N/A	N/A	3	2015	BIPOLAR FLAKE	Obsidian	1
19/05/15	071	001	Sefra Aboun	N/A	N/A	N/A	N/A	2	2015	BIPOLAR FLAKE	Obsidian	1
22/05/15	97A	N/A	N/A	N/A	N/A	N/A	N/A	1	2015	BIPOLAR FLAKE	Obsidian	1
22/05/15	97A	N/A	N/A	N/A	N/A	N/A	N/A	1	2015	ANGULAR WASTE	Obsidian	1
29/05/15	79A	N/A	N/A	N/A	N/A	N/A	N/A	2	2015	BIPOLAR FLAKE	Obsidian	3
29/05/15	79A	N/A	N/A	N/A	N/A	N/A	N/A	2	2015	Angular waste	Obsidian	2

06/05/2015	999	001	Adi Abiselam	N/A	N/A	N/A	N/A	2	2015	END SCRAPER FLAKE	Obsidian	1
06/05/2015	999	001	Adi Abiselam	N/A	N/A	N/A	N/A	2	2015	FLAKE DISTAL FRAGMENT	Obsidian	2
06/05/2015	999	001	Adi Abiselam	N/A	N/A	N/A	N/A	2	2015	FLAKE PROXMAL FRAGMENT	Obsidian	1
08/05/2015	078A	N/A	N/A	N/A	N/A	N/A	N/A	1	2015	FLAKE	Obsidian	1
29/05/15	029	002	Mai Fesasi	N/A	N/A	N/A	N/A	2	2015	CONVEX SCRAOER	Obsidian	1
29/05/15	029	002	Mai Fesasi	N/A	N/A	N/A	N/A	2	2015	bipolar core	Obsidian	1
29/05/15	029	002	Mai Fesasi	N/A	N/A	N/A	N/A	2	2015	FLAKE	Obsidian	5
29/05/15	029	002	Mai Fesasi	N/A	N/A	N/A	N/A	2	2015	OUTIL ECAILLE	Obsidian	1
29/05/15	029	002	Mai Fesasi	N/A	N/A	N/A	N/A	2	2015	FLAKE PROXMAL FRAGMENT	Obsidian	3
29/05/15	029	002	Mai Fesasi	N/A	N/A	N/A	N/A	2	2015	FLAKE MEDIAL FRAGMENT	Obsidian	1
29/05/15	029	002	Mai Fesasi	N/A	N/A	N/A	N/A	2	2015	FLAKE DISTAL FRAGMENT	Obsidian	1
29/05/15	029	002	Mai Fesasi	N/A	N/A	N/A	N/A	2	2015	Angular waste	Obsidian	3
29/05/15	029	002	Mai Fesasi	N/A	N/A	N/A	N/A	2	2015	BIPOLAR FLAKE	Obsidian	4
17/05/15	071	002	Mai Eungug	N/A	N/A	N/A	N/A	1	2015	FLAKE	Obsidian	3
17/05/15	071	002	Mai Eungug	N/A	N/A	N/A	N/A	1	2015	BIPOLAR FLAKE	Obsidian	4
17/05/15	071	002	Mai Eungug	N/A	N/A	N/A	N/A	1	2015	bipolar core	Obsidian	1
17/05/15	071	002	Mai Eungug	N/A	N/A	N/A	N/A	1	2015	FLAKE PROXMAL FRAGMENT	Obsidian	1
17/05/15	071	002	Mai Eungug	N/A	N/A	N/A	N/A	1	2015	FLAKE MEDIAL FRAGMENT	Obsidian	2
17/05/15	071	002	Mai Eungug	N/A	N/A	N/A	N/A	1	2015	FLAKE DISTAL FRAGMENT	Obsidian	4
17/05/15	071	002	Mai Eungug	N/A	N/A	N/A	N/A	1	2015	bipolar flake fragment	Obsidian	2
17/05/15	071	002	Mai Eungug	N/A	N/A	N/A	N/A	1	2015	Angular waste	Obsidian	2
17/05/15	071	001	Sefra-Aboun	N/A	N/A	N/A	N/A	2	2015	FLAKE	Obsidian	9
17/05/15	071	001	Sefra-Aboun	N/A	N/A	N/A	N/A	2	2015	bipolar flake	Obsidian	2
17/05/15	071	001	Sefra-Aboun	N/A	N/A	N/A	N/A	2	2015	bipolar core	Obsidian	3
17/05/15	071	001	Sefra-Aboun	N/A	N/A	N/A	N/A	2	2015	FLAKE DISTAL FRAGMENT	Obsidian	4
17/05/15	071	001	Sefra-Aboun	N/A	N/A	N/A	N/A	2	2015	STRAIGHT BACKED	Obsidian	1
29/05/15	079	001	Da'ero Arat/St. Gabriel Church	N/A	N/A	N/A	N/A	2	2015	FLAKE	Obsidian	5
29/05/15	079	001	Da'ero Arat/St. Gabriel Church	N/A	N/A	N/A	N/A	2	2015	bipolar flake	Obsidian	6
29/05/15	079	001	Da'ero Arat/St. Gabriel Church	N/A	N/A	N/A	N/A	2	2015	bipolar core	Obsidian	7
29/05/15	079	001	Da'ero Arat/St. Gabriel Church	N/A	N/A	N/A	N/A	2	2015	FLAKE PROXMAL FRAGMENT	Obsidian	1
29/05/15	079	001	Da'ero Arat/St. Gabriel Church	N/A	N/A	N/A	N/A	2	2015	FLAKE DISTAL FRAGMENT	Obsidian	2
29/05/15	079	001	Da'ero Arat/St. Gabriel Church	N/A	N/A	N/A	N/A	2	2015	Angular waste	Obsidian	3
29/05/15	079	001	Da'ero Arat/St. Gabriel Church	N/A	N/A	N/A	N/A	2	2015	CONVEX SCRAPER	Obsidian	1
09/06/2015	006	001	Beta Samati	B	36	24	1	20	2015	BIPOLAR FLAKE	Obsidian	1

14/06/15	002	001	Enda Cha'atat	N/A	N/A	N/A	N/A	2	2015	bipolar flake	Obsidian	12
14/06/15	002	001	Enda Cha'atat	N/A	N/A	N/A	N/A	2	2015	bipolar core	Obsidian	3
14/06/15	002	001	Enda Cha'atat	N/A	N/A	N/A	N/A	2	2015	FLAKE	Obsidian	18
14/06/15	002	001	Enda Cha'atat	N/A	N/A	N/A	N/A	2	2015	Angular waste	Obsidian	15
14/06/15	002	001	Enda Cha'atat	N/A	N/A	N/A	N/A	2	2015	BURIN SPALL	Obsidian	1
14/06/15	002	001	Enda Cha'atat	N/A	N/A	N/A	N/A	2	2015	FLAKE PROXMAL FRAGMENT	Obsidian	1
14/06/15	002	001	Enda Cha'atat	N/A	N/A	N/A	N/A	2	2015	FLAKE MEDIAL FRAGMENT	Obsidian	2
14/06/15	002	001	Enda Cha'atat	N/A	N/A	N/A	N/A	2	2015	FLAKE DISTAL FRAGMENT	Obsidian	4
14/06/15	002	001	Enda Cha'atat	N/A	N/A	N/A	N/A	2	2015	burin	Obsidian	1
14/06/15	002	001	Enda Cha'atat	N/A	N/A	N/A	N/A	2	2015	BACKED CRECENT	Obsidian	1
14/06/15	002	001	Enda Cha'atat	N/A	N/A	N/A	N/A	2	2015	backed fragment	Obsidian	1
14/06/15	002	001	Enda Cha'atat	N/A	N/A	N/A	N/A	2	2015	NOTCHED	Obsidian	1
09/05/2015	069	004	Kawhi Aboi Haftom	N/A	N/A	N/A	N/A	2	2015	bipolar core	Obsidian	4
09/05/2015	069	004	Kawhi Aboi Haftom	N/A	N/A	N/A	N/A	2	2015	ANGULAR WASTE	Obsidian	5
09/05/2015	069	004	Kawhi Aboi Haftom	N/A	N/A	N/A	N/A	2	2015	bipolar flake	Obsidian	7
09/05/2015	069	004	Kawhi Aboi Haftom	N/A	N/A	N/A	N/A	2	2015	FLAKE	Obsidian	3
09/05/2015	069	004	Kawhi Aboi Haftom	N/A	N/A	N/A	N/A	2	2015	UTILIZED FLAKE	Obsidian	1
09/05/2015	069	004	Kawhi Aboi Haftom	N/A	N/A	N/A	N/A	2	2015	FLAKE PROXMAL FRAGMENT	Obsidian	1
09/05/2015	069	004	Kawhi Aboi Haftom	N/A	N/A	N/A	N/A	2	2015	FLAKE DISTAL FRAGMENT	Obsidian	3
09/05/2015	069	004	Kawhi Aboi Haftom	N/A	N/A	N/A	N/A	2	2015	UNIFACIAL POINT	Obsidian	1
10/06/2015	006	001	Beta Samati	A	66	51	1	N/A	2015	FLAKE DISTAL FRAGMENT	Obsidian	2
08/05/2015	77A	N/A	N/A	N/A	N/A	N/A	N/A	2	2015	ANGULAR WASTE	Obsidian	1
12/05/2016	006	001	Beta Samati	B	35	60	1	3	2016	BIPOLAR FLAKE	Obsidian	1
12/05/2016	006	001	Beta Samati	B	35	61	1	5	2016	DIST FRAGMENT	Obsidian	1
17/05/16	006	001	Beta Samati	B	45	64	2	15	2016	UTILIZED FLAKE	Obsidian	1
17/05/16	006	001	Beta Samati	B	45	60	1	22	2016	NOTCHED SCRAPER?	Obsidian	1
18/05/16	006	001	Beta Samati	B	45	60	2	6	2016	FLAKE	Obsidian	1
16/05/16	006	001	Beta Samati	B	38	65	1	19	2016	BACKED FRAGMENT	Obsidian	1
16/05/16	006	001	Beta Samati	B	35	70	1	9	2016	BIPOLAR FRAG	Obsidian	1
15/05/16	006	001	Beta Samati	B	35	70	1	1	2016	DIST FRAGMENT	Obsidian	1
16/05/16	006	001	Beta Samati	B	48	67	2	3	2016	FLAKE	Obsidian	1
13/05/16	006	001	Beta Samati	B	45	60	1	12	2016	FLAKE	Obsidian	1
15/05/16	006	001	Beta Samati	B	45	64	2	3	2016	BIPOLAR FRAG	Obsidian	1
15/05/16	006	001	Beta Samati	B	35	68	1	5	2016	BIPOLAR CORE	Obsidian	1

15/05/16	006	001	Beta Samati	B	35	68	1	5	2016	UTILIZED FLAKE	Obsidian	1
21/05/16	006	001	Beta Samati	B	28	62	2	4	2016	BIPOLAR FLAKE	Obsidian	1
21/05/16	006	001	Beta Samati	B	28	62	2	4	2016	MEDIAL FRAG	Obsidian	1
16/05/16	006	001	Beta Samati	B	48	62	1	18	2016	BIPOLAR FRAG	Obsidian	1
15/05/16	006	001	Beta Samati	B	45	64	1	7	2016	BIPOLAR CORE	Obsidian	1
15/05/16	006	001	Beta Samati	B	45	64	1	7	2016	FLAKE	Obsidian	1
12/05/2018	006	001	Beta Samati	B	48	62	1	2	2016	DIST FRAGMENT	Obsidian	2
12/05/2016	006	001	Beta Samati	B	45	60	1	3	2016	DIST FRAGMENT	Obsidian	1
17/05/16	006	001	Beta Samati	B	38	62	1	7	2016	FLAKE	Obsidian	1
17/05/16	006	001	Beta Samati	B	38	62	1	7	2016	PROX FRAG	Obsidian	1
02/06/2016	006	001	Beta Samati	B	28	98	1	6	2016	BACKED FRAGMENT	Obsidian	1
02/06/2016	006	001	Beta Samati	B	28	98	1	6	2016	ANGULAR WASTE	Obsidian	1
02/06/2016	006	001	Beta Samati	B	28	98	1	6	2016	FLAKE	Obsidian	1
25/05/16	006	001	Beta Samati	B	38	74	1	13	2016	FLAKE	Obsidian	1
26/05/16	006	001	Beta Samati	B	28	62	3	17	2016	DIST FRAGMENT	Obsidian	1
02/06/2016	006	001	Beta Samati	B	26	96	1	15	2016	FLAKE	Obsidian	1
02/06/2016	006	001	Beta Samati	B	26	96	1	15	2016	BACKED CRESENT	Obsidian	1
01/06/2016	006	001	Beta Samati	B	26	96	1	6	2016	DIST FRAGMENT	Obsidian	1
01/06/2016	006	001	Beta Samati	B	26	96	1	6	2016	PROX FRAG	Obsidian	1
02/06/2016	006	001	Beta Samati	B	38	104	1	3	2016	FLAKE	Obsidian	2
02/06/2016	006	001	Beta Samati	B	38	104	1	3	2016	BIPOLAR FLAKE	Obsidian	4
02/06/2016	006	001	Beta Samati	B	38	104	1	3	2016	MEDIAL FRAG	Obsidian	2
30/05/16	006	001	Beta Samati	B	27	92	1	7	2016	DIST FRAGMENT	Obsidian	1
17/05/16	006	001	Beta Samati	B	25	90	1	4	2016	MEDIAL FRAG	Obsidian	1
26/05/16	006	001	Beta Samati	B	25	82	1	11	2016	MEDIAL FRAG	Obsidian	1
28/05/16	006	001	Beta Samati	B	26	85	1	9	2016	FLAKE	Obsidian	1
30/05/16	006	001	Beta Samati	B	28	89	1	15	2016	PROX FRAG	Obsidian	1
01/06/2016	006	001	Beta Samati	B	25	81	1	8	2016	BIPOLAR FLAKE	Obsidian	1
30/05/16	006	001	Beta Samati	B	26	96	1	3	2016	BIPOLAR FLAKE	Obsidian	1
29/05/16	006	001	Beta Samati	B	45	90	1	4	2016	ANGULAR WASTE	Obsidian	1
02/06/2016	006	001	Beta Samati	B	37	0	1	4	2016	FLAKE	Obsidian	1
02/06/2016	006	001	Beta Samati	B	37	0	1	4	2016	MEDIAL FRAG	Obsidian	1
26/05/16	006	001	Beta Samati	B	26	85	1	3	2016	FLAKE	Obsidian	1
23/05/16	006	001	Beta Samati	B	25	60	2	6	2016	FLAKE	Obsidian	2

23/05/16	006	001	Beta Samati	B	25	60	2	6	2016	BIPOLAR FLAKE	Obsidian	1
25/05/16	006	001	Beta Samati	B	28	62	2	31	2016	FLAKE	Obsidian	1
23/05/16	006	001	Beta Samati	B	28	62	2	9	2016	MEDIAL FRAG	Obsidian	1
24/05/16	006	001	Beta Samati	B	25	81	1	2	2016	BACKED CRESENT	Obsidian	1
26/05/16	006	001	Beta Samati	B	27	0	1	5	2016	DIST FRAGMENT	Obsidian	1
24/05/16	006	001	Beta Samati	B	25	80	1	5	2016	BIPOLAR FRAG	Obsidian	2
24/05/16	006	001	Beta Samati	B	28	62	2	13	2016	DIST FRAGMENT	Obsidian	2
29/05/16	006	001	Beta Samati	B	26	85	1	13	2016	END SCRAPER	Obsidian	1
29/05/16	006	001	Beta Samati	B	26	85	1	13	2016	BIPOLAR FRAG	Obsidian	1
06/07/2012	002	001	Enda Cha'atat	N/A	N/A	N/A	N/A	2	2012	bipolar flake	Obsidian	1
06/07/2012	002	001	Enda Cha'atat	N/A	N/A	N/A	N/A	2	2012	bipolar core fragment flake	Obsidian	1
06/07/2012	002	001	Enda Cha'atat	N/A	N/A	N/A	N/A	2	2012	backed fragment	Obsidian	1
31/5/2016	067	001	Aoudi Welka	N/A	N/A	N/A	N/A	2	2016	bipolar flake	Obsidian	3
31/5/2016	067	001	Aoudi Welka	N/A	N/A	N/A	N/A	2	2016	Flake	Obsidian	2
31/5/2016	067	001	Aoudi Welka	N/A	N/A	N/A	N/A	2	2016	burin	Obsidian	1
31/5/2016	067	001	Aoudi Welka	N/A	N/A	N/A	N/A	2	2016	bipolar core	Obsidian	1
12/06/2015	006	001	Beta Samati	B	47	49	2	6	2015	Flake	Obsidian	1

Table II. 10 SRSAH Obsidian Sites.

#	Survey Unit	Site	Site Name	Survey Unit and Site Number	Obsidian Count	Comments
1	006	001	Beta Samati	006-001	297	
2	013	001	Dem Elal	013-001	81	
3	071	001	Sefra Aboun	071-001	209	
4	071	002	Mai Eungug	071-002	19	
5	022	001	Enda Balata Dista	022-001	42	
6	022	002	Enda Aboy Meles	022-002	51	
7	022	003	Dungur	022-003	1	
8	067	001	Aoudi Welka	067-001	32	
9	024	001	Gembes	024-001	6	
10	024	002	N/A	024-002	7	
11	024	003	N/A	024-003	17	
12	024B	N/A	N/A	024B	4	
13	044	001	Sekoualou	044-001	100	
14	026	001	Hchen	026-001	23	
15	025A	N/A	N/A	025A	3	
16	008	001	N/A	008-001	1	
17	082A	N/A	N/A	082A	2	
18	042	001	N/A	042-001	2	
19	061A	N/A	N/A	061A	1	
20	016	001	N/A	016-001	3	
21	081A	N/A	N/A	081A	1	
22	014	001	Adi Helafa 1	014-001	18	
23	014	002	Adi Helafa 2	014-002	4	
24	009A	N/A	N/A	009A	3	
25	014A	N/A	N/A	014	1	

26	008A	N/A	N/A	008A	1	
27	013A	N/A	N/A	013A	2	
28	017	001	Endaba Hailu	017-001	2	
29	068	001	Mirai Abune Afsea	068-001	11	
30	027	001	Sefra Tourkui	027-001	626	
31	010	001	Adi Abiselam 2	010-001	2	
32	051A	N/A	N/A	051A	1	
33	069	001	Tseratsur	069-001	2	Obsidian was uncovered in 069a – the survey unit that 069-001 is part of. I am including these samples with the data from 069-001 as it is unclear whether they were collected at the site and because of their physical proximity (notwithstanding their initial designation).
34	069	004	Kawhi Aboi Haftom	069-004	25	
35	077A	N/A	N/A	077A	1	
36	002	001	Enda Cha'atat	002-001	63	
37	081	001	Adi Krumbe/Tahtay Gundam	081-001	2	
38	029	003	Zban Ma'ekune/Beloho	029-003	1	
39	97A	N/A	N/A	97A	2	
40	79A	N/A	N/A	79A	5	
41	999	001	Adi Abiselam	999-001	4	
42	078A	N/A	N/A	078A	1	
43	029	002	Mai Fesasi	029-002	20	
44	079	001	Da'ero Arat/St. Gabriel Church	079-001	25	
45	042	002	Enda Giordis Mogu'o	042-002	1	
Total					**1705**	

Table II. 11 Obsidian from Beta Samati 006-001 (analyzed by Dr. Elizabeth Peterson).

Date	Survey Unit	Site	Site Name	Area	Quad	Locus	Lot	Bag #	Season	Type	Raw Material	Count
04/08/11	006	001	Beta Samati	A		11	1	8	2011	flake fragments distal	Obsidian	1
05/08/11	006	001	Beta Samati	A		10	2	10	2011	bipolar flake	Obsidian	1
05/08/11	006	001	Beta Samati	A		10	2	10	2011	flake fragments distal	Obsidian	1
05/08/11	006	001	Beta Samati	A		10	2	10	2011	backed cresent	Obsidian	1
03/08/11	006	001	Beta Samati	A		20	4	14	2012	bipolar flake fragment	Obsidian	1
03/08/11	006	001	Beta Samati	A		20	4	14	2012	bipolar flake	Obsidian	2
23/07/11	006	001	Beta Samati	A		4	1	7	2011	flake	Obsidian	1
23/07/11	006	001	Beta Samati	A		4	1	7	2011	microflake	Obsidian	1
26/07/11	006	001	Beta Samati	A		4	1	12	2011	flake fragment	Obsidian	2
26/07/11	006	001	Beta Samati	A		4	1	12	2011	bipolar flake fragment	Obsidian	1
26/07/11	006	001	Beta Samati	A		4	1	12	2011	bipolar flake fragment	Obsidian	3
29/07/11	006	001	Beta Samati	A		10	1	5	2011	flake fragments medial	Obsidian	1

29/07/11	006	001	Beta Samati	A		10	1	5	2011	bipolar flake	Obsidian	1
29/07/11	006	001	Beta Samati	A		10	1	5	2011	flake	Obsidian	2
29/07/11	006	001	Beta Samati	A		10	1	5	2011	outil ecaill	Obsidian	1
27/07/11	006	001	Beta Samati	A		5	1	2	2011	bipolar flake	Obsidian	1
27/07/11	006	001	Beta Samati	A		4	1	20	2011	flake fragments distal	Obsidian	1
27/07/11	006	001	Beta Samati	A		4	1	20	2011	flake fragments medial	Obsidian	1
27/07/11	006	001	Beta Samati	A		4	1	20	2011	bipolar flake	Obsidian	2
27/07/11	006	001	Beta Samati	A		4	1	20	2011	flake	Obsidian	1
27/07/11	006	001	Beta Samati	A		4	1	20	2011	backed cresent	Obsidian	1
25/07/11	006	001	Beta Samati	A		3	1	8	2011	flake fragments distal	Obsidian	2
25/07/11	006	001	Beta Samati	A		3	1	8	2011	flake fragments medial	Obsidian	1
25/07/11	006	001	Beta Samati	A		3	1	8	2011	bipolar flake	Obsidian	2
20/07/11	006	001	Beta Samati	A		1	1	2	2011	bipolar flake	Obsidian	1
20/07/11	006	001	Beta Samati	A		1	1	2	2011	bipolar flake	Obsidian	1
05/08/11	006	001	Beta Samati	A		14	1	2	2011	flake fragments proximal	Obsidian	1
04/08/11	006	001	Beta Samati	A		10	2	5	2011	flake fragments distal	Obsidian	3
04/08/11	006	001	Beta Samati	A		10	2	5	2011	flake fragments medial	Obsidian	1
04/08/11	006	001	Beta Samati	A		10	2	5	2011	flake	Obsidian	1
20/06/12	006	001	Beta Samati	A		25	1	12	2012	backed cresent	Obsidian	1
20/06/12	006	001	Beta Samati	A		10	1	30	2011	utilized flake	Obsidian	1
10/08/11	006	001	Beta Samati	B				2	2011	denticulate side scraper	Obsidian	1
10/08/11	006	001	Beta Samati	B				2	2011	bipolar flake fragment	Obsidian	3
10/08/11	006	001	Beta Samati	B				2	2011	blade	Obsidian	1
10/08/11	006	001	Beta Samati	B				2	2011	bipolar flake	Obsidian	1
10/08/11	006	001	Beta Samati	B				2	2011	flake	Obsidian	1
19/06/12	006	001	Beta Samati	A		20	2	13	2012	flake	Obsidian	1
19/06/12	006	001	Beta Samati	A		20	2	13	2012	Angular waste	Obsidian	1
16/06/12	006	001	Beta Samati	B		6	1	88	2012	flake fragment	Obsidian	1
13/06/12	006	001	Beta Samati	B		6	1	49	2012	flake fragment	Obsidian	1
23/06/12	006	001	Beta Samati	A		200	4	14	2012	proximal flake fragment	Obsidian	1
23/06/12	006	001	Beta Samati	A		200	4	14	2012	Flake	Obsidian	2
21/06/12	006	001	Beta Samati	A		25	1	22	2012	utilized flake fragment	Obsidian	1
21/06/12	006	001	Beta Samati	A		25	1	22	2012	crecent backed	Obsidian	1
21/06/12	006	001	Beta Samati	A		25	1	22	2012	utilized flake fragment	Obsidian	1

21/06/12	006	001	Beta Samati	A		25	1	22	2012	bipolar core	Obsidian	1
06/06/12	006	001	Beta Samati	A		15	1	2	2012	flake fragments proximal	Obsidian	2
06/06/12	006	001	Beta Samati	A		15	1	2	2012	bipolar flake	Obsidian	1
26/06/12	006	001	Beta Samati	B		10	2	275	2012	bipolar flake	Obsidian	1
26/06/12	006	001	Beta Samati	B		10	2	275	2012	flake fragments distal	Obsidian	1
23/06/12	006	001	Beta Samati	B		10	2	228	2012	blade	Obsidian	1
23/06/12	006	001	Beta Samati	B		10	2	228	2012	partially backed	Obsidian	1
09/06/12	006	001	Beta Samati	B		1	NA	10	2012	bipolar flake	Obsidian	1
24/06/12	006	001	Beta Samati	B		16	1	285	2012	backed flake pice broken	Obsidian	1
26/06/12	006	001	Beta Samati	B		14	1	282	2012	flake fragment	Obsidian	1
16/06/12	006	001	Beta Samati	A		20	2	4	2012	blade distal fragment	Obsidian	1
16/06/12	006	001	Beta Samati	A		20	2	4	2012	flake	Obsidian	1
16/06/12	006	001	Beta Samati	A		20	2	4	2012	bipolar flake	Obsidian	1
16/06/12	006	001	Beta Samati	A		20	2	4	2012	backed crescent	Obsidian	1
16/06/12	006	001	Beta Samati	A		20	2	4	2012	bipolar core	Obsidian	1
07/06/12	006	001	Beta Samati	A		15	1	6	2012	bipolar flake	Obsidian	2
07/06/12	006	001	Beta Samati	A		15	1	6	2012	flake fragments distal	Obsidian	1
23/06/12	006	001	Beta Samati	A		27	1	30	2012	bipolar flake fragment	Obsidian	2
16/06/12	006	001	Beta Samati	B		6	1	91	2012	CRF	Obsidian	1
27/06/12	006	001	Beta Samati	B		15	1	300	2012	bipolar flake	Obsidian	1
21/06/12	006	001	Beta Samati	B		11	2	139	2012	flake	Obsidian	1
21/06/12	006	001	Beta Samati	A		25	1	17	2012	flake	Obsidian	1
21/06/12	006	001	Beta Samati	A		25	1	17	2012	proximal flake fragment	Obsidian	1
21/06/12	006	001	Beta Samati	A		27	1	15	2012	MEDIAL BLADE FRAGMENT	Obsidian	1
21/06/12	006	001	Beta Samati	A		27	1	15	2012	proximal fragment	Obsidian	1
21/06/12	006	001	Beta Samati	A		27	1	15	2012	bipolar flake fragment	Obsidian	1
21/06/12	006	001	Beta Samati	B		12	1	138	2012	bipolar flake	Obsidian	1
20/06/12	006	001	Beta Samati	B		11	1	116	2012	bipolar flake	Obsidian	1
15/06/12	006	001	Beta Samati	B		7	1	67	2012	utilized flake fragment	Obsidian	1
22/06/12	006	001	Beta Samati	B		10	1	212	2012	flake fragments distal	Obsidian	1
22/06/12	006	001	Beta Samati	A		20	4	2	2012	flake	Obsidian	1
22/06/12	006	001	Beta Samati	A		20	4	2	2012	bipolar flake fragments	Obsidian	1
19/06/12	006	001	Beta Samati	A		20	3	5	2012	bipolar flake	Obsidian	2
19/06/12	006	001	Beta Samati	A		20	3	5	2012	blade	Obsidian	2

19/06/12	006	001	Beta Samati	A		20	3	5	2012	utilized blade	Obsidian	1
19/06/12	006	001	Beta Samati	A		20	3	5	2012	flake	Obsidian	1
19/06/12	006	001	Beta Samati	A		20	3	5	2012	bipolar core fragment	Obsidian	1
19/06/12	006	001	Beta Samati	A		20	3	5	2012	flake fragments medial	Obsidian	1
23/06/12	006	001	Beta Samati	A		25	2	10	2012	bipolar flake	Obsidian	1
23/06/12	006	001	Beta Samati	A		25	2	10	2012	bipolar flake fragment	Obsidian	3
07/06/12	006	001	Beta Samati	B		1	NA	5	2012	BURIN SPALL	Obsidian	1
07/06/12	006	001	Beta Samati	B		1	NA	5	2012	flake fragments proximal	Obsidian	14
07/06/12	006	001	Beta Samati	B		1	NA	5	2012	blade fragment proxmal end	Obsidian	1
07/06/12	006	001	Beta Samati	B		1	NA	5	2012	flake fragments medial	Obsidian	3
07/06/12	006	001	Beta Samati	B		1	NA	5	2012	bipolar flake fragments	Obsidian	2
07/06/12	006	001	Beta Samati	B		1	NA	5	2012	flake fragments distal	Obsidian	4
07/06/12	006	001	Beta Samati	B		1	NA	5	2012	flakes	Obsidian	13
07/06/12	006	001	Beta Samati	B		1	NA	5	2012	blade	Obsidian	2
07/06/12	006	001	Beta Samati	B		1	NA	5	2012	bipolar flake	Obsidian	2
07/06/12	006	001	Beta Samati	B		1	NA	5	2012	bipolar core	Obsidian	4
07/06/12	006	001	Beta Samati	B		1	NA	5	2012	CTF	Obsidian	1
07/06/12	006	001	Beta Samati	B		1	NA	5	2012	utilized blades	Obsidian	3
07/06/12	006	001	Beta Samati	B		1	NA	5	2012	backed crescent	Obsidian	5
07/06/12	006	001	Beta Samati	B		1	NA	5	2012	backed blade	Obsidian	1
07/06/12	006	001	Beta Samati	B		1	NA	5	2012	backed flake piece broken	Obsidian	3
07/06/12	006	001	Beta Samati	B		1	NA	5	2012	side scraper	Obsidian	1
07/06/12	006	001	Beta Samati	B		1	NA	5	2012	partially backed	Obsidian	1
16/06/12	006	001	Beta Samati	B		10	1	86	2012	flake fragment	Obsidian	1
13/06/12	006	001	Beta Samati	B		1	1	48	2012	bipolar flake fragment	Obsidian	1
20/06/12	006	001	Beta Samati	A		27	1	3	2012	flake fragment	Obsidian	1
20/06/12	006	001	Beta Samati	A		27	1	3	2012	bipolar flake fragment	Obsidian	1
20/06/12	006	001	Beta Samati	A		27	1	3	2012	CTF	Obsidian	1
05/08/11	006	001	Beta Samati	A		11	2	5	2011	modified flake	Obsidian	1
05/08/11	006	001	Beta Samati	A		11	2	5	2011	blade fragment	Obsidian	1
26/07/11	006	001	Beta Samati	A		3		15	2011	bipolar flake fragment	Obsidian	1
07/06/15	006	001	Beta Samati	A	?	64	1	6	2015	SIDE SCRAPER	Obsidian	1
23/05/15	006	001	Beta Samati	A	66	29	1	2	2015	BIPOLA CORE	Obsidian	1
17/05/15	006	001	Beta Samati	A	75	29	1	7	2015	FLAKE MEDIAL FRAGMENT	Obsidian	1

17/05/15	006	001	Beta Samati	A	75	29	1	7	2015	FLAKE DISTAL FRAGMENT	Obsidian	1
17/05/15	006	001	Beta Samati	A	75	29	1	7	2015	ANGULAR WASTE	Obsidian	3
14/05/15	006	001	Beta Samati	A	76	29	1	1	2015	BIPOLAR FLAKE	Obsidian	1
14/05/15	006	001	Beta Samati	A	76	29	1	1	2015	FLAKE	Obsidian	1
20/05/15	006	001	Beta Samati	A	76	31	1	3	2015	BIPOLAR FLAKE	Obsidian	1
05/06/15	006	001	Beta Samati	A	75	64	1	1	2015	FLAKE DISTAL FRAGMENT	Obsidian	2
05/06/15	006	001	Beta Samati	A	75	64	1	1	2015	ANGULAR WASTE	Obsidian	1
20/05/15	006	001	Beta Samati	A	75	40	2	3	2015	FLAKE	Obsidian	1
23/05/15	006	001	Beta Samati	A	65	45	8	4	2015	FLAKE	Obsidian	1
23/05/15	006	001	Beta Samati	A	65	45	8	4	2015	FLAKE PROXMAL FRAGMENT	Obsidian	2
22/05/15	006	001	Beta Samati	A	75	37	1	3	2015	MEDIAL BLADE FRAGMENT	Obsidian	1
09/06/15	006	001	Beta Samati	A	75	64	1	7	2015	LOUTIL ECAILLES	Obsidian	1
05/06/15	006	001	Beta Samati	A	76	45	1	4	2015	FLAKE DISTAL FRAGMENT	Obsidian	1
05/06/15	006	001	Beta Samati	A	76	45	1	4	2015	FLAKE MEDIAL FRAGMENT	Obsidian	1
05/06/15	006	001	Beta Samati	A	76	45	1	4	2015	BIPOLAR FLAKE	Obsidian	1
25/05/15	006	001	Beta Samati	A	66	51	1	2	2015	SCRAPER FRAGMENT	Obsidian	1
25/05/15	006	001	Beta Samati	A	66	51	1	2	2015	BURIN SPAULL	Obsidian	1
25/05/15	006	001	Beta Samati	A	66	51	1	2	2015	BIPOLAR FLAKE	Obsidian	1
25/05/15	006	001	Beta Samati	A	76	31	1	5	2015	SCRAPER FRAGMENT	Obsidian	1
07/06/15	006	001	Beta Samati	A	67	47	1	4	2015	FLAKE	Obsidian	2
07/06/15	006	001	Beta Samati	A	67	47	1	4	2015	FLAKE DISTAL FRAGMENT	Obsidian	2
08/06/15	006	001	Beta Samati	A	75	66	1	2	2015	FLAKE	Obsidian	2
08/06/15	006	001	Beta Samati	A	75	66	1	2	2015	OUTIL ECAILLE	Obsidian	1
09/06/15	006	001	Beta Samati	B	36	25	3	3	2015	OUTIL ECAILLE	Obsidian	1
07/06/15	006	001	Beta Samati	B	36	24	1	11	2015	BIPOLAR CORE	Obsidian	1
07/06/15	006	001	Beta Samati	B	36	24	1	11	2015	BIPOLAR FLAKE	Obsidian	1
25/05/15	006	001	Beta Samati	B	34	18	1	8	2015	FLAKE PROXMAL FRAGMENT	Obsidian	1
04/06/15	006	001	Beta Samati	B	37	45	1	6	2015	END SCRAPER ON FLAKE	Obsidian	1
28/05/15	006	001	Beta Samati	B	37	25a	1	2	2015	FLAKE DISTAL FRAGMENT	Obsidian	1
08/06/15	006	001	Beta Samati	B	37	45	2	15	2015	BACKED FRAGMENT	Obsidian	1
09/06/15	006	001	Beta Samati	A	75	66	1	7	2015	FLAKE	Obsidian	1
10/06/15	006	001	Beta Samati	A	73	63	3	8	2015	FLAKE	Obsidian	1
10/06/15	006	001	Beta Samati	A	73	63	3	8	2015	BIPOLAR FLAKE	Obsidian	1
11/06/15	006	001	Beta Samati	B	37	52	1	11	2015	FLAKE PROXMAL FRAGMENT	Obsidian	1

10/06/15	006	001	Beta Samati	B	36	45	3	3	2015	BACKED CRESCENT	Obsidian	1
08/06/15	006	001	Beta Samati	B	36	24	1	17	2015	BIPOLAR FLAKE	Obsidian	1
20/05/15	006	001	Beta Samati	B	36	24	1	3	2015	FLAKE	Obsidian	1
07/06/15	006	001	Beta Samati	B	46	49	1	5	2015	FLAKE DISTAL FRAGMENT	Obsidian	1
10/06/15	006	001	Beta Samati	B	37	50	1	3	2915	BIPOLAR FLAKE	Obsidian	2
12/06/15	006	001	Beta Samati	B	37	51	1	14	2015	BIPOLAR FLAKE	Obsidian	1
12/06/15	006	001	Beta Samati	B	37	44	2	6	2015	FLAKE	Obsidian	1
12/06/15	006	001	Beta Samati	B	37	44	2	6	2015	FLAKE	Obsidian	1
11/06/15	006	001	Beta Samati	A	75	53	1	1	2015	FLAKE DISTAL FRAGMENT	Obsidian	1
09/06/15	006	001	Beta Samati	B	36	24	1	20	2015	BIPOLAR FLAKE	Obsidian	1
10/06/15	006	001	Beta Samati	A	66	51	1		2015	FLAKE DISTAL FRAGMENT	Obsidian	2
12/05/16	006	001	Beta Samati	B	35	60	1	3	2016	BIPOLAR FLAKE	Obsidian	1
12/05/16	006	001	Beta Samati	B	35	61	1	5	2016	DIST FRAGMENT	Obsidian	1
17/05/16	006	001	Beta Samati	B	45	64	2	15	2016	UTILIZED FLAKE	Obsidian	1
17/05/16	006	001	Beta Samati	B	45	60	1	22	2016	NOTCHED SCRAPER?	Obsidian	1
18/05/16	006	001	Beta Samati	B	45	60	2	6	2016	FLAKE	Obsidian	1
16/05/16	006	001	Beta Samati	B	38	65	1	19	2016	BACKED FRAGMENT	Obsidian	1
16/05/16	006	001	Beta Samati	B	35	70	1	9	2016	BIPOLAR FRAG	Obsidian	1
15/05/16	006	001	Beta Samati	B	35	70	1	1	2016	DIST FRAGMENT	Obsidian	1
16/05/16	006	001	Beta Samati	B	48	67	2	3	2016	FLAKE	Obsidian	1
13/05/16	006	001	Beta Samati	B	45	60	1	12	2016	FLAKE	Obsidian	1
15/05/16	006	001	Beta Samati	B	45	64	2	3	2016	BIPOLAR FRAG	Obsidian	1
15/05/16	006	001	Beta Samati	B	35	68	1	5	2016	BIPOLAR CORE	Obsidian	1
15/05/16	006	001	Beta Samati	B	35	68	1	5	2016	UTILIZED FLAKE	Obsidian	1
21/05/16	006	001	Beta Samati	B	28	62	2	4	2016	BIPOLAR FLAKE	Obsidian	1
21/05/16	006	001	Beta Samati	B	28	62	2	4	2016	MEDIAL FRAG	Obsidian	1
16/05/16	006	001	Beta Samati	B	48	62	1	18	2016	BIPOLAR FRAG	Obsidian	1
15/05/16	006	001	Beta Samati	B	45	64	1	7	2016	BIPOLAR CORE	Obsidian	1
15/05/16	006	001	Beta Samati	B	45	64	1	7	2016	FLAKE	Obsidian	1
12/05/18	006	001	Beta Samati	B	48	62	1	2	2016	DIST FRAGMENT	Obsidian	2
12/05/16	006	001	Beta Samati	B	45	60	1	3	2016	DIST FRAGMENT	Obsidian	1
17/05/16	006	001	Beta Samati	B	38	62	1	7	2016	FLAKE	Obsidian	1
17/05/16	006	001	Beta Samati	B	38	62	1	7	2016	PROX FRAG	Obsidian	1
02/06/16	006	001	Beta Samati	B	28	98	1	6	2016	BACKED FRAGMENT	Obsidian	1

02/06/16	006	001	Beta Samati	B	28	98	1	6	2016	ANGULAR WASTE	Obsidian	1
02/06/16	006	001	Beta Samati	B	28	98	1	6	2016	FLAKE	Obsidian	1
25/05/16	006	001	Beta Samati	B	38	74	1	13	2016	FLAKE	Obsidian	1
26/05/16	006	001	Beta Samati	B	28	62	3	17	2016	DIST FRAGMENT	Obsidian	1
02/06/16	006	001	Beta Samati	B	26	96	1	15	2016	FLAKE	Obsidian	1
02/06/16	006	001	Beta Samati	B	26	96	1	15	2016	BACKED CRESENT	Obsidian	1
01/06/16	006	001	Beta Samati	B	26	96	1	6	2016	DIST FRAGMENT	Obsidian	1
01/06/16	006	001	Beta Samati	B	26	96	1	6	2016	PROX FRAG	Obsidian	1
02/06/16	006	001	Beta Samati	B	38	104	1	3	2016	FLAKE	Obsidian	2
02/06/16	006	001	Beta Samati	B	38	104	1	3	2016	BIPOLAR FLAKE	Obsidian	4
02/06/16	006	001	Beta Samati	B	38	104	1	3	2016	MEDIAL FRAG	Obsidian	2
30/05/16	006	001	Beta Samati	B	27	92	1	7	2016	DIST FRAGMENT	Obsidian	1
17/05/16	006	001	Beta Samati	B	25	90	1	4	2016	MEDIAL FRAG	Obsidian	1
26/05/16	006	001	Beta Samati	B	25	82	1	11	2016	MEDIAL FRAG	Obsidian	1
28/05/16	006	001	Beta Samati	B	26	85	1	9	2016	FLAKE	Obsidian	1
30/05/16	006	001	Beta Samati	B	28	89	1	15	2016	PROX FRAG	Obsidian	1
01/06/16	006	001	Beta Samati	B	25	81	1	8	2016	BIPOLAR FLAKE	Obsidian	1
30/05/16	006	001	Beta Samati	B	26	96	1	3	2016	BIPOLAR FLAKE	Obsidian	1
29/05/16	006	001	Beta Samati	B	45	90	1	4	2016	ANGULAR WASTE	Obsidian	1
02/06/16	006	001	Beta Samati	B	37	0	1	4	2016	FLAKE	Obsidian	1
02/06/16	006	001	Beta Samati	B	37	0	1	4	2016	MEDIAL FRAG	Obsidian	1
26/05/16	006	001	Beta Samati	B	26	85	1	3	2016	FLAKE	Obsidian	1
23/05/16	006	001	Beta Samati	B	25	60	2	6	2016	FLAKE	Obsidian	2
23/05/16	006	001	Beta Samati	B	25	60	2	6	2016	BIPOLAR FLAKE	Obsidian	1
25/05/16	006	001	Beta Samati	B	28	62	2	31	2016	FLAKE	Obsidian	1
23/05/16	006	001	Beta Samati	B	28	62	2	9	2016	MEDIAL FRAG	Obsidian	1
24/05/16	006	001	Beta Samati	B	25	81	1	2	2016	BACKED CRESENT	Obsidian	1
26/05/16	006	001	Beta Samati	B	27	0	1	5	2016	DIST FRAGMENT	Obsidian	1
24/05/16	006	001	Beta Samati	B	25	80	1	5	2016	BIPOLAR FRAG	Obsidian	2
24/05/16	006	001	Beta Samati	B	28	62	2	13	2016	DIST FRAGMENT	Obsidian	2
29/05/16	006	001	Beta Samati	B	26	85	1	13	2016	END SCRAPER	Obsidian	1
29/05/16	006	001	Beta Samati	B	26	85	1	13	2016	BIPOLAR FRAG	Obsidian	1
12/06/15	006	001	Beta Samati	B	47	49	2	6	2015	Flake	Obsidian	1
Total												297

Table II. 12 Obsidian from Dem Elal 013-001 (analyzed by Dr. Elizabeth Peterson).

Date	Survey Unit	Site	Site Name	Bag #	Season	Type	Raw Material	Count
10/08/11	013	001	Dem Elal	2	2011	Utilized flake	Obsidian	2
10/08/11	013	001	Dem Elal	2	2011	Bipolar core fragment	Obsidian	3
10/08/11	013	001	Dem Elal	2	2011	Bipolar core	Obsidian	15
10/08/11	013	001	Dem Elal	2	2011	CTF	Obsidian	1
10/08/11	013	001	Dem Elal	2	2011	Prismatic core	Obsidian	1
10/08/11	013	001	Dem Elal	2	2011	Outil ecaille	Obsidian	5
10/08/11	013	001	Dem Elal	2	2011	Blade	Obsidian	2
10/08/11	013	001	Dem Elal	2	2011	Bipolar flake	Obsidian	10
10/08/11	013	001	Dem Elal	2	2011	Bipolar flake fragment	Obsidian	5
10/08/11	013	001	Dem Elal	2	2011	Flake medial fragment	Obsidian	7
10/08/11	013	001	Dem Elal	2	2011	Flake proximal fragment	Obsidian	5
10/08/11	013	001	Dem Elal	2	2011	Flake distal fragment	Obsidian	8
10/08/11	013	001	Dem Elal	2	2011	flake	Obsidian	9
10/08/11	013	001	Dem Elal	2	2011	Notched scraper fragments	Obsidian	3
10/08/11	013	001	Dem Elal	2	2011	denticulate scraper on flake	Obsidian	3
10/08/11	013	001	Dem Elal	2	2011	End scraper flake	Obsidian	1
10/08/11	013	001	Dem Elal	2	2011	Unifacial point	Obsidian	1
Total								81

Table II. 13 Obsidian from Sefra Aboun 071-001 (analyzed by Dr. Elizabeth Peterson).

Date	Survey Unit	Site	Site Name	Bag #	Season	Type	Raw Material	Count
10/08/2011	071	001	Sefra Aboun	1	2011	bipolar core	Obsidian	2
10/08/2011	071	001	Sefra Aboun	1	2011	awl	Obsidian	1
10/08/2011	071	001	Sefra Aboun	1	2011	flake fragments	Obsidian	12
02/07/2012	071	001	Sefra Aboun	3	2012	flake	Obsidian	20
02/07/2012	071	001	Sefra Aboun	3	2012	bipolar flake	Obsidian	30
02/07/2012	071	001	Sefra Aboun	3	2012	bipolar flake fragment	Obsidian	6
02/07/2012	071	001	Sefra Aboun	3	2012	flake proximal fragment	Obsidian	2
02/07/2012	071	001	Sefra Aboun	3	2012	flake medial fragment	Obsidian	3
02/07/2012	071	001	Sefra Aboun	3	2012	flake distal fragment	Obsidian	13
02/07/2012	071	001	Sefra Aboun	3	2012	outil ecaille	Obsidian	2
02/07/2012	071	001	Sefra Aboun	3	2012	end and side scraper	Obsidian	1
02/07/2012	071	001	Sefra Aboun	3	2012	bipolar core fragment	Obsidian	14
02/07/2012	071	001	Sefra Aboun	3	2012	bipolar core	Obsidian	9
02/07/2012	071	001	Sefra Aboun	3	2012	backed crescent	Obsidian	3
02/07/2012	071	001	Sefra Aboun	3	2012	backed fragment	Obsidian	6
02/07/2012	071	001	Sefra Aboun	3	2012	burin spall	Obsidian	2
02/07/2012	071	001	Sefra Aboun	3	2012	Angular waste	Obsidian	44
19/05/2015	071	001	Sefra Aboun	2	2015	bipolar flake	Obsidian	1
17/05/2015	071	001	Sefra Aboun	2	2015	flake	Obsidian	9
17/05/2015	071	001	Sefra Aboun	2	2015	bipolar flake	Obsidian	2
17/05/2015	071	001	Sefra Aboun	2	2015	bipolar core	Obsidian	3
17/05/2015	071	001	Sefra Aboun	2	2015	flake distal fragment	Obsidian	4
17/05/2015	071	001	Sefra Aboun	2	2015	straight backed	Obsidian	1
Total								190

Table II. 14 Obsidian from Mai Eungug 071-002 (analyzed by Dr. Elizabeth Peterson).

Date	Survey Unit	Site	Site Name	Bag #	Season	Type	Raw Material	Count
17/05/2015	071	002	Mai Eungug	1	2015	Flake	Obsidian	3
17/05/2015	071	002	Mai Eungug	1	2015	bipolar flake	Obsidian	4
17/05/2015	071	002	Mai Eungug	1	2015	bipolar core	Obsidian	1
17/05/2015	071	002	Mai Eungug	1	2015	flake proximal fragment	Obsidian	1
17/05/2015	071	002	Mai Eungug	1	2015	flake medial fragment	Obsidian	2

17/05/2015	071	002	Mai Eungug	1	2015	flake distal fragment	Obsidian	4
17/05/2015	071	002	Mai Eungug	1	2015	bipolar flake fragment	Obsidian	2
17/05/2015	071	002	Mai Eungug	1	2015	angular waste	Obsidian	2
Total								19

Table II. 15 Obsidian from Enda Balata Dista 022-001 (analyzed by Dr. Elizabeth Peterson).

Date	Survey Unit	Site	Site Name	Bag #	Season	Type	Raw Material	Count
10/08/2011	022	001	Enda Balata Dista	2	2011	flake	Obsidian	7
10/08/2011	022	001	Enda Balata Dista	2	2011	bipolar flake	Obsidian	7
10/08/2011	022	001	Enda Balata Dista	2	2011	backed crescent	Obsidian	1
10/08/2011	022	001	Enda Balata Dista	2	2011	side scrape denticulate	Obsidian	1
10/08/2011	022	001	Enda Balata Dista	2	2011	angular waste	Obsidian	9
10/08/2011	022	001	Enda Balata Dista	2	2011	burin spaul	Obsidian	2
10/08/2011	022	001	Enda Balata Dista	2	2011	CTF	Obsidian	1
10/08/2011	022	001	Enda Balata Dista	2	2011	bipolar core	Obsidian	3
10/08/2011	022	001	Enda Balata Dista	2	2011	flake proximal fragment	Obsidian	2
10/08/2011	022	001	Enda Balata Dista	2	2011	flake distal fragment	Obsidian	3
10/08/2011	022	001	Enda Balata Dista	2	2011	flake medial fragment	Obsidian	6
Total								42

Table II. 16 Obsidian from Enda Aboy Meles 022-002 (analyzed by Dr. Elizabeth Peterson)

Date	Survey Unit	Site	Site Name	Bag #	Season	Type	Raw Material	Count
10/08/2011	022	002	Enda Aboy Meles	2	2011	denticulate scraper	Obsidian	1
10/08/2011	022	002	Enda Aboy Meles	2	2011	angle burin	Obsidian	1
10/08/2011	022	002	Enda Aboy Meles	2	2011	side scraper	Obsidian	1
10/08/2011	022	002	Enda Aboy Meles	2	2011	bipolar flake	Obsidian	4
10/08/2011	022	002	Enda Aboy Meles	2	2011	flake fragments	Obsidian	36
10/08/2011	022	002	Enda Aboy Meles	2	2011	bipolar core	Obsidian	5
10/08/2011	022	002	Enda Aboy Meles	2	2011	single platform core	Obsidian	1
10/08/2011	022	002	Enda Aboy Meles	2	2011	backed fragment	Obsidian	1
10/08/2011	022	002	Enda Aboy Meles	2	2011	backed flake pice broken	Obsidian	1
Total								51

Table II. 17 Obsidian from Dungur 022-003 (analyzed by Dr. Elizabeth Peterson).

Date	Survey Unit	Site	Site Name	Bag #	Season	Type	Raw Material	Count
10/08/2011	022	003	Dungur	2	2011	outil ecaille	Obsidian	1
Total								1

Table II. 18 Obsidian from Aoudi Welka 067-001 (analyzed by Dr. Elizabeth Peterson).

Date	Survey Unit	Site	Site Name	Bag #	Season	Type	Raw Material	Count
09/08/2011	067	001	Aoudi Welka	2	2011	blade	Obsidian	1
09/08/2011	067	001	Aoudi Welka	2	2011	flake	Obsidian	4
09/08/2011	067	001	Aoudi Welka	2	2011	bipolar flake	Obsidian	3
09/08/2011	067	001	Aoudi Welka	2	2011	bipolar core	Obsidian	2
09/08/2011	067	001	Aoudi Welka	2	2011	burin angular	Obsidian	1
09/08/2011	067	001	Aoudi Welka	2	2011	side scraper	Obsidian	1
09/08/2011	067	001	Aoudi Welka	2	2011	CTF	Obsidian	1
09/08/2011	067	001	Aoudi Welka	2	2011	outil ecaille	Obsidian	1
09/08/2011	067	001	Aoudi Welka	2	2011	utilized flake	Obsidian	2
09/08/2011	067	001	Aoudi Welka	2	2011	flake medial fragment	Obsidian	4
09/08/2011	067	001	Aoudi Welka	2	2011	flake distal fragment	Obsidian	5
31/05/2016	067	001	Aoudi Welka	2	2016	bipolar flake	Obsidian	3
31/05/2016	067	001	Aoudi Welka	2	2016	flake	Obsidian	2

31/05/2016	067	001	Aoudi Welka	2	2016	burin	Obsidian	1
31/05/2016	067	001	Aoudi Welka	2	2016	bipolar core	Obsidian	1
Total								32

Table II. 19 Obsidian from 024-001 (analyzed by Dr. Elizabeth Peterson).

Date	Survey Unit	Site	Site Name	Bag #	Season	Type	Raw Material	Count
09/06/2012	024	001	N/A	2	2012	bipolar flake fragment	Obsidian	5
09/06/2012	024	001	N/A	2	2012	bipolar core	Obsidian	1
Total								6

Table II. 20 Obsidian from 024-002 (analyzed by Dr. Elizabeth Peterson).

Date	Survey Unit	Site	Site Name	Bag #	Season	Type	Raw Material	Count
09/06/2012	024	002	N/A	3	2012	burin spall	Obsidian	1
09/06/2012	024	002	N/A	3	2012	flake	Obsidian	1
09/06/2012	024	002	N/A	3	2012	bipolar flake fragment	Obsidian	1
09/06/2012	024	002	N/A	3	2012	double side scraper	Obsidian	1
09/06/2012	024	002	N/A	3	2012	bipolar flake	Obsidian	1
09/06/2012	024	002	N/A	3	2012	flake fragment	Obsidian	1
09/06/2012	024	002	N/A	3	2012	bipolar flake fragment	Obsidian	1
Total								7

Table II. 21 Obsidian from 024-003 (analyzed by Dr. Elizabeth Peterson).

Date	Survey Unit	Site	Site Name	Bag #	Season	Type	Raw Material	Count
09/06/2012	024	003	N/A	2	2012	flake	Obsidian	3
09/06/2012	024	003	N/A	2	2012	bipolar flake	Obsidian	2
09/06/2012	024	003	N/A	2	2012	angular waste	Obsidian	3
09/06/2012	024	003	N/A	2	2012	flake proximal fragment	Obsidian	1
09/06/2012	024	003	N/A	2	2012	flake distal fragment	Obsidian	1
09/06/2012	024	003	N/A	2	2012	flake medial fragment	Obsidian	3
09/06/2012	024	003	N/A	2	2012	bipolar core	Obsidian	2
09/06/2012	024	003	N/A	2	2012	bipolar core fragment	Obsidian	2
Total								17

Table II. 22 Obsidian from Survey Unit 024b (analyzed by Dr. Elizabeth Peterson).

Date	Survey Unit	Bag #	Season	Type	Raw Material	Count
09/06/2012	24B	1	2012	outil ecaille	Obsidian	1
09/06/2012	24B	1	2012	flake proximal fragment	Obsidian	1
09/06/2012	24B	1	2012	Alternate edge point	Obsidian	1
09/06/2012	24B	1	2012	utilized bipolar flake	Obsidian	1
Total						**4**

Table II. 23 Obsidian from Sekoualou 044-001 (analyzed by Dr. Elizabeth Peterson).

Date	Survey Unit	Site	Site Name	Bag #	Season	Type	Raw Material	Count
04/07/12	044	001	Sekoualou	3	2012	flake distal fragment	Obsidian	1
04/07/12	044	001	Sekoualou	2	2012	blade	Obsidian	3
04/07/12	044	001	Sekoualou	2	2012	end scraper flake	Obsidian	2
04/07/12	044	001	Sekoualou	2	2012	burin spall	Obsidian	2
04/07/12	044	001	Sekoualou	2	2012	outil ecaille	Obsidian	1
04/07/12	044	001	Sekoualou	2	2012	bipolar core fragment	Obsidian	3
04/07/12	044	001	Sekoualou	2	2012	bipolar flake fragment	Obsidian	3

04/07/12	044	001	Sekoualou	2	2012	flake proximal fragment	Obsidian	4
04/07/12	044	001	Sekoualou	2	2012	flake medial fragment	Obsidian	4
04/07/12	044	001	Sekoualou	2	2012	flake distal fragment	Obsidian	5
04/07/12	044	001	Sekoualou	2	2012	bipolar flake	Obsidian	29
04/07/12	044	001	Sekoualou	2	2012	bipolar core	Obsidian	15
04/07/12	044	001	Sekoualou	2	2012	flake	Obsidian	20
04/07/12	044	001	Sekoualou	2	2012	angular waste	Obsidian	8
Total								100

Table II. 24 Obsidian from Hchen 026-001 (analyzed by Dr. Elizabeth Peterson).

Date	Survey Unit	Site	Site Name	Bag #	Season	Type	Raw Material	Count
04/0720/12	026	001	Hchen	2	2012	partial uniface point	Obsidian	1
04/0720/12	026	001	Hchen	2	2012	angular waste	Obsidian	8
04/0720/12	026	001	Hchen	2	2012	utilized flake	Obsidian	1
04/0720/12	026	001	Hchen	2	2012	backed fragment	Obsidian	1
04/0720/12	026	001	Hchen	2	2012	bipolar flake	Obsidian	5
04/0720/12	026	001	Hchen	2	2012	Flake	Obsidian	3
04/0720/12	026	001	Hchen	2	2012	flake medial fragment	Obsidian	3
04/0720/12	026	001	Hchen	3	2012	bipolar flake	Obsidian	1
Total								23

Table II. 25 Obsidian from Survey Unit 025a (analyzed by Dr. Elizabeth Peterson).

Date	Survey Unit	Bag #	Season	Type	Raw Material	Count
09/06/2012	025A	2	2012	angular waste	Obsidian	1
09/06/2012	025A	2	2012	flake	Obsidian	1
09/06/2012	025A	2	2012	burin	Obsidian	1
Total						3

Table II. 26 Obsidian from 008-001 (analyzed by Dr. Elizabeth Peterson).

Date	Survey Unit	Site	Site Name	Bag #	Season	Type	Raw Material	Count
15/06/2012	008	001	N/A	2	2012	flake distal fragment	Obsidian	1
Total								1

Table II. 27 Obsidian from Survey Unit 082a (analyzed by Dr. Elizabeth Peterson).

Date	Survey Unit	Bag #	Season	Type	Raw Material	Count
12/06/2012	082A	1	2012	flake	Obsidian	1
12/06/2012	082A	1	2012	flake fragment	Obsidian	1
Total						

Table II. 28 Obsidian from 042-001 (analyzed by Dr. Elizabeth Peterson).

Date	Survey Unit	Site	Site Name	Bag #	Season	Type	Raw Material	Count
08/06/2012	042	001	N/A	1	2012	outil ecaille	Obsidian	1
18/05/2015	042	001	N/A	3	2015	bipolar flake	Obsidian	1
Total								2

Table II. 29 Obsidian from Survey Unit 061a (analyzed by Dr. Elizabeth Peterson).

Date	Survey Unit	Bag #	Season	Type	Raw Material	Count
12/06/2012	061A	1	2012	bipolar flake	Obsidian	1
Total						1

Table II. 30 Obsidian from 016-001 (analyzed by Dr. Elizabeth Peterson).

Date	Survey Unit	Site	Site Name	Bag #	Season	Type	Raw Material	Count
11/06/2012	016	001	N/A	2	2012	alternate edge point	Obsidian	1
11/06/2012	016	001	N/A	2	2012	bipolar flake	Obsidian	1
11/06/2012	016	001	N/A	2	2012	bipolar core	Obsidian	1
Total								3

Table II. 31 Obsidian from Survey Unit 081a (analyzed by Dr. Elizabeth Peterson).

Date	Survey Unit	Bag #	Season	Type	Raw Material	Count
11/06/2012	081A	1	2012	flake proximal fragment	Obsidian	1
Total						1

Table II. 32 Obsidian from Adi Helafa 014-001 (analyzed by Dr. Elizabeth Peterson).

Date	Survey Unit	Site	Site Name	Bag #	Season	Type	Raw Material	Count
26/07/2011	014	001	Adi Helafa	2	2011	flake	Obsidian	3
10/08/2011	014	001	Adi Helafa	2	2011	bipolar flake	Obsidian	1
10/08/2011	014	001	Adi Helafa	2	2011	flake proximal fragment	Obsidian	2
10/08/2011	014	001	Adi Helafa	2	2011	bipolar flake fragment	Obsidian	5
10/08/2011	014	001	Adi Helafa	2	2011	notched	Obsidian	2
10/08/2011	014	001	Adi Helafa	2	2011	unifaced unfinished	Obsidian	2
10/08/2011	014	001	Adi Helafa	2	2011	triangular flake	Obsidian	1
10/08/2011	014	001	Adi Helafa	2	2011	outil ecaille	Obsidian	2
Total								18

Table II. 33 Obsidian from Adi Helafa 014-002 (analyzed by Dr. Elizabeth Peterson).

Date	Survey Unit	Site	Site Name	Bag #	Season	Type	Raw Material	Count
12/06/2012	014	002	Adi Halefa		2012	bipolar core	Obsidian	1
12/06/2012	014	002	Adi Halefa		2012	bipolar flake fragment	Obsidian	1
14/06/2012	014	002	Adi Halefa	2	2012	bipolar flake	Obsidian	1
14/06/2012	014	002	Adi Halefa	2	2012	flake distal fragment	Obsidian	1
Total								4

Table II. 34 Obsidian from Survey Unit 009a (analyzed by Dr. Elizabeth Peterson).

Date	Survey Unit	Bag #	Season	Type	Raw Material	Count
15/06/2012	009A	2	2012	bipolar flake fragment	Obsidian	3
Total						3

Table II. 35 Obsidian from Survey Unit 014a (analyzed by Dr. Elizabeth Peterson).

Date	Survey Unit	Bag #	Season	Type	Raw Material	Count
15/06/2012	014A	2	2012	bipolar flake fragment	Obsidian	1
Total						1

Table II. 36 Obsidian from Survey Unit 008a (analyzed by Dr. Elizabeth Peterson).

Date	Survey Unit	Bag #	Season	Type	Raw Material	Count
15/06/2012	008A	1	2012	bipolar core fragment	Obsidian	1
Total						1

Table II. 37 Obsidian from Survey Unit 013a (analyzed by Dr. Elizabeth Peterson).

Date	Survey Unit	Bag #	Season	Type	Raw Material	Count
13/06/2012	013A	1	2012	flake fragment	Obsidian	1
13/06/2012	013A	1	2012	flake	Obsidian	1
Total						2

Table II. 38 Obsidian from Endaba Hailu 017-001 (analyzed by Dr. Elizabeth Peterson).

Date	Survey Unit	Site	Site Name	Bag #	Season	Type	Raw Material	Count
12/06/2012	017	001	Endaba Hailu	2	2012	bipolar core fragment	Obsidian	1
11/06/2012	017	001	Endaba Hailu	2	2012	flake fragment	Obsidian	1
Total								2

Table II. 39 Obsidian from Mirai Abune Afsea 068-001 (analyzed by Dr. Elizabeth Peterson).

Date	Survey Unit	Site	Site Name	Bag #	Season	Type	Raw Material	Count
09/08/2011	068	001	Mirai Abune Afsea	2	2011	flake medial fragment	Obsidian	4
09/08/2011	068	001	Mirai Abune Afsea	2	2011	bipolar flake fragment	Obsidian	2
09/08/2011	068	001	Mirai Abune Afsea	2	2011	bipolar flake	Obsidian	2
09/08/2011	068	001	Mirai Abune Afsea	2	2011	bipolar core fragment	Obsidian	1
09/08/2011	068	001	Mirai Abune Afsea	2	2011	utilized flake	Obsidian	2
Total								11

Table II. 40 Obsidian from Sefra Tourkui 027-001 (analyzed by Dr. Elizabeth Peterson).

Date	Survey Unit	Site	Site Name	Bag #	Season	Type	Raw Material	Count
04/07/2012	027	001	Sefra Tourkui	2	2012	flake	Obsidian	1
04/07/2012	027	001	Sefra Tourkui	2	2012	blade proximal fragment	Obsidian	1
04/07/2012	027	001	Sefra Tourkui	2	2012	angular waste	Obsidian	1
04/07/2012	027	001	Sefra Tourkui	2	2012	angular waste	Obsidian	132
04/07/2012	027	001	Sefra Tourkui	2	2012	bipolar flake	Obsidian	74
04/07/2012	027	001	Sefra Tourkui	2	2012	bipolar flake fragments	Obsidian	31
04/07/2012	027	001	Sefra Tourkui	2	2012	utilized flake	Obsidian	8
04/07/2012	027	001	Sefra Tourkui	2	2012	CTF	Obsidian	3
04/07/2012	027	001	Sefra Tourkui	2	2012	modified flake	Obsidian	1
04/07/2012	027	001	Sefra Tourkui	2	2012	flake proximal fragment	Obsidian	19
04/07/2012	027	001	Sefra Tourkui	2	2012	flake distal fragment	Obsidian	34
04/07/2012	027	001	Sefra Tourkui	2	2012	flake medial fragment	Obsidian	36
04/07/2012	027	001	Sefra Tourkui	2	2012	blade proximal fragment	Obsidian	5
04/07/2012	027	001	Sefra Tourkui	2	2012	blade distal fragment	Obsidian	5
04/07/2012	027	001	Sefra Tourkui	2	2012	bipolar core fragment	Obsidian	24
04/07/2012	027	001	Sefra Tourkui	2	2012	backed fragment	Obsidian	9
04/07/2012	027	001	Sefra Tourkui	2	2012	burin spall	Obsidian	10
04/07/2012	027	001	Sefra Tourkui	2	2012	blade	Obsidian	5
04/07/2012	027	001	Sefra Tourkui	2	2012	bipolar core	Obsidian	13
04/07/2012	027	001	Sefra Tourkui	2	2012	outil ecaille	Obsidian	8
04/07/2012	027	001	Sefra Tourkui	2	2012	shatter	Obsidian	123
04/07/2012	027	001	Sefra Tourkui	2	2012	flake	Obsidian	62
04/07/2012	027	001	Sefra Tourkui	2	2012	side scraper	Obsidian	4
04/07/2012	027	001	Sefra Tourkui	2	2012	end scraper flake	Obsidian	1
04/07/2012	027	001	Sefra Tourkui	2	2012	double side scraper	Obsidian	1
04/07/2012	027	001	Sefra Tourkui	2	2012	straight backed	Obsidian	1
04/07/2012	027	001	Sefra Tourkui	2	2012	partial uniface point	Obsidian	3
04/07/2012	027	001	Sefra Tourkui	2	2012	backed crescent	Obsidian	11

Total								626

Table II. 41 Obsidian from Adi Abiselam 2 010-001 (analyzed by Dr. Elizabeth Peterson).

Date	Survey Unit	Site	Site Name	Bag #	Season	Type	Raw Material	Count
06/05/2015	010	001	Adi Abiselam 2	3	2015	bipolar flake	Obsidian	1
06/05/2015	010	001	Adi Abiselam 2	3	2015	flake medial fragment	Obsidian	1
Total								2

Table II. 42 Obsidian from Survey Unit 051a (analyzed by Dr. Elizabeth Peterson).

Date	Survey Unit	Site	Bag #	Season	Type	Raw Material	Count
09/05/2015	051A	001	2	2015	bipolar core	Obsidian	1
Total							1

Table II. 43 Obsidian from 069-001 Tseratsur (analyzed by Dr. Elizabeth Peterson).

Date	Survey Unit	Site	Site Name	Bag #	Season	Type	Raw Material	Count
08/05/2015	069	001	Tseratsur	2	2015	flake	Obsidian	2
Total								2

Table II. 44 Obsidian from Kawhi Aboi Haftom 069-004 (analyzed by Dr. Elizabeth Peterson).

Date	Survey Unit	Site	Site Name	Bag #	Season	Type	Raw Material	Count
09/05/2015	069	004	Kawhi Aboi Haftom	2	2015	bipolar core	Obsidian	4
09/05/2015	069	004	Kawhi Aboi Haftom	2	2015	angular waste	Obsidian	5
09/05/2015	069	004	Kawhi Aboi Haftom	2	2015	bipolar flake	Obsidian	7
09/05/2015	069	004	Kawhi Aboi Haftom	2	2015	flake	Obsidian	3
09/05/2015	069	004	Kawhi Aboi Haftom	2	2015	utilized flake	Obsidian	1
09/05/2015	069	004	Kawhi Aboi Haftom	2	2015	flake proximal fragment	Obsidian	1
09/05/2015	069	004	Kawhi Aboi Haftom	2	2015	flake distal fragment	Obsidian	3
09/05/2015	069	004	Kawhi Aboi Haftom	2	2015	unifacial point	Obsidian	1
Total								25

Table II. 45 Obsidian from Survey Unit 077a (analyzed by Dr. Elizabeth Peterson).

Date	Survey Unit	Bag #	Season	Type	Raw Material	Count
08/05/2015	077A	2	2015	angular waste	Obsidian	1
Total						**1**

Table II. 46 Obsidian from Enda Cha'atat 002-001 (analyzed by Dr. Elizabeth Peterson).

Date	Survey Unit	Site	Site Name	Bag #	Season	Type	Raw Material	Count
14/06/2015	002	001	Enda Cha'atat	2	2015	bipolar flake	Obsidian	12
14/06/2015	002	001	Enda Cha'atat	2	2015	bipolar core	Obsidian	3
14/06/2015	002	001	Enda Cha'atat	2	2015	flake	Obsidian	18
14/06/2015	002	001	Enda Cha'atat	2	2015	Angular waste	Obsidian	15
14/06/2015	002	001	Enda Cha'atat	2	2015	burin spall	Obsidian	1
14/06/2015	002	001	Enda Cha'atat	2	2015	flake proximal fragment	Obsidian	1
14/06/2015	002	001	Enda Cha'atat	2	2015	flake medial fragment	Obsidian	2
14/06/2015	002	001	Enda Cha'atat	2	2015	flake distal fragment	Obsidian	4
14/06/2015	002	001	Enda Cha'atat	2	2015	burin	Obsidian	1
14/06/2015	002	001	Enda Cha'atat	2	2015	backed crescent	Obsidian	1
14/06/2015	002	001	Enda Cha'atat	2	2015	backed fragment	Obsidian	1

14/06/2015	002	001	Enda Cha'atat	2	2015	notched	Obsidian	1
06/07/2012	002	001	Enda Cha'atat	2	2012	bipolar flake	Obsidian	1
06/07/2012	002	001	Enda Cha'atat	2	2012	bipolar core fragment flake	Obsidian	1
06/07/2012	002	001	Enda Cha'atat	2	2012	backed fragment	Obsidian	1
Total								63

Table II. 47 Obsidian from Adi Krumbe/Tahtay Gundam 081-001 (analyzed by Dr. Elizabeth Peterson).

Date	Survey Unit	Site	Site Name	Bag #	Season	Type	Raw Material	Count
20/05/2015	081	001	Adi Krumbe/Tahtay Gundam	2	2015	flake	Obsidian	1
20/05/2015	081	001	Adi Krumbe/Tahtay Gundam	2	2015	bipolar core	Obsidian	1
Total								2

Table II. 48 Obsidian from Mai Fesasi 029-002 (analyzed by Dr. Elizabeth Peterson).

Date	Survey Unit	Site	Site Name	Bag #	Season	Type	Raw Material	Count
29/05/15	029	002	Mai Fesasi	2	2015	convex scraper	Obsidian	1
29/05/15	029	002	Mai Fesasi	2	2015	bipolar core	Obsidian	1
29/05/15	029	002	Mai Fesasi	2	2015	flake	Obsidian	5
29/05/15	029	002	Mai Fesasi	2	2015	outil ecaille	Obsidian	1
29/05/15	029	002	Mai Fesasi	2	2015	flake proximal fragment	Obsidian	3
29/05/15	029	002	Mai Fesasi	2	2015	flake medial fragment	Obsidian	1
29/05/15	029	002	Mai Fesasi	2	2015	flake distal fragment	Obsidian	1
29/05/15	029	002	Mai Fesasi	2	2015	Angular waste	Obsidian	3
29/05/15	029	002	Mai Fesasi	2	2015	bipolar flake	Obsidian	4
Total								20

Table II. 49 Obsidian from Zban Ma'ekune/Beloho 029-003 (analyzed by Dr. Elizabeth Peterson).

Date	Survey Unit	Site	Site Name	Bag #	Season	Type	Raw Material	Count
28/05/2015	029	003	Zban Ma'ekune/Beloho	2	2015	flake distal fragment	Obsidian	1
Total								**1**

Table II. 50 Obsidian from Survey Unit 097a (analyzed by Dr. Elizabeth Peterson).

Date	Survey Unit	Bag #	Season	Type	Raw Material	Count
22/05/2015	097A	1	2015	bipolar flake	Obsidian	1
22/05/2015	097A	1	2015	angular waste	Obsidian	1
Total						2

Table II. 51 Obsidian from Survey Unit 079a (analyzed by Dr. Elizabeth Peterson).

Date	Survey Unit	Bag #	Season	Type	Raw Material	Count
29/05/2015	079A	2	2015	bipolar flake	Obsidian	3
29/05/2015	079A	2	2015	angular waste	Obsidian	2
Total						5

Table II. 52 Obsidian from Adi Abiselam 999-001 (analyzed by Dr. Elizabeth Peterson).

Date	Survey Unit	Site	Site Name	Bag #	Season	Type	Raw Material	Count
06/05/2015	999	001	Adi Abiselam	2	2015	end scraper flake	Obsidian	1
06/05/2015	999	001	Adi Abiselam	2	2015	flake distal fragment	Obsidian	2
06/05/2015	999	001	Adi Abiselam	2	2015	flake proximal fragment	Obsidian	1
Total								4

Table II. 53 Obsidian from Survey Unit 078a (analyzed by Dr. Elizabeth Peterson).

Date	Survey Unit	Bag #	Season	Type	Raw Material	Count
08/05/2015	078A	1	2015	flake	Obsidian	1
Total						1

Table II. 54 Obsidian from Da'ero Arat 079-001 (analyzed by Dr. Elizabeth Peterson).

Date	Survey Unit	Site	Site Name	Bag #	Season	Type	Raw Material	Count
29/05/2015	079	001	Da'ero Arat/St. Gabriel Church	2	2015	flake	Obsidian	5
29/05/2015	079	001	Da'ero Arat/St. Gabriel Church	2	2015	bipolar flake	Obsidian	6
29/05/2015	079	001	Da'ero Arat/St. Gabriel Church	2	2015	bipolar core	Obsidian	7
29/05/2015	079	001	Da'ero Arat/St. Gabriel Church	2	2015	flake proximal fragment	Obsidian	1
29/05/2015	079	001	Da'ero Arat/St. Gabriel Church	2	2015	flake distal fragment	Obsidian	2
29/05/2015	079	001	Da'ero Arat/St. Gabriel Church	2	2015	angular waste	Obsidian	3
29/05/2015	079	001	Da'ero Arat/St. Gabriel Church	2	2015	convex scraper	Obsidian	1

Table II. 55 Obsidian Samples Analyzed with Brucker Tracer III-V p-XRF.

#	Site Name	Site Type	Site Number	Time Period	Sources (excluding R)	Number of Sources (excluding R)	Total Analyzed Samples (includes R)	C	D	E	F	G	H	R
1	Sefra Aboun	Settlement	071-001	Pre-Aksumite to Middle Aksumite	C, E, F, G	4	53	39	0	3	2	9	0	0
2	Beta Samati	Settlement	006-001	Pre-Aksumite to Post-Aksumite	C, E, F, G, H	5	46	33	0	4	2	3	1	3
3	Tseratsur	Settlement	069-001	Classic to Late Aksumite	C, E	2	7	5	0	2	0	0	0	0
4	Sekoualou	Settlement	044-001	Pre-Aksumite	C, F, G	3	10	7	0		1	1		1
5	Da'ero Arat/St. Gabriel Church	Settlement	079-001	Classic to Middle Aksumite	C, E	2	7	5	0	2	0	0	0	0
6	Mai Eungug	Find Spot	071-002	Pre- to Classic Aksumite	C, E	2	7	3	0	4	0	0	0	0
7	N/A	Survey Unit	052	Indeterminate	C	1	1	1	0		0	0	0	0
8	Sefra Tourkui	Settlement	027-001	Pre-Aksumite	C, E	2	56	55	0	1	0	0	0	0

9	N/A	Find Spot	016-001	Post-Aksumite	C	1	3	3	0	0	0	0	0	0
10	Endaba Hailu	Artifact Scatter	017-001	Late to Post-Aksumite	C	1	1	1	0	0	0	0	0	0
11	Hchen	Artifact Scatter	026-001	Pre- to Early Aksumite	C, G	2	5	4	0	0	0	1	0	0
12	N/A	Find Spot	042-001	Post-Aksumite	C	1	1	1	0	0	0	0	0	0
13	N/A	Survey Unit	009a	Indeterminate	C, E, F	3	4	1	0	2	1	0	0	0
14	N/A	Survey Unit	008a	Indeterminate	C	1	1	1	0	0	0	0	0	0
15	N/A	Survey Unit	61a	Indeterminate	C	1	1	1	0	0	0	0	0	0
16	N/A	Survey Unit	25a	Indeterminate	C	1	1	1	0	0	0	0	0	0
17	Adi Halefa	Find Spot	014-002	Proto to Early Aksumite	C	1	4	4	0	0	0	0	0	0
18	Mirai Abune Afsea	Artifact Scatter	068-001	Pre-Aksumite	C, G	2	4	3	0	0	0	1	0	0
19	Dungur	Settlement	022-003	Pre-Aksumite to Late Aksumite	C	1	1	1	0	0	0	0	0	0
20	N/A	Survey Unit	24b	Indeterminate	C, E	2	2	1	0	1	0	0	0	0
21	Gembes	Artifact Scatter	024-001	Late to Post-Aksumite	C, G	2	6	5	0	0	0	1	0	0
22	Adi Helafa	Settlement	014-001	Post-Aksumite	C	1	5	5	0	0	0	0	0	0
23	Aoudi Welka	Artifact Scatter	067-001	Pre-Aksumite to Early Aksumite	C	1	5	5	0	0	0	0	0	0
24	Enda Balata Dista	Settlement	022-001	Pre-Aksumite	C	1	3	3	0	0	0	0	0	0
25	Enda Aboy Meles	Settlement	022-002	Pre-Aksumite	C	1	4	4	0	0	0	0	0	0
26	N/A	Find Spot	024-003	Classic Aksumite	C, E	2	7	3	0	4	0	0	0	0
27	N/A	Artifact Scatter	024-002	Classic Aksumite	C, F	2	5	1	0	0	4	0	0	0
28	Dem Elal	Settlement	013-001	Pre-Aksumite to Post-Aksumite	C	1	6	6	0	0	0	0	0	0
29	Mai Fesasi	Settlement	029-002	Middle to Post Aksumite	C	1	19	19	0	0	0	0	0	0
30	Kawhi Aboi Haftom	Artifact Scatter	069-004	Early Aksumite	C	1	3	3	0	0	0	0	0	0
31	Enda Cha'atat	Settlement	002-001	Classic to Middle Aksumite	C, E, F, G	4	25	20	0	1	3	1	0	0
32	N/A	Survey Unit	078	Indeterminate	C	1	1	1	0	0	0	0	0	0
33	N/A	Survey Unit	079a	Indeterminate	C, H	2	5	4	0	0	0	0	1	0
34	Zban Ma'ekune/ Beloho	Find Spot	029-003	Indeterminate	C	1	1	1	0	0	0	0	0	0
35	N/A	Survey Unit	097a	Indeterminate	C, E	2	2	1	0	1	0	0	0	0
36	Adi Krumbe/ Tahtay Gundam	Find Spot	081-001	Pre-Aksumite	C	1	2	2	0	0	0	0	0	0
37	Adi Abisalem	Artifact Scatter	999-001	Middle Aksumite	C, F	2	4	2	0	0	2	0	0	0
38	N/A	Survey Unit	13a	Indeterminate	D, E	2	2	0	1	1	0	0	0	0
39	N/A	Survey Unit	081a	Indeterminate	E	1	1	0	0	1	0	0	0	0

40	Adi Abisalem 2	Find Spot	010-001	Classic to Middle Aksumite	E	1	1	0	0	1	0	0	0	0
41	N/A	Survey Unit	069	Indeterminate	E	1	2	0	0	2	0	0	0	0
42	Enda Giordis Mogu'o	Settlement	042-002	Middle Aksumite	E	1	1	0	0	1	0	0	0	0
43	N/A	Find Spot	008-001	Middle to Post Aksumite	G	1	1	0	0	0	0	1	0	0
44	N/A	Survey Unit	077a	Indeterminate	H	1	1	0	0	0	0	0	1	0
	Totals	**44**	-	-	-	-	**328**	**256**	**1**	**31**	**15**	**18**	**3**	**4**

Table II. 56a: Obsidian Groups at Pre-Aksumite Single Period Sites

Site	Obsidian Group C	Obsidian Group D	Obsidian Group E	Obsidian Group F	Obsidian Group G	Obsidian Group H	Total Sources
Sefra Tourkui (027-001)	1	0	1	0	0	0	2
Adi Krumbe/Tahtay Gundam (081-001)	1	0	0	0	0	0	1
Mirai Abune Afsea (068-001)	1	0	0	0	1	0	2
Enda Balata Dista (022-001)	1	0	0	0	0	0	1
Sekoualou (044-001)	1	0	0	1	1	0	3
Enda Aboy Meles (022-002)	1	0	0	0	0	0	1

Table II. 56b: Obsidian Groups at Pre-Aksumite Sites (includes survey collections from units that contain an obsidian site).

Site	Obsidian Group C	Obsidian Group D	Obsidian Group E	Obsidian Group F	Obsidian Group G	Obsidian Group H	Total
Sefra Tourkui (027-001)	1	0	1	0	0	0	2
*Adi Krumbe/Tahtay Gundam (081-001) + SU 081a (contains source E)	1	0	1	0	0	0	2
Mirai Abune Afsea (068-001)	1	0	0	0	1	0	2
Enda Balata Dista (022-001)	1	0	0	0	0	0	1
Sekoualou (044-001)	1	0	0	1	1	0	3
Enda Aboy Meles (022-002)	1	0	0	0	0	0	1

* Adi Krumbe/Tahtay Gundam (081-001) is a site contained by SU 081a.

Table II. 57a: Obsidian Groups at Pre-Aksumite and Multi-period Sites.

Site	Obsidian Group C	Obsidian Group D	Obsidian Group E	Obsidian Group F	Obsidian Group G	Obsidian Group H	Total Sources
Sefra Aboun (071-001)	1	0	1	1	1	0	4
Beta Samati (006-001)	1	0	1	1	1	1	5
Mai Eungug (071-002)	1	0	1	0	0	0	2
Sefra Tourkui (027-001)	1	0	1	0	0	0	2
Hchen (026-001)	1	0	0	0	1	0	2
Dem Elal (013-001)	1	0	0	0	0	0	1

Adi Krumbe/Tahtay Gundam (081-001)	1	0	0	0	0	0	1
Mirai Abune Afsea (068-001)	1	0	0	0	1	0	2
Dungur (022-003)	1	0	0	0	0	0	1
Aoudi Welka (067-001)	1	0	0	0	0	0	1
Enda Balata Dista (022-001)	1	0	0	0	0	0	1
Sekoualou (044-001)	1	0	0	1	1	0	3
Enda Aboy Meles (022-002)	1	0	0	0	0	0	1

Table II. 57b: Obsidian Groups at Pre-Aksumite and Multi-period Sites (includes survey collections from units that contain an obsidian site).

Site	Obsidian Group C	Obsidian Group D	Obsidian Group E	Obsidian Group F	Obsidian Group G	Obsidian Group H	Total
Sefra Aboun (071-001)	1	0	1	1	1	0	4
Beta Samati (006-001)	1	0	1	1	1	1	5
Mai Eungug (071-002)	1	0	1	0	0	0	2
Sefra Tourkui (027-001)	1	0	1	0	0	0	2
Hchen (026-001)	1	0	0	0	1	0	2
*Dem Elal (013-001) + SU 013a (contains sources D and E)	1	1	1	0	0	0	3
Adi Krumbe/Tahtay Gundam (081-001) + SU 081a (contains source E)	1	0	1	0	0	0	2
Mirai Abune Afsea (068-001)	1	0	0	0	1	0	2
Dungur (022-003)	1	0	0	0	0	0	1
Aoudi Welka (067-001)	1	0	0	0	0	0	1
Enda Balata Dista (022-001)	1	0	0	0	0	0	1
Sekoualou (044-001)	1	0	0	1	1	0	3
Enda Aboy Meles (022-002)	1	0	0	0	0	0	1

* Dem Elal (013-001) is a site contained by SU 013a.

Table II. 58a: Obsidian Groups at Proto-Aksumite and Multi-period Sites.

Site	Obsidian Group C	Obsidian Group D	Obsidian Group E	Obsidian Group F	Obsidian Group G	Obsidian Group H	Total
Sefra Aboun (071-001)	1	0	1	1	1	0	4
Beta Samati (006-001)	1	0	1	1	1	1	5
Mai Eungug (071-002)	1	0	1	0	0	0	2
Hchen (026-001)	1	0	0	0	1	0	2
Dem Elal (013-001)	1	0	0	0	0	0	1
Adi Halefa (014-002)	1	0	0	0	0	0	1
Dungur (022-003)	1	0	0	0	0	0	1
Aoudi Welka (067-001)	1	0	0	0	0	0	1

Table II. 598b: Obsidian Groups at Proto-Aksumite and Multi-period Sites (includes survey collections from units that contain an obsidian site).

Site	Obsidian Group C	Obsidian Group D	Obsidian Group E	Obsidian Group F	Obsidian Group G	Obsidian Group H	Total
Sefra Aboun (071-001)	1	0	1	1	1	0	4
Beta Samati (006-001)	1	0	1	1	1	1	5
Mai Eungug (071-002)	1	0	1	0	0	0	2
Hchen (026-001)	1	0	0	0	1	0	2
*Dem Elal (013-001) + SU 013a (contains sources D and E)	1	1	1	0	0	0	3
Adi Halefa (014-002)	1	0	0	0	0	0	1
Dungur (022-003)	1	0	0	0	0	0	1
Aoudi Welka (067-001)	1	0	0	0	0	0	1

* Dem Elal (013-001) is a site contained by SU 013a.

Table II. 59a: Obsidian Groups at Early Aksumite Single Period Sites.

Site	Obsidian Group C	Obsidian Group D	Obsidian Group E	Obsidian Group F	Obsidian Group G	Obsidian Group H	Total
Kawhi Aboi Haftom (069-004)	1	0	0	0	0	0	1

Table II. 59b: Obsidian Groups at Early Aksumite Single Period Sites (includes survey collections from units that contain an obsidian site).

Site	Obsidian Group C	Obsidian Group D	Obsidian Group E	Obsidian Group F	Obsidian Group G	Obsidian Group H	Total
* Kawhi Aboi Haftom (069-004) + SU 069 (contains group E)	1	0	1	0	0	0	2

* Kawhi Aboi Haftom (069-004) is a site contained by SU 069.

Table II. 60a: Obsidian Groups at Early Aksumite and Multi-period Sites.

Site	Obsidian Group C	Obsidian Group D	Obsidian Group E	Obsidian Group F	Obsidian Group G	Obsidian Group H	Total
Sefra Aboun (071-001)	1	0	1	1	1	0	4
Beta Samati (006-001)	1	0	1	1	1	1	5
Mai Eungug (071-002)	1	0	1	0	0	0	2
Hchen (026-001)	1	0	0	0	1	0	2
Dem Elal (013-001)	1	0	0	0	0	0	1
Dungur (022-003)	1	0	0	0	0	0	1
Aoudi Welka (067-001)	1	0	0	0	0	0	1
Kawhi Aboi Haftom (069-004)	1	0	0	0	0	0	1
Adi Halefa (014-002)	1	0	0	0	0	0	1

Table II. 60b: Obsidian Groups at Early Aksumite and Multi-period Sites (includes survey collections from units that contain an obsidian site).

Site	Obsidian Group C	Obsidian Group D	Obsidian Group E	Obsidian Group F	Obsidian Group G	Obsidian Group H	Total
Sefra Aboun (071-001)	1	0	1	1	1	0	4
Beta Samati (006-001)	1	0	1	1	1	1	5
Mai Eungug (071-002)	1	0	1	0	0	0	2
Hchen (026-001)	1	0	0	0	1	0	2
*Dem Elal (013-001) + SU 013a (contains sources D and E)	1	1	1	0	0	0	3
Dungur (022-003)	1	0	0	0	0	0	1
Aoudi Welka (067-001)	1	0	0	0	0	0	1
* Kawhi Aboi Haftom (069-004) + SU 069 (contains group E)	1	0	1	0	0	0	2

* Dem Elal (013-001) is a site contained by SU 013a.

* Kawhi Aboi Haftom (069-004) is a site contained by SU 069.

Table II. 61 Obsidian Groups at Classic Aksumite Single Period Sites.

Site	Obsidian Group C	Obsidian Group D	Obsidian Group E	Obsidian Group F	Obsidian Group G	Obsidian Group H	Total
024-002	1	0	0	1	0	0	2
024-003	1	0	1	0	0	0	2

Table II. 62a: Obsidian Groups at Classic Aksumite and Multi-period Sites.

Site	Obsidian Group C	Obsidian Group D	Obsidian Group E	Obsidian Group F	Obsidian Group G	Obsidian Group H	Total
Sefra Aboun (071-001)	1	0	1	1	1	0	4
Beta Samati (006-001)	1	0	1	1	1	1	5
Tseratsur (069-001)	1	0	1	0	0	0	2
Da'ero Arat/St. Gabriel Church (079-001)	1	0	1	0	0	0	2
Mai Eungug (071-002)	1	0	1	0	0	0	2
Dem Elal (013-001)	1	0	0	0	0	0	1
Dungur (022-003)	1	0	0	0	0	0	1
024-002	1	0	0	1	0	0	2
024-003	1	0	1	0	0	0	2
Enda Cha'atat (002-001)	1	0	1	1	1	0	4
Adi Abiselam 2 (010-001)	0	0	1	0	0	0	1

Table II. 62b: Obsidian Groups at Classic Aksumite and Multi-period Sites (includes survey collections from units that contain an obsidian site).

Site	Obsidian Group C	Obsidian Group D	Obsidian Group E	Obsidian Group F	Obsidian Group G	Obsidian Group H	Total
Sefra Aboun (071-001)	1	0	1	1	1	0	4
Beta Samati (006-001)	1	0	1	1	1	1	5

Tseratsur (069-001)	1	0	1	0	0	0	2
*Da'ero Arat/St. Gabriel Church (079-001) + SU 079a (contains sources C and H)	1	0	1	0	0	1	3
Mai Eungug (071-002)	1	0	1	0	0	0	2
*Dem Elal (013-001) + SU 013a (contains sources D and E)	1	1	1	0	0	0	3
Dungur (022-003)	1	0	0	0	0	0	1
*024-002 + SU 024b (contains sources C and E)	1	0	1	1	0	0	3
024-003	1	0	1	0	0	0	2
Enda Cha'atat (002-001)	1	0	1	1	1	0	4
Adi Abiselam 2 (010-001)	0	0	1	0	0	0	1

* Da'ero Arat/St. Gabriel Church (079-001) is a site contained by SU 079a.

* Dem Elal (013-001) is a site contained by SU 013a.

* 024-002 is a site contained by SU 024b.

Table II. 63a: Obsidian Groups at Middle Aksumite Single Period Sites.

Site	Obsidian Group C	Obsidian Group D	Obsidian Group E	Obsidian Group F	Obsidian Group G	Obsidian Group H	Total
Enda Giordis Mogu'o (042-002)	0	0	1	0	0	0	1
Adi Abiselam (999-001)	1	0	0	1	0	0	2

Table II. 63b: Obsidian Groups at Middle Aksumite Single Period Sites (includes survey collections from units that contain a site).

Site	Obsidian Group C	Obsidian Group D	Obsidian Group E	Obsidian Group F	Obsidian Group G	Obsidian Group H	Total
Enda Giordis Mogu'o (042-002)	0	0	1	0	0	0	1
Adi Abiselam (999-001)	1	0	0	1	0	0	2
*Luhuts (077-001) + SU 077a	0	0	0	0	0	1	1

* Luhuts (077-001) is a Middle Aksumite single period settlement (0.66 ha) discovered within SU 077a. No lithics have been associated with this settlement per se; however, lithics from obsidian group H were discovered in the environs of this site and, for the purposes of this model, will be analyzed together with data from this site.

Table II. 64a: Obsidian Groups at Middle Aksumite and Multi-period Sites.

Site	Obsidian Group C	Obsidian Group D	Obsidian Group E	Obsidian Group F	Obsidian Group G	Obsidian Group H	Total
Sefra Aboun (071-001)	1	0	1	1	1	0	4
Beta Samati (006-001)	1	0	1	1	1	1	5
Tseratsur (069-001)	1	0	1	0	0	0	2
Da'ero Arat/St. Gabriel Church (079-001)	1	0	1	0	0	0	2
Dem Elal (013-001)	1	0	0	0	0	0	1
008-001	1	0	0	0	1	0	2
Dungur (022-003)	1	0	0	0	0	0	1
Mai Fesasi (029-002)	1	0	0	0	0	0	1

Enda Cha'atat (002-001)	1	0	1	1	1	0	4
Adi Abiselam 2 (010-001)	0	0	1	0	0	0	1
Enda Giordis Mogu'o (042-002)	0	0	1	0	0	0	1
Adi Abiselam (999-001)	1	0	1	1	0	0	3

Table II. 654b: Obsidian Groups at Middle Aksumite and Multi-period Sites (includes survey collections from units that contain a site).

Site	Obsidian Group C	Obsidian Group D	Obsidian Group E	Obsidian Group F	Obsidian Group G	Obsidian Group H	Total
Sefra Aboun (071-001)	1	0	1	1	1	0	4
Beta Samati (006-001)	1	0	1	1	1	1	5
Tseratsur (069-001)	1	0	1	0	0	0	2
*Da'ero Arat/St. Gabriel Church (079-001) + SU 079a (contains groups C and H)	1	0	1	0	0	1	3
*Dem Elal (013-001) + SU 013a (contains groups D and E)	1	1	1	0	0	0	3
008-001	1	0	0	0	1	0	2
Dungur (022-003)	1	0	0	0	0	0	1
Mai Fesasi (029-002)	1	0	0	0	0	0	1
Enda Cha'atat (002-001)	1	0	1	1	1	0	4
Adi Abiselam 2 (010-001)	0	0	1	0	0	0	1
Enda Giordis Mogu'o (042-002)	0	0	1	0	0	0	1
Adi Abiselam (999-001)	1	0	1	1	0	0	3
*Luhuts (077-001) + SU 077a (contains group H)	0	0	0	0	0	1	1

* Da'ero Arat/St. Gabriel Church (079-001) is a site contained by SU 079a.

* Dem Elal (013-001) is a site contained by SU 013a.

* Luhuts (077-001) is a Middle Aksumite single period settlement (0.66 ha) discovered within SU 077a. No lithics have been associated with this settlement per se; however, lithics from obsidian group H were discovered in the environs of this site and, for the purposes of this model, will be analyzed together with data from this site.

Table II. 65a: Obsidian Groups at Late Aksumite and Multi-period Sites.

Site	Obsidian Group C	Obsidian Group D	Obsidian Group E	Obsidian Group F	Obsidian Group G	Obsidian Group H	Total
Beta Samati (006-001)	1	0	1	1	1	1	5
Tseratsur (069-001)	1	0	1	0	0	0	2
Endaba Hailu (017-001)	1	0	0	0	0	0	1
Dem Elal (013-001)	1	0	0	0	0	0	1
008-001	1	0	0	0	1	0	2
Dungur (022-003)	1	0	0	0	0	0	1
Gembes (024-001)	1	0	0	0	1	0	2
Mai Fesasi (029-002)	1	0	0	0	0	0	1

Table II. 65b: Obsidian Groups at Late Aksumite and Multi-period Sites (includes survey collections from units that contain a site).

Site	Obsidian Group C	Obsidian Group D	Obsidian Group E	Obsidian Group F	Obsidian Group G	Obsidian Group H	Total
Beta Samati (006-001)	1	0	1	1	1	1	5
Tseratsur (069-001)	1	0	1	0	0	0	2
Endaba Hailu (017-001)	1	0	0	0	0	0	1
*Dem Elal (013-001) + SU 013a (contains groups D and E)	1	1	1	0	0	0	3
008-001	1	0	0	0	1	0	2
Dungur (022-003)	1	0	0	0	0	0	1
*Gembes (024-001) + SU 024b (contains groups C and E)	1	0	1	0	1	0	3
Mai Fesasi (029-002)	1	0	0	0	0	0	1

* Dem Elal (013-001) is a site contained by SU 013a.

* Gembes (024-001) is a site contained by SU 024b.

Table II. 66 All SRSAH Obsidian Sites by Time Period.

Time Period	Number of Sites
Pre-Aksumite	13
Proto-Aksumite	8
Early Aksumite	9
Classic Aksumite	11
Middle Aksumite	13
Late Aksumite	8

Table II. 67a Longitudinal Overview of Centrality Measures by Node (Pre-Aksumite to Early Aksumite).

	Pre-Aksumite					Proto Aksumite					Early Aksumite					
Site	DC	BP	FBC	BCFP	CCSG	DC	BP	FBC	BCFP	CCApF	CCSGF	DC	BP	FBC	BCFP	CCApF	CCSGF
071001	21	4267.021	12.483	0	1	12	2423.25	6.476	0	42.004	7	13	2641.828	7.45	0	56.001	8
006001	21	4267.021	12.483	0	1	12	2423.25	6.476	0	42.004	7	13	2641.828	7.45	0	56.001	8
071002	15	2999.851	11.121	0	1	9	1830.428	5.921	0	42.004	7	10	2033.074	6.958	0	56.001	8
027001	15	2999.851	11.121	0	1	N/A	N/A	N/A	N/A	N/A	N/A	N/A	N/A	N/A	N/A	N/A	N/A
026001	16	3236.38	11.085	0	1	9	1830.428	5.921	0	42.004	7	10	2033.074	6.958	0	56.001	8
013001	12	2309.904	10.159	0	1	7	1358.547	5.563	0	42.004	7	8	1553.908	6.654	0	56.001	8
081001	12	2309.904	10.159	0	1	N/A	N/A	N/A	N/A	N/A	N/A	N/A	N/A	N/A	N/A	N/A	N/A
068001	16	3236.38	11.085	0	1	N/A	N/A	N/A	N/A	N/A	N/A	N/A	N/A	N/A	N/A	N/A	N/A
022003	12	2309.904	10.159	0	1	7	1358.547	5.563	0	42.004	7	8	1553.908	6.654	0	56.001	8
067001	12	2309.904	10.159	0	1	7	1358.547	5.563	0	42.004	7	8	1553.908	6.654	0	56.001	8

022001	12	2309.904	10.159	0	1	N/A	N/A	N/A	N/A	N/A	N/A	N/A	N/A	N/A	N/A	N/A	N/A	N/A
044001	18	3717.981	11.236	0	1	N/A	N/A	N/A	N/A	N/A	N/A	N/A	N/A	N/A	N/A	N/A	N/A	N/A
022002	12	2309.904	10.159	0	1	N/A	N/A	N/A	N/A	N/A	N/A	N/A	N/A	N/A	N/A	N/A	N/A	N/A
026001	N/A	N/A	N/A	N/A	N/A	N/A	N/A	N/A	N/A	N/A	N/A	N/A	N/A	N/A	N/A	N/A	N/A	N/A
014002	N/A	N/A	N/A	N/A	N/A	7	1358.547	5.563	0	42.004	7	8	1553.908	6.654	0	56.001	8	
069004	N/A	N/A	N/A	N/A	N/A	N/A	N/A	N/A	N/A	N/A	N/A	8	1553.908	6.654	0	56.001	8	
069001	N/A	N/A	N/A	N/A	N/A	N/A	N/A	N/A	N/A	N/A	N/A	N/A	N/A	N/A	N/A	N/A	N/A	N/A
079001	N/A	N/A	N/A	N/A	N/A	N/A	N/A	N/A	N/A	N/A	N/A	N/A	N/A	N/A	N/A	N/A	N/A	N/A
024002	N/A	N/A	N/A	N/A	N/A	N/A	N/A	N/A	N/A	N/A	N/A	N/A	N/A	N/A	N/A	N/A	N/A	N/A
024003	N/A	N/A	N/A	N/A	N/A	N/A	N/A	N/A	N/A	N/A	N/A	N/A	N/A	N/A	N/A	N/A	N/A	N/A
002001	N/A	N/A	N/A	N/A	N/A	N/A	N/A	N/A	N/A	N/A	N/A	N/A	N/A	N/A	N/A	N/A	N/A	N/A
010001	N/A	N/A	N/A	N/A	N/A	N/A	N/A	N/A	N/A	N/A	N/A	N/A	N/A	N/A	N/A	N/A	N/A	N/A
008001	N/A	N/A	N/A	N/A	N/A	N/A	N/A	N/A	N/A	N/A	N/A	N/A	N/A	N/A	N/A	N/A	N/A	N/A
029002	N/A	N/A	N/A	N/A	N/A	N/A	N/A	N/A	N/A	N/A	N/A	N/A	N/A	N/A	N/A	N/A	N/A	N/A
042002	N/A	N/A	N/A	N/A	N/A	N/A	N/A	N/A	N/A	N/A	N/A	N/A	N/A	N/A	N/A	N/A	N/A	N/A
999001	N/A	N/A	N/A	N/A	N/A	N/A	N/A	N/A	N/A	N/A	N/A	N/A	N/A	N/A	N/A	N/A	N/A	N/A
017001	N/A	N/A	N/A	N/A	N/A	N/A	N/A	N/A	N/A	N/A	N/A	N/A	N/A	N/A	N/A	N/A	N/A	N/A
024001	N/A	N/A	N/A	N/A	N/A	N/A	N/A	N/A	N/A	N/A	N/A	N/A	N/A	N/A	N/A	N/A	N/A	N/A

Table II. 67b Longitudinal Overview of Centrality Measures by Node (Classic Aksumite to Late Aksumite).

	Classic Aksumite						**Middle Aksumite**						**Late Aksumite**					
Site	DC	BP	FBC	BCFP	CCApF	CCSGF	DC	BP	FBC	BCFP	CCApF	CCSGF	DC	BP	FBC	BCFP	CCApF	CCSGF
071001	21	4204.314	11.786	0.429	88.841	10	22	4399.769	14.507	1.333	106.689	11	N/A	N/A	N/A	N/A	N/A	N/A
006001	21	4204.314	11.786	0.429	88.841	10	22	4399.769	14.507	1.333	106.689	11	10	1970.913	6.587	0	42.004	7
071002	16	3154.834	10.476	0.429	88.841	10	N/A	N/A	N/A	N/A	N/A	N/A	N/A	N/A	N/A	N/A	N/A	N/A
027001	N/A	N/A	N/A	N/A	N/A	N/A	N/A	N/A	N/A	N/A	N/A	N/A	N/A	N/A	N/A	N/A	N/A	N/A
026001	N/A	N/A	N/A	N/A	N/A	N/A	N/A	N/A	N/A	N/A	N/A	N/A	N/A	N/A	N/A	N/A	N/A	N/A
013001	9	1799.441	5.48	0	89.254	11	9	1779.949	6.047	0	107.583	13	7	1398.632	5.702	0	42.004	7
081001	N/A	N/A	N/A	N/A	N/A	N/A	N/A	N/A	N/A	N/A	N/A	N/A	N/A	N/A	N/A	N/A	N/A	N/A

068001	N/A	N/A	N/A	N/A	N/A	N/A	N/A	N/A	N/A	N/A	N/A	N/A	N/A	N/A	N/A	N/A	N/A	N/A
022003	9	1799.441	5.48	0	89.254	11	9	1779.949	6.047	0	107.583	13	7	1398.632	5.702	0	42.0 04	7
067001	N/A	N/A	N/A	N/A	N/A	N/A	N/A	N/A	N/A	N/A	N/A	N/A	N/A	N/A	N/A	N/A	N/A	N/A
022001	N/A	N/A	N/A	N/A	N/A	N/A	N/A	N/A	N/A	N/A	N/A	N/A	N/A	N/A	N/A	N/A	N/A	N/A
044001	N/A	N/A	N/A	N/A	N/A	N/A	N/A	N/A	N/A	N/A	N/A	N/A	N/A	N/A	N/A	N/A	N/A	N/A
022002	N/A	N/A	N/A	N/A	N/A	N/A	N/A	N/A	N/A	N/A	N/A	N/A	N/A	N/A	N/A	N/A	N/A	N/A
026001	N/A	N/A	N/A	N/A	N/A	N/A	N/A	N/A	N/A	N/A	N/A	N/A	N/A	N/A	N/A	N/A	N/A	N/A
014002	N/A	N/A	N/A	N/A	N/A	N/A	N/A	N/A	N/A	N/A	N/A	N/A	N/A	N/A	N/A	N/A	N/A	N/A
069004	N/A	N/A	N/A	N/A	N/A	N/A	N/A	N/A	N/A	N/A	N/A	N/A	N/A	N/A	N/A	N/A	N/A	N/A
069001	16	3154.834	10.476	0.429	88.841	10	16	3103.61	13.106	1.333	106.689	11	8	1613.872	5.81	0	42.0 04	7
079001	16	3154.834	10.476	0.429	88.841	10	16	3103.61	13.106	1.333	106.689	11	N/A	N/A	N/A	N/A	N/A	N/A
024002	12	2522.729	6.155	0	89.254	11	N/A	N/A	N/A	N/A	N/A	N/A	N/A	N/A	N/A	N/A	N/A	N/A
024003	16	3154.834	10.476	0.429	88.841	10	N/A	N/A	N/A	N/A	N/A	N/A	N/A	N/A	N/A	N/A	N/A	N/A
002001	21	4204.314	11.786	0.429	88.841	10	22	4399.769	14.507	1.333	106.689	11	N/A	N/A	N/A	N/A	N/A	N/A
010001	7	1535.599	2.536	0	90	13	7	1500.451	4.571	0	108.361	15	N/A	N/A	N/A	N/A	N/A	N/A
008001	N/A	N/A	N/A	N/A	N/A	N/A	12	2534.646	6.653	0	107.583	13	9	1811.808	6.087	0	42.0 04	7
029002	N/A	N/A	N/A	N/A	N/A	N/A	9	1779.949	6.047	0	107.583	13	7	1398.632	5.702	0	42.0 04	7
042002	N/A	N/A	N/A	N/A	N/A	N/A	7	1500.451	4.571	0	108.361	15	N/A	N/A	N/A	N/A	N/A	N/A
999001	N/A	N/A	N/A	N/A	N/A	N/A	19	3817.634	13.497	1.333	106.689	11	N/A	N/A	N/A	N/A	N/A	N/A
017001	N/A	N/A	N/A	N/A	N/A	N/A	N/A	N/A	N/A	N/A	N/A	N/A	7	1398.632	5.702	0	42.0 04	7
024001	N/A	N/A	N/A	N/A	N/A	N/A	N/A	N/A	N/A	N/A	N/A	N/A	9	1811.808	6.087	0	42.0 04	7

Bibliography

Adams, Robert M. (1975). The emerging place of trade in civilizational studies. *Ancient Civilization and Trade, University of New Mexico Press, Albuquerque*, 451–466.

Adams, Robert MacCormick. (1974). *The evolution of urban society: Early Mesopotamia and prehispanic Mexico*. Weidenfeld and Nicholson.

Agbe-Davies, A. S., & Bauer, A. A. (2010). Rethinking trade as a social activity: An introduction. *Social Archaeologies of Trade and Exchange: Exploring Relationships among People, Places, and Things*, 13–28.

Aksoy, Ö. C. (2018). Functions and uses of metallic axe-heads and arrowheads from Safah, Oman: An analysis of metalwork wear and weapon design. *Journal of Archaeological Science: Reports*, *19*, 727–752.

al-Naboodah, H. M. (1992). The Commercial Activity of Bahrain and Oman in the Early Middle Ages. *Proceedings of the Seminar for Arabian Studies*, *22*, 81–96.

al-Shanfari, A. B., & Weisgerber, G. (1989). A late bronze age warrior burial from Nizwa (Oman). *Oman Studies. Papers on the Archaeology and History of Oman*, 17–30.

Alchian, A. A., & Demsetz, H. (1973). The property right paradigm. *The Journal of Economic History*, *33*(1), 16–27.

Algaze, G. (2001). *Uruk Mesopotamia & its neighbors: Cross-cultural interactions in the era of state formation*. James Currey Publishers.

Algaze, G. (2005). *The Uruk world system: The dynamics of expansion of early Mesopotamian civilization*. University of Chicago Press.

Al-Jahrwari, N. S. A. (2008). *Settlement Patterns, Development and Cultural Change in Northern Oman Peninsula: A multi-tiered approach to the analysis of long-term settlement trends* (PhD Thesis). Durham University.

Al-Jahwari, N. S. (2009). The agricultural basis of Umm an-Nar society in the northern Oman peninsula (2500–2000 BC). *Arabian Archaeology and Epigraphy*, *20*(2), 122–133.

Anfray, F. (2012a). Matara: Enquête archéologique sur une cité antique d'Érythrée. *Palethnologie de l'Afrique, Lethnologie*, *4*, 11–48.

Anfray, F. (2012b). The archaeological excavation of a city of Ancient Eritrea. *Palethnology of Africa. Palethnology, Revue Bilingue de Préhistoire*, *4*, 11–48.

Anfray, Francis. (1967). Matara. *Annales d'Ethiopie*, *7*, 33–53.

Anfray, Francis. (1968). Aspects de l'archéologie éthiopienne. *The Journal of African History*, *9*(3), 345–366.

Anfray, Francis. (1990). *Les anciens Ethiopiens: Siècles d'histoire*.

Arensberg, C., Pearson, H. W., & Polanyi, K. (1957). The economy as instituted process. *Trade and Market in Early Empires*, 243.

Arrow, K. J. (1974). *The limits of organization*. WW Norton & Company.

Assefa, Z., Lam, Y. M., & Mienis, H. K. (2008). Symbolic use of terrestrial gastropod opercula during the Middle Stone Age at Porc-Epic Cave, Ethiopia. *Current Anthropology*, *49*(4), 746–756.

Ayres, C. (1978). *The Theory of Economic Progress*. New Issues Press.

Ayres, C. E. (1952). *The Industrial Economy: Its technological basis and institutional destiny*. Houghton Mifflin.

Azzarà, V. (2013). Architecture and building techniques at the Early Bronze Age site of HD-6, Rāʾs al-Ḥadd, Sultanate of Oman. *Proceedings of the Seminar for Arabian Studies*, 11–26.

Azzarà, V. M., & De Rorre, A. P. (2018). Socio-cultural innovations of the Final Umm an-Nar period (c. 2100–2000 BCE) in the Oman peninsula: New insights from Ra's al-Jinz RJ-2. *Arabian Archaeology and Epigraphy*, *29*(1), 10–26.

Bandyopadhyay, S., Rao, A. R., & Sinha, B. K. (2011). *One Introduction to Social Network Analysis*.

Bandyopadhyay, S., Rao, A. R., Sinha, B. K., & Sinha, B. K. (2011). *Models for social networks with statistical applications* (Vol. 13). Sage.

Barber, B. (1995). All economies are" embedded": The career of a concept, and beyond. *Social Research*, 387–413.

Barberi, F., Tazieff, H., & Varet, J. (1972a). Volcanism in the Afar depression: Its tectonic and magmatic significance. *Tectonophysics*, *15*(1–2), 19–29.

Barberi, F., Tazieff, H., & Varet, J. (1972b). Volcanism in the Afar depression: Its tectonic and magmatic significance. *Tectonophysics*, *15*(1–2), 19–29.

Bard, K. A., DiBlas, M. C., Koch, M., Crescenz, L., D Andrea, A. C., Fattovich, R., … Harris, M. S. (2003). The joint archaeological project at Bieta Giyorgis (Aksum, Ethiopia) of the Istituto Universitario Orientale, Naples (Italy), and Boston University, Boston (USA): Results, research procedures and preliminary computer applications. *BAR International Series*, *1151*, 1–14.

Bard, K. A., Fattovich, R., Manzo, A., & Perlingieri, C. (1997). Archaeological investigations at Bieta Giyorgis (Aksum), Ethiopia: 1993–1995 field seasons. *Journal of Field Archaeology*, *24*(4), 387–403.

Bard, K. A., Fattovich, R., Manzo, A., & Perlingieri, C. (2014). The chronology of Aksum (Tigrai, Ethiopia): A view from Bieta Giyorgis. *Azania: Archaeological Research in Africa*, *49*(3), 285–316.

Barjamovic, G. (2011). *A historical geography of Anatolia in the Old Assyrian colony period* (Vol. 38). Museum Tusculanum Press.

Barnes, J. A. (1954). Class and committees in a Norwegian island parish. *Human Relations*, *7*(1), 39–58.

Bavay, L., De Putter, T., Adams, B., Navez, J., & Andre, L. (2000). The origin of obsidian in predynastic and early dynastic upper Egypt. *Mitteilungen Des Deutschen Archäologischen Instituts. Abteilung Kairo*, *56*, 5–20.

Bavelas, A. (1948). A mathematical model for group structures. *Human Organization*, *7*(3), 16.

Bavutti, E., Borgi, F., Maini, E., & Kenoyer, J. M. (2015a). Shell fish-hook production at Ras al-Hadd HD-5, Sultanate of Oman (fourth millennium BC): Preliminary archaeological and experimental studies (poster). *Proceedings of the Seminar for Arabian Studies*, 15–20.

Béchennec, F., Roger, J., Le Métour, J., Wyns, R., & Chevrel, S. (1992). *Geological Map of Ibri Sheet NF 40—02. Scale 1: 250,000*. Bureau de Recherches Géologiques et Minieres.

Beck, R. (2003). EO-1 user guide v. 2.3. *Department of Geography University of Cincinnati*.

Beech, M. J. (2004). *In the Land of the Ichthyophagi: Modelling fish exploitation in the Arabian Gulf and Gulf of Oman from the 5th millennium BC to the Late Islamic Period* (Vol. 1217). British Archaeological Reports Limited.

Begemann, Freidrich, Hauptmann, A., Schmitt-Strecker, S., & Weisgerber, G. (2010). Lead isotope and chemical signature of copper from Oman and its occurrence in Mesopotamia and sites on the Arabian Gulf coast. *Arabian Archaeology and Epigraphy*, *21*(2), 135–169.

Begemann, Friedrich, & Schmitt-Strecker, S. (2009). Über das Frühe Kupfer Mesopotamiens. *Iranica Antiqua*, *44*.

Beldados, A., & Costantini, L. (2011). Sorghum exploitation at Kassala and its environs, Northeastern Sudan in the second and first millennium BC. *Nyame Akuma*, *75*, 33–39.

Bentley, R. A., & Maschner, H. D. (2003). *Complex systems and archaeology*. University of Utah Press Salt Lake City.

Benton, J. (2006). *Burial practices of the third millennium BC in the Oman Peninsula: A reconsideration*.

Berman, M. (2010). All That Is Solid Melts into Air: The Experience of Modernity. *London*, *13*, 15.

Bernardini, W. (2007). Jeddito yellow ware and Hopi social networks. *Kiva*, *72*(3), 295–328.

Berthoud, T., & Cleuziou, S. (1983). Farming communities of the Oman peninsula and the copper of Makkan. *The Journal of Oman Studies*, *6*(2), 239–246.

Bibby, G. (1970). *Looking for Dilmun*. Knopf Books for Young Readers.

Biggs, N., Lloyd, E. K., & Wilson, R. J. (1986). *Graph Theory, 1736-1936*. Oxford University Press.

Blake, E. (2013). Social networks, path dependence, and the rise of ethnic groups in pre-Roman Italy. *Network Analysis in Archaeology: New Approaches to Regional Interaction*, 203–221.

Blake, E. (2014). *Social networks and regional identity in Bronze Age Italy*. Cambridge University Press.

Blanton, R. E., & Fargher, L. F. (2012). Neighborhoods and the civic constitutions of premodern cities as seen from the perspective of collective action. *The Neighborhood as a Social and Spatial Unit in Mesoamerican Cities*, 27–52.

Blau, P. (1964). Power and exchange in social life. *NY: John Wiley & Sons*.

Boissevain, J. (1979). Network analysis: A reappraisal. *Current Anthropology*, *20*(2), 392–394.

Bonacich, P. (1972). Factoring and weighting approaches to status scores and clique identification. *Journal of Mathematical Sociology*, *2*(1), 113–120.

Bonacich, P. (1987). Power and centrality: A family of measures. *American Journal of Sociology*, *92*(5), 1170–1182.

Bonacich, P. (2007). Some unique properties of eigenvector centrality. *Social Networks*, *29*(4), 555–564.

Borengasser, M., Hungate, W. S., & Watkins, R. (2007). Hyperspectral remote sensing: Principles and applications.

Borgatti, S. P. (1995). Centrality and AIDS. *Connections*, *18*(1), 112–114.

Borgatti, S. P. (2005). Centrality and network flow. *Social Networks*, *27*(1), 55–71.

Borgatti, S. P., & Halgin, D. S. (2011a). Analyzing affiliation networks. *The Sage Handbook of Social Network Analysis*, *1*, 417–433.

Borgatti, S. P., & Halgin, D. S. (2011b). On network theory. *Organization Science*, *22*(5), 1168–1181.

Bott, E. (1971). *Family and social network: Roles, norms, and external relationships inordinary urban families*. Tavistock publications.

Bott, E. (2017). Urban families: Conjugal roles and social networks. In *Man in Adaptation* (pp. 76–104). Routledge.

Bott, R. (1957). Homogeneous vector bundles. *Annals of Mathematics*, 203–248.

Boucharlat, R. (2003). Iron Age water-draining galleries and the Iranian 'Qanat.' *Archaeology of the United Arab Emirates*, 159–172.

Boudier, F., & Nicolas, A. (1995). Nature of the Moho transition zone in the Oman ophiolite. *Journal of Petrology*, *36*(3), 777–796.

Bradley, R., & Edmonds, M. (2005). *Interpreting the axe trade: Production and exchange in Neolithic Britain*. Cambridge University Press.

Brandes, U., Robins, G., McCranie, A., & Wasserman, S. (2013). What is network science? *Network Science*, *1*(1), 1–15.

Brandt, Steve A. (1980). Archaeological investigations at Lake Besaka, Ethiopia. *Proceedings of the Eight Panafrican Congress of Prehistory and Quaternary Studies. Nairobi: The International Louis Leakey Memorial Institute of African Prehistory*, 239–43.

Brandt, Steven A. (1996). The ethnoarchaeology of flaked stone tool use in southern Ethiopia. *Aspects of African Archaeology*, 733–738.

Brandt, Steven A., Fisher, E. C., Hildebrand, E. A., Vogelsang, R., Ambrose, S. H., Lesur, J., & Wang, H. (2012). Early MIS 3 occupation of Mochena Borago Rockshelter, Southwest Ethiopian Highlands: Implications for Late Pleistocene archaeology, paleoenvironments and modern human dispersals. *Quaternary International*, *274*, 38–54.

Brint, S. (1992). Hidden meanings: Cultural content and context in Harrison White's structural sociology. *Sociological Theory*, *10*(2), 194–208.

Brown, A. R. (1957). *A natural science of society*. Free Press of Glencoe.

Brughmans, T. (2010). Connecting the dots: Towards archaeological network analysis. *Oxford Journal of Archaeology*, *29*(3), 277–303.

Brughmans, T. (2011). *Facebooking the past: A critical social network analysis approach for archaeology*.

Brughmans, T. (2013). Thinking through networks: A review of formal network methods in archaeology. *Journal of Archaeological Method and Theory*, *20*(4), 623–662.

Brughmans, T., & Peeples, M. (2017). Trends in archaeological network research: A bibliometric analysis. *Journal of Historical Network Research*, *1*(1), 1–24.

Buffa, V., & Vogt, B. (2001). Sabir–cultural identity between Saba and Africa. *Migration Und Kulturtransfer*, 437–450.

Burt, R. S. (1982). *Toward a structural theory of action: Network models of social structure, perception, and action*. Academic Pr.

Burt, R. S. (1983). *Corporate profits and cooptation: Networks of market constraints and directorate ties in the American economy*. Academic Press New York.

Cable, C. M., & Thornton, C. P. (2013). Monumentality and the third-millennium "towers" of the Oman Peninsula. *Connections and Complexity: New Approaches to the Archaeology of South Asia*, 375–99.

Cain, C. R. (2000). *Animals at Axum: Initial Zooarchaeological Research in the Later Prehistory of the Northern Ethiopian Highlands* (PhD Thesis). Washington University.

Carter, T., Grant, S., Kartal, M., Coşkun, A., & Özkaya, V. (2013). Networks and neolithisation: Sourcing obsidian from Körtik Tepe (SE Anatolia). *Journal of Archaeological Science*, *40*(1), 556–569.

Cattani, M. (2003). Il sistema informativo dello scavo di HD6 (Ra's al Hadd–Sultanato d'Oman). *Ocnus*, *11*, 77–96.

Chakrabarti, D. K. (1990). *The external trade of Indus civilization*. Munshiram Manoharlal Publishers.

Charpentier, V. (2008). Hunter-gatherers of the" empty quarter of the early Holocene" to the last Neolithic societies: Chronology of the late prehistory of south-eastern Arabia (8000-3100 BC). *Proceedings of the Seminar for Arabian Studies*, 93–115.

Charpentier, V., Berger, J.-F., Crassard, R., Borgi, F., Davtian, G., Méry, S., & Phillips, C. S. (2013). Conquering new territories: When the first black boats sailed to Masirah Island. *Proceedings of the Seminar for Arabian Studies*, 85–98.

Chen, X., Warner, T. A., & Campagna, D. J. (2007). Integrating visible, near-infrared and short-wave infrared hyperspectral and multispectral thermal imagery for geological mapping at Cuprite, Nevada. *Remote Sensing of Environment*, *110*(3), 344–356.

Cheng, C. F., & Schwitter, C. M. (1957). Nickel in ancient bronzes. *American Journal of Archaeology*, *61*(4), 351–365.

Christaller, W., & Baskin, C. W. (1933). *Die Zentralen Orte in Süddeutschland. Central Places in Southern Germany; Translated by Carlisle W. Baskin*. Prentice-Hall.

Christides, V. (1994). New Light on Navigation and Naval Warfare in the Eastern Mediterranean, the Red Sea and the Indian Ocean (6th-14th centuries AD). *Nubica, Internationales Jahrbuch Für Koptische, Meroitisch-Nubische, Äthiopische Und Verwandte Studien*, *3*(1), 3–42.

Clark, J. D., & Williams, M. A. J. (1978). Recent archaeological research in southeastern Ethiopia. 1974-1975. *Annales d'Ethiopie*, *11*, 19–44. Editions de la Table Ronde.

Clark, R.N. (1991). *Spectroscopy 101. The problems with NIRA. Unpublished manuscript.* Denver, CO: US Geological Survey.

Clark, Roger N. (1999). Spectroscopy of rocks and minerals, and principles of spectroscopy. *Manual of Remote Sensing*, *3*(3–58), 2–2.

Clarke, D. (1973). Archaeology: The loss of innocence. *Antiquity*, *47*(185), 6–18.

Cleuziou, S. (1981). *Oman peninsula and its relations eastwards during the 3rd millennium BC*. CNRS.

Cleuziou, S. (1992). The Oman peninsula and the Indus civilization: A reassessment. *Man and Environment*, *17*(2), 93–103.

Cleuziou, S. (1996). *The Emergence of Oases and Town in Eastern and Southern Arabia*. na.

Cleuziou, S. (2002). The early Bronze Age of the Oman Peninsula: From chronology to the dialectics of tribe and state formation. *Essays on the Late Prehistory of the Arabian Peninsula*, 191–246.

Cleuziou, S. (2003). Early Bronze Age trade in the Gulf and the Arabian Sea: The society behind the boats. *Archaeology of the United Arab Emirates*, 133–150.

Cleuziou, S. (2007). Evolution toward complexity in a coastal desert environment: The early bronze age in the Ja'alan, Sultanate of Oman. *The Model-Based Archaeology of Socionatural Systems*, 209–227.

Cleuziou, S. (2009). Extracting wealth from a land of starvation by creating social complexity: A dialogue between archaeology and climate? *Comptes Rendus Geoscience*, *341*(8–9), 726–738.

Cleuziou, S., & Méry, S. (2002). In-between the great powers: The Bronze Age Oman peninsula. *Essays on the Late Prehistory of the Arabian Peninsula*, 273–316.

Cleuziou, S., & Tosi, M. (1993). Black boats of Magan: Some thoughts on Bronze Age water transport in Oman and beyond from the impressed bitumen slabs of Ra's al-Junayz. *Annales Academiae Scientiarum Fennicae. Series B*, *273*, 745–761. Suomalainen tiedeakatemia.

Cleuziou, S., & Tosi, M. (2000). Ra's al-Jinz and the prehistoric coastal cultures of the Ja'alan. *Journal of Oman Studies*, *11*, 19–73.

Cleuziou, S., & Tosi, M. (2007). *In the shadow of the ancestors: The prehistoric foundations of the early Arabian civilization in Oman*. Ministry of Heritage & Culture, Sultanat of Oman.

Cleuziou, S., & Tosi, M. (2018). *In the Shadow of the Ancestors. The Prehistoric Foundations of the Early Arabian Civilization in Oman (second expanded edition).* (Second Expanded Edition). Sultanate of Oman: Ministry of Heritage and Culture.

Coase, R. H. (1937). The nature of the firm. *Economica*, *4*(16), 386–405.

Coleman, R. G. (1993). Geological evolution of the Red Sea. *Oxford Monographs on Geology and Geophysics. Oxford University Press, New York*, *186*.

Coleridge, S. T. (1884). *Table Talk of Samuel Taylor Coleridge: And the Rime of the Ancient Mariner, Christabel, &c* (Vol. 14). George Routledge and Sons.

Collar, A., Coward, F., Brughmans, T., & Mills, B. J. (2015). Networks in archaeology: Phenomena, abstraction, representation. *Journal of Archaeological Method and Theory*, *22*(1), 1–32.

Collins, R. (1988). *Theoretical sociology*. Harcourt College Pub.

Connah, G. (2015). *African civilizations: An archaeological perspective*. Cambridge University Press.

Constantinou, G. (1982). Geological features and ancient exploitation of the cupriferous sulphide orebodies of Cyprus. *Early Metallurgy in Cyprus*, *400*, 13e23.

Cook, S. (1974). 'Structural Substantivism': A Critical Review of Marshall Sahlins' Stone Age Economics. *Comparative Studies in Society and History*, *16*(3), 355–379.

Coward, F. (2010). Small worlds, material culture and ancient Near Eastern social networks. *Social Brain, Distributed Mind*, 449–79.

Coward, F., & Knappett, C. (2013). Grounding the net: Social networks, material culture and geography in the Epipalaeolithic and Early Neolithic of the Near East (~ 21,000–6,000 cal BCE). *Network Analysis in Archaeology: New Approaches to Regional Interaction*, 247–280.

Craddock, P. T. (1995). *Early metal mining and production*.

Craddock, P. T., La Niece, S., & Hook, D. R. (2003). *Evidences for the production, trading, and refining of copper in the Gulf of Oman during the third millenium BC*. na.

Crawford, H. E. (1973). Mesopotamia's invisible exports in the third millennium BC. *World Archaeology*, *5*(2), 232–241.

Crawford, H. E. (1998). *Dilmun and its Gulf neighbours*. Cambridge university press.

Crosta, A. P., Sabine, C., & Taranik, J. V. (1998). Hydrothermal alteration mapping at Bodie, California, using AVIRIS hyperspectral data. *Remote Sensing of Environment*, *65*(3), 309–319.

Crowley, J. K., Brickey, D. W., & Rowan, L. C. (1989). Airborne imaging spectrometer data of the Ruby Mountains, Montana: Mineral discrimination using relative absorption band-depth images. *Remote Sensing of Environment*, *29*(2), 121–134.

Curtis, B. (2004). Ancient interaction across the southern Red Sea: New suggestions for investigating cultural exchange and complex societies during the first millennium. *BAR International Series*, 57–70.

Curtis, M. C., & Schmidt, P. R. (2008). Landscape, people, and places on the ancient Asmara plateau. *The Archaeology of Ancient Eritrea*, 64–108.

Curtis, Matthew C. (2008). New perspectives for examining change and complexity in the northern Horn of Africa during the first millennium BCE. *The Archaeology of Ancient Eritrea*, 329–348.

Curtis, Matthew C. (2010). *Laurel Phillipson, Using Stone Tools: The Evidence from Aksum, Ethiopia*. Springer.

Dalton, G. (1966). Bridewealth" vs." Brideprice. *American Anthropologist*, *68*(3), 732–738.

Dalton, G. (1982). Barter. *Journal of Economic Issues*, *16*(1), 181–190.

Dalton, J. B., Bove, D. J., Mladinich, C. S., & Rockwell, B. W. (2004). Identification of spectrally similar materials using the USGS Tetracorder algorithm: The calcite–epidote–chlorite problem. *Remote Sensing of Environment*, *89*(4), 455–466.

D'Andrea, A. C., Manzo, A., Harrower, M. J., & Hawkins, A. L. (2008). The Pre-Aksumite and Aksumite settlement of NE Tigrai, Ethiopia. *Journal of Field Archaeology*, *33*(2), 151–176.

D'Andrea, A. C., Schmidt, P. R., & Curtis, M. C. (2008). Paleoethnobotanical analysis and agricultural economy in early first millennium BCE sites around Asmara. *The Archaeology of Ancient Eritrea*, 207–216.

D'Andrea, A. Catherine. (2008). T'ef (Eragrostis tef) in ancient agricultural systems of highland Ethiopia. *Economic Botany*, *62*(4), 547–566.

D'Andrea, A. Catherine, Richards, M. P., Pavlish, L. A., Wood, S., Manzo, A., & Wolde-Kiros, H. S. (2011). Stable isotopic analysis of human and animal diets from two pre-Aksumite/Proto-Aksumite archaeological sites in northern Ethiopia. *Journal of Archaeological Science*, *38*(2), 367–374.

D'Andrea, C., Lyons, D., Haile, M., & Butler, A. (1999). Ethnoarchaeological approaches to the study of prehistoric agriculture in the highlands of Ethiopia. In *The exploitation of plant resources in ancient Africa* (pp. 101–122). Springer.

David, H. (2002). Soft stone mining evidence in the Oman Peninsula and its relation to Mesopotamia. *Essays of the Late Prehistory of the Arabian Peninsula. Serie Orientale Roma*, *93*, 317–335.

De Cardi, B. (1970). *Excavations at Bampur: A third millennium settlement in Persian Baluchistan, 1966* (Vol. 51). American Museum of National History.

De Cardi, B., Collier, S., & Doe, D. B. (1976). Excavations and survey in Oman, 1974-1975. *Journal of Oman Studies*, *2*, 101–187.

de Contenson, H. (2006). Antiquités éthiopiennes: D'Axoum à Haoulti.

de Contenson, Henri. (1981). Pre-aksumite culture. *UNESCO General History of Africa*, *2*, 341–361.

de Goeje, M. J. (1873). *Kitāb al-masālik wa-al-mamālik* (Vol. 1). Brill.

Desruelles, S., Fouache, E., Eddargach, W., Cammas, C., Wattez, J., Beuzen-Waller, T., … Thornton, C. (2016). Evidence for early irrigation at Bat (Wadi Sharsah, northwestern Oman) before the advent of farming villages. *Quaternary Science Reviews*, *150*, 42–54.

Dillian, C. D., & White, C. L. (2010a). Introduction: Perspectives on Trade and Exchange. In C. D. Dillian & C. L. White (Eds.), *Trade and Exchange: Archaeological Studies from History and Prehistory* (pp. 3–14).

Dillian, C. D., & White, C. L. (2010b). *Trade and exchange*. Springer.

Dixon, J. E., Cann, J. R., & Renfrew, C. (1968). *Obsidian and the origins of trade*. na.

Douglas, M. (2002). Foreword: No free gifts. In *The Gift*.

Drennan, R. D., Earle, T., Feinman, G. M., Fletcher, R., Kolb, M. J., Peregrine, P., … Smith, M. L. (2011). Comparative archaeology: A commitment to understanding variation. In *The Comparative Archaeology of Complex Societies* (pp. 1–3). Cambridge University Press.

Drennan, R. D., Earle, T., Feinman, G. M., Fletcher, R., Kolb, M. J., Peregrine, P., … Stark, Miriam T. (2012). Comparative archaeology: A commitment to understanding variation. In *The Comparative Archaeology of Complex Societies* (pp. 1–3). Cambridge University Press.

Dumitru, I.A., & Harrower, M. J. (2018a). Mapping Ancient Production and Trade of Copper in Oman and Obsidian in Ethiopia. In *Stories of Globalization: The Red Sea and the Persian Gulf from Late Prehistory to Early Modernity.*

Dumitru, I. A., & Harrower, M. J. (2018b). From Rural Collectables to Global Commodities: Copper from Oman and Obsidian from Ethiopia. In *Globalization in Prehistory: Contact, Exchange, and the "People Without History."*

During Caspers, E. (1984). Sumerian trading communities residing in Harappan society. *Frontiers of the Indus Civilization, Wheeler Commemoration Volume*, 363–370.

Durkheim, E. (1893). Pre-Contractual Solidarity. *The Durkheimian Tradition*.

Durkheim, E. (2014). *The division of labor in society*. Simon and Schuster.

Earle, T. (2002). Commodity flows and the evolution of complex societies. *Theory in Economic Anthropology*, 81–104.

Earle, T. (2010). Exchange Systems in Prehistory. In C. D. Dillian & C. L. White (Eds.), *Trade and Exchange: Archaeological Studies from History and Prehistory* (pp. 205–217).

Earle, T. (2018). *Bronze Age Economics: The first political economies*. Routledge.

Earle, T. K. (1977). A reappraisal of redistribution: Complex Hawaiian chiefdoms. In *Exchange systems in prehistory* (pp. 213–229). Elsevier.

Earle, T. K. (1997). *How chiefs come to power: The political economy in prehistory*. Stanford University Press.

Eckstein, D., Liese, W., & Stieber, J. (1987). Holzversorgung im prähistorischen Kupferbergbau in Oman. *Naturwissenschaftliche Rundschau*, *40*(11), 426–430.

Edens, C. (1992). Dynamics of trade in the ancient Mesopotamian "world system." *American Anthropologist*, *94*(1), 118–139.

Edens, C. (1993). Indus-Arabian interaction during the Bronze Age: A review of evidence. *Harappan Civilization: A Recent Perspective*, *2*, 335–363.

Edwards, David N. (2004). *The Nubian Past: An Archaeology of the Sudan*.

Edwards, D.N. (2004). The Nubian past: An archaeology of the Sudan.

Ericson, R. E. (2008). Command economy. *The New Palgrave Dictionary of Economics: Volume 1–8*, 897–907.

Esposti, M. D., Renzi, M., & Rehren, T. (2016). *Iron Age metallurgy at Salūt (Sultanate of Oman): A preliminary note*. 8.

Fattovich, R., & Bard, K. A. (2006). *Joint Archaeological Expedition at Mersa/Wadi Gawasis (Red Sea, Egypt) of the University of Naples» l'Orientale «(Naples, Italy), Istituto*

Italiano per l'Africa e l'Oriente (Rome, Italy), and Boston University (Boston, USA)– 2005-2006 Field Season.

Fattovich, Rodolfo. (1978). Traces of a possible African component in the Pre-Aksumite culture of northern Ethiopia. *Documents Pour Servir à l'Histoire Des Civilisations Ethiopiennes Paris*, (9), 25–30.

Fattovich, Rodolfo. (1988). Remarks on the late prehistory and early history of northern Ethiopia. *Proceedings of the Eighth International Conference of Ethiopian Studies*, *1*, 85–104. Institute of Ethiopian Studies Addis Ababa.

Fattovich, Rodolfo. (1990a). Remarks on the Pre-Aksumite period in northern Ethiopia. *Journal of Ethiopian Studies*, *23*, 1–33.

Fattovich, Rodolfo. (1990b). The peopling of the northern Ethiopian-Sudanese borderland between 7000 and 1000 BP: A preliminary model. *Nubica*, *1*(2), 3–45.

Fattovich, Rodolfo. (1996). The Afro-Arabian Circuit Contacts between the Horn of Africa and Southern Arabia in the 3rd-2nd Millennia BC. *Interregional Contacts in the Later Prehistory of Northeastern Africa, Eds. L. Krzyzaniak, K. Kroeper, and M. Kobusiewicz*, 395–402.

Fattovich, Rodolfo. (1997). *The contacts between Southern Arabia and the Horn of Africa in late prehistoric and early historical times: A view from Africa*.

Fattovich, Rodolfo. (1999). The development of urbanism in the northern Horn of Africa in ancient and medieval times. *The Development of Urbanism in Africa from a Global Perspective.*

Fattovich, Rodolfo. (2005). The archaeology of the Horn of Africa. *Afrikas Horn*, *22*, 3.

Fattovich, Rodolfo. (2009). Reconsidering Yeha, c. 800–400 bc. *African Archaeological Review*, *26*(4), 275–290.

Fattovich, Rodolfo. (2010a). The development of ancient states in the northern Horn of Africa, c. 3000 BC–AD 1000: An archaeological outline. *Journal of World Prehistory*, *23*(3), 145–175.

Fattovich, Rodolfo. (2010b). The development of ancient states in the northern Horn of Africa, c. 3000 BC–AD 1000: An archaeological outline. *Journal of World Prehistory*, *23*(3), 145–175.

Fattovich, Rodolfo. (2012a). The northern Horn of Africa in the first millennium BCE: Local traditions and external connections. *Rassegna Di Studi Etiopici*, *4*, 1–60.

Fattovich, Rodolfo. (2012b). The southern Red Sea in the 3rd and 2nd Millennia BC: An archaeological overview. *Navigated Spaces, Connected Places: Proceedings of the Red Sea Project V*, 39–46.

Fattovich, Rodolfo, & Bard, K. (2006). Marsa Gawasis (Wadi Gawasis) and the Egyptian Seafaring Expeditions to Punt. *Essam El-Saeed et El-Sayed Mahfouz (Éd.) The Festschrift Volume. A Collection of Studies Presented to Professor Abdel Monem Abdel Haleem Sayed, Alexandrie*, 18–38.

Fattovich, Rodolfo, & Bard, K. A. (1994). The origins of Aksum: A view from Ona Enda Aboi Zague (Tigray). *New Trend in Ethiopian Studies. Papers of the 12th International Conference of Ethiopian Studies*, *1*, 16–25.

Fattovich, Rodolfo, & Bard, K. A. (2001). The Proto-Aksumite period: An overview. *Annales d'Ethiopie*, *17*, 3–24. Editions de la Table Ronde.

Fattovich, Rodolfo, Bard, K., Petrassi, L., & Pisano, V. (2000). *The Aksum archaeological area: A preliminary assessment* (Vol. 1). Isituto Universitario Orientale.

Faust, K. (1997). Centrality in affiliation networks. *Social Networks*, *19*(2), 157–191.

Feinman, G. M. (2013). The emergence of social complexity. *Cooperation and Collective Action: Archaeological Perspectives*, 35–56.

Field, S., Frank, K. A., Schiller, K., Riegle-Crumb, C., & Muller, C. (2006). Identifying positions from affiliation networks: Preserving the duality of people and events. *Social Networks*, *28*(2), 97–123.

Finneran, N. (2007). *The archaeology of Ethiopia*. Routledge.

Finneran, N. (2013). Lucy to Lalibela: Heritage and identity in Ethiopia in the twenty-first century. *International Journal of Heritage Studies*, *19*(1), 41–61.

Finneran, N., Boardman, S., & Cain, C. (2000a). A new perspective on the Late Stone Age of the northern Ethiopian highlands: Excavations at Anqqer Baahti, Aksum, Ethiopia 1996. *AZANIA: Journal of the British Institute in Eastern Africa*, *35*(1), 21–51.

Finneran, N., Boardman, S., & Cain, C. (2000b). Excavations at the Late Stone Age Site of Baahti Nebait, Aksum, Northern Ethiopia, 1997. *AZANIA: Journal of the British Institute in Eastern Africa*, *35*(1), 53–73.

Firth, R. (2013). *Elements of social organisation*. Routledge.

Flannery, K. V. (1973). Archaeology with a capital S. *Research and Theory in Current Archaeology*, 47–53.

Fleming, D. E. (2004). *Democracy's ancient ancestors: Mari and early collective governance*. Taylor & Francis US.

Foucault, M. (1977). *Discipline and punish: The birth of the prison, trans. Alan Sheridan*. New York: Vintage Books.

Francaviglia, V. (1990). Obsidian Tools from Ethiopia to Yemen. *Paper Delivered at the" Eleventh Conference of Ethiopian Studies", Addis Ababa*.

Francaviglia, V. M. (1990). Obsidian sources in ancient Yemen. *The Bronze Age Culture of Khawlan At-Tiyal and al-Hada (Yemen Arab Republic). Roma: IsMEO*, 129–36.

Francaviglia, V. M. (1996). Il existait déjà au Néolithique un commerce d'obsidienne à travers la Mer Rouge. *Revue d'archéométrie*, 65–70.

Frayne, D. R. (1993). *Sargonic and Gutian Periods (2334-2113). Toronto*.

Freeman, L. C. (2004). The development of social network analysis: A study in the sociology of science. *Vancouver, BC: Empirical Press. Xii*.

Freeman, L.C. (n.d.). Centrality in networks: I. Conceptual clarification. *Social Networks*, *1*, 215–239.

Freeman, Linton C., Borgatti, S. P., & White, D. R. (1991). Centrality in valued graphs: A measure of betweenness based on network flow. *Social Networks*, *13*(2), 141–154.

Freidel, D., & Reilly III, F. K. (2010). The Flesh of the God: Cosmology. *Food, And*.

Frenez, D., Genchi, F., al-Wardi, M., & al-Bakri, S. (2017). *An inscribed Kassite eye-stone amulet bead from the Early Iron Age grave LCG-1 at Daba, Sultanate of Oman*.

Fried, M. H. (1967). *The evolution of political society: An essay in political anthropology* (Vol. 7). Random House.

Frifelt, K. (1991). The island of Umm an-Nar, vol. 1. Third millennium graves. *Aarhus: Jutland Archaeological Society Publications XXVI: I*.

Frifelt, Karen. (1970). Jamdat Nasr graves in the Oman. *Kuml*, *1970*, 355–383.

Frifelt, Karen. (1975). On prehistoric settlement and chronology of the Oman Peninsula. *East and West*, *25*(3/4), 359–424.

Frifelt, Karen. (1995). *The island of Umm an-Nar: The third millennium settlement* (Vol. 26). Aarhus Universitetsforlag.

Gallagher, J. P. (1977). Contemporary stone tools in Ethiopia: Implications for archaeology. *Journal of Field Archaeology*, *4*(4), 407–414.

Garraty, C. P. (n.d.). Investigating Market Exchange in Ancient Societies: A Theoretical Review. In *Archaeological Approaches to Market Exchange in Ancient Societies* (pp. 3–32).

Garraty, C. P., & Stark, B. L. (2010). *Archaeological approaches to market exchange in ancient societies*. University Press of Colorado.

Gasse, E., & Street, F. A. (1978). Late Quaternary lake-level fluctuations and environments of the northern Rift Valley and Afar region (Ethiopia and Djibouti). *Palaeogeography, Palaeoclimatology, Palaeoecology*, *24*(4), 279–325.

Geertz, C. (1971). *Islam observed: Religious development in Morocco and Indonesia* (Vol. 37). University of Chicago Press.

Genchi, F. (n.d.). Genchi F. 2019—The Iron Age collective graves of Daba. *Dreamers. 40 Years of Italian Archaeological Research in Oman*.

Genchi, F., Giardino, C., & Yule, P. (2018). An early Iron Age metal-working atelier just inside the Empty Quarter in Oman. In *In the shadow of the ancestors. The Prehistoric Foundations of the Early Arabian Civilization in Oman* (Second Expanded Edition).

Genchi, F., Giardino, C., & Yule, P. (n.d.). ʿUqdat al-Bakrah. An Early Iron Age Metal-working Atelier just inside the Empty Quarter in Oman. In *In the Shadow of the Ancestors. The*

Prehistoric Foundations of the Early Arabian Civilization in Oman (second expanded edition).

Gerlach, I. (2012). Yeha: An Ethio-Sabaean site in the highlands of Tigray (Ethiopia). *New Research in Archaeology and Epigraphy of South Arabia and Its Neighbors*, 215–240.

Giardino, C. (2010). *I metalli nel mondo antico: Introduzione all'archeometallurgia*.

Giardino, C. (2015). The beginning of copper metallurgy in Oman. *Proceedings of the Symposium The Archaeological Heritage of Oman, UNESCO, Paris–September 7th 2012*, 115–125. Ministry of Heritage & Culture (Sultanate of Oman) Muscat.

Giardino, C. (2017). *Magan—The Land of Copper: Prehistoric Metallurgy of Oman*. Sultanate of Oman: Ministry of Heritage and Culture.

Giles, A. B., Massom, R. A., & Warner, R. C. (2009). A method for sub-pixel scale feature-tracking using Radarsat images applied to the Mertz Glacier Tongue, East Antarctica. *Remote Sensing of Environment*, *113*(8), 1691–1699.

Giraud, J., & Cleuziou, S. (2009). Funerary landscape as part of the social landscape and its perceptions: 3000 Early Bronze Age burials in the eastern Jaʾlān (Sultanate of Oman). *Proceedings of the Seminar for Arabian Studies*, 163–180. JSTOR.

Gjesfjeld, E., & Phillips, S. C. (2013). Evaluating adaptive network strategies with geochemical sourcing data: A case study from the Kuril Islands. *Network Analysis in Archaeology: New Approaches to Regional Interaction*, 281–305.

Glassner, J.-J. (1996). Dilmun, Magan and Meluhha: Some observations on language, toponymy, anthroponymy and theonymy. *The Indian Ocean in Antiquity*, 235–50.

Glennie, K. A., Boeuf, M. G. A., Hughes-Clark, M. W., Moody-Stuart, M., Pilaar, W. F. H., & Reinhardt, B. M. (1974). Geology of the Oman Mountains (Parts one, two, and three). *The Hague, Martinus Nijhoff*.

Glennie, K. W. (2005). *The desert of southeast Arabia: Desert environments and sediments*. Gulf PetroLink.

Goetz, Alexande. F., & Srivastava, V. (1985). *Mineralogical mapping in the Cuprite mining district, Nevada*.

Goldfrank, W. L. (1990). Fascism and the great transformation. *The Life and Work of Karl Polanyi*, 87–92.

Golitko, M., & Feinman, G. M. (2015). Procurement and distribution of pre-Hispanic Mesoamerican obsidian 900 BC–AD 1520: A social network analysis. *Journal of Archaeological Method and Theory*, *22*(1), 206–247.

Golitko, M., Meierhoff, J., Feinman, G. M., & Williams, P. R. (2012). Complexities of collapse: The evidence of Maya obsidian as revealed by social network graphical analysis. *Antiquity*, *86*(332), 507–523.

Goodenough, K. M., Styles, M. T., Schofield, D., Thomas, R. J., Crowley, Q. C., Lilly, R. M., Carney, J. N. (2013). Architecture of the Oman–UAE ophiolite: Evidence for a multi-phase magmatic history. In *Lithosphere Dynamics and Sedimentary Basins: The Arabian Plate and Analogues* (pp. 23–42). Springer.

Goschen, G. J. (1893). Ethics and economics. *The Economic Journal*, *3*(11), 377–387.

Granovetter, M. (1983). *The strength of weak ties: A network theory revisited*.

Granovetter, M. (1985). Economic action and social structure: The problem of embeddedness. *American Journal of Sociology*, *91*(3), 481–510.

Gudeman, S. (2012). Vital energy: The current of relations. *Social Analysis*, *56*(1), 57–73.

Gudeman, S. (2016). *Anthropology and economy*. Cambridge University Press.

Hage, P. (1977). Centrality in the kula ring. *The Journal of the Polynesian Society*, *86*(1), 27–36.

Hage, P., & Harary, F. (1981). Mediation and power in Melanesia. *Oceania*, *52*(2), 124–135.

Hage, P., & Harary, F. (1983). *Structural models in anthropology: Cambridge studies in social anthropology*.

Hage, P., & Harary, F. (1991a). *Exchange in Oceania: A graph theoretic analysis*. Oxford University Press.

Hage, P., & Harary, F. (1991b). *Exchange in Oceania: A graph theoretic analysis*. Oxford University Press.

Hage, P., & Harary, F. (1996a). *Island networks: Communication, kinship, and classification structures in Oceania*. Cambridge University Press.

Hage, P., & Harary, F. (1996b). *Island networks: Communication, kinship, and classification structures in Oceania*. Cambridge University Press.

Hakimi, S. L. (1964). Optimum locations of switching centers and the absolute centers and medians of a graph. *Operations Research*, *12*(3), 450–459.

Halperin, R. (1994). *Cultural economics past and present*. Austin, TX: The University of Texas Press.

Halperin, R. H. (1988). *Economies across cultures: Towards a comparative science of the economy*. Springer.

Halperin, Rhoda. (1991). Karl Polanyi's concept of householding: Resistance and livelihood in an Appalachian region. *Research in Economic Anthropology*, *13*, 93–116.

Hanneman, R. A., & Riddle, M. (2005). *Introduction to social network methods*. University of California Riverside.

Hanotte, O., Bradley, D. G., Ochieng, J. W., Verjee, Y., Hill, E. W., & Rege, J. E. O. (2002). African pastoralism: Genetic imprints of origins and migrations. *Science*, *296*(5566), 336–339.

Harrower, M. J. (2016). *Water histories and spatial archaeology: Ancient Yemen and the American West*. Cambridge University Press.

Harrower, M. J., & D'Andrea, A. C. (2014). Landscapes of state formation: Geospatial analysis of Aksumite settlement patterns (Ethiopia). *African Archaeological Review*, *31*(3), 513–541.

Harrower, M. J., David-Cuny, H., Nathan, S., Dumitru, I. A., & Al-Jabri, S. (2016). First discovery of ancient soft-stone (chlorite) vessel production in Arabia: Aqir al-Shamoos (Oman). *Arabian Archaeology and Epigraphy*, *27*(2), 197–207.

Harrower, M. J., McCorriston, J., & D'Andrea, A. C. (2010). General/specific, local/global: Comparing the beginnings of agriculture in the Horn of Africa (Ethiopia/Eritrea) and southwest Arabia (Yemen). *American Antiquity*, *75*(3), 452–472.

Hart, J. P., Birch, J., & St-Pierre, C. G. (2017). Effects of population dispersal on regional signaling networks: An example from northern Iroquoia. *Science Advances*, *3*(8), e1700497.

Hart, J. P., & Engelbrecht, W. (2012). Northern Iroquoian ethnic evolution: A social network analysis. *Journal of Archaeological Method and Theory*, *19*(2), 322–349.

Hassig, R. (1982). Periodic markets in precolumbian Mexico. *American Antiquity*, *47*(2), 346–355.

Hatke, G. (2011). *Africans in Arabia Felix: Aksumite relations with Himyar in the sixth century CE (Dissertation)*. Princeton University.

Hauptmann, A. (1985). *5000 Jahre Kupfer in Oman: Die Entwicklung der Kupfermetallurgie vom 3. Jahrtausend bis zur Neuzeit* (Vol. 4). Dt. Bergbaumuseum.

Hauptmann, A. (2007). *The archaeometallurgy of copper: Evidence from Faynan, Jordan*. Springer Science & Business Media.

Hauptmann, A., & Weisgerber, G. (1981). Third millenium BC copper production in Oman. *ArchéoSciences, Revue d'Archéométrie*, *1*(1), 131–138.

Hauptmann, A., Weisgerber, G., & Bachmann, H. G. (1988). *Early copper metallurgy in Oman.* Zhengzhou, China.

Hauptmann, A., Weisgerber, G., & Bachmann, H.-G. (1986). Early copper metallurgy in Oman. *The Beginning of the Use of Metals and Alloys*, 34–51.

Hazlitt, W. (1894). *The Spirit of the Age: Or, contemporary portraits*. George Bell.

Heimpel, W. (1987). Das Untere Meer. *Zeitschrift Für Assyriologie Und Vorderasiatische Archäologie*, *77*(1), 22–91.

Helwing, B. (2014). East of Eden? A review of Turkey's eastern neighbors in the Neolithic. In *The Neolithic in Turkey Vol. 6-10500-5200BC: Environment Settlement, Flora, Fauna, dating, Symbols of Belief, with View from North, South, East, and West* (pp. 321–377). Archaeology and Art Publications Istanbul.

Herrmann, J. T., Casana, J., & Qandil, H. S. (2012). A sequence of inland desert settlement in the Oman peninsula: 2008–2009 excavations at Saruq al-Hadid, Dubai, UAE. *Arabian Archaeology and Epigraphy*, *23*(1), 50–69.

Hinton, J., Veiga, M. M., & Beinhoff, C. (2003). Women and artisanal mining: Gender roles and the road ahead. *The Socio-Economic Impacts of Artisanal and Small-Scale Mining in Developing Countries*, 149–88.

Hirsch, H. (1963). Die Inschriften der Könige von Agade. *Archiv Für Orientforschung*, *20*, 1–82.

Hirth, K., & Andrews, B. (2002). Pathways to Prismatic Blades. *Cotsen Institute of Archaeology, Monograph*, *45*.

Hirth, K. G. (1998). The distributional approach: A new way to identify marketplace exchange in the archaeological record. *Current Anthropology*, *39*(4), 451–476.

Hodges, R. (1988). *Primitive and peasant markets*. Basil Blackwell Oxford.

Højgaard, K. (1980). Dentition on Umm an-Nar (Trucial Oman), 2500 BC. *European Journal of Oral Sciences*, *88*(5), 355–364.

Homans, G.C. (1961). *Social Behaviour: Its Elementary Forms*. New York: Harcourt Brace.

Homans, George Caspar. (1968). The study of groups. *International Encyclopedia of the Social Sciences*, *6*, 259–264.

Hoyland, R. G. (2002). *Arabia and the Arabs: From the Bronze Age to the coming of Islam*. Routledge.

Hunt, G. R., Salisbury, J. W., & Lenhoff, C. J. (1971). Visible and near infrared reflectance spectra of minerals and rocks: III. *Oxides and Hydroxides. Mod. Geol*, *2*, 195–205.

Hunt, T. L. (1988). Graph theoretic network models for Lapita exchange: A trial application. *Archaeology of the Lapita Cultural Complex: A Critical Review. Thomas Burke Memorial Washington State Museum Research Reports*, (5), 135–155.

Huntingford, G. W. (1980). *The Periplus of the Ethyrean Sea (London, Hakluyt Society)*.

Huot, J.-L. (2001). De l'île de Dalma au Ra's al-Jinz: Les céramiques mésopotamiennes dans la péninsule d'Oman aux V - III millénaires. In *Études mésopotamiennes: Recueil de textes offert à Jean-Louis Huot*. Éds. Recherche sur les Civilisations.

Ibrahim, M., & ElMahi, A. T. (2000). Metallurgy in Oman during the Early Islamic Period. In *The Archaeology of Jordan and Beyond: Essays in Honor of James A. Sauer* (pp. 207–221).

Ingram, J. K. (1888). *A history of political economy*. Macmillan.

Irwin, G. J. (1978). The development of Mailu as a specialized trading and manufacturing centre in Papuan prehistory: The causes and the implications. *The Australian Journal of Anthropology*, *11*(3), 406.

Irwin, Geoffrey J. (1977). Pots and entrepots: A study of settlement, trade and the development of economic specialization in Papuan prehistory. *World Archaeology*, *9*(3), 299–319.

Jacobsen, T. (1943). Primitive democracy in ancient Mesopotamia. *Journal of Near Eastern Studies*, *2*(3), 159–172.

Jevons, W. S. (1879). *The theory of political economy*. Macmillan and Company.

Kabesh, M., Refaat, A. M., Abdallah, Z., Kabesh, M. L., Refaat, A. M., & Abdallah, Z. M. (1980). Geochemistry of Quaternary volcanic rocks, Dhamar-Rada'Field, Yemen Arab Republic. *Neues Jahrbuch Für Mineralogie, Monatshefte*, *138*, 292–311.

Kennet, D. (2004). *Sasanian and Islamic pottery from Ras al-Khaimah (eBook version): Classification, chronology and analysis of trade in the Western Indian Ocean.* (Vol. 1). Archaeopress.

Kenoyer, J. M. (1991). The Indus valley tradition of Pakistan and western India. *Journal of World Prehistory*, *5*(4), 331–385.

Keynes, J. N. (2017). *The scope and method of political economy*. Routledge.

Khalidi, L. (2010). Holocene obsidian exchange in the Red Sea region. In *The evolution of human populations in Arabia* (pp. 279–291). Springer.

Khalidi, L., Gratuze, B., & Boucetta, S. (2009). Provenance of obsidian excavated from Late Chalcolithic levels at the sites of Tell Hamoukar and Tell Brak, Syria. *Archaeometry*, *51*(6), 879–893.

Khalidi, L., Inizan, M.-L., Gratuze, B., & Crassard, R. (2013). Considering the Arabian Neolithic through a reconstitution of interregional obsidian distribution patterns in the region. *Arabian Archaeology and Epigraphy*, *24*(1), 59–67.

Khalidi, L., Oppenheimer, C., Gratuze, B., Boucetta, S., Sanabani, A., & Al-Mosabi, A. (2010). Obsidian sources in highland Yemen and their relevance to archaeological research in the Red Sea region. *Journal of Archaeological Science*, *37*(9), 2332–2345.

Kitchen, K. A. (2004). The elusive land of Punt revisited. *BAR INTERNATIONAL SERIES*, 25–32.

Knapp, A. B. (2011). *Cyprus, copper and Alashiya*. INSTAP Academic Philadelphia.

Knapp, A. B. (2013). *The archaeology of Cyprus: From earliest prehistory through the Bronze Age*. Cambridge University Press.

Knappett, C. (2011). *An archaeology of interaction: Network perspectives on material culture and society*. Oxford University Press Oxford.

Knappett, C. (2012). A regional network approach to Protopalatial complexity. *Back to the Beginning: Reassessing Social and Political Complexity on Crete during the Early and Middle Bronze Age*, 384–402.

Knappett, C. (2013a). Introduction: Why networks. *Network Analysis in Archaeology: New Approaches to Regional Interaction*, 3–16.

Knappett, C. (2013b). *Network analysis in archaeology: New approaches to regional interaction*. Oxford University Press.

Knappett, C., Evans, T., & Rivers, R. (2008). Modelling maritime interaction in the Aegean Bronze Age. *Antiquity*, *82*(318), 1009–1024.

Knoke, D., & Yang, S. (2008). *Social Network Analysis*. SAGE.

Knox, H., Savage, M., & Harvey, P. (2006). Social networks and the study of relations: Networks as method, metaphor and form. *Economy and Society*, *35*(1), 113–140.

Kristiansen, K. (2010). Decentralized Complexity: The Case of Bronze Age Northern Europe. In *Pathways to Power* (pp. 169–192). Springer.

Kronenfeld, D. B. (2005). *Structural models in Anthropology*.

Kruse, F.A. (1988). Use of airborne imaging spectrometer data to map minerals associated with hydrothermally altered rocks in the northern grapevine mountains, Nevada, and California.

Kruse, Fred A., Lefkoff, A. B., Boardman, J. W., Heidebrecht, K. B., Shapiro, A. T., Barloon, P. J., & Goetz, A. F. H. (1993). The spectral image processing system (SIPS)—Interactive visualization and analysis of imaging spectrometer data. *Remote Sensing of Environment*, *44*(2–3), 145–163.

La Lone, D. E. (1982). The Inca as a nonmarket economy: Supply on command versus supply and demand. In *Contexts for prehistoric exchange* (pp. 291–316). Elsevier.

Lancaster, W., & Lancaster, F. (1992). Tribe, community and the concept of access to resources: Territorial behaviour in South-East Ja'alan. *Mobility and Territoriality: Social and Spatial Boundaries among Foragers, Fishers, Pastoralists and Peripatetics*, 343–64.

Larson, K. A. (2013). A Network Approach to Hellenistic Sculptural Production. *Journal of Mediterranean Archaeology*, *26*(2).

Laughton, A. S., Whitmarsh, R. B., & Jones, M. T. (1970). A discussion on the structure and evolution of the Red Sea and the nature of the Red Sea, Gulf of Aden and Ethiopia rift junction-The evolution of the Gulf of Aden. *Philosophical Transactions of the Royal Society of London. Series A, Mathematical and Physical Sciences*, *267*(1181), 227–266.

Laumann, E. O., Marsden, P. V., & Prensky, D. (1992). The boundary specification problem in network analysis. *Research Methods in Social Network Analysis*, *61*, 87.

Lazear, E. P. (1979). Why is there mandatory retirement? *Journal of Political Economy*, *87*(6), 1261–1284.

Leemans, W. F. (1960). The trade relations of Babylonia and the question of relations with Egypt in the Old Babylonian Period. *Journal of the Economic and Social History of the Orient*, *3*(1), 21–37.

Legrain, L. (1947). *Business Documents of the Third Dynasty of Ur*. Harrison and Sons.

Lehner, J. W., & Yener, K. A. (2014). Organization and specialization of early mining and metal technologies in Anatolia. In *Archaeometallurgy in global perspective* (pp. 529–557). Springer.

Leigh, B. (2016). Metal. In *The Bronze Age Towers at Bat, Sultanate of Oman: Research by the Bat Archaeological Project 2007–12* (Vol. 143, pp. 229–235). University of Pennsylvania Press.

Leontief, W. (1982). Academic economics. *Science*, *217*(4555), 104–107.

Leslie, T. E. C. (1879). "The Love of Money," "On the Philosophical Method in Political Economy," and "Political Economy and Sociology." In *Essays in Political Economy*.

Levine, D. N. (1974). Greater Ethiopia: The evolution of a multiethnic society.

Lévi-Strauss, C. (1969). *The elementary structures of kinship*. Beacon Press.

Lie, J. (1991). Embedding Polanyi's market society. *Sociological Perspectives*, *34*(2), 219–235.

Lillesand, T. M., Kiefer, R. W., & Chipman, J. W. (2000). Remote sensing and image interpretation. John Willey & Sons. *New York*, *724*.

Livarda, A., & Orengo, H. A. (2015). Reconstructing the Roman London flavourscape: New insights into the exotic food plant trade using network and spatial analyses. *Journal of Archaeological Science*, *55*, 244–252.

Lutz, J., & Pernicka, E. (2004). *Neutronenaktivierungsanalysen*. na.

MacDonald, K. C. (1992). The domestic chicken (Gallus gallus) in sub-Saharan Africa: A background to its introduction and its osteological differentiation from indigenous fowls (Numidinae and Francolinus sp.). *Journal of Archaeological Science*, *19*(3), 303–318.

Maddin, R. (1988). *The beginning of the use of metals and alloys: Papers from the Second International Conference on the Beginning of the Use of Metals and Alloys, Zhengzhou, China, 21-26 October 1986*.

Magee, P. (1996). The chronology of the southeast Arabian Iron Age. *Arabian Archaeology and Epigraphy*, *7*(2), 240–252.

Magee, P. (2004). The impact of southeast Arabian intra-regional trade on settlement location and organization during the Iron Age II period. *Arabian Archaeology and Epigraphy*, *15*(1), 24–42.

Magee, P. (2014). *The archaeology of prehistoric Arabia: Adaptation and social formation from the Neolithic to the Iron Age*. Cambridge University Press.

Malinowski, B. (1922). *Argonauts of the western Pacific*. Routledge.

Malinowski, B. (1941). Man's culture and man's behavior. *Sigma Xi Quarterly*, *29*(3/4), 182–196.

Manzo, A. (2003). Skeuomorphism in Aksumite pottery? Remarks on the origins and meanings of some ceramic types. *Aethiopica*, *6*, 7–46.

March, J. G., & Simon, H. A. (1958). Organizations. *New York: Willey*.

Mauss, M. (1925). *The gift: The form and reason for exchange in archaic societies*. Routledge.

McCann, J. C. (1995). *People of the plow: An agricultural history of Ethiopia, 1800–1990*. Univ of Wisconsin Press.

McCorriston, J. (1997). Textile extensification, alienation, and social stratification in ancient mesopotamia. *Current Anthropology*, *38*(4), 517–535.

McCorriston, J. (2006). Breaking the rain barrier and the tropical spread of Near Eastern agriculture into southern Arabia. *Behavioral Ecology and the Transition to Agriculture*, 217–264.

McCorriston, J. (2011). *Pilgrimage and household in the Ancient Near East*. Cambridge University Press.

McCorriston, J., Harrower, M., Martin, L., & Oches, E. (2012). Cattle cults of the Arabian Neolithic and early territorial societies. *American Anthropologist*, *114*(1), 45–63.

Mead, M. (1928). *Coming of Age in Samoa*. New York: Harper Collins.

Merkel, J. (1985). Ore beneficiation during the late Bronze/early Iron age at Timna, Israel. *MASCA Journal*, *3*(5), 164–169.

Merrick, H. V., Brown, F. H., & Nash, W. P. (1994). Use and movement of obsidian in the Early and Middle Stone Ages of Kenya and northern Tanzania. *Society, Culture, and Technology in Africa*, *11*(6), 29–44.

Merrillees, R. S. (1984). *Ambelikou-Aletri: A preliminary report*. Department of Antiquities.

Mertens, K. C., De Baets, B., Verbeke, L. P., & De Wulf, R. R. (2006). A sub-pixel mapping algorithm based on sub-pixel/pixel spatial attraction models. *International Journal of Remote Sensing*, *27*(15), 3293–3310.

Mery, S. (1995). Archaelogy of the Borderlands: 4th Millennium BC Mesopotamian Pottery at Ra's al-Hamra RH-5 (Sultanate of Oman). *Annali Dell'Università Degli Studi Di Napoli "L'Orientale". Rivista Del Dipartimento Di Studi Asiatici e Del Dipartimento Di Studi e Ricerche Su Africa e Paesi Arabi*, *1995*(55/2), 193–206.

Méry, S., Phillips, C., & Calvet, Y. (1998). Dilmun pottery in Mesopotamia and Magan from the end of the 3rd and beginning of the 2nd millennium BC. *Abiel II*, 165–180.

Méry, Sophie. (1991). Origine et production des récipients de terre cuite dans la péninsule d'Oman à l'Âge du Bronze. *Paléorient*, 51–78.

Méry, Sophie. (1996). *Ceramics and patterns of exchange across the Arabian Sea and the Persian Gulf in the Early Bronze Age*. na.

Méry, Sophie. (2000). *Les céramiques d'Oman et l'Asie moyenne: Une archéologie des échanges à l'Âge du Bronze* (Vol. 23). CNRS.

Méry, Sophie, & Blackman, M. J. (1996). Black-jars of Meluhha: Production and diffusion of Indus pottery ware during the second half of the 3rd millennium BC. *Text Prepared for Harappan Studies-3*.

Méry, Sophie, & Schneider, G. (1996). Mesopotamian Pottery Wares in Eastern Arabia from the 5th to the 2nd Millennium BC: A Contribution of Archaeometry to the Economic History. *Proceedings of the Seminar for Arabian Studies*, 79–96.

Meyers, M. L. (1983). The Soul of Modern Economic Man: Ideas of Self-interest. *Thomas Hobbes to Adam Smith, Chicago*.

Michels, J. W. (2005). Changing settlement patterns in the Aksum-Yeha region of Ethiopia: 700 BC-AD 850. *BAR International Series*, *1446*.

Milgram, S. (1967). The small world problem. *Psychology Today*, *2*(1), 60–67.

Mill, J. S. (1836). *On the definition of political economy; and on the method of investigation proper to it* (Vol. 4). University of Toronto Press Toronto.

Mill, J. S. (1844). Of the influence of consumption on production. *Some Unsettled Questions of Political Economy*.

Miller, N. F. (1984). The use of dung as fuel: An ethnographic example and an archaeological application. *Paléorient*, 71–79.

Mills, B. J. (2016). Communities of consumption: Cuisines as constellated networks of situated practice. In *Knowledge in Motion: Constellations of Learning Across Time and Place* (pp. 247–270). University of Arizona Press.

Mills, B. J. (2017). Social network analysis in archaeology. *Annual Review of Anthropology*, *46*, 379–397.

Mills, B. J., Clark, J. J., Peeples, M. A., Haas, W. R., Roberts, J. M., Hill, J. B., Clauset, A. (2013a). Transformation of social networks in the late pre-Hispanic US Southwest. *Proceedings of the National Academy of Sciences*, *110*(15), 5785–5790.

Mills, B. J., Peeples, M. A., Haas, W. R., Borck, L., Clark, J. J., & Roberts, J. M. (2015a). Multiscalar perspectives on social networks in the late prehispanic Southwest. *American Antiquity*, *80*(1), 3–24.

Mills, B. J., Roberts Jr, J. M., Clark, J. J., Haas Jr, W. R., Huntley, D., Peeples, M. A., Breiger, R. L. (2013b). The dynamics of social networks in the Late Prehispanic US Southwest. *Network Analysis in Archaeology: New Approaches to Regional Interaction*, 181–202.

Mische, A. (2011). Relational sociology, culture, and agency. *The SAGE Handbook of Social Network Analysis*, 80–97.

Mizoguchi, K. (2009). Nodes and edges: A network approach to hierarchisation and state formation in Japan. *Journal of Anthropological Archaeology*, *28*(1), 14–26.

Mizoguchi, K. (2013). Evolution of prestige good systems: An application of network analysis to the transformation of communication systems and their media. *Network Analysis in Archaeology: New Approaches to Regional Interaction*, 151–178.

Mohr, P. (1983). Perspectives on the Ethiopian volcanic province. *Bulletin Volcanologique*, *46*(1), 23–43.

Mohr, P. A. (1971). Ethiopian rift and plateaus: Some volcanic petrochemical differences. *Journal of Geophysical Research*, *76*(8), 1967–1984.

Mohr, Paul. (1983). Ethiopian flood basalt province. *Nature*, *303*(5918), 577.

Mohr, Paul. (1989). Nature of the crust under Afar: New igneous, not thinned continental. *Tectonophysics*, *167*(1), 1–11.

Mohr, Paul, & Zanettin, B. (1988). The Ethiopian flood basalt province. In *Continental flood basalts* (pp. 63–110). Springer.

Moreno, J. L. (1934). *Who shall survive?: A new approach to the problem of human interrelations.*

Muhly, James D. (2005). *Kupfer und Bronze in der spätbronzezeitlichen Ägäis*. na.

Muhly, James D. (2009). Oxhide ingots in the Aegean and in Egypt. *Oxhide Ingots in the Central Mediterranean*, 17–40.

Muhly, James David. (1973). *Copper and tin. The distribution of mineral resources and the nature of the metals trade in the Bronze Age*.

Mundt, J. T., Street, N. G., Streutker, D. R., & Glenn, N. F. (2007). *Partial Unmixing of Hyperspectral Imagery: Theoyr and Methods*. 12.

Mundt, J. T., Streutker, D. R., & Glenn, N. F. (2007). Partial unmixing of hyperspectral imagery: Theory and methods. *Proceedings of the American Society of Photogrammetry and Remote Sensing*, *2007*.

Munro-Hay, S. (1993). State development and urbanism in northern Ethiopia. *The Archaeology of Africa: Food, Metals and Towns*, 608–621.

Munro-Hay, S. C. (1991). *Aksum: An African civilisation of late antiquity*. Edinburgh University Press Edinburgh.

Munro-Hay, S., & Tringali, G. (1991). The Ona sites of Asmara and Hamasien. *Rassegna Di Studi Etiopici*, *35*, 135–170.

Murra, J. V. (1968). An Aymara Kingdom in 1567. *Ethnohistory*, *15*(2), 115–151.

Murra, J. V., & Morris, C. (1976). Dynastic oral tradition, administrative records and archaeology in the Andes. *World Archaeology*, *7*(3), 269–279.

Nadel, S. F. (2013). *The theory of social structure*. Routledge.

Negash, A., Brown, F., & Nash, B. (2011). Varieties and sources of artefactual obsidian in the Middle Stone Age of the Middle Awash, Ethiopia. *Archaeometry*, *53*(4), 661–673.

Negash, A., & Shackley, M. S. (2006). Geochemical provenance of obsidian artefacts from the MSA site of Porc Epic, Ethiopia. *Archaeometry*, *48*(1), 1–12.

Newman, M. (2018). *Networks*. Oxford University Press.

Newman, M. E. (2004). Detecting community structure in networks. *The European Physical Journal B*, *38*(2), 321–330.

Newman, M. E. (2011). Complex systems: A survey. *ArXiv Preprint ArXiv:1112.1440*.

Nowak, M. A., Page, K. M., & Sigmund, K. (2000). Fairness versus reason in the ultimatum game. *Science*, *289*(5485), 1773–1775.

Oka, R., & Kusimba, C. M. (2008). The archaeology of trading systems, part 1: Towards a new trade synthesis. *Journal of Archaeological Research*, *16*(4), 339–395.

Oppenheim, A. L. (1954). The seafaring merchants of Ur. *Journal of the American Oriental Society*, *74*(1), 6–17.

Opsahl, T. (2013). Triadic closure in two-mode networks: Redefining the global and local clustering coefficients. *Social Networks*, *35*(2), 159–167.

O'Shea, J. M. (2013). *Villagers of the Maros: A portrait of an Early Bronze Age society*. Springer Science & Business Media.

Pankhurst, Richard. (1961). *An introduction to the economic history of Ethiopia, from early times to 1800*. Lalibela House.

Pankhurst, Rita. (1997). The coffee ceremony and the history of coffee consumption in Ethiopia. *ICES: International Conference of Ethiopian Studies*, Vol. 2–516.

Papo, D., Buldú, J. M., Boccaletti, S., & Bullmore, E. T. (2014). *Complex network theory and the brain*. The Royal Society.

Pareto, V. (1906). Manual of Political Economy. 1971 translation of 1927 edition. *New York: Augustus M. Kelley*.

Park, K., & Willinger, W. (2005). *The Internet as a large-scale complex system* (Vol. 3). Oxford University Press, USA.

Parpola, S., Parpola, A., & Brunswig Jr, R. H. (1977). The Meluhha Village. *Journal of the Economic and Social History of the Orient*, *20*(2), 129–165.

Parry, J. (1986). The gift, the Indian gift and the'Indian gift'. *Man*, 453–473.

Peake, H. (1928). The copper mountain of Magan. *Antiquity*, *2*(8), 452–457.

Peate, I. U., Kent, A. J., Baker, J. A., & Menzies, M. A. (2008). Extreme geochemical heterogeneity in Afro-Arabian Oligocene tephras: Preserving fractional crystallization and mafic recharge processes in silicic magma chambers. *Lithos*, *102*(1–2), 260–278.

Peeples, M. A. (2011). *Identity and social transformation in the Prehispanic Cibola world: AD 1150–1325*. Arizona State University.

Peeples, M. A. (2018). *Connected Communities: Networks, identity, and social change in the ancient Cibola world*. University of Arizona Press.

Peeples, M. A. (2019). Finding a Place for Networks in Archaeology. *Journal of Archaeological Research*, 1–49.

Peeples, M. A., Mills, B. J., Randall Haas, W., Clark, J. J., & Roberts, J. M. (2016). Analytical challenges for the application of social network analysis in archaeology. *The Connected Past: Challenges to Network Studies in Archaeology and History*, 59–84.

Persky, J. (1995). The ethology of homo economicus. *Journal of Economic Perspectives*, *9*(2), 221–231.

Peterson, E. (2017). *Development of craft specialization during the Pre-Aksumite period in Eastern Tigrai, Ethiopia: A study of hide working traditions (Dissertation)*.

Phillips, Jackie. (1997). Punt and Aksum: Egypt and the horn of Africa. *The Journal of African History*, *38*(3), 423–457.

Phillips, Jackie. (1995). Egyptian and Nubian material from Ethiopia and Eritrea. *Sudan Archaeological Research Society Newsletter*, *9*, 2–10.

Phillipson, D. W. (1977). The excavation of Gobedra rock-shelter, Axum: An early occurrence of cultivated finger millet in northern Ethiopia. *AZANIA: Journal of the British Institute in Eastern Africa*, *12*(1), 53–82.

Phillipson, D. W. (1998). *Ancient Ethiopia: Aksum, its antecedents and successors*. British Museum Press.

Phillipson, D. W. (2009). The first millennium BC in the highlands of Northern Ethiopia and South–Central Eritrea: A reassessment of cultural and political development. *African Archaeological Review*, *26*(4), 257–274.

Phillipson, D. W. (2012). *Foundations of an African Civilisation: Aksum & the Northern Horn, 1000 BC-1300 AD*. Boydell & Brewer Ltd.

Phillipson, D. W., & Phillips, J. (2000). *Archaeology at Aksum, Ethiopia, 1993-7, Volume II*.

Phillipson, L. (2000). A functional consideration of Gudit scrapers from Aksum, Ethiopia. *Recent Research on the Stone Age of Northeastern Africa*, 259–76.

Phillipson, Laurel. (2000). Aksumite lithic industries. *African Archaeological Review*, *17*(2), 49–63.

Phillipson, Laurel. (2004). Lithic Tools: A hitherto unrecognised component of Aksumite material culture. *Lithics in Action*, 254–69.

Phillipson, Laurel. (2009a). Lithic artefacts as a source of cultural, social and economic information: The evidence from Aksum, Ethiopia. *African Archaeological Review*, *26*(1), 45–58.

Phillipson, Laurel. (2009b). *Using stone tools: The evidence from Aksum, Ethiopia* (Vol. 196). British Archaeological Reports Limited.

Phillipson, Laurel. (2012). Grindstones and related artefacts from Pre-Aksumite Seglamen, northern Ethiopia, and their wider implications. *Azania: Archaeological Research in Africa*, *47*(4), 509–530.

Phillipson, Laurel. (2013a). Lithic tools used in the manufacture of pre-Aksumite ceramics. *Azania: Archaeological Research in Africa*, *48*(3), 380–402.

Phillipson, Laurel. (2013b). Parchment production in the first millennium BC at Seglamen, northern Ethiopia. *African Archaeological Review*, *30*(3), 285–303.

Phillipson, Laurel. (2017). Lithic evidence for the peopling of northern Ethiopia. *African Archaeological Review*, *34*(2), 177–191.

Phillipson, Laurel, & Sulas, F. (2005). Cultural continuity in Aksumite lithic tool production: The evidence from Mai Agam. *AZANIA: Journal of the British Institute in Eastern Africa*, *40*(1), 1–18.

Pickin, J., & Timberlake, S. (1988). Stone hammers and fire-setting: A preliminary experiment at Cwmystwyth mine, Dyfed. *Bulletin of the Peak District Mines Historical Society*, *10*, 165–167.

Pillevuit, A., Marcoux, J., Stampfli, G., & Baud, A. (1997). Pillevuit: The Oman Exotics: A key to the understanding of the Neotethyan geodynamic evolution.

Plattner, S. (1989). *Economic anthropology*. Stanford University Press.

Polanyi, K. (1944). *The great transformation* (Vol. 2). Beacon press Boston.

Polanyi, K. (2001). The Economy as Instituted Process. *The Sociology of Economic Life (Oxford, Westview Press, 1992)*.

Polanyi, K., Arensberg, C. M., & Pearson, H. W. (1957). *Trade and market in the early empires: Economies in history and theory*. Free Press.

Possehl, G. L. (1986). *Kulli: An Exploration of Ancient Civilization in Asia*. Carolina Academic Press.

Possehl, G. L. (1996). *Meluhha*. Kegan Paul International.

Possehl, G. L. (2002). *The Indus civilization: A contemporary perspective*. Rowman Altamira.

Possehl, G., Thornton, C., & Cable, C. (2009). Bat 2009. *A Report from the American Team. Report Compiled for the Department of Excavations and Archaeological Studies, Ministry of Heritage and Culture, Muscat*.

Potts, D. T. (1993a). Four seasons of excavation at Tell Abraq (1989-1993). *Proceedings of the Seminar for Arabian Studies*, 117–126.

Potts, D. T. (1993b). Rethinking some aspects of trade in the Arabian Gulf. *World Archaeology*, *24*(3), 423–440.

Potts, D. T. (1999). 'The Plant for the Heart Grows in Magan…': Redefining Southeastern Arabia's Role in Ancient Western Asia. *Australian Archaeology*, *48*(1), 35–41.

Potts, D. T. (2003). A Soft-Stone Genre from Southeastern Iran: Zig-zag bowls from Magan to Margiana,'. *Culture Through Objects. Ancient Near Eastern Studies in Honour of PRS Moorey*, 77–91.

Potts, Daniel T. (1990). *The Arabian Gulf in Antiquity: From Alexander the Great to the Coming of Islam*. Clarendon.

Potts, Daniel T. (2005). In the beginning: Marhashi and the origins of Magan's ceramic industry in the third millennium BC. *Arabian Archaeology and Epigraphy*, *16*(1), 67–78.

Potts, Daniel T. (2008). An Umm an-Nar-type compartmented soft-stone vessel from Gonur Depe, Turkmenistan. *Arabian Archaeology and Epigraphy*, *19*(2), 168–181.

Potts, Daniel T. (2009). The archaeology and early history of the Persian Gulf. In *The Persian Gulf in History* (pp. 27–56). Springer.

Potts, Daniel T. (2012). *In the Land of the Emirates: The Archaeology and History of UAE*. Trident Press Abu Dhabi/London.

Prange, M. (2001). 5000 Jahre Kupfer im Oman, Band II. *Bochum: Metalla*, *8*.

Prange, M., & Hauptmann, A. (2001). The chemical composition of bronze objects from 'Ibri/Selme. *The Metal Hoard from 'Ibri/Selme, Sultanate of Oman*, 75–84.

Puglisi, S. M. (1946). *Industria litica di Aksum nel Tigrai occidentale*.

Pulak, Ç. (2000). *The copper and tin ingots from the Late Bronze Age shipwreck at Uluburun*. na.

Radivojević, M., & Grujić, J. (2017). Community structure of copper supply networks in the prehistoric Balkans: An independent evaluation of the archaeological record from the 7th to the 4th millennium BC. *Journal of Complex Networks*, *6*(1), 106–124.

Radivojević, Miljana, & Rehren, T. (2016). Paint It Black: The Rise of Metallurgy in the Balkans. *Journal of Archaeological Method and Theory*, *23*(1), 200–237.

Rashid, S. (1985). Adam Smith's acknowledgements: Neo-plagiarism and the Weath of Nations. *BEBR Faculty Working Paper; No. 1180*.

Rathje, W. L. (1975). The last tango in Mayapan: A tentative trajectory of production-distribution systems. *Ancient Civilization and Trade*, 409–448.

Ratnagar, S. (2004). *Trading encounters: From the Euphrates to the Indus in the Bronze Age*. Oxford University Press New Delhi.

Reade, J. (1995). Magan and Meluhha merchants at Ur. *Finkbeiner et Al*, 597–599.

Renfrew, C. (1969). Trade and culture process in European prehistory. *Current Anthropology*, *10*(2/3), 151–169.

Renfrew, C. (1975). Trade as action at a distance: Questions of integration and communication. *Ancient Civilization and Trade*, *3*, 3–59.

Renfrew, C. (1977). Alternative models for exchange and spatial distribution. In *Exchange systems in prehistory* (pp. 71–90). Elsevier.

Renfrew, C., Cann, J. R., & Dixon, J. E. (1965). Obsidian in the Aegean. *Annual of the British School at Athens*, *60*, 225–247.

Renfrew, C., Dixon, J. E., & Cann, J. R. (1966). Obsidian and early cultural contact in the Near East. *Proceedings of the Prehistoric Society*, *32*, 30–72. Cambridge University Press.

Rocha, L. E. (2017). Dynamics of air transport networks: A review from a complex systems perspective. *Chinese Journal of Aeronautics*, *30*(2), 469–478.

Rosen, S. (1982). Authority, control, and the distribution of earnings. *The Bell Journal of Economics*, 311–323.

Rosenthal, F. (1958). The Muqaddimah. *An Introduction to History*, *3*.

Rossini, C. C. (1928). *Storia d'Etiopia* (Vol. 3). Officina d'arte grafica A. Lucini.

Rothman, M. S. (1987). Graph theory and the interpretation of regional survey data. *Paléorient*, 73–91.

Rothman, M. S. (2001). *The local and the regional: An introduction*.

Rouse, L. M., & Weeks, L. (2011). Specialization and social inequality in Bronze Age SE Arabia: Analyzing the development of production strategies and economic networks using agent-based modeling. *Journal of Archaeological Science*, *38*(7), 1583–1590.

Ryan, L., & D'Angelo, A. (2018). Changing times: Migrants' social network analysis and the challenges of longitudinal research. *Social Networks*, *53*, 148–158.

Sabidussi, G. (1966). The centrality index of a graph. *Psychometrika*, *31*(4), 581–603.

Sabloff, J. A., & Friedel, D. A. (1975). A model of a pre-Colombian trading center. In *Ancient Civilization and Trade* (pp. 369–408). Albuquerque: University of New Mexico Press.

Sadr, K. (1991). *The development of nomadism in ancient northeast Africa*. University of Philadelphia Press Philadelphia.

Sahlins, M. (2004). *Apologies to Thucydides: Understanding history as culture and vice versa*. University of Chicago Press.

Sahlins, M. (2017). *Stone age economics*. Routledge.

Santoro, M. (2008). Framing Notes. An Introduction to "Catnets." *SO*, 0–0.

Savage, S. H., Levy, T. E., & Jones, I. W. (2012). Prospects and problems in the use of hyperspectral imagery for archaeological remote sensing: A case study from the Faynan copper mining district, Jordan. *Journal of Archaeological Science*, *39*(2), 407–420.

Schiavo, F. L., Muhly, J. D., Maddin, R., & Giumlia-Mair, A. (2009). *Oxhide ingots in the central Mediterranean*. AG Leventis Foundation.

Schmidt, C. and Döpper, S. (2019). The Hafit period at Al-Khashbah, Sultanate of Oman: results of four years of excavations and material studies. *Proceedings of the Seminar for Arabian Studies, 49, 265 – 274.*

Schmidt, P. R., Curtis, M. C., & Teka, Z. (2008). *The archaeology of ancient Eritrea*. Red Sea Press, Inc.

Schotter, A. (2008). *The economic theory of social institutions*.

Scott, J. (2011). Social physics and social networks. *The SAGE Handbook of Social Network Analysis*, 55–66.

Scott, J., & Carrington, P. J. (2011). *The SAGE handbook of social network analysis*. SAGE publications.

Searle, M. P., Warren, C. J., Waters, D. J., & Parrish, R. R. (2004). Structural evolution, metamorphism and restoration of the Arabian continental margin, Saih Hatat region, Oman Mountains. *Journal of Structural Geology*, *26*(3), 451–473.

Searle, Michael P. (2007). Structural geometry, style and timing of deformation in the Hawasina Window, Al Jabal al Akhdar and Saih Hatat culminations, Oman Mountains. *GeoArabia*, *12*(2), 99–130.

Sellet, F. (1993). Chaîne opératoire; the concept and its applications. *Lithic Technology*, *18*(1–2), 106–112.

Sergew, H. (1972). The problem of Gudit. *Journal of Ethiopian Studies*, *1*(10), 112–124.

Sergew Hable, S. (1972). Ancient and medieval Ethiopian history to 1270. *United Printers, Addis Ababa*.

Serpico, M., White, R., Nicholson, P. T., & Shaw, I. (2000). *Ancient Egyptian materials and technology*. Edited by Nicholson P, Shaw I. Cambridge: Cambridge University Press.

Servet, J.-M. (2007). Le principe de réciprocité chez Karl Polanyi, contribution à une définition de l'économie solidaire. *Revue Tiers Monde*, (2), 255–273.

Service, E. R. (1971). *Primitive social organization: An evolutionary perspective*.

Shaw, M. E. (1954). Group structure and the behavior of individuals in small groups. *The Journal of Psychology*, *38*(1), 139–149.

Shepherd-Popescu, E. (2003). The Neolithic settlement sites on the islands of Dalma and Marawah. *Archaeology of the United Arab Emirates, Proceedings of the First International Conference on the Archaeology of the UAE*, 45–54. Trident Press.

Shubik, M. (1984). *A Game Theoretic Approach to Political Economy: Game Theory in the Social Sciences*.

Shugar, A. (2009). Peaking your interest: An introductory explanation of how to interpret XRF data. *WAAC Newsletter*, *31*(3), 8–10.

Shugar, A. N., & Mass, J. L. (2012). *Handheld XRF for art and archaeology* (Vol. 3). Leuven University Press.

Sigrist, M. (1988). *Isin year names*. Andrews University Press.

Smith, A. (2010). *The Wealth of Nations: An inquiry into the nature and causes of the Wealth of Nations*. Harriman House Limited.

Smith, M. E. (2011). *The comparative archaeology of complex societies*. Cambridge University Press.

Solomon Woldekiros, H. (2014). *The Afar Caravan Route: Insights into Aksumite (50 BCE-CE 900) Trade and Exchange from the Low Deserts to the North Ethiopian Plateau (Dissertation)*.

Spar, I., Von Dassow, E., Lambert, W. G., & Jursa, M. (1988). *Cuneiform Texts in the Metropolitan Museum of Art: Tablets, cones, and bricks of the third and second millennia, BC* (Vol. 1). Metropolitan Museum of Art.

Stanfield, J. Ron. (1990). Karl Polanyi and contemporary economic thought. *The Life and Work of Karl Polanyi. Quebec: Black Rose*.

Stanfield, James Ronald. (1986). *The economic thought of Karl Polanyi: Lives and livelihood*. Springer.

Stanish, C. (2017). The Evolution of Human Co-operation: Ritual and Social Complexity in Stateless Societies

Stein, G. J. (2002). From passive periphery to active agents: Emerging perspectives in the archaeology of interregional interaction. *American Anthropologist*, *104*(3), 903–916.

Steward, J. H. (1972a). *Theory of culture change: The methodology of multilinear evolution*. University of Illinois Press.

Steward, J. H. (1972b). *Theory of culture change: The methodology of multilinear evolution*. University of Illinois Press.

Strogatz, S. H. (2001). Exploring complex networks. *Nature*, *410*(6825), 268.

Suitor, J. J., Wellman, B., & Morgan, D. L. (1997). It's about time: How, why, and when networks change. *Social Networks*, *19*(1), 1–7.

Swayze, G. A. (1997). *The hydrothermal and structural history of the Cuprite Mining District, southwestern Nevada: An integrated geological and geophysical approach*.

Tazieff, H., Varet, J., Barberi, F., & Giglia, G. (1972). Tectonic significance of the Afar (or Danakil) depression. *Nature*, *235*(5334), 144.

Terrell, J. (1976). Island biogeography and man in Melanesia. *Archaeology & Physical Anthropology in Oceania*, *11*(1), 1–17.

Terrell, J. (1977a). Geographic systems and human diversity in the North Solomons. *World Archaeology*, *9*(1), 62–81.

Terrell, J. (1977b). Human biogeography in the Solomon Islands. *Fieldiana. Anthropology*, *68*(1), 1–47.

Terrell, J. E. (2010). Language and material culture on the Sepik coast of Papua New Guinea: Using social network analysis to simulate, graph, identify, and analyze social and cultural boundaries between communities. *Journal of Island & Coastal Archaeology*, *5*(1), 3–32.

Thompson, G. F. (2003). *Between hierarchies and markets: The logic and limits of network forms of organization*. Oxford University Press on Demand.

Thompson, R. C. (1933). *The British Museum Excavations at Nineveh, 1931-32*. University Press.

Thompson, R. C., & Assyria), A. (King of. (1933). *The British Museum Excavations at Nineveh, 1931-32*. University Press.

Thornton, C. P., & Giardino, C. (2012). Serge Cleuziou and the 'tin problem.' In *Aux marges de l'archéologie: Hommage à Serge Cleuziou, de Boccard, Travaux de la Maison René-Ginouvès Paris* (pp. 253–260).

Thornton, Christopher P. (2014). The emergence of complex metallurgy on the Iranian Plateau. In *Archaeometallurgy in Global Perspective* (pp. 665–696). Springer.

Thornton, Christopher P., Cable, C. M., & Possehl, G. L. (2016). *The Bronze Age Towers at Bat, Sultanate of Oman: Research by the Bat Archaeological Project, 2007-12* (Vol. 143). University of Pennsylvania Press.

Thornton, M. W., Atkinson, P. M., & Holland, D. A. (2006). Sub-pixel mapping of rural land cover objects from fine spatial resolution satellite sensor imagery using super-resolution pixel-swapping. *International Journal of Remote Sensing*, *27*(3), 473–491.

Thurow, L. C. (1983). *Dangerous currents: The state of economics*. Random House New York.

Tiercelin, J. J., Taieb, M., & Faure, H. (1980). Continental sedimentary basins and volcano-tectonic evolution of the Afar Rift. *Atti Convegni Lincei*, *47*, 491–504.

Tikriti, W. Y. (2002). The south-east Arabian origin of the falaj system. *Proceedings of the Seminar for Arabian Studies*, 117–138.

Torrence, R. (1986). *Production and exchange of stone tools*. Cambridge University Press, Cambridge.

Tosi, M. (1975). Notes on the distribution and exploitation of natural resources in ancient Oman. *Journal of Oman Studies*, *1*, 187–206.

Travers, J., & Milgram, S. (1977). An experimental study of the small world problem. In *Social Networks* (pp. 179–197). Elsevier.

Trigger, B. G. (2003). *Understanding early civilizations: A comparative study*. Cambridge University Press.

Tringali, G. (1965). Cenni sulle ʿona di Asmara e dintorni. *Annales d'Ethiopie*, *6*, 143–161. Editions de la Table Ronde.

Tripcevich, N. (2007). *Quarries, caravans, and routes to complexity: Prehispanic obsidian in the south-central Andes* (PhD Thesis). University of California, Santa Barbara.

Turner, J. H. (1987). *The structure of sociology theory*. Jaipur, India: Dorsey.

Tylecote, R. F., & Merkel, J. F. (1985). Experimental Smelting Techniques: Achievements and Future.(Retroactive Coverage). *British Museum Publications Ltd., Furnaces and Smelting Technology in Antiquity,* 3–20.

Verhagen, P., Brughmans, T., Nuninger, L., & Bertoncello, F. (2013). The long and winding road: Combining least cost paths and network analysis techniques for settlement location analysis and predictive modelling. *Archaeology in the Digital Era*, 357.

Verhoeye, J., & De Wulf, R. (2002). Land cover mapping at sub-pixel scales using linear optimization techniques. *Remote Sensing of Environment*, *79*(1), 96–104.

Villey, M., Le Metour, J., & Gramont, X. (1986). *Geological map of Fanjah. Sheet NF 40-3F, Scale 1:100,000.* Directorate General of Minerals, Oman Ministry of Petroleum and Minerals.

Vogt, B. (1985). *Zur Chronologie und Entwicklung der Gräber des späten 4.-2. Jtsd. v. Chr. auf der Halbinsel Oman: Zusammenfassung, Analyse und Würdigung publizierter wie auch unveröffentlichter Grabungsergebnisse*. Georg-August-Universität zu Göttingen.

Vogt, B., & Sedov, A. (1998). The Sabir culture and coastal Yemen during the second millennium BC-the present state of discussion. *Proceedings of the Seminar for Arabian Studies*, *28*, 261–270.

Voigt, R. (1999). Κολόη und Ḳoñayto ('Auf-/Ausblick'): Studien zur äthiopischen Toponomastik. 1. *Aethiopica*, *2*, 90–102.

von Kardorff, E. (2019). Barnes (1954): Class and Committees in a Norwegian Island Parish. In *Schlüsselwerke der Netzwerkforschung* (pp. 31–34). Springer.

Wagner, G., & Yule, P. (2007). *Thermoluminescence Dating of Early Ceramics from Oman*.

Waller Jr, W. T. (1982). The evolution of the veblenian dichotomy: Veblen, Hamilton, Ayres, and Foster. *Journal of Economic Issues*, *16*(3), 757–771.

Warner, T. A., Nellis, N. D., & Foody, G. M. (2009). Remote sensing scale and data selection issues. In *The SAGE Handbook of Remote Sensing*. Thousand Oaks, CA.: SAGE Publications Inc.

Wasserman, S., & Faust, K. (1994). *Social network analysis: Methods and applications* (Vol. 8). Cambridge university press.

Wasserman, S., & Faust, K. (1997). Social network analysis, methods and applications. *American Ethnologist*, *24*(1), 219–220.

Watts, D. J. (2004). The "new" science of networks. *Annu. Rev. Sociol.*, *30*, 243–270.

Watts, D. J., & Strogatz, S. H. (1998). Collective dynamics of 'small-world'networks. *Nature*, *393*(6684), 440.

Weedman, K. J. (2002). On the spur of the moment: Effects of age and experience on hafted stone scraper morphology. *American Antiquity*, *67*(4), 731–744.

Weeks, L. (1999). Lead isotope analyses from Tell Abraq, United Arab Emirates: New data regarding the 'tin problem'in Western Asia. *Antiquity*, *73*(279), 49–64.

Weeks, L. (2004). *Early metallurgy of the Persian Gulf: Technology, trade, and the Bronze Age World*. Brill.

Weeks, L. (2007a). Coals to Newcastle, copper to Magan? Isotopic analyses and the Persian Gulf metals trade. *Metals and Mines: Studies in Archaeometallurgy*, 89–96.

Weeks, L. (2007b). Coals to Newcastle, copper to Magan? Isotopic analyses and the Persian Gulf metals trade. *Metals and Mines: Studies in Archaeometallurgy*, 89–96.

Weeks, L. (2008). The 2007 early Iranian metallurgy workshop at the University of Nottingham. *Iran*, *46*(1), 335–345.

Weeks, L. R. (1997). Prehistoric metallurgy at Tell Abraq, UAE. *Arabian Archaeology and Epigraphy*, *8*(1), 11–85.

Weeks, Lloyd R. (2003). Prehistoric Metallurgy in the UAE: Bronze Age-Iron Age Transitions. *Proceedings of the First Archaeological Conference on the UAE Trident Press, Galway*, 11.

Weisgerber, G. (2007). Sites of multi-period copper production in the Sultanate of Oman. *Proceedings of the International Symposium: Archaeology of the Arabian Peninsula through the Ages (7th–9th May 2006)*. Ministry of Heritage and Culture.

Weisgerber, Gerd. (1977). Beobachtungen zum alten Kupferbergbau im Sultanat Oman. *Der Anschnitt*, 190–211.

Weisgerber, Gerd. (1978). Evidence of ancient mining sites in Oman: A preliminary report. *Journal of Oman Studies*, *4*, 15–28.

Weisgerber, Gerd. (1980a). Patterns of Early Islamic Metallurgy in Oman. *Proceedings of the Seminar for Arabian Studies*, *10*, 115–126. Retrieved from JSTOR.

Weisgerber, Gerd. (1980b). Patterns of early Islamic metallurgy in Oman. *Proceedings of the Seminar for Arabian Studies*, 115–126. JSTOR.

Weisgerber, Gerd. (1980c). Und Kupfer in Oman. *Der Anschnitt*, *32*(2–3), 61–110.

Weisgerber, Gerd. (1981). Makan and Meluhha: Third millennium BC copper production in Oman and the evidence of contact with the Indus Valley. *South Asian Archaeology*, *1981*, 19.

Weisgerber, Gerd. (1982). Aspects of Late Iron Age Archaeology in Oman—The Samad Civilization. *Proceedings of the Seminar for Arabian Studies*, 81–93. JSTOR.

Weisgerber, Gerd. (1983). Copper production during the third millennium BC in Oman and the question of Makan. *Journal of Oman Studies*, *6*(2), 269–276.

Weisgerber, Gerd. (1987). Archaeological evidence of copper exploitation at ‘Arja. *Journal of Oman Studies*, *9*, 145–172.

Weisgerber, Gerd. (2008). Metallurgy in Arabia. *Encyclopedia of the History of Science, Technology, and Medicine in Non-Western Cultures*, 1613–1622.

Weisgerber, Gerd, & Yule, P. (1999). Preliminary report of the 1996 season of excavation in the Sultanate of Oman. *Studies in the Archaeology of the Sultanate of Oman. Verlag Maria Leidorf, Rahden*, 97–117.

Weisgerber, Gerd, & Yule, P. (2003). Al-Aqir near Bahlā’–an Early Bronze Age dam site with planoconvex ‘copper’ ingots. *Arabian Archaeology and Epigraphy*, *14*(1), 24–53.

Wertime, T. A., & Wertime, S. F. (1982). *Early pyrotechnology: The evolution of the first fire-using industries. Papers presented at a seminar on early pyrotechnology held at the Smithsonian Institution, Washington, DC, and the National Bureau of Standards, Gaithersburg, Maryland, April 19-20, 1979; One of the Smithsonian Institution-National Bureau of Standards seminars on the application of the Materials and Measurement Sciences to Archaeology and Museum Conservation, organized by Alan D. Franklin and Jacqueline S. Olin*.

Whitcomb, D. S. (n.d.). The Archaeology of al-Hasa’ Oasis in the Islamic Period. *Atlal*, *2*, 95–115.

White, D. A., & Barber, S. B. (2012). Geospatial modeling of pedestrian transportation networks: A case study from precolumbian Oaxaca, Mexico. *Journal of Archaeological Science*, *39*(8), 2684–2696.

White, H. C. (2008a). Notes on the Constituents of Social Structure. Soc. Rel. 10-Spring'65. *Sociologica*, *2*(1), 0–0.

White, H. C. (2008b). Notes on the Constituents of Social Structure. Soc. Rel. 10-Spring'65. *Sociologica*, *2*(1), 0–0.

Whitten, N. E., & Wolfe, A. W. (1973). Network analysis. *Handbook of Social and Cultural Anthropology*, 717–746.

Wilkinson, J. C. (1973). Arab-Persian Land Relationships in Late Sasānid Oman. *Proceedings of the Seminar for Arabian Studies*, 40–51. JSTOR.

Wilkinson, John C. (1983a). The origins of the aflaj of Oman. *The Journal of Oman Studies, Vol. 6, Pt. 1*, 177–198.

Wilkinson, John Craven. (1972). *The origins of the Omani state*. SOAS.

Williamson, O. E. (1975). Markets and hierarchies. *New York*, *2630*.

Williamson, O. E. (1979). Transaction-cost economics: The governance of contractual relations. *The Journal of Law and Economics*, *22*(2), 233–261.

Williamson, O. E. (1981). The economics of organization: The transaction cost approach. *American Journal of Sociology*, *87*(3), 548–577.

Williamson, O. E., & Ouchi, W. G. (1981). The markets and hierarchies and visible hand perspectives. *Perspectives on Organizational Design and Behavior. NY: Wiley*, 347–70.

Wissink, M., Düvell, F., & Mazzucato, V. (2017). The evolution of migration trajectories of sub-Saharan African migrants in Turkey and Greece: The role of changing social networks and critical events. *Geoforum*.

Witter, W. (1938). *Die Kenntnis von Kupfer und Bronze in der alten Welt*. Curt Rabitzsch.

Wolf, E. R. (1956). Aspects of Group Relations in a Complex Society: Mexico 1. *American Anthropologist*, *58*(6), 1065–1078.

Wolfe, A. W. (1970). On structural comparisons of networks. *Canadian Review of Sociology/Revue Canadienne de Sociologie*, *7*(4), 226–244.

Yon, S. A., & Pieters, C. M. (1988). Interactions of light with rough dielectric surfaces-Spectral reflectance and polarimetric properties. *Lunar and Planetary Science Conference Proceedings*, *18*, 581–592.

Yule, P., & Weisgerber, G. (2015). a. Al-Wāsiṭ Tomb W1 and other Sites, Materials for a Definition of the Second Half of the 2nd Millennium BCE. *Archaeological Research in the Sultanate of Oman*, 9–108.

Yule, P., Weisgerber, G., Kunter, M., & Bemmann, M. (1993). *Wadi Suq Burial Structures in Oman*. Warszawa: Litterae et Artes.

Yule, Paul, & Weisgerber, G. (1996). *Die 14. Deutsche Archäologische Oman-Expedition 1995*.

Yule, Paul, Weisgerber, G., Prange, M., & Hauptmann, A. (2001). *The Metal Hoard from ʾIbrī/Selme, Sultanate of Oman*. Franz Steiner Verlag.

Zarins, Juri. (1987). Obsidian and the Red Sea trade: Prehistoric aspects. *South Asian Archaeology*, *1*, 507–541.

Zarins, Juris. (1989). Ancient Egypt and the Red Sea trade: The case for obsidian in the predynastic and archaic periods. *Essays in Ancient Civilization Presented to Helene J. Kantor*, 339–68. Studies in Ancient Oriental Civilization, 47.

Zarins, Juris. (1996). Obsidian in Predynastic/Archaic Egyptian Red Sea trade. *The Indian Ocean in Antiquity. London: Kegan Paul*.

Ioana Andrada Dumitru

Curriculum Vitae

Johns Hopkins University
Dept. of Near Eastern Studies
Gilman Hall 113, 3400 N. Charles Street
Baltimore, MD 21218

Email: idumitr1@jhu.edu
idumitru@culturalsite.com

EDUCATION

2019 Ph.D., Near Eastern Studies, Johns Hopkins University. Dissertation: A Comparative Approach to the Development of Ancient Copper Supply Networks in Oman and Obsidian Supply Networks in Ethiopia. Advisors: Michael J. Harrower, Glenn M. Schwartz (defended 24 Sept.; to be conferred 30 Dec.)

2016 M.A., Near Eastern Studies, Johns Hopkins University

2011 B.A., Cum Laude with Honors in Majors, Classical and Near Eastern Archaeology, Philosophy (double major), Bryn Mawr College

PROFESSIONAL APPOINTMENTS AND EMPLOYMENT

2019 Official Rapporteur, 2019 UNESCO Meeting on the Management of Public Archaeological Sites (Practical Applications of the Salalah Guidelines)

2019 Senior GIS/ Remote Sensing Specialist and Grant Proposal Writer, Cultural Site Research and Management Foundation, Baltimore, MD

2016 GIS/ Remote Sensing Specialist, CSRM Foundation, Baltimore, MD

PUBLICATIONS

Refereed Journal Articles

(in review) Harrower, M.J., S. Nathan, J.C. Mazzariello, K. Zerue, **I.A. Dumitru**, Y. Meresa, J. Bongers, G. Gebreegziabher, B. Zaitchik, M. Anderson – Water Availability and the Empire of Aksum: The Southern Red Sea Archaeological Histories (SRSAH) Project Survey (2009 – 2016). *African Archaeological Review*.

(in review) Sivitskis, A.J., J.W. Lehner, M.J. Harrower, **I.A. Dumitru**, P.E. Paulsen, S. Nathan, D.R. Viete, S. Al-Jabri, B. Helwing, F. Wiig, D. Moraetis, B. Pracejus, B. Zaitchick (in prep): Detecting and Mapping Slag Heaps at Ancient Copper Production Sites in Oman. *Remote Sensing*.

2019 Comer, D.C., J.A Comer, **I.A. Dumitru**, W.A. Ayres, M.J. Levin, K. Seikel, D. White, M.J. Harrower (2019): Airborne LiDAR Reveals a Vast Archaeological Landscape at the Nan Madol World Heritage Site. *Remote Sensing*.

2019 Harrower, M.J., **I.A. Dumitru**, C. Perlingieri, S. Nathan, K. Zerue, J.L. Lamont, A. Bausi, J.L. Swerida, J.L. Bongers, H.S. Woldekiros, L.A. Poolman, C.M. Pohl, S.A. Brandt, E.A. Peterson (December 2019): Beta Samati: Discovery and Excavation of an Aksumite Town. *Antiquity.*

2018 Wiig, F., M.J. Harrower, A. Braun, S. Nathan, J.W. Lehner, K.M. Simon, J.O. Strum, J. Trinder, **I.A. Dumitru**, S. Hensley, T. Clark (2018): Mapping a Subsurface Water Channel with X- Band and C-Band Synthetic Aperture Radar at the Iron Age Archaeological Site of 'Uqdat al- Bakrah(Safah), Oman. *Geosciences 8, 1 – 15.*

2018 Sivitskis, A.J., M.J. Harrower, H. David-Cuny, **I.A. Dumitru**, S. Nathan, F. Wiig, D.R Viete, K.W. Lewis, A. Taylor, E.N. Dollarhide, B. Zaitchik, S. Al-Jabri, K.J.T. Livi, A. Braun (2018): Hyperspectral satellite imagery detection of ancient raw material sources: Soft stone vessel production at Aqir al-Shamoos (Oman). *Archaeological Prospection, 1 – 12*.

2016 Harrower, M.J., H. David-Cuny, S. Nathan, **I.A. Dumitru**, S. Al-Jabri (2016): First discovery of ancient soft-stone (chlorite) vessel production in Arabia: Aqir al-Shamoos (Oman). *Arabian Archaeology and Epigraphy, 27, 197-207*.

2014 Harrower, M.J., K. O'Meara, J.J. Basile, J.L. Swerida, **I.A. Dumitru**, C.J. Hickman, J.L. Bongers, C.J. Bailey, E. Fieldhouse (2014): If a picture is worth a thousand words… 3D modeling a Bronze Age Tower in Oman. *World Archaeology, 46(1), 43-62.*

Refereed Book Chapters

2018 **Dumitru, I.A.**, M.J. Harrower (2018): From Rural Collectables to Global Commodities: Copper from Oman and Obsidian from Ethiopia, in *Globalization in Prehistory: Contact, Exchange and 'People Without History,'* pp. 232 – 262, N. Boivin and M. Frachetti (editors), Cambridge University Press: Cambridge.

2018 **Dumitru, I.A.**, M.J. Harrower (2018): Mapping Ancient Production and Trade of Copper in Oman and Obsidian in Ethiopia, in *Stories of Globalization: The Red Sea and the Persian Gulf from Late Prehistory to Early Modernity*, pp. 74 – 94, A. Manzo, C. Zazzaro, and D.J. De Falco (editors), Brill: Leiden.

Other Publications

2017 Harrower, M.J. and **I.A. Dumitru** (2017): Archaeology: Digital maps illuminate ancient trade routes. *Nature 543: 188 – 189.*

2016 Harrower, M.J., **I.A. Dumitru**, S. Nathan, F. Wiig, H. David-Cuny, A.J. Sivitskis, A.F. Buffington, S. Al-Jabri (2016): The Archaeological Water Histories of Oman (ArWHO) Project: Recent Research in Al-Dhahirah Governorate of Oman. *Bulletin of the British Foundation for the Study of Arabia 21: 16 – 18*.

AWARDS AND HONORS

2014 Cornelia G. Harcum Scholarship, Department of Near Eastern Studies, Johns Hopkins University.

GRANTS AND FELLOWSHIPS

2019 Dean's Prize Fellowship, Johns Hopkins University, $6,500 USD.

2019 Lewis and Clark Fund for Exploration and Field Research – "Huaca La Meseta: Exploring a Monumental Stone Complex in a Peruvian Cloud Forest" (J.L. Bongers – Co-PI and **I.A. Dumitru** – Co-PI) - $4,500 USD.

2018 Australian Research Council – Discovery Early Career Research Award – "Strategic resources and human cooperation in the rise of social complexity in southeastern Arabia" (J. Lehner – PI, **I.A. Dumitru** – Collaborator) $384,983 AUS.

2018 United States Ambassadors Fund Large Grant for Cultural Preservation – "Conservation of the Endangered World Heritage Site of Nan Madol: A Ceremonial Center of Eastern Micronesia" (D. Comer – PI, **I.A. Dumitru** – Research collaborator) $375,000 USD.

2017 Teaching-as-Research (TAR) Fellowship, Center for the Integration of Research, Teaching and Learning (CIRTL).

2016 NASA EPSCoR GEOCORE Grant – "Modelling Fish Spawning Aggregation Sites" (D. Comer – PI, **I.A. Dumitru** – Research collaborator).

2016 Center for Advanced Spatial Technologies (CAST), SPARC Fieldwork Support Grant – "Mapping the Iron Age Metalworking Site of As-Safah (Oman)" (M. Harrower – PI, F. Wiig – Co-PI, **I.A. Dumitru** – Co-PI)

2016 National Geographic Society, Committee for Research and Exploration Grant – "Beita Semati and the Empire of Aksum: Political and Religious Change at an African Crossroads" (M. Harrower – PI, **I.A. Dumitru** – Co-PI, C. Perlingieri – Co-PI) $24,945 USD.

2016 Dean's Teaching Fellowship, Johns Hopkins University, $11,500 USD.

2015 Internal Mellon Foundation Summer Research Stipend, $500 USD.

2015 Internal Travel Grant, Dept. of Near Eastern Studies, Johns Hopkins University, $1000 USD.

2014 Internal Mellon Foundation Summer Research Stipend, $500 USD.

2013 Sigma Xi Grants-in-Aid, $1,000 USD

2013 Islamic Studies Initiative KSAS, Johns Hopkins University, Language Training Grant, $1,800 USD.

2013 Internal Mellon Foundation Summer Research Stipend, $500 USD.

2013 Internal Research Travel Grant, Dept. of Near Eastern Studies, Johns Hopkins, $1,000 USD.

2012 Internal Mellon Foundation Summer Research Stipend, $500 USD.

2012 Internal Research Travel Grant, Dept. of Near Eastern Studies, Johns Hopkins University, $1,000 USD.

INVITED TALKS

2018 **Dumitru, I.A.** and M.J. Harrower – "Mapping and Modeling Obsidian Trade Networks in Northern Ethiopia," 2018 ASOR Annual Meeting, Denver, Colorado November 14 –17, 2018.

2015 Harrower, M.J., K.M. O'Meara, **I.A. Dumitru**, C.J. Hickman, J.L. Bongers – "3D Modeling – Breakthrough or Fad? Bronze Age Towers in Oman and Excavations of an Aksumite Town in Ethiopia", Society for American Archaeology (SAA) Meetings, San Francisco, CA, April 15 – 19, 2015.

2014 **Dumitru, I.A.** and M.J. Harrower – "GPS in Archaeology," GIS Science Workshop, University of Bucharest, June 3 – 5, 2014.

2014 Harrower, M.J. and **I.A. Dumitru** – "Globalization and Entanglement in Ancient Arabia: Reconsidering Core and Periphery in the Archaeology of the Ancient Near East," Dept. of Near Eastern Languages and Cultures, University of California, Los Angeles, April 21, 2014.

2013 Harrower, M.J., **I.A. Dumitru**, J.L. Swerida, J.L. Bongers – "The Red Sea and Persian Gulf: Long-Term Conduits of Ancient Interchange, Entanglement, and Hybridity," *Ancient Globalization and People without History*, Society for American Archaeology (SAA) Meetings, Honolulu, HI, April 5, 2013.

CONFERENCE ACTIVITY

Sessions Organized

2018 Earley-Spadoni, T. and **I.A. Dumitru** – *GIS and Remote Sensing in Archaeology*. 2018 ASOR Annual Meeting, Denver, Colorado, November 14 – 17, 2018.

Papers Presented

2019 **Dumitru, I.A.** – "Introduction to Key Issues and Thematic Areas to discuss in round tables," The International Workshop of the Practical Application of the Salalah Guidelines for the Management of Public Archaeological Sites (UNESCO Workshop), Nizwa, Oman, September 16 – 19, 2019.

2019 Harrower, M.J. and **I.A. Dumitru** – "Community Participation at Beta Semati, Ethiopia," The International Workshop of the Practical Application of the Salalah

Guidelines for the Management of Public Archaeological Sites (UNESCO Workshop), Nizwa, Oman, September 16 – 19, 2019.

2018 **Dumitru, I.A.** and M.J. Harrower – "Modelling Networks of Obsidian Production in Northern Ethiopia and of Copper Production in Northern Oman: A Comparative Study," The Connected Past 2018, Oxford, UK, December 6 – 7, 2018.

2018 **Dumitru, I.A.**, J.W. Lehner, and M.J. Harrower – "Modelling the Connectivity of Socioeconomic Networks of Copper Production in Ancient Oman," 2018 Society for American Archaeology (SAA) 83rd Annual Meeting, Washington, DC., April 11 – 15, 2018.

2018 Harrower, M.J., **I.A. Dumitru**, C. Perlingieri, J.L. Lamont – "An Ancient Basilica: Monumental Architecture at Beita Semati, Ethiopia,"2018 Society of Africanist Archaeologists (SAfA) 24th Biennial Meeting, Toronto, Canada, June 18 – 21, 2018.

2016 Harrower, M.J., C. Perlingieri, **I.A. Dumitru**, S. Nathan, J.C. Mazzariello – "The rise and decline of Aksum beyond the capital: The Southern Red Sea Archaeological Histories (SRSAH) Project (2009 – 2015)," 2016 Society of Africanist Archaeologists (SAfA) 23rd Biennial Meeting, Toulouse, France, June 26 – July 2, 2016.

2016 **Dumitru, I.A.**, M.J. Harrower, C. Perlingieri – "Discovery and excavations of an Aksumite town, Bieta Semati (Ethiopia)," 2016 Society of Africanist Archaeologists (SAfA) 23rd Biennial Meeting, Toulouse, France, June 26 – July 2, 2016.

2016 Harrower, M.J., **I.A. Dumitru**, S. Nathan, A. Buffington, H. David-Cuny, A. Sivitskis – "The Archaeological Water Histories of Oman (ArWHO) Project: Results of Archaeological Survey and Satellite Imagery Analysis," 2016 American Schools of Oriental Research (ASOR) Meeting, San Antonia, TX, November 2016.

2016 **Dumitru, I.A.** and M.J. Harrower – "Mapping Economic Networks of Production and Trade: Copper in Oman and Obsidian in Ethiopia," Raw Materials Exploitation in Prehistory: Sourcing, Processing, and Distribution, Faro, Portugal, March 10 – 12, 2016.

2015 Sivitskis, A.J., M.J. Harrower, and **I.A. Dumitru** – "Satellite Imagery Detection of Archaeological Deposits: Experiments with Field Measured Spectral Signatures of Agricultural Sediments and Ancient Copper Mining in Oman (poster)," 2015 Geological Society of America Annual Meeting in Baltimore, MD, November 1 – 4, 2015.

2015 **Dumitru, I.A.** and M.J. Harrower – "Mapping Ancient Production and Trade of Copper from Oman and Obsidian from Ethiopia," Red Sea Conference VII, Procida, Italy, May 27, 2015.

2014 **Dumitru, I.A.**, and M.J. Harrower – "Mapping Ancient Copper in Oman: Application of Hyperspectral EO-1 Hyperion Satellite Imagery," Early Arabian

Metallurgy Workshop, Seminar for Arabian Studies, British Museum, London, UK, July 26, 2014.

2013 Harrower, M.J., **I.A. Dumitru**, J. Swerida, S. Nathan, J. Bongers – "The Red Sea and the Persian Gulf: Long-Term Conduits of Ancient Interchange, Entanglement, and Hybridity," American Schools of Oriental Research (ASOR) Meetings, Baltimore, MD, Nov. 20 – 23, 2013.

CAMPUS TALKS

2013 **Dumitru, I.A. –** "Using GIS Applications and Remote Sensing Technologies in Archaeology," Johns Hopkins Archaeological Museum, April 20, 2013.

2012 **Dumitru, I.A.** – "Create your own Cuneiform Tablet," Johns Hopkins Archaeological Museum.

TEACHING EXPERIENCE

2019 Instructor of record, "Freshman Seminar: The Development of Useful Things: A Comparative Approach to the Study of Technology and Economy in the Ancient World," Department of Near Eastern Studies, Johns Hopkins University.

2017 Teaching Assistant, "Geographic Information Systems in Archaeology," Department of Near Eastern Studies, Johns Hopkins University.

2017 Instructor of record, "The Development of Useful Things: Technology and Economy in the Ancient World," Department of Near Eastern Studies, Johns Hopkins University.

2015 Teaching Assistant, "World Prehistory," Department of Near Eastern Studies, Johns Hopkins University.

2013 Teaching Assistant, "Introduction to Archaeology," Department of Near Eastern Studies, Johns Hopkins University.

RESEARCH AND ARCHAEOLOGICAL FIELD EXPERIENCE

2019 Director, Africa Social Networks Project (AfroNet) (Co-Director, Kifle Zerue, Chair of Archaeology Department, Aksum University; Co-Director, Michael J. Harrower, Associate Professor of Archaeology, Department of Near Eastern Studies, Johns Hopkins University).

2018 GIS/Remote Sensing Analyst, Ambassadors Fund Large Grant for Cultural Preservation – "Conservation of the Endangered World Heritage Site of Nan Madol: A Ceremonial Center of Eastern Micronesia," CSRM Foundation.

2017 Design lead and technical consultant, Meroe Visitor Center, UNESCO World Heritage Site of the Island of Meroe, Sudan, CSRM Foundation.

2016 Co-Director Southern Red Sea Archaeological Histories Project (SRSAH)

2016 GIS/Remote Sensing Analyst, Fort Irwin: Direct Detection Modelling Project (NASA Legacy funded), CSRM Foundation.

2016 GIS/Remote Sensing Analyst, Fort Benning: Direct Detection Modelling Project (NASA Legacy funded), CSRM Foundation.

2016 GIS/Remote Sensing Analyst, Nasca Lines Project, CSRM Foundation.

2015 Field Director for Geospatial Analysis, Archaeological Water Histories of Oman (ArWHO) Project (2015, 2017).

2014 Field Archaeologist, Tayinat Lower Town Project (TLTP), Turkey.

2014 Geospatial Technician, Mochena Borago Archaeological Project, Ethiopia.

2012 Field Director, Southern Red Sea Archaeological Histories (SRSAH) Project (2012, 2014, 2015).

2012 Field Photographer, for Excavation and Small Finds, Southern Red Sea Archaeological Histories (SRSAH) Project (2012, 2014 – 2016).

2012 Field Photographer, Archaeological Water Histories of Oman (ArWHO) Project (2012 – 2013, 2015, 2017).

2012 Remote Sensing Analyst, Archaeological Water Histories of Oman (ArWHO) Project (2012 – 2013, 2015, 2017).

2011 Graduate Student Researcher, Spatial Observation Lab for Archaeological Research (SOLAR), Johns Hopkins University.

RESEARCH REPORTS

2018 Harrower, M., C. Perlingieri, **I.A. Dumitru**, et al. Southern Red Sea Archaeological Histories (SRSAH) Project. 2016 Field Report, May 17, 2018.

2017 Harrower, M., **I.A. Dumitru**, et al. Archaeological Water Histories of Oman (ArWHO) Project. Report 2017, Sept. 4, 2017.

2015 Harrower, M., **I.A. Dumitru**, et al. Archaeological Water Histories of Oman (ArWHO) Project. Report 2015, Jan. 25, 2015.

2015 Harrower, M., C. Perlingieri, **I.A. Dumitru**, et al. Southern Red Seas Archaeological Histories (SRSAH) Project. Report 2015, June 22, 2015.

2014 Harrower, M., C. Perlingieri **I.A. Dumitru**, et al. Southern Red Seas Archaeological Histories (SRSAH) Project. Report 2014, Oct. 10, 2014.

2013 Harrower, M., C. Perlingieri, **I.A. Dumitru**, et al. Southern Red Seas Archaeological Histories (SRSAH) Project. July 21, 2013.

2013 Harrower, M., K. O'Meara, J. Swerida, **I. A. Dumitru**, et al. Archaeological Water Histories of Oman (ARWHO) Project, Report 2013, Mar 22, 2013.

2012 Harrower, M., J. Swerida, J. Bongers, **I. A. Dumitru**, et al. Southern Red Sea Archaeological Histories Project: Baita Semati and Aksumite Societies of Yeha Region. Report Jul 10, 2012.

2012 Harrower, M., J. Swerida, **I. A. Dumitru**, J. Bongers. Archaeological Water Histories of Oman (ARWHO) Project Report Jan 22, 2012.

CAMPUS AND DEPARTMENTAL SERVICE

2018 *Co-Organizer*, 2018 ANŠHE Lecture, Emily Hammer (University of Pennsylvania, Near Eastern Languages and Civilizations Department) – "Digital Approaches to Historical Landscapes of the Ancient Near East," Johns Hopkins University, May 1, 2018.

2015 *Co-Organizer*, 2015 ANŠHE Lecture, Heather Baker (University of Toronto, Near and Middle Eastern Civilizations Department) – "The Babylonian City in Long-Term Perspective: Investigating Urban Processes Using Texts and Archaeology," Johns Hopkins University, April 20, 2015.

2014 *Co-Organizer*, 2014 ANŠHE Lecture, Rita Wright (New York University, Anthropology Department) – "A Comparative Perspective on Gender in Specialized Economies: Craft Specialization, Kinship, and Technology," Johns Hopkins University, April 21, 2014.

MEDIA COVERAGE

(in prep) Stirn, M. (in prep): Introducing the Visitor Center, Archaeological Sites of the Island of Meroe UNESCO World Heritage Site. *National Geographic Traveler Magazine*.

2018 Buchanan, M. (2018): Protecting the legacy of Nan Madol, a lost city in the Pacific. *Share America* (published online September 4th, 2018; https://share.america.gov/protecting-nan-madol-lost-city-in-pacific/?fbclid=IwAR1Vet9HmpVPd-3pbRHmIxR9qsWqW7wEr6htLoyhvw1rzMDhpyR9rD1aep4)

2017 Iron Age soft-stone vessels discovered in Sultanate. *Times of Oman* (published online January 18, 2017; https://timesofoman.com/article/100894/Oman/Heritage/Iron-Age-soft-stone-vessels-discovered-in-Sultanate)

2017 Oman TV – First Discovery of Soft-Stone (Chlorite) Vessel Production in Arabia (published online January 16, 2017; https://youtu.be/FIg-IezdMsY)

RELATED PROFESSIONAL SKILLS

Network Analysis	UCINET 6, Gephi, visone
GIScience	GIS (ESRI ArcMap 10.6, ArcGIS Pro, QGIS), Remote Sensing (Hexagon Geospatial ERDAS IMAGINE 2018, Harris Geospatial ENVI 5.3)
Chemical Analysis	Brucker Tracer III-V XRF Analyzer, Thermo Niton XL3t GOLDD+
Statistics	R 3.5.1, JMP Pro 14

Mapping	Trimble GeoXH, Trimble Geo7x, Trimble R4 base station
Photography	Digital Photograph, Adobe Photoshop CC 2018
Illustration	Adobe Illustrator CC 2018, Adobe InDesign 2018

LANGUAGES

Modern

Romanian	Native
English	Native
Spanish	Excellent
French	Excellent
Italian	Good
Portuguese	Can read with dictionary
German	Can read with dictionary
Arabic	Beginner (Speaking only)
Tigrinya	Beginner (Speaking only)

Ancient

Ancient Greek	Can read with dictionary
Akkadian	Can read with dictionary
Sumerian	Can read with dictionary

PROFESSIONAL MEMBERSHIPS/ AFFILIATIONS

Society of Africanist Archaeologists (SAfA)

American Schools of Oriental Research (ASOR)

International Council on Monuments and Sites (ICOMOS)

University Consortium for Geographic Information Science (UCGIS)